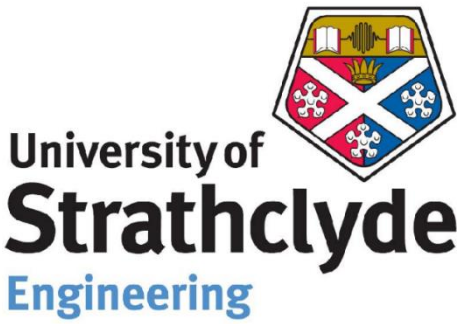

Department of Civil and Environmental Engineering

University of Strathclyde

GEOCHEMISTRY OF GROUNDWATER OF SHALLOW COASTAL AQUIFERS OF EASTERN DAHOMEY BASIN, SOUTHWESTERN NIGERIA

A Thesis submitted in fulfilment of the requirement for the Degree of Doctor of Philosophy

By

JAMIU ABIMBOLA ALADEJANA

2020

Declaration

This thesis is the result of the author's original research. It has been composed by the author and has not been previously submitted for any examination which has led to the Award of a degree.

Signature: ……..

Date: ……..

Dedication

This work is dedicated to Almighty God who grant me the grace to complete it when life became challenging that I could not see beyond my nose

Acknowledgement

I give honour and adoration to the merciful God whose Covenant never failed. My sincere gratitude goes to Almighty God the creator of the universe, "The Beginning and The End". I am indeed grateful to my parents. My special appreciation to my wife for her love and sacrifice, and also, my sincere gratitude to my children for their love and passion despite me, being an absentee father throughout my study.

I am highly indebted to my Supervisor, Prof. Robert M. Kalin, for the guidance, constant motivation, moral support and invaluable knowledge given to me during my study. Prof Kalin, you are indeed a great father, leader and mentor.

I also wish to extend my sincere appreciation to my second supervisor, Dr Philippe Sentenac, for his contributions and moral support.

I want to express my sincere appreciation to the Petroleum Technology and Development Fund (PTDF) for funding my PhD study under the Overseas PhD scholarship scheme. Also for the support of the Scottish Government under the Climate Justice Fund Water Futures Programme, awarded to the University of Strathclyde.

I will like to express my sincere appreciation to my colleague, Ibrahim Hassan, for your love and support at every opportunity for the last three years we met here at the University of Strathclyde. You have been a wonderful brother and friend to me. I will like to thank Christopher Ibeh, Ibrahim Lawal, Emmanuel Salifu, Charles Mbama, Ibrahim Labaran Ali, Cedric Sachet, Jackson Kawala, and all my friends and colleagues who have assisted at various occasions generously with their knowledge and expertise in preparing this thesis. Their views and tips are indeed useful.

My appreciation goes to Mara Knapp, Tatyana Peshkur and Valerio Cappadona for the assistance during the laboratory work. Ademola Ologbe, and Davies Akpan for their help during the fieldwork.

My appreciation goes to Prof. Moshood Tijani and Dr. (Mrs) S. Tijani, for their kindness to me. My sincere gratitude to Prof Alan MacDonald of the British Geological Survey (BGS), who played a vital role in my choice of University and

Supervisor during my decision making. Dr Nasir Kolade and his wonderful family who ensured I did not feel lonely throughout my stay here in Glasgow. Your support has been incredible. To the entire family of Aladejana, I appreciate your help. Mr and Mrs Akintola, Dr Olumide Odeyemi, Mr Lanre Adebayo and all those family and friends that gave me support one way or the other, I appreciate you all.

Publications from the Thesis

Refereed Journal Articles

1. Aladejana, Jamiu A, Kalin, R.M., Sentenac, P., Hassan, I., 2020. Hydrostratigraphic Characterisation of Shallow Coastal Aquifers of Eastern Dahomey Basin, S / W Nigeria, Using Integrated Hydrogeophysical Approach ; Implication for Saltwater Intrusion. Geoscience 10, 65. https://doi.org/10.3390/geosciences10020065 [Open access]

2. Aladejana, Jamiu A., Kalin, R.M., Sentenac, P., Hassan, I., 2020. Assessing the Impact of Climate Change on Groundwater Quality of the Shallow Coastal Aquifer of Eastern Dahomey Basin, Southwestern Nigeria. Water 12, 224. https://doi.org/10.3390/w12010224 [Open access]

3. Aladejana, Jamiu A, Kalin, R.M., Sentenac, P., Hassan, I., 2020. Groundwater Quality Index as a Hydrochemical Tool for Monitoring Saltwater Intrusion into Coastal Freshwater Aquifer of Eastern Dahomey Basin, Southwestern Nigeria. ***Accepted for publication*** in Elsevier Journal; *Groundwater for Sustainable Development. Manuscript ID: GSD-2019-398*

4. Jamiu A. Aladejana, Robert M. Kalin, Ibrahim Hassan, Moshood N. Tijani and Philippe Sentenac. 2020. Hydrogeochemical and Isotopic Characterization of Coastal Groundwater of Eastern Dahomey Basin, Southwestern Nigeria. ***Under review*** in Elsevier Journal; *Results in Geochemistry*. *Manuscript ID: RINGEO-D-20-00006*

5. Jamiu A. Aladejana, Robert M. Kalin, Ibrahim Hassan, Philippe Sentenac and Moshood N. Tijani. 2020. Assessing the Impact of Land Use Patterns on the Groundwater in the Shallow Coastal Aquifer of Eastern Dahomey Basin, Nigeria Using Statistical and Water Quality Analysis. ***Under review*** in Elsevier Journal; *African Journal of Earth Sciences. Manuscript ID: AES8466*

6. Jamiu A. Aladejana, Robert M. Kalin, Ibrahim Hassan, Philippe Sentenac and Moshood N. Tijani. 2020. Origin and residence time of groundwater in the shallow coastal aquifer of Eastern Dahomey Basin using $\delta^{18}O$ and δD Isotopes. ***To be submitted*** to MDPI; *Applied Science (Earth Science and Geography)* [Open access]

Conference Papers

a) Young Water Professionals Conference, International Water Association, United Kingdom. Edinburgh, United Kingdom. June 2019.
Paper Presented; Jamiu A. Aladejana, Robert M. Kalin, Philippe Sentenac and Ibrahim Hassan. (2019). *Delineating Saltwater Intrusion into Coastal Freshwater Aquifers of Eastern Dahomey Basin, Southwestern Nigeria.*

b) 1st Doctoral School Multidisciplinary Symposium, University of Strathclyde, United Knigdom. June 19, 2019.
Paper Presented; Jamiu A. Aladejana, Robert M. Kalin, Philippe Sentenac and Ibrahim Hassan. (2019). *Groundwater Quality Index as a Hydrochemical Tools for Monitoring Saltwater Intrusion into Coastal Freshwater Aquifer of Eastern Dahomey Basin, Southwestern Nigeria. Book of Abstract, p36.*

c) International Conference on water, informatics, Sustainability and Environment, Carleton University, Ottawa, Canada. August 7-9, 2019.
Paper Presented; Jamiu A. Aladejana, Ibrahim Hassan, Robert M. Kalin and Philippe Sentenac. (2019***)***. *Assessing the impact of Climate Change on Groundwater quality of Shallow Coastal Aquifer of Eastern Dahomey Basin, Southwestern Nigeria, Using Seasonal Biogeochemical Processes of Nitrate, Sulphate, Iron and Manganese*. *Book of Abstract, p78*

Abstract

Coastal basins offer valuable land, water and economic resources and have high economic contribution to national and global development; hence the high population of coastal cities around the world due to their commercial, industrial and agricultural significance. Some of the cities and towns situated in coastal parts of Africa rely on the freshwater of the coastal aquifers to meet the vast shortage in water supply resulting from infrastructural deficiency and decay. Complexity of groundwater occurrence and distribution in basement aquifers lead most of the developing countries to depending on basins to meet their daily water demand as these basins are known for high freshwater potential. The Eastern Dahomey Basin (EDB) is not an exemption. The high rate of population growth, unpredictable rainfall patterns, rise in sea-levels, coupled with over abstraction and seawater intrusion, land-use activities, climate conditions, and the geological setting have significant influence on groundwater chemistry and quality. Recently, groundwater resources management has become preferentially higher in the agenda of the sustainable development goal of the United Nations with much attention on developing countries where groundwater remains their source of water demand for various usages. As data and information on groundwater is critical to its sustainable management, especially at a basin scale. This study presents a comprehensive groundwater geochemistry of the Eastern Dahomey basin to contribute to the amount of knowledge available to better increase the effective frame work of integrated water resources management in Sub-Saharan Africa.

A total of 230 water samples were collected between May 2017 and April 2018, a period which spanned through wet and dry seasons, from the shallow boreholes and

hand-dug wells. These 230 groundwater samples (97 in wet season and 133 in dry season) were analysed for essential water quality parameters such as pH, Electrical Conductivity (EC), Total Dissolved solid (TDS), Total Hardness (TH), Ca, Mg, Na, K, HCO_3, Cl, SO_4, NO_3, F and the trace metals As, Cd, Fe, Mn, Pb and Si and stable Environmental Isotopes of $\delta^{18}O$ and $\delta^{2}H$. In addition to these, stable isotopes of $\delta^{18}O$ and $\delta^{2}H$ in precipitation data from three selected GNIP stations, Douala, Cotonou and Kano within the West Africa, were collected for comparative analysis. These data were subjected to evaluation for different quality indices such as GQIswi, SMI, GWQI and Ionic ratios, while modelling, plotting and statistical were carried out using analysis using ArcGIS, MATLAB, Geochemist Workbench, SPSS, Origin pro and Microsoft Excel. Electrical resistivity prospecting and borehole logging were carried out in locations with enhanced electrical conductivity around the coastal communities. Three traverses A-B, C-D and E-F were selected along which ERT and IP were carried out in directions perpendicular and parallel to the coastline and correlated with borehole logs.

Higher salinities above 1000 µS/cm were observed in wells located around communities in Seme, Lekki, Eleko, Okun-Ajah, Ode-Mahin and Igbokoda. HFE-D revealed that mixed groundwater of Na+Ca-HCO_3, Na-Cl and Ca-Cl dominate the area due to gravity-driven flow leading to groundwater freshening inland from the coastline towards the northern part of the basin. The groundwater quality index from SMI and GQIswi show areas within 3 km from the coastline that are more sensitive vulnerable to seawater intrusion. This result therefore guided our selection of areas for electrical resistivity geophysical investigation. Electrical resistivity tomography (ERT) and induced polarisation (IP) indicated a saline water-saturated layer of fine-grained sand and silty clay which is overlaid by the unconsolidated unconfined freshwater aquifer

in area around Lekki and Okun Ajjah while low resistivity of clay lenses were found at Igbokoda, Ugbonla and Ode-Mahin. Correlation of selected ERT results with borehole logs further affirmed the suspected lithology from the sections.

Results of the hydrochemical model revealed Ca-HCO3 and Na-Cl as dominant water types with other mixing water types such as Ca-SO_4, Ca-Cl, Na-SO_4 and K-Mg-HCO_3 which characterised early stage of groundwater transformation in the shallow coastal basin. In addition, a comparison of the $\delta^{18}O$ and $\delta^{2}H$ isotopic compositions of groundwater and precipitation in the three selected stations, with their respective D-excess values established low evapotranspiration induced isotope enrichment, which could be due to higher precipitation and humidity in the region resulting in low isotope fractionation, hence, little effect of seasonal variations.

Assessing the future use of groundwater for irrigation suggests some parts of the aquifer may have unsuitable quality based on the percentage sodium (%Na), Kelly's ratio (KR), magnesium ratio (MR) and total hardness. Results of GQWI revealed 44.8, 22.9 and 12.5% of water samples during the wet season fell in the class of excellent, good and moderate-quality respectively, while 8.3 %, 1.0 and 10.4 % fell in a class of poor, very poor and none potable water quality. Correlating the spatial distribution of the GWQI with the land use pattern map of the area revealed the least potable water is clustered around settlement areas, indicating groundwater quality has been impacted by municipal, industrial and agricultural waste. The linear regression modelling established significant relationships between SWL, SO_4^{2-}, NO_3^{-}, Fe, and Eh for both wet and dry seasons with the *p*-value falling between 75% and 95%, which can also be seen in the plots of Eh/ORP against Fe^{2+}, Mn^{2+}, SO_4^{2-}, and NO_3^{-}.

This study has identified groundwater quality deterioration within the shallow coastal aquifers of the eastern Dahomey basin. Hydrochemical and geophysical approach established saltwater intrusion into freshwater aquifer occurred both as seawater intrusion, dissolution of evaporites within the clay lenses and sea spraying within the close proximity to the sea. Hydrochemical and environmental Isotopes classified as young from a meteoric source, which is still in the early stage of geochemical evolution with short residence time. A combination of groundwater quality indices (GWQI) and biogeochemical (redox) analysis also established the influence of natural and anthropogenic effect of climate change, urbanisation, industrialisation and agriculture on the groundwater quality of the basin. The present study provides information of value to planners and policy-makers for the sustainable management and protection of coastal groundwater resources in the Eastern Dahomey Basin. There is a need for waste management policy review and enforcement to support sustainable groundwater resource management and sustainable development goal number 6 (SDG6).

Keywords: Groundwater; Saltwater intrusion; Groundwater quality index; freshwater; Coastal aquifer; Clay lenses; Saline water; Freshwater; Geoelectrical Layers; Hydrogeochemistry; mineral dissolution; Saturation Index; Stable Isotopes; Environmental Isotopes; Precipitation; Groundwater Origin; Residence time; Climate change; Biogeochemical Processes; Redox and Metals mobilisation; land use; seasonal effects; Anthropogenic; water resource management.

Table of Content

List of Figure

List of Tables

List of Bullet

LIST OF ABBREVIATION

AGI	Advance geophysical instrument	NDDC	Niger Delta Development Commission
AQC	Analytical quality control	1-D	One dimension
CAI	Chloroalkaline Index	ORP	Oxidation and reduction potential
DO	Dissolved oxygen	%Na	Percentage sodium
DS	Dry season	PI	Permeable Index
EDB	Eastern Dahomey Basin	PCA	Principal component analysis
EC	Electrical conductivity	QC	Quality control
ERT	Electrical resistivity tomography	QCCS	Quality control check standards
FA	Factor analysis	RWML	Regional meteoric water line
FW	Fresh water	RSC	Residual sodium carbonate
FW	Fresh water	SW	Saline water
GIS	Geographical Information System	SW	Saline water
GMWL	Global meteoric water line	SMI	Saltwater mixing index
GNIP	Global Network of isotope in precipitation	SMI	Saltwater mixing index
GDP	Gross domestic product	SI	Saturation index
GWQI	Groundwater quality index	SLR	Sea level rise
GQIswi	Groundwater quality index for saltwater intrusion	SAR	Sodium absorption ratio
HCA	Hierarchical cluster analysis	SWL	Static water level
HFE-D	Hydrochemical facies evolution diagram	SWL	Static water level
IP	Induced polarization	SDG6	Sustainable development goal number 6
IWRM	Integrated water resources management	TDS	Total dissolved solids
IPCC	Intergovernmental Panel on Climate Change	TH	Total hardness
IAP	Ion activity product	TEM	Transient electromagnetic
IC	Ion chromatography	2-D	Two dimension
KR	Kelly ratio	UNDP	United Nations Development Programme
LMWL	Local meteoric water line	VES	Vertical electrical sounding
MR	Magnesium ratio	V-SMOW	Vienna Standard Mean Ocean Water
MWL	Meteoric water line	WS	Wet season
MQL	Method quantification limit	WHO	World health organisation
MSI	Mineral saturation index	WMO	World meteorological organisation
MSI	Mineral saturation index		

CHAPTER 1

1.0 INTRODUCTION

1.1 Background Introduction

Groundwater is a natural resource essential for the economic and secure provision of potable water supply in both urban and rural environments (Nowroozi et al., 1999). The level of appreciation of water as an invaluable resource ever shown by man is far less than its importance in the daily well-being of his existence.

According to Biswas and Tortajada, (2019) “thousands have left without love, no one without good quality water”. This quote underline trend of groundwater quality deterioration in developing countries in Sub-Saharan Africa and Asia (Biswas and Tortajada, 2019), which prompted development of integrated water resource management (IWRM) as a strategy to halt further groundwater quality deterioration as millions depends on it for different purpose ranging from domestic, agricultural and industrial usage.

The rapid expansion of industries and urbanisation has triggered unplanned groundwater development leading to severe stress on groundwater resources in the groundwater basin around the world (Priyantha Ranjan et al. 2006,). Complexity of groundwater occurrence and distribution in basement aquifers also push people to focus on the sedimentary basin, which has higher water potential to meet their daily freshwater demand.

Coastal freshwater aquifers are generally susceptible to degradation due to its proximity to seawater, in combination with the intensive water demands that

accompany higher population densities of coastal zones around the world especially in developing countries of Asia and Sub-Saharan Africa (Chang et al., 2011; Werner et al., 2013). Higher competition for space and resources in coastal cities also pose a challenges of the resources and environmental management, which also put additional stress on the quantity and quality of the coastal freshwater that complement sources for water supply. Basically, when there is poor aquifer management, groundwater pollution such as serious salinization and metals contaminations problems appear, even at isolated and localised cases to regional basin scale (Nwankwoala, 2011). This could impair quality of life and jeopardise economic growth of such society.

The Sub-Sahara Africa is known to have extensive coast, which is the host for some of the most populated cities in Africa. The Eastern Dahomey basin is the Nigeria part of the transboudary basin known as Dahomey which cut across the Benin, Togo, Ghana and Ivory Coast. The Basin covers the southern areas of Lagos, Ogun and Ondo which hosts cities like Lagos, Abeokuta, Shagamu, Okitipupa, Ilaro, Igbokoda with other towns and villages and accommodates about 27% of the country population.

The current condition of Nigeria's coastal aquifers is challenging to ascertain, because comprehensive investigations have only been completed for coastal systems in the Niger Delta Basin (Nwankwoala, 2011, 2013). In the case of Eastern Dahomey Basin, few seawater intrusion studies appear to have been undertaken with focus on the coastal areas of Lagos. The assessment appears to be linked to the economic value of the groundwater resource. Though few local studies around Lagos metropolis have reported saltwater intrusion occurrence in the confined aquifers of the Coastal Plain Sands in a zone stretching from Apapa to Lekki. The saltwater bearing sands overlie freshwater aquifers, which are exploited by boreholes (Adepelumi et al., 2009; Oteri

and Atolagbe, 2003). In the coastal area of Ondo state, Omosuyi et al., 2008; and Talabi et al., 2012 reported saltwater intrusion in shallow coastal aquifer around Igbokoda, Ugbonla and Aiyetoro, which lead to abandonment of several boreholes constructed by the Niger Delta Development Commission (NDDC) while inhabitants resulting into importing water from the towns and villages located at the norther part of the basin through private individuals at a higher cost. In addition, to this problem, an ample number of researchers have reported series of groundwater contamination and pollution at specific areas within the basin especially around the major cities and towns.

Adegbola et al, 2013; Ayolabi et al, 2013; and Edet, 2016 have reported elevated concentrations of ions, heavy and trace metals in groundwater of shallow aquifers of the coastal cities of Nigeria, many of which were attributed to indiscriminate waste disposal, effluents from sewage, industrial and agricultural waste. Groundwater and surface water pollution and quality deterioration within the Eastern Dahomey basin have also been reported by Oteri; 1988, Longe et al.; 1987, Adeoti et al.; 2010, and Ayolabi et al.; 2013. Groundwater pollution and contamination in urban area of the Basin was linked to unregulated and indscriminate waste disposal practice that characterised the municipalities. This is further compounded by the incensant flooding driven by extreme precipitation from climate change which promote groundwater interaction with contaminated surface water from rivers, lagoon and drainage channels. This creates a direct passage for metals and nutrients to leaching into groundwater and deteroriate its quality. Upon these challenges, inadequate information, knowledge and paucity of data in aspect of groundwater science and management is confronting proper implementation of Integrated water resources management in this area and other part of the country at large. Therefore,

understanding the geochemistry of water on a basin scale is crucial for effective water resource management and protection (Dragon and Gorski, 2014).

According to the United nation SDG6, *"2 billion people are living with the risk of reduced access to freshwater resources, and by 2050, at least one in four people is likely to live in a country affected by chronic or recurring shortages of freshwater"* (UNDP, (2017). Consequently, more than 2 million people die every year from water-borne related diseases while 4.3 and 6.4 per cent of Sub-Sahara African and India's GDP resulting from adverse economy impacted cost due to inadequate sanitation. Nigeria is currently ranked poorly in the race to achieving Sustainable Development Goal 6 (SDG6), a challenge which requires among others proper understanding of relationships between any of land use, sea level rise, climate change and groundwater quality.

Monitoring groundwater is necessary to detect emerging pollution and contamination early enough to prevent damage to the resource since remediation remains expensive and nearly impossible to implement after water quality deterioration. This task requires adequate knowledge and information on groundwater chemistry to develop a novel aproach to achieve an inclusive and efficient integrated water resources framework that will ensure acelerated steps towards achieving sustainable development goal number 6 (SDG6) in Nigeria and Sub-Sahara Africa at large.

1.2 The Aim of the Study

The proposed study aims to evaluate the groundwater resources of Eastern Dahomey basin, using integrated hydrogeology and stable environmental isotopes to understand hydrochemical processes that control groundwater geochemistry of the

basin with a view to assessing the possible impact of natural and anthropogenic drivers on the groundwater quality of shallow coastal aquifer system for sustainable water resources management. This will allow formulation of adaptive strategies for sustainable coastal groundwater resources management.

1.3 Research Objectives

To achieve the stated aim, the following set of objectives will be addressed.

1. To employed electrical conductivity (EC) in combination with some groundwater quality indices and ionic ratios as a hydrochemical tool for preliminary studies of fingerprints of salinity and other groundwater quality parameters in shallow coastal aquifers of Eastern Dahomey Basin.
2. To characterise the Hydrostratigraphic units of the shallow coastal aquifers of the Eastern Dahomey Basin with focus on origin and distribution of saltwater intrusion into the coastal freshwater aquifer using a physicochemical approach through the electrical conductivity and geophysical method of Electrical Resistivity Tomography (ERT), Induced Polarisation (IP) complemented with borehole logs.
3. To identify the main Hydrogeochemical processes that control groundwater chemistry across the Eastern Dahomey Basin using GIS and interpolation techniques.
4. To evaluate groundwater chemistry variations across different geological units and formation within the basin using stable environmental isotopes of $\delta^{18}O$ and $\delta^{2}D$ in combination with key hydrochemical parameters as contribution to the groundwater conceptual model.
5. To assess the impact of land use on groundwater quality in the EDB using the groundwater quality index and statistical analysis for various groundwater usage.

6. To investigate the impacts of climate change through flooding on groundwater quality of the shallow coastal groundwater of the Eastern Dahomey basin, using variations of seasonal redox biogeochemical process of some selected redox-sensitive ions such as Fe, Mn, NO_3, SO_4.

1.4 Scope of the Study

The study will be carried out within the following scope;

- Well and borehole inventory and field measurement of physicochemical parameters such as Electrical Conductivity (EC), Salinity, pH, Eh, Total Dissolved Solid (TDS) and temperature.
- Sampling and preservation of groundwater from shallow Hand-dug wells and open boreholes within the study area.
- Gathering data from boreholes and hydraulic conductivity and other relevant aquifer parameters within the study area.
- Analysis of major anions HCO_3^-, Cl^-, F^-, SO_4^{2-}, and NO_3^- using IC. Major cations Ca^{2+}, Mg^{2+}, Na^+, K^+, Fe, Cu, Mn, Cr, Co, Pb, As, Li, Ba, Yt, Zn and other relevant trace elements using ICP-MS and stable environmental isotopes such as ^{18}O and ^{2}H analysis using Accelerator Mass Spectrometry (AMS)
- Geophysical investigation along selected profile using electrical methods of Electrical Resistivity Tomography (ERT) and Induced Potential (IP) with borehole logs of some selected wells within the study area.
- Producing groundwater quality and saltwater temporal maps of the area from the results of the hydrochemical studies using Arc and QGIS tools to see its quality and identify the vulnerable zones in the area.

1.5 Limitation of the Study

1 In a multi-aquifer setting like the Eastern Dahomey Basin, sampling from different levels of aquifer will help in better understanding the vertical trend in groundwater salinity. Due to lack of groundwater monitoring well that provide this within the basin, this work only focused on wells and boreholes representing the shallow aquifers.

2 The sampling and data acquisition was influenced by accessibility and the consent of the wells and boreholes owners which had slight effect on the sampling distribution.

3 Lack of enough borehole data that could well represent the basin limit the amount of information across the geologic units.

1.6 Structure of the Thesis

This thesis describes a comprehensive approach for hydrogeological assessment of groundwater of the shallow aquifers of the eastern Dahomey basin, southwestern Nigeria, as part of the basic requirements for the integrated water resources management in Sub-Saharan Africa. In addition to the current chapter, nine chapters form this document which is stated as follows;

- ✓ Chapter 2 presents the review of the previous studies fundamental principles and key information relating to groundwater chemistry, stable isotopes and hydrogeophysical application to groundwater studies.
- ✓ Chapter 3 presents the Description of the study area, physical settings, geology and hydrogeology settings of the area which include Regional geology, local geology of Dahomey basin.
- ✓ Chapter 4 presents the methodology of the study. Which also include desk/ reconnaissance survey, hydrogeological field studies, groundwater inventories, in-situ

measurement of physicochemical parameters, groundwater sampling, Geophysical data acquisition and interpretations, Laboratory analysis, data analysis, evaluation and interpretation.

- ✓ Chapter 5 Hydrostratigraphy and aquifer characterisation which includes; (a) "Groundwater Quality Index as a Hydrochemical Tool for Monitoring Saltwater Intrusion into Coastal Freshwater Aquifer of Eastern Dahomey Basin, Southwestern Nigeria" (b) "Hydrostratigraphic Characterisation of Shallow Coastal Aquifers of Eastern Dahomey Basin, Southwestern Nigeria, Using Integrated Hydrogeophysical Approach".
- ✓ Chapter 6 presents "Hydrogeochemical and Isotopic Characterization of Coastal Groundwater of Eastern Dahomey Basin, Southwestern Nigeria".

  Chapter 7 presents "Origin and residence time of groundwater in the shallow coastal aquifer of Eastern Dahomey Basin using $\delta^{18}O$ and δD Isotopes".
- ✓ Chapter 8 presents the impact natural and anthropogenic on groundwater quality which includes (a) "Assessing the Impact of Land Use Patterns on the Groundwater in the Shallow Coastal Aquifer of Eastern Dahomey Basin, Nigeria Using Statistical and Water Quality Analysis". (b) "Assessing the Impact of Climate Change on Groundwater Quality of the Shallow Coastal Aquifer of Eastern Dahomey Basin, Southwestern Nigeria".
- ✓ Chapter 9 presents the implications of the study on integrated water resources management in Nigeria and Sustainable development goal 6 current outlook and way forward.
- ✓ Chapter 10 presents the main conclusions of this research with a list of specific topics suggested for future research.

All references cited are presented at the end of the thesis. This is followed by Appendices referred to within the thesis.

CHAPTER 2

2.0 LITERATURE REVIEW

2.1 Introduction

This chapter presents the relevant literature necessary to achieve the aims stated in Chapter One and highlights the research gap and justification of this research, which are presented in subsequent chapters. The problem addressed in this research was introduced in Chapter One, which also includes the objectives and the scope required to achieve the aim. Understanding key hydrogeological processes, especially groundwater chemistry, is one of the keys to groundwater quality assessment and monitoring. Groundwater quality has been an essential issue in sustainable water resources management, thus, regularly monitoring its quality could help understand the necessary framework required to accelerate the global goal of providing safe and clean water to the people of Sub-Saharan Africa. Groundwater administration in Nigeria is structured on the scale of the basin. Eastern Dahomey is one of the critical eight hydrogeological provinces, which serves the water demand for more than a quarter of the country's population.

2.2 Common sediment of the coastal environment

Suspended matter characterized the estuaries environment due to the nature of water movement in tidal areas of the coastal basins system (Posma, 1967). These processes lead to particles entrapment within the basin structures. Common sources of sediment to estuaries are fluvial from streams and rivers, marine, shores, barrier, anthropogenic, eolian from the desert, volcanic, and glacial (Nicholas and Boon, 1994;

Harbison, 2007). The unconsolidated sediments found within estuarine plains are mainly of either fluvial or marine origin.

Estuarine sediments are generally more homogeneous than catchment soils. Sediments derived from streams and rivers are fine-grained than marine sediments. Still, this trend varies regionally and also depends on the surrounding rocks and dominant weathering process and intensity of the area. In estuaries, the marine contribution of sediment is likely to be less than in a flat tidal sea, but still significant. Based on mineralogy (Wakeland, 1978) and sediment flux deficit, marine-derived sediments depend on the amount of fluvial input escaping to the ocean (Kim and Bokuniewicz, 1991).

The dynamics of circulation in estuary is associated with density differences, mainly caused by salinity variations, and is only second to tidal influences in importance for sediment deposition (Posma, 1967).

In light of the above, the typical sediments in the coastal environment are listed as follow;

Sand

Quartz, commonly known as *sands*, and carbonate (shell material) are abundant at the outer shoals and barriers via delta abandonment (Penland *et al.*; 1988). Generally, sand is trapped along beaches, and this setting covers a smaller area than accumulation sites for finer-grained material, largely tidal flats and river mouths. Tidal lag effects are not crucial for the material of diameter greater than 100 μm (Postma, 1967).

Clay minerals

Minor variations in the land – derived clays occur upon contact with salt water. Typically, there is no significant variation in clay – mineral assemblage throughout estuaries. Illite, Kaolinite, Vermiculite, and Montmorillonite exhibit differential settling rates that are salinity – dependent (Postma, 1967; see Table 3). Montmorillonite is least likely to flocculate due to its highly negative charge and stronger cation double layer. Primary minerals, mica and feldspar, are of fluvial origin and therefore are lowest where seawater dominates (Reinson, 1977).

Iron minerals

In the coastal environment, the occurrence and abundance of diagenetic iron minerals are related to the depositional setting (Berner, 1971). In anoxic sediments, pyrite concentrations above that derived from interstitial marine water sulfate suggest that pyritisation in many bottom sediments occur at the sediment-waterer interface. Pyrite is protected against oxidation by its association with lignite and fine-grained sediments (Brown *et al.*; 1999). The occurrence of iron oxide concentrations in association with pyrite in coastal sediments indicates the oxidation of pyrite (e.g. Logan *et al.*; 1999). The occurrence of marcasite indicates the oxidation of pyrite and reprecipitation under low pH (Brown *et al.*; 1999).

Evaporites

In hypersaline supratidal areas, mineralisation is common. Soil salinities in bare supratidal mud are as high as 88 parts per thousand (ppt) in mangrove communities at the tropical region. The gypsum and halite are attributed to capillary rise of pore-water rather than evaporation of ponded water. While calcite and aragonite

may be of either biogenic or evaporitic origin, dolomite normally occurs via mineralization of calcite. In temperate lagoons, Wright, (1999) primary dolomite forms in association with seasonal desiccation and sulfate reduction. In overlying oxidizing conditions, soluble iron and sulfate cause precipitation of ferric oxy-hydroxides and acid – sulfate minerals, dominated by jarosite. The coexistence of reduced and oxidized minerals (e.g. pyrite, gypsum and jarosite) may indicate sea-level variations (Arakel and Ridley, 1986), or alternately may be produced in microenvironments around plant roots (Lord and church, 1983).

Organic matter

Significant organic matter production occurs in intertidal zones, a high proportion of which may then be either incorporated into sediments or exported. Organic material is also imported to the estuarine environment as ‘’ marine snow’’, i.e. large diameter organic particles (Chin *et al.*; 1998). These particles affect the sedimentation rate and allow the incorporation of organic matter in sand facies. Subsequently, this incorporation in sand leads to abrasion and re-suspension in the water column.

2.2.1 Mineral resources of the Eastern Dahomey basin

The Eastern Dahomey basin is characterised with multi-aquifer layers of different lithological units, as described in chapter 3. The Basin is known for numerous valuable minerals deposit and therefore holds a huge prospect for mineral exploration. The minerals found within this basin are: sand, bitumen, limestone, feldspar, kaolin, granite, gemstones, bentonite, gypsum and phosphorous (Oli et al., 2019). The dominant mineral is commonly based on the solubility of this mineral, which is

considered relatively high, which could aid the mineral dissolution processes when other relevant conditions favour their chemical reactions, (Abimbola et al.; 1999).

2.3 Saltwater intrusion and hydrostratigraphy characterisation

2.3.1 Concept of Saltwater intrusion

Saltwater intrusion is the movement of saline water into freshwater aquifers, which can result in the pollution and contamination of drinking freshwater resources and other consequences. According to Carrera et al. (2010) and Meyer et al. (2019), saltwater intrusion progression into the coastal freshwater aquifer is a function of (1) geological heterogeneity of coastal aquifers, (2) type of inland boundary conditions, (3) coastal topography and water management, (4) relative sea-level rise and (5) initial salt distribution.

Saltwater intrusion occurs as part of natural phenomena in most coastal aquifers, owing to the hydraulic connection between groundwater and seawater. Actions of man could induce this process by creating a reverse pressure, which advances the boundary of the seawater-freshwater contacts towards the continental zone. Because of higher mineral content in saltwater compared to freshwater, it is denser and has higher water pressure. As a result, saltwater can push inland beneath the freshwater (Oteri 2010). Certain human activities, especially groundwater pumping from coastal freshwater wells, could induced rate of saltwater intrusion in many coastal aquifers. When there is uncontrolled water extraction, it lowers the level of fresh groundwater, reversing the pressure and causing saltwater to flow further inland. Factors such as navigation channels or agricultural and drainage channels could also provide conduits for saltwater to move inland, and sea-level rise (Barlow and Paul,

2003). This phenomenon is better to explain in Figure 2.1, which show the interface between coastal freshwater and seawater, where the movement originates depending on the dominant factors.

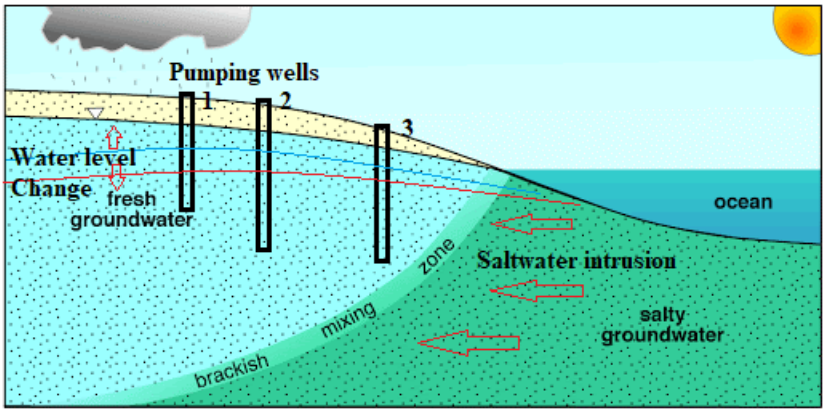

Figure 2.1 Sketch of fresh-sea water interface in a coastal area

Another concept of saltwater intrusion into the coastal freshwater aquifer is through the dissolution of evaporites deposited with the coastal sediments as a result of ocean transgression in the past, which were followed by evaporation and subsequent deposition of sediments which further buried deep in the soil. They form lenses-like structure of clay within the sandy aquifers which, when dissolved in groundwater, could raise their salinity and cause significant contaminations and render the water non-potable. Some researchers (Cary et al., 2015; Giambastiani et al., 2007; Oteri, 1991) have reported this type of phenomenon in coastal basins around the world.

2.3.2 Monitoring and assessment of saltwater intrusion

Saltwater within the geological environment is characterised by certain physicochemical parameters that differentiate them from the fresh and brackish water. Elevation of parameters such as electrical conductivity (EC), total dissolved solids (TDS), sodium and chloride ions concentration is a fingerprint to higher salinity in groundwater. Because of these characteristics, saltwater behaves like electrolytes

within the aquifer pore spaces (Ayolabi et al., 2013; Post et al., 2013; Tran et al., 2012). According to the work of Oteri and Atolagbe, 2003, successful management of coastal groundwater resources depends, not only on planning and regulation but also on the accurate assessment and prediction of the behaviour of the saltwater interface to both natural and anthropogenic drivers.

Generally, hydrochemical method and hydrogeophysical methods remain the two common methods used in assessment and monitoring saltwater intrusion in coastal aquifers. Studies from various locations around the world (Bouzourra et al., 2015; Ebrahimi et al., 2016; Gime´nez-Forcada, 2014; Giménez-Forcada et al., 2010; Isa and Aris, 2015; Werner and Gallagher, 2006) have demonstrated effectiveness of hydrochemical methods ranging from groundwater quality indices to ionic ratios related to saltwater intrusion. While hydrogeophysical methods of electrical resistivity, electromagnetic and electronic/logging have also been applied by several researchers (Adepelumi et al., 2009; Ayolabi et al., 2013; Bauer-Gottwein et al., 2010; Hodlur et al., 2006; Khalil, 2006; Kouzana et al., 2010; Oyeyemi et al., 2015) in mapping and delineating saltwater intrusion in the coastal basin around the world. These methods have been very helpful in the sustainable management of saltwater intrusion in coastal zones around the world.

2.4 Occurrence of saltwater intrusion into the shallow coastal freshwater aquifer of Eastern Dahomey Basin

The lithological disposition of the aquifers gives rise to artesian and sub-artesian conditions in places. In the Lagos metropolitan area, the Coastal Plain Sands were the major aquifers exploited in the past but drilling for water supply over the past decade target the deeper Abeokuta Formation. This is because of excessive drawdown

(progressive decline in the head) associated with boreholes tapping the phreatic aquifers of the Coastal Plain Sands and the consequent problem of saline water intrusion already manifest in some localities. Saltwater intrusion into shallow coastal aquifers of the Eastern Dahomey Basin occurs below the freshwater lens in a layer extended within 5km of the coastline in some places (Oteri and Atolagbe, 2003). The occurrence of saltwater intrusion is also discovered in the confined aquifer of the Coastal Plain Sands in locations around Apapa, Lekki, Lakwe, Oniru, Sangotedo, Akodo, which are all within the proximity of the sea. The saltwater is said to overlie the freshwater aquifers which are exploited by boreholes in most cases (Adepelumi et al, 2009 and Oladapo, 2014). In some parts of the basin around Lakwe, saltwater occurred in form of lances trapped within the clay layers intercalated sand and sandy clay layer while some are trapped within the sandy layer as salt lenses in Nigeria, there have been few studies aimed at assessing freshwater resources in coastal areas of the country, and most of these works were conducted by researchers from the academic institutions (Oteri, 2008). Potable water supply to inhabitants in some of the communities in the coastal belt of Nigeria has been a significant problem due to saltwater intrusion (Oteri and Atolagbe, 2003). In these regards, Oyedele and Momoh (2009) evaluated seawater intrusion in the freshwater aquifers in the coastal area around the University of Lagos Lagoon, southwestern Nigeria, using a combination of VES and IP method correlated with borehole logs carried out within the study area. The result revealed that the depth to the saline water surfaces is shallower towards the lagoon and deeper as one moves farther away from the coastline. The study shows that the area suffers from acute saline water intrusion. It was concluded that the saltwater intrusion could be due to the deposition of sediments during transgression inland areas

and the influence of meteoric water which aids the push some of these sediments in the subsurface.

Adeoti et al, (2010) employed electrical resistivity and induced polarization methods in Oniru area, Lekki, Lagos State Nigeria, to study saline water intrusion problem of the area. The quality of groundwater was detected to vary from poorly polluted saline water-saturated sand/clay through intermediate water quality clayey sand/sand to freshwater sand as observed from three 1-D geoelectric sections carried out. They observed that depth to fresh–saltwater interface varied between 19.47 and 105.69 m, which becomes shallower towards the coastline.

Combined geophysical and geochemical techniques were used to map saltwater intrusion into coastal aquifers. Ayolabi et al. (2013) employed this combined method in studying saltwater intrusion into the coastal aquifers of the University of Lagos Campus. In this work, pollutant sources were linked to brackish water infiltration from the creek and surrounding lagoon, wastewater accumulation and percolation through unlined drainage/canal within the university, wastewater from the adjoining water channel, infiltration from a polluted stream. All these were pointing to anthropogenic sources.

Oladapo et al. (2014) studied the saline water intrusion in Lagos municipality using a total of 52 borehole logs consisting of natural gamma-ray, single-point resistance, short and long normal resistivity. The result revealed that saline water incursion was most severe at the southern flank of the city towards the coast; Apapa, Kirikiri, Ijora, Satellite Town, Iganmu, Bariga, Lagos Island, Victoria Island, Lekki, Ajah, Badore, Sangotedo, Awoyaya, Lakowe and Akodo.

Despite all this, the report still shows that systematic and detailed groundwater quality assessment and monitoring are insufficient for sustainable management of groundwater in the face of the menace of saltwater intrusion and climate change. This challenge results from a combination of factors, such as costs associated with water quality monitoring, the relatively low levels of funding for research in Sub-Sahara Africa over the past decade and limited national regulation of high-intensity rainfall events which pose a risk to shallow and poorly protected groundwater sources (Coode & Akute Geo-Resource, 1996; *Lapworth et al., 2016).* Also, groundwater as dynamic resources upon which its quality requires constant regimented monitoring for early detection of contamination and pollution to ensure a sustainability and health safety measure of life, and possibly plant and animals which depends on it for survival. Moreover, there is a vital need to monitor the possible risk of saline water intrusion of the coastal aquifers because, once saline intrusion into coastal aquifer has occurred, it is challenging to overcome and to improve the management of the water resources based on long-term strategy. Protection of groundwater resources in coastal areas and their sustainable management, in conjunctive use with other water resources (e.g., surface water, seawater), require an understanding of the coastal aquifer hydrogeology.

2.4.1 Application of Hydrochemical methods insaltwater moitoring and assessment

About 99% of total ions in natural waters comprises of a small number of principal ions called major ions (Custodio, 1987). Groundwater is typically classified into “water types” on the basis of the absolute and relative abundances of the major ions. These water types can be used to catigorise environments with associated predominant hydrogeochemical reactions. However, due to the predominance of Na

and Cl in saline waters, major ion differences presented by trilinear diagrams can be inconclusive in differentiating saline water from freshwater bodies (Howard and Lloyd, 1984).

Consequently, Tomaszkiewicz et al., (2014) and Trabelsi et al., (2016) proposed a modified water-type classification known as HFE-D and modified piper diagram system for groundwater indices for saltwater intrusion and mixing which were developed into temporal map and applied in monitoring and investigating saltwater intrusion into coastal freshwater aquifer.

The main features of this system were salinity, total dissolved solids, water type and indices for seawater intrusion. Some ionic ratios of major ions are also useful in understanding processes relating to chemical evolution in coastal groundwater. Therefore, determination of salinity source is usually through chemical methods. For example, Mg/Ca ratio is usually much greater in seawater than in continental waters (Gattacceca et al., 2009). Discrimination based on relative major ion abundances is more successful where recharging freshwater is of continental (Ca-HCO3 type) rather than of marine origin (Na-Cl type. In the Rhodope area of Greece, the Cl/HCO3 ratio was initially used to discriminate sources of salinity (Petalas and Diamantis, 1999). Kumar, 2014; Ebrahimi et al., 2016; Edet, 2016; Mohanty and Rao, 2019 distinguished groundwater types by consideration of Na/Cl, Mg/Ca, SO4/Cl, Cl/Br and saltwater mixing index (SMI).

2.4.2 Applications of electrical resistivity tomography and Induced potentials in delineating Saltwater intrusion

Rock resistivity is of particular interest for hydrogeological purposes. It allows, delineation of freshwater from saltwater, between soft-rock sandy aquifers and clayey

material, between hard rock porous/fractured aquifers and low-permeable claystone and marlstones, and between a water-bearing fractured rock and its solid host rock. (Kirsch, 2011 Ernstson et al.. 2009; Ernstson and Scherer 1986;)

This effectiveness of this method in delineating and characterisation of coastal aquifers has been revealed in several studies in different basins across the world.

Balia and Viezzoli, (2015) applied integrated resistivity, IP, and Transient Electromagnetic (TEM) geophysical techniques to characterize coastal aquifers of Muravera (Sardinia, Italy). Result revealed a near seashore the shallow aquifer, hosted in the lower horizon of the top layer, contains brackish-salt water. In contrast, at distances exceeding 1 km from the seashore, it has freshwater. The salt was attributed to near-surface transport mechanism such as lateral infiltration of seawater through the natural or human-made channels communicating with the sea, and sea spray conveyed inland by the wind and fertilizers. The authors suggested that the salt could be credited to classical seawater intrusion or probably to the fact that in geological past, the shoreline was about 2km inland with regard to its current position.

Researchs such as Land *et al.*, 2004; Adepelumi *et al.*, 2009; Adeoti et al., 2010; Odunaike *et al.*, 2010; Kirsch, 2011; Amadi et al., 2012; Igboekwe et al., 2012; Di Maio *et al.*, 2013; Oyeyemi et al., 2015;Akinbinu, 2015; Ayolabi et al., 2013; Francés et al., 2015; and McInnis et al., 2013 have applied ERT or a combination of ERT and IP to differentiate lithology at different coastal aquifers. A combination of these methods helps to determine naturally low resistance layers from the salt-bearing units with almost similar resistivity values (Abdulrahman et al., 2016; Elijah A Ayolabi et al., 2013; Buselli and Lu, 2001; Günther and Dlugosch, 2010; W. Ali, H. Hötzl, S. Geyer, E. Salameh, A. Flexer, Y. Guttman, 2004).

In this study, a combination of electrical resistivity methods was integrated with borehole logs to characterise the stratigraphy of the Eastern Dahomey Basin with respect to saltwater intrusion with a view of finding clue to origin and distribution of saltwater within the coastal freshwater aquifer.

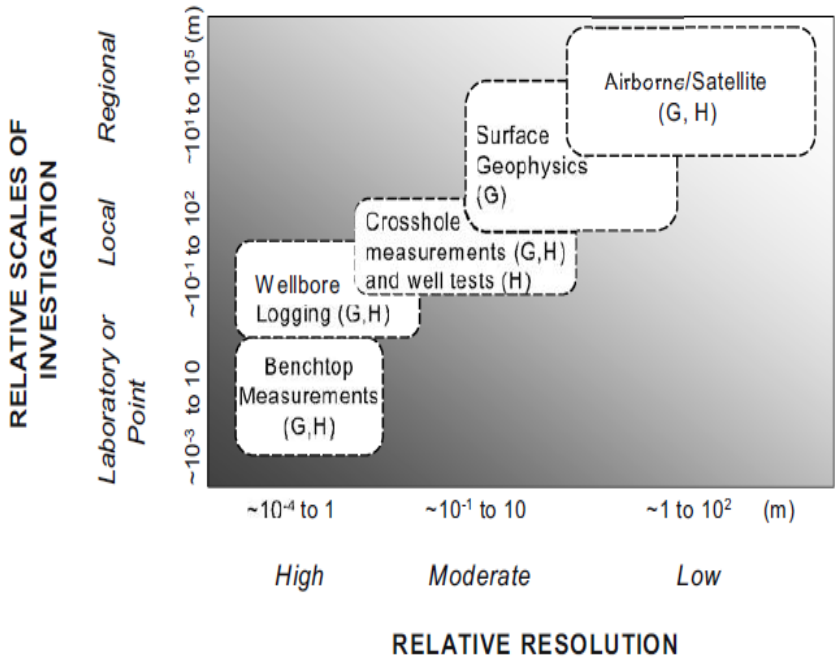

Figure 2.2 Chart showing the trade-off between the relative resolutions of different methods.

Chart showing the trade-off between the relative resolutions of the information obtained using different yet typical geophysical (G) and hydrological (H) measurement acquisition approaches and the relative scale of the investigations for which those acquisition geometries are typically used. Benchtop measurements refer to those such as core, column, and tank measurements collected within a laboratory. (Source: Rubin and Hubbard, 2005).

Bullet 1

Seawater intrusion investigation remains a critical task with intensive demand for resources, and the current scientific challenges of coastal aquifer management in Nigeria are as complex and diverse as the system in itself. Monitoring and investigation requires accounting for the unique characteristic of each coastal aquifer and this leads to the development of basin-specific approaches which involves the design and implementation of novel studies.

2.5 Groundwater geochemistry

Understanding the geochemistry of water provides the clues to its hydrochemical evolution and critical for effective water resource management and protection (Dragon and Gorski, 2014). Studies hydrochemical changes in groundwater can help in delineating the flow pattern occurring in the aquifers. This knowledge is essential in groundwater systems, especially where there is complex hydrogeology as a result of multiple aquifers. In such case, multilayer aquifer systems like the Eastern Dahomey basin, the spatial variations in groundwater chemistry can give a clue determining the groundwater transformation as it flows between different aquifers (Chukwura et al., 2015; Shin et al., 2017).

Groundwater chemistry evolves as a result of hydrogeochemical processes during infiltration and flows in aquifers over space and time (Bodrud-Doza et al., 2019; Kalin, 1995; Narany et al., 2014; Prasanna et al., 2011; Talabi and Tijani, 2013). In watershed and groundwater aquifers, hydrochemical processes such as cation exchange, evaporation, dissolution/ precipitation of minerals, seawater intrusion, oxidation-reduction and biological processes play significant roles in the hydrochemical evolution of groundwater (Adimalla and Kumar, 2020; Narany et al., 2014; Somaratne and Frizenschaf, 2013)

2.5.1 Origin of Dissolved Ions

As groundwater evolved from precipitation through infiltration within soil and rocks aquifer, it trapped dissolve ions either from gas in atmosphere or minerals within the zones which it circulates. The origin or source of dissolved ions is either natural or artificial, which are termed geogenic and anthropogenic, respectively. Depending on prevailing factors such as Solubility of minerals, concentration, temperature, Eh and pH and ion exchange capacity of groundwater determines its hydrochemical status (Davis De West, 1966).

Table 2.1 Major components of groundwater and their common sources (Todd, 1980)

Major Constituent	Source in Water
Calcium	Primarily from carbonates, gypsum, feldspars
Magnesium	Feldspars, olivine, pyroxene, amphiboles, mica, Mg-calcite
Sodium	Feldspars, evaporite, cation exchange, seawater, industrial waste
Potassium	Feldspar, fertiliser, K-evaporite, glauconite
Silicic Acid	silicates
Ammonia	Pollution, degradation of organic matter, reduced NO_3, cation-exchange
Sulphate	Dissolution of gypsum and anhydrite, oxidation of pyrite, seawater, windborne fertiliser salts
Chloride	Windborne rainwater, seawater and brines, evaporite deposits, pollution
Nitrate	Atmospheric deposition, the decay of nitrogen-fixing plants, oxidation of ammonia or organic nitrogen, contamination
Carbonate	soil and atmospheric CO_2, carbonate rocks, oxidation of organic material, volcanic gases
Oxygen	soil gas and atmosphere

2.5.2 Common hydrochemical reaction in groundwater

2.5.2.1 Redox Reactions

Many reactions in groundwater involve the transfer of electrons between dissolved, gaseous and solid constituents. Electron loss results in oxidation and

election gain results in a reduction, but since free elections do not exist in solution, oxidation and reduction coincide and the overall reaction is called Redox reaction, e.g.

$Fe + 2H^+ \leftrightarrow Fe^{2+} + H_2$

Fe is oxidized to Fe^{2+} and protons are simultaneously reduced to hydrogen. In most case it is convenient to write redox reactions in terms of half reactions, which can then be added so that the elections cancel;

$Fe \longrightarrow Fe^{2+} + 2e$ oxidation

$2((H^+ + e) \longrightarrow \frac{1}{2} H_2$ reduction

$Fe + 2H^+ \longrightarrow Fe^{2+} + H_2$ complete reaction

Water may participate in Redox reactions in the following four ways:

- It may be an inert solvent, in which case it does not appear in the reaction equation.
- It may fulfil an acid-base role, in which case water appears on one side of the equation and H^+ or OH^- on the other side.
- It may be oxidized as; $O^{2-} + 4H^+ + 4e \rightarrow 2H_2O$
- It may be reduced as $2H^+ + 2e \rightarrow H_2$ (In this reaction water is reduced since hydrogen ions come from the reaction:
- $H_2O \rightarrow H^+ + OH$

This is an example of an acid-base reaction occurring simultaneously with another reaction. As the reaction proceeds, the solution becomes progressively more alkaline because of loss of protons as hydrogen. The dominant oxidation-reduction reactions that have taken place in the groundwater can be deduced from the presence of the product of these reactions in groundwater and surface.

As groundwater passes through an aquifer, oxidizing agents in the water are consumed progressively by reaction with reducing agents in the aquifer, starting with

the most powerful oxidizing agents (dissolved oxygen (DO), NO_3 reduction and SO_4 reduction). It should be noted that the presence of oxidizing species might indicate recent groundwater recharge.

Bacteria and other micro-organisms catalyse many of the redox reactions in groundwater. Most bacteria-derived the energy for their metabolism from the oxidation of organic matter, and this oxidation must be accompanied by simultaneous reduction. If O_2 is available, i.e. the water is aerobic, the preferred reduction is that of oxygen to water. In the absence of reducing reactions e.g. the reduction of NO_3, to N_2 by denitrifying bacteria and the reduction of SO_4 to sulphide by sulfate-reducing bacteria as indicated by the following reactions:

$$2NO_3^{2-} + 12H^+ + 10e \longrightarrow N_2 + 2H_2O$$

$$SO_4^{2-} + 10H^+ + 8e \longrightarrow H_2S + 4H_2O$$

Given favourable physical conditions, the other requirements for significant bacteria activity is; - an adequate supply of materials such as N-, P- and S- compounds, trace elements, organic carbon and a suitable oxidizing agent. However, the persistence of oxy-anions (Oxo-anions) such as SO_4, NO_3 etc. in reducing H_2O probably indicates a lack of adequate nutrient.

2.5.2.2 Mineral dissolution and precipitation

An equilibrium relationship can describe the solution of a mineral in water: when water is brought in contact with an excess of mineral, the concentration of the solution increases to a maximum (for a given physical condition) after which the solution is said to be saturated.

The concentration of the saturated solution is the solubility of the mineral involved, and in general, it depends on temperature and pressure and sometimes upon

external chemical factors. The Table 2.2 shows the solubility of commonly encountered sedimentary minerals. Precipitation reactions result in minerals being formed (precipitated) from ions that are dissolved in water. This type of response can be observed during the precipitation of iron, which is common in areas where water seeps into the ground or springs. In this type of environment, the solid iron hydroxide is formed when iron dissolved in groundwater comes in contact with dissolved oxygen in surface water.

Table 2.2 Selected rock minerals and their solubility

Mineral	**Formula**	**Solubility at pH 7 (mg/I)**
Gibbsite	$Al_2O_3.2H_2O$	0.001
Quartz	SiO_2	12
Fluorite	CaF_2	160
Dolomite	$CaMg\ (CO_3)_2$	90(at PCO_2 of 10^{-3})
Calcite	$CaCO_3$	100
Gypsum	$CaSO_4.2H_2O$	2,100
Sylvite	KCI	264,000
Epsomite	$MgSO_4.7H_2O$	267,000
Mirabillite	$NaSO4.10H_2O$	280,000
Halite	NaCI	360,000

Source: Seidell, (1958)

The solution reactions caused the ions to release into the water by minerals dissolution. The release of calcium (Ca^{2+}) and bicarbonate (HCO_3) ions during the dissolution of calcite ($CaCO_3$) in limestone is an example of this type of reaction. Due to the powerful solvent properties of water, solution-precipitation reactions with the aquifer matrix are frequently crucial in controlling groundwater chemistry.

Note that all the minerals listed above dissolve congruently in pure H_2O: i.e. no solid phases are produced as a result of the dissolution reaction. On the other hand, most

rock-forming silicates, except for quartz, dissolve congruently producing a solid phase during dissolution reaction, e.g. orthoclase (a common mineral in granites) may dissolves in water according to the reaction:

Kaolinite is left as solid phase, although it too may dissolve via its dissolution reaction, which is also incongruent.

$$11H_2O + 2KAISi_3O_8(s) \rightarrow 2K + 2OH + 4Si(OH)4 + AI\ Si_2O_5(OH)_3\ (s)$$

(Kaolinite)

Incongruent dissolution processes may also arise when two or more minerals each of which dissolves congruently in pure water dissolves successively in the same water; a common example is the dissolution of gypsum in a solution which is already saturated with calcite. The dissolution of gypsum will contribute Ca_2+ion;

$$CaSO_4.2H_2O \rightarrow Ca^{2+} + SO_4^{2-} + 2H_2O$$

If the Ca^{2+} ion concentration is increased, as shown in the equation and reference to le Chatelier's principle means that the solubility of calcite must be decreased. Thus in this situation/circumstance gypsum dissolution is incongruent as it is accompanied by calcite precipitation.

When a product of a dissolution reaction is present in a solution at a higher concentration than would occur in equilibrium with undissolved solid, the solution is said to be super-saturated. Under this condition, precipitation may occur. However, mineral precipitation, unlike mineral dissolution, is not well described by equilibrium chemistry. Certain minerals particularly calcite, dolomite, and most silicates are reluctant to precipitate from solution despite considerable supersaturation. Thus caution must be taken in using solution-precipitation equilibrium in groundwater

chemistry because equilibrium chemistry is useful in prediction when a mineral may dissolve. Still, it is not necessarily valuable for predicting when it will precipitate.

2.5.2.3 Cations exchange and sorption

The ion exchange between the groundwater and its host environment during residence or travel in the study area was verified by employing the chloroalkaline indices CAI-1 and CAI-2 which was employed by (Schoeller 1967). The indices are defining as follow;

CAI-1 = [Cl – (Na + K)]/Cl and

CAI-2 = [Cl – (Na + K)]/ (SO_4 + HCO_3 + CO_3 + NO_3)

CAI is negative when there is an exchange between sodium and potassium in the water with calcium and magnesium in the rocks. If the ratio is positive, then there is no base exchange.

2.5.3 Groundwater chemistry of coastal aquifers of Nigeria

The hydrochemical evaluation identified the natural variations and changes, which are intrinsic to coastal areas. The assessment also reveals hydrochemical alterations resulting from human impacts through urbanisation, agriculture and industrialisation, especially around the major cities within the basin. These findings may be valuable for achieving sustainable use of coastal ecosystems in the Eastern Dahomey Basin. We selected some of the reviewed literature from the coastal area of Nigeria which gives relevant information about the controlling geochemical processes that determines the chemical characteristics of the groundwater of the shallow coastal aquifers, especially from the Eastern Dahomey basin. Ionic concentration sequences, groundwater facies and the controlling processes as deduced from various Authors are

presented in Table 2.3. Most of these studies show rock-water interaction, minerals and evaporite dissolution, sea spraying and seawater intrusion as the dominants hydrochemical processes in this basin.

Table 2.3 Selected previous studies on groundwater geochemistry of shallow coastal aquifers in Nigeria

		Ion Concentration Sequence			
Author	**Formation/Aquifer**	**Cations**	**Anions**	**Water types**	**Controlling processes**
Abimbola et, 1999	Abeokuta formation	Ca > Na > Mg > K	HCO_3 > Cl > SO_4	Ca-HCO_3 and Na-Cl	Rock-water interaction and Sea spraying
Olobaniyi and Owoyemi, 2006	Niger Delta	Ca > Na > K > Mg	HCO_3 > Cl > SO_4	Ca-HCO_3 and Na-Cl	Rock-water interaction and Sea water influence
Aladejana and Talabi 2012	Abeokuta formation	Na > Ca > K > Mg	HCO3 > Cl > SO_4	Na -HCO_3, Na - Cl and Ca - Cl	
Aboyeji and Ogunkoya, 2015	Basement rock	Na > Ca > K > Mg	Cl > SO_4 > HCO_3	Na-Cl and Ca-SO_4	Rock-water interaction/ mineral dissolution
Talabi et al 2012	Coastal Plain Sand	Na > K > Ca > Mg	Cl > HCO_3 > SO_4	Na-(K)-Cl-SO_4 and Ca-((Mg)-HCO3	Saltwater intrusion and sea spraying
Odukoya et al, 2013	Coastal Plain Sand	Na > K > Ca > Mg	Cl > S	Na - Cl and Na - SO_4	Rock weathering and sea water influence
Tijani et al, 2005	Coastal Plain Sand	Na > K > Ca > Mg	Cl > HCO_3 > SO_4	Ca-(Mg)-HCO_3 and Na-Cl-(SO4)-HCO_3	Rock weathering and sea water influence
Longe et al, 1987	Coastal Plain sand	Na > K > Ca > Mg	SO4 > HCO_3 > Cl	Na - Cl and Na - SO_4	Evaporite dissolution and Saltwater influence
Abel Talabi, 2013	Basement rock	Ca > Mg > Na > K	Cl > HCO_3 > NO_3	Ca -(Mg) - Cl	Rock-water interaction/ mineral dissolution
Talabi and Tijani, 2013	Basement rock	Ca > K > Na > Mg	HCO_3 > Cl > SO_4	Ca(Mg)-HCO_3, Na(K)-HCO_3	Rock-water interaction/ mineral dissolution
Aniekan Edet, 2019	C. River Basin	Ca > Na > Mg > K	Cl > HCO_3 > SO_4	Ca > Cl and Na -Cl	Rock-water interaction/ Saltwater influence

Bullet 2

There are many studies with a focus on specific site and location within the Dahomey basin, none of the studies considered the regional groundwater geochemical studies that assess the influence of different geology on the hydrochemical evolution of groundwater across the basin. To achieve this objective, a combination of chemistry and stable isotopes to assess groundwater evolution with insight into the origin and hydrochemical dynamics.

2.6 Stable Isotopes of Oxygen and Hydrogen

The natural isotopes $\delta^{18}O$ and δD are referred to as an intrinsic component of the water molecule and therefore considered ideal tracers. During the hydrological water cycles direct evaporation over the ocean through condensation and precipitation to groundwater recharge and runoff back to the seas, these isotopes are selectively partitioned at each step within the cycle (Figure 2.2). The principal hydrological processes that affect the distribution of isotopes through the hydrological cycle, according to Clerk and Fritz 2015 include the following:

1. Evaporation and formation of atmospheric vapour
2. Condensation and rainout with decreasing temperature
3. Re-evaporation from soils and surface waters, which enriches the residual water in both isotopes
4. Mixing during recharge and groundwater flow
5. And, rarely, isotope exchange during mineral–water and gas–water reactions, a process that is only important in an exceptional circumstance of low water/rock or water/gas ratios.

2.6.1 Origin of Water Vapor from Deuterium Excess

Deuterium intercept is another parameter that defining a meteoric water line (MWL). Accordingly, the deuterium excess or *d* of precipitation is calculated from the δ 18O and δ D for any water sample, as

$$d = D - 8(\delta 18O) \text{ ---------- (2.1)}$$

Deuterium excess can vary regionally from much less than 10‰ to over 20‰ (Kalin et al; 1997). This excess is as a result of kinetic evaporation (nonequilibrium) during the formation of the primary vapour mass, and it provides an additional tool to trace the origin of the water.

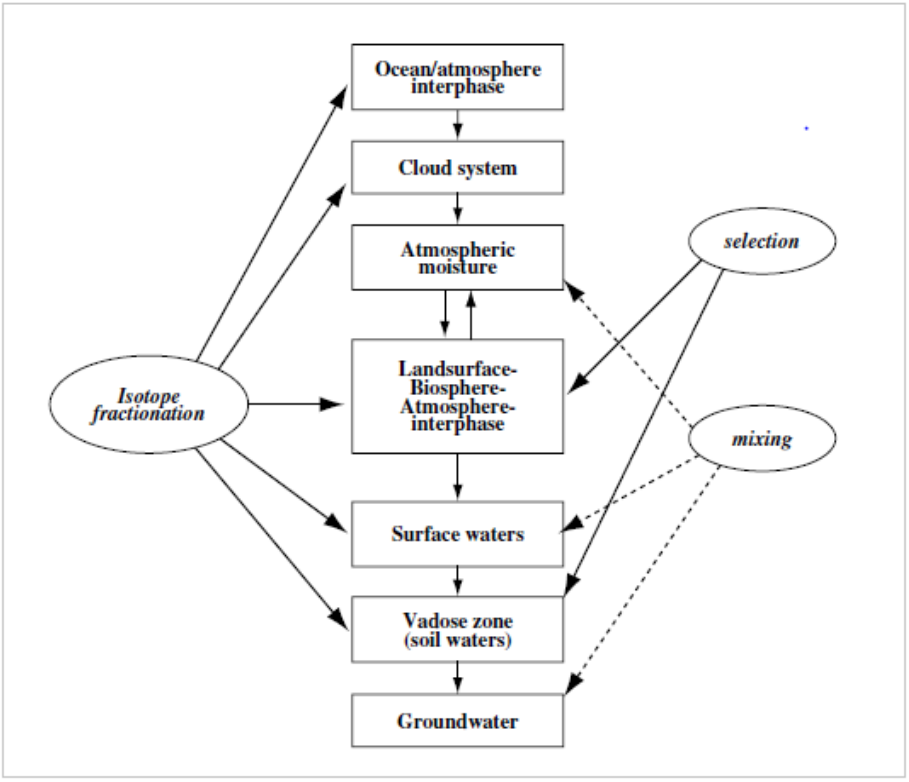

Figure 2.3 Isotope composition changes along the components of the hydrogeologic cycle. The diagram indicates the sites where isotope fractionation, selection or mixing processes operate. (Source: Gat, 2010)

The evaporation effect also plays a role during the formation of primary water vapour, which is a nonequilibrium or *kinetic* process that proceeds at a greater rate in the forward direction (evaporation) than the reverse (condensation). The process becomes increasingly kinetic with lower humidity. Nonequilibrium evaporation preferentially enhances fractionation of ^{18}O (with only minor enhanced fractionation of δD), and so the vapour is more depleted in $\delta^{18}O$ than for equilibrium conditions as this vapour condenses to produce precipitation. Because of differences in the origin of water vapour and rainout along the trajectory from its source, any given region will have its own characteristic MWL. This, therefore, become a datum with which the surface and groundwater in that region can be compared.

2.6.2 Groundwater recharge using Stable Isotopes of $\delta^{18}O$ and δD

Transformation of the isotope status in precipitation into groundwater is a significant step in the application of stable isotopes as tracers of groundwater from which information about its origin could be provided although the various temperature-sensitive processes of rainout distribute isotopes in precipitation over a wide range. This range characterized by high attenuation as precipitation infiltrates the subsurface (Clerk and Firtz 1997). The seasonal variations of precipitation influenced this behaviour, especially where groundwater is recharged only at certain times of the year like the tropical coast of West Africa. As a result of the seasonal effect, the $\delta^{18}O$ content of precipitation may vary over 8‰, while it is usually less than 1‰ in groundwater.

2.6.3 Seasonal variation of groundwater recharge

The isotopic composition of groundwater can be traced to that of precipitation in the recharge area. Typically, the weighted mean annual value of $\delta^{18}O$ and δD in precipitation is considered to represent the isotopic signature of groundwater. A good example is in tropical regions with strong seasonal bias in the amount of precipitation which is synonymous to the Eastern Dahomey basin. Using the mean monthly value to represent groundwater would overly bias toward the isotopically enriched dry months, whereas using the weighted mean of monthly precipitation gives a value that is more representative of groundwater. Although the $\delta^{18}O$ and δD in precipitation during these transition seasons approximate that of mean annual precipitation, there can be little deviations either isotopic depletion or enrichment. The weighted mean annual isotopic composition of precipitation is often enriched over local groundwater.

Isotopes approach is more of a younger scientific but interdisciplinary field, that evolved since around the 1950s when it was first realised the methods of nuclear physics for the detection of isotopes could have useful applications in hydrology, which is considered to be a current method in hydrogeological studies across the world. In this study, $\delta^{18}O$ and δD will be applied based on the objectives, the study location and cost of analysis. Using the data obtained, these will give an insight into the origin, flow pattern and recharge of groundwater within Eastern Dahomey Basin. The effectiveness has been employed in studies include (Ako et al., 2012; Al-Charideh and Kattaa, 2016; Avrahamov et al., 2010; Cary et al., 2015; Gattacceca et al., 2009; He et al., 2015, n.d.; Krishnaraj et al., 2012; Saravana Kumar et al., 2009; Sivan et al., 2005; Usama A. Abu Risha1, 2016); and several others with significant discoveries.

Bullet 3

Several studies carried out on groundwater evolution of shallow aquifer of the Eastern Dahomey basin only focused on local or specific site mostly with hydrochemical approach. This study employed environmental isotopes of $\delta^{18}O$ and $\delta^{2}D$ in regional precipitation and groundwater samples, in combination with some key hydrochemical parameters of major ions across the entire basin to regionally assess the origin and the residence time of groundwater of shallow coastal aquifers to increase the knowledge required for sustainable management of the groundwater resources.

2.7 Groundwater Quality

Abimbola et al. (1999) worked on the aspect of groundwater quality in Abeokuta. He was able to characterise the water from both sedimentary and basement in the area as Ca-HCO_3 type with low TDS. Water from the borehole located within the sedimentary settings noticed to have low Chloride and pH indicating the possible aggressive or corrosive character as compared to the shallow dug wells in the basement area with relative high Chloride and pH value. Although water from basement rock aquifers is generally known to have very low chloride (Freeze and Cherry 1989) the observed chloride, in this case, is attributed to the sea spray due to the relative closeness of the area to the coast, and the fact that the recharge is predominantly from precipitation.

This direct interaction of contaminated and polluted surface water with groundwater degrades the quality of groundwater in the unconfined top aquifer in this coastal area as observed in the work of Ayolabi and Oyelayo (2005) and Ayolabi *et al.*, (2013, 2014). In the search for potable freshwater, most wells and boreholes in this area are drilled to the second aquifer, which is a confined aquifer underlying the coastal area of the basin which is most densely populated, to meet their daily water demand. This development has put pressure on groundwater and lead to saltwater intrusion into

the freshwater aquifer through up conning wedge shift resulting from over-abstraction of groundwater (Oteri & Atolagbe, 2003; Oteri, 2008; Adepelumi *et al.*, 2009; Oyeyemi et al., 2015; Edet, 2016). Proximity to the sea also encourages saltwater intrusion into the freshwater of the coastal aquifer due to sea-level rise (SLR) and destruction of the coastal barrier due to indiscriminate sand mining along the coastline of the basin. Another school of thought has also suggested possible dissolution of evaporite minerals trapped within the basin lithology during a past event of ocean transgression and regression into groundwater causing their enhanced salinity and electrical conductivity (Cary et al., 2015; Tran et al., 2012).

The work of Longe et al. (1987), Oteri (1991, 2008), Oteri & Atolagbe (2003), Adepelumi *et al.* (2009), Adeoti et al. (2010), Longe (2011),; Ayolabi *et al.* (2013), Ayolabi et al. (2013) and Odukoya *et al.* (2013) have employed different methods such as electrical resistivity tomography (ERT), induced polarization (IP) and hydrochemistry on groundwater in some selected and specific locations within this basin. Some of these studies which have identified saltwater intrusion in the upper aquifers mainly in the eastern coast of Lagos, such as Lekki, Ajjah, Victoria Island, Sagontedo. The deterioration of water quality in parts of Lekki phase 1 and Oniru environs of Lagos metropolis due to saltwater infiltration into the freshwater aquifer which has become a significant concern (Adepelumi et al., 2009).

Despite all this, the report still shows that systematic and detailed groundwater quality assessment and monitoring are insufficient for sustainable management of groundwater in the face of the menace of saltwater intrusion. This challenge results from a combination of factors, such as costs associated with water quality monitoring, the relatively low levels of funding for research in Sub-Sahara Africa over the past

decade and limited national regulation of high-intensity rainfall events, which pose a risk to shallow and poorly protected groundwater sources (Coode & Akute Geo-Resource, 1996 *Lapworth et al., 2016).* Table 2.1 present major constituents of water and their possible source.

2.7.1 Land use impact on groundwater quality

Groundwater quality is influenced by the land use and hydrological parameters such as evaporation, interception infiltration rate, and runoff that may also be altered or controlled by land-use patterns (Senthilkumar et al., 2018). Urbanisation and agriculture activities release waste with an adverse effect on groundwater quality. Inappropriate waste management practice that characterised developing countries of Sub-Sahara African increases the challenges facing groundwater quality.

Different land use classification map of the Eastern Dahomey Basin (Figure 2.4) revealed Water bodies, Plantation, Bare soil, Agriculture, Agriculture in shallows and recession, Cropland and fallow with oil palms, Forest, Savannah, Wetland-floodplain and settlement. With this diverse outlook of the land-use pattern in the study area, it is necessary to compare how this correlates with the groundwater quality distribution within the basin.

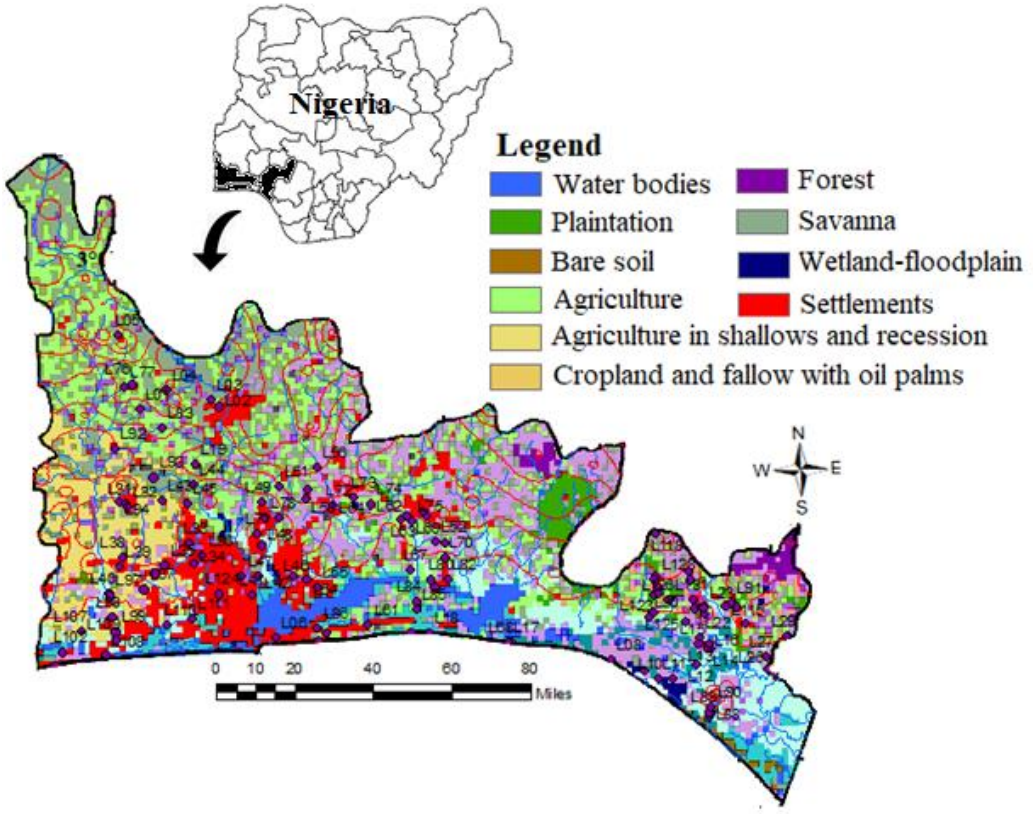

Figure 2.4 Land use map of the Eastern Dahomey Basin

2.7.1 Groundwater quality in the shallow coastal aquifer of Nigeria

Groundwater pollution and quality deterioration within EDB has been reported by others including Oteri; 1988, Longe et al.; 1987, Adeoti et al.; 2010, and Ayolabi et al.; 2013. According to the United nation SDG6, "2 billion people are living with the risk of reduced access to freshwater resources, and by 2050, at least one in four people is likely to live in a country affected by chronic or recurring shortages of freshwater" (UNDP, (2017). Consequently, more than 2 million people die every year from water-borne related diseases. At the same time, 4.3 and 6.4 per cent of Sub-Sahara African and India's GDP resulting from adverse economy impacted cost due to inadequate sanitation.

Nigeria is ranked poorly in the planning to achieve Sustainable Development Goal 6 (SDG6), a challenging which requires, among others, a proper understanding of relationships between land use and groundwater quality. Monitoring groundwater is necessary to detect emerging pollution and contamination early enough to prevent damage to the resource since remediation remains expensive and nearly impossible to implement after water quality deterioration.

To improve the quality of freshwater resources, policies that support investment planning for the management of freshwater ecosystems and sanitation facilities at a local level is necessary. This study assessed the impact of land use on groundwater quality in the EDB using the groundwater quality index and statistical analysis.

Bullet 4

Monitoring groundwater is necessary to detect emerging pollution and contamination early enough, to prevent damage to the resource since remediation remains expensive and nearly impossible to implement after water quality deterioration. This study focuses on the need to understand the groundwater quality distribution within the basin to establish possible link with the land use pattern

2.8 Climate change impacts on Groundwater quality of shallow coastal aquifers

The relationship between climate change and drinking water is casual and complicated (Aladejana et al, 2020). This is because of climate change-related effects of extreme precipitation, temperature rise and water-borne diseases systematically interrelated with different types of microorganisms, geographical area, season, type of water supply, water source and watershed characteristics (Can et al.,, 2019).

Hinkel et al. (2011) projected that the populations of Mozambique and Nigeria are projected to be most affected by sea-level rise in terms of the absolute number of

people flooded annually, among the Sub-Saharan African region. Herrador, et al., (2015), stated there are substantial knowledge gaps regarding systemic causes and effects with considerable uncertainty about how heavy rainfall, microbial pollution of water supplies and increased turbidity interrelated. In recent time, several outbreaks of waterborne diseases which were attributed to the extreme hydrological events like flooding were reported in sub-Sahara Africa, and other parts of the world (Kasei, 2009; Babanyara et al., 2010; Serdeczny *et al.*, 2016; Pfeiffer et al., 2015; and Cann, 2019). In the densely populated coastal areas of developing country like Nigeria, waste management is a challenge due to indiscriminate dumping of waste from municipal, industries and agricultural activities across the cities (Ojolowo and Wahab, 2017).

Furthermore, the IPCC Fourth Assessment Report failed to broadly capture the impacts of climate change on water quality in great details. In recent time, researchers have established the effect of climate change-driven flooding on surface water quality, especially in the coastal zones of the world where extreme precipitations occur (Priyantha, et al., 2006; Doug Linzey, 2011; Hiyama et al., 2014; Unsal et al., 2014; Nistor *et al.*, 2016). While research in the area of climate change impact on groundwater quality is still in the early stage (Unsal, et al., 2014; Serdeczny *et al.*, 2016), this is probably due to invisibility of the groundwater from the surface while groundwater quality monitoring data in the study area is rarely conducted.

Studies within the Eastern Dahomey Basin and the adjoining southern coast (Edet et al., 2003; Adegbola et al, 2013; Ayolabi et al, 2013; Hashmi *et al.*, 2014; Edet, 2016) have identified elevated concentrations of ions, heavy and traced metals in groundwater in shallow aquifers of the coastal cities of Nigeria. Many of which

attributed its groundwater contaminations to indiscriminate waste disposal, effluents from sewage, industries and agriculture waste.

Ojolowo and Wahab, 2017 reported annual flooding in coastal areas of Nigeria which are linked to extreme precipitation driven by climate change. This menace, coupled with indiscriminate waste disposal practices that characterized this area which lead to uncontrolled solid waste blocks drainages, causes flooding. The debris within the river channels and floodplains triggered some biogeochemical processes which cause metals and ions to leaching down into the groundwater and leads to contamination. Assessing the biogeochemical process on groundwater within the shallow aquifer in this zone could present the key the link between climate and groundwater quality through some groundwater quality parameters which are sensitive to biogeochemical processes of redox reaction such as NO_3, SO_4, Fe, As and Mn. (Ahmed et al., 2019a) in his work linked the occurrence of this element with the anthropogenic sources in groundwater from Surma basin, Bangladesh. (Banu et al., 2013; Helena et al., 2000; Wang et al., 2017) linked nitrate, trace and heavy metals contamination in groundwater to irrigation and municipal leachates. Examining this elements using relevant statistics in groundwater of seasonally flooded coastal zones could establish a link between groundwater quality and climate change which is necessary management of water resources, especially in Sub-Saharan Africa where devastating effects climate change has been predicted (Duran-Encalada et al., 2017; Lapworth1 et al., 2018).

Finally, the importance of groundwater to the life, health, and economy of developing countries cannot be overemphasised. There is need to understand the impact of climate change on groundwater quality. This is necessary to ensure the

protection of water resources of coastal basins in Sub-Saharan Africa where groundwater remain the sources of the freshwater supply.

Bullet 5

In recent time, researchers have established the impact of climate change-driven flooding on surface water quality, especially in the coastal zones of the world where extreme precipitations becomes a common occurrence (Priyantha, et al., 2006; Doug Linzey, 2011; Hiyama et al., 2014; Unsal et al., 2014; Nistor *et al.*, 2016). While research in the area of climate change impact on groundwater quality is still in the early stage (Unsal, et al., 2014; Serdeczny *et al.*, 2016), no study in this part of Africa has looked in the direction of possible relationship between groundwater and climate change, especially with emphases on biogeochemical processes.

CHAPTER 3

3.0 DESCRIPTION OF STUDY AREA AND PHYSICAL SETTINGS

3.1 Study Area

The Eastern Dahomey Basin is located within the southwestern part of Nigeria (Figure 3.1). It is a transboundary coastal sedimentary basin, which extends from Ghana through Togo and Benin to Nigeria. This basin is bounded by Okitipupa Ridge, which is the boundary it shares with Niger Delta basin (Jones and Hockey, 1964). It lies between Latitudes $2^0 41^{'} 10.00''$ - $4^0 59'5900''$N and Longitudes $6^0 21'1300''$ - $7^0 52'42.00''$E along the coast of the Gulf of Guinea. The basin is bounded in the south by the Atlantic Ocean, and thin out at the north by the Precambrian basement rocks. The area of investigation is hilly at the north and flattening in to plain towards the ocean with several points virtually at or below the sea level. The highest elevation is observed around Abeokuta. Eastern Dahomey Basin is characterised by two distinct seasons, wet and dry. The wet season occurs between April and October with a break in August and features average rainfall, which ranges from 1800mm – 2500mm, while the dry season lasts from November to April (Ukhurebor and Abiodun, 2018).

The major rivers Ogun, Ose and Oluwa drain the basin into the delta and to the Atlantic Ocean. The basin hosts two major administrative water basins authorities in Nigeria and the Ogun-Osun and Benin-Owena river basins and accommodates about 40% population of the country residence including the metropolitan city of Lagos. The study area is vital to the economy of Nigeria and West-Africa.

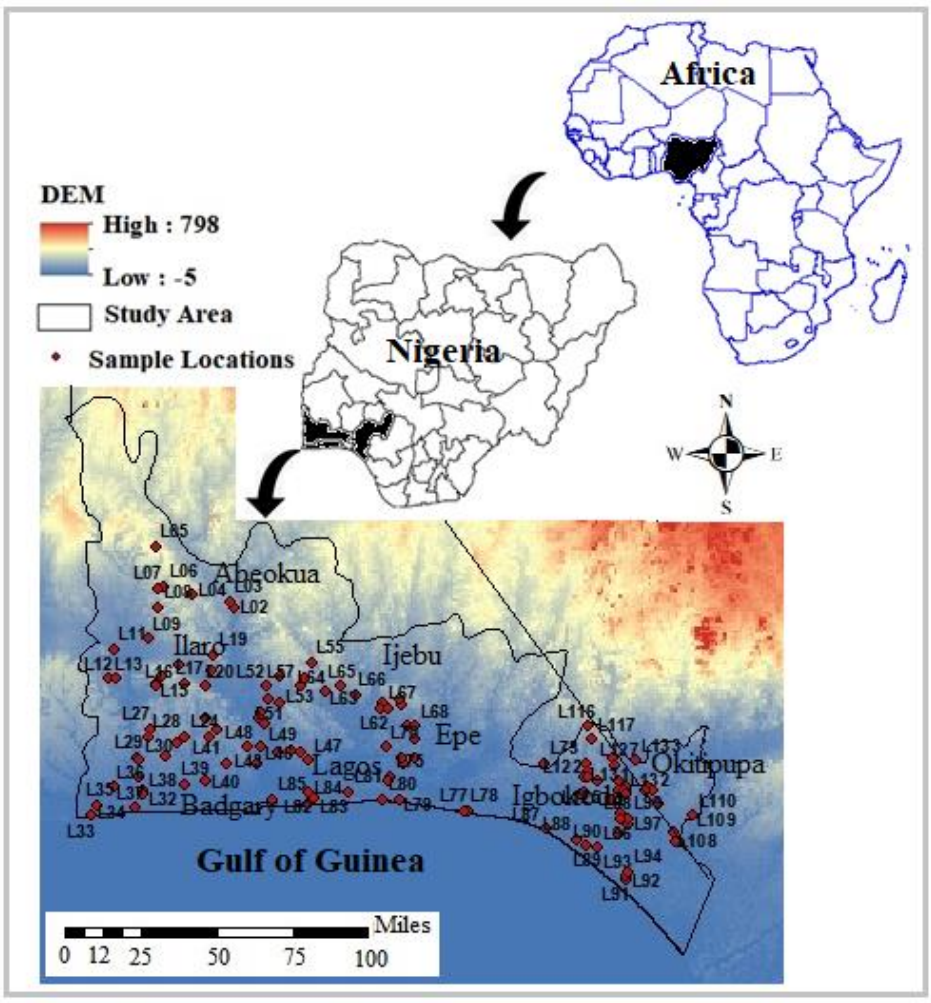

Figure 3.1 Map of the Study Area with Africa and Nigeria inset maps showing the DEM

3.2 Climate and Vegetation

The Eastern Dahomey Basin is characterised by a tropical wet and dry climate. It experiences two rainy seasons, with the most torrential rains falling from April to July and a weaker rainy season from September to November. A brief relative dry spell is experienced in August and a longer dry season from December to March. The climates in these areas are typically coastal, with high annual rainfall ranging from 2250mm in their northern borders to over 2,600mm at the coast. The humidity is very high, over 80%, and an average annual temperature of about 21°C.

3.3 Geomorphology / Topography of Dahomey Basin

The area is characterised by a relatively high elevation area with about 400-500m in the northern part of Ogun-Oshun Basin. The area whose elevation is less than 200m widely extends in the remaining part of Ogun-Oshun Basin. The low land area and lagoons extend along the coastal area (Figure 3.1). The central to the northern part of Ogun-Oshun is classified into high land area called "Western Plateau". On the other hand, the lowland, which is called as "West Nigeria Inland Low Area", is distributed in the south of above area. The coastal area is distributed in the southern end of Ogun-Oshun Basin area with elevation of less than 100m

3.4 Geology

3.4.1 Regional Geology of Western Nigeria

The geology of Nigeria comprises of three major rock types, which are named, (a) the Basement Complex (b) the Younger Granites (c) the Sedimentary Basins. The Basement Complex, which is Precambrian in age, is made up of the Migmatite-Gneiss Complex, the Schist Belts and the Older Granites. The Younger Granites is made of numerous Jurassic magmatic ring complexes centered around Jos and few other areas in north-central Nigeria (Obaje, 2009). The Younger Granites have structure and petrology compared from the Older Granites.

The Sedimentary Basins, composed of sediments of Cretaceous to Tertiary ages, comprise the Dahomey Basin, the Niger Delta, the Anambra Basin, the Lower, Middle and Upper Benue Trough, the Chad Basin, the Sokoto Basin, and the Bida-Nupe Basin (Figure 3.2). More detailed Geology of Nigeria can be found in Obaje 2009 with summary presented in Figure 3.2.

The Nigerian basement complex forms the Southern part of the Tran-Sahara Pan-African mobile belt (Coby 1989) of the Late Proterozoic (500 – 750Ma) age laying between the Achaean blocks of the West African craton is bounded to the West and East by the mobile belt. The mobile belt West African craton extends from sierra Leone (Where it is called the Rokellide belts) northwards (where it is called Mauritanide belts). The evolution of the Basement Complex of Nigeria is associated with the general evolution of the African continent. It comprises gneisss and migmatites with supral crustal relics, which have yielded Archean (c. 2700Ma) and Proterozoic (c.2000Ma) ages (Annor 1995, Dada et al., 1998). The rocks of the Precambrian crystalline complex of Nigeria were differentiated, by Oyawoye 1964 into four different groups, which include:

(i) The Ancient Metasediment.

(ii) The Gneisses Migmatites and Older granites.

(iii) The Pegmatite and dolerite dykes, considered as a special minor group.

Four major Orogenies punctuate the Precambrian history of Africa. These are:

- Liberian Orogeny (2,800 – 2,500Ma).
- Eburnean Orogeny (2,200 – 1,800Ma).
- Kibaran Orogeny (1,300 – 900Ma).
- Pan African Orogeny (600 – 400Ma).

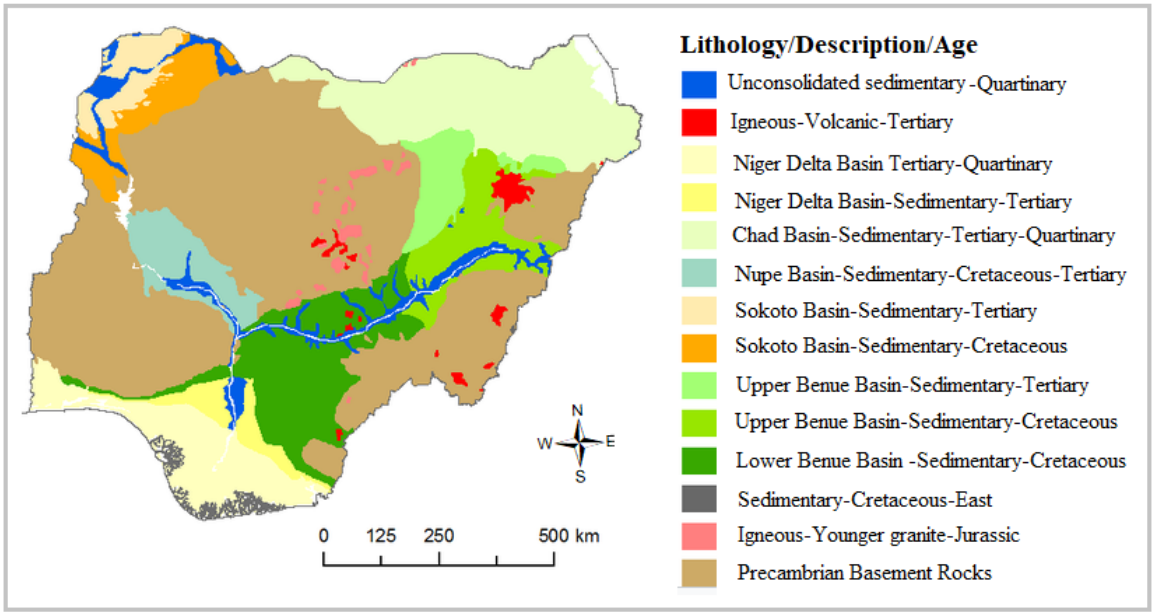

Figure 3.2 Geology Map of Nigeria (Adapted from NGSA, 2019)

3.4.2 The Geology of the Eastern Dahomey Basin

The Dahomey basin was initiated during the Mesozoic, probably during the cretaceous period. This was responsible to separation of the Africa-S/America land masses and the subsequent opening of Atlantic Ocean. The sedimentary sequence in the W/African coast is very similar to that of the Brazilian coastal basin. Available stratigraphy evidence suggests that deposition was initiated in fault control depression on crystalline basement complex. The depression were as a result of rift- generated basement subsidence, during the early cretaceous(Neoconian), the subsidence gave rise to the deposition of a very thick sequence of continental grit and pebbly sands/conglomerate, over the entire basin, and, in most cases the depocentre is usually thick in sediments compare to the sides) over 1,400m sediments are preserved in the coastal area of Nigeria offshore in Benin republic (Billman 1976, Omatsola and Adegoke 1981) During the early to late cretaceous (Santonian). There was another episode of major tectonic activities probably associated with closure and folding of the Benue trough. The basement rocks (the granite gneiss and the associated pegmatites)

as well as sediments in the Dahomey were filled and blocks faulted forming a series of horsts and grabben. Considerable erosional activities accompany the uplift and block faulting and the extensive Lower cretaceous sediment will also eroded from the horst.

3.4.3 Stratigraphy of Eastern Dahomey Basin

The stratigraphy of the eastern Dahomey basin (Figure 2.3) has been studied using both outcrop and sub-surface data by various workers and several classification schemes have been proposed (Figure.2.4). The stratigraphic description of the sediments has been presented by Jones and Hockey (1964): Reyment (1965); Adegoke (1969) Fayose (1970); Billman (1976); Ako et al. (1980); Omatsola and Adegoke (1981); Agagu (1985); Nwachukwu et al. (1992); Nton (2001); Elueze and Nton (2004) and Adeleye et al. (2005) among others. However, there are still controversies on age assignment and nomenclatures of the different litho-units.

The lithostratigraphic formations range from cretaceous to Tertiary ages. The successions from the oldest to youngest include: Abeokuta group (comprises Ise Formation, Afowo Formation and Araromi Formation), Ewekoro Formation, Akinbo Formation, Oshosun Formation, Ilaro Formation and Benin Formation.

General stratigraphy

The general Stratigraphy of the Dahomey basin include:

1. The Abeokuta Formation
2. The Ewekoro Formation
3. Ilaro Formation
4. Alluvium.

5. Coastal plain sands (Benin Formation)

Abeokuta Formation

This is the oldest sedimentary unit in the Dahomey basin. it consists of lower cretaceous sandstone and grits with interbedded mudstone unconformity overlain the basement complex fine detrital sandstone, siltstone and shale overlying the formation in the upperparts. The youngest sets of strata are marginal to fully marine sand and shale of the Maestrichian AGE. This formation has been raised to the status of the group as described, by Omatsola and Adegoke (1981). The Abeokuta group now consist of Ise formation, Afowo formation and Araromi formation.

Ise Formation

This formation overlies the basement complex of southwestern Nigeria, and consists of rift continental sands, grits, silts, conglomerate and sandstones. At the base of the Ise Formation are conglomerates which are overlain by coarse to medium grained loose, sandstones and grits with inter-bedded Kaolinite (Omatsola and Adegoke, 1981). The conglomerates are unimbricated and at some locations, ironstones occur. Both the cross-bedding azimuths of the sandstones and the pebble alignments point to a NE- paleo -current system (Nton, 2001). The age is Necomian to Albian.

Afowo Formation

The formation is composed of medium grained sandstones with friable, but thick inter-bedded shales, siltstones and claystones. The shale component increases progressively from the base to the top. The sandy facies are tar bearing around Okitipupa, while the shales are organic-rich (Enu, 1990). The lower part of this

formation is transitional with mixed brackish to marginal horizons that alternate with well sorted, sub-rounded sands. This indicates a littorals or estuarine near-shore environment in which the water level fluctuates. Billman (1992) assigned a Turonian age to this formation while the upper part ranges into the Maastrichtian. This formation lies conformably on Ise formation; however, it is found overlying unconformably on basement complex in some area.

Araromi Formation

This is the youngest of the cretaceous sediments in the eastern Dahomey basin (Omatsola and Adegoke, 1981). It is composed of fine to medium grained sandstone at the base, overlain by shales and siltstones with inter-bedded limestone, marl and lignite (Ogbe, 1972; Okosun, 1990). The shales are light grey to black, mostly marine and with very high organic content. The Formation is highly fossiliferous, containing abundant planktonic foraminifera, Ostracordes, Pollen and spores. The age is Maastrichian to paleocene.

Ewekoro Formation

The Ewekoro Formation overlies the Araromi Formation and is composed predominantly of fossiliferous limestones which become arenaceous towards the base (Reyment, 1965). It is an exclusive limestone body, which is traceable over a distance of about 320km continuously from Ghana eastward, towards the eastern margin of the Dahomey basin in Nigeria. The limestone is thickly bedded and colour banded. The formation is associated with shallow marine environment due to abundance of coralline algae, Gastropods, Echinoids fragments and other skeletal debris (Nton, 2001). The age is Paleocene.

Ilaro Formation

The Ilaro formation overlies the Oshosun formation and consist massive, yellowish, poorly consolidated, cross-bedded sandstones, which are fine to medium grained and poorly sorted according to Kogbe (1976), the sedimentation of Oshosun formation was followed by a regression that resulted in the deposition of the sandstone unit of the Ilaro formation. The formation is Eocene in age.

Benin Formation/Coastal plains sands

This is the youngest stratigraphic sequence in the eastern Dahomey basin. The Ilaro Formation underlies it. It consists of soft, very poorly sorted clayey sands, pebbly sands, sandy clays and rare thin lignite. The sands are in parts cross-bedded and show transitional to continental characteristics. The age is from Oligocene to Recent (Reyment, 1965).

Basement rocks of Abeokuta

The northern part of the Abeokuta area lies within the Precambrian Basement rock. Geology of Abeokuta can be said to have divided into two major groups as mentioned above which include; The ancient gneisss-migmatite suite (Complex) which has been distinguished into three major divisions due to the penetration of Pan-African (600Ma) bodies of granodiorites, Porphyritic granites, Quartz diorites and pegmatites (Oyawoye 1972, Kayode, 1974) The major division include;

Biotite Granite Gneiss.

Porphyroblastic Gneiss

Porphyritic Biotite Granite

Biotite Schist

Migmatite

The remaining small portion are covered by the Ise Formation of the Abeokuta Group, which consists of conglomerates and grits at base and in turn overlain by coarse to medium grained loose sands (Figure 3.4). This formation is notable in the south-eastern and south-western parts of the study area (Figure 3.3).

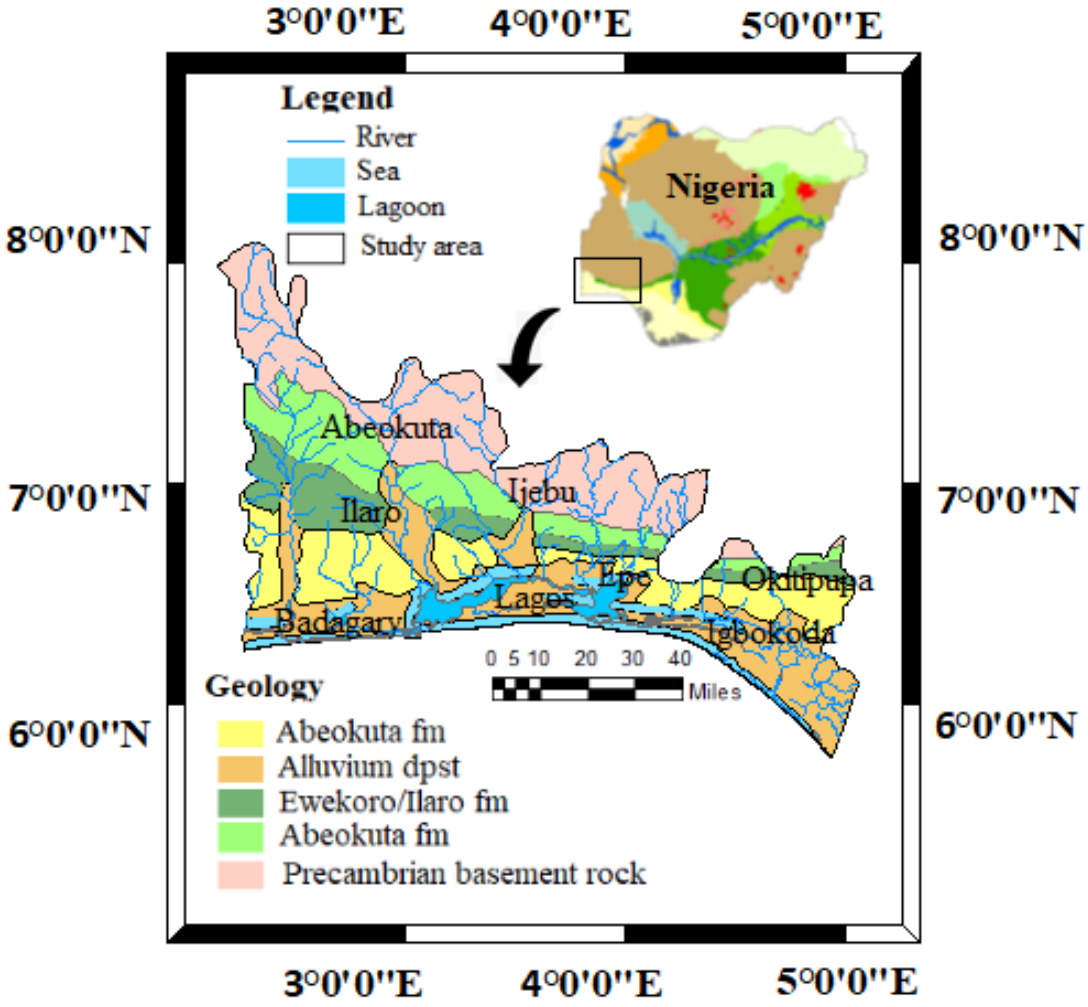

Figure 3.3 Geological Map of the Eastern Dahomey Basin (Modified from Nigerian Geological Survey Agency 2006)

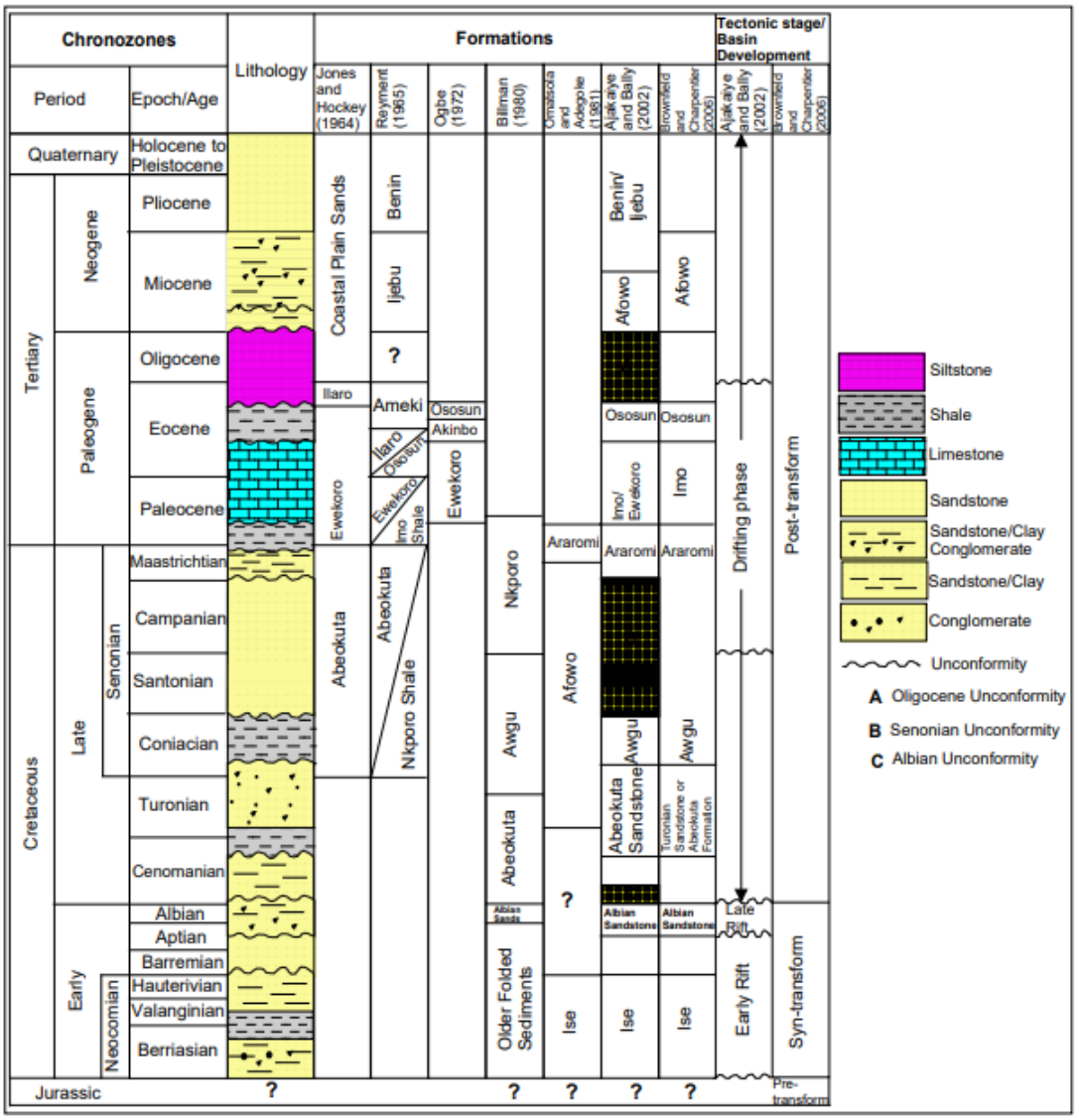

Figure 3.4 Regional geology and stratigraphic profile of eastern part of Dahomey Basin including the study area. (Adapted from Olabode and Mohammed. 2016)

3.5 Hydrogeology

3.5.1Groundwater Potential of Dahomey Basin

The Dahomey basin was initiated during the Mesozoic, probably during the cretaceous period. This was responsible for the separation of the Africa-S/America landmasses and the subsequent opening of Atlantic Ocean. The sedimentary sequence in the W/African coast is very similar to that of the Brazilian coastal basin. Available

stratigraphy evidence suggests that deposition was initiated in fault control depression on crystalline basement complex. The depression was as a result of the rift- generated basement subsidence, during the early cretaceous (Neoconian), the subsidence gave rise to the deposition of a very thick sequence of continental grit and pebbly sands/conglomerate, over the entire basin and in most cases, the depocentre is usually thick in sediments compare to the sides) over 1,400m sediments are preserved in the coastal area of Nigeria offshore in Benin republic (Billman 1976, Omatsola and Adegoke 1981). During the early to late cretaceous (Santonian). There was another episode of major tectonic activities probably associated with closure and folding of the Benue trough. The basement rocks (the granite gneiss and the associated pegmatites), as well as sediments in the Dahomey, were filled and blocks faulted forming a series of horsts and graben. Considerable erosional activities accompany the uplift and block faulting, and the extensive Lower Cretaceous sediment will also have eroded from the horst. The geological structure of the basins forms a simple monocline against the Basement. It outcrops to the north with only a little evidence of faulting (Figure 3.3). The dips are reportedly 1° or less to the south and south-west. (Jones et al., 1964).

Table 3.1 Showing River Basin Province and Respective Underlying Stratigraphic Units

Age	**Ogun river Basin**	**Owena river Basin**
Quaternary	Deltaic Plains Benin Formation	Deltaic Plains Benin Formation
Tertiary	Ilaro Formation Oshosun Formation Ewekoro Formation	 Ameki Formation Imo Shale
Cretaceous	Abeokuta Formation Basement	 Basement

In the Ogun and Osse River Basin, the oldest outcropping sedimentary formation is the Abeokuta Formation which appears to overlie the Basement Complex directly. This formation is in turn overlain by the Ewekoro, Oshoun, Ilaro and Benin Formations. Sedimentary rock is distributed only along narrow belt expanding from the east to the west along the coast facing Guinean Gulf. There is the considerable development of alluvium in the coastal areas and along the course of the major drainage systems of the Rivers Ogun and Osse.

The groundwater resource in the basin is contained in four aquifers in the sedimentary basin. The first aquifer is shallow of Recent Sediments along the Atlantic Sea coast and along river valleys. It is used for very small private domestic supplies through dug wells and shallow boreholes. The second and third aquifers are in the Coastal Plains Sands Formation. They are exploited through dug wells in places, shallow - and deep - boreholes (maximum depth of 300 m at the coast). These aquifers provide substantial quantities of water for private-, public- and industrial–water supplies as the main aquifer exploited. The fourth aquifer is the deep and highly productive Abeokuta formation. Only a few boreholes located mainly in Ikeja industrial area, extract water from the fourth aquifer. The water from this aquifer is hot with temperatures as high as 80 °C recorded in a few of the boreholes (Coode Blizard Ltd et al., 1966). This aquifer is undergoing massive development in adjoining Ogun State in recent times where it is encountered at shallower depths of between 300 to 550 m.

Abeokuta Formation

In the Ogun Basin, the Abeokuta Formation is the oldest sedimentary formation, which unconformably overlies the rocks of the Basement. It is reported to

be 250 - 300m thick (Reyment 1965). The Abeokuta Formation consists of arkosic sandstones and grits, tending to be carbonaceous towards the base. The formation has excellent potential for groundwater except that the bituminous materials associated with the sands could affect the quality of the water. (Offidile 2002). The thickness increases from about 120m in the east, to 240m, to the west, towards the Benin border. (Jones et al. 1964). However, with its proximity to the Basement and its high permeability, a considerable quantity of water should be held above the crystalline bedrock. Carter, (Undated GSN Rpt. 1185).

Table 3.2 Summary of Lithostratigraphic description of selected boreholes from Abeokuta Formation

S/N	Lithological Description	Depth to Top (m)	Thickness (m)
1	Laterite, hard concretionary	0	1.5
2	Pale sandy Clay	1.5	0.9
3	Shale	2.4	0.3
4	Ferruginised sandstone	2.7	45.0
5	Conglomerate	47.7	0.6
6	Basement rock	48.3	--

Successful boreholes were reported at Ijebu Ode and Aiyetoro. Carter also reported specific capacity, of between 63 and 17,550 lits/hr/rn (1300 gift). Other successes were reported from Iboro, Ishaga and Imushin. Eastwards, in the Osse basin, the Abeokuta formation appears to thicken in the higher regions of Agenebode and Auchi, where the water table is low, 120-300m. The shallow water table observed in this area is thought to be due to the high permeability of the aquifer, as also exemplified by the Kern Kern Formation, in the Upper Benue basin and the Nanka sands of the Anambra Basin.

Ewekoro/Akinbo/Oshosun Formation

Ewekoro Formation as defined by Jones et al. 1964, and has been subdivided into the Ewekoro and Oshosun Formations by Reyment (1965) and Later into the Ewekoro, Akinbo and Oshosun as outlined by Adegoke (1980). However, for convenience, the hydrogeology is treated under the Ewekoro Formation as defined by Jones et al. (1964).

It consists of a sequence of sandstone, shale's, limestone and clays varying between 100 - 300m thick (Carter GSN. Report 1185). At the type section, the formation reportedly comprises 120m of overlying shale 30m of Limestone. The top section of the formation has poor groundwater potential because of the argillaceous nature of the rock (Offidile 2002). However, the limestone sequence within the formation consists of highly fractured and sometimes pulverised limestones with interconnected voids and crevices that hold enormous quantities of water, giving yields of up to 10 to 20 litres per second from most of the boreholes in the area.

Ilaro Formation

The Ilaro Formation consists of fine to coarse sands alternating with shales and clays which overlies the Oshosun, Akinbo and Ewekoro Formations (Offodile, 2002). Comparing the geological characteristics, Ilaro Formation like the Ameki formation, its Lateral part equivalent, could be a suitable aquifer and can yield a considerable quantity of water. Jones et al. (1964) reported a well to be about 57m deep, giving a low yield of about 2975 Ltr/hr and a specific capacity of 1023 Ltr/hr/m.

Benin Formation

The Benin Formation is also very important in the Osse Owena basin where it is the primary source of groundwater. It is very well developed in the Osse river and underlies more than half of the basin's sedimentary area. It also forms a significant part of the Ogun basin. The Benin Formation, underlain by the sandstones and shales of the upper Ilaro Formation, consists of a sequence of predominant continental sands and some lenses of shales and clays proved to be up to 107.7 m thick in this area. (Jones et, al. 1964).

The Benin Formation gives copious yields of up to 45,000 Ltr/hr or 12 Ltr/sec in many areas. The water table is high between 20-25m, and the water quality is excellent. The area underlain by this formation stretches from the Ado-Odo, Ilaro, Mushin, Ikeja area, through Okitipupa of Ogun Basin, into a broad area in Benin - Ugheli - Agbo region of the Osse basin in Edo and Delta States (Offodile 2002). At Mushin, a well penetrating a similar sequence, 108.6m deep, gave a yield of 32,850 Ltr/hr or 9 Ltr/sec and a specific capacity of 1930.5 Ltr/hr/rn. These prolific yields are typical of the Benin Formation all over the south-western River basins.

Deltaic Formation

The Deltaic Formation consists of alluvial deposits associated with the coastal areas of Lagos and the areas of the Osse basin adjoining the Niger Delta. The hydrogeological situations in these areas is similar to that of Niger Delta Basin. Suffice it to mention that the sandstone beds are limited in thickness and variable in lateral extent. Moreover, such aquifers have been subjected to saline intrusion due to overdevelopment and seawater incursions. Also, the Limitations in thickness and

extent of the aquifers have the effect of reducing the specific capacity of the boreholes considerably (Offidile 2002).

Alluvial Deposits

The broad valleys of the Yewa, Ogun and Osun river systems show an extensive alluvial development which has substantial groundwater potential. The available drilling records have not distinguished this formation. However, (Jones et al. 1964) recorded a 49,275 lits/hr. The output from at Ibefun, with a specific capacity of 9234 lits/hr/m. This is an excellent yield and underlines the high potential of the alluvial deposits of these river systems. (Offidile 2002).

Three to four different hydrogeological units have been identified within the Eastern Dahomey Basins. The alluvial aquifers along Delta line and major rivers (creek lines), shallow coastal plain sands and intercalations of Clay, Limestone, Tar Sands, Shale, Peats and Upper coal measure underlying different locations within the study area defined the layer boundaries because of their relatively low to very low permeability. The alternating sequence of this low and high permeability layer define the layers of the three confined aquifers which responsible for groundwater resources of the study area. An overview of the aquifer productivity of the entire Nigeria is presented in Figure 3.5 which form the primary outlook of the groundwater potential of the hydrogeological basins of the country. The groundwater situation varies rapidly from place to place. In the areas of Lagos where the formation appears to be Least developed and has been contaminated, the underlying Benin Formation provides a ready answer to the groundwater problems (Offidile 2002).

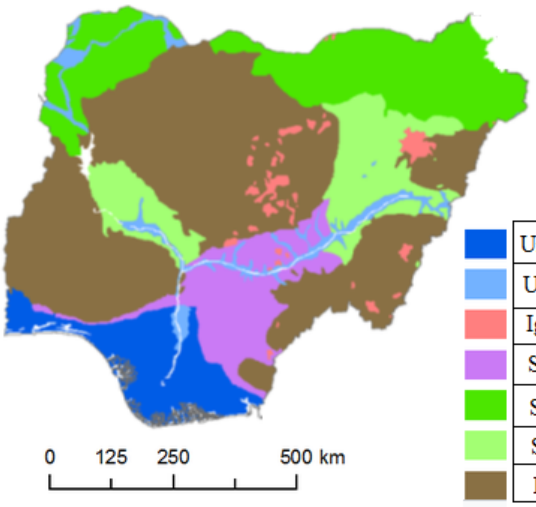

AquiferDescription	Aquifer Production
Unconsolidated	High to Very High
Unconsolidate	High
Igneous	Low to Moderate
Sedimentary Intergranular/Fracture	Moderate (locally High)
Sedimentary Intergranular	Moderate to High
Sedimentary Intergranular	Low to High
Basement	Low to Moderate

Figure 3.5 Aquifer production map of Nigeria (After NMGS 2019)

3.5.2. Hydrostratigraphic description of Eastern Dahomey Basin

Hydraulic conductivity values presented in this report are considered representative based on literature review and field investigations across the Eastern Dahomey Basin. Due to the high variability in hydraulic conductivity in the alluvium, Coastal Plain sand, Ewekoro, Ilaro and Abeokuta formations. Hydraulic data from available and accessible boreholes were collected from the few available studies The layers are represented in order of unconfined aquifer, and two-three confined aquifers within the alluvium and coastal plain sand, within the upper Benin formation which is necessary to groundwater resources of the Eastern Dahomey Basins. Virtually all the water boreholes in these areas are terminated within the coastal plain sand of the Benin formation. These layers are depicted in the stratigraphic section in Figure 3.7 and 3.8. In these basin especially the alluvium and coastal plain sands, there are unconfined aquifers with unconsolidated fine to medium grain sands with a depth range from 1-45m depending on locations. Low permeable aquitard underlies these with clay, shale, peats and some organic materials (Adeoti et al, 2010; Faleye & Olorunfemi, 2015; Fatoba, Omolayo, & Adigun, 2014; Longe, Malomo, & Olorunniwo, 1987) with a little

fraction of sands in some locations with a thickness ranging from 8-45m. The thickness of the second aquifer ranges from 10–35m while the third aquifer is about 10-35m with depth ranging from 150-240m thick. The fourth aquifer starts from 200m to 250m depending on the locations (Longe et al, 1987, 2009). The variation in the aquifer characteristics begin from Abeokuta formation (Figure 3.6) in the North as the lateritic top soil thinning out as it passes through Ilaro, Ewekoro, into Coastal Plain Sand and Alluvium units towards the sea. This is more peculiar to area around the cross-sections XX' and YY' at the western part of the study area Figure 3.6. Underlining the uppermost sandy unconfined aquifer are intercalations of Clay, Shale, limestone and peats with disseminated sands at different proportions which reduced their permeability to serve as the boundary between the aquifer units as presented in Figure3.6 and 3.7.

The thicknesses and depths to the top of the aquifer units within each geologic unit were determined (Faleye and Olorunfemi, 2015), and four aquifer units are identified within the Coastal Alluvium/Coastal Plain Sands. Within the area underlying the Eastern parts of the study area around the cross-section AA' and BB', four aquifer units are delineated through Borehole and some complementary geophysical investigation. Depth to the aquifer units was in the range of 5–23m for the primary unconfined aquifer while depth to three confined aquifers is in the range of 7–80m, 63-188m and 245–261m respectively while their thicknesses range from 7–26m, 6–67m, 20-143m and 61–117m respectively. The aquifers are bounded by intercalation of Shale, Tar sands, and sandy clays layers with relatively low hydraulic conductivity. Two main aquifer units were identified within the Upper Coal Measures. The depths to the top/thicknesses of the aquifer units are 9.8 m (1.7m) and 23 m (5.3m) respectively.

The Nkporo Shale had a thickness and depth to the top of the only identified aquifer unit as 10m and 16 m respectively, (Faleye and Olorunfemi, 2015).

The aquifer parameters required for this model development are the hydraulic conductivity and porosity. A summary of hydraulic property estimates for aquifers from the study area is presented in Table 3.3.

Table 3.3 Summary of hydraulic conductivity values from different Authors across the study area.

S/N	Author	Hydraulic Conductivity Range	Zone	Geology
1	Salami & Olorunfemi., (2014)	56.55 - 99.22m /day	East	Abeokuta Formation
2	Longe et al., (1987)	0.295×10^{-3}- 2.5×10^{-4} m/s	West	Coastal Plain Sand
3	Fatoba et al., (2014)	0.8 - 65.3 m/day	West	Coastal Plain Sand

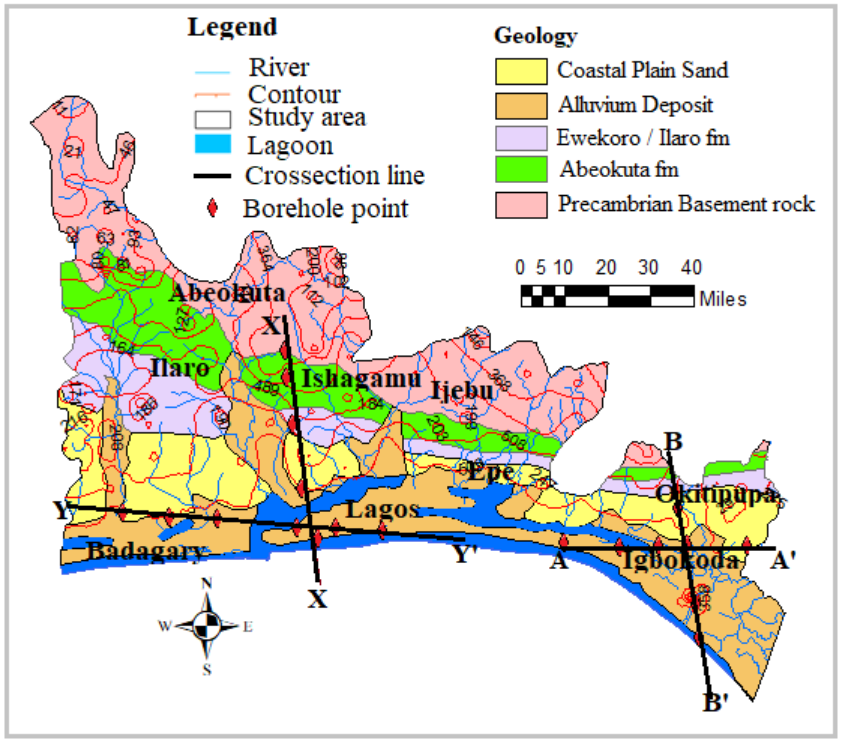

Figure 3.6 Geological map of the Eastern Dahomey Basin with stratigraphical cross-sections

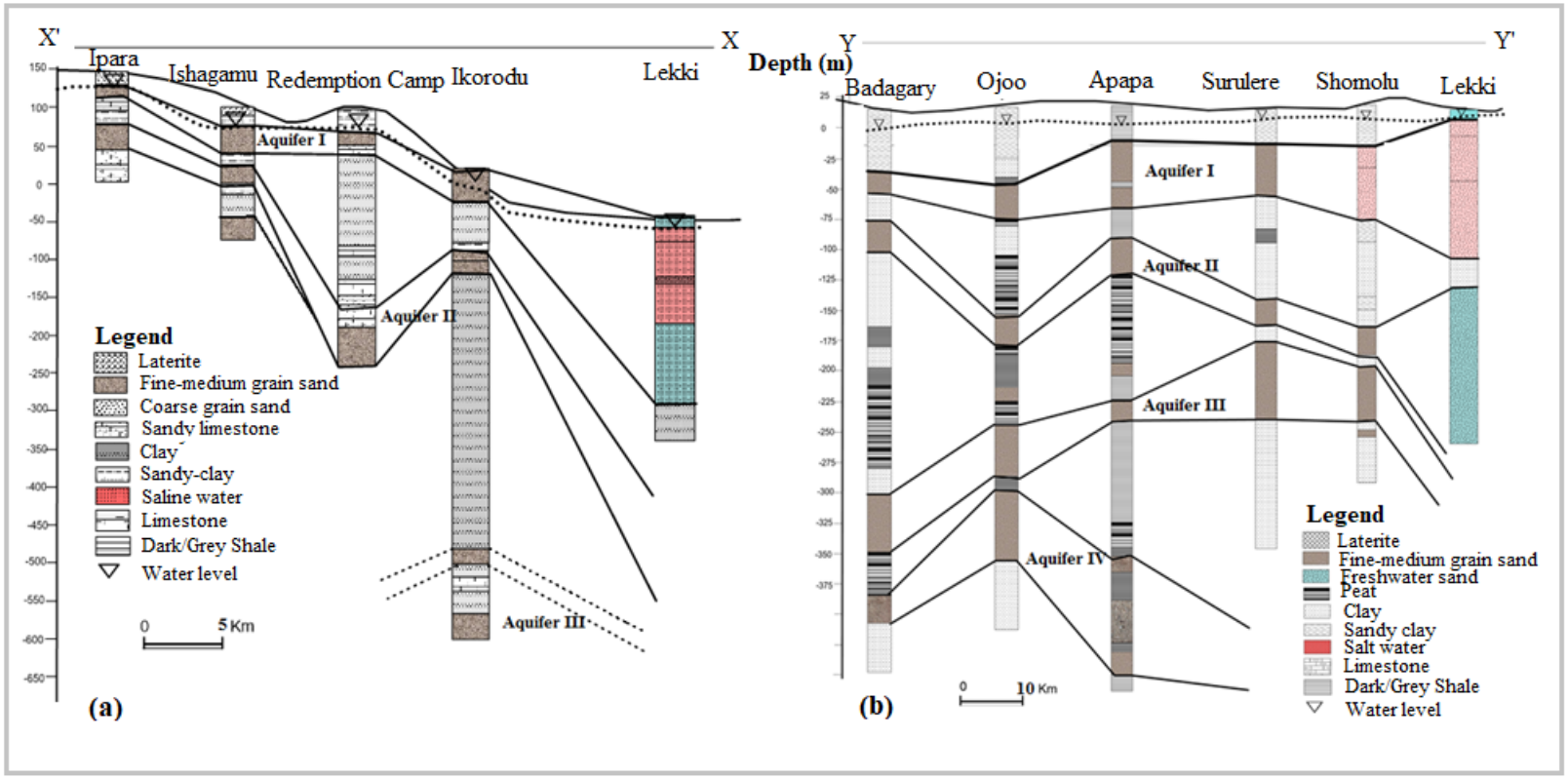

Figure 3.7 Hydrostratigraphy cross-section along (a) XX' and (b) YY'

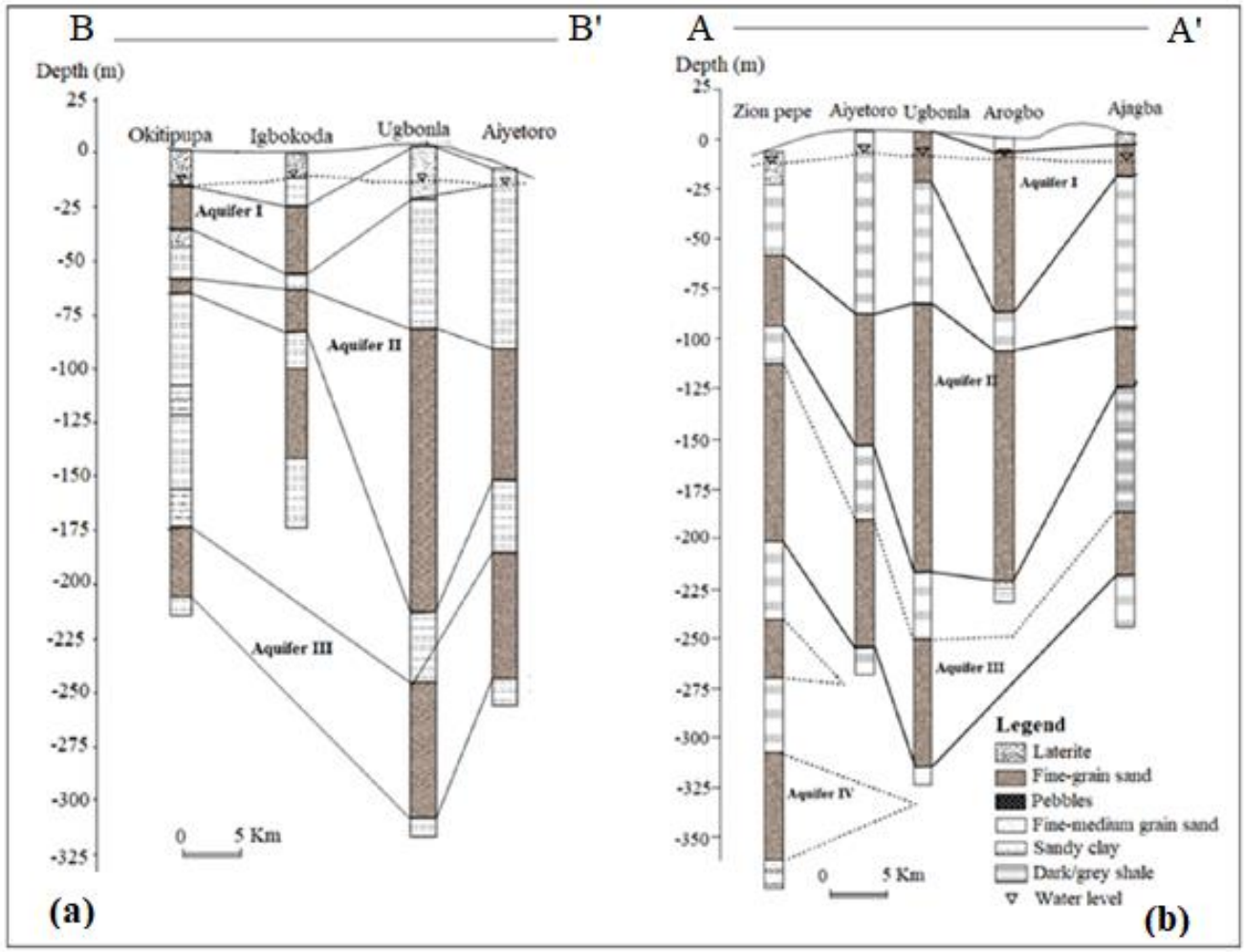

Figure 3.8 Hydrostratigraphic cross-section along (a) BB' (b)

CHAPTER 4

4.0 METHODOLOGY

4.1 Preamble

Fieldwork is very important, almost unavoidable to achieve the best hydrogeological studies of any area. This fact, therefore, necessitated the fieldwork across the Nigeria Eastern Dahomey Basin to carried the following activities in agreement with the objectives of the research study;

a. Carried out well inventories in some selected boreholes and recorded information such as well type, well depth and depth to water level as shown Appendix 1.
b. Carried out some physicochemical field measurements such as electrical conductivity (EC), pH, total dissolved solids (TDS), salinity, redox potential (ORP) and temperature, from all the sampled wells.
c. Collection of water samples in polystyrene bottles of about 50ml for Laboratory analysis of major ions and some relevant trace metals / Elements after preservation.

4.2 Desk/Reconnaissance Study

Desk study is an essential prerequisite to any hydrogeological field investigation, according to Rick Brassington, (1988). This study enables details examination of both geological and hydrogeological information available in the study area. From this study, information on aquifer and their characteristics were deduced which serve as a guide in planning the fieldwork. Topographical map of the area was also studied to have idea about access to the area to save time and cost, and also to come up with the best mapping and sampling method that produced a systematic

approach for better representative sampling. identification of hydro-lithostratigraphic units was carried out from the previous studies, which guided the selection of the areas for details investigation and also have the idea of possible challenges that could hinder fieldwork in this area. Finally, possible risks associated with fieldwork in the area was identified for development of risk management.

The reconnaissance survey was also necessary to see reality on the field to check up the area to be investigated and to make adequate plans on how the field exercise would be achieved. It also involves making the map of the study area and carrying out a detailed desk study of the map. This will also help in the selection of some vital equipment that will help in aiding the smooth running of the fieldwork. During this events, the visit was made to some community leaders for familiarities and liaising. It is also necessary for security purpose to intimate and educate the community the objective and scope of the study mainly in more sensitive and volatile areas within the area.

4.3 Hydrogeological field procedure

Specific equipment was used for the field exercise which include Global Positioning System GPS, water level meter, pH meter, temperature meter, electrical conductivity meter, containers (fetcher) and a sampling basin, sample collection bottles of about 50cl size, sample bags, polythene bags, permanent markers, masking tape, field notebook and concentrated nitric acid HNO_3 for sample digestion.

4.3.1 Field physicochemical measurement

Well-inventories were carried out on a total number of 230 (96 in the wet season and 134 in dry season) shallow hand-dug wells, shallow tube wells and

boreholes from the Eastern Dahomey Basin (EDB) between May 2017 and April 2018. The physicochemical parameters were measured in the field using a Model 99720 pH/Conductivity meter capable of measuring total dissolved solids (TDS), salinity, temperature and Eh/ORP (Figure 4.1). The depth of the wells and static water level were measured with the aid of a water depth meter while the coordinates of each sampled well were recorded using GPS.

Figure 4.1 Some of the field activities during sample physicochemical measurement and sampling of water samples.

4.3.2 Sampling and Preservation

The water samples were collected from the shallow hand-dug wells and machine drilled boreholes. The wells were sampled using a water sampler and collected into three separate 60ml polyethylene bottles after rinse. The bottles each labelled LXA, LXB, ISX where X represents location number while A, B and IS represented the acidified samples for metals, unacidified samples for the major anions and ISX for isotopes analysis respectively (Figure 4.3). The samples were acidified with two drops

of concentrated HNO_3 in 50 ml of water. The samples were all kept at a lower temperature of about 4°C in cooler box and transferred to refrigerator before transferred to the laboratory. The groundwater sampling distribution (Figure 4.2) is largely controlled by the accessibility and well and borehole availability and consent by the owners.

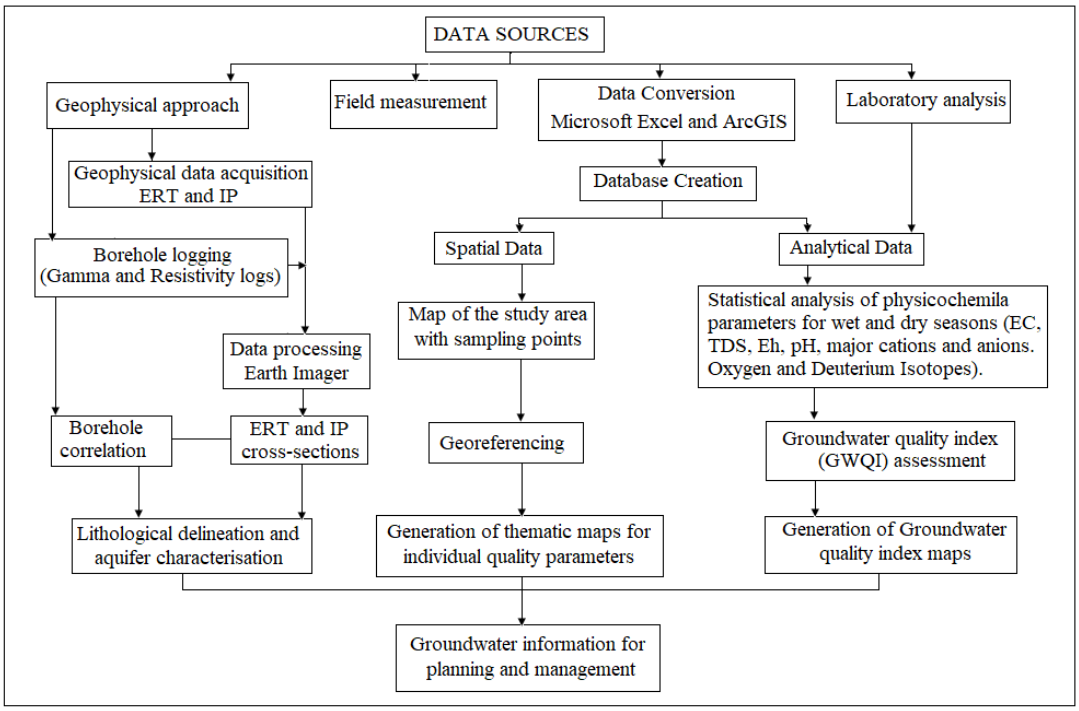

Figure 4.2 Flow chart for the groundwater study approach

4.3.3 Laboratory analysis

4.3.3.1 Cations Analysis

Inductively coupled plasma optical emission spectroscopy (ICP-OES, iCAP 6200, Thermo Fisher Scientific) was used to quantify $Ca^{2+,}$ Mg^{2+}, Na^{+}, K^{+}, Fe, Cu, Mn, Cr, Co, Pb, As, Li, Ba, Cd, Zn, Hg, Sr and Si. Water samples were collected from shallow hand-dug and boreholes across Eastern Dahomey Basin, Nigeria and acidified with concentrated HNO_3 (69%). The water samples were first shaken a few times and then roughly 15 ml were filtered through 0.45 µm acetate cellulose syringe filter (VWR

international LLC) and collected in clean centrifuge tubes. Matrix matching (2% HNO_3) standards were prepared by dilution of certified standards for all the elements of interest and used to obtain a four-point calibration curve. Yttrium (Y^{3+}) at concentration of 5 ppm was used as internal standard. Element carry over effect was assessed by running samples containing only acid mix (no elements) and blank samples immediately after the highest of the standard used for calibration purposes. Quality control (QC) samples containing the analytes of interest at known concentrations were prepared and analysed every 20 samples to check instrument performances throughout the sample analysis. Samples whose concentration exceeded the highest standard were adequately diluted to fit in the linear range of the calibration curve. Method quantification limit (MQL) for all the elements ranged from 0.0001 to 0.1194 mg/L.

4.3.3.2 Anions Analysis

Step 1: Sample handling storage preservation and preparation

Groundwater samples were refrigerated at 4^{o}C in 500 ml HDPE bottles. A representative aliquot was passed through a Millex syringe filter (0.45 µm pore size, 33 mm diameter housing with mixed cellulose ester membrane, Millipore) into Peak IC Autosampler sample tubes (12 mls polystyrene, Metrohm). Samples with concentrations of dissolved anions exceeding the highest standard were diluted using ultrapure water to fit into a middle of the linear range of an individual anion calibration curve.

Step 2: Analysis

A single- column chemically suppressed IC technique was employed for the simultaneous determination of six inorganic anions (fluoride, chloride, bromide,

nitrate, phosphate, sulphate). The equipment used was a Metrohm 850 Professional IC system comprised of a guard column (Metrosep A Supp 5 Guard/4.0), analytical column (Metrosep A Supp 5), Metrohm Suppressor Module (MSM) and Metrohm CO_2 Suppressor (MCS), electrical conductivity detector (Microprocessor-controlled Digital Signal Processing, DSP technology), eluent and sample degassers and an autosampler (858 Professional Sample Processor) with 2-channel peristaltic pump. Before every run the instrument was equilibrated for at least 30 minutes then electrical conductivity and anion pump pressure monitored. Analyses proceeded only when the IC system performed within the accepted range of pressure and conductivity. Full details are provided in Table 1 below.

The sample volume used was 10 µL. Separation of analytes was achieved by using a mobile phase (eluent) of 1 mM sodium bicarbonate and 3.2 mM sodium carbonate, delivered at a flow rate of 0.7 ml/min. Retention times for the analytes are provided in Table 2 below. Concentrations were calculated by peak area using MagIC Net software (version 3.3). Multi-analyte calibration standards of 0.1, 1, 2, 5 and 10 ppm (Table 3) were prepared from 1000 ppm single element stock standard solutions (Fisher Scientific) using 18.2 MΩ cm^{-1} ultrapure water (Triple Red water purification system). Data was accepted when calibration curves generated correlation coefficients (R^2) >0.9980. In a brief method validation study, the linear ranges of fluoride, nitrite, nitrate, bromide, and phosphate were found to be 0.1 to 10 ppm, and the linear ranges of chloride and sulphite were 0.1 to 50 ppm.

Method detection limits for the anions of interest were from 0.01 to 0.02 mg/l (Table The precision of the method was tested at three different concentration levels (Blank, 0.1 and 5 mg/L). Analytical precision ranged from 0.01 to 5 % for n=7. Quality Control Check Standards (QCCS) were included at the start, middle and end of each

analytical run. These were comprised of 0.5 mg/L and 5 mg/L of each analyte prepared from a different stock solution than the calibration standards. Changes in the sensitivity of the instrument were monitored by analysing 2 and 5 mg/L Analytical Quality Control (AQC) standards for each analyte. These were run after each twentieth sample. QCCS and AQC results were accepted when measured values had been within 10 % of expected control values.

Table 4.1 IC system and a method detail.

IC Parameter	**CEE'S System and Method Details**
Anion column type	Metrosep A Supp 5
Guard column	Metrosep A Supp 5 Guard/4.0
Column thermostat temperature, ^{o}C	24
Eluent composition and concentration, mM	$NaHCO_3$ - 1 and Na_2CO_3 - 3.2
Detector electrical conductivity, uS/cm	0.8 – 1.2
Eluent flow, mL/min	0.7
Anion pump pressure, MPa	8.5 - 10
Suppressor regenerant, 100 mMol/L	H_2SO_4
Rinse	ultrapure water
Sample loop, uL	20
Sample size, uL	10
Sample replicates	1
Peristaltic pump tubing	Tygon Long Flex Life

Table 4.2 Analytes retention time and method detection limit

Analyte	**Retention Time, min**	**MDL, mg/l**
Fluoride, F^-	3.50	0.01
Chloride, Cl-	5.19	0.01
Bromide, Br^-	7.89	0.02
Nitrate, NO_3^-	9.09	0.02
Phosphate, PO_4^{3-}	11.93	0.01
Sulphate, SO_4^{2-}	13.75	0.01

4.3.3.3 Bicarbonate Alkalinity Measurement

Alkalinity (HCO_3^-) was determined using a Digital Titrator (Model: 16900, HACH International) and 1.6 N and 0.16 N H_2SO_4 cartridge.

List of used materials

1. 0.16N Sulfuric Acid Cartridge
2. 1.6 N Sulfuric Acid Cartridge
3. Bromcresol Green-Methyl red indicator powder pillow
4. Phenolphthalein indicator powder pillow
5. Buffers (4.01 and 7.00)
6. Deionized water
7. 150 ml Glass Beaker
8. Stir Bar
9. 100 ml Graduated Cylinder
10. Digital Titrator

After placing the sulfuric acid cartridge in position in the Hach Digital Titrator, we connected the delivery tube carefully and ensured titrant is forced out of the delivery tip to remove the air bubbles trapped within the tube. Proper check was conducted for leaks where the tip connects to the cartridge. The instrument was rinsed with the deionized water after which, the counter was reset to zero before the start of titration.

Sample preparation

The samples were grouped based on the values of total dissolved solids (TDS). Group 1 consists the samples with TDS values below 40 mg/l while the group 2 are those samples above 40 mg/l. This guided the choice of molarity of the sulfuric acid as titrant, in this regard, 0.16M H_2SO_4 was used for group 1, while group 2 were titrated with 1.6 M H_2SO_4.

Titration procedure

The following steps were taken for the titration;

Step 1: Volume V in ml of the sample was added into the 150 ml glass beaker.

Step 2: 1 pillow of Phenolphthalein indicator was added to the sample.

Step 3: The titrant added to the samples from zero digit on the titrator until the solution become colorless. Then the digit number was recorded as **A** which is referred to P-Alkalinity.

Step 4: 1 pillow of Bromcresol Green-Methyl red indicator was added to the solution.

Step 5: The titration continued from where the Phenolphthalein endpoint occurred until the colour changed to slight pink from green. Then the digit was recorded as B which is referred to as total alkalinity.

Calculation of Alkalinity concentration was done as present below;

$CaCO_3$ alkalinity (mg/l) = Multiplier × Total digit used. For Phenolphthalein alkalinity.

$CaCO_3$ total alkalinity (mg/l) = Multiplier ×Total digit used. For Bromcresol Green-Methyl red

If $CaCO_3$ alkalinity (mg/l) = X and $CaCO_3$ total alkalinity (mg/l) =Y and Z = Bicarbonate alkalinity.

Then Hydroxide alkalinity = 2X – Y and

And total alkalinity = X +Y+Z

Z = Total alkalinity – (X+Y) = Bicarbonate alkalinity

The above procedure was performed on all the water samples with selection of volume and molar concentration of H_2SO_4 based on Total dissolved solid of the samples.

4.3.3.4 $\delta^{18}O$ and δD Isotopes analysis

Then, samples labelled IS were shipped to the Ministry of Agriculture, Irrigation and Water Development Isotope Laboratory, Blantyre, Malawi under a temperature below 4°C for the stable isotope of $\delta^{2}H$ and $\delta^{18}O$ analysis. The groundwater samples and analysis were carried out following the same method of isotope water samples as described in Banda et al., 2019 and analysis which was conducted in line with International Standard Procedures with appropriate quantification and validation of results.

4.3.3.5 Selection Regional Precipitation $\delta^{18}O$ and δD Isotope Data

Regional precipitation isotope data was needed for this study to identify any possible deviation from the Global Meteoric Water Line (GMWL) to better characterise local meteoric conditions. The closest Global Network of Isotope in Precipitation (GNIP) data stations to the study location in the Eastern Dahomey Basin are Cotonou (Republic of Benin) to the west and Douala (Cameroon) to the east. The only station in Nigeria is situated in Kano, at the northern savannah region of Nigeria. Meanwhile, Cotonou and Douala, located along the coast of West Africa, share similar climate conditions with the study area (Figure 4.3) In light of this, a total of 134 regional and annual precipitation isotope data of $\delta^{18}O$ and $\delta^{2}H$ were collected from the Douala, Cameroon (50), Cotonou, Republic of Benin (50) and Kano, Nigeria (33) meteorological stations during 2009 – 2018. These isotope data were downloaded from the GNIP and are presented in Table 2. The results are expressed as δ-values relative to V-SMOW (Vienna Standard Mean Ocean Water), and the measurement precision is 0.01‰ and 0.2‰ for $\delta^{18}O$ and $\delta^{2}H$, respectively.

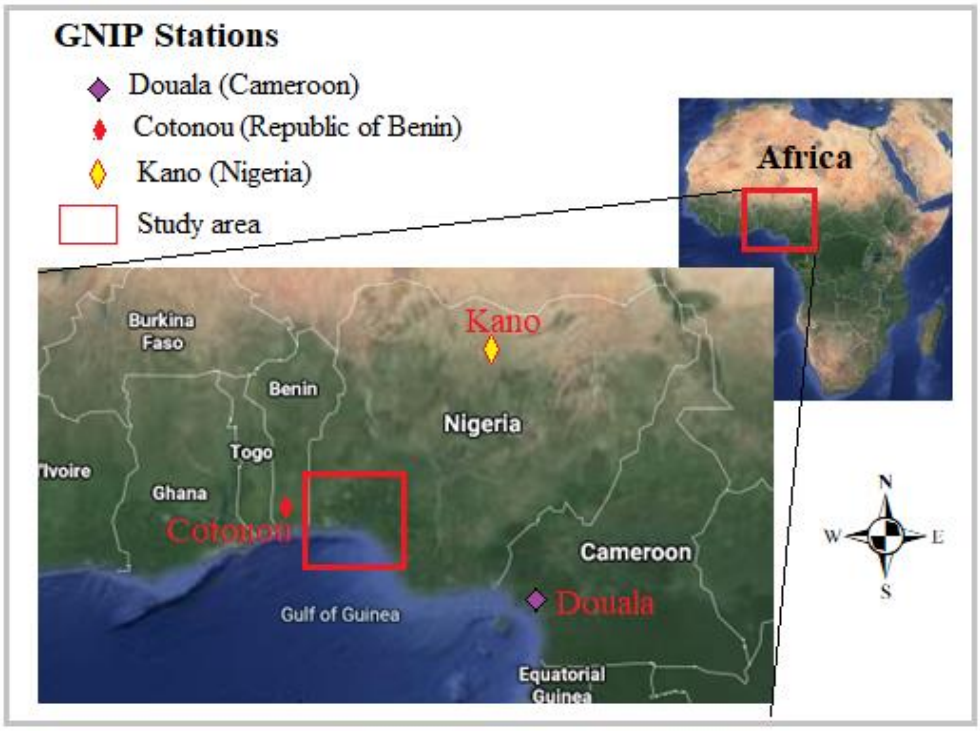

Figure 4.3 Map of West Africa coast showing all

Figure 4.4 Picture of field and Laboratory sample preservation and preparation

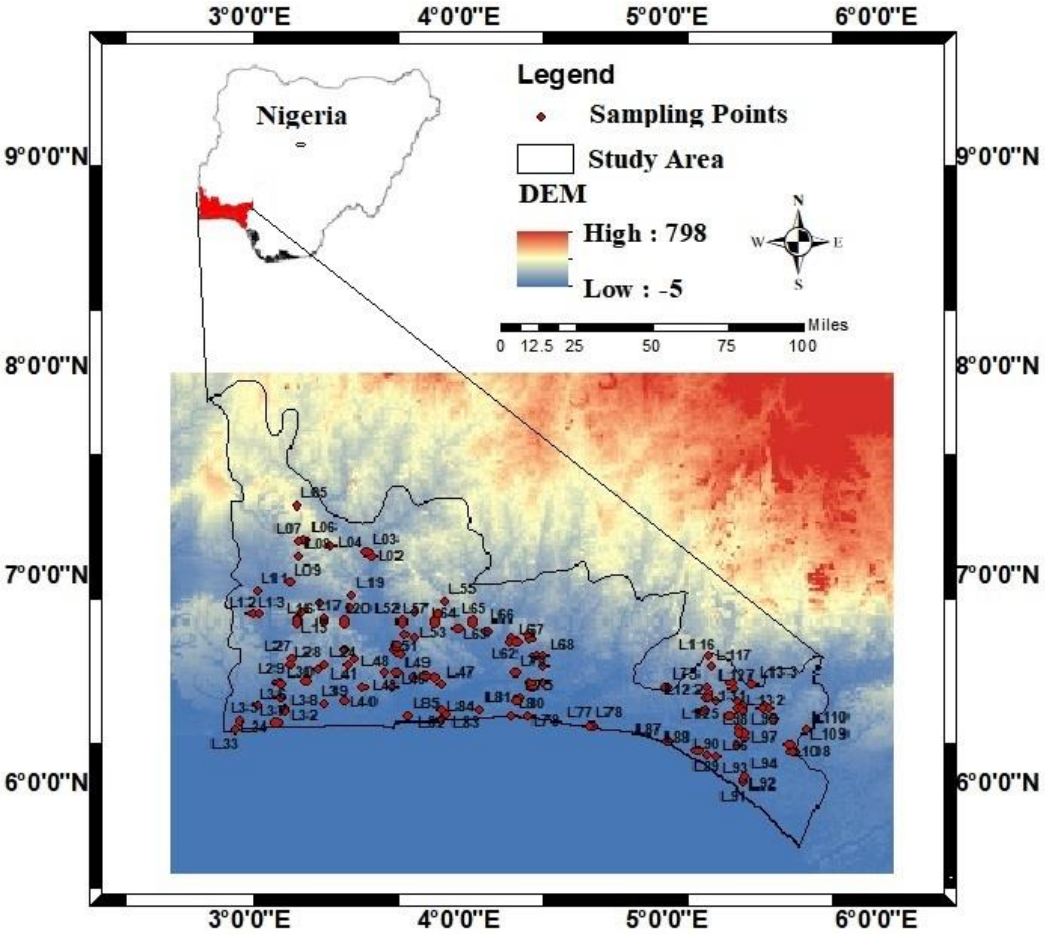

Figure 4.5 Map of the study area showing the sampling points

4.4 Field Geophysical Data Acquisition Procedure

Various geophysical techniques are commonly employed for groundwater investigation in the coastal environment. However, electrical resistivity methods are unique because of their ability to detect increases in the conductivity of an aquifer that result from increases in pore-water conductivity (Abdul Nassir et al. 2000). Electrical resistivity method was chosen for this work based on existing results obtained by previous workers like Goldman et al. (1991) and Nowroozi et al. (1999) that confirmed the existence of distinct resistivity contrast between freshwater and saline-waters in coastal aquifers of Isreal.

Sounding and profiling can be combined in a single process (2D resistivity imaging) to investigate complicated geological structures with lateral resistivity changes. This combination provides detailed information, both laterally and vertically along the profile. In the 2D case, it is assumed that the resistivity of the ground varies only in the vertical and one horizontal direction along with the profile. There is no resistivity variation perpendicular to it (strike direction). 2D resistivity surveys (2D imaging) have played an increasingly important role in the last few years. The advantages of 2D measurements are their high vertical and lateral resolution along the profile, comparatively low cost due to computer-driven data acquisition, which means only a small field crew is needed (one operator and, depending on terrain roughness and profile lengths, one or two assistants) Ernstson and Kirsch, 2006. (Kirsch, 2011)

In this study, the earlier result of the in-situ test for electrical conductivity across the area revealed high conductivity in some of the wells especially in locations very close to the coast as shown in the figure below. This was the basis for the application of this method in order delineate the subsurface lithology that shows the signature of saltwater in this aquiferous layers.

In the light of the above, geophysical data acquisition for the delineation of areas with low resistivity was also conducted. In this context, total of ten electrical resistivity tomography (ERT) and Induced polarisation (IP) were carried out in the selected parts of the study area. Each of these profiles is 500 meters long in a different direction to the coastline as shown in the Figure 4.5 and 4.6 which was controlled by accessibility and terain factor. There are many dodgeries in this areas because of swampiness and natural characteristics of sand bars which are generally parallel to the coastline arising from their depositional process.

Electrical resistivity tomography was conducted along those profiles as using Wenner and Dipole-Dipole arrays at each location using a multichannel Advanced Geophysical Instrument (AGI) SAS 4000 with 84 electrodes with 6m electrode spacing, see Figure 4.8.

4.5 Data Processing and Evaluation

4.5.1 Hydrochemical data processing and Interpretation

Descriptive statistics and correlation analysis were useful tools to obtain significant information from hydrochemical data sets in studies of groundwater (Adimalla, 2019a; Edet, 2019, 2016; Narany et al., 2014; Shakerkhatibi et al., 2019; Thilagavathi et al., 2017). To evaluate the analytical data descriptive and multivariate statistical techniques i.e., correlation analysis was used in this present study, by using SPSS_26_Win_64. Parametric descriptive statistical methods were also employed to calculate minimum, maximum, mean and standard deviation of the analytical data. Pearson's correlation matrix was used to identify the relationship between the pairs of parameters.

Table 4.3 Location and coordinates of ERT profiles

		Starting Point		**Ending Point**				Length **(m)**
S/N	**Location**	**Northing**	**Easting**	**Northing**	**Easting**	**Orientation**		
1	Igbokoda 1	$6^0$22’20.24’’	$4^0$45’46.00’’	$6^0$22’14.91’’	$4^0$46’01.34’’	East-West	290NW	500
2	Ugbonla Ebute	$6^0$09’14.20’’	$4^0$47’22.38’’	$6^0$08’58.91’’	$4^0$47’17.13’’			500
3	Ipare-Aboto Rd	$6^0$16’00.17’’	$4^0$41’50.22’’	$6^0$16’04.48’’	$4^0$42’06.08’’	233SW	60NE	500
4	Araromi	$6^0$20’15.92”	$4^0$29’19.74”	$6^0$20’08.66”	$4^0$29’34.47”		135SE	500
5	Abule Obi	$6^0$18’59.93’’	$4^0$33’13.44’’	$6^0$19’14.98’’	$4^0$33’19.84’’		8.0N	500
6	Aboto-Igbokoda Rd 2	$6^0$17’32.4”	$4^0$45’06.05”	$6^0$17’16.00”	$4^0$45’08.35”		32NE	500
7	Igbokoda-Okitipupa Rd 2	$6^0$23’48.32”	$4^0$46’25.48”	$6^0$23’33.00”	$4^0$46’20.07”		11N	500

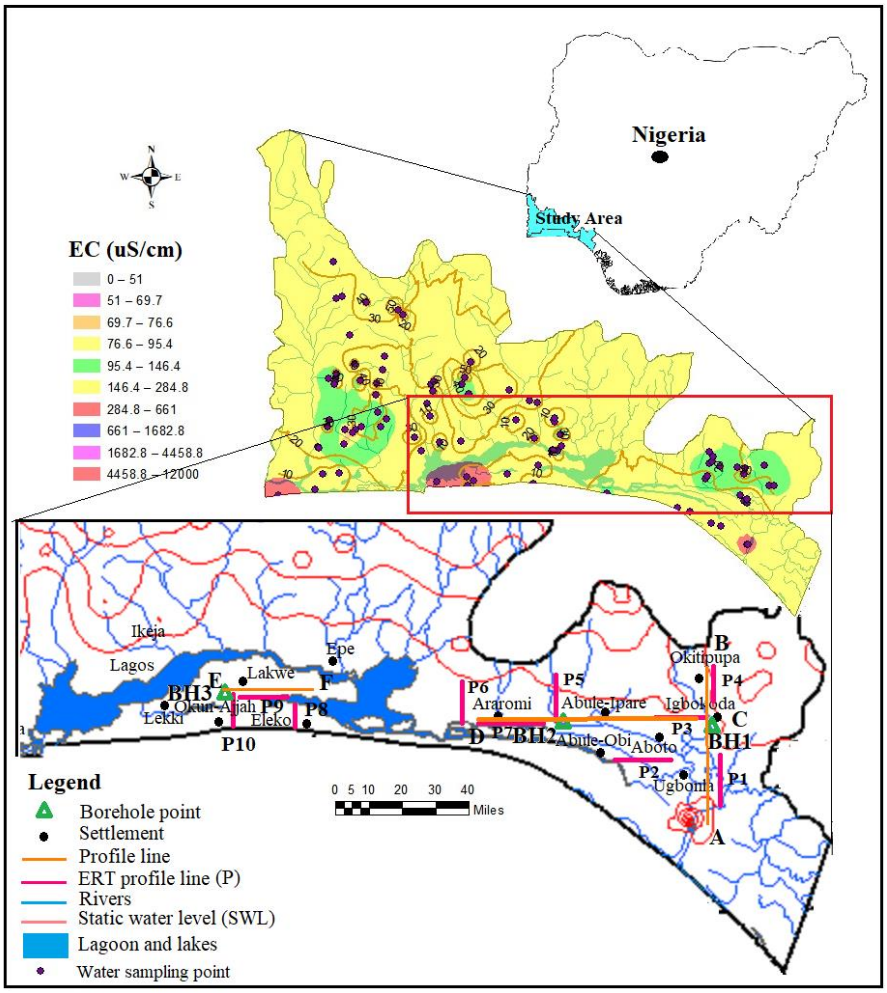

Figure 4.6 Map of the Eastern Dahomey Basin showing well sampling points, borehole points and geoelectrical profile and spatial distribution map of electrical conductivity (EC)

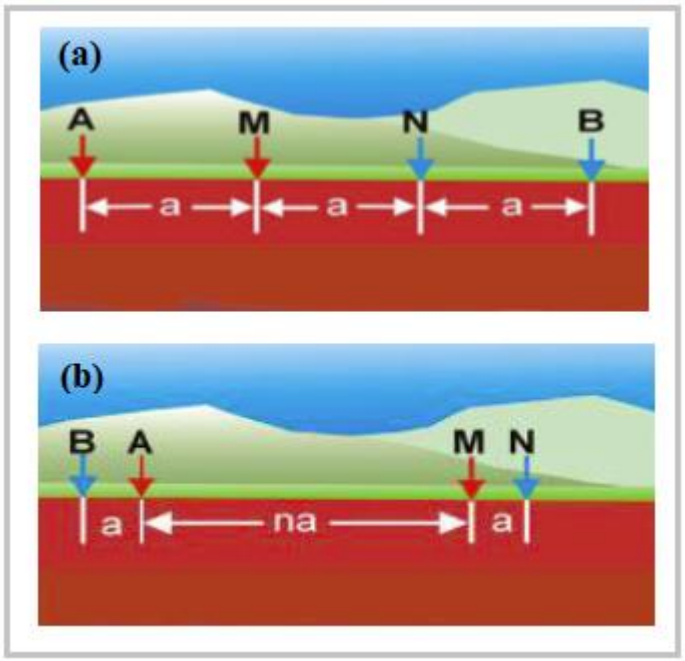

Figure 4.7 The Electrode arrays used (a) Wenner array with a = 6m for the electrical resistivity tomography (ERT) (b) Dipole-dipole array for the induced polarisation (IP)

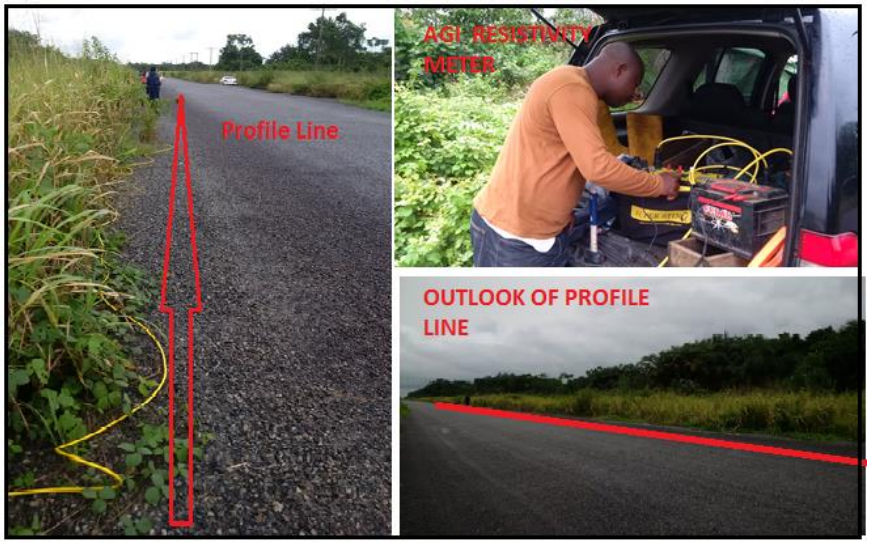

Figure 4.8 Picture showing field geophysical data acquisition

Spatial analysis for the distribution of mineral saturation zones

Geostatistics is a subset of statistics which specialises in analysis and interpretation of geographically referenced data. Geographical information system (GIS) and geostatistical techniques provide an integrated tool to investigate the spatial

distribution of selected minerals. The minerals were calculated through the Geochemist Work Bench Geochemical tool. The minerals include Calcite, Dolomite, Aragonites, Gypsum, Halite and Anhydrite. The spatial distribution maps of each mineral were generated using the ordinary kriging method, which is one of the best interpolation methods in ArcGIS geostatistical extension (Adimalla and Kumar, 2020; Ahmed et al., 2019b; Bodrud-Doza et al., 2019; Wang et al., 2017). This method is for optimum linear interpolation with a minimum square error of the sampled location, based on the equation 1 below;

$$Z^*(x_0) = \sum_{i=1}^{n} n\lambda_i Z(x_i) \qquad (1)$$

where $Z*(x)$ is the estimated value at location x_0, n is the number of points, $Z(xi)$ is the known value at location xi, and λi is the weight of the kriging.

4.5.2 Geophysical Data processing and interpretation

Effects of lateral changes in resistivity and chargeabilities can be separated from changes with depth using modern day computers. For this to be done, data must be collected along the whole length of a traverse at a number of different spacing that are multiples of a fundamental spacing as was the principle adopted in the use of the dipole-dipole array for both ERT and IP data acquisition. The results can be displayed as contoured pseudo-sections that give rough visual impressions of the way in which resistivity and chargeability vary with depth. The acquired ERT and IP data was inverted to produce sections with vertical scales in depth rather than electrode separation, which give greatly improved pictures of actual resistivity and chargeabilities variations (Figure 4.7). The AGI EarthImager 2D software was used to analyse the acquired ERT and IP data. Results were presented in sections/profiles.

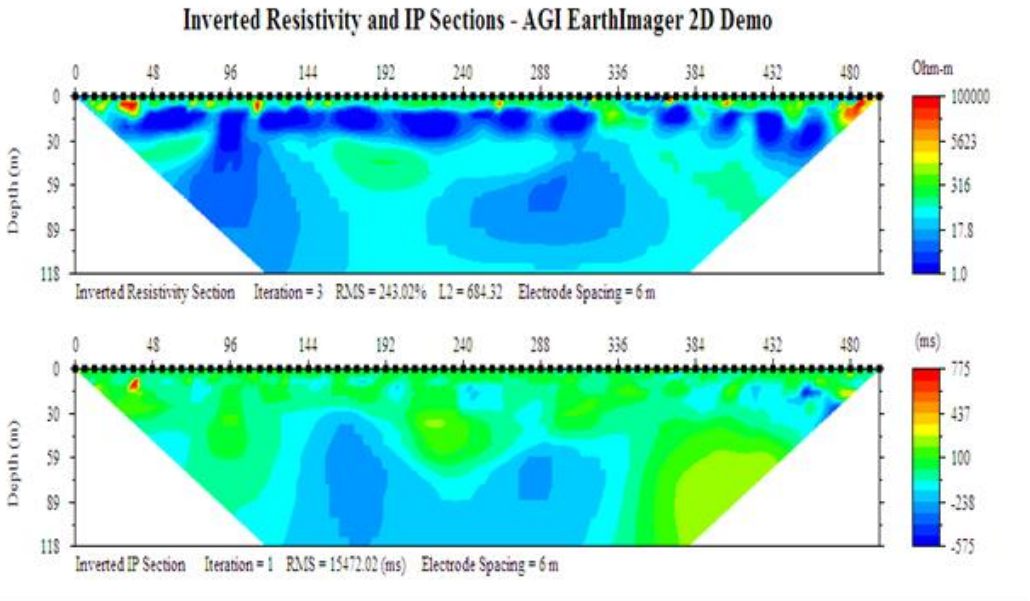

Figure 4.9 Both ERT and IP Pseudo-sections after inversion

Data quality control

The multiparameter pH/conductivity tester was usually calibrated with a buffer solution of pH 4 and 7 with errors of +/-0.02, while conductivity and total dissolved solid was calibrated in solution with 1413 µS/cm and 940 ppm respectively. This procedure was repeated before the commencement of groundwater sampling. The instrument was also rinsed to avoid cross-contamination of samples. The accuracy of the chemical analyses was determined by using the ion charge balance equation (Somaratne and Frizenschaf, 2013). Some selected major ions were repeated in ten (10) randomly selected samples from which their correlation values fell well above 0.8.

CHAPTER 5

5.0 HYDROSTRATIGRAPHY AND AQUIFER CHARACTERISATION

5.1 Preamble

The general geology and hydrogeology have been described in Chapter 3 to give an overview of the geohydrology of the Eastern Dahomey Basin. Due to the heterogeneity of the aquifers resulting from the multilayer and complex geology that characterises the basin, there is a requirement for details of the aquifer characterisation in some selected representative locations in order to have a clear picture of the aquifer geometry and lithology to give an insight into the potential implication on groundwater resources of the basin. In addition to this, one of the major groundwater issues popular among the literature from this basin is saltwater intrusion. Therefore, the preliminary studies were designed to use the enhanced electrical conductivity (EC) and major ions which are critical to groundwater quality to investigate the basin. In order to achieve this, field physicochemical measurement coupled with groundwater sampling were carried out while electrical conductivity along with other groundwater quality relating to saltwater intrusion was used for selection of areas at which hydrogeophysical and borehole analysis were carried out. Results of this were presented in the following two papers;

- Aladejana, Jamiu A, Kalin, R.M., Sentenac, P., Hassan, I., 2020. Groundwater Quality Index as a Hydrochemical Tool for Monitoring Saltwater Intrusion into Coastal Freshwater Aquifer of Eastern Dahomey Basin, Southwestern Nigeria. ***Accepted for***

publication in Elsevier Journal; *Groundwater for Sustainable Development.* Manuscript number GSD-2019-398.

- Aladejana, Jamiu A, Kalin, R.M., Sentenac, P., Hassan, I., 2020. Hydrostratigraphic Characterisation of Shallow Coastal Aquifers of Eastern Dahomey Basin, S/W Nigeria, Using Integrated Hydrogeophysical Approach ; Implication for Saltwater Intrusion. *Geoscience* 10, 65. https://doi.org/10.3390/geosciences10020065

These articles represent the preliminary studies to establish focus and further detail research work, especially due to the extensiveness of this study basin. With the help of my supervisor, Prof. Robert M. Kalin, my second supervisor, Dr Philippe Sentenac and my research colleague, Ibrahim Hassan, we were able to design and criticise the method for improvement, which lead to the first draft of these manuscripts with further reviews leading to the publications as stated above.

5.2 Paper 1

Aladejana, Jamiu A, Kalin, R.M., Sentenac, P., Hassan, I., 2020. Groundwater Quality Index as a Hydrochemical Tool for Monitoring Saltwater Intrusion into Coastal Freshwater Aquifer of Eastern Dahomey Basin, Southwestern Nigeria. *waiting to be accept for publication* in Elsevier Journal; *Groundwater for Sustainable Development*

Groundwater Quality Index as a Hydrochemical Tool for Monitoring Saltwater Intrusion into Coastal Freshwater Aquifer of Eastern Dahomey Basin, Southwestern Nigeria

Jamiu A. Aladejana[1,2], Robert M. Kalin[1], Philippe Sentenac[1] and Ibrahim Hassan[1,3]

[1] *Department of Civil and Environmental Engineering University of Strathclyde Glasgow;*

[2] *Department of Geology, University of Ibadan*

[3] *Department of Civil Engineering Abubakar Tafawa Balewa University Bauchi, Nigeria;*

Email; Jamiu.aladejana@strath.ac.uk

5.2.1 Abstract

Saltwater intrusion into coastal freshwater aquifers is a threat to groundwater quality globally. This study determines the extent of saltwater intrusion into the coastal freshwater aquifer of the Eastern Dahomey Basin (EDB), Nigeria. Groundwater chemistry was sampled and analysed for ionic ratios and interpreted using a hydrochemical facie evolution diagram (HFE-D), the saltwater mixing index (SMI) and the Groundwater quality index for saltwater intrusion (GQIswi). High electrical conductivity (EC) and total dissolved solids (TDS) and the concentration of dissolved ions showed increased salinity as a result of seawater intrusion in wells located around

communities in Seme, Lekki, Eleko, Okun-Ajah, Ode-Mahin and Igbokoda. Correlation of ions in the wet season also suggests higher salinities which originate partly from industrial and municipal effluents especially from wells which are close to river channels, while dry season groundwater shows the dominant influence of seawater intrusion. HFE-D revealed that mixed groundwater of Na+Ca-HCO_3, Na-Cl and Ca-Cl dominate the area due to gravity-driven flow leading to groundwater freshening inland from the coastline towards the northern part of the basin. The groundwater quality index from SMI and GQIswi shows areas within 3 km from the coastline that are more sensitive to saltwater intrusion based on abstraction rate and depth of the wells. The present study provides information of value to planners and policy-makers for the sustainable management and protection of coastal groundwater resources in the Eastern Dahomey Basin.

Keywords: *Saltwater intrusion; Groundwater quality index; freshwater; Coastal aquifer*

5.2.2 Introduction

Coastal aquifers around the world are at risk of increasing salinity resulting from saltwater intrusion. Rapid growth in urbanisation, population and the associated over-abstraction of groundwater in coastal regions has worsened the situation. Mapping the intrusion and extent of saltwater coverage or mixing zones is difficult and costly due to the hydrogeologic complexity, the multifaceted nature of the problem, and the high cost of drilling multiple level wells needed for detailed study (Cardno, 2011).

Nigeria, the most populous nation in Africa, has some of its largest cities on the southwestern coast (UNDP, 2012). The high population density has resulted in

over-abstraction of groundwater from the fragile coastal aquifer, and the proximity to the sea has led to a saltwater intrusion into the coastal freshwater aquifer. Studies have shown that saline groundwater can lead to severe problems for water supply, especially under heavy groundwater abstraction (Tirkey et al., 2017). Seawater intrusion is a widespread problem of coastal aquifers associated with urbanisation (Hwang et al., (2004), Oteri (1988), Longe et al.; (1987), Adepelumi et al.; (2009), Adeoti et al.; (2010), Ayolabi et al.; (2013) and Talabi et al., (2012). These studies identified saline water in some boreholes and wells, especially at the upper-aquifer in part of Lagos. Some of the locations experiencing saline water intrusion include the eastern coast of Lagos such as Lekki, Ajjah, Victoria Island and coastal communities in Ondo state such as Aiyetoro, Ugbonla, Mahin and Igbokoda. The origin of saltwater was linked to the incursion of seawater from the ocean during the flooding of canals and dissolved evaporites trapped within the aquifers sediments. Adepelumi et al., (2009) observed that deterioration of water quality in the coastal zones of Lekki phase 1 and Oniru environs of Lagos metropolis is due to saltwater intrusion which was of concern among the owner of properties in the vicinity. They also found several boreholes constructed in Naira were abandoned due to saline water intrusion.

Cities underlying by the Eastern Dahomey Basin, like other coastal cities in the world, rely heavily on the groundwater resources as one source of potable water for domestic, industrial and agricultural purposes to complement the erratic pipe-borne water supply. There are a few specific-sites hydrogeological studies of the area within the basin especially approaching the border with Lagos (Longe et al, 1987; Oteri & Atolagbe, 2003; Longe and Balogun, 2010) while few or none have looked at hydrogeological processes across the entire basin to study the relative distribution and extent of saline intrusion and its effect on groundwater quality. These aquifers

constitute a vital source of freshwater in the regions, and with the continuous increase in water demand there is vital need to monitor the risk of saline water intrusion as once this problem occurs it is difficult to remediate. A long-term water resource management strategy is needed which will require investment. Less than 2% of seawater intrusion in the freshwater can diminish the water's potability according to Custodio (2002). Presently, there is no groundwater monitoring well within this basin, necessary for routine saltwater intrusion monitoring. Assessment of major ions is vital to identify the source of determination of water quality (Saha et al., 2018). The chemical composition of groundwater changes as it flows through geologic media, so full chemical analysis is useful to identify a saltwater intrusion (Saha et al., 2019; Seddique et al., 2019).

This study employed hydrochemical methods using selected groundwater indices and ionic ratios to fingerprint saline water intrusion in freshwater. The conclusions are expected to be considered as one monitoring tool for the annual assessment of groundwater in the coastal aquifers of the EDB. The indices used include hydrochemical evolution facies diagram HEF diagram, Groundwater Quality Index for Saltwater Intrusion (GQIswi) and Seawater Mixing Index (SMI), combined with the ionic ratios Br/Cl and Cl/HCO3 and Revelle coefficient. These methods had proven effective in the work of Kennedy, (2012), Christina and Alexandros, (2014); Amiri *et al.*, (2016) and Edet, (2016). Comparing these indices and ratios should support policy for groundwater monitoring for saltwater intrusion. The outcomes will add to available information and knowledge on the saltwater intrusion of the coastal freshwater aquifer of the EDB. This information is necessary for sustainable groundwater resources management in this coastal zone in the face of both anthropogenic and natural drivers, such as climate change.

5.2.2.1 Study Area and Geomorphology

The Eastern Dahomey Basin is located within the southwestern part of Nigeria (figure 5.1). It is a transboundary coastal sedimentary basin which extends from Ghana through Togo and Benin to Nigeria. This basin is bounded in the east by Okitipupa Ridge, which is the boundary it shares with Niger Delta basin (Jones and Hockey, 1964). It lies between Latitudes $2^0$41'10.00'' - $4^0$59'5900''N and Longitudes $6^0$21'1300'' - $7^0$52'42.00''E along the coast of the Gulf of Guinea. The basin is progrades into the Atlantic Ocean in the south, and thin out at the north on the Precambrian basement rocks. The area of investigation is undulated at the north and flatting in to plane towards the ocean with several points virtually at or below the sea level. The highest elevation is observed around Abeokuta. Eastern Dahomey Basin is characterised by two distinct seasons, wet and dry. The wet season occurs between April and October with a break in August and features average rainfall which ranges from 1800mm – 2500mm, while the dry season lasts from November to April (Ukhurebor and Abiodun, 2018).

The major rivers in this area include Ogun, Ose and River Oluwa which drain the basin into the delta and discharge into the Atlantic Ocean. The basin hosts two major administrative water basins authorities in Nigeria, and the Ogun-Osun and Benin-Owena river basins and accommodates about 40% population of the country residence including the metropolitan city of Lagos. The study area is vital to the economy of Nigeria and West-Africa.

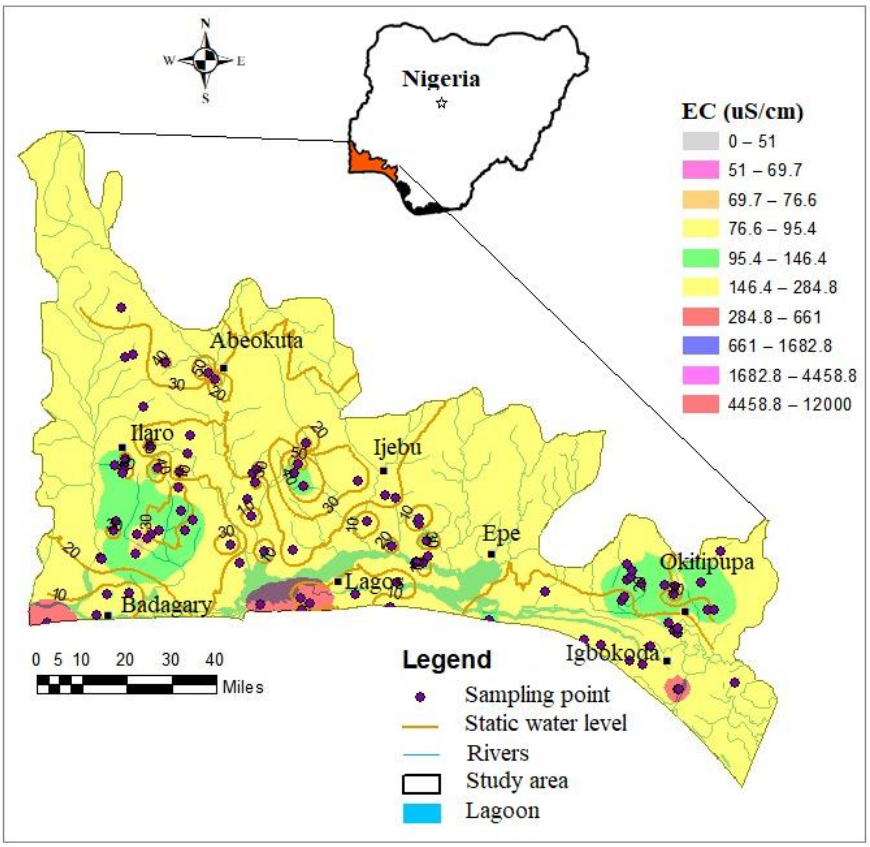

Figure 5.1 Map of the Eastern Dahomey Basin showing the sampling points and spatial distribution of electrical conductivity

5.2.2.2 Geology and Hydrogeology of Eastern Dahomey Basin

The lithological character of the sediments is formed by a regime of transgressions and regressions of the sea since the Cretaceous era, these transgressions come from the south (Jones and Hockey, 1964). The stratigraphic description of the sediments has been provided by various authors including Jones and Hockey, (1964); Adegoke, and Omatsola, (1981), Elueze and Nton, (2004); Okosun (1990) Omatsola and Adegoke (1981); Ako et al. (1980); Billman (1976); Kogbe (1974); Fayose (1970); Jones and Hockey, (1964), summarised in Table 5.1 and presented in Figure 5.2. The Oligocene to Recent Alluvium deposits and coastal plain sands consist of soft, very poorly sorted clayey-sands, pebbly sands, sandy clays and thin layer of lignite

(Reyment, 1965). This is underlain by Ilaro formation, which consists of massive, yellowish, poorly consolidated, cross-bedded sandstones, which are fine-medium-grained and poorly sorted (Kogbe (1976). This layer is followed by Ewekoro formation which consists of predominantly paleocene fossiliferous limestone that becomes arenaceous towards the base (Reyment, 1965) and below the Abeokuta formation consists of lower Cretaceous sandstone and grits with interbedded mudstone unconformity overlaying the basement complex fine detrital sandstone, siltstone and shale.

The Coastal Plains Sands represents the main aquifer in the southern parts of the EDB, in which most of the wells and boreholes extract water (Aladejana et al., 2020). This is a multi-aquifer system consisting of three aquifer horizons separated by silty or clayey layers (Aladejana et al., 2020; Longe et al., 1987). The aquifer shows high thickness at the northern part of Abeokuta, through Ewekoro, Ilaro, and thin-out at the coast. The percentage composition of sands in lithology also increases towards the coast (Longe et al., 1987).

Longe et al. (1987) characterised coastal plain and alluvium deposits into different units. The first is an unconfined water table aquifer prone to pollution. The second and third are confined aquifers composed of an alternating sequence of sand and clay. They are tapped by boreholes as the basis of mini water-works in Lagos area (Longe, 2011). These aquifers belong to the continental Ilaro Formation. The third aquifer appears to be the most productive facies with a high level of groundwater exploitation as most production terminates in this unit. This aquifer is in an under confined to semi-confined condition (Longe et al., 1987; Adelana *et al.*, 1996; Longe, 2011). Generally, the piezometric surface ranges from 2.0 to 15.0 m below ground

level (b.g.l) in the area. The average annual precipitation is above 1700 mm and serves as a primary source of groundwater recharge.

Table5.1 Stratigraphic Sequence in the Eastern Dahomey Basin (Modified from Adelana et al., 2004)

Formation	**Age**	**Rock Type**	**Approximate Depth of Base (m.b.s.l)**
Coastal Plain Sands	Tertiary (Oligocene – Pleistocene)	Clays, Silty Clays, Sands	130
Ilaro	Tertiary Eocene	Clays and Shales	280
Ewekoro	Tertiary Paleocene	Shales, limestone and sands	550
Abeokuta	Upper Cretaceous	Sandstone, Siltstone, Shale, Conglomerate	350-600
Basement complex rock	Paleozoic to Precambrian	Granites and Migmatite	>400

m.b.s.l represents metre below the sea level

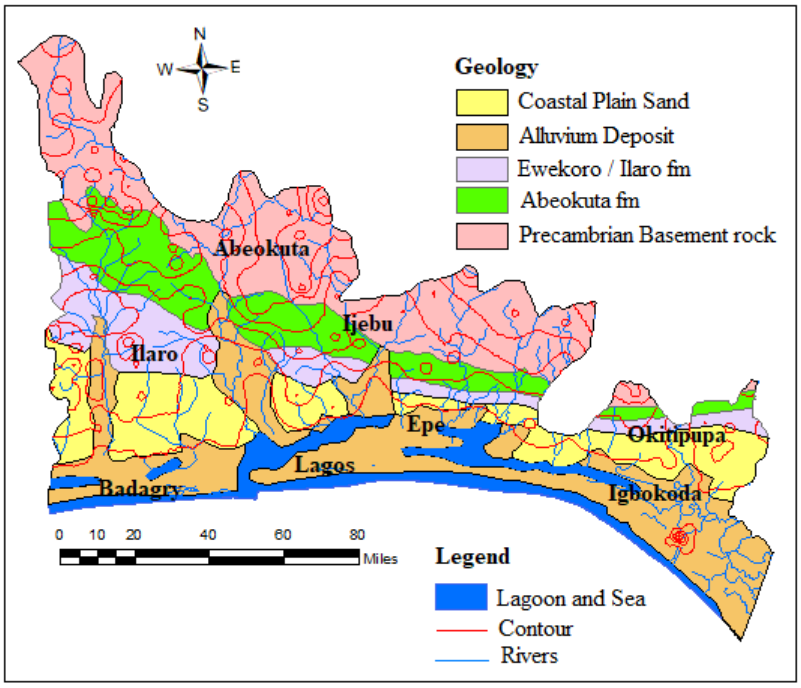

Figure 5.2 Geology map of Eastern Dahomey Basin showing the contour, drainage and Lagoon

5.2.3 Materials and method

5.2.3.1 Field physicochemical measurement and groundwater sampling

A topographical map of the study area was gridded to determine accessible locations within the area in which to carry out a systematic and representative groundwater sampling. Physicochemical measurements of electrical conductivity (EC), pH, total dissolved solids (TDS) salinity, redox potential (Eh) and temperature were measured and recorded in the field using Model 99720 microprocessor pH/Conductivity meter. A total of 229 water samples were collected from shallow boreholes and hand-dug wells, 96 in the dry season and 133 in the wet season, across the Eastern Dahomey Basin. The samples were collected in three separate polyethene bottles labelled A, B and IS Samples labelled A were acidified to a pH < 2 after

collection with 0.4ml of concentrated nitric acid (HNO_3). Samples B and IS were filtered with a 0.45µm filter and preserved in an ice-packed cooler to keep samples temperature below 4°C before being transported to the laboratory for further analysis. Samples labeled A and B were meant for cations and and anions analysis respectively, while samples labeled IS were meant for the Oxygen and hydrogen isotopes analysis.

5.2.3.2 Laboratory analysis

Cations and anions analyses were carried out using inductively coupled plasma - optical emission spectrometry (ICP-OES) and Ion Chromatography (IC) with standard methods after filtering with <0.45µm. Alkalinity and bicarbonate were determined using HACH digital titrator using Bromcresol Green-Methyl red and Phenolphthalein indicator using 0.16 and 1.6M of sulphuric acid. Results were checked for error using calculated error equations recommended by Appelo and Postma (1993).

5.2.3.3 Data quality control

Quality control was conducted on hydrochemical laboratory results of the ions using ionic balance using (sum of cations versus the sum of anions). About 75% of the samples fall within ±5 acceptable error limit as described in Appelo and Postma (1993) with 12 (dry season) and 19 (wet season) samples recorded above this threshold. Total dissolved solids (TDS) and calculated total dissolved ions (TDI) were plotted on a scatter diagram and showed a regression correlation of 0.78 and 0.86 respectively for both wet and dry seasons. The values are both below the limits recommended for hydrochemical analysis by the World Meteorological Organisation (WMO) in 1994.

5.2.3.4 Data evaluation and analysis

5.2.3.4.1 Theoretical Background

1. HFE-Diagram approach

The Hydrochemical Facies Evolution Diagram (HFE-D) proposed by Gimenez Forcada (2010) presents a simple method to identify the state of a coastal aquifer with respect to freshening /intrusion phases, as deduced from the distribution of anion and cation percentages as presented in Figure 4. The HFE-D uses only the percentage of the major cations (Ca^{2+} and Na^{+}) and anions (HCO_3^-, SO_4^{2-} and Cl^-) to determine the dynamics of saline/saltwater intrusion. The authors suggest conventional diagrams such as the Piper diagram do not allow for full recognition of the facies evolution sequence during recharge and intrusion events. Therefore, Gimenez Forcada (2010) suggested that the HFE-D diagram is more informative for this purpose. This diagram is well explained in Amiri et al. (2016).

2. Groundwater Quality Index for Saltwater Intrusion (GQIswi)

This method accounts for hydrochemical processes associated with saltwater intrusion and is explained using graphical methods like the Piper diagram and Chaddah or Hydrochemical facies evolution diagram. As these graphical methods are not georeferenced for use by policymakers, the approach of GQIswi is used to simplify multiple non-linear processes involving several water quality pollutants into an indicator that can be quantified and spatially referenced into a single map, (Tomaszkiewicz et al., 2014). Singhal and Gupta, (2010); El-Fadel et al., (2013) and Amiri et al., (2015) all successfully applied this method in their studies. GQIswi is numerically derived as shown in equations below;

GQI*cation* = $[(1 - \%(Na + K) \times 50]$ if %Ca < 50% or

$[(1 - \%(Mg) \times 50]$ if %Ca ≥50% ----------eq (1)

GQI*anion* == $[(1 + \%(CO3 + HCO3) \times 25]$ if %Cl < 50% or

$[(\%(SO_4^{2+}) \times 50]$ if %Cl ≥ 50%----------eq (2)

$GQI_{EC} = \left[\frac{20{,}000 - EC_{loc}}{20{,}000 - 200}\right]$ if 200 ≤ EC_{loc} ≤ 20,000 or 0 if EC_{loc} ≥ 20,000 ---------eq (3)

$GQI_{SWI} = \frac{GQI_{cation} + GQI_{anion} + GQI_{EC}}{2}$ ---------- eq (4)

3. Seawater Mixing Index (SMI)

The "Saltwater Mixing Index" (SMI) proposed by Park and Aral, (2008) is based on the work of Aniekan Edet, (2016) and used to estimate the relative degree of saltwater/brackish water mixing with freshwater. SMI value can be computed as follows:

$SMI = a \times \frac{CNa}{TNa} + b \times \frac{CMg}{TMg} + C \times \frac{CCl}{TCl} + d\frac{CSO4}{TSO4}$ ---------- eq (5)

where letters a, b, c and d represent the relative degree concentration proportion of ions such as Na, Mg, Cl, and SO_4 in seawater respectively where (a = 0.31, b = 0.04, c = 0.57, d = 0.08); **C** is the measured concentration (in mg/l) of the ions in groundwater. The letter **T** represents the regional threshold values estimated from the interpretation of the probability curves as presented in Edet, (2016). From the regional results in this study, the computed threshold values for Na, Mg, Cl, and SO_4 were 107, 18.4, 218 and 37.9 mg/l, respectively. SMI for each sample is computed using the

calculated threshold values. The water is said to be affected by seawater mixing where the SMI is greater than 1 (Edet, 2016).

5.2.3.4.2 Data processing and statistical analysis

Geochemist Workbench student edition 12.0 and GW-Chart by the USGS were used to plot data and determination of water type from the hydrochemical results. Descriptive statistics and Pearson's correlation coefficient between the physicochemical parameters were carried out using SPSS and Microsoft Origin Pro. The correlation coefficient (r-value) ranges between -1 to +1 provide an insight into the relationship between the pairs of the physicochemical parameters. Pearson's correlation coefficient value lies between +1 to −1, and the degree of correlation is said to be a perfect correlation if the correlation coefficient value is near +1. For values ranging between +0.75 and +1, is considered a high degree of correlation, similarly a moderate degree of correlation for values between +0.25 and +0.75 and a low degree of correlation for values between 0 and +0.25, and vice vasa for the negative correlation values (Kumar et al., 2011). A correlation matrix was carried out on the data set from the two seasons separately.

5.2.3.4.3 GIS approach

Results of the calculated numerical indices and water types were plotted on the map of the study area using ArcGIS version 10.60 after converting the imported CSV files to shapefiles and then plotted on a study area map extracted from a global administrative boundary map downloaded from the DIVA-GIS website. The maps present the georeferenced spatial distribution of the electrical conductivities, water type and groundwater quality index for saltwater intrusion GQIswi.

5.2.4 Results and discussions

5.2.4.1 Groundwater chemical analysis

The physical and chemical characteristics of groundwater samples from the shallow boreholes and hand-dug wells during wet (June to July 2017) and dry (February to March 2018) seasons within Eastern Dahomey Basin (EDB) coastal aquifer in Nigeria are presented in Table 5,2 and Figure 5.3. Total dissolved solids (TDS) varies from below detection (BD) in rainwater to 8,500 of the seawater from the Gulf of Guinea coast with an average of 201.8 mg/l in the wet season. In the dry season samples, TDS ranges from 2.3 to 9300 mg/l with an average of 233 mg/l. The increase in TDS during the dry season samples could be attributed to the effect of evaporation which encourages increase in mineral concentrations in groundwater compared to the dilution process driven by precipitation in the wet season. Similarly, electrical conductivity (EC) (see Table 5.2) of the groundwater is higher in the dry season compared to the wet season. Major ions in groundwater, such as Cl^-, Na^+, SO_4^{2+} and Mg^{2+}, are used as an indication of saltwater intrusion into freshwater aquifer and are presented in Table 5.2. The concentration of Cl^- ranges from 0.1 to 18,970 mg/l with an average value of 218 mg/l in wet season samples while those from the dry season range from 0.9 mg/l to 19,230 mg/l with an average value of 32 mg/l. Chloride concentration shows a slight increase in concentration during the dry season. The concentration of Na^+ for wet and dry seasons ranges from 0.1 to 8,857 mg/l and 0.6 to 9,420 mg/l with an average of 107 and 104 mg/l respectively. The correlation coefficient between chloride and sodium (Table 5.3 and 5.4) in the wet season ($r = 0.01$) compared to dry season ($r = 0.98$) indicate the diverse source of chloride, which could be attributed to anthropogenic contribution possibly effluent from sewage or

leachates (Longe and Balogun, 2010; Ayolabi et al., 2013; Lapworth *et al.*, 2017). We cannot discount the impact of precipitation and evaporation, which causes mineral precipitation from the seawater and halite which characterised the dry season; however, the concentrations of sodium and chloride are far below equilibrium halite saturation.

SO_4^{2-} concentration ranges from 0.1 to 2,211 mg/l with an average of 245 mg/l in the wet season and 0.3 to 576 mg/l and the average concentration of 17.6 mg/l in groundwater samples collected during the dry season. Mg^{2+} concentration ranges from 0.04 to 1,377 mg/l with an average value of 18.4 mg/l in the wet season and 0.1 to 1416 mg/l with an average concentration of 18.6 mg/l in the dry season. High correlation of SO_4^{2+} with Cl^- (r = 1.0) and conversely low correlation (r = 0.05) with Na and the relatively high correlation between Cl^- and NO_3^- (r = 0.60) further affirm the anthropogenic influence (see Table 5.3 and 5.4). Most of the increases observed in Cl^-, Na^+, Mg^{2+} and SO_4^{2-} occurred in locations within the proximity of the sea. Cl^- also shows higher correlation with all the major ions except NO_3^- in water samples from dry season. This could be attributed to the effect of salinisation resulted from saltwater intrusion and evaporation / dissolution with dominant Na-Cl and Ca-Cl water type (see Table 5.5 and 5.6).

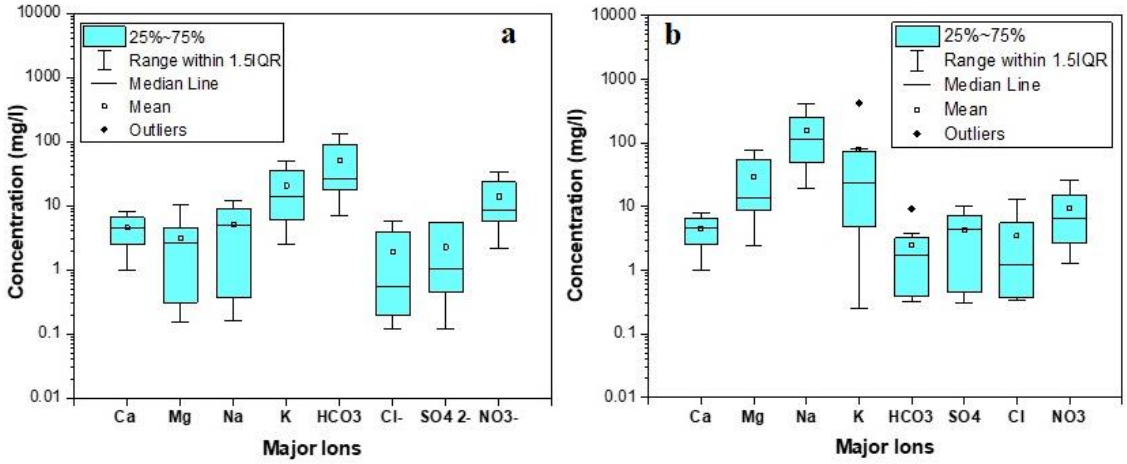

Figure 5.3 Box plot for the major ions (a) wet season (b) dry season

Table 5.2 Statistical summary of the physicochemical properties of the groundwater samples for both seasons

	Wet Season N=97				Dry Season N=133			
Parameter	Min	Max	Aver	Stdev	Min	Max	Aver	Stdev
EC (µScm)	0	12000	295.4	1219	5.5	10009	385	1138
TDS	0	8500	201.8	864	2.3	6750	233	671
Ca (mg/l)	0.3	374	16.5	41.2	0.24	428	21	53.9
Mg (mg/l)	0.04	1377	18.4	140	0.14	1417	18.6	127
Na (mg/l)	0.1	8857	106.8	903	0.6	9420	104	829
K (mg/l)	0.1	447.1	10.5	46.2	0.1	488	9.1	42.9
HCO3 (mg/l)	1.04	563.6	59.7	93.6	0	8390	138	765
Cl (mg/l)	0.1	18970.2	218.1	1934	1.0	1289	32	116
SO4 (mg/l)	0.1	2211.	37.9	245	0.3	576	17.6	56.3
NO3 (mg/l)	0.02	259	31.8	54	0.3	312	30.5	54.6
F (mg/l)	0	1.10	0.1	0.15	0.01	1.5	0.1	0.2
Br (mg/l)	0	54.7	1.0	6.3	0.01	22	0.3	1.9

Table 5.3 Pearson correlation for the physicochemical parameters for wet season samples

Param	EC	TDS	Ca	Mg	Na	K	HCO3	Cl-	SO4	NO3-	F	Br
EC	1											
TDS	1.00	1.00										
Ca^{2+}	**0.94**	**0.94**	1.00									
Mg^{2+}	**0.99**	**0.99**	**0.91**	1.00								
Na^{+}	**0.99**	**0.99**	**0.90**	1.00	1.00							
K^{+}	**0.98**	**0.98**	**0.93**	**0.98**	**0.98**	1.00						
HCO_3^{-}	0.15	0.14	0.46	0.09	0.05	0.14	1.00					
Cl-	0.06	0.05	0.14	0.00	0.01	0.12	0.26	1.00				
SO_4^{2-}	0.10	0.10	0.18	0.04	0.05	0.16	0.28	1.00	1.00			
NO_3^{-}	0.32	0.32	0.33	0.26	0.27	0.38	0.19	**0.60**	0.48	1.00		
F^{-}	0.05	0.04	0.22	0.01	-0.02	0.08	**0.63**	**0.50**	**0.50**	0.16	1.00	
Br^{-}	**0.52**	**0.51**	**0.55**	0.47	0.48	**0.57**	0.25	**0.88**	**0.90**	0.29	0.43	1

2-Tailed Test of Significance

Table 5.4 Pearson correlation for the physicochemical parameters for dry season samples

Para	EC	TDS	Ca	Mg	Na	K	HCO_3	Cl	SO_4	NO_3	F	Br
EC	1											
TDS	1.00	1.00										
Ca^{2+}	**0.90**	**0.90**	1.00									
Mg^{2+}	**0.97**	**0.97**	**0.82**	1.00								
Na^{+}	**0.99**	**0.99**	**0.76**	**0.99**	1.00							
K^{+}	0.44	0.44	**0.72**	**0.96**	**0.98**	1.00						
HCO_3^{-}	**0.86**	**0.87**	**0.85**	**0.99**	**0.98**	**0.94**	1.00					
Cl^{-}	**0.95**	**0.95**	**0.65**	**0.88**	**0.98**	0.45	0.33	1.00				
SO_4^{2-}	0.43	0.43	**0.75**	**0.60**	0.28	0.31	**0.85**	0.30	1.00			
NO_3^{-}	0.27	0.28	0.27	0.12	0.27	**0.63**	0.20	0.25	0.16	1.00		
F^{-}	0.30	0.30	0.42	0.37	0.23	0.13	0.49	0.18	0.25	0.15	1.00	
Br^{-}	**0.88**	**0.88**	**0.50**	**0.84**	**0.94**	0.30	0.19	**0.96**	0.16	0.05	0.13	1.00

2-Tailed Test of Significance

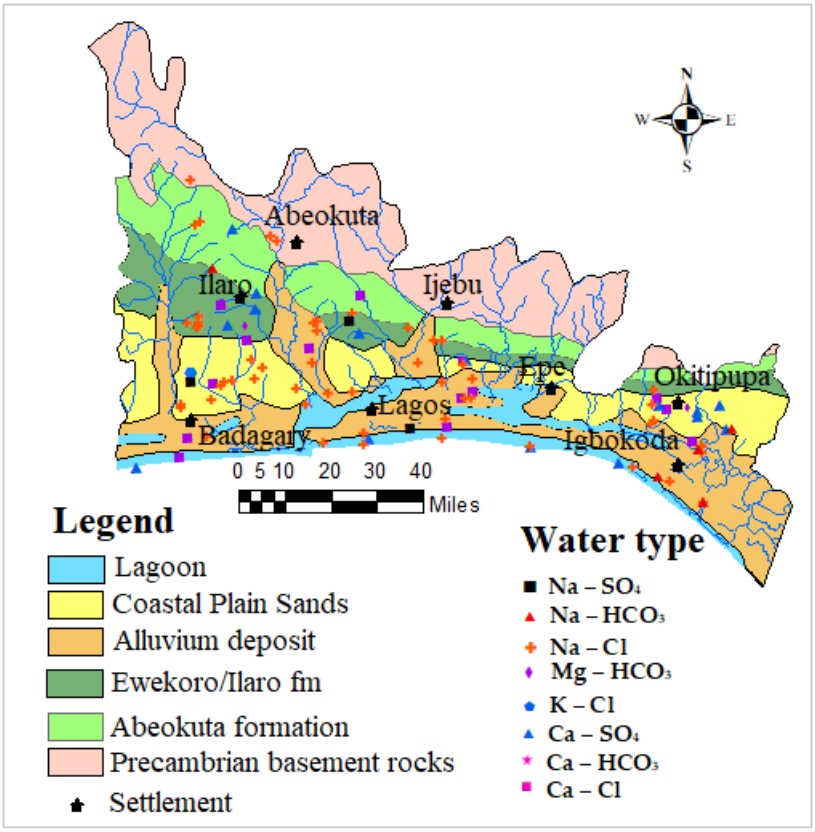

Figure 5.4 Distribution of groundwater types for the water samples during the wet season

Table 5.5 Groundwater type with water their respective sample locations for wet season

Water Type	Sample	% Sample	Sample Location
Na-Cl	56	58.3	L02, L04, L05, L07, L08, L09, L12, L13, L14, L15, L16, L22, L23, L24, L25, L26, L28, L29, L32, L33, L36, L38, L39, L41, L42, L43, L45, L46, L47, L48, L49, L49, L50, L52, L53, L55, L56, L57, L58, L60, L62, L63, L65, L67, L69, L71, L72, L74, L76, L77, L80, L81, L82, L85, L87, L88 and L89
Na-SO4	3	3.1	L31, L51 and L68
Na-HCO_3	5	7.3	L10, L75, L78, L79 and L96
Ca-HCO_3	15	15.6	L03, L06, L17, L18, L19, L35, L54, L66, L70, L73, L84, L92, L93, L94 and L95
Ca-Cl	14	14.6	L01, L11, L21, L27, L34, L37, L40, L44, L59, L61, L64, L83, L86 and L90
K-Cl	1	1	L30
Mg-HCO_3	2	2.1	L20 and L91

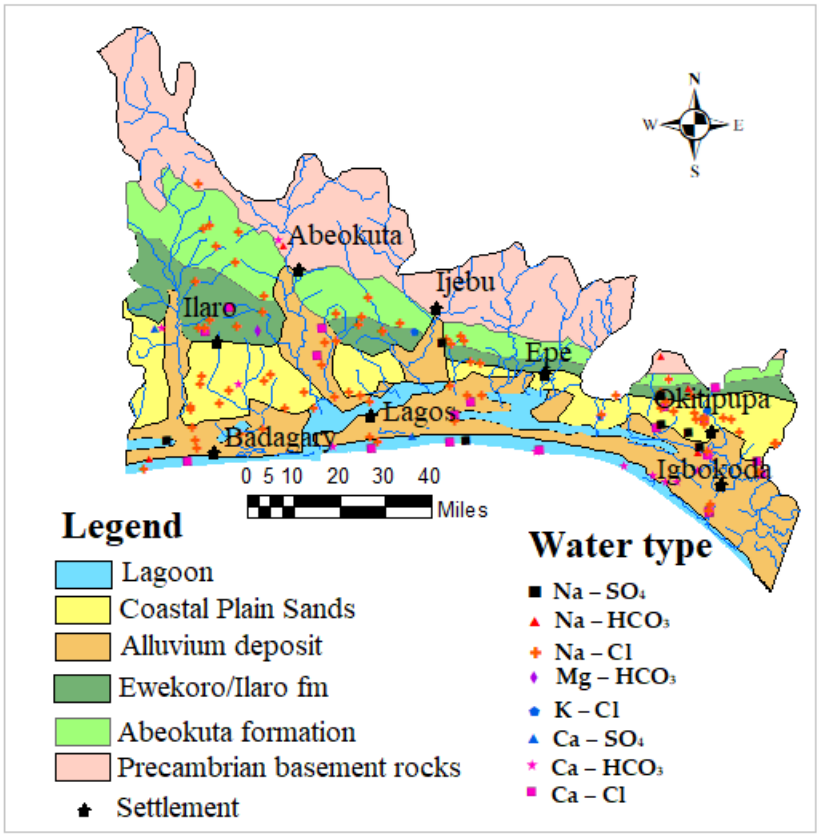

Figure 5.5 Distribution of groundwater types in the dry season

Table 5.6 Groundwater type with water their respective sample locations for dry season

Water Type	Sample	% Sample	Sample Location
Na-Cl	81	60.9	L01, L04, L05, L06, L07, L08, L09, L11, L14, L15, L17, L18, L19, L22, L23, L25, L26, L27, L28, L29, L30, L31, L32, L33, L34, L38, L39, L40, L41, L42, L43, L44, L45, L46, L47, L48, L49, L51, L53, L54, L55, L56, L57, L58, L59, L60, L61, L63, L64, L65, L67, L68, L69, L70, L72, L73, L74, L76, L82, L83, L94, L96, L99, L101, L104, L105, L107, L110, L112, L114, L115, L117, L118, L120, L121, L125, L127, L129, L130, L131 and L132
Na-SO_4	7	5.3	L36, L62, L79, L100, L119, L124 and L128
Na-HCO_3	6	4.5	L02, L35, L111, L116, L126 and L134
Ca-HCO_3	12	9	L03, L13, L24, L78, L85, L86, L87, L88, L89, L90, L95 and L98
Ca-Cl	21	15.8	L10, L102, L106, L108, L109, L122, L123, L133, L16, L37, L50, L52, L71, L75, L77, L80, L84, L91, L92, L93 and L97
Ca-SO_4	3	2.3	L12, L81 and 113
K-Cl	2	1.5	L66 and L103
Mg-HCO_3	1	0.8	L20

5.2.4.2 Groundwater characterisation using HEF diagram

The Hydrochemical Facies Evolution Diagram (HFE-D) developed by Giménez-Forcada et al. (2010) was employed in this study. The method has been used by several authors namely Wu *et al.*, (2010); Li *et al.*, (2015); Amiri *et al.*, (2016); Han et al., (2016) and Shi *et al.*, (2018) and provides a simple way to identify the state of the coastal aquifer with respect to intrusion/freshening phases. The processes are identified by the distribution of anions and cations percentages in the square diagram (Figure 5.6). In the HFE-Diagram, four main facies are recognised which include Na–Cl, sea/saltwater, Ca–HCO3, natural freshwater, Ca–Cl, salinised water with reverse cation exchange, and Na–HCO3, salinised water with direct cation exchange (Figure 5.6). The facies explained two, almost simultaneous, processes which occur during the intrusion stage of saltwater into freshwater.

The facies types located above and to the left of the conservative mixing line are representative of the freshening phase whereas facies types situated below and to the right of the line characterise the sea/saltwater intrusion phase. Facies types located in the centre of HFE-diagram can be considered as a mixing phase for both fresh and saltwater representing the transformation phase for either freshening or intrusion phases. In the intrusion and freshening fields, different sub-steps can be identified, following the salinity evolution through the Cl^- percentage. The freshening sub-steps include f-1, f-2, f- 3, f-4, and FW (representative of freshwater composition). In this diagram, the intrusion sub-steps related to the sea/saltwater intrusion phase are represented as i-1, i-2, i-3, i-4, and SW (representative sea/saltwater composition).

During the recharge of the aquifer, the groundwater is said to be in the freshening phase with f4 with dominant Ca-HCO_3 in the inland towards the northern

parts of the basin bounded by the Precambrian rock which is unconformably overlain by the oldest Abeokuta formation groundwater aquifer. This facies is gradually transforming to mixed Ca+Na-HCO_3 rock. This begins from an initial state because the aquifer contains kaolinite which releases more Na^+ ions into the groundwater to form a mixed water of facies f-3 (MixNa-MixHCO_3, Ca- MixHCO_3 and Mix). As the water continues to flow within the basin, the groundwater gradually transforms to f-2 (MixNa-MixCl) probably due to the influence of sea spraying and possible effluents from the industries as the industrial activities increase towards the same trend as groundwater flow down south. Finally, the f-1 facies represents water type which has experienced influence of saltwater intrusion and is mostly close to the coastline (see Figure 5.4, 5.5). Na-Cl water type dominates the coastal plain sands and alluvium deposits aquifer and some locations along river channels and lagoon, especially in the rainy season. A summary of water types is shown in Table 5.4 and 5.5 while figure 5.4 and 5.5 show their spatial distribution across EDB for both wet and dry season, respectively. Finally, the intrusion process (salinisation) of the aquifer is reduced as the freshening increases northward towards the inland of the basin.

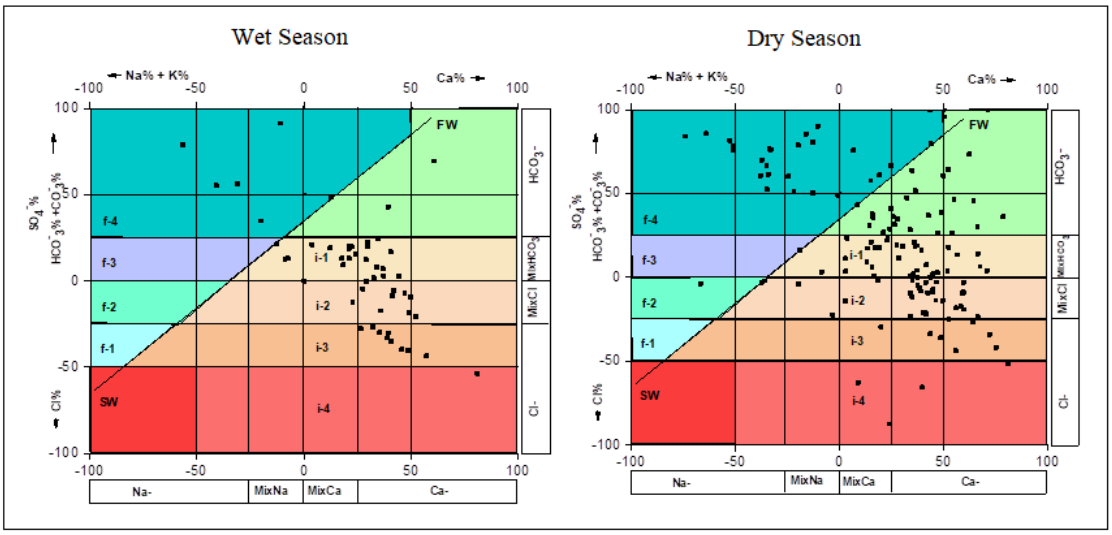

Figure 5.6 Hydrochemical plots for major ions in analysed groundwater samples from Eastern Dahomey Basin aquifers. (A)HEF diagram which indicates mixing of saline water in a few locations within the coastal plain sand aquifers.

5.2.4.3 Ionic ratio

Ionic ratios have been used to evaluate seawater intrusion in coastal areas at different locations around the world (Custodio and Alcala 2008; Khaska et al., 2012; Li et al., 2015; Katz et al., 2010; Aniekan Edet 2016). The ionic ratio of water samples for both wet and dry season in the basin are presented in Table 5.7. Tables 5.8 and 5.9 contain the correlation between EC, saltwater mixing index (SMI) and these ratios. These ratios are considered to be a good indicator of seawater intrusion. They include Na^+/Ca^{2+}, Ca^{2+}/Cl-, Na^+/Ca^{2+}, Cl^-/HCO_3^-, Mg^{2+}/Cl^-, Ca^{2+}/SO_4^{2-}, SO_4^{2-}/Cl^- and Cl^-/Br^-. The ratio Mg^{2+}/Cl^- shows moderate positive correlation (r = 0.946) with Na^+/Cl^- in the wet season and (r = 0.919) in the dry season. This correlation indicates seawater mixed in groundwater for both seasons. The Cl^-/Br^- in groundwater ranges from 4.46 to 346 (wet) and 6.45 to 460 (dry) with an average of 170 and 49 respectively. There is a weak correlation between EC and Cl^-/Br^- (Tables 5.8 and 5.9) with (r = 0.192 and 0.297) for the wet and dry seasons respectively. Higher correlation values between EC

and Cl^-/Br^- in water samples during the dry season indicates more influence of seawater in the dry as compared to the wet season. This is confirmed by EC and SMI correlation which is 0.516 in the wet season and 0.931 in the dry season. This process suggests chloride in the groundwater in the wet season is more from non-seawater sources (e.g. effluent), while the groundwater in the dry season has more influence of seawater. The ratios of Na^+/Cl^- showed significant correlation with EC (r = 0.73) (see Tables 5.8 and 5.9) in the wet season and very weak (r = 0.070) in the dry season which also confirmed the earlier statement.

Table 5.7 Statistical summary of TDS, SMI and some selected Ionic ratio.

	Wet Season N = 96				Dry Season N = 133			
Ionic Ratio	Min	Max	Aver	Stdev	Min	Max	Aver	Stdev
HCO_3/Cl	0.01	39.09	4.23	6.63	0.063	77.58	6.78	16.03
Na/Cl	0.01	67.83	1.55	6.88	0.02	53.13	3.76	10.91
Na/Ca	0.09	23.68	2.27	3.01	0.574	7.22	2.71	1.51
Ca/Cl	0.00	11.43	1.04	1.73	0.01	14.81	1.41	3.13
K/Cl	0.00	3.42	0.32	0.49	0.006	19.18	1.50	3.98
Cl/HCO_3	0.03	67.42	1.25	6.84	0.013	15.96	1.36	3.25
Mg/Cl	0.00	10.55	0.34	1.13	0.006	6.48	0.50	1.33
Ca/SO_4	0	0	0	0	0.035	33.41	4.64	8.73
SO4/Cl	0.00	5.88	0.53	0.87	0.041	3.171	0.598	0.83
Cl/Br	4.46	346.96	170.96	53.08	6.449	460.3	49.18	100.28
SMI	0.00	54.68	0.99	6.29	0.009	0.31	0.056	0.08

Table 5.8 Correlations between the ionic ratios for wet season water sample

Ionic ratio	EC	Ca/Cl	Na/Cl	Na/Ca	Cl/HCO_3	Mg/Cl	Ca/SO_4	SO_4/Cl	Cl/Br	SMI
EC	1.000									
Ca/Cl	0.123	1.000								
Na/Cl	**0.985**	0.148	1.000							
Na/Ca	**0.707**	-0.157	**0.735**	1.000						
Cl/HCO_3	0.042	-0.092	-0.033	0.008	1.000					
Mg/Cl	**0.934**	0.299	**0.946**	**0.632**	-0.046	1.000				
Ca/SO_4	-0.018	-0.016	-0.029	-0.008	-0.033	-0.021	1.000			
SO4/Cl	0.043	0.303	0.074	-0.027	-0.083	0.091	-0.208	1.000		
Cl/Br	0.192	-0.017	0.128	0.013	-0.004	0.099	0.282	-0.038	1.000	
SMI	**0.516**	-0.004	0.450	0.333	0.875	0.414	-0.048	-0.038	0.077	1.000

2-Tailed Test of Significance

Table 5.9 Correlations between the ionic ratios for dry season water sample

Ionic ratio	EC	Ca/Cl	Na/Cl	Na/Ca	Cl/HCO_3	Mg/Cl	Ca/SO_4	SO_4/Cl	Cl/Br	SMI
EC	1.000									
Ca/Cl	**0.097**	1.000								
Na/Cl	0.070	**0.755**	1.000							
Na/Ca	-0.007	-0.269	0.063	1.000						
Cl/HCO_3	0.042	-0.165	-0.082	0.048	1.000					
Mg/Cl	0.127	**0.824**	**0.919**	-0.068	-0.123	1.000				
Ca/SO_4	0.006	0.382	0.378	-0.082	-0.118	0.452	1.000			
SO4/Cl	0.078	0.179	0.009	-0.122	-0.085	0.046	-0.256	1.000		
Cl/Br	0.297	-0.061	-0.101	-0.228	0.232	-0.079	0.049	0.019	1.000	
SMI	**0.931**	0.061	-0.007	**0.504**	-0.017	0.113	-0.014	0.139	0.381	1.000

2-Tailed Test of Significance

5.2.4.3.1 Revelle Coefficient, $[Cl/(CO_3+HCO_3)]$ Ratio

The Revelle Coefficient **(**$Cl/(CO_3+HCO_3)$) ratio has been used as a criterion to evaluate the saltwater intrusion in previous groundwater studies (Abdalla, 2016; Edet, 2016; Kumar et al., 2010). Chloride is one of the dominant ions in seawater and mostly occurs in small amounts in groundwater. HCO_3 is usually the most abundant negative ion in groundwater while it occurs in low concentration in seawater. The ration of these anions is used as a measure of the degree of contamination of freshwater by saltwater.

The classification is shown in Table 5.10. In this study, 55.2 and 45.9 % of the sampled groundwater fell into the category of good quality water with respect to Cl/HCO3 ratio for wet and dry seasons respectively, while 39.6 and 42.9% of the samples showed slight seawater influence for the respective season. Seawater influence was observed on 2.25 % of the samples from the dry season and 0% from the wet season. The highest seawater impact is observed in water samples from wells located around Okun-Ajjah, Ode-Mahin and Gbetomey. These are less than 500m from the coastline except Ode-Mahin which is within 100m from the sea lagoon. Only one sample collected showed extreme influence expected from seawater.

Table 5.10 Groundwater Quality Classification based on Cl/HCO3 ratio

		Wet Season		Dry Season	
Classification	Cl/HCO_3	Samples	% Sample	Sample	%Sample
Good Quality	< 0.5	53	55.21	61	45.9
Slightly Contaminated	0.5 - 1.3	36	39.58	57	42.9
Moderately Contaminated	1.3 -2.8	6	6.25	12	9.02
Highly Contaminated	2.8 - 6.6	0	0	3	2.25
Extremely Contaminated	> 6.6	1	1.04	0	0

This result further confirms the applicability of this method in the evaluation of groundwater quality with regard to saltwater intrusion (Narany et al., 2014). Comparing the results of the wet season with the dry season, there is a slightly higher intrusion in the dry season which could be attributed to over-abstraction of groundwater when common rain harvesting stopped while dilution could be responsible for low salinity in the wet season (Table 5.10).

Chloride concentration was classified into fresh, fresh-brackish, brackish, brackish-salt, salt and hyperhaline as shown in Table 5.11. The results revealed 97.92 % and 95.5% water fall within the freshwater class for wet and dry seasons respectively. This method only shows the slight effect of seasonal variation on

saltwater intrusion with 1.0 % and 0.7 % which represent the only sample collected from the sea as the saltwater among the samples while 2.3% of the dry season groundwater samples indicate brackish-salt water compared to 0 % of the wet season.

Table 5.11 Classification of water, based on Chloride Content

		Wet Season		Dry Season	
Water Class	Chloride (mg/l)	No. of sample	%Sample	No. of sample	%Sample
Fresh	≤ 150	94	97.9	128	95.5
Fresh-brackish	150 - 300	1	1.1	2	1.5
Brackish	300 - 1000	0	0	0	0
Brackish-Salt	1000 – 10,000	0	0	3	2.3
Salt	10,000 – 20,000	1	1.1	1	0.7
Hyperhaline	> 20,000	0	0	0	0

5.2.4.4 Assessment of intrusion using saltwater mixing index (SMI)

The seawater mixing index (SMI) which was proposed by Par et al. (2005) was also employed in this study to further assess the groundwater of the Eastern Dahomey Basin with respect to seawater pollution. The results of this method are presented in Table 5.12. The results show that 96.9 and 93.2 per cent of the groundwater samples from both wet and dry seasons fall within a freshwater category with SMI values below 1.0, while 1.1 and 2.3 % of respective wet and dry season samples areslightly polluted based on SMI with values falling between 1.0 - 2.0. 2.08 and 3.0% of wet and dry season water samples revealed SMI values between 10.0 – 150.0, which indicate dangerously polluted groundwater with saltwater intrusion. This represents the groundwater from Gbetomey in Badagary, Ogombo, Okun-Ajjah and Ode-Mahin in the wet and dry season. Hydrochemical results around Isheri and Adesanya areas near Lekki also shows that during the dry season, the samples have high SMI values. This is further supported by the moderate to high correlation between SMI, EC and

Cl/HCO_3 of 0.51 and 0.88 (Table 5.8) during the wet season, while SMI, EC and Na/Cl revealed a correlation of 0.93 and 0.50. However, a low correlation value of -0.02 was obtained between SMI and Cl/HCO_3 during the dry season (Table 5.9). The variation in correlations could be attributed to effect of sea spraying resulting from NaCl dissolution in precipitation during the wet season and evapoconcentration /mineral dissolution which could lead to a higher concentration of NaCl in the coastal groundwater systems during the dry season (Vengosh and Rosenthal, 1994; Abimbola, et al., 1999; Edet, 2019). Common practice of municipal, agricultural and industrial waste being discharged into drainages and river channels which interact directly with groundwater of the shallow unconfined aquifer understudy (Lapworth et al., 2017c; Ofomola, 2015; Ojolowo and Wahab, 2017; Palamuleni, 2002). This situation is aggravated by the coastal plains sands and alluvium deposit that characterised by relatively higher hydraulic connection between the groundwater and contaminated surface water from drainages, rivers and lagoons of the shallow unconfined aquifers in this area (Longe et al., 1987; Longe and Balogun, 2010; Morsy et al., 2018).

Table 5.12 Classification of Seawater Mixing Index (SMI)

		Wet Season		Dry Season	
SMI Range	Classification	Sample	%Sample	Sample	%Sample
< 1	Freshwater	93	96.9	124	93.2
1.0 – 2.0	Slightly polluted	1	1.04	3	2.3
2.0 – 6.0	Moderately polluted	0	0	1	0.75
6.0 – 10.0	Seriously polluted	0	0	1	0.75
10.0 – 150.0	Dangerously polluted	2	2.08	4	3.01
>150	Seawater	0	0	0	0

Higher Cl correlation with EC, TDS and some major ions such as Na^+, SO_4^{2-} and Mg^{2+} in groundwater are among the important diagnosis of saltwater intrusion

(Eissa et al., 2018; Salman et al., 2019). This suggest that the chloride found in groundwater samples during the wet season is influenced by both anthropogenic and geogenic source resulting from the weak correlation between EC, TDS and Na^{+}, Ca^{2+}, Mg^{2+}, SO_4^{2-} with Cl^{-} (Table 5.3).

Furthermore, Cl^{-} also shows strong correlation with these parameters during the dry season which revealed geogenic source of saltwater intrusion with mineral dissolution of possible gypsum and other evaporite minerals (Guendouz et al., 2003; Laluraj et al., 2005; Paris et al., 2010) and assisted by higher evaporation and abstraction rate of groundwater compared to wet season.

5.2.4.5 Groundwater quality index in relation to saltwater intrusion

The aquifer monitoring and vulnerability maps for saltwater intrusion were prepared based on calculations of GQI_{SWI} and HFE diagrams for both wet and dry seasons. Based on GQI_{SWI} method, the spatial distribution maps (Figure 5.7) revealed that the study area is dominated by freshwater in both wet (mean GQI_{SWI} = 21.0) and dry seasons (mean GQI_{SWI} = 70.4). However, some fingerprint of saltwater intrusion was identified in both seasons in locations along the coastline due to their proximity to the Gulf of Guinea. Saline water was identified in some locations far inland into the basin especially along the rivers during the wet season. Low correlation of Na and Cl (r = 0.01) in wet season and a conversely high value (r = 0.98) implies a different origin of Cl in groundwater. Higher correlation of Cl with NO3 (r = 0.60) in the wet season suggests anthropogenic influence which could be attributed to high recharge and soil saturation rate, while a relatively low correlation value (r = 0.25) between Cl and NO_3 suggests geogenic sources of seawater intrusion and evapoconcentration in the dry season. A few boreholes within 500m of the coastline located at the south-

central to the southwestern part within the coastal plain sand and alluvium deposit show relatively higher salinity. This higher salinity is suspected to be an indication of a saltwater intrusion. Processes such as over-abstraction of water from the shallow aquifer, flooding triggered by sea-level rise due to climate change and effluence from domestic and municipal waste might contribute to future increases in the salinity of groundwater within this basin (Aladejana et al., 2020). Total evaporation with precipitation of halite minerals along the riverbed has been reported in a few areas (Ayolabi et al., 2013; Odukoya et al., 2013). It is important to note that halite is not considered a major source of salinity as freshwater predominates the areas along the coastline, where most of the shallow wells tap the unconfined aquifer that is directly recharged by the precipitation. The GQIswi show mixed groundwater types as predominant groundwater across the Eastern Dahomey Basin. This predomination of mixed groundwater type based on GQIswi is also supported by the hydrochemical facies evolution diagram (HFE-D) earlier presented in Figure 5.6. The mixing characteristics observed across this Basin could be attributed to the nature (geology) of the basin through rock-water interaction and also to topography (gravity) driven flow generally in a north-south direction (Figure 5.7).

Table 5.13 Summary of Indices evaluated for Wet and Dry season

	Wet Season N = 96				Dry Season N = 133			
Index	Min	Max	Aver	Stdev	Min	Max	Aver	Stdev
GQIpiper(mix)	11.84	90.84	45.88	16.87	17.12	90.3	45.55	15.49
GQIpiper(dom)	22.12	84.29	45.36	6.4	18.91	87.58	51.43	12.24
Fsea(%)	-0.11	99.01	1.04	10.21	-0.11	6.7	0.05	0.65
GQIfsea	-4.34	111.19	-3.85	1020.96	-1.94	111.26	95.32	64.96
GQIswi	-9.67	99.68	21.02	511.89	-10	99.27	70.43	34.46

Table 5.14 Results of GQIswi calculated for water samples in wet and dry seasons

Water type	Typical GQIswi		Wet Season		Dry Season	
	Min	Max	Samples	% Sample	Samples	%Sample
Freshwater	75	100	30	32	58	43.6
Mixed GW	50	75	64	68.75	67	50.4
Saline GW	10	50	1	1.04	6	4.5
Saltwater	0	10	1	1.04	2	1.5

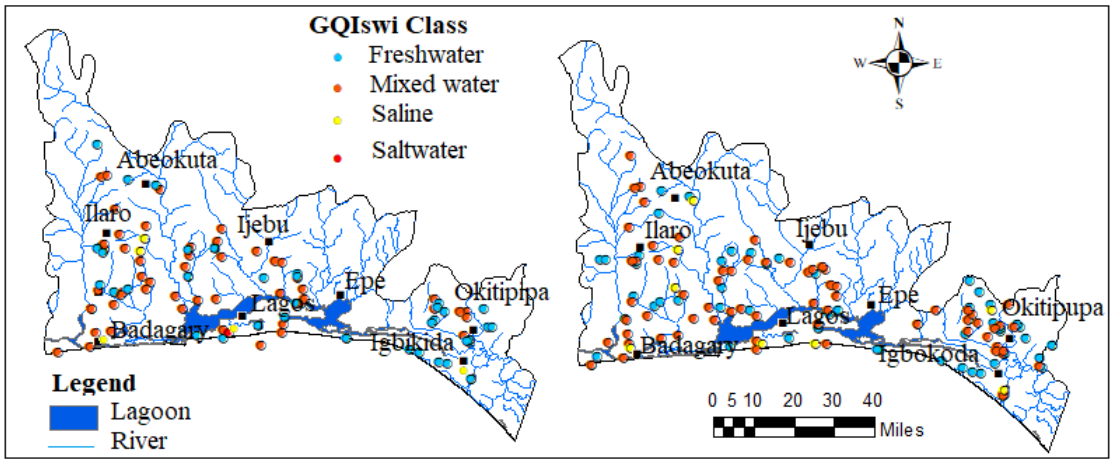

Figure 5.7 Spatial variation of the seawater intrusion for groundwater quality index (GQIswi) of the Eastern Dahomey Basin (EDB).

5.2.5 Conclusion

In this study, saltwater intrusion into the freshwater aquifer of the Eastern Dahomey Basin, Southwestern Nigeria, was monitored using a seasonal hydrochemical quality index and ionic ratios such as HFE-D, SMI and GQIswi and Ionic ratio such as Cl/Br, Cl/HCO_3 that are used to evaluate seawater intrusion. Pearson correlation analysis physicochemical parameters, especially Na^+, Ca^{2+}, Mg^{2+}, Cl^-, HCO_3^- and SO_4^{2-} and EC values revealed the influence of seawater intrusion in some of the water samples from wells that are relatively deeper within the proximity

of the coastline of Seme, Lekki, Eleko, Okun-Ajjah, Ode-Mahin and Igbokoda. It further revealed the anthropogenic influence of industrial and municipal effluent especially in samples from wells within the alluvium deposit which are generally closer to the river channels flood plain. Results of HFE-D, Ionic ratios, SMI and GQIswi revealed that mixed groundwater of Na+Ca-HCO_3 and Na-Cl dominate the area due to gravity-driven flow.

Spatial distribution of groundwater revealed freshening, which increases inland from the coastline towards the northern part of the basin. Results of the groundwater quality index confirmed this and identified few locations of saline water around Lekki, Okun-Ajjah and the Ode-Mahin in both wet and dry seasons. Most sampled boreholes show freshwater during the wet season above the units characterised by saltwater intrusion. The present study provides important information to support planners and policy-makers to develop sustainable water resources management plans for the region to prevent deterioration of the freshwater resources of coastal groundwater in the Eastern Dahomey Basin.

5.2.6 Acknowledgements

The author is grateful to the Petroleum Technology and Development Fund (PTDF) under the Overseas PhD scholarship scheme for funding this research and also for the support of the Scottish Government under the Climate Justice Fund Water Futures Programme, awarded to the University of Strathclyde (Prof R.M. Kalin).

5.2.7 References

A. Vengosh, E.R., 1994. Saline groundwater in Israel: its bearing on the water crisis in the country. J. Hydrol. 156, 389–430.

Abdalla, F., 2016. Ionic ratios as tracers to assess seawater intrusion and to identify salinity sources in Jazan coastal aquifer, Saudi Arabia. Arab. J. Geosci. 9, 1–12. https://doi.org/10.1007/s12517-015-2065-3

Abimbola, A. F., Tijani M. N and Nurudeen, A., 1999. Some aspect of groundwater quality assessment of Abeokuta. J. Min. Geol. 32, 23–32.

Adegoke, O.S. and Omatsola, M.E., 1981. Tectonic Evolution and Cretaceous Stratigraphy of the Dahomey Basin. Niger. J. Min. Geol. 18, 130–137.

Adelana, S.M.A., Olasehinde, P.I., Bale, R.B., Vrbka, P., Edet, A.E., Goni, I.B., 1996. An overview of the geology and hydrogeology of Nigeria. Q. J. Eng. Geol. Hydrogeol. 29, S1–S12. https://doi.org/10.1144/GSL.QJEGH.1996.029.S1.01

Aladejana, Jamiu A, Kalin, R.M., Sentenac, P., Hassan, I., 2020. Hydrostratigraphic Characterisation of Shallow Coastal Aquifers of Eastern Dahomey Basin , S / W Nigeria , Using Integrated Hydrogeophysical Approach ; Implication for Saltwater Intrusion. Geoscience 10, 65. https://doi.org/10.3390/geosciences10020065

Aladejana, Jamiu A., Kalin, R.M., Sentenac, P., Hassan, I., 2020. Assessing the Impact of Climate Change on Groundwater Quality of the Shallow Coastal Aquifer of Eastern Dahomey Basin, Southwestern Nigeria. Water 12, 224. https://doi.org/10.3390/w12010224

Amiri, V., Nakhaei, M., Lak, R., Kholghi, M., 2016. Assessment of seasonal groundwater quality and potential saltwater intrusion: a study case in Urmia coastal aquifer (NW Iran) using the groundwater quality index (GQI) and hydrochemical facies evolution diagram (HFE-D). Stoch. Environ. Res. Risk Assess. 30, 1473–1484. https://doi.org/10.1007/s00477-015-1108-3

Ayolabi, E. a, Folorunso, A.F., Odukoya, A.M., Adeniran, A.E., 2013. Mapping saline water intrusion into the coastal aquifer with geophysical and geochemical techniques : the University of Lagos campus case (Nigeria). Springer plus 2, 1–14. https://doi.org/10.1186/2193-1801-2-433

Ayolabi, E.A., Folorunso, A.F., Kayode, O.T., 2013. Integrated Geophysical and Geochemical Methods for Environmental Assessment of Municipal Dumpsite System.

Int. J. Geosci. 4, 850–862. https://doi.org/10.4236/ijg.2013.45079

Charette, M.A., Allen, M.C., 2006. Precision ground water sampling in coastal aquifers using a direct-push, shielded-screen well-point system. Gr. Water Monit. Remediat. 26, 87–93. https://doi.org/10.1111/j.1745-6592.2006.00076.x

Christina, G., Alexandros, G., 2014. Seawater Intrusion and Nitrate Pollution in Coastal Aquifer of Almyros – Nea Anchialos Basin , Central Greece. WSEAS Trans. Environ. Dev. 10, 211–222.

Custodio, E., 2002. Coastal aquifers as important natural hydrogeological structures. Groundw. Hum. Dev. 1905–1918.

Edet, A., 2019. Seasonal and spatio-temporal patterns, evolution and quality of groundwater in Cross River State, Nigeria: implications for groundwater management. Sustain. Water Resour. Manag. 5, 667–687. https://doi.org/10.1007/s40899-018-0236-6

Edet, A., 2016. Hydrogeology and groundwater evaluation of a shallow coastal aquifer, southern Akwa Ibom State (Nigeria). Appl. Water Sci. https://doi.org/10.1007/s13201-016-0432-1

Eissa, M.A., de Dreuzy, J.R., Parker, B., 2018. Integrative management of saltwater intrusion in poorly-constrained semi-arid coastal aquifer at Ras El-Hekma, Northwestern Coast, Egypt. Groundw. Sustain. Dev. 6, 57–70. https://doi.org/10.1016/j.gsd.2017.10.002

Giménez-Forcada, E., Bencini, A., Pranzini, G., 2010. Hydrogeochemical considerations about the origin of groundwater salinization in some coastal plains of Elba Island (Tuscany, Italy). Environ. Geochem. Health 32, 243–257. https://doi.org/10.1007/s10653-009-9281-2

Guendouz, A., Moulla, A.S., Edmunds, W.M., Zouari, K., Shand, P., Mamou, A., 2003. Hydrogeochemical and isotopic evolution of water in the Complexe Terminal aquifer in the Algerian Sahara. Hydrogeol. J. 11, 483–495. https://doi.org/10.1007/s10040-003-0263-7

Han, D., Song, X., Currell, M.J., 2016. Identification of anthropogenic and natural inputs

of sulfate into a karstic coastal groundwater system in northeast China: Evidence from major ions, δ13CDICand δ34SSO4. Hydrol. Earth Syst. Sci. 20, 1983–1999. https://doi.org/10.5194/hess-20-1983-2016

Jones, H. A and Hockey, R.., 1964. The Geology of part of Southwestern Nigeria. GSN Bull. No. 31-10.

K.M. Hiscock, P.F. Dennis, P.R. Saynor, M.O.T., 1996. Hydrochemical and stable isotope evidence for the extent and nature of the effective Chalk aquifer of north Norfolk, UK. J. Hydrol. 180, 79–107. https://doi.org/10.5923/j.geo.20110101.02

Kennedy, G.W., 2012. Development of a Gis-Based Approach for the Assessment of Relative Seawater Intrusion Vulnerability in Nova Scotia , Canada.

Krishnaraj, S., Murugesan, V., K, V., Sabarathinam, C., Paluchamy, A., Ramachandran, M., 2012. Use of Hydrochemistry and Stable Isotopes as Tools for Groundwater Evolution and Contamination Investigations. J. Geo-sciences 1, 16–25. https://doi.org/10.5923/j.geo.20110101.02

Kumar, K.S., Kumar, P.S., BABU, M.J.R., RAO, C.H., 2010. Assessment and Mapping of Ground Water Quality Using Geographical Information Systems. Int. J. Eng. Sci. Technol. 2, 6035–6046.

Kumar, P.J.S., Jegathambal, P., James, E.J., 2011. Multivariate and Geostatistical Analysis of Groundwater Quality in Palar River Basin. Int. J. Geol. 5, 108–119.

Laluraj, C.M., Gopinath, G., Dineshkumar, P.K., 2005. Groundwater chemistry of shallow aquifers in the coastal zones of Cochin, India. Appl. Ecol. Environ. Res. 3, 133–139.

Lapworth, D.J., Nkhuwa, D.C.W., Okotto-Okotto, J., Pedley, S., Stuart, M.E., Tijani, M.N., Wright, J., 2017. Urban groundwater quality in sub-Saharan Africa: current status and implications for water security and public health. Hydrogeol. J. 25, 1093–1116. https://doi.org/10.1007/s10040-016-1516-6

Li, W., Wang, M.-Y., Liu, L.-Y., Yan, Y., 2015. Assessment of Long-Term Evolution of Groundwater Hydrochemical Characteristics Using Multiple Approaches: A Case Study in Cangzhou, Northern China. Water 7, 1109–1128.

https://doi.org/10.3390/w7031109

Longe, E.O., 2011. Groundwater Resources Potential in the Coastal Plain Sands Aquifers , Lagos, Nigeria 3, 1–7.

Longe, E.O., Balogun, M.R., 2010. Groundwater quality assessment near a municipal landfill, Lagos, Nigeria. Res. J. Appl. Sci. Eng. Technol. 2, 39–44.

Longe, E. O., Malomo, S., Olorunniwo, M.A., 1987. Hydrogeology of Lagos metropolis. J. African Earth Sci. 6, 163–174. https://doi.org/10.1016/0899-5362(87)90058-3

Morsy, K.M., Morsy, A.M., Hassan, A.E., 2018. Groundwater sustainability: Opportunity out of threat. Groundw. Sustain. Dev. 7, 277–285. https://doi.org/10.1016/j.gsd.2018.06.010

Narany, T.S., Ramli, M.F., Aris, A.Z., Nor, W., Sulaiman, A., Juahir, H., Fakharian, K., 2014. Identification of the Hydrogeochemical Processes in Groundwater Using Classic Integrated Geochemical Methods and Geostatistical Techniques , in Amol-Babol Plain, Iran. Sci. World J. 2014, 1–15.

Odukoya, A.M., Folorunso, A.F., Ayolabi, E.A., Adeniran, E.A., 2013. Groundwater Quality and Identification of Hydrogeochemical Processes within University of Lagos, Nigeria. J. Water Resour. Prot. 5, 930–940. https://doi.org/10.4236/jwarp.2013.510096

Ofomola, 2015. Mapping of Aquifer Contamination Using Geoelectric Methods at a Municipal Solid Waste Disposal site in Warri, Southern Nigeria. IOSR J. Appl. Geol. Geophys. Ver. I 3, 2321–990. https://doi.org/10.9790/0990-03313947

Ojolowo, S., Wahab, B., 2017. Municipal solid waste and flooding in Lagos metropolis , Nigeria : Deconstructing the evil nexus. J. Geogr. Reg. Plan. Full 10, 174–185. https://doi.org/10.5897/JGRP2016.0614

Oteri, A.U., & Atolagbe, F.P., 2003. Saltwater Intrusion into Coastal Aquifers in Nigeria, in: The Second International Conference on Saltwater Intrusion and Coastal Aquifers Monitoring, Modeling, and Management. Mérida, Yucatán, México, March 30 - April 2, 2003. Merida Yucatan, pp. 1–15.

Palamuleni, L.G., 2002. Effect of sanitation facilities, domestic solid waste disposal and hygiene practices on water quality in Malawi's urban poor areas: A case study of South Lunzu Township in the city of Blantyre. Phys. Chem. Earth 27, 845–850. https://doi.org/10.1016/S1474-7065(02)00079-7

Paris, G., Gaillardet, J., Louvat, P., 2010. Geological evolution of seawater boron isotopic composition recorded in evaporites. Geology 38, 1035–1038. https://doi.org/10.1130/G31321.1

Park, C.H., Aral, M.M., 2008. Saltwater intrusion hydrodynamics in a tidal aquifer. J. Hydrol. Eng. 13, 863–872. https://doi.org/Doi 10.1061/(Asce)1084-0699(2008)13:9(863)

Saha, R., Dey, N.C., Rahman, M., Bhattacharya, P., Rabbani, G.H., 2019. Geogenic Arsenic and Microbial Contamination in Drinking Water Sources: Exposure Risks to the Coastal Population in Bangladesh. Front. Environ. Sci. 7, 1–12. https://doi.org/10.3389/fenvs.2019.00057

Saha, R., Dey, N.C., Rahman, S., Galagedara, L., Bhattacharya, P., 2018. Exploring suitable sites for installing safe drinking water wells in coastal Bangladesh. Groundw. Sustain. Dev. 7, 91–100. https://doi.org/10.1016/j.gsd.2018.03.002

Salman, S.A., Arauzo, M., Elnazer, A.A., 2019. Groundwater quality and vulnerability assessment in west Luxor Governorate, Egypt. Groundw. Sustain. Dev. 8, 271–280. https://doi.org/10.1016/j.gsd.2018.11.009

Seddique, A.A., Masuda, H., Anma, R., Bhattacharya, P., Yokoo, Y., Shimizu, Y., 2019. Hydrogeochemical and isotopic signatures for the identification of seawater intrusion in the paleobeach aquifer of Cox's Bazar city and its surrounding area, south-east Bangladesh. Groundw. Sustain. Dev. 9. https://doi.org/10.1016/j.gsd.2019.100215

Shi, X., Wang, Y., Jiao, J.J., Zhong, J., Wen, H., Dong, R., 2018. Assessing major factors affecting shallow groundwater geochemical evolution in a highly urbanized coastal area of Shenzhen City, China. J. Geochemical Explor. 184, 17–27. https://doi.org/10.1016/j.gexplo.2017.10.003

Talabi, A.O., Tijani, M.N., Aladejana, A.J., 2012. Assessment of impact of climatic change

on groundwater quality around Igbokoda Coastal area , southwestern Nigeria . J. Environ. Earth Sci. 2, 39–50.

Tirkey, P., Bhattacharya, T., Chakraborty, S., Baraik, S., 2017. Assessment of groundwater quality and associated health risks: A case study of Ranchi city, Jharkhand, India. Groundw. Sustain. Dev. https://doi.org/10.1016/j.gsd.2017.05.002

Tomaszkiewicz, M., Abou Najm, M., El-Fadel, M., 2014. Development of a groundwater quality index for seawater intrusion in coastal aquifers. Environ. Model. Softw. 57, 13–26. https://doi.org/10.1016/j.envsoft.2014.03.010

Ukhurebor, K.E., Abiodun, I.C., 2018. Variation in annual rainfall data of forty years (1978-2017) for south-south, Nigeria. J. Appl. Sci. Environ. Manag. 22, 511. https://doi.org/10.4314/jasem.v22i4.13

Wu, M.-L., Wang, Y.-S., Sun, C.-C., Wang, H., Dong, J.-D., Yin, J.-P., Han, S.-H., 2010. Identification of coastal water quality by statistical analysis methods in Daya Bay, South China Sea. Mar. Pollut. Bull. 60, 852–860. https://doi.org/10.1016/j.marpolbul.2010.01.007

5.3 Paper 2

Aladejana, Jamiu A, Kalin, R.M., Sentenac, P., Hassan, I., 2020. Hydrostratigraphic Characterisation of Shallow Coastal Aquifers of Eastern Dahomey Basin, S/W Nigeria, Using Integrated Hydrogeophysical Approach ; Implication for Saltwater Intrusion. Geoscience 10, 65. https://doi.org/10.3390/geosciences10020065 [Open access]

Hydrostratigraphic Characterisation of Shallow Coastal Aquifers of Eastern Dahomey Basin, S/W Nigeria Using Integrated Hydrogeophysics; implication for saltwater intrusion

Jamiu A. Aladejana[1,2]*, Robert M. Kalin[1], Philippe Sentenac[1] and Ibrahim Hassan[1,3]

[1] *Department of Civil and Environmental Engineering, University of Strathclyde, Glasgow, UK;* [2] *Department of Geology, University of Ibadan, Nigeria;*
[3] *Department of Civil Engineering Abubakar Tafawa Balewa University Bauchi, Nigeria;*
* *Correspondence: jamiu.aladejana@strath.ac.uk*

5.3.1 Abstract

This study employed electrical resistivity tomography (ERT) in characterising the shallow groundwater aquifers of Eastern Dahomey Basin in southwestern Nigeria to assess the possible distribution of saltwater within the aquifers. Electrical resistivity tomography (ERT) and borehole logging were carried in locations with relatively enhanced electrical conductivity within the coastal communities through 97 sampled groundwater samples from shallow wells and boreholes. Three traverses A-B, C-D and E-F were selected along which ERT and induced polarization (IP) were carried out in directions perpendicular and parallel to the coastline. Three geoelectrical layers were identified along traverse line A-B which comprises cross-sections 1, 2, 3 and 4 located around Ugbonla, Aboto and Igbokoda with layers' resistivity and chargeability values ranging from (1 - 1000, 33 – 200 and 1 - 1700 Ωm), and (-50 – 200 Ωm, -30 – 200 Ωm

and -50 – 120 Ωm respectively from the top to the bottom layer. These values indicated unconsolidated sand/lateritic silty clay, underlain by a sandy/silty clay layer with underlying fine-grained sand with disseminated clay lenses. The average thickness of the first two layers is 16 and 53 m while that of the third layer is undetermined. Resistivity and chargeability results from ERT and IP cross-sections along profile C-D exhibited characteristics similar to that of profile A-B with unconsolidated sands which are underlain by intercalation of sandy/silty clay and fine-grained sands with suspected clay lenses saturated with saline water. Profile E-F revealed a geoelectrical layer with low resistivity which ranges from 1 - 30 Ωm with the corresponding chargeability between -150 – 400 ms. This indicates a saline water-saturated layer of fine-grained sand and silty clay which is overlaid by the unconsolidated unconfined freshwater aquifer. Correlation of selected ERT results with borehole logs further affirmed the suspected lithology from the sections. Two scenarios of saltwater intrusions into coastal freshwater aquifer were suggested which include the presence of trapped salt-saturated clay lenses within aquifer lithology and seawater incursion induced by over-drafting of groundwater in this basin. The study has provided valuable information to contribute to sustainable coastal groundwater resources management. It, therefore, identified further investigation which will involve a combination of hydrochemical and isotopes to further understand the hypothesis of paleowater.

Keywords: Coastal aquifer; Clay lenses; Saline water; Freshwater; Geoelectrical Layers and Intrusion

---

5.3.2 Introduction

Seawater intrusion is gradually becoming an inevitable problem of coastal aquifer especially in coastal zones of the world (1). Coastal regions have been described as the

area of the world that is fast becoming home to high and growing population which is consequently undergoing a series of environmental degradation, (Mulrennan and Woodroffe, 1998; Creel, 2003). High population contributes significantly to this environmental decline. As at the year 2003, approximately three billion people, about half of the world's population, live within 200 kilometres of the coastline, a figure which will likely double by the year 2025 (Creel, 2003). Coastal areas account for approximately 40 and 45 % of the world's and Nigeria's population respectively (Oteri and Atolagbe, 2003; Wu et al., 2010)

Rural-urban migration associated with economic, industrial and agricultural opportunities among other factors lead to this rapid population growth. In most of the developing countries around the world, there is associated infrastructural deficiency which includes erratic pipe-borne water supply among others. This, therefore, puts significant pressure on coastal freshwater aquifer which remains the only alternative source of water, to meet water required for domestic, agricultural, industrial and recreational purposes.

Eastern Dahomey Basin in Nigeria comprises two major inland river basins which include, Ogun-Osun and Benin-Owena river basin, with the addition to the coastal aquifer. This basin contributes significantly to the water resources of Nigeria and is also the major source of freshwater supply to various households. There are several reports from different sectors, ranging from government agencies, non-governmental organisations, research and academic institutions to "ad-hoc" and uncoordinated individuals and private companies, on the alarming degradation and the threat to groundwater quality, especially in the coastal area. Here, the groundwater level is generally higher which permits constant interaction with the polluted surface water The daily water demand in Lagos, the most populous city in Subsaharan Africa

underlain by this basin is about 724 Million gallons with production standing at 317 million gallons, this leaves a gap of about 407 million gallons which is complemented through the groundwater from shallow hand-dug wells and boreholes. Worse still, some of the pipe-borne water never reached households due to constant defects from burst transmission pipes and old trunk lines (Oluwafemi et al., 2016). This further emphasised the importance of this invaluable resource to the economic and health status of inhabitants of the country's southwest coast. Indiscriminate waste disposal and management also pollute surface water which recharges the groundwater. This direct interaction of contaminated and polluted surface water with groundwater degrades the quality of groundwater in the unconfined top aquifer in this coastal area as observed in the work of (Ayolabi et al., 2013; Ayolabi et al., 2014; Ayolabi and Oyelayo, 2005). In the search for potable freshwater, most wells and boreholes in this area are drilled to the second aquifer, which is a confined aquifer (Figure 5.9) underlying the coastal area of the basin which is most densely populated, in order to meet their daily water demand. This development has put pressure on groundwater and lead to saltwater intrusion into the freshwater aquifer through up conning wedge shift resulting from over-abstraction of groundwater (Adepelumi et al., 2009; Edet, 2016; Oteri and Atolagbe, 2003; Oteri, 2008). Proximity to the sea also encourages saltwater intrusion into the freshwater of the coastal aquifer due to sea-level rise (SLR) and destruction of the coastal barrier due to indiscriminate sand mining along the coastline of the basin (Izbicki, 1996). Another school of thought has also suggested possible dissolution of evaporite minerals trapped within the basin lithology during a past event of ocean transgression and regression into groundwater causing their enhanced salinity and electrical conductivity (Cary et al., 2015; Tran et al., 2012). The work of (Adeoti et al., 2010; Adepelumi et al., 2009; E. a Ayolabi et al., 2013; Elijah Adebowale

Ayolabi et al., 2013; E.O. Longe et al., 1987; Longe, 2011; Odukoya et al., 2013; Oteri and Atolagbe, 2003; Oteri, 1991, 2008) have employed different methods such as electrical resistivity tomography (ERT), induced polarization (IP) and hydrochemistry on groundwater in some selected and specific locations within this basin. Some of these studies which have identified saltwater intrusion in the upper aquifers mainly in the eastern coast of Lagos, such as Lekki, Ajjah, Victoria Island, Sagontedo. The deterioration of water quality in parts of Lekki phase 1 and Oniru environs of Lagos metropolis due to saltwater infiltration into the freshwater aquifer has become a significant concern (Adepelumi et al., 2009).

Despite all this, the report still shows that systematic and detailed groundwater quality assessment and monitoring are insufficient for sustainable management of groundwater in the face of the menace of salty water. This challenge results from a combination of factors, such as costs associated with water quality monitoring, the relatively low levels of funding for research in Sub-Sahara Africa over the past decade and limited national regulation of high-intensity rainfall events which pose a risk to shallow and poorly protected groundwater sources (Lapworth et al., 2017a; Oteri, 2008). Also, groundwater as dynamic resources upon which its quality requires constant regimented monitoring for early detection of contamination and pollution to ensure a sustainability and health safety measure of life, and possibly plant and animals which depends on it for survival.

Moreover, there is a vital need to monitor the possible risk of saline water intrusion of the coastal aquifers because, once saline intrusion into coastal aquifer has occurred, it is challenging to overcome and to improve the management of the water resources based on long-term strategy. Within this location, several boreholes have had to be

abandoned, and other water sources sought, often at a high cost. Furthermore, subsurface data are generally scarce because invasive methods such as borehole drilling and associated aquifer tests are expensive and time-consuming. The current lack of hydrogeological information of the existing commercial boreholes is also a factor. Therefore, non- invasive hydrogeophysical methods of subsurface data acquisition provide an alternative, or a complement to, direct observations. Protection of groundwater resources in coastal areas and their sustainable management, in conjunctive use with other water resources (e.g., surface water, seawater), require an understanding of the coastal aquifer hydrogeology.

This study, therefore, focusses on the delineation of origin and distribution of saltwater intrusion in the coastal freshwater aquifer of Eastern Dahomey Basin using a physicochemical approach through the electrical conductivity and geophysical method of electrical resistivity tomography (ERT), induced polarization (IP) complemented with borehole logs with the objective of identify saltwater bearing lithological units that are responsible for salinisation of freshwater. Complimentary use of these methods improves the extensive coverage of hydrogeological investigations due to the difference between their characteristics and capability.

5.3.2.1 Study Area and Geomorphology

The Eastern Dahomey Basin lies in the southwestern part of Nigeria, which is the eastern part of Dahomey Basin (also called Benin or Keta Basin in Nigerian literature). It is a transboundary basin that extends from Ghana through Togo and Benin to Nigeria. This basin is bounded by Okitipupa Ridge, which is the boundary it shares with Niger Delta basin (Adegoke, and Omatsola, 1981). It lies between Latitudes $2^0$41ˈ10.00’’ and $4^0$59’5900’’N and Longitudes $6^0$21’1300’’ and $7^0$52’42.00’’E along the coast of the Gulf of Guinea (see Figure 5.8). The basin is bounded in the south by

the Atlantic Ocean, west by the Republic of Benin and thin out at the north by the Precambrian basement rocks. The area of investigation towards the south is low lying with several points virtually at sea level which are prone to flooding. The highest elevation is found around the city of Abeokuta in the northern parts of the study Basin. Two major climatic seasons can be recognised, a dry one from November to March and a wet one which starts in April and ends in October with a short break in mid-August. Major rivers such as the Ogun, Ose, and Oluwa drain the basin into the delta and the Atlantic Ocean. The basin hosts two major administrative water basins authorities in Nigeria which include Ogun-Osun and Benin-Owena river basins and accommodates about 40% population of the country's residents including the metropolitan city of Lagos which signifies it is essential to the economy of Nigerian and West-Africa.

5.3.2.2. Geology and Hydrogeology of Eastern Dahomey Basin

The lithological character of the sediments was dictated by the regime of transgressions and regressions of the sea since the Cretaceous age, and the transgressions are found to have been coming from the south. The stratigraphic description of the sediments has been provided by various authors including (Adegoke and Omatsola, 1981; Jones and Hockey, 1964; Offodile, 1971; Okunlola et al., 2009), as presented in Table 5.15. Some of these authors have proven the area to be composed of the following stratigraphic units from youngest to the oldest. The Alluvium Deposits and coastal plain sands consist of soft, very poorly sorted clayey sands, pebbly sands, sandy clays and rare thin lignite of Oligocene to Recent age. This is underlain by Ilaro formation which consists of massive, yellowish, poorly consolidated, cross-bedded sandstones, which are fine to medium-grained and poorly sorted (Adegoke and Omatsola, 1981). This is followed by Ewekoro formation which consists of

predominantly Paleocene fossiliferous limestone which becomes arenaceous towards the base (Jones and Hockey, 1964) and Abeokuta formation which consists of lower Cretaceous sandstone and grits with interbedded mudstone unconformity overlain the basement complex fine detrital sandstone, siltstone and shale overlying the formation in the upper parts. The youngest sets of strata are marginal to fully marine sand and shale of the Maastrichtian Age.

The Coastal Plains Sands represents the main aquifer in the southern parts of the basin which most of the well and boreholes exploit. This has resulted in a multi-aquifer system consisting of three aquifer horizons separated by silty or clayey layers (Longe et al., 1987). The aquifer shows high thickness at the northern part of Abeokuta, through Ewekoro, Ilaro, and thin-out into the coastal plain sands, in locations closer to the coast in the south. The percentage of sands in lithology also increases towards the south (Longe et al., 1987). The geology map of the basin is presented in Figure 5.8.

Table 5.15 Stratigraphic Sequence in the Eastern Dahomey Basin. Modified from Adelana et al., (2004).

Formation	**Age**	**Rock Type**	**Approximate Depth of Base (m.b.s.l)**
Coastal Plain Sands	Tertiary (Oligocene – Pleistocene)	Clays, Silty Clays, Sands	130
Ilaro	Tertiary Eocene	Clays and Shales	280
Ewekoro	Tertiary Paleocene	Shales, limestone and sands	550
Abeokuta	Upper Cretaceous	Sandstone, Siltstone, Shale, Conglomerate	350-600
Crystalline Basement	Paleozoic to Precambrian	Granites and Migmatite	>400

The coastal plain and alluvium deposits of the Eastern Dahomey Basin are characterised with a multi-layer aquifer, which is classified into three types (Longe et al., 1987). The first aquifer is a water table aquifer which is prone to pollution because of its nearness to the ground surface. The second and third are confined aquifers composed of an alternating sequence of sand and clay. They are harnessed through boreholes and are the basis of mini water-works in Lagos area and other parts of the Basin. These aquifers belong to the continental Ilaro Formation. The third aquifer seems to be the most productive and faces the highest level of groundwater exploitation within which most boreholes terminated. Within it, groundwater exists under confined to the semi-confined condition (Adelana et al., 1996; Longe et al., 1987; Longe, 2011). Generally, the water-table ranges from 2.0 to 15.0 m below ground level (b.g.l) in the area. Also, the study area is well-drained by rivers and streams that flows southerly into the lagoon and the Atlantic Ocean. The average annual precipitation is above 1700 mm and serves as a primary source of groundwater replenishment.

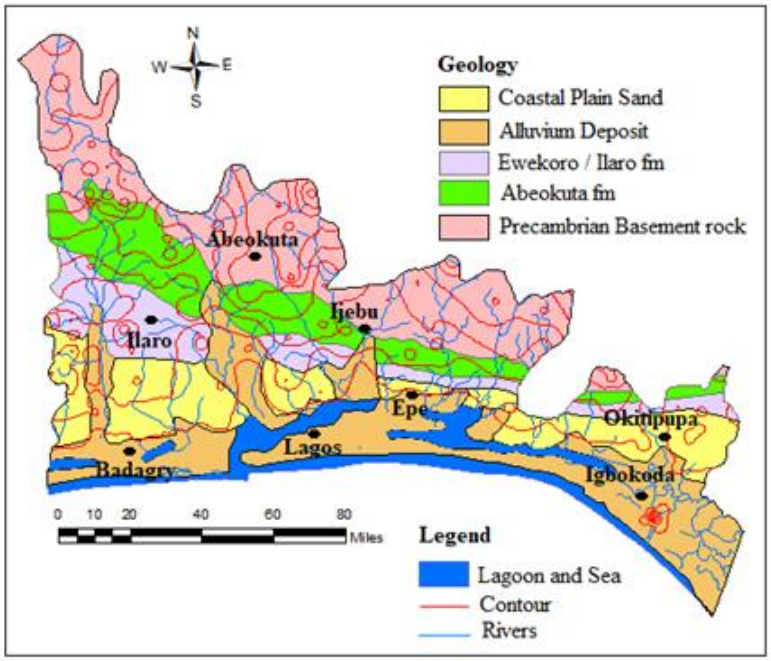

Figure 5.8 Geology map of Eastern Dahomey Basin.

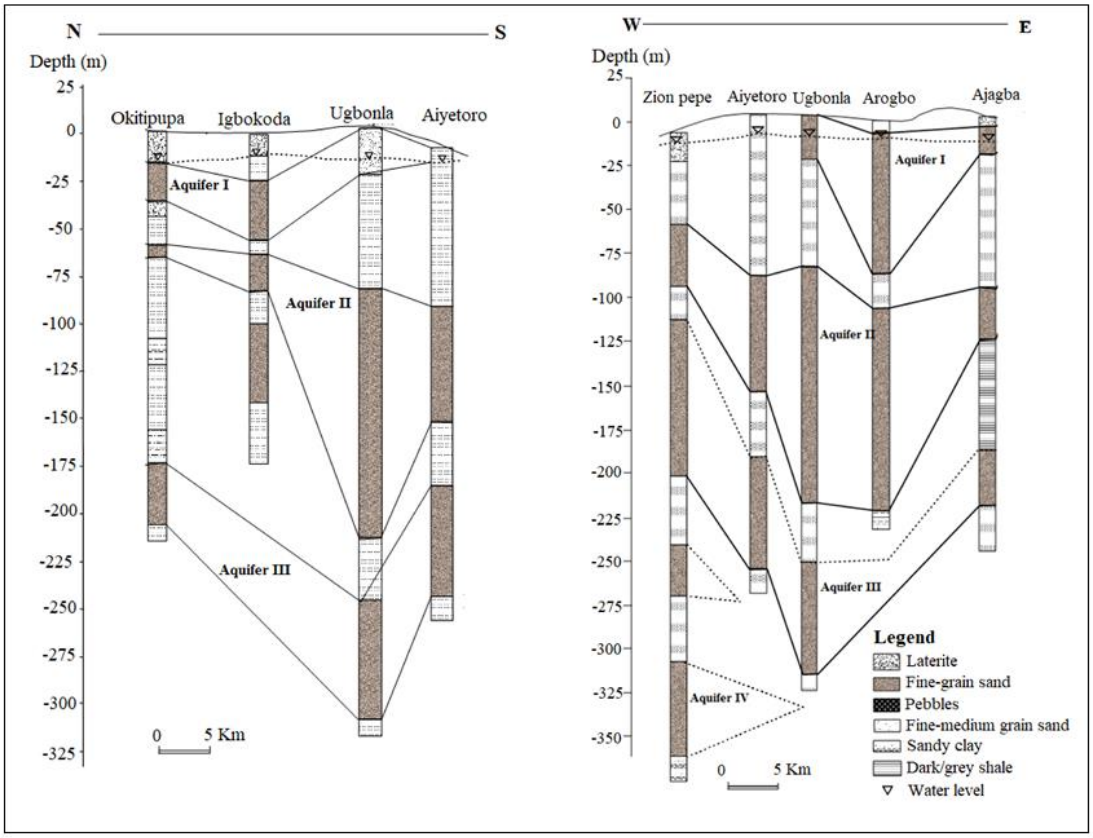

Figure 5.9 Generalised aquifer description in parts of Eastern Dahomey basin. Modified from Omosuyi, et al., (2008)

5.3.3 Materials and Methods

5.3.3.1. Field Physico-chemical Measurement

The physicochemical field measurement of electrical conductivity, salinity and water level are groundwater parameters that are critical to water quality regarding the saltwater intrusion. Monitoring change in conductivity could provide a clue to the early stage of saltwater intrusion into the freshwater aquifer (Edet, 2016; Longe et al., 1987). This was therefore employed as a preliminary approach to the selection of locations for geophysical investigation. This was also necessary to save time and cost. The physicochemical parameters were measured in the field using a Model 99720

microprocessor pH/Conductivity meter capable of measuring total dissolved solids (TDS), salinity, temperature and oxidation and reduction potential (Eh/ORP). The depth of the wells and static water level were measured with the aid of a water depth meter while the coordinates of each sampled well were recorded using GPS. Conductivity from 6.7 to 12000 µS/cm. were found in water samples from wells in locations around Igbokoda, Ungbonla, Ibeju-Lekki and Okun-Ajjah. (Figure 5.10 and Table 5.17). It was challenging to select a continuous length of resistivity profile due to the marshy nature of the coastal area. Also, the isolated and drained sandbars which could have served as the survey are built-up for residential use especially in part of the coast near to the metropolitan city of Lagos. Hence, the selection of the profile lines is mainly controlled by the available space (Figure 5.10).

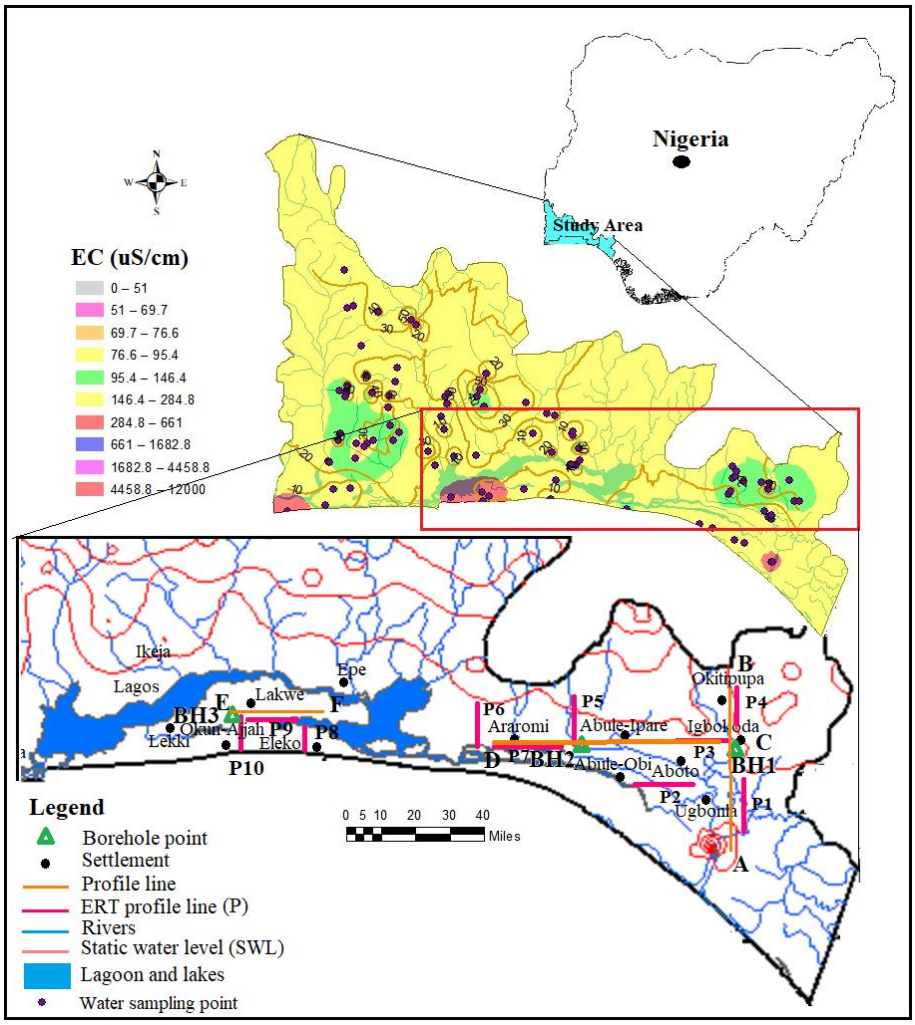

Figure 5.10 Map of the Eastern Dahomey Basin.

5.3.3.2 Hydro-geophysical Approach

Electrical near-surface-geophysical methods used in this study, such as Electrical Resistivity Tomography (ERT) and Induced Polarisation (IP) have been employed in various areas in the field of Hydrogeology for groundwater studies (Khalil, 2006). This method was chosen over Vertical Electrical sounding (VES) because, the latter only presented a limited vertical overview of resistivity distribution below the survey point which does not capture the lateral stratigraphic relationship of the different layers (Aluko et al., 2017). The IP and ERT are integrated in this study because of the common ambiguous and challenges poised when lithology such as clay and sand units

or other factors such as contaminants and saltwater which are characterized with low resistivity values are faced during interpretation of electrical resistivity data. IP method is very important since it measured chargeability of lithology which is a key parameter that differentiate clayey and sandy units within similar resistivity range.

The principle of the ERT method is based on the measurement of the soil apparent resistivity, using a large number of electrodes placed along the profile or in the area. The electrodes are interconnected by a special cable that enables connection to the electrodes as current and potential electrode step by step. This allows measurement for a large number of variants of a 4-electrodes array with differing geometry and penetration depth. The measurement proceeds automatically and is controlled by a computer/laptop. Details of this method can be found in the work of (Abdulrahman et al., 2016; Elijah A Ayolabi et al., 2013; Buselli and Lu, 2001; Günther and Dlugosch, 2010).

Induced Potential (IP) method targets electrical resistivity and chargeability of the subsurface lithology, which applies to delineate the zones of freshwater and saltwater contact, permeable sands aquifers and impermeable clayey aquitard and their overall geometry. Groundwater applications of this methods include delineating aquifer depth and thickness, mapping aquitards or confining units, identifying fluid migration paths such as fractures and fault zones and mapping contamination to the groundwater such as saltwater intrusion (de Franco et al., 2009; McInnis et al., 2013; Oteri and Atolagbe, 2003; Oteri, 1991, 1981).

5.3.3.3. Geophysical Field Data Acquisition

Ten geoelectrical profiles (L1 – L10), each of 500 m length with electrode spacing of 6 m, were carried out for both electrical resistivity tomography (ERT) and induced

potential (IP) using an Advance Geophysical Instrument (AGI) SuperSting R8/IP8 Earth Resistivity meter, an 8 channel Memory Resistivity and IP Meter with inbuilt processor for 84 multi-electrodes systems. Resistivity profiles were carried out around Igbokoda, Ungbonla, Araromi Eleko, Lakowe and Okun-Ajjah within the coastal area of the Basin. The selection of the location of the profile was based on both enhanced electrical conductivity (EC) results (Figure 5.10) and accessibility as observed during the groundwater well inventory. The sections were conducted along two directions, North-South and West-East respectively A-B, C-D and E-F as shown in Figure 3. Traverse A-B which consists of ERT and IP profiles sections 1 and 4 was carried out around Ugbonla, Aboto, and Igbokoda, and perpendicular to the shoreline. Traverse C-D consisted of profile sections 2, 3, 5, 6 and 7 with 2, 3 and 7 ran parallel to the shoreline profile sections while 5 and 7 ran at an angle almost perpendicular to the shoreline around Abule-Ipare, Abule-Obi and Araromi (Figure 5.10). The third traverse is E-F which consists of profile section 8 and 10 ran at an at almost perpendicular to the shoreline while profile section 9 ran parallel to the shoreline in location between 8 and 10. The traverse E-F which ran parallel to the shoreline was carried out around the Eleko, Lakowe and Oku-Ajjah area of the metropolitan city of Lagos. There was constrained to the length of the traverse line due to high water level which is above the ground surface in most of the area. Details of the profiles and coordinates are shown in Figure 5.10.

5.3.3.4 Geophysical Data Processing

The ERT and IP data acquired were processed and analysed using the AGI EarthImager 2D software. The results presented were inverted using the standard method of inversion (L2-norm approach) after the 5th iteration. For all sections results,

an RMS model error below 96.7% was obtained. On the IP, the resistivity and chargeability variations were displayed as contoured pseudo-sections that give rough visual impressions of the variability of resistivity and chargeability with depth below the profiles. The acquired ERT and IP data were inverted to produce sections with vertical scales in depth, which give significantly improved pictures of actual resistivity and chargeabilities variations.

In addition to ERT and IP measurements, data from borehole drilling and geophysical well loggings were correlated with information from ERT and IP results for validation. These borehole logging points were selected in locations along or sufficiently close to the ERT sections. The respective sections were therefore interpreted using resistivity classifications of groundwater types as shown in Table 5.16 below.

Table 5.16 Classification of aquifer based on resistivity value After (Oyeyemi et al., 2015).

S/N	Resistivity Value (Ωm)	Description
1	0 - 55	Saline water
2	55 - 90	Brackish water (Interface)
3	>90	Freshwater

5.3.4 Results

5.3.4.1. Results of Well and Borehole Field Inventories

Results of some physicochemical parameters such as electrical conductivity (EC), total dissolved solids (TDS) salinity static water level, well depth and others parameters which could serve as a fingerprint to saltwater intrusion were carried out

on 93 shallow boreholes, and hand-dug wells across the Eastern Dahomey basin are presented in Table 5.17.

Table 5.17 Regional Electrical Conductivity

Parameters	Min	Max	Average	Stdev	Variance
Elevation (m)	-1.00	230.00	46.30	39.80	1584
pH	3.97	8.10	5.57	1.00	1.00
EC (µS/cm)	6.7	12000.00	295.40	1219.42	1486983.00
TDS (mg/l)	0.00	8500.00	201.83	863.57	745754.00
ORP (Mv	-136.00	330.00	222.90	74.88	5606.00
Salinity (mg/l)	0.00	5000.00	136.79	508.98	259062.00
Temp (^{0}C)	25.50	34.60	29.44	1.72	2.96
Alkalinity (mg/l)	0.20	96.40	9.05	15.59	242.98
SWL (m)	0.20	67.00	18.27	15.36	235.98
Well Depth (m)	2.10	125.00	26.62	18.85	355.16219

The respective ranges of EC, TDS, salinity, static water level and well depth are 6.7 – 12,000 µS/cm, 3.2 – 8500 mg/l, 2 – 5000 mg/l, 0.2 – 67 m and 2.10 – 125 m (Table 3). EC, TDS and salinity increase from the north towards the shoreline which shows the influence of seawater. These two parameters also decrease with the depth of the well and static water level (SWL) which could increase the influence of surface and groundwater interaction causing pollution and contamination of groundwater and positively altering these values (Edet, 2016, 2014; Edet et al., 2003; Oyelami et al, 2013). Enhanced EC showed by the value of standard deviation and variance (Table 5.17) were observed in some wells around Igbokoda, Ode-Mahin, Ugbonla, Ogombo, Okun-Ajjah and Lekki.

5.3.4.2. Results of Electrical Resistivity Tomography (ERT) and Induced Polarisation (IP)

The 500m long ERT-IP sections from some selected locations based on enhanced EC revealed different geoelectrical layers across the profile sections with maximum depth probed ranging between 105 and 118m. Traverse A-B consists of 1, 2, 3 and 4 ERT and IP profile sections which out of P1 and P4 are perpendicular while P2 and P3 are parallel to the coastline. On the ERT and IP section P1 (Figure 5.11), located at the front of the palace of the Olugbo of the Ugbo Kingdom in Ode-Ugbo, three geoelectric layers were delineated with resistivity values /chargeability range between (1 – 30 Ωm /-50 – 45 Ms), (70 – 200 Ωm/-30 - 20 Ms) and (1 – 30 Ωm / -50 – 70 Ms) figure 3a, with respective average depth of 23, 47 and 70 m (Table 5.18).

These ERT and IP values are delineated to be silty sand and clay which represent the topsoil, sandy clay and underlain by fine-grain sands which have the impression of saltwater saturated clay lenses. This could be attributed to low resistivity within this unit, hence the saline water that characterised abandoned deep boreholes in this area.

Table 5.18 Lithological interpretation of Geoelectrical sections from Profile A-B.

Ugbonla geoelectrical section			
Depth (m)	Resistivity (Ωm)	Chargeability (ms)	Lithological Description
0 - 23	1 - 130	-50 - 45	Unconsolidated dry-Sand (Top soil)
23 - 70	70 - 200	-30 – 20	Clayey sand
70 - 105	1 - 130	-50 - 70	Fine grain Sand
Aboto geoelectrical section			
Depth (m)	Resistivity (Ωm)	Chargeability (ms	Lithological Description
0 - 14	300 - 700	5 - 75	Unconsolidated sand (Top soil)
14 - 118	10 - 40	-5 – 100	Saturated fine grain sand with clay lenses.
Igbokoda geoelectrical section			
Depth (M)	Resistivity (Ωm)	Chargeability (ms)	Lithological Description
0 - 13	700 - 1000	15 - 30	Unconsolidated dry-sand (Top soil)
13 - 55	33 - 50	1 - 128	Clayey sand
55 - 105	10 - 20	-12 - 100	Fine grain clay with clay lenses
Okitipupa Rd geoelectrical section			
Depth (m)	Resistivity (Ωm)	Chargeability (ms	Lithological Description
0 - 13	60 - 300	100 - 200	Lateritic clay (Top soil)
13 - 36	300 - 1700	80 – 200	Sandy Clay
36 - 105	200 - 700	300 - 120	Fine grain Sands with clay lenses

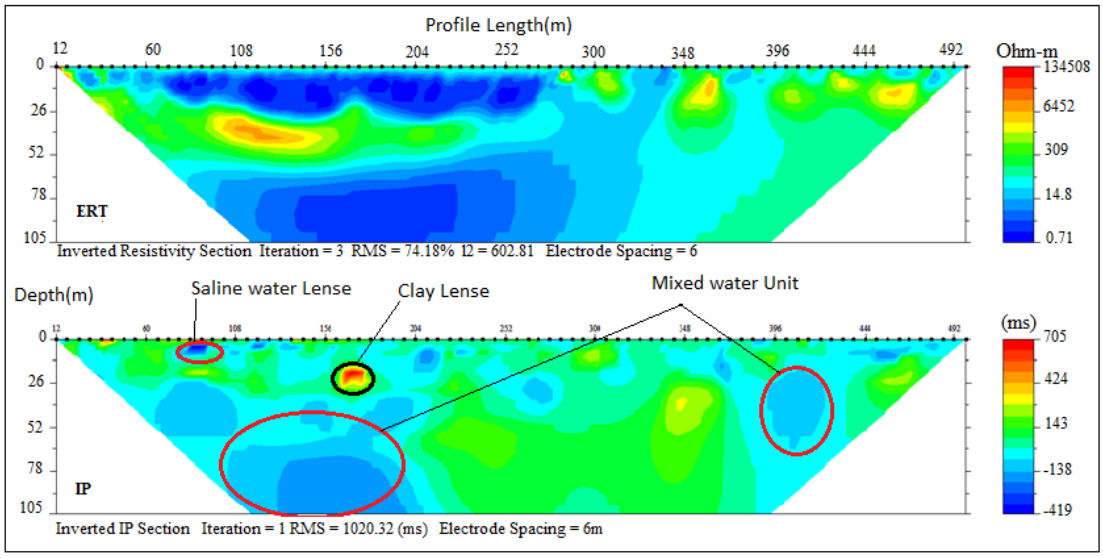

Figure 5.11 Inverted Resistivity and IP Cross-sections Ugbonla Profile (Section 1).

The ERT and IP section P2 (Figure 5.12), located at Aboto village, revealed two geoelectric layers with resistivity/chargeability values between (300 – 700 Ωm/10 – 40 ms) and (5 – 75 Ωm /-5 – 100 ms). These values indicate silty sand topsoil and fine-grain sand with clay lenses saturated with saline water with respective depths of 14 m and above 104 m. The presence of clay lenses is responsible for low resistivity values within the layers. Three geoelectric layers were delineated along ERT and IP section P3 (Figure 5.13), located at the south-eastern part of Igbokoda along Aboto Road. Resistivity / chargeability of the layers from top to bottom range between (700 – 1000 Ωm/15 – 30 Ms), (33 – 50 Ωm/1 – 128 ms) and (10 – 20 Ωm and -12 – 100 Ms) which are indication of silty sand topsoil, clayey sand/sandy clay and fine-grain sands with respective average thicknesses of 25m, 42m and more than 25 m. The low resistivity with corresponding high chargeability within the layers indicate clay lenses saturated with saline water which characterised the second and third layers.

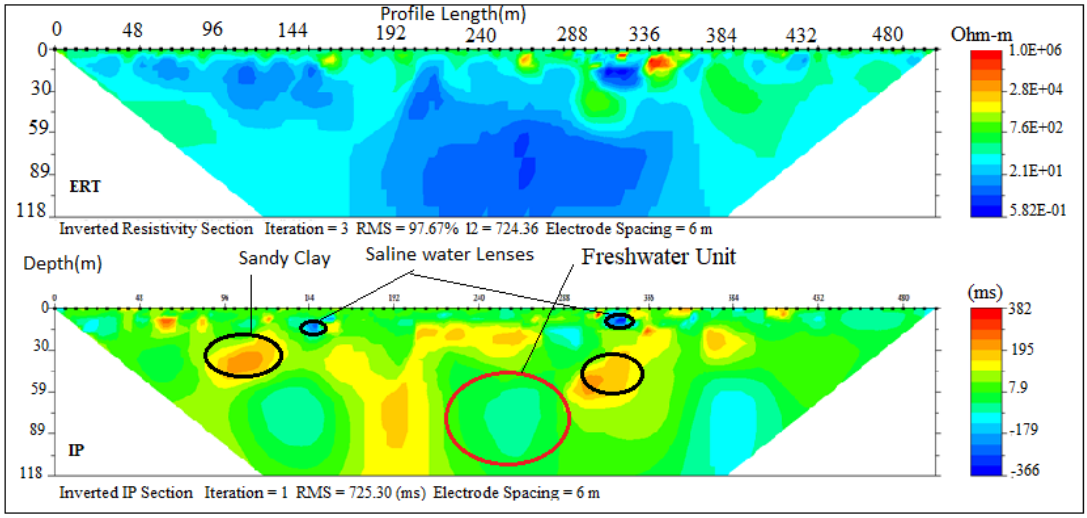

Figure 5.12 Inverted Resistivity and IP Cross-sections Aboto (Profile section 2).

The last ERT and IP sections P4 (Figure 5.14) at the northern end for profile A-B were carried out along the Igbokoda Okitipupa road. These sections revealed three geoelectrical layers with resistivity/chargeability values ranging between (60 – 300Ωm/100 – 200 ms), (300 - 1700Ωm/80 – 150 ms) and (200 – 700 Ωm /30 – 120 ms) suspected to be lateritic topsoil, sandy clay and fine grain sand with clay lenses. The resistivity values indicate a freshwater aquifer with depth ranges between 13m to 36 m underlying the lateritic clay topsoil which serve as a protective layer for the aquifer. Hence the relatively good groundwater quality observed in wells around this area. The overall results on this profile show an improved water quality along the northern part of the study area away from the coast, which is due to hydraulic properties of the lithology.

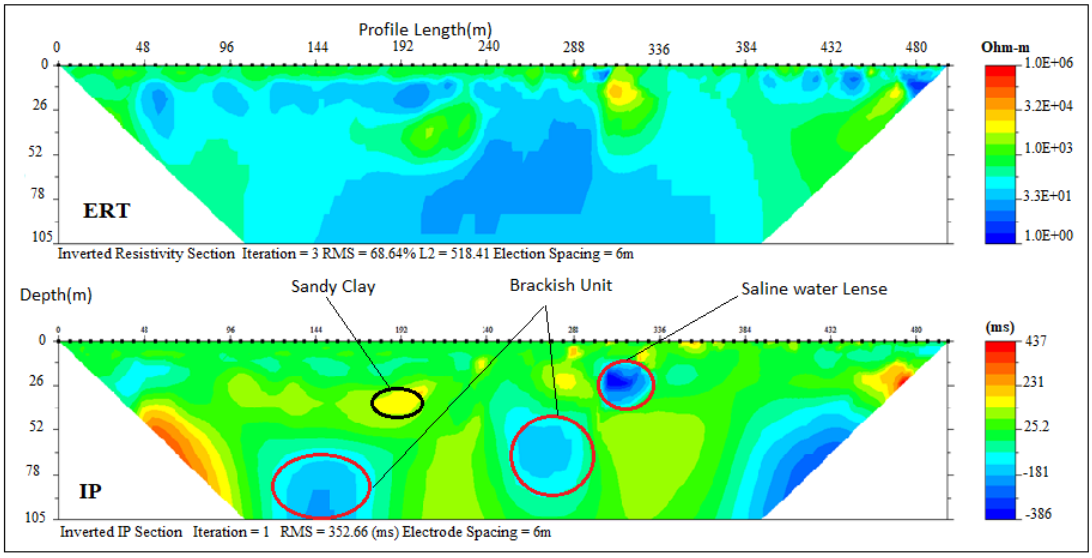

Figure 5.13 Inverted Resistivity and IP Cross-sections of Igbokoda (Profile section 3).

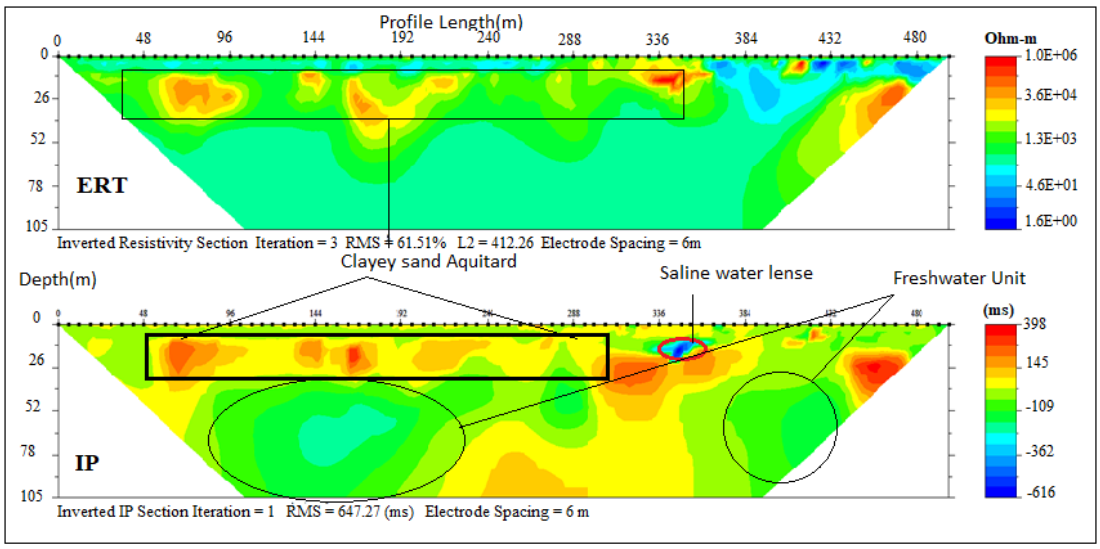

Figure 5.14 Inverted Resistivity and IP Cross-sections of Okitipupa road (Profile section 4).

Profile C-D (figure 5.10) is parallel to the coastline and consists of three ERT, with their respective IP sections (2, 3, 5, 6 and 7) carried out at Aboto, Abule-Ipare, Abule-Obi and Araromi towns respectively. ERT and IP section P5 (Figure 5.15) revealed three geoelectrical layers with resistivity/chargeability values ranges between (50 – 496 Ωm /-100 – 40 ms), (32 – 300 Ωm /0 – 100 ms) and (40 – 180 Ωm/-40– 20

ms). These results revealed unconsolidated wet sand, sandy clay and fine-grain sand with clay lenses. The average thickness of the first and second layers are 25m and 35m, respectively while the second layer has thickness beyond 58 m. Saline water intrusion was observed around some lensoid shape clay with low resistivity, and high chargeability observed within the layers. Sandy clay with an average thickness of 35 m formed a semi-aquitard layer. A lensoid shape area within the geoelectric section with resistivity of about 4200 Ωm and Chargeability of 400 ms was suspected to be buried hardpan of ferruginised clay or mudstone found at the a very shallow depth.

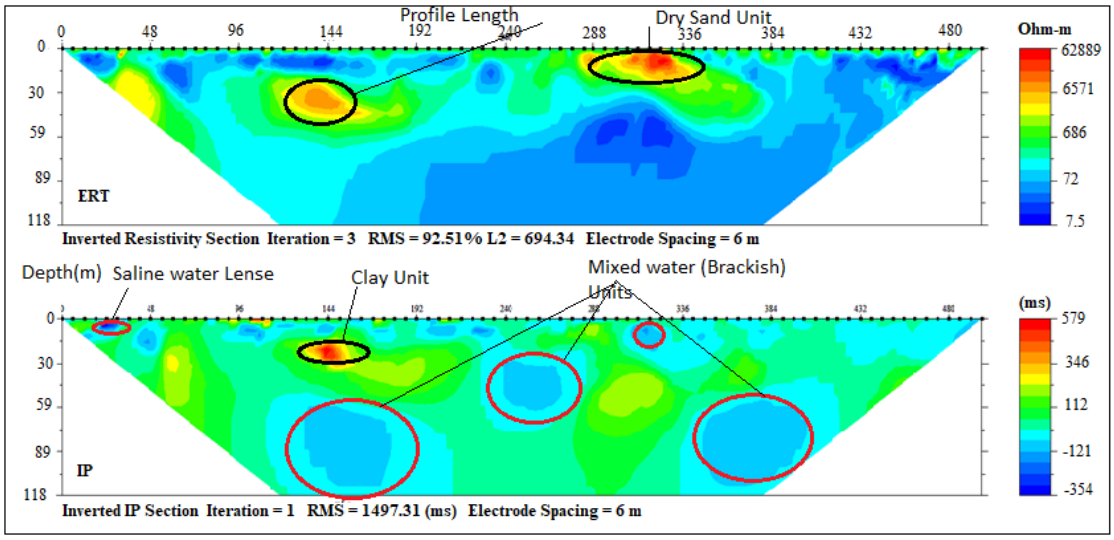

Figure 5.15 Inverted Resistivity and IP Cross-sections Ebute Ipare (Profile section 5).

At Abule-Obi, integrated ERT and IP sections P7 (Figure 5.16) also delineated three geoelectrical layers with resistivity and chargeability values ranges between (10 – 130 Ωm/80 – 300 ms), (1 – 70 Ωm/ 20 – 120 ms) and (1 – 50 Ωm/ 10 – 60 ms) which were indication of silty clay topsoil, sandy clay and fine-grain sand with clay lenses similar to Abule-Ipare section. The average thickness of these layers is 15, 27, and 63 m. Low resistivity and chargeability of the third layer indicate saline water intrusion.

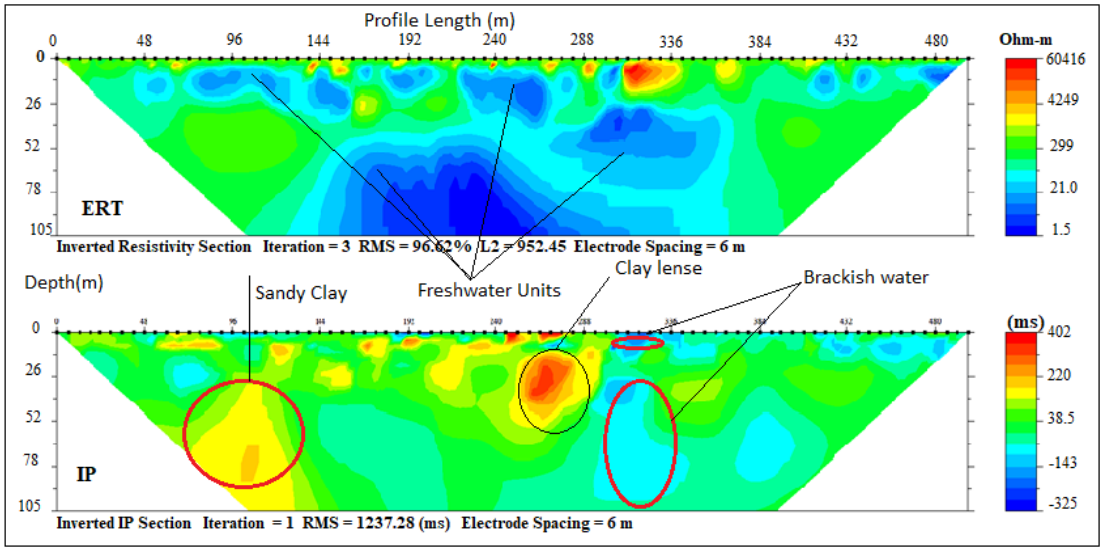

Figure 5.16 Inverted Resistivity and IP Cross-sections Abule-Obi (Profile section 7).

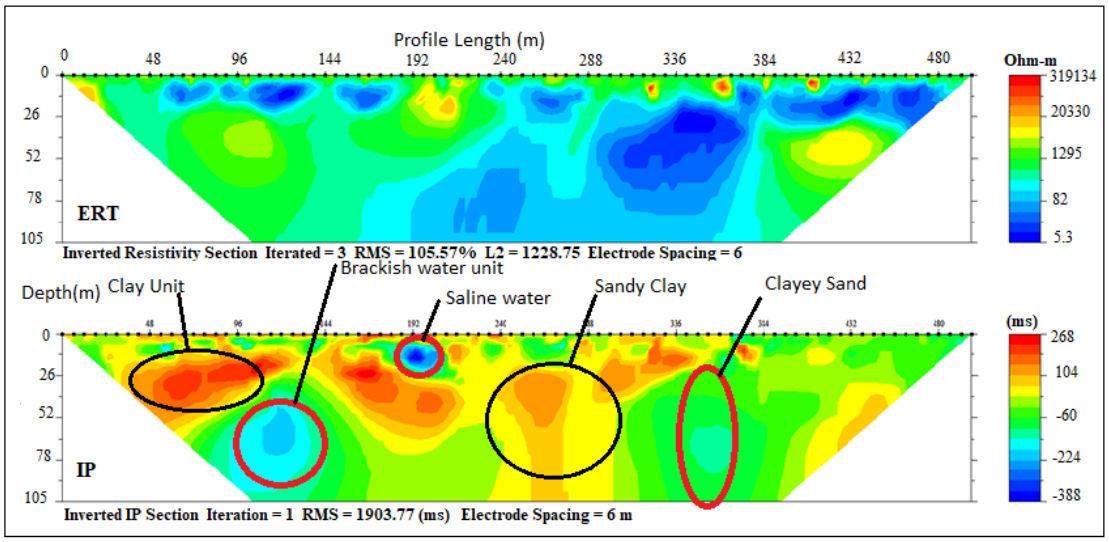

Figure 5.17 Inverted Resistivity and IP Cross-sections Araromi (Profile section 6).

ERT and IP Section P6 (Figure 5.17) carried out around Araromi village delineated only two distinct geoelectrical layers with resistivity values range between (1 - 20 /-200 Ωm – 10 ms) and (5 – 150 Ωm/80 – 20 ms) which is an indication of a silty sand topsoil and fine-grain sand with silty/clay lenses with 23 m and >76 m thick respectively (Figure 5.18). The second layer though predominantly clay has a portion of sandy clay which can be classified as the freshwater aquifer in the area which is well protected by the first layer of sandy clay, thus responsible for the relatively

improved water quality in this zone compared to Ugbonla and Igbokoda salt lenses trapped within the clayey layers. The general low resistivity observed in form of salt lenses in most of the sections which could be due to the effect of the ocean transgression and regression which occurred along this coast in past ages (Cretaceous to Tertiary), responsible for the deposition of the sediments that formed the strata (Francés et al., 2015; Igel et al., 2013; Obiora and Onwuka, 2005). Both resistivity and chargeability interpretations of these section with depths are presented in table 5.19.

Table 5.19 Lithological interpretation of Geoelectrical sections from Profile B-C.

Ebute – Ipare geoelectrical section			
Depth (m)	Resistivity (Ωm)	Chargeability (ms)	Lithological Description
0 - 25	50 - 496	-100 - 40	Unconsolidated sand (Top soil)
25 - 60	32 - 300	0 – 100	Sandy Clay
60 - 118	40 - 180	-40 - 20	Fine grain Sands
Abule-Obi geoelectrical section			
Depth (m)	Resistivity (Ωm)	Chargeability (ms)	Lithological Description
0 - 15	10 - 130	380 - 300	Silty Clay (Top soil)
15 - 42	1 - 70	20 – 120	Sandy Clay
42 - 105	1 - 50	10 - 60	Fine-grain sands with clay lenses
Araromi geoelectrical section			
Depth (m)	Resistivity (Ωm)	Chargeability (ms)	Lithological Description
0 - 23	1 - 120	-200 - 10	Saturated fine Sand (Top soil)
23 - 70	5 - 150	-80 – 200	Fin grain sandy with silt and clay

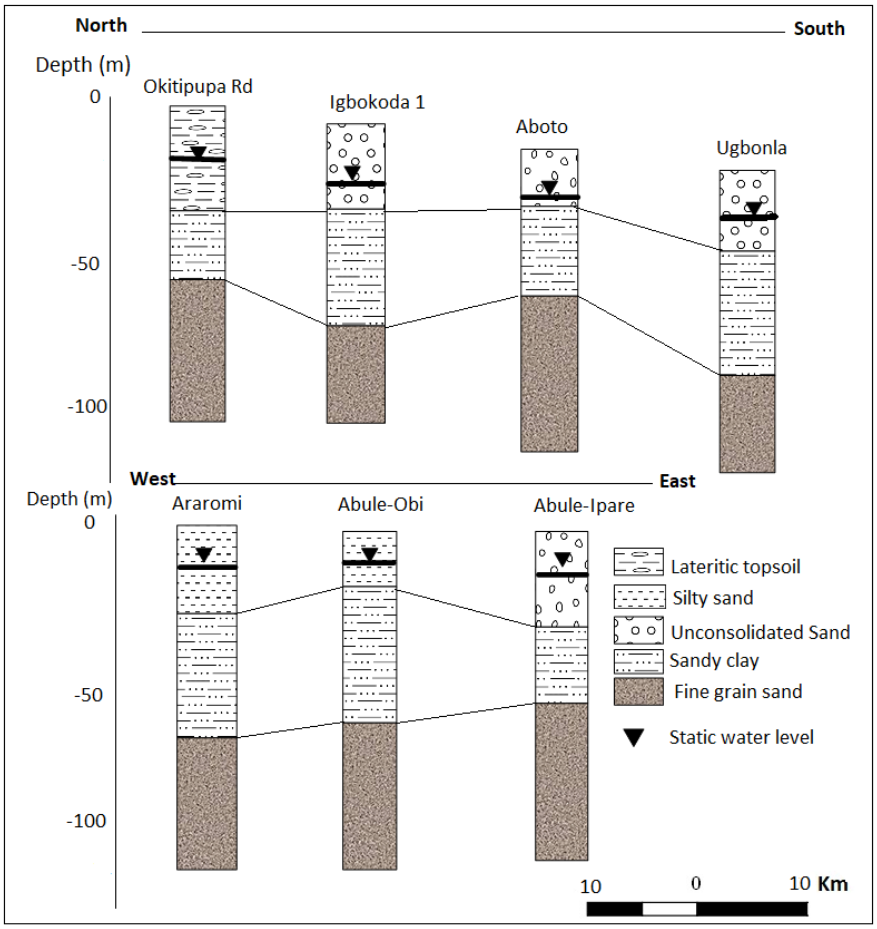

Figure 5.18 Lithological description of profile A-B and C-D.

Profile E-F (Figure 5.10) is located parallel to the coastline of Lagos and very close to areas with wells with enhanced electrical conductivity (EC) values suspected to be a fingerprint of saltwater intrusions as presented earlier in Figure 5.10. Locations such as Eleko, Lakowe and Okun-Ajjah were selected along profile line E-F.

Three (3) geoelectrical layers delineated under ERT and IP section P8 (Figure 5.19) with resistivity/chargeability ranging from (300 – 6000 Ωm/ -100 – 301 ms) – 300 and 300 – 400 Ωm /, 1 – 20 and 10 – 400 ms respectively. These lithological units are suspected to be dry loose sand, ferruginised clayey sand and sandy clay with the depth ranging 0 – 6, 6 – 45, and 45 – 118 m respectively.

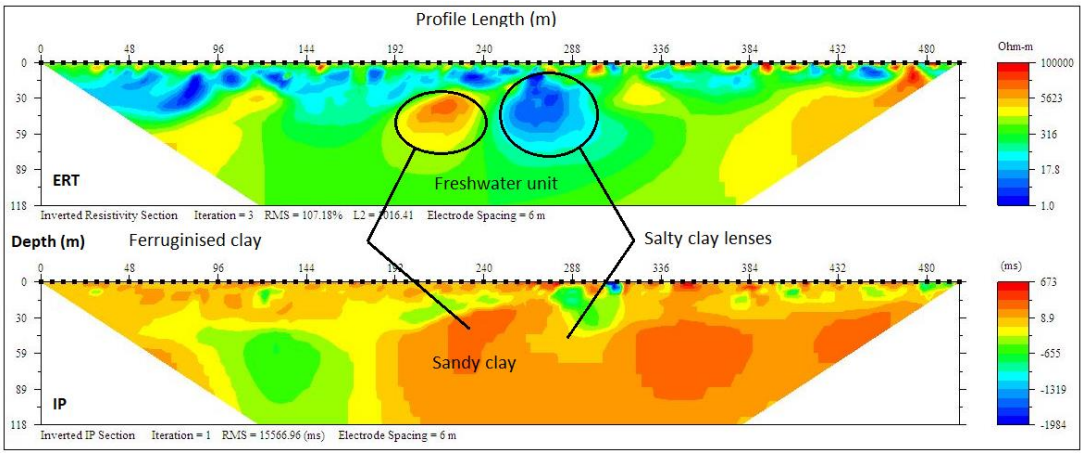

Figure 5.19 Inverted Resistivity and IP Cross-sections Eleko Profile E-F (Profile section 8).

The ERT and IP profile section P9 (Figure 5.20) at Lakwe revealed three layers with resistivity and chargeability (470 – 1605 Ωm/10 – 30 ms), (100 – 200 Ωm/-80 – 10 ms) and (200 -500 Ωm/-100 – 110 ms) respectively. These layers are suspected to be dry loose sand topsoil, sandy clay with lenses of brackish water and fine grain sands saturated with freshwater with a respective average depth of 8. 23 and 79 m.

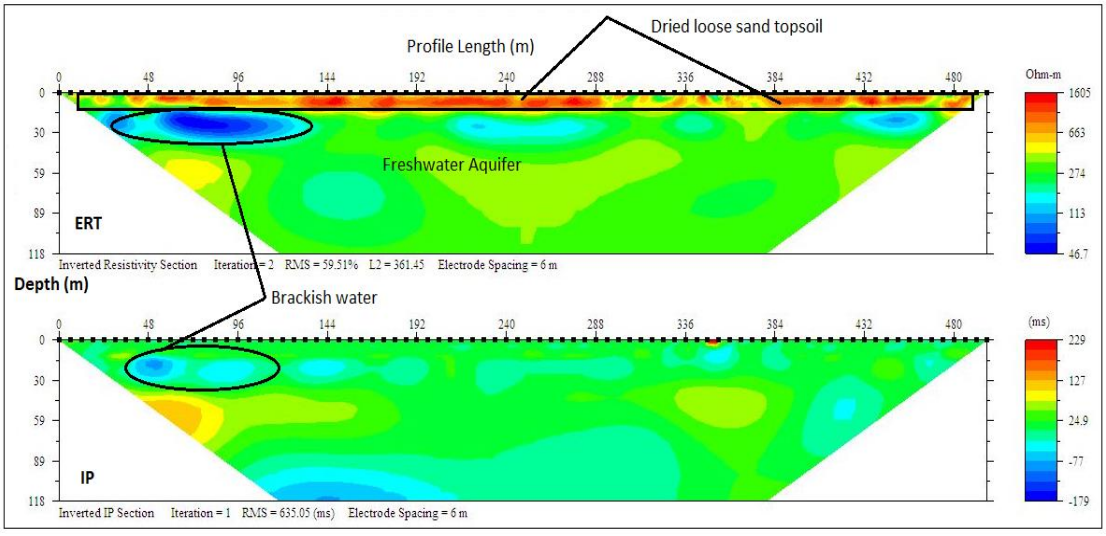

Figure 5.20 Inverted Resistivity and IP Cross-sections Lakowe (Profile section 9).

ERT and IP profile section P10 at Okun- Ajjah (Figure 5.21), like the previous ones, delineated three layers with resistivity/chargeability values ranging between

(100 -1000 Ωm/-10 – 60ms), (50 – 200 Ωm/-150 – 1 ms) and (7 – 30 Ωm/50 – 143 ms) from the top to the third layer. These values indicate loose dry sand and fine-medium grain sand and clay/sandy clay, with an average thickness of 15, 28 and 79 m. The first layers contain freshwater, while the underlining layers are saturated with saline water which could be attributed to the enhanced conductivity observed in water sampled from wells which are below 15 m at Okun Ajjah and Ogumbo. However, most of the wells in this zones are shallow wells which are generally below 20 m which are vulnerable to contamination and pollution from the surface water, while deeper wells are around Lekki, Victoria Island and Okun-Ajjah are tapping saline water. The interpretations of the three sections along this profile line is presented in Table 5.20 with lithostratigraphical sections presented in Figure 5.22.

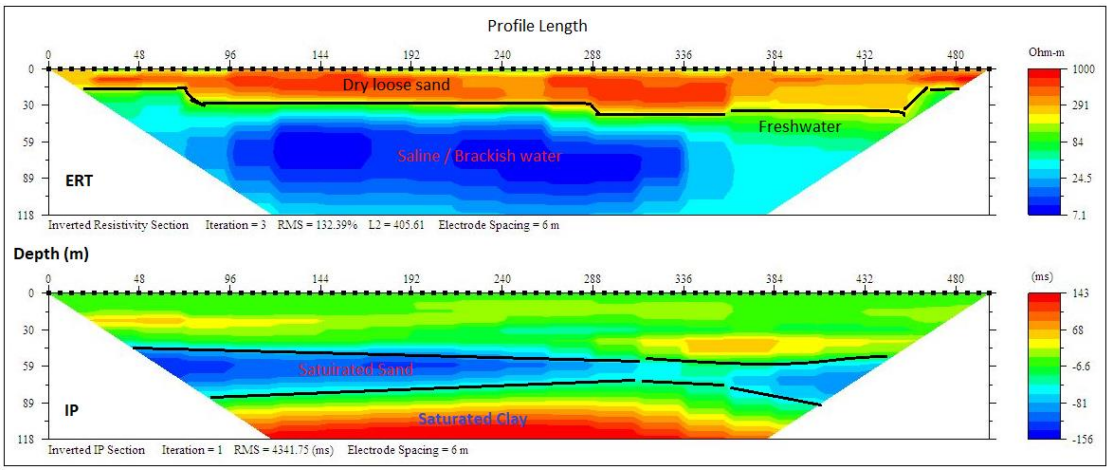

Figure 5.21 Inverted Resistivity and IP Cross-sections Okun-Ajjah (Profile section 10).

Table 5.20 Lithological interpretation of Geoelectrical sections from Profile E-F.

Eleko geoelectrical section			
Depth (m)	Resistivity (Ωm)	Chargeability (ms)	Lithological Description
0 - 6	300 - 6000	-100 - 30	Lateritic clayey sand
6 - 45	1 - 300	1 - 20	Clayey sand with clay lenses
45 - 118	300 - 400	10 - 400	Sandy clay
Lakowe geoelectrical section			
Depth (m)	Resistivity (Ωm)	Chargeability (ms)	Lithological Description
0 - 13	470 - 1605	10 - 30	Dry Loose sand
13 - 30	100 - 200	-80 – 10	Sandy Clay
30 - 118	200 - 500	-100 - 110	Fine grain Sands
Okun-Ajjah geoelectrical section			
Depth (m)	Resistivity (Ωm)	Chargeability (ms	Lithological Description
0 - 30	100 - 1000	-10 - 60	Dry loose sand
15 - 40	50 - 200	-150 – 1	Fine-medium grain sand
40 - 118	7 - 30	50 - 143	Clay –Sandy clay

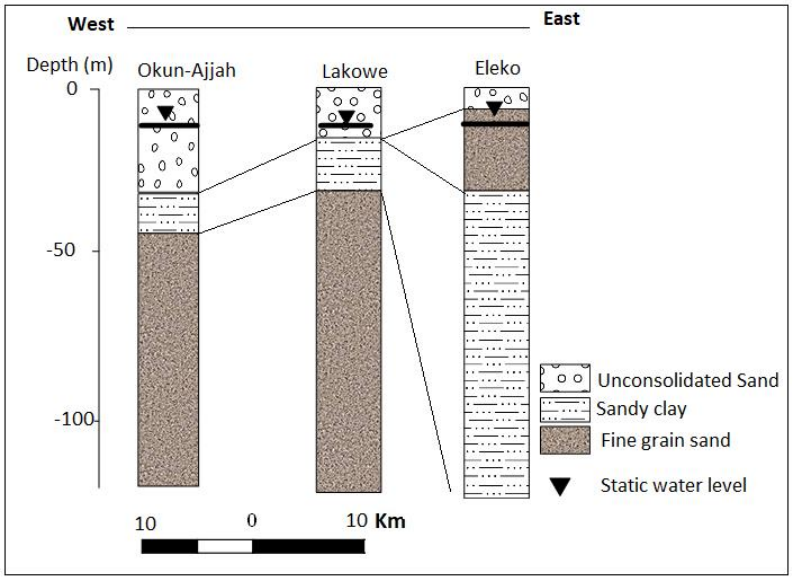

Figure 5.22 Litho-Log from ERT and IP from Profile E-F.

5.3.4.3 Correlation of the geoelectrical sections with borehole logs

Challenges are resulting from complex geo-electrical and hydrogeological characteristics such as electrical conductivity /resistivity and porosity / hydraulic conductivity of coastal lithology. This is commonly attributed to cumulative error from data acquisition and processing; it is necessary to apply this method together with other direct tools such as borehole logging for the subsurface investigation to increase confidence in results and outcome. The result of the ERT is therefore correlated with two borehole logs from both ends of the basin along profile A-B and E-F in a bid to confirm the lithological surface boundary as established from ERT and IP. Gama and ERT profiles alongside lithological log description are presented in Figures 5.23 and 5.24. The results confirm the presence of lower hydraulic conductivity in the second layer of sandy/silty clay which separated it from the top unconsolidated sandy to the silty sand unconfined aquifer and the third layer of confined fine-grained with clay lenses aquifer around Igbokoda and Ugbonla which experience enhanced conductivity in a few of the sampled boreholes. Also, correlation of sections with a borehole log (Figure 5.24) along with profile/traverse line E-F revealed a thick layer of saltwater saturated fine-grained sands, and silty clay around the Okun-Ajjah area of Lekki. The layers are overlain by unconsolidated loose sand which is common to entire Cretaceous to the recent coastal plain sand of the basin.

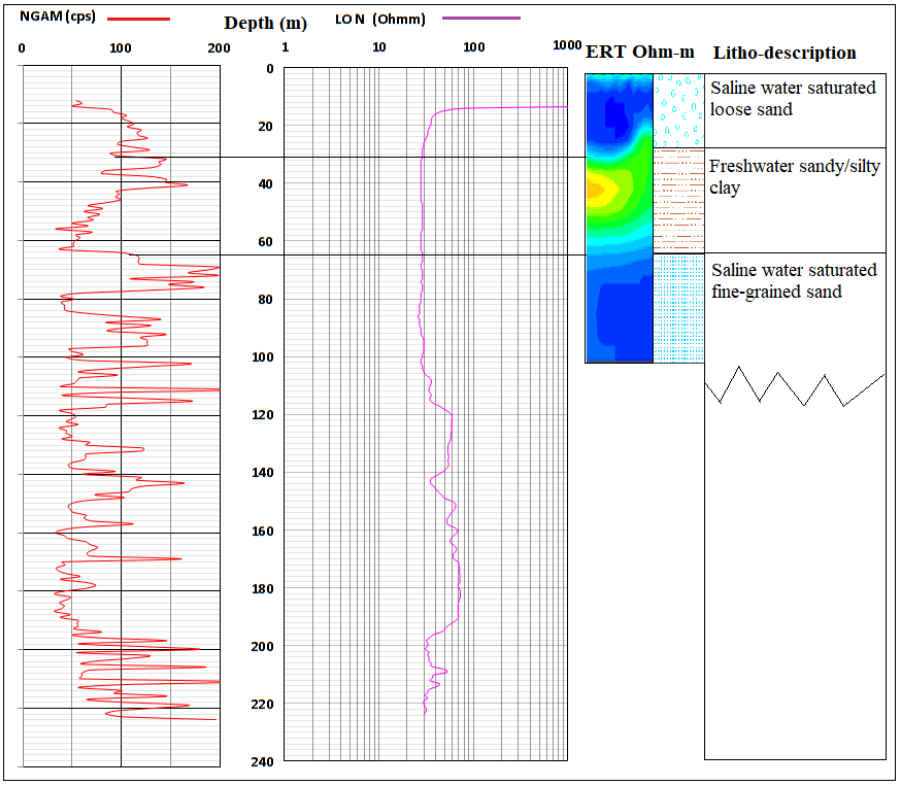

Figure 5.23 Correlation of Borehole Log with ERT Along Profile **A-B.**

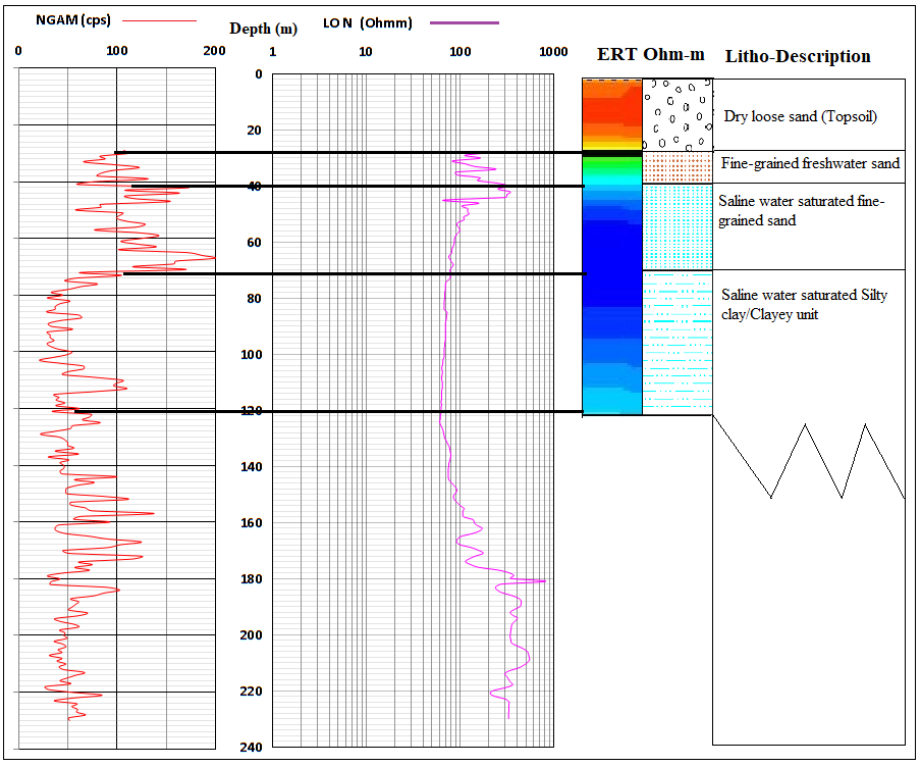

Figure 5.24 Correlation of Borehole Log at with ERT Along Profile **E-F.**

5.3.5 Conclusions

This study has conducted investigations to characterize the hydrostratigraphy of shallow coastal aquifer of the Eastern Dahomey Basin, Southwestern Nigeria. Enhanced electrical conductivity revealed from field physicochemical measurement across the basin, geophysical method of ERT and IP and a few borehole-loggings were carried out in locations around Igbokoda, Aboto, Ugbonla, Abule-Ipare, Abule Obi and Araromi, Okun-Ajjah, Lakowe and Eleko across the coastal communities of the basin.

These approaches have demonstrated a high level of efficiency and effectiveness in delineating lithological layers underlying the coaster aquifers and detected clay lenses which are possible sources of saltwater intrusion into the freshwater aquifer in the area. The results of the ERT and IP revealed intercalation of sand and clay underlying the coastal area. However, the maximum depth delineated along the traverses are 105m and 118 m from which 3 to 4 geoelectrical layers were mapped from which the resistivity and chargeability values indicated lateritic topsoil, unconsolidated sand, sandy clay/clayey sandy, fine grain sand with clay lenses.

Unconsolidated sands at the top constitute the unconfined aquifer which is underlain in most areas by sandy clay / clayey sand which serves as a semi-aquifer unit with depth ranges between 13m and 45 m while the third layer represents the fine-grained sands with clay lenses in some areas which characterised the Ondo-State axis of the coast. The results reveal the clay lenses in the second and third layers, which could be the trap of saltwater attributed to evaporite deposited within the basin during the ancient transgression and regression that produced deposition sediments. Some clay lenses suspected to contain saltwater also were delineated under the sections in Lakowe while thick sandy aquifer with an average thickness of 25 m saturated with

saline water was observed in the Okun-Ajjah profile sections. There is a thin layer of freshwater overlying this unit which is the source of freshwater recharging the shallow wells less than 20 m deep. This layer is highly vulnerable and sensitive to saline water intrusion if groundwater exploitation exceeds the current state. This type of intrusion is responsible for the enhanced electrical conductivity in most wells in the area which are drilled beyond 25 m. This situation is quite unsustainable since most of the freshwater units in this area generally reside within the unconfined or semi-confined aquifer which is vulnerable to contamination from polluted surface water and leachates from industrial and municipal waste that characterise this densely populated coastal zone.

Finally, the methods used have identified two possible sources of saltwater intrusion into the coastal freshwater aquifer of Eastern Dahomey Basin; namely dissolution of evaporite/salt lenses within the clay layer and direct (flow boundary) connection between the sea and the coastal aquifer in areas very close to the sea due to lack of hydraulic boundary. For a further understanding of the saltwater within the coastal areas of this basin, it is, therefore, necessary to use another method such as hydrochemistry and Isotope. Finally, a detail saltwater vulnerability map of the area is necessary to develop a sustainable groundwater management strategy to protect this fragile resource from further deterioration.

Author Contributions: J.A. A. and R.M.K. designed the research; J.A. A. wrote the original draft.; R.M.K., P. S. and I. H. reviewed and edited the manuscript; R.M.K. gave critical views on the manuscript for further improvement.

Funding: This research was funded by the Nigeria Tertiary Education Trust Fund (TETFUND and supported by the Scottish Government under the Climate Justice Fund Water Futures Programme, awarded to the University of Strathclyde (R.M. Kalin)

Acknowledgments: The authors would like to gratefully acknowledge Ismail Babatunde, Sanni Babatunde and Damilola Bolaji Ajibola for field assistance durin data acquisition.

Conflicts of Interest: The authors declare no conflict of interest.

5.3.6 References

Abdulrahman, A., Nawawi, M., Saad, R., Abu-Rizaiza, A.S., Yusoff, M.S., Khalil, A.E., Ishola, K.S., 2016. Characterization of active and closed landfill sites using 2D resistivity/IP imaging: case studies in Penang, Malaysia. Environ. Earth Sci. 75, 1–17. https://doi.org/10.1007/s12665-015-5003-5

Adegoke, O.S. and Omatsola, M.E., 1981. Tectonic Evolution and Cretaceous Stratigraphy of the Dahomey Basin. Niger. J. Min. Geol. 18, 130–137.

Adelana, S.M.A., Olasehinde, P.I., Bale, R.B., Vrbka, P., Edet, A.E., Goni, I.B., 1996. An overview of the geology and hydrogeology of Nigeria. Q. J. Eng. Geol. Hydrogeol. 29, S1–S12. https://doi.org/10.1144/GSL.QJEGH.1996.029.S1.01

Adeoti, L., Alile, O.M., Uchegbulam, O., 2010. Geophysical investigation of saline water intrusion into freshwater aquifers: A case study of Oniru, Lagos State. Sci. Res. Essays 5, 248–259.

Adepelumi, A.A., Ako, B.D., Ajayi, T.R., Afolabi, O., Omotoso, E.J., 2009. Delineation of saltwater intrusion into the freshwater aquifer of Lekki Peninsula, Lagos, Nigeria. Environ. Geol. 56, 927–933. https://doi.org/10.1007/s00254-008-1194-3

Aluko, K.O., Raji, W.O., Ayolabi, E.A., 2017. Application of 2-D resistivity survey to groundwater aquifer delineation in a sedimentary terrain : A case study of south-western Nigeria 71–79.

Ayolabi, E. a, Folorunso, A.F., Odukoya, A.M., Adeniran, A.E., 2013. Mapping saline water intrusion into the coastal aquifer with geophysical and geochemical techniques : the University of Lagos campus case (Nigeria). Springer plus 2, 1–14. https://doi.org/10.1186/2193-1801-2-433

Ayolabi, Elijah A, Enoh, I.J.E., Folorunso, A.F., 2013. Engineering Site Characterisation Using 2-D and 3-D Electrical Resistivity Tomography. Earth Sci. Res. 2. https://doi.org/10.5539/esr.v2n1p133

Ayolabi, E.A., Epelle, E.S., Lucas, O.B., Ojo, A., 2014. Geophysical and geochemical site investigation of eastern part of Lagos metropolis, southwestern Nigeria. Arab. J. Geosci. 8, 7445–7453. https://doi.org/10.1007/s12517-014-1688-0

Ayolabi, Elijah Adebowale, Folorunso, A.F., Kayode, O.T., 2013. Integrated Geophysical and Geochemical Methods for Environmental Assessment of Municipal Dumpsite System. Int. J. Geosci. 4, 850–862. https://doi.org/10.4236/ijg.2013.45079

Ayolabi, E.A., Oyelayo, F.J., 2005. Geophysical and hydrochemical assessment of groundwater pollution due to a dumpsite in Lagos state, Nigeria. J. Geol. Soc. India 66, 617–622.

Buselli, G., Lu, K., 2001. Groundwater contamination monitoring with multichannel electrical and electromagnetic methods. J. Appl. Geophys. 48, 11–23. https://doi.org/10.1016/S0926-9851(01)00055-6

Cary L., Petelet-Giraud E., Bertrand G., Kloppmann W., Aquilina L., Martins V., Hirata R., Montenegro S., Pauwels H., Chatton E., Franzen, M. and Aurouet A., 2015. Origins and processes of groundwater salinization in the urban coastal aquifers of Recife (Pernambuco, Brazil): A multi-isotope approach. Sci. Total Environ. 530–531, 411–429. https://doi.org/10.1016/j.scitotenv.2015.05.015

Creel, L., 2003. Ripple effects: Population and coastal regions. Popul. Ref. Bur. 8.

de Franco, R., Biella, G., Tosi, L., Teatini, P., Lozej, A., Chiozzotto, B., Giada, M., Rizzetto, F., Claude, C., Mayer, A., Bassan, V., Gasparetto-Stori, G., 2009. Monitoring the saltwater intrusion by time lapse electrical resistivity tomography: The Chioggia test site (Venice Lagoon, Italy). J. Appl. Geophys. 69, 117–130. https://doi.org/10.1016/j.jappgeo.2009.08.004

Edet, A., 2016. Hydrogeology and groundwater evaluation of a shallow coastal aquifer, southern Akwa Ibom State (Nigeria). Appl. Water Sci. https://doi.org/10.1007/s13201-016-0432-1

Edet, A., 2014. An aquifer vulnerability assessment of the Benin Formation aquifer, Calabar, southeastern Nigeria, using DRASTIC and GIS approach. Environ. Earth Sci. 71, 1747–1765. https://doi.org/10.1007/s12665-013-2581-y

Edet, A.E., Merkel, B.J., Offiong, O.E., 2003. Trace element hydrochemical assessment of the Calabar Coastal Plain Aquifer, southeastern Nigeria using statistical methods. Environ. Geol. 44, 137–149. https://doi.org/10.1007/s00254-002-0738-1

Francés, A.P., Ramalho, E.C., Fernandes, J., Groen, M., Hugman, R., Khalil, M.A., De Plaen, J., Monteiro Santos, F.A., 2015. Contributions of hydrogeophysics to the hydrogeological conceptual model of the Albufeira-Ribeira de Quarteira coastal aquifer in Algarve, Portugal. Hydrogeol. J. 23, 1553–1572. https://doi.org/10.1007/s10040-015-1282-x

Günther, T., Dlugosch, R., 2010. Aquifer characterization using coupled inversion of DC/IP and MRS data on a hydrogeophysical test-site. 23rd EEGS Symp. 302–307. https://doi.org/doi:10.4133/1.3445447

Igel, J., Günther, T., Kuntzer, M., 2013. Ground-penetrating radar insight into a coastal aquifer: The freshwater lens of Borkum Island. Hydrol. Earth Syst. Sci. 17, 519–531. https://doi.org/10.5194/hess-17-519-2013

Izbicki, J.A., 1996. Seawater intrusion in a coastal California aquifer. Califonia.

Jones, H. A and Hockey, R.., 1964. The Geology of part of Southwestern Nigeria. GSN Bull. No. 31-10.

Khalil, M.H., 2006. Geoelectric resistivity sounding for delineating salt water intrusion in the Abu Zenima area, west Sinai, Egypt. J. Geophys. Eng. 3, 243. https://doi.org/10.1088/1742-2132/3/3/006

Lapworth, D.J., Krishan, G., MacDonald, A.M., Rao, M.S., 2017. Groundwater quality in the alluvial aquifer system of northwest India: New evidence of the extent of anthropogenic and geogenic contamination. Sci. Total Environ. 599–600, 1433–1444. https://doi.org/10.1016/j.scitotenv.2017.04.223

Longe, E.O., 2011. Groundwater Resources Potential in the Coastal Plain Sands Aquifers , Lagos, Nigeria 3, 1–7.

Longe, E.O., Malomo, S., Olorunniwo, M.A., 1987. Hydrogeology of Lagos metropolis. J. African Earth Sci. 6, 163–174. https://doi.org/10.1016/0899-5362(87)90058-3

McInnis, D., Silliman, S., Boukari, M., Yalo, N., Orou-Pete, S., Fertenbaugh, C., Sarre, K., Fayomi, H., 2013. Combined application of electrical resistivity and shallow groundwater sampling to assess salinity in a shallow coastal aquifer in Benin, West Africa. J. Hydrol. 505, 335–345. https://doi.org/10.1016/j.jhydrol.2013.10.014

Mulrennan, M.E., Woodroffe, C.D., 1998. Saltwater intrusion into the coastal plains of the Lower Mary River, Northern Territory, Australia. J. Environ. Manage. 54, 169–188. https://doi.org/10.1006/jema.1998.0229

Obiora, D.N., Onwuka, O.S., 2005. Groundwater Exploration in Ikorodu , Lagos-Nigeria : A Surface Geophysical Survey Contribution. Pacific J. Sci. Technol. 6.

Odukoya, A.M., Folorunso, A.F., Ayolabi, E.A., Adeniran, E.A., 2013. Groundwater Quality and Identification of Hydrogeochemical Processes within University of Lagos, Nigeria. J. Water Resour. Prot. 5, 930–940. https://doi.org/10.4236/jwarp.2013.510096

Offodile, M.E. (1971), 1971. The Hydrogeology of Coastal Areas of Southeastern states of Nigeria., Unpublished Geological survey of Nigeria Report.

Okunlola, O.A., Adeigbe, O.C., Oluwatoke, O.O., 2009. Compositional and Petrogenetic Features of Schistose rocks of Ibadan area , Southwestern Nigeria. Earth Sci. Res. J. 13, 119–133.

Oluwafemi, A., Jakpor, P., Bohme, S., Kishimoto, S., Lobina, E., 2016. Lagos Water Crisis Alternative Roadmap for Water Sector. Lagos.

Omosuyi, G.O., Ojo, J.S., Olorunfemi, M.O., 2008. Geoelectric Sounding to Delineate

Shallow Aquifers in the Coastal Plain Sands of. Pacific J. Sci. Technol. 9, 62–77.

Oteri, A.U., & Atolagbe, F.P., 2003. Saltwater Intrusion into Coastal Aquifers in Nigeria, in: The Second International Conference on Saltwater Intrusion and Coastal Aquifers Monitoring, Modeling, and Management. Mérida, Yucatán, México, March 30 - April 2, 2003. Merida Yucatan, pp. 1–15.

Oteri, A.U., 1991. Geophysical investigations of sea water intrusion into the Cainozoic aquifers of South Coast Kenya - a review. J. African Earth Sci. 13, 221–227. https://doi.org/10.1016/0899-5362(91)90006-K

Oteri, A.U., 1981. Geoelectric investigation of saline contamination of a chalk aquifer by mine drainage water at Tilmanstone, England. Geoexploration 19, 179–192. https://doi.org/10.1016/0016-7142(81)90002-8

Oteri, A.U. and R.A.A., 2008. The Lagos Megacity Project :, Water, Megacities and Global Change.

Oyelami A. C., Ojo O. A., Aladejana J. A. and Agbede O.O., 2013. Assessing the Effect of a Dumpsite on Groundwater Quality : A Case Study of Aduramigba Estate within Osogbo Metropolis . J. Environ. Earth Sci. 3, 120–131.

Oyeyemi, K.D., Aizebeokhai, A.P., Oladunjoye, M.A., 2015. Integrated Geophysical and Geochemical Investigations of Saline Water Intrusion in a Coastal Alluvial Terrain, Southwestern Nigeria. Int. J. Appl. Environ. Sci. ISSN 10, 973–6077.

Tran, L.T., Larsen, F., Pham, N.Q., Christiansen, A. V., Tran, N., Vu, H. V., Tran, L. V., Hoang, H. V., Hinsby, K., 2012. Origin and extent of fresh groundwater, salty paleowaters and recent saltwater intrusions in Red River flood plain aquifers, Vietnam. Hydrogeol. J. 20, 1295–1313. https://doi.org/10.1007/s10040-012-0874-y

Wu, M.-L., Wang, Y.-S., Sun, C.-C., Wang, H., Dong, J.-D., Yin, J.-P., Han, S.-H., 2010. Identification of coastal water quality by statistical analysis methods in Daya Bay, South China Sea. Mar. Pollut. Bull. 60, 852–860. https://doi.org/10.1016/j.marpolbul.2010.01.007

5.4 Concluding remarks

This chapter presented the preliminary investigation of the hydrogeological assessment of groundwater in the Eastern Dahomey Basin. Due to the size of the

Nigerian part of the basin and its economic importance, it also offers with realistic scope for a PhD research, however, a comprehensive and detailed hydrogeology studies are required. It was necessary strategic to conduct a preliminary study to gain an idea of possible hot spots for detailed investigation.

In light of the above, a combination of hydrochemical and geophysical approaches was employed that lead to the two article publications. The primary aim was to characterise the shallow aquifers of the basin to give an idea of the aquifer geometry concerning different lithology and the groundwater chemistry to identify possible hydrogeochemical anomalies that serve as a fingerprint for groundwater quality status.

Field physicochemical parameters and major ions analysis and groundwater quality indices such as electrical conductivity, hydrochemical facies evolution diagram (HFE-D), ionic ratios, chloride concentrations, saltwater mixing index (SMI) and groundwater quality index for saltwater intrusion (GQIswi), were employed. Integrating these results identified groundwater samples with enhanced conductivity in some areas which was attributed to possible saltwater intrusions and anthropogenic influence. This result led to the selection of area where the geophysical investigation was carried out.

For effective hydrostratigraphical characterisation of the shallow groundwater aquifers of the basin, non-invasive geophysical method electrical resistivity tomography (ERT) and induced polarization (IP) which have historical success in such a task was used. The results identified sandy units and clay lenses within the aquifer units in areas within 2-5 km from the coastlines especially regions where groundwater abstraction is relatively higher.

One or a combination of these two methods have been used in hydrogeological studies around the world especially in case studies. However, this study is the first to combine all these methods to characterise a basin as large as Eastern Dahomey in southwestern Nigeria. Due to the paucity of data in developing countries of sub-Saharan Africa, the data and results from this study have advanced the data gathering and information on groundwater studies for policymakers and further research. Further sampling and more detailed studies on groundwater quality are conducted in the subsequent chapters.

5.5 Supplementary Information

Paper 1

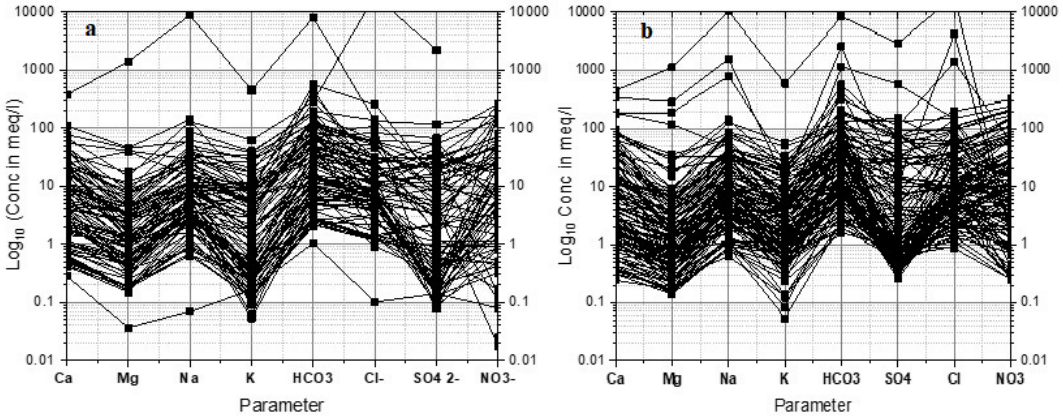

Schoeller diagram for regional groundwater samples (a) Wet season (b) dry season

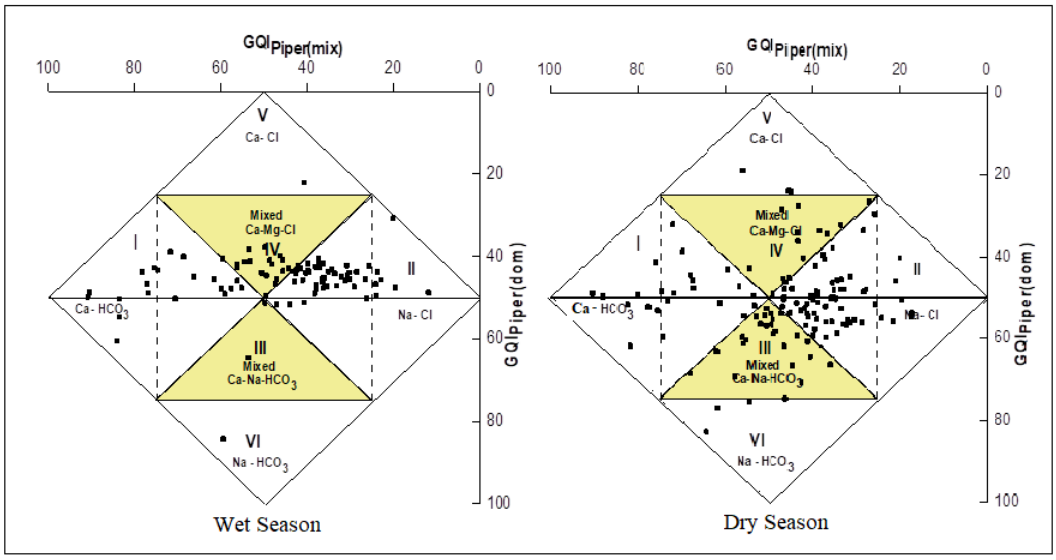

Modified Piper diagram for saltwater mixing for both wet and dry seasons

Paper 2

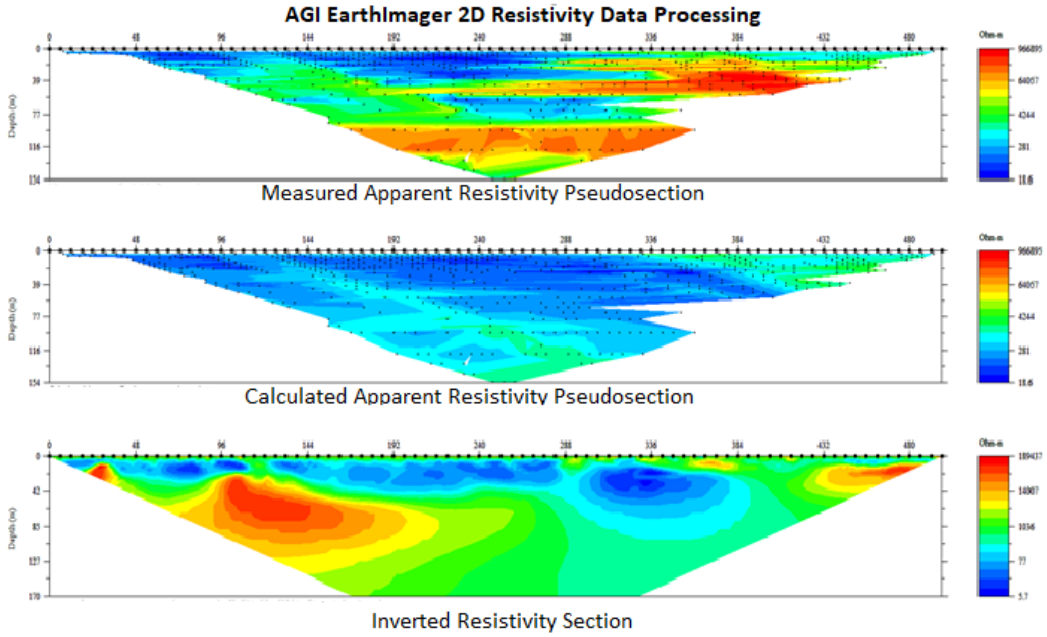

Computer Simulation for electrical resistivity data processing Image

Chargeability of some minerals, materials and rocks (Telford et al. 1990)

S/N	Material	Chargeabilities (ms)
1	Groundwater	0
2	Alluvium	1 - 4
3	Gravels	3 – 9
4	Sandstones Materials	3 - 12
5	Argillites	3 - 10
6	Quartzites	5- 12
7	20% Sulfides	2000 - 3000
8	8-20% Sulfides	1000 - 2000
9	2-8% Sulfides	500 - 1000
10	Sandstone Siltstone	100 - 500
11	Shale	50 - 100
12	Limestone	10 - 20

Chargeability of some minerals (Telford et al. 1990)

S/N	Mineral	Chargeabilities (ms)
1	Pyrite	13.4
2	Chalcocite	13.2
3	Copper	12.3
4	Graphite	11.2
5	Chalcopyrite	9.4
6	Bornite	6.3
7	Galena	3.7
8	Magnetite	2.2
9	Malachite	0.2
10	Hematite	0.0

Resistivity values range for different lithological unit

S/N	Resistivity (Ω-m)	Sediment/Rock	Description	TDS (mg/l)
1	0.5 - 2.0	Very porous sand, or saturated clay	Seawater, very saline water	20,000
2	2.0 - 4.5	Porous Sand, or Saturated Clay	Saline water	10,000
3	4.5 - 10.0	Sandy Saturated or Sandy Clay	Salty Brackish water	10,000 -1,500
4	10.0 - 15.0	Sandy Clay, Sandy gravel	Brackish water	1,500 - 700
5	15.0 - 30.0	Sand, gravel, some clay	Poor quality freshwater	700 - 100
6	30.0 - 70.0	Sand, gravel, minor clay	Intermediate quality fresh water	100 - 50
7	70.0 - 100.0	Sand, gravel, no clay	Good quality fresh water	50 - 20
8	More than 100.0	Coarse sand, gravel, no clay	Very good quality fresh water	Less than 20

CHAPTER 6

6.0 GEOCHEMISTRY OF SHALLOW AQUIFER'S GROUNDWATER

6.1 Preamble

The outcome of Chapter 5 revealed impact of both natural and human activities within the Eastern Dahomey Basin. Elevation in the concentration of major ions and trace metals found in some of the wells and boreholes sampled are evident in this conclusion. Most of the affected wells are said to be within the proximity of the sea and some within the flood plain of the channels of the river. There is a need to employ an integrated hydrochemical and stable isotopes method to better understand the evolution of the groundwater of the study basin especially with regard to the multi-aquifer system and complex geology that characterise this basin.

The current chapter employed hydrochemical and stable isotopes of oxygen and hydrogen to understand hydrogeochemical processes which control the evolution of groundwater within the basin. The study lead to a research article which is under review in an Elsevier Journal; Results in Geochemistry (2020) as presented below;

- Jamiu A. Aladejana, Robert M. Kalin, Ibrahim Hassan, Moshood N. Tijani and Philippe Sentenac. 2020. Hydrogeochemical and Isotopic Characterization of Coastal Groundwater of Eastern Dahomey Basin, Southwestern Nigeria. ***Under review*** in Elsevier Journal; *Results in Geochemistry*. Manuscript number; RINGEO-D-20-00006

  The article presents the efforts in characterisation of the groundwater of the shallow aquifer of the basin with a view to identifying the dominant hydrogeological processes that influence the groundwater chemistry. The research was designed

under the supervision of my supervisor, Prof. Robert M. Kalin with critical review of the manuscript, while technical contributions were made by Dr Philippe Sentenac, Ibrahim Hassan and Prof. Moshood N. Tijani.

6.2 Paper 3

Jamiu A. Aladejana, Robert M. Kalin, Ibrahim Hassan, Moshood N. Tijani and Philippe Sentenac. 2020. Hydrogeochemical and Isotopic Characterization of Coastal Groundwater of Eastern Dahomey Basin, Southwestern Nigeria. *Under review* in Elsevier Journal; *Results in Geochemistry*

Hydrogeochemical and Isotopic Characterization of Coastal Groundwater of Eastern Dahomey Basin, Southwestern Nigeria

Jamiu A. Aladejana[1,2], Robert M. Kalin[1], Ibrahim Hassan[1,3] Moshood N. Tijani[2] and Philippe Sentenac[1]

[1] *Department of Civil and Environmental Engineering University of Strathclyde Glasgow;*
[2] *Department of Geology, University of Ibadan*
[3] *Department of Civil Engineering Abubakar Tafawa Balewa University Bauchi, Nigeria;*
Corresponding email; Jamiu.aladejana@strath.ac.uk

6.2.1 Abstract

Hydrogeochemical and isotopic evolution of groundwater was investigated in the multi-aquifer system within the geological units of the Eastern Dahomey Basin (EDB), Southwestern Nigeria. The EDB is the eastern part of a large sedimentary sequence of the transboundary Benin Basin which runs along the West African coast. The EDB is characterised by Abeokuta, Ewekoro, Ilaro, Alluvium deposits and Coastal plain sands aquifer with 2 to 5 aquiferous layers. A total of 250 water samples were collected between May 2017 and April 2018 from the shallow boreholes and hand-dug wells for physicochemical, and Oxygen and Hydrogen isotopes analysis. The groundwaters were mainly Na–Cl, Ca-HCO_3 and Ca–Cl types and Ca–Na–NO_3–Cl–HCO_3 with mixed facies such as Na–HCO_3, Na-SO_4, Ca-SO_4, K-Cl, K-SO_4 and Mg–HCO_3 types. The groundwaters were dominantly classified as fresh on the basis of TDS results, which were generally less than 1000mg/l except in a few locations. Inferred water-rock interactions with calcite and aragonite (possible dolomite), gypsum/anhydrite,

and secondary halite correlate with the geology of the basin. When plotted using Gibbs diagrams major ion chemistry suggests mineral dissolution through rock-water interaction, carbonate precipitation and evaporation/sea spraying as the geogenic factors controlling the water chemistry, with secondary contributions from anthropogenic sources such as industrial, agricultural and municipal waste. The isotopic contents of groundwaters ranged from -5.19 to 0.33 ‰ and -4.03 to 0.83 ‰ for $\delta^{18}O$ and -32.5 to 2.3 ‰ and -19.7 to 7.5 ‰ for δD in wet and dry seasons respectively. These results showed isotopic enrichment in the dry season due to evaporation. The conventional δD-$\delta^{18}O$ diagram with data points plotted along the Global Meteoric Water Line (GMWL) indicates that the groundwaters from the wet season are recent and are of meteoric origin, and have not been affected by evaporation while those of the dry season show short-range clustering, which signifies a similar origin with the fingerprint of evaporation effect. Groundwater in shallow aquifer of the Eastern Dahomey Basin was classified as being young from a meteoric source, which is still in the early stage of geochemical evolution.

Keywords; Hydrogeochemistry; Mineral dissolution; Saturation Index; Groundwater; Stable Isotopes

6.2.2 Introduction

Groundwater is an essential natural resource needed in both urban and rural environments (Stephen et al. 2004). The level of appreciation of this resource is far less than its importance (Oke *et al.*, 2016). In many areas groundwater is preferred as a water supply in homes, farms and industries because it is considered to be relatively safe from contamination and pollution, and is also cheaper in terms of cost of development and accessibility. Coastal basins offer valuable land, water and economic

resources and have high economic contribution to national and global development; hence the high population of coastal cities around the world due to their commercial, industrial and agricultural significance. The rapid expansion of industries and urbanisation trigger unplanned groundwater development leading to severe stress on groundwater resources in the coastal groundwater basins around the world (Guendouz *et al.*, 2003; Priyantha Ranjan *et al,* 2006; Narany *et al.*, 2014). Some of the cities and towns situated in coastal parts of Africa and Asia rely on the freshwater of the coastal aquifers to meet the vast shortage in water supply resulting from infrastructural deficiency and decay (Adimalla and Kumar, 2020) (Kumar, 2010).

In most developing countries especially in sub-Saharan Africa, due to the complexity of groundwater occurrence and distribution in basement aquifers, the source of freshwater depends on the groundwater resources within these basins, known for high freshwater potential. The Eastern Dahomey Basin (EDB) is not an exemption. This basin hosts cities such as Lagos, Abeokuta, Ijebu, Okitipupa, Igbokoda, Epe and other towns and villages. The high rate of population growth, unpredictable rainfall patterns, rise in sea-levels, coupled with over abstraction and seawater intrusion due to human activities impact groundwater resources.

Groundwater chemistry evolves as a result of hydrogeochemical processes during infiltration and flow in aquifers over space and time (Bodrud-Doza et al., 2019; Kalin, 1995; Narany et al., 2014; Prasanna et al., 2011; Talabi and Tijani, 2013). In watershed and groundwater aquifers, hydrochemical processes such as cation exchange, evaporation, dissolution / precipitation of minerals, seawater intrusion, oxidation-reduction and biological processes play significant roles in the hydrochemical evolution of groundwater (Adimalla and Kumar, 2020; Narany et al.,

2014; Somaratne and Frizenschaf, 2013). Land-use activities, climate conditions, and the geological setting have significant influence on groundwater chemistry. Un-engineered irrigation and drainage system which characterise coastal areas increase the vulnerability of the freshwater to contamination and alteration of groundwater chemistry as metals and nutrient leach through the soil and end up in the water as it percolates through the vadose zone.

Studies of the major ions have been used to identify the hydrochemical facies of groundwater (Edet, 2016; Kalin, R.M. and Long, 1994; Tijani et al., 2014). Several researchers have carried out assessments of groundwater chemistry and considered hydrogeochemical processes by developing geochemical modelling and adopting graphical methods for the interpretation of water quality indices. The EDB is endowed with mineral resources which include Kaolin, Gypsum, Limestone, Bentonite, Phosphate, Silica sand, Bitumen, Feldspar, Gemstone, Granite and some accessory minerals that occur in association with these major minerals (Alfred et al., 2016; Oke, 2015; Olabode and Mohammed, 2016). Furthermore, due to the alternation of the wet and dry season in this area, the weathering rate is high, enhancing the leaching of ions and metals into groundwater during flow within the aquifer.

Abimbola *et. al.* (1999) identified groundwater of Calcium-bicarbonate and Sodium and Calcium-Chloride water types around Abeokuta and its environs which were attributed to both rocks and sea influence. Talabi et al, (2012); Oke et al, (2016), in their studies also identified similar groundwater types in areas around the Abeokuta formation which was attributed to sea spraying from the Gulf of guinea. High sodium bicarbonate water type in part of the Eastern Dahomey Basin was attributed to the chemical weathering of Kaolinite to Albite (Abimbola et la, 1999; Oke and Aladejana 2012). Several studies indicated the role of other processes such as evaporation and

limited discharge, which lead to mineral precipitation in the aquifer. Longe et al, 1987; Longe and Balogun, 2010; Ayolabi et al, 2013; Ayolabi *et al.*, 2014 identified the impact of sewage and leachates from the landfill site and municipal wastes on groundwater quality within the metropolitan city of Lagos. Oteri & Atolagbe, 2003; Adepelumi *et al.*, 2009; Ayolabi *et al.*, 2014 identified elevated salinity in groundwater collected from tube wells and boreholes around Oniru, Victoria Island area of Lagos, attributed to saltwater intrusion. None of these studies evaluated the combination of chemistry and stable isotopes to see how the groundwater evolved with insight to origin and hydrochemical dynamics. This study is among the first to look into the groundwater chemistry and origin across the EDB in relation to groundwater flows and hydrochemical dynamism across the Basin, and was carried out to delineate the main hydrogeochemical processes that control groundwater chemistry. It provides an overview of the spatial distribution of selected minerals that characterised typical basin groundwater, using GIS and interpolation techniques. It was conducted on two sets of groundwater samples collected in different seasons to determine the possible influence of seasonal variations on groundwater recharge and hydrochemical processes.

6.2.2.1 Study area

The Eastern Dahomey Basin is located in the South-Western part of Nigeria. It lies between Latitudes 2° 41'10.00" and 4° 59'59.00" N and Longitudes 6°21'13.00" and 7°52'42.00"E along the coast of the Gulf of Guinea (Figure 6.1). The Dahomey Basin is one of the sedimentary basins located along the Gulf of Guinea which stretches through four countries which include Nigeria, Ghana, Benin Republic and the Republic of Togo. The other basins located around this area are; Ivory Coast, Tano, Saltpond, Central and Keta. The Dahomey Basin, also known as the Benin Embayment, is part of a system of West African peri-cratonic (margin sag). The basin

covers much of the continental margin of the Gulf of Guinea, extending from the Volta-delta in Ghana on the West to the Okitipupa Ridge in Nigeria on the East (Adegoke and Omatsola, 1981; Brownfield et al, 2016). The Romanche (apparently an offset extension of the Ghana Ridge) and Chain (supposedly an offset extension of the Benin Hinge Line) fractures zones delimited the Dahomey Embayment which was formed during the opening of Equatorial Atlantic starting in the Late Jurassic and continuing into the Cretaceous (Adegoke and Omatsola, 1981) periods. The crustal separation, typically preceded by crustal thinning, was accompanied by an extended period of thermally induced basin subsidence through the Middle-Upper Cretaceous to Tertiary periods as the South American and the African plates entered a drift phase to accommodate the emerging Atlantic Ocean (Akinmosin et al., 2013). The onshore part of the basin covers a broad arc-shaped profile of about 600 km^2 in extent, and a maximum width of some 130 km, along its N-S axis, near the Nigerian-Republic of Benin border. The Nigerian part of this basin is known as the Eastern Dahomey Basin which underlies the three states of Lagos, Ogun and Ondo. Due to the economic importance of these areas, there has been a large influx of people into the cities within this basin, especially Lagos, which is the economic hub of Nigeria. The area of investigation is low lying, with several points virtually at sea level, which are prone to flooding. The highest elevation, 265 m above sea level is around Abeokuta town where the basin thins out into the Precambrian basement rocks. The climate around the basin is characterised by wet and dry seasons, within the tropical rain forest belt. Precipitation in this area occurs as rainfall ranges between 750 and 1000 mm mostly between March and October (wet season) and 250 mm and 500 mm between November and March (dry season) (Oloruntola et al., 2019).

6.2.2.2 Geology/Hydrogeology

The Dahomey Basin spans through onshore and offshore across the above mentioned three states. At the onshore part toward the northern part of the basin, cretaceous and tertiary sediments are found in some road cuts, river channels and quarries (Olabode and Mohammed, 2016). Previous authors (Jones and Hockey, 1964; Adegoke, and Omatsola, 1981) presented detailed geology, evolution, stratigraphy and hydrocarbon occurrence of the basin most of which recognised two structural elements (Figure 6.2). These structural aspects comprise the Benin basin and the Okitipupa structure. They have identified three blocks which include the onshore geoblock (Bodashe, Ileppa—Ojo geoblock), the Okitipupa structure (Union – Gbekebo geoblock) and offshore geoblock (Olabode and Mohammed, 2016).

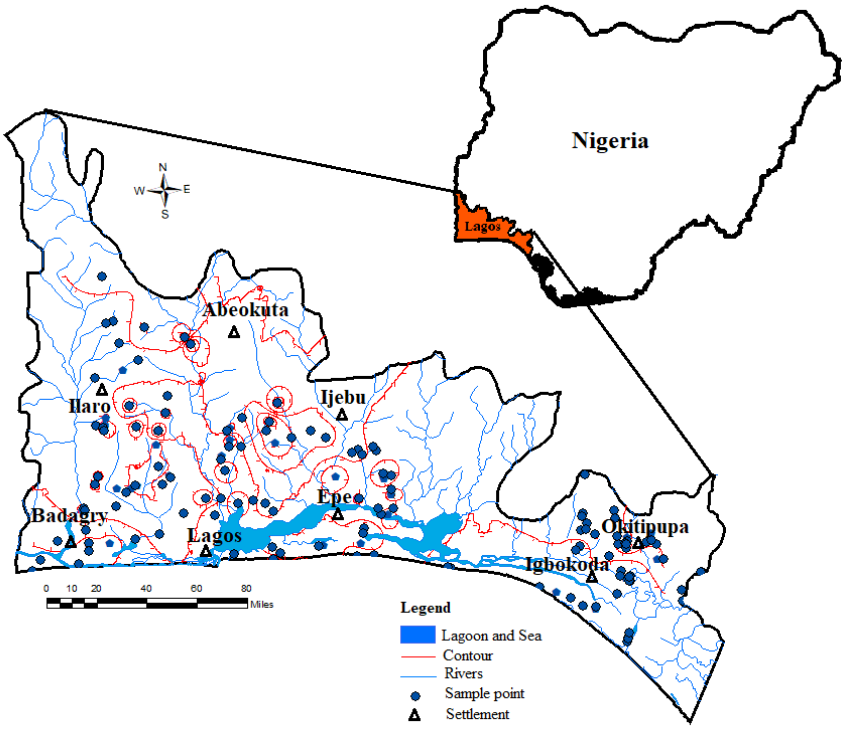

Figure 6.1 Map of the study area showing sampling location

The geoblocks have gone through three main stages of basin evolution (Olabode and Mohammed, 2016). These stages are classified into (1) the initial graben

(pre-drift) phase prolonged (2) the transitional stage and (3) the open marine (drift) phase. In the early studies, stratigraphy and age of the basin (Figure 6.2) were described as Cretaceous and Tertiary sediments, while subsequent authors recognised three chronostratigraphic units: (1) pre-lower Cretaceous folded sequence, (2) Cretaceous sequence and (3) Tertiary sequence (Jones and Hockey, 1964; Adegoke and Omatsola, 1981). The Cretaceous stratigraphy is compiled from outcrops, borehole logs consist of the Abeokuta Group sub-divided into three informal formational units namely Ise, Afowo, and Araromi, the Ise Formation unconformably overlies the basement complex and comprises coarse conglomeratic sediments. The Afowo Formation comprises transitional to marine sands and sandstone with variable but thick interbedded shales and siltstone, while Araromi remains the uppermost formation and is made up of shales and siltstone with interbeds of limestone and sands. The Tertiary sediments consist of Ewekoro, Akinbo, Oshosun, Ilaro and Benin (coastal plain sand) Formations. The Ewekoro Formation consists of fossiliferous well-bedded limestone while Akinbo and Oshosun Formations are made up of flaggy grey and black shales (Figure 6.3). Glauconitic rock bands and phosphatic beds define the boundary between Ewekoro and Akinbo Formations. Ilaro and Benin Formations are predominantly coarse sandy estuarine, deltaic and continental beds. In this study and for the hydrogeological significant, Abeokuta, Ewekoro, Ilaro formation, Alluvium deposit and Coastal Plain Sands are considered (Figure 6.3).

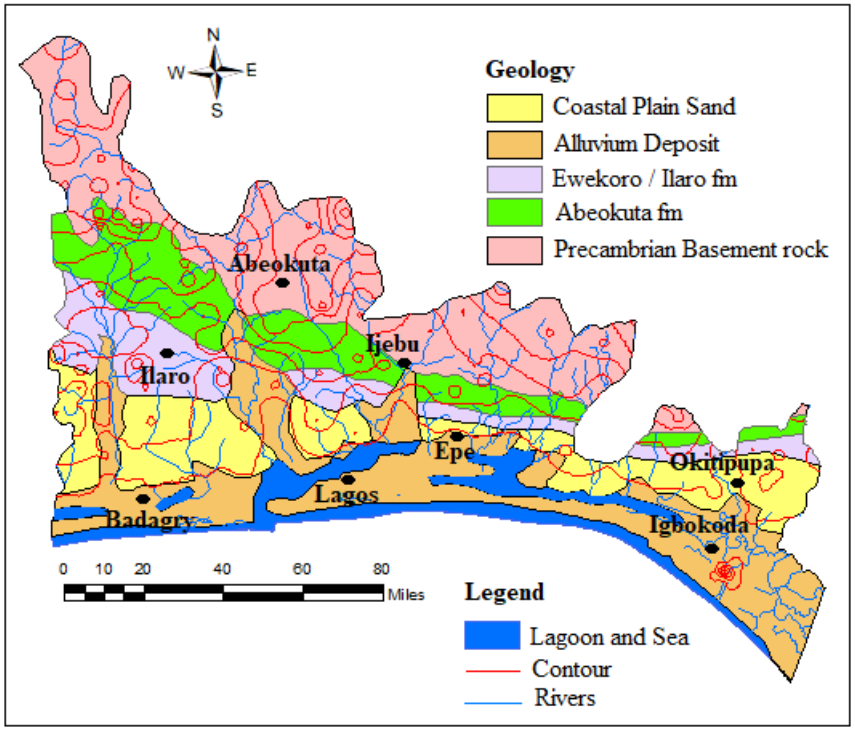

Figure 6.2 Geology map of Eastern Dahomey Basin showing the different geological formations

Groundwater aquifer in Eastern Dahomey Basin was described as a multi-aquifer system consisting of three aquifer horizons separated by Shally, Silty or Clayey layers (Adeoti et al., 2010; Longe, 2011; Oloruntola et al., 2019). Multi-layer aquifers characterised coastal plain and alluvium deposits; (Longe et al, 1987) classified the aquifer into three types. The first aquifer is a water table aquifer prone to pollution because of its direct interaction with surface water and drainages. The second and third are confined aquifers composed of an alternating sequence of sand and clay. These aquifers belong to the continental Ilaro Formation. The third aquifer is the most productive and faces the highest level of groundwater exploitation. Within this layer, groundwater exists under confined to the semi-confined condition (Longe et al 1987; Adelana *et al.*, 1996; Longe, 2011). Generally, water-table ranges from 2.0 to 15.0 m below ground level (b.g.l) in the area. The aquifer shows high thickness at the northern part of Abeokuta, through Ewekoro, Ilaro, and extended to the coastal plain sands, in

locations closer to the coast in the south. The percentage of sands in lithology also increases towards the south (Longe et al, 1987). Finally, the study area is well-drained by rivers and streams that flow southerly into the lagoon and the Atlantic Ocean. The average annual precipitation is above 1700 mm and serves as a primary source of groundwater replenishment.

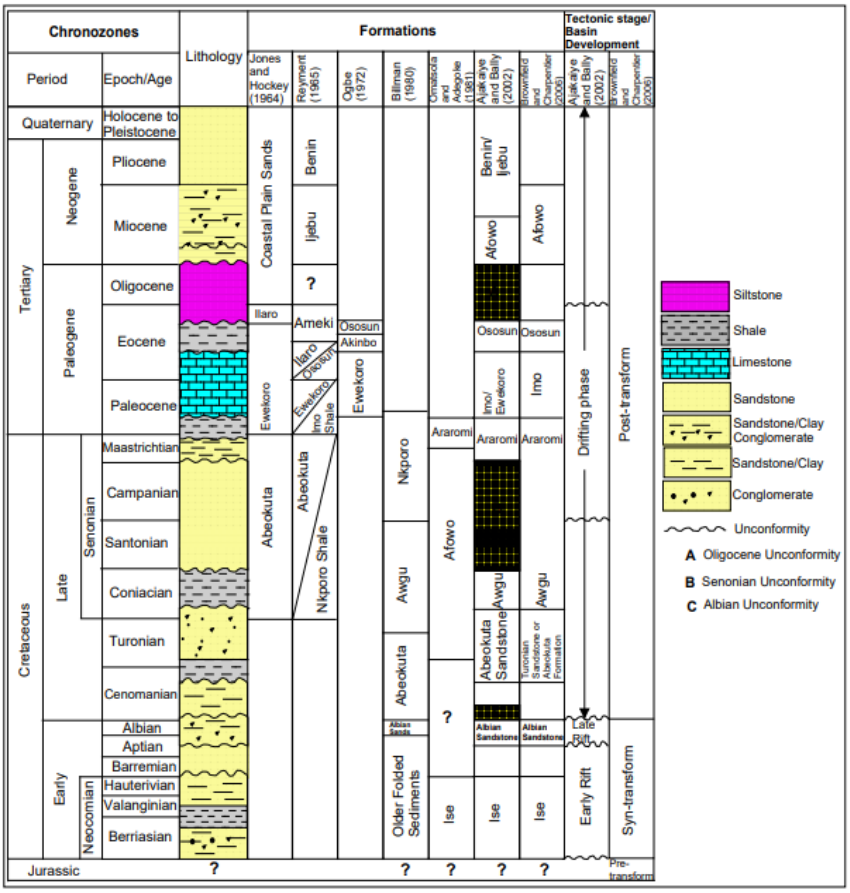

Figure 6.3 Generalised Stratigraphic of Dahomey Basin showing age, Lithology, and sequence of the formations and tectonic stage of its development in the eastern part. (Adapted from Olabode and Mohammed, 2016)

6.2.3. Methodology

6.2.3.1Field physicochemical measurement

Well inventory was carried out on a total number of 250 (96 in the wet season and 134 in dry season) shallow hand-dug wells, shallow tube wells and boreholes from the Eastern Dahomey Basin (EDB) between May 2017 and April 2018. The physicochemical parameters were measured in the field using a Model 99720 pH/Conductivity meter capable of measuring total dissolved solids (TDS), salinity, temperature and Eh/ORP. The depth of the wells and static water level were measured with the aid of a water depth meter while the coordinates of each sampled well were recorded using GPS. The 250 groundwater samples were collected in three separate 50 ml polypropylene tubes labelled A, B and IS. Samples labelled A were acidified to a pH < 2 after collection with 0.4 ml of concentrated nitric acid (HNO_3). Samples B and IS were filtered with 0.45µm filter and preserved in an ice-packed cooler to keep the samples' temperature below 4°C before being transported to the laboratory for further analysis.

6.2.3.2 Laboratory procedure

The 250 acidified water samples labelled A were prepared by collecting 10 ml of each sample in a centrifuge tube and arranging them serially for Inductively Coupled Plasma (ICP-MS) analysis of cations and Ion Chromatography (IC) for the anions concentrations in the Environmental Laboratory, Department of Civil and Environmental Engineering, University of Strathclyde. Alkalinity (HCO_3^-) was determined using a Digital Titrator (Model: 16900, HACH International) and 1.6 N H_2SO_4 cartridge. Then, samples labelled IS were shipped to the Ministry of

Agriculture, Irrigation and Water Development Isotope Laboratory, Blantyre, Malawi, for isotope analysis.

6.2.3.3. Data quality control

The multiparameter pH/conductivity tester was usually calibrated with a buffer solution of pH 4 and 7 with errors of +/-0.02, while conductivity and total dissolved solid was calibrated in solution with 1413 µS/cm and 940 ppm respectively. This procedure was repeated before the commencement of groundwater sampling. The instrument was also rinsed to avoid cross-contamination of samples. The accuracy of the chemical analyses was determined by using the ion charge balance equation (Somaratne and Frizenschaf, 2013). Some selected major ions were repeated in ten (10) randomly selected samples from which their correlation values fell well above 0.8.

6.2.3.4. Data Processing/ Interpretation

Descriptive statistics and correlation analysis were useful tools to obtain significant information from hydrochemical data sets in studies of groundwater (Adimalla, 2019a; Edet, 2019, 2016; Narany et al., 2014; Shakerkhatibi et al., 2019; Thilagavathi et al., 2017). To evaluate the analytical data descriptive and multivariate statistical techniques i.e., correlation analysis was used in this present study, by using SPSS_26_Win_64. Parametric descriptive statistical methods were also employed to calculate minimum, maximum, mean and standard deviation of the analytical data. Pearson's correlation matrix was used to identify the relationship between the pairs of parameters.

6.2.3.5 Spatial analysis for the distribution of mineral saturation zones

Geostatistics is a subset of statistics which specialises in analysis and interpretation of geographically referenced data. Geographical information system (GIS) and geostatistical techniques provide an integrated tool to investigate the spatial distribution of selected minerals. The saturation index of some selected minerals were calculated through the Geochemist Work Bench Geochemical tool. The minerals include Calcite, Dolomite, Aragonites, Gypsum, Halite and Anhydrite. The spatial distribution maps of each mineral were generated using the ordinary kriging method, which is one of the best interpolation methods in ArcGIS geostatistical extension (Adimalla and Kumar, 2020; Ahmed et al., 2019b; Bodrud-Doza et al., 2019; Wang et al., 2017). This method is for optimum linear interpolation with a minimum square error of the sampled location, based on the equation 1 below.

$$Z^*(x_0) = \sum_{i=1}^{n} n\lambda_i Z(x_i) \quad (1)$$

where $Z*(x)$ is the estimated value at location x_0, n is the number of points, $Z(xi)$ is the known value at location xi, and λi is the weight of the kriging.

6.2.4 Results and Discussion

Hydrochemical results of groundwater samples collected from the study area are summarised in Table 6.1. The measured pH of groundwater varies within a range of 3.8 – 8.1 and 3.9 – 8.0 with mean values of 5.6 and 5.5 for wet and dry season respectively. The EC varies from 0.00 to 11000 µs/cm and 5.50 to 12009 µS/cm with an average of 295.4 and 347.8 µs/cm for respective wet and dry seasons. The total dissolved solids (TDS) concentrations of the groundwater range from <ND to 7500 mg/l and 2.30 to 8750 mg/l with average values of 201.8 and 232.8 mg/l for the

respective seasons. The relative concentrations of the cations occur in the order of Na>K>Ca>Mg and Na>Ca >Mg>K, while anions are in the order of HCO_3 >Cl>SO_4 and Cl>SO_4>HCO_3 for both wet and dry seasons respectively. The concentrations of dissolved major ions in both seasons showed wide variabilities in the groundwater samples from EDB. Such a wide range of ionic concentrations are attributed to multiple hydrochemical processes influencing the water chemistry within the Basin.

Table 6.1 Statistical Summary of major ions in water samples for both seasons

	Rainy Season					**Dry Season**				
Para	N	Mean	SD	Min	Max	N	Mean	SD	Min	Max
Ca^{2+}	96	16.50	41.19	0.28	374.00	133	21.46	54.99	0.24	448.5
Mg^{2+}	96	18.39	140.38	0.04	1377.00	133	15.99	101.85	0.14	1125
Na^{+}	96	106.83	902.75	0.07	8857.00	133	111.87	903.99	0.64	10310
K^{+}	96	10.51	46.17	0.05	447.10	133	10.07	51.46	0.05	590.2
HCO_3	96	142.34	818.70	1.04	8028.45	134	137.47	761.99	0.00	8390.05
SO_4^{2-}	81	37.87	245.14	0.08	2210.66	133	39.39	258.80	0.26	2932
Cl^{-}	96	218.06	1934.34	0.10	18270.20	133	204.83	1671.35	0.87	18833
NO_3^{-}	95	31.76	54.14	0.02	258.56	133	29.91	54.14	0.25	311.92
TDS	96	201.83	863.57	0.00	7500.00	133	232.77	668.10	2.30	8750
EC	96	295.39	1219.42	0.00	11000.0	133	347.81	995.09	5.50	12009
pH	96	5.567	1.00	3.97	8.10	133	5.45	0.94	3.85	7.96

6.2.4.1 Correlation of Major Ions

Correlation coefficient analysis was carried out on the hydrochemical data of major ions to study the relationships between the parameters (Kumar et al, 2011; Bouderbala *et al.*, 2016; Edet, 2016; Adimalla, 2019). Table 6.2, Figures 6.4 and 6.5 show the relationship between the major ions in groundwater for both wet and dry season. High positive correlation (mostly above 0.5) has been obtained between Ca and Mg, Na, K, HCO_3^{-}, TDS, EC and pH but weak correlation with Cl^{-}, SO_4^{2-} and NO_3^{-} in the wet season water samples while Ca shows high correlation with Mg, Na, K, HCO_3-, Cl^{-}, SO_4^{2-}, TDS, EC, and pH but weak correlation with $NO_3^{-}$for the dry

season. NO_3^- shows high correlation with Cl^- and SO_4^{2-} in wet season contrary to weak or low correlation with Cl^- and SO_4^{2-} in the dry season groundwater samples.

The observed trend indicates possibly anthropogenic inputs from agricultural and industrial waste, in combination with rock weathering and mineral dissolution in groundwater of EDB during the wet season. In the dry season water samples indicating the predominance of chemical weathering along with leaching of secondary salts. Scatter diagrams of Na against Cl for both seasons are presented in Figure 6.4 and 6.5, the distribution revealed both Na and Cl play a significant role in the hydrochemical evolution of the groundwater during the wet and dry season. Scatter plots between Na + K against Ca +Mg also confirm the dominant of these ions.

Table 6.2 Pearson Correlation for major physicochemical parameters of samples from rainy and dry seasons.

Parameter	Ca^{2+}	Mg^{2+}	Na^{+}	K^{+}	HCO_3^{-}	SO_4^{2-}	Cl^{-}	NO_3^{-}	TDS	EC	pH
	Raining Season										
Ca^{2+}	1										
Mg^{2+}	0.915*	1									
Na^{+}	0.904*	0.999*	1								
K^{+}	0.927*	0.979*	0.979*	1							
HCO_3^{-}	0.938*	0.998*	0.995*	0.982*	1						
SO_4^{2-}	0.182	0.044	0.049	0.165	0.066	1					
Cl^{-}	0.139	0.004	0.009	0.123	0.025	0.998*	1				
NO_3^{-}	0.325	0.264	0.266	0.375	0.276	0.482*	0.605*	1			
TDS	0.936*	0.995*	0.993*	0.985*	0.997*	0.096	0.054	0.319	1		
EC	0.938*	0.994*	0.992*	0.985*	0.997*	0.100	0.058	0.322	1.000	1	
PH	0.520*	0.288*	0.268*	0.290*	0.327*	0.150	0.120	-0.051	0.315*	0.318*	1
	Dry Season										
Ca^{2+}	1										
Mg^{2+}	0.851*	1									
Na^{+}	0.772*	0.986*	1								
K^{+}	0.721*	0.949*	0.978*	1							
HCO_3^{-}	0.857*	0.988*	0.977*	0.940	1						
SO_4^{2-}	0.747*	0.955*	0.967*	0.973	0.950*	1					
Cl^{-}	0.795*	0.990*	0.998*	0.966	0.984*	0.955*	1				
NO_3^{-}	0.088	-0.031	-0.033	0.065	-0.024	-0.010	-0.037	1			
TDS	0.894*	0.959*	0.989*	0.321	0.867*	0.217*	0.966*	0.106	1		
EC	0.894*	0.960*	0.988*	0.319	0.864*	0.219*	0.964*	0.103	1.000*	1	
PH	0.496*	0.296*	0.257*	0.259	0.303*	0.289*	0.254*	-0.074	0.235*	0.237*	1

**: Correlation is significant at the 0.05 level*

.

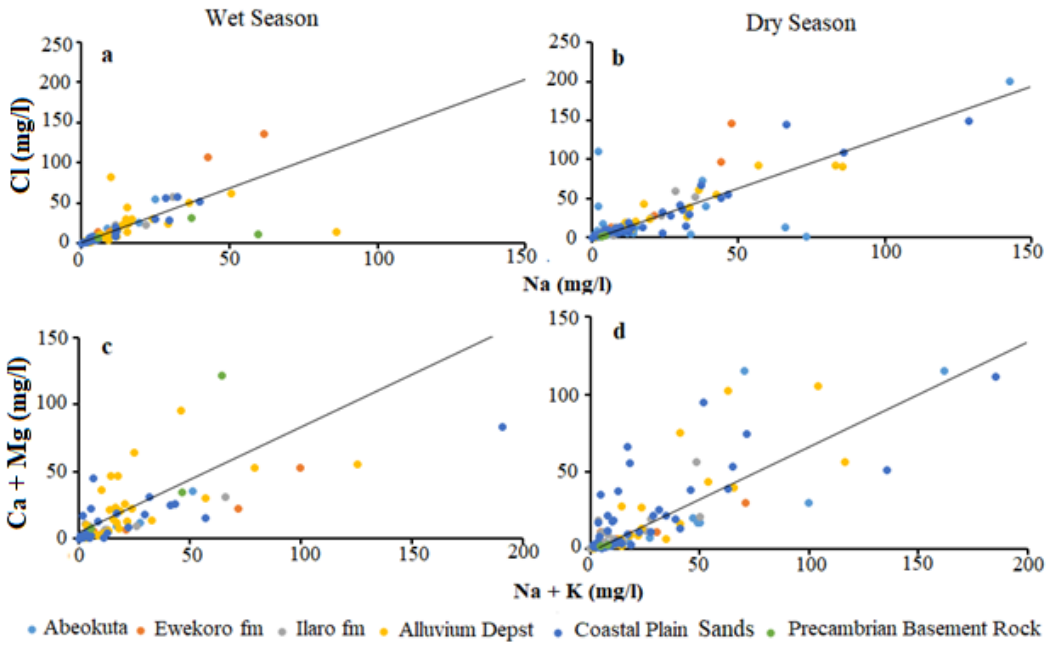

Figure 6.4 Scatter plots between (a) Na vs Cl wet season (b) Na vs Cl (c) Na +K vs Ca + Mg wet season (d) Na + K vs Ca + Mg dry season

Table 6.3 The linear relationship between Na Vs Cl and Na + K vs Ca + Mg

Na vs Cl	**Wet Season**		**Dry Season**	
Lithology	**Y**	**R^2**	**Y**	**R^2**
Abeokuta formation	1.97x – 1.81	0.91	0.95x + 3.51	0.49
Ewekoro formation	2.41x – 6.34	0.99	0.74x – 9.38	0.92
Ilaro formation	1.77x – 3.10	0.91	1.61x – 2.42	0.90
Alluvium Deposit	1.35x + 1.22	0.68	2.50x – 53.40	0.98
Coastal Plain Sands	-0.02X +57.8	0.01	1.31x – 1.73	0.88
Precambrian	0.14x + 12.29	0.08	0.81x – 1.46	1.00
Na+K vs Ca+Mg				
Abeokuta formation	0.67x – 1.59	0.95	0.68x - 1.91	0.72
Ewekoro formation	0.46x – 0.45	0.91	2.14x – 8.49	0.28
Ilaro formation	0.39x + 3.45	0.82	0.69x + 0.84	0.61
Alluvium Deposit	0.78x + 5.12	0.65	0.39x + 17.16	0.97
Coastal Plain Sands	0.19x + 8.14	0.99	0.14x + 17.7	0.99
Precambrian	1.71x – 12.14	0.76	0.36x + 0.08	1.00

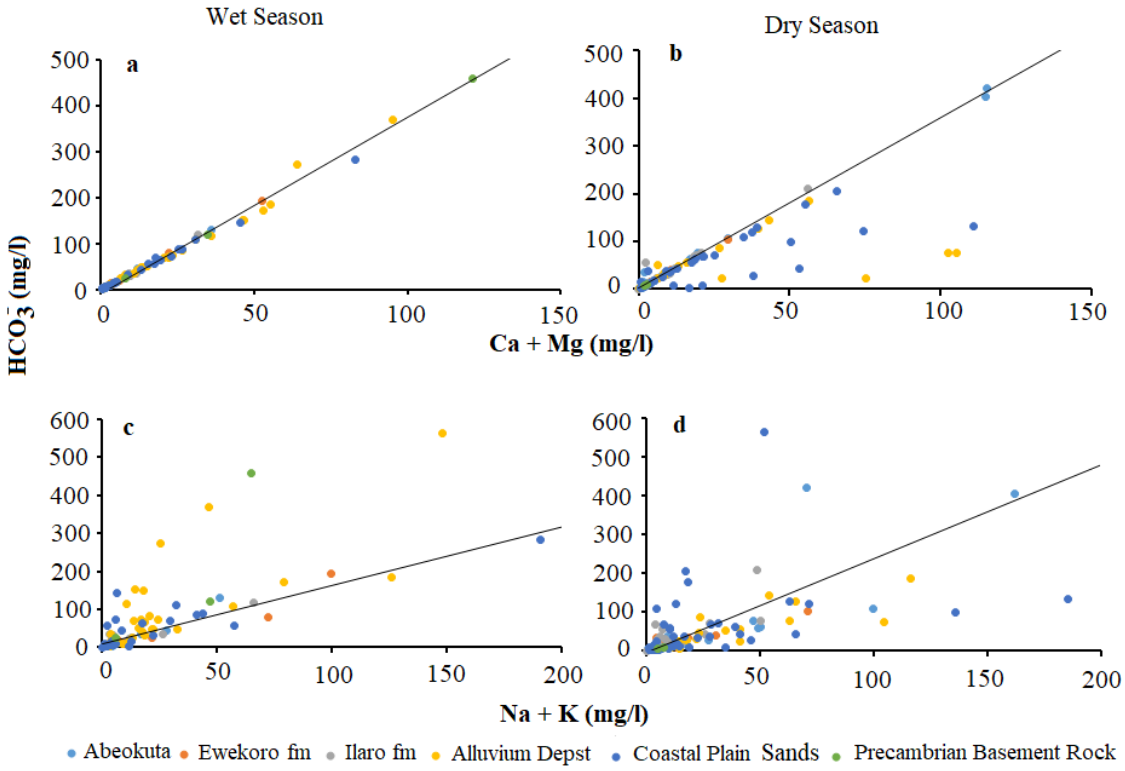

Figure 6.5 Scatter plots (a) Ca +Mg vs HCO_3 wet season (b) Ca +Mg vs HCO_3 dry season (c) Na + K vs HCO_3 wet season (d) Na + K vs HCO_3 dry season

Table 6.4 The linear relationship between Ca + Mg vs HCO_3 and Na + K vs HCO_3

Ca + Mg vs HCO3	**Wet Season**		**Dry Season**	
Lithology	**Y**	**R^2**	**Y**	**R^2**
Abeokuta formation	3.63x – 0.34	0.99	3.57x + 1.67	0.99
Ewekoro formation	3.68x – 0.42	0.99	3.82x – 1.94	0.99
Ilaro formation	3.78 – 1.85	0.98	3.64x + 2.48	0.94
Alluvium Deposit	3.67x – 3.20	0.99	3.38x + 65.40	0.80
Coastal Plain Sands	4.59x – 13.18	0.99	5.33x - 54.84	0.99
Precambrian	3.83x – 8.74	0.99	3.40x + 0.23	1.00
Na + K vs HCO_3				
Abeokuta formation	2.45x – 6.22	0.96	2.41x - 4.96	0.71
Ewekoro formation	1.67x – 1.93	0.91	8.09x – 32.67	0.28
Ilaro formation	1.53x + 10.33	0.88	2.51x + 5.25	0.59
Alluvium Deposit	2.79x + 17.21	0.61	1.40x - 19.61	0.87
Coastal Plain Sands	0.86x + 24.03	0.99	0.77x + 38.53	0.99
Precambrian	6.49x – 52.71	0.74	1.23x + 0.51	1.00

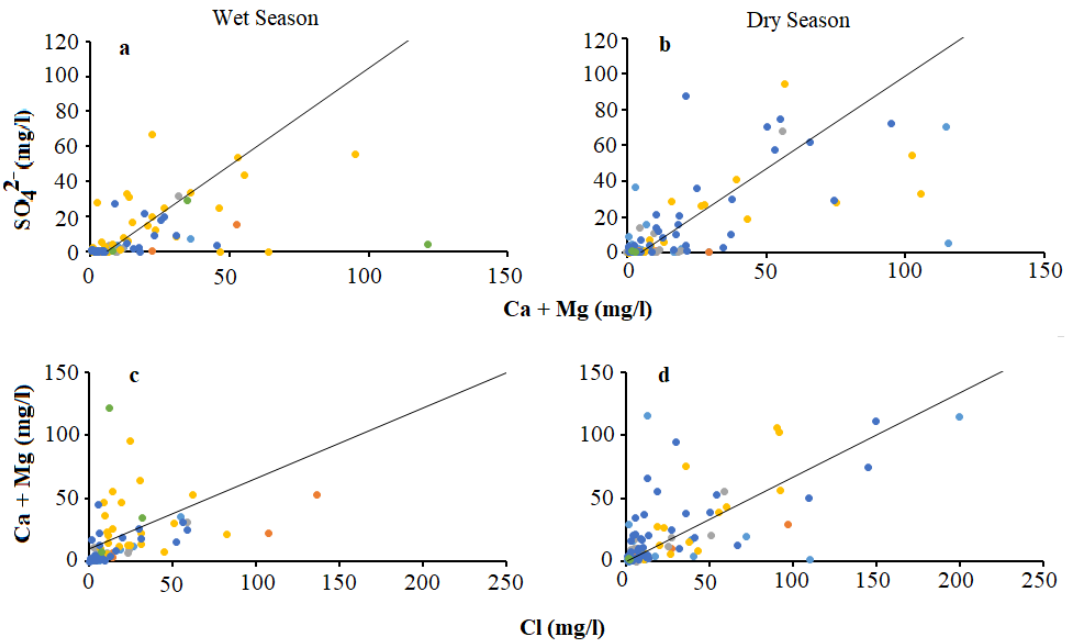

Figure 6.6 Scatter plots (a) Ca +Mg vs SO_4 wet season (b) Ca +Mg vs SO_4 dry season (c) Cl vs HCO_3 wet season (d) Cl vs HCO_3 dry season

Table 6.5 The linear relationship between Ca + Mg vs SO42- and Cl vs Ca + Mg

Ca +Mg vs SO_4^{2-}	**Wet Season**		**Dry Season**	
Lithology	**Y**	**R^2**	**Y**	**R^2**
Abeokuta formation	0.21x – 0.06	0.91	0.30x + 1.43	0.37
Ewekoro formation	0.29x – 1.18	0.83	1.93x - 13.86	0.99
Ilaro formation	1.11x – 6.26	0.88	1.04x - 4.91	0.72
Alluvium Deposit	0.22x + 9.90	0.14	0.07x + 20.55	0.11
Coastal Plain Sands	0.08x + 67.04	0.04	1.86x - 17.16	0.99
Precambrian	-0.05x + 13.74	0.03	-0.41x + 1.62	1.00
Cl vs Ca +Mg				
Abeokuta formation	0.65x – 1.76	0.98	0.41x + 3.04	0.35
Ewekoro formation	0.31x + 1.04	0.89	1.64x – 14.87	0.75
Ilaro formation	0.43x + 2.99	0.75	0.67x + 0.58	0.69
Alluvium Deposit	0.56x + 10.13	0.59	0.15x + 32.94	0.92
Coastal Plain Sands	0.002x + 61.41	0.0003	0.08x – 19.48	0.99
Precambrian	-0.48x + 62.75	0.01	-1.48x + 4.81	1.00

6.2.4.2 Hydrochemical Facies characterisation of Groundwater

Groundwater types

Different graphical procedures have been useful in geochemical data interpretation for characterising groundwater into types based on the dominant ions (Prasanna et al, 2011; Talabi and Tijani, 2013; Anomohanran *et al.*, 2014; Amiri *et al.*, 2016; Hussien and Faiyad, 2016; Lapworth *et al.*, 2017; Adimalla and Kumar, 2020). A Piper diagram (Figure 6.7) was used in combination with a Durov plot (Figure 6.8) to characterise the groundwater from both seasons across different rock units and geological formation to see the possible trend in water types and their distribution across the Basin. Piper and Durov diagrams (Figure 6.7 and 6.8) were modelled using Geochemist Work Bench (GWB12) from which groundwater types were determined. The projection of some points at the central part of the diamond-shaped area signified the heterogeneity of the hydrochemical status of the groundwater samples at both seasons in this area. Based on the Piper diagram (Figure 6.7), both Alkali water (Na + K) and Alkaline earth metals (Ca + Mg) water types evolved from the EDB alongside with other mixing groundwater types. From the diagram, out of the 96 water samples collected during the wet season, Na-Cl (39 %), Na-SO_4 (5 %), Na-HCO_3 (7 %), Ca-HCO_3 (18 %), Ca-Cl (18 %), Ca-SO_4(8 %), K-Cl (3 %), Mg-HCO_3 (1 %) and K-SO_4 (1 %) (Table. 3) were observed. In the dry season, out of 134 sampled groundwater, Na-Cl (60 %), Na-SO_4 (6 %), Na-HCO_3 (5 %), Ca-HCO_3 (9 %), Ca-Cl (15%), Ca-SO_4 (2%), K-Cl (2%) and Mg-HCO_3 (1%) (Table. 3) were observed.

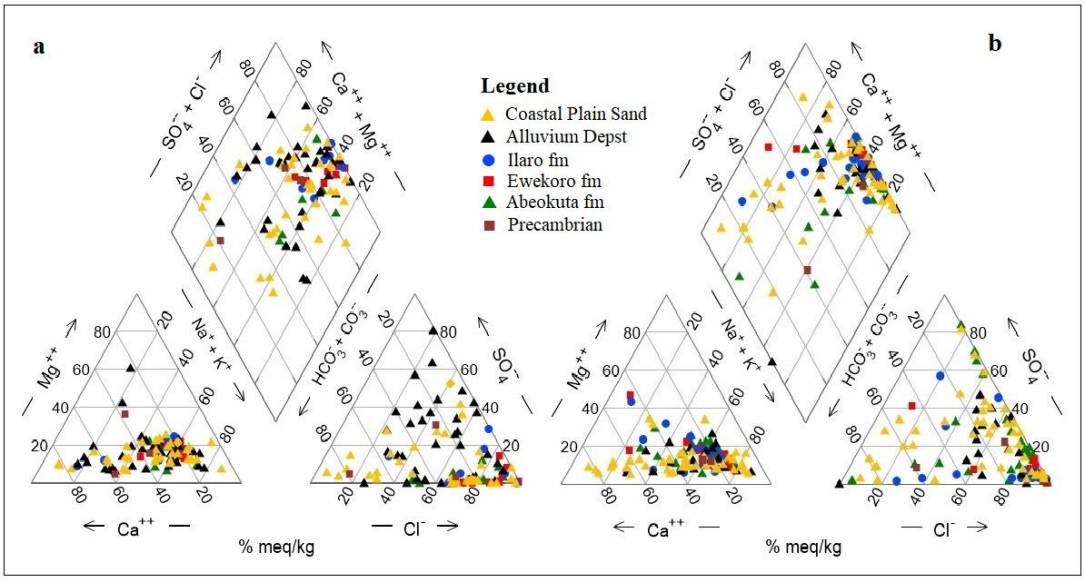

Figure 6.7 Piper Diagram for both (a) rainy and (b) dry seasons

The results show the hydrochemical dynamic of groundwater from the basin is a combination of influence from rocks interaction and anthropogenic inputs. It is clear that in all the waters, alkali metals of Na-Cl dominate the samples in both seasons. The abundance of the alkali metals could be attributed to sea spray process due to the proximity of the area to sea as suggested in the work of Abimbola *et al.*, (1999) on one hand and the influence of the municipal waste on the other hand, also the dissolution of Ca and Mg-rich silicate minerals in the aquifer matrix plays a significant role in hydrochemical evolution. Some of the samples fall in the sub-field, which also suggests alkali metals exceed alkaline earth. The higher concentration of alkali ions present in the water may influence ion-exchange reactions between the solid and aqueous phases, resulting in sodium-enriched sediments.

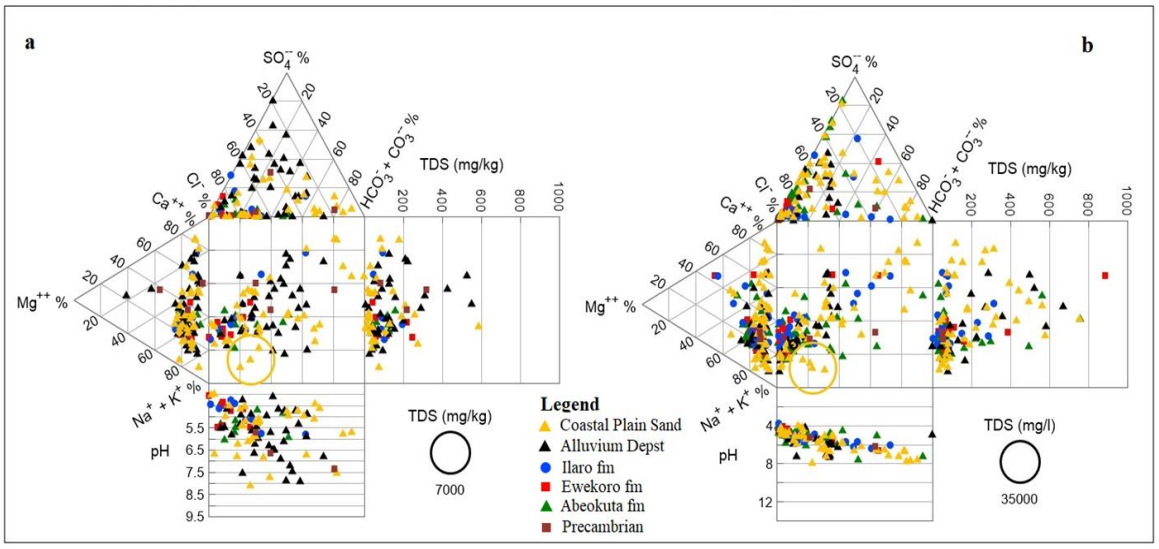

Figure 6.8 Durov diagram for groundwater major ions for (a) Wet Season and (b) Dry season

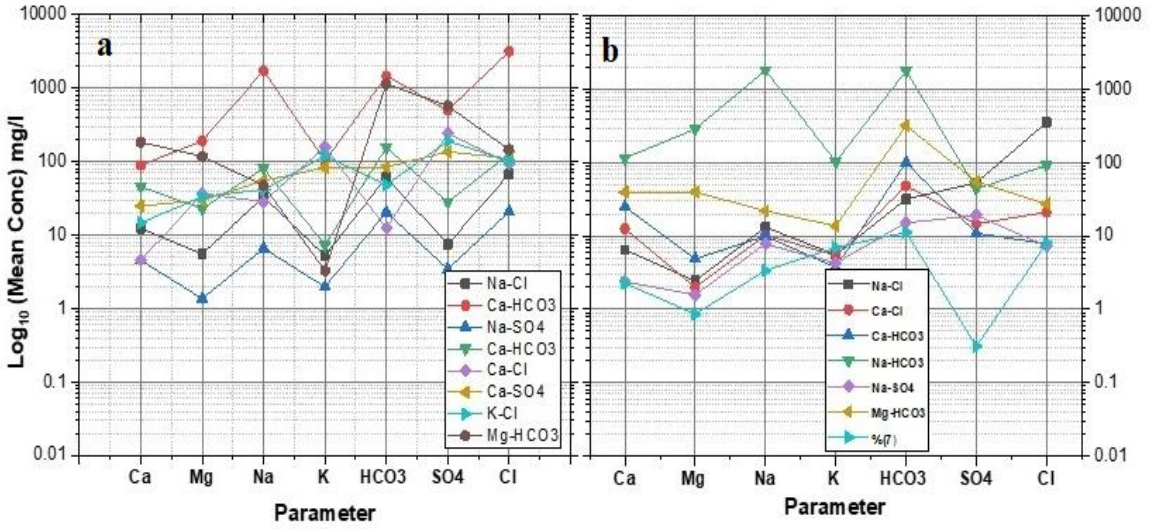

Figure 6.9 Schoeller diagram showing different water types and distribution with major ions

6.2.4.3 Geochemical evolution of the groundwater of the EDB aquifers

To further understand the dominant hydrochemical process controlling the groundwater chemistry of EDB, the analysis of the major ions was plotted on Gibbs (1971) (Birks et al., 2019; Hussien and Faiyad, 2016; Srinivasamoorthy et al., 2014)

from which $Na^+/(Na^+ + Ca^{2+})$ and $Cl^-/(Cl^- + HCO_3^-)$ were plotted against log of TDS (Figure 6.10) in two separate charts for both wet and dry seasons. The diagram (Figure 6.10) reveals clustering of the points around rock-dominant which indicates that rock-water interaction is the dominant factor controlling the chemistry of the water with the influence of precipitation in the wet season samples, while that of the dry season tends towards evaporation effect (Figure 6.10) which reveals the possible seasonal influence. Evaporation increases all forms of ions in groundwater (Prasanna et al, 2011; Sheikhy Narany *et al.*, 2014; Srinivasamoorthy and Sarma, 2014; Adimalla, 2019).

The scatter diagrams of some selected major ions also supports the earlier deductions, which further confirm the possible hydrochemical processes controlling the groundwater in the area. major ions relationships as explained by the linear correlation graphs (Figure 6.4 – 6.6) show the relationships between the selected ions with their correlation coefficient (R^2) and related equation in Table 6.3, 6.4 and 6.5. Scatter plots of Na vs Cl^+ for both season samples from wet season plotted more on equal line and on almost equal with their coefficient of correlation values more than 0.5 across all the geological formations (Abeokuta, Ewekoro, Ilaro formations and Alluvium deposit and coastal plain sands' aquifers of the basin). In the dry season, the samples plotted on both sides of the line (Figure 6.4), which indicates dissolution of halite whereas samples above equal line suggest the presence of an excess of sodium contents.

Excess of the sodium salt is due to various anthropogenic activities as well as the contribution of marine salt through sea spraying (Prasanna et al, 2011). This type of phenomenon is possibly responsible for the dominant Na-Cl water type observed in EDB. The relationship between Na + K vs Ca +Mg also shows a similar trend. The

clustering of the points closer to the Ca + Mg half signify rock mineral dissolution as the hydrochemical controlling factor.

Table 6.6 Percentage groundwater sample types for both wet and dry seasons across EDB

	Wet Season N =96		**Dry Season N =134**	
Water Type	**Sample**	**% Sample**	**Sample**	**% Sample**
Na-Cl	37	39	76	60
Na-SO4	5	5	7	6
Na-HCO_3	7	7	6	5
Ca-HCO_3	17	18	12	9
Ca-Cl	17	18	19	15
Ca-SO_4	8	8	2	2
K-Cl	3	3	3	2
Mg-HCO_3	1	1	1	1
K-SO_4	1	1	0	0

The wide range of the plots in the dry season samples indicates precipitation and seasonal effects on the hydrochemical evolution of the basin. Ca + Mg vs HCO_3^- plots show high correlation coefficient >0.5 (Table 6.4) across aquifers in all the geologic units in both seasons suggests early stage of recharge with mineral dissolution (carbonate minerals mostly) in the wet season groundwater samples, while dry season water samples display evidence of mixing and precipitation. This is responsible for calcite, dolomite and aragonite saturation observed in some of the wells sampled in both seasons. The relationship between Na + K vs HCO_3 also explains the effect of seasonal variation with most of the point plotted on the side of HCO_3 (Figure 6.5) on wet season groundwater samples showing early water from precipitation while those of dry season tending towards Na + K indicating a mixed water from which weathering of kaolinite to albite has released Na into the water on one hand and evaporation causing precipitation on the other hand. Their coefficient shows high correlation

values (Table 6.5) across the rock units except in Ewekoro formations which have more carbonate minerals from the limestone and associated weathering product. Figure 6.6 showed the relationship between Ca + Mg vs SO_4 and Ca + Mg vs Cl through scatter plots. This revealed the evidence of evaporation on the groundwater which was possibly responsible for mineral precipitation which is more prominent during the dry season in the basin.

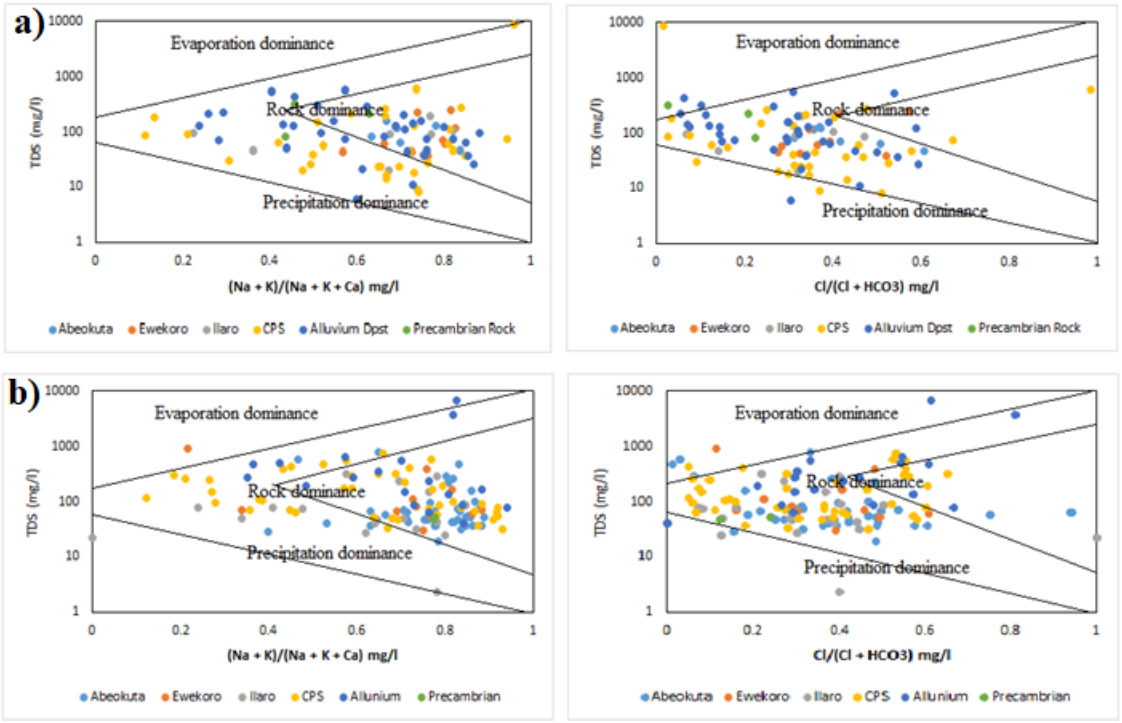

Figure 6.10 Gibbs diagram of Anions and Cations for both (a) wet and (b) dry seasons

6.2.4.4 Mineral saturation index (mineral dissolution and precipitation)

One of the methods employed thermodynamic principle related to water-rock interaction processes by calculation of mineral dissolution in groundwater. This phenomenon provides information on the mineral phases involved in the water-rock interaction processes. By using the saturation index (SI), it is possible to understand the common minerals that have a significant dominant influence on the evolution of groundwater chemistry of each water sample. Linking this to the geology of the area,

it provides a good insight into the hydrochemical process through the evolved groundwater hydrochemistry. In this study, to determine the chemical equilibrium between minerals and waters, saturation indices of carbonate and silicate minerals such as calcite, dolomite, aragonite, gypsum, anhydrite and halite were calculated (Table 6.6) using the following equation by Heathcode 1985 (Krishnaraj et al., 2012).

$$SI = \log(IAP/Ks)$$

Where IAP represents ion activity product, and Ks represents the mineral's solubility product.

The calculated values of SI for calcite, dolomite and aragonite showed values above zero saturation line (Figure 6.15) which is an indication of oversaturation in some groundwater samples within the study area in both seasons' water samples. Figures 6.13 and 6.14 present spatial distribution maps of the selected minerals for wet and dry seasons. The statistical summary also presented in Table 6.7. Gypsum, anhydrite is near saturation in some locations especially, in the wet season while dry season water samples are under saturated with same minerals. Scatter plots of TDS against calcite, dolomite, aragonite and gypsum (Figure 6.11 and 6.12) show a trend of mineralisation, which is more consistent during the dry season compared to the wet season. This indicates dissolution of minerals in the groundwater of the Basin as a dominant factor controlling the chemistry. Oversaturation of calcite, dolomite and aragonite in the Ewekoro and Ilaro formation parts of the basin could be as a result of weathering and dissolution of carbonate minerals from limestone within the area, which is evident in the mining sites of Dangote and Lafarge cement industries in the area.

Table 6.7 Statistical summary of mineral saturation status of the sampled groundwater

Minerals	Min	Max	Mean	St dev
Wet Season				
Calcite	-8.134	2.468	-4.51417	2.64433
Dolomite	-15.4	6.78	-8.41605	5.20171
Aragonite	-8.298	2.304	-4.67827	2.64427
Gypsum	-6.569	0	-3.61593	2.02927
Anhydrite	-6.742	0	-3.73003	2.0674
Halite	-12.67	-4.482	-8.70445	1.21007
Dry Season				
Calcite	-13.71	2.163	-8.3875	2.66226
Dolomite	-27.5	6.056	-16.2475	5.23115
Aragonite	-13.87	1.998	-8.55125	2.66446
Gypsum	-5.242	-4.78	-5.1	0.24201
Anhydrite	-5.42	-4.958	-5.27825	0.24218
Halite	-10.13	-9.281	-9.7825	0.4298

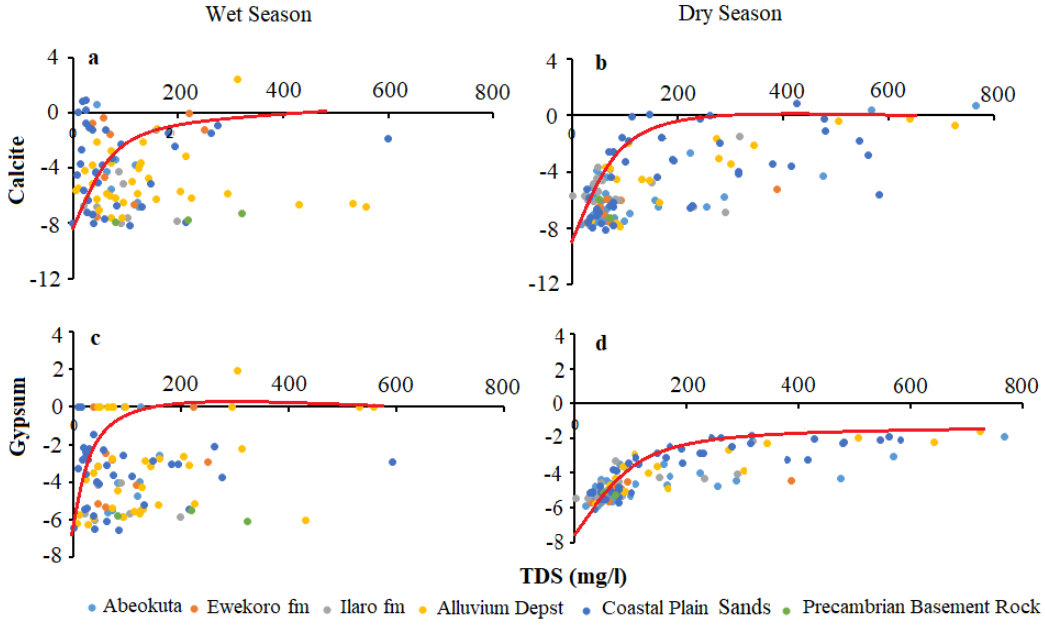

Figure 6.11 Scatter plots of TDS vs (a) Calcite WS (b) Calcite DS (c) Gypsum WS (d) Gypsum DS

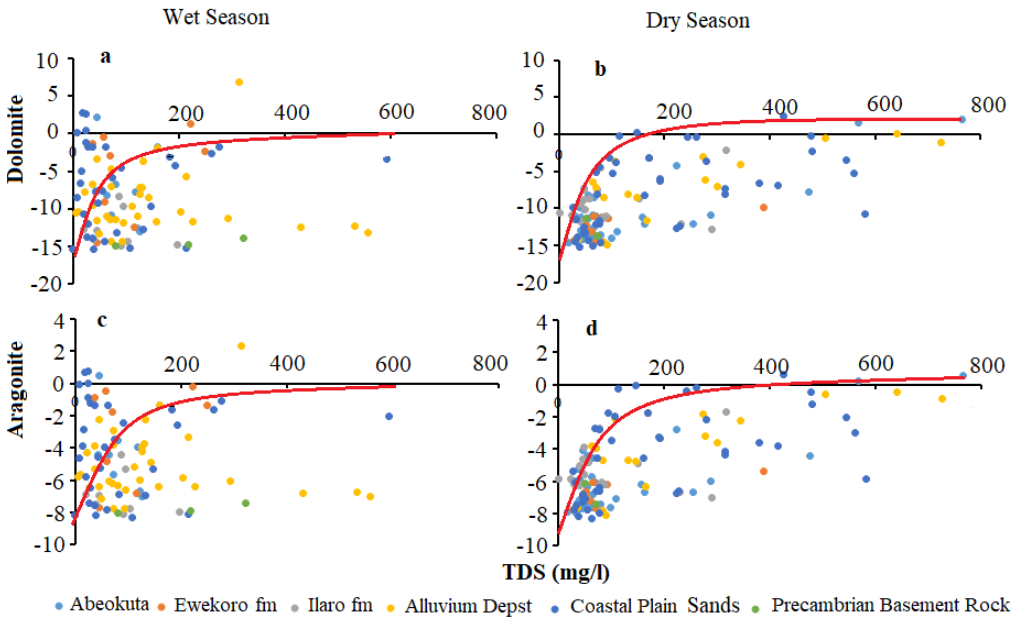

Figure 6.12 Scatter diagram showing TDS vs (a) Dolomite WS (b) Dolomite DS (c) Aragonite WS (d) Aragonite DS

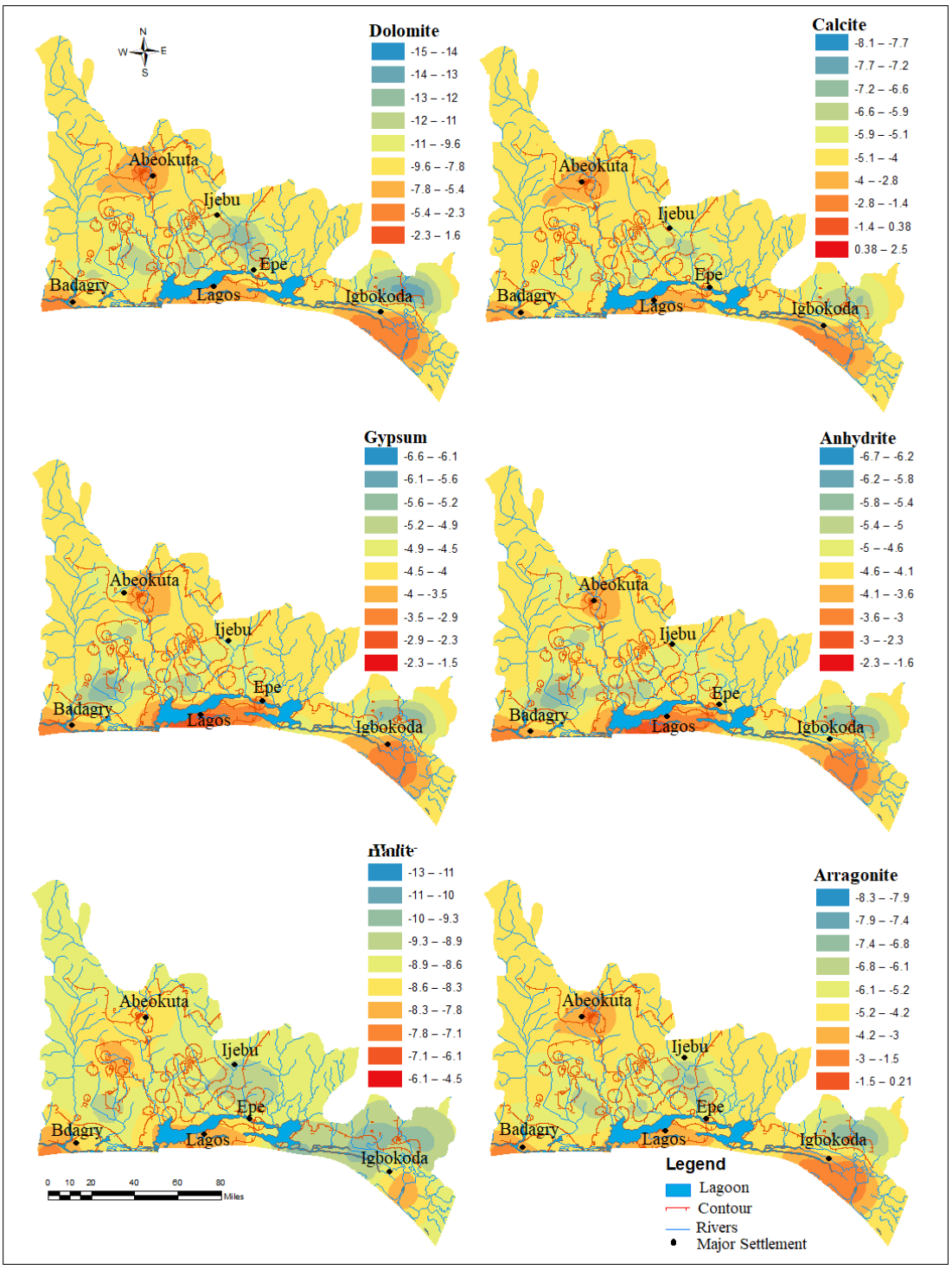

Figure 6.13 Saturation index map for the rainy season water samples

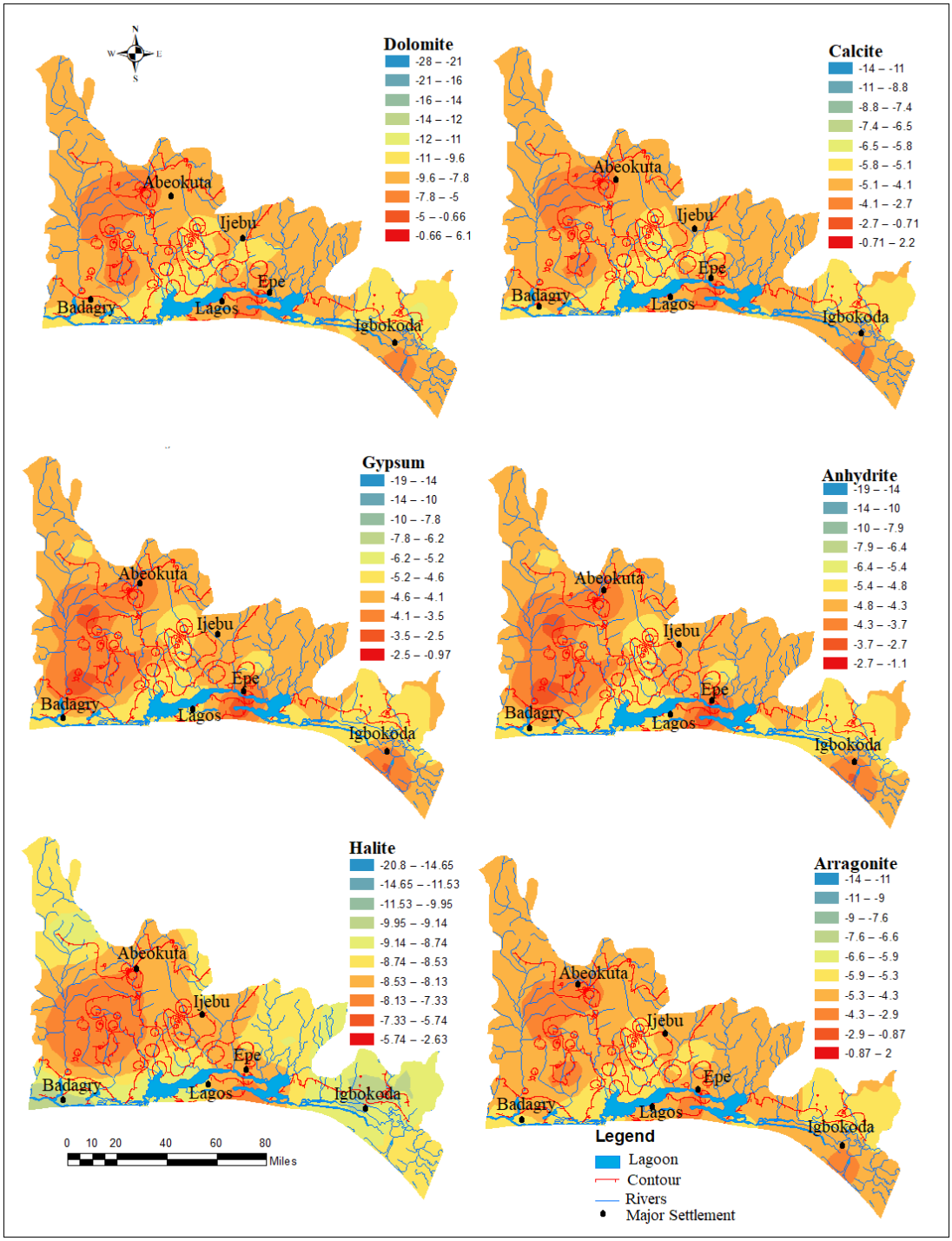

Figure 6.14 Saturation index map for the dry season water samples

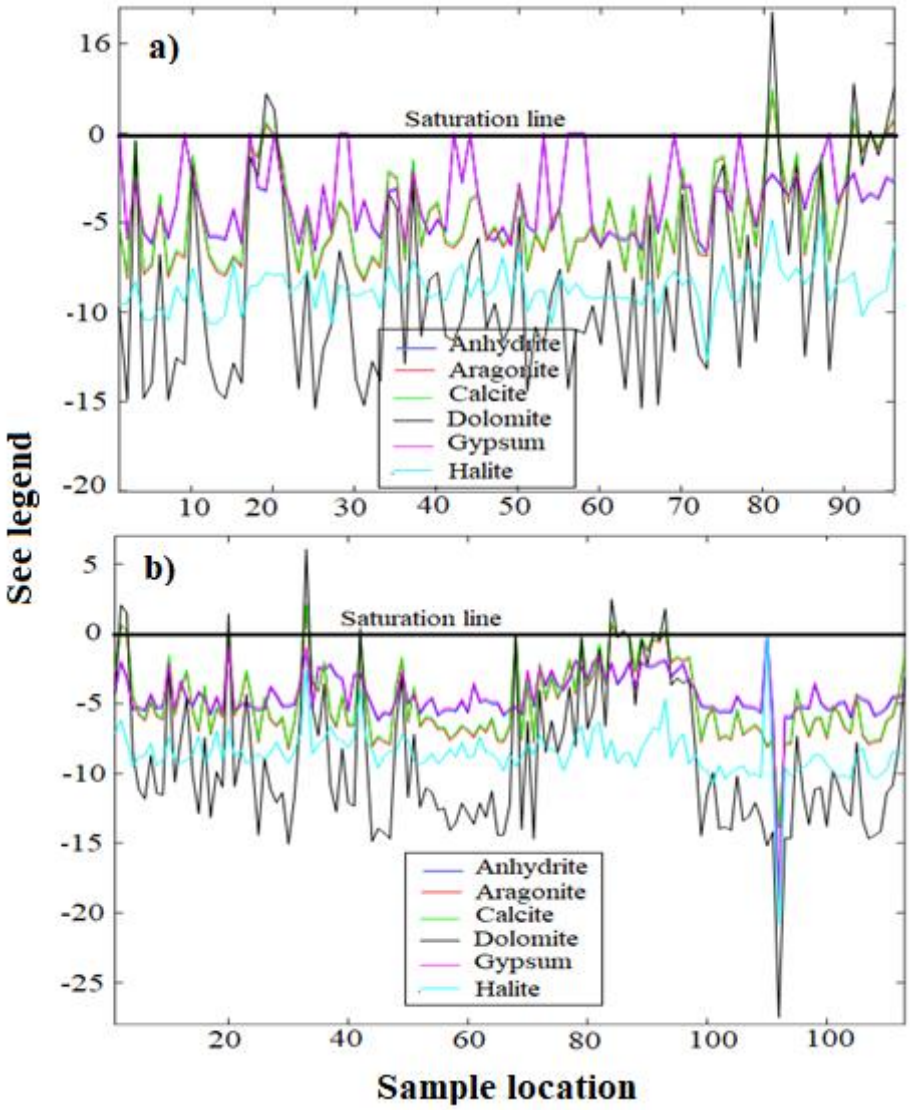

Figure 6.15 Linear graph showing the saturated index of groundwater samples for (a)wet season (b) dry season

6.2.4.5 Stable isotopes ($\delta^{18}O$ and δD ‰) evaluation

Stable isotopes of Oxygen and Hydrogen isotope ratios provide insight into physical processes that govern the hydrosphere and lower atmosphere (Guendouz *et al.*, 2003; Prasanna et al, 2011; Bakari *et al.*, 2012; Cary *et al.*, 2015; Awaleh *et al.*, 2017). Isotope techniques can be used to solve problems such as identification of the origin of groundwater, determination of its age, flow velocity and direction, interrelations between surface waters and groundwater, possible connections between

different aquifers, local porosity, transmissivity and dispersivity of an aquifer (Banda et al., 2019; Kalin, 1995; Kalin R.M., 2000). Different origin of surface or groundwater is distinguished in these natural and conservative tracers. Their conservative nature is preserved even in low-temperature environments. Isotopic composition of the aqueous substance is influenced by different environmental processes which often occur through fractionation, or preferential expression of a particular isotope of an element in one species or phase over another (Krishnaraj et al., 2012; Talabi and Tijani, 2013). Stable Isotope fractionation results from associated mass-differences bond vibration frequencies and zero-point energies. This process results in phase segregation in which lighter molecules move to a less dense phase while the heavier molecules favour the denser phase. These fractionations occurred mostly in predictable phase. Using the hydrochemical approach in combination with $^{2}D/H$ and ^{18}O values of fluids provides even more powerful signatures of the origins of aqueous fluids and the processes that transform one type into another.

Statistical summary of the data of δD and $\delta^{18}O$ values for the sampled groundwater in the wet and dry season from shallow groundwater aquifers of the Eastern Dahomey Basin is presented in Table 6.8. The values vary from -5.19 to 0.33‰ and -4.03 to 0.83‰ for $\delta^{18}O$ at both wet and dry seasons, respectively. The values for δD vary from -32.5 to 2.3 ‰ and -19.7 to 7.5 ‰ for the wet season and dry season respectively. $\delta^{18}O$ has average values of -3.02 and -3.05 ‰, while δD has average values of -13.11 and -12.44 ‰ for the respective wet and dry season groundwater samples. D-excess values ranged from -27.31 to 1.97 ‰ and -15.76 to 6.67 ‰ with average values of -10.1 and -9.39 ‰ for wet and dry seasons respectively. The results of the oxygen and hydrogen isotopic analysis for both wet and dry seasons are plotted on $\delta D/\delta^{18}O$ diagrams (Figure 6.16) alongside the Global Meteoric Water

Line (GMWL), defined by Craig (1961), regional meteoric water line (RMWL) and local meteoric water line (LMWL) as applied by several authors in groundwater research. The $\delta D/\delta^{18}O$ diagrams show that the groundwater for both seasons plotted on/close to the GMWL, which shows they were young water from precipitation with slight influence of evaporation. The wet season $\delta D/\delta^{18}O$ diagram (Figure 6.16) showed wider range along the LMWL which indicated precipitation dominant with rapid infiltration into the shallow coastal aquifers of the Eastern Dahomey Basin compared to dry season samples plotted within a shorter/narrow range (Figure 6.16) which tends towards mixed water with significant influence of evaporation before infiltrating the aquifer. This also suggests relatively higher residence time of the groundwater travelling from the surface or recharge area through the vadose zone into the aquifers within the basin during the dry season. This relative longer residence time likely interacts with transpirative evaporation from the water table during the hot drier periods and is likely responsible for the slight enrichment observed in the isotopes composition of the water in the dry season compared to wet season, the later preserves the δD and δ18O composition which is very similar or the same as that of the rainwater in the area.

Table 6.8 Statistical summary of the results of Hydrogen and Oxygen Isotopes

Descp Stat	**$\delta^{2}H$**	**$\delta^{18}O$**	**D-Excess**
	Wet Season		
Min	-32.5	-5.19	-27.31
Max	2.3	0.33	1.97
Aver	-13.11	-3.02	-10.10
Stdev	3.59	0.55	3.08
	Dry Season		
Min	-19.7	-4.03	-15.76
Max	7.5	0.83	6.67
Aver	-12.44	-3.05	-9.39
Stdev	2.83	0.50	2.36

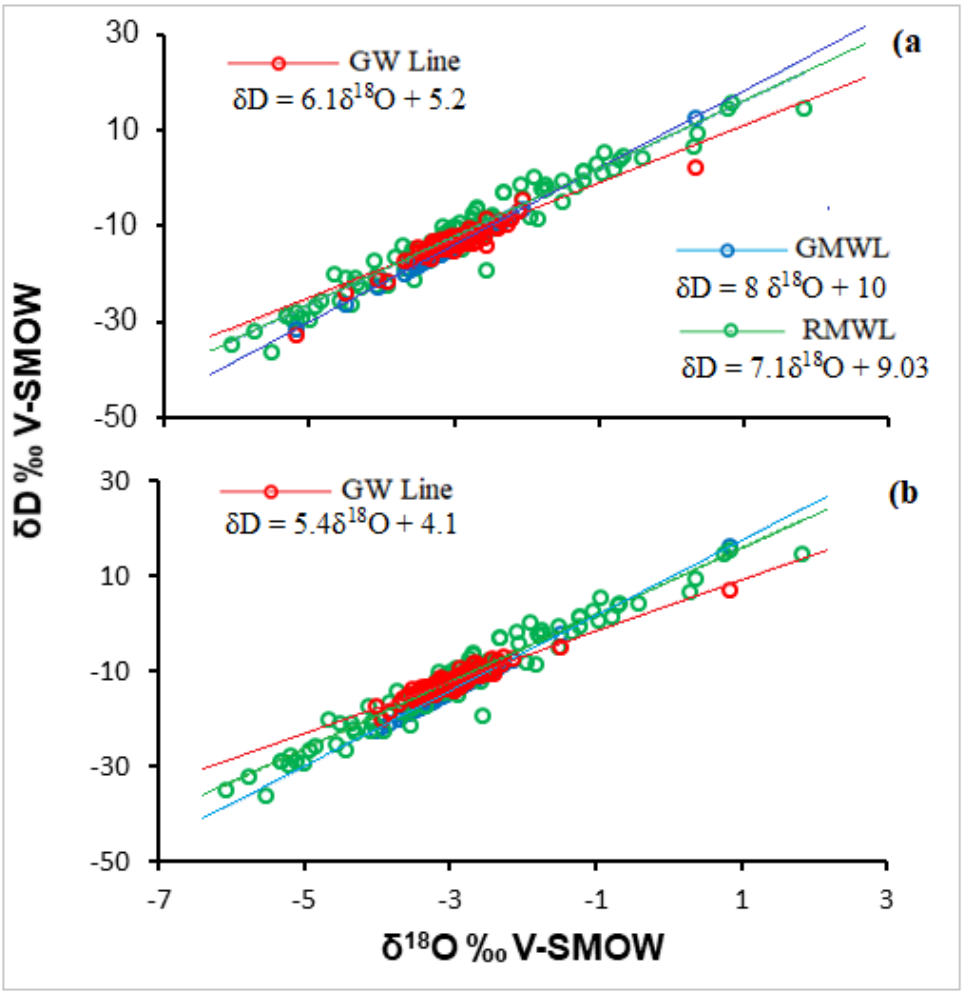

Figure 6.16 $\delta D/\delta^{18}O$ diagram of groundwater samples for (a) wet season (b) dry season

6.2.5 Conclusions

The results of this study provides an insight into the geochemical processes controlling the groundwater chemistry in the Eastern Dahomey Basin. The hydrochemical types in the area can be divided into two major groups. The first group includes mixed Na–Cl, Ca-HCO_3 and Ca–Cl types in both wet and dry seasons, which indicate recent meteoric water in contact with atmospheric CO_2 and water at the intermediate zone of groundwater discharge area which influences rocks mineral dissolution and possible sea spraying due to proximity to the ocean. The other class of

water comprises mixed Na–HCO_3, Na-SO_4, Ca-SO_4, K-Cl, K-SO_4 and Mg–HCO_3 types, indicating the groundwater recharge areas within the Basin. The concentrations of TDS in most groundwater samples are below 1,000 mg/l, except in a few locations within the alluvium deposit and coastal plain sands where higher concentrations were recorded which could be linked to geogenic influence of saltwater intrusion and anthropogenic, from municipal waste.

The relative concentrations of the ions occur in the order of Na>K>Ca>Mg and Na>Ca >Mg>K, while anions are in order of HCO_3 >Cl>SO_4 and Cl>SO_4>HCO_3 for both wet and dry seasons respectively. In the multi-aquifer of the EDB, mineral dissolution from the rock weathering, precipitation and evaporation seem to be the major hydrogeochemical processes controlling the concentration of major ions in groundwater. Calcite, dolomite and aragonite have high SI values in some locations especially the area underlain by limestone and other carbonate rocks, which indicates influence of precipitation as the result of evaporation, whereas gypsum and anhydrite saturation in areas within coastal sands and alluvium deposits could be due to the influence of evaporite dissolution. Halite is undersaturation in all the sampled groundwater in both wet and dry season. The stable isotopes analysis from $\delta D/\delta^{18}O$ showed recent groundwater with precipitation having a significant influence on the chemistry of water samples from the wet season from wide range of clustering along the local meteoric water line (LMWL) and almost on global meteoric water line (GMWL) with much depletion in their isotopic composition of both δD and $\delta^{18}O$. In the case of water samples from the wet season, the plots displayed short range of cluster along the water lines which indicates relative influence of evaporation and effect of seasonal variation with accompanying enrichment of δD and $\delta^{18}O$ composition. The study has contributed information that will be useful to relevant

planners and policymakers for sustainable management of this vital groundwater resource especially given the rapid population surge with attendant groundwater demand.

Acknowledgements The Author is grateful to the Petroleum Technology and Development Fund (PTDF) under the Overseas PhD scholarship scheme for funding this research and also for the support of the Scottish Government under the Climate Justice Fund Water Futures Programme, awarded to the University of Strathclyde (Prof R.M. Kalin).

6.2.6 References

Adegoke, O.S. and Omatsola, M.E., 1981. Tectonic Evolution and Cretaceous Stratigraphy of the Dahomey Basin. Niger. J. Min. Geol. 18, 130–137.

Adelana, S.M.A., Olasehinde, P.I., Bale, R.B., Vrbka, P., Edet, A.E., Goni, I.B., 1996. An overview of the geology and hydrogeology of Nigeria. Q. J. Eng. Geol. Hydrogeol. 29, S1–S12. https://doi.org/10.1144/GSL.QJEGH.1996.029.S1.01

Adeoti, L., Alile, O.M., Uchegbulam, O., 2010. Geophysical investigation of saline water intrusion into freshwater aquifers: A case study of Oniru, Lagos State. Sci. Res. Essays 5, 248–259.

Adepelumi, A.A., Ako, B.D., Ajayi, T.R., Afolabi, O., Omotoso, E.J., 2009. Delineation of saltwater intrusion into the freshwater aquifer of Lekki Peninsula, Lagos, Nigeria. Environ. Geol. 56, 927–933. https://doi.org/10.1007/s00254-008-1194-3

Adimalla, N., 2019. Controlling factors and mechanism of groundwater quality variation in semiarid region of South India: an approach of water quality index (WQI) and health risk assessment (HRA). Environ. Geochem. Health 18–19. https://doi.org/10.1007/s10653-019-00374-8

Adimalla, N., Kumar, A., 2020. Hydrogeochemical investigation of groundwater quality in the hard rock terrain of South India using Geographic Information System (GIS) and

groundwater quality index (GWQI) techniques. Groundw. Sustain. Dev. 10.

Ahmed, N., Reza, A., Hossain, S., Deb, N., Quaiyum, A., 2019. Appraising spatial variations of As , Fe , Mn and NO_3 contaminations associated health risks of drinking water from Surma basin, Bangladesh. Chemosphere 218, 726–740. https://doi.org/10.1016/j.chemosphere.2018.11.104

Akinmosin, A.A., Omosanya, O., Ige, T., 2013. The Occurrence of Tar Sands at Ijebu-Itele, Eastern Dahomey Basin, SW, Nigeria 3, 98–105.

Alfred, G., Kaki, C., Adeoye, J.A., 2016. Benin and Western Nigeria Offshore Basins : A Stratigraphic Nomenclature Comparison 2016, 177–188.

Amiri, V., Nakhaei, M., Lak, R., Kholghi, M., 2016. Assessment of seasonal groundwater quality and potential saltwater intrusion: a study case in Urmia coastal aquifer (NW Iran) using the groundwater quality index (GQI) and hydrochemical facies evolution diagram (HFE-D). Stoch. Environ. Res. Risk Assess. 30, 1473–1484. https://doi.org/10.1007/s00477-015-1108-3

Anomohanran, O., 2014. Characterization by factor analysis of the chemical facies of groundwater in the deltaic plain sands aquifer of Warri, western Niger delta, Nigeria. Int. J. Water Resour. Environ. Eng. 3, 155–163. https://doi.org/10.4314/ajst.v7i1.55201

Awaleh, M.O., Baudron, P., Soubaneh, Y.D., Boschetti, T., Hoch, F.B., Egueh, N.M., Mohamed, J., Dabar, O.A., Masse-Dufresne, J., Gassani, J., 2017. Recharge, groundwater flow pattern and contamination processes in an arid volcanic area: Insights from isotopic and geochemical tracers (Bara aquifer system, Republic of Djibouti). J. Geochemical Explor. 175, 82–98. https://doi.org/10.1016/j.gexplo.2017.01.005

Ayolabi, E.A., Epelle, E.S., Lucas, O.B., Ojo, A., 2014. Geophysical and geochemical site investigation of eastern part of Lagos metropolis, southwestern Nigeria. Arab. J. Geosci. 8, 7445–7453. https://doi.org/10.1007/s12517-014-1688-0

Ayolabi, E.A., Folorunso, A.F., Kayode, O.T., 2013. Integrated Geophysical and Geochemical Methods for Environmental Assessment of Municipal Dumpsite System.

Int. J. Geosci. 4, 850–862. https://doi.org/10.4236/ijg.2013.45079

Bakari, S.S., Aagaard, P., Vogt, R.D., Ruden, F., Brennwald, M.S., Johansen, I., Gulliksen, S., 2012. Groundwater residence time and paleorecharge conditions in the deep confined aquifers of the coastal watershed, South-East Tanzania. J. Hydrol. 466–467, 127–140. https://doi.org/10.1016/j.jhydrol.2012.08.016

Banda, L.C., Rivett, M.O., Kalin, R.M., Zavison, A.S.K., Phiri, P., Kelly, L., Chavula, G., Kapachika, C.C., Nkhata, M., Kamtukule, S., Mleta, P., Nhlema, M., 2019. Water-isotope capacity building and demonstration in a developing world context: Isotopic baseline and conceptualization of a Lake Malawi catchment. Water (Switzerland) 11. https://doi.org/10.3390/w11122600

Birks, S.J., Fennell, J.W., Gibson, J.J., Yi, Y., Moncur, M.C., Brewster, M., 2019. Applied Geochemistry Using regional datasets of isotope geochemistry to resolve complex groundwater flow and formation connectivity in northeastern Alberta , 101, 140–159. https://doi.org/10.1016/j.apgeochem.2018.12.013

Bodrud-Doza, M., Bhuiyan, M.A.H., Islam, S.M.D.U., Rahman, M.S., Haque, M.M., Fatema, K.J., Ahmed, N., Rakib, M.A., Rahman, M.A., 2019. Hydrogeochemical investigation of groundwater in Dhaka City of Bangladesh using GIS and multivariate statistical techniques. Groundw. Sustain. Dev. https://doi.org/10.1016/j.gsd.2018.11.008

Bouderbala, A., Remini, B., Saaed Hamoudi, A., Pulido-Bosch, A., 2016. Application of multivariate statistical techniques for characterization of groundwater quality in the coastal aquifer of Nador, Tipaza (Algeria). Acta Geophys. 64, 670–693. https://doi.org/10.1515/acgeo-2016-0027

Brownfield, B.M.E., Jewell, S., Survey, U.S.G., 2016. Assessment of Undiscovered Oil and Gas Resources of the Niger Delta Province , Nigeria and Cameroon , Africa.

Cary L., Petelet-Giraud E., Bertrand G., Kloppmann W., Aquilina L., Martins V., Hirata R., Montenegro S., Pauwels H., Chatton E., Franzen, M. and Aurouet A., 2015. Origins and processes of groundwater salinization in the urban coastal aquifers of Recife (Pernambuco, Brazil): A multi-isotope approach. Sci. Total Environ. 530–531, 411–429. https://doi.org/10.1016/j.scitotenv.2015.05.015

Edet, A., 2019. Seasonal and spatio-temporal patterns, evolution and quality of groundwater in Cross River State, Nigeria: implications for groundwater management. Sustain. Water Resour. Manag. 5, 667–687. https://doi.org/10.1007/s40899-018-0236-6

Edet, A., 2016. Hydrogeology and groundwater evaluation of a shallow coastal aquifer, southern Akwa Ibom State (Nigeria). Appl. Water Sci. https://doi.org/10.1007/s13201-016-0432-1

Guendouz, A., Moulla, A.S., Edmunds, W.M., Zouari, K., Shand, P., Mamou, A., 2003. Hydrogeochemical and isotopic evolution of water in the Complexe Terminal aquifer in the Algerian Sahara. Hydrogeol. J. 11, 483–495. https://doi.org/10.1007/s10040-003-0263-7

He, J., Ma, J., Zhao, W., Sun, S., n.d. Groundwater evolution and recharge determination of the Quaternary aquifer in the Shule River basin, Northwest China.

Hussien, B.M., Faiyad, A.S., 2016. Modeling the Hydrogeochemical Processes and Source of Ions in the Groundwater of Aquifers within Kasra-Nukhaib Region 2016, 1156–1181. https://doi.org/10.4236/ijg.2016.710087

Jones, H. A and Hockey, R.., 1964. The Geology of part of Southwestern Nigeria. GSN Bull. No. 31-10.

Kalin, R.M. and Long, A., 1994. Application of hydrogeochemical modelling for validation of hydrologie flow modelling in the Tucson basin aquifer, Arizona, United States of America, in: Mathematical Models and Their Applications to Isotope Studies in Groundwater Hydrology. IAEA TECDOC-777, Viena, pp. 209–254.

Kalin R.M., 2000. Radiocarbon Dating of Groundwater Systems, in: Cook P.G., H.A.L. (eds (Ed.), Environmental Tracers in Subsurface Hydrology. Springer. Kluwer Academic Publishers, Boston, Boston, pp. 111–144. https://doi.org/https://doi.org/10.1007/978-1-4615-4557-6_4

Kalin, R.M., 1995. Basic concepts and formulations for isotope-geochemical process investigations, procedures and methodologies of geochemical modelling of groundwater systems, in: Y Yurtsever (Ed.), Manual on Mathematical Models in Isotope Hydrology. IAEA TECHDOC 910, Viena, pp. 155–206.

Krishnaraj, S., Murugesan, V., K, V., Sabarathinam, C., Paluchamy, A., Ramachandran, M., 2012. Use of Hydrochemistry and Stable Isotopes as Tools for Groundwater Evolution and Contamination Investigations. J. Geo-sciences 1, 16–25. https://doi.org/10.5923/j.geo.20110101.02

Kumar, P.J.S., Jegathambal, P., James, E.J., 2011. Multivariate and Geostatistical Analysis of Groundwater Quality in Palar River Basin. Int. J. Geol. 5, 108–119.

Lapworth, D.J., Nkhuwa, D.C.W., Okotto-Okotto, J., Pedley, S., Stuart, M.E., Tijani, M.N., Wright, J., 2017. Urban groundwater quality in sub-Saharan Africa: current status and implications for water security and public health. Hydrogeol. J. 25, 1093–1116. https://doi.org/10.1007/s10040-016-1516-6

Longe, E.O., 2011. Groundwater Resources Potential in the Coastal Plain Sands Aquifers , Lagos, Nigeria 3, 1–7.

Longe, E.O., Balogun, M.R., 2010. Groundwater quality assessment near a municipal landfill, Lagos, Nigeria. Res. J. Appl. Sci. Eng. Technol. 2, 39–44.

Longe, E. O., Malomo, S., Olorunniwo, M.A., 1987. Hydrogeology of Lagos metropolis. J. African Earth Sci. 6, 163–174. https://doi.org/10.1016/0899-5362(87)90058-3

Longe, E.O., Malomo, S., Olorunniwo, M.A., 1987. Hydrogeology of Lagos metropolis. J. African Earth Sci. 6, 163–174. https://doi.org/10.1016/0899-5362(87)90058-3

Narany, T.S., Ramli, M.F., Aris, A.Z., Nor, W., Sulaiman, A., Juahir, H., Fakharian, K., 2014. Identification of the Hydrogeochemical Processes in Groundwater Using Classic Integrated Geochemical Methods and Geostatistical Techniques, in Amol-Babol Plain, Iran. Sci. World J. 2014, 1–15.

Nicaise, Y., Gérard, D., Flavien, D., 2013. Hydrogeophysical estimation of an unconfined sandy aquifer parameters using gravimetric and geoelectrical methods. Appl. Sci. Reports 2, 1–9.

Oke, S.A., 2015. Evaluation of the Vulnerability of Selected Aquifer Systems in the Eastern Dahomey Basin, South Western Nigeria.

Oke, S.A., Vermeulen, D., Gomo, M., 2016. Aquifer vulnerability assessment of the

Dahomey Basin using the RTt method. Environ. Earth Sci. 75, 1–9. https://doi.org/10.1007/s12665-016-5792-1

Olabode, S.O., Mohammed, M.Z., 2016. Depositional Facies and Sequence 2016, 210–228.

Oloruntola, M.O., Adeyemi, G.O., Bayewu, O., Obasaju, D.O., 2019. Hydro-geophysical mapping of occurrences and lateral continuity of aquifers in coastal and landward parts of Ikorodu, Lagos, Southwestern Nigeria. Int. J. Energy Water Resour. 3, 219–231. https://doi.org/10.1007/s42108-019-00026-8

Oteri, A.U., and Atolagbe, F.P., 2003. Saltwater Intrusion into Coastal Aquifers in Nigeria, in: The Second International Conference on Saltwater Intrusion and Coastal Aquifers Monitoring, Modeling, and Management. Mérida, Yucatán, México, March 30 - April 2, 2003. Merida Yucatan, pp. 1–15.

Prasanna, M. V, Chidambaram, S., Kumar, G.S., 2011. Hydrogeochemical assessment of groundwater in Neyveli Basin , Cuddalore District , South India. Arab J. Geosci. 4, 319–330. https://doi.org/10.1007/s12517-010-0191-5

Priyantha Ranjan, S., Kazama, S., Sawamoto, M., 2006. Effects of climate and land use changes on groundwater resources in coastal aquifers. J. Environ. Manage. 80, 25–35. https://doi.org/10.1016/j.jenvman.2005.08.008

Shakerkhatibi, M., Mosaferi, M., Pourakbar, M., Ahmadnejad, M., Safavi, N., Banitorab, F., 2019. Comprehensive investigation of groundwater quality in the north-west of Iran: Physicochemical and heavy metal analysis. Groundw. Sustain. Dev. https://doi.org/10.1016/j.gsd.2018.10.006

Sheikhy Narany, T., Ramli, M.F., Aris, A.Z., Sulaiman, W.N.A., Juahir, H., Fakharian, K., 2014. Identification of the hydrogeochemical processes in groundwater using classic integrated geochemical methods and geostatistical techniques, in Amol-Babol Plain, Iran. Sci. World J. 2014. https://doi.org/10.1155/2014/419058

Singh, R. D.Kumar, C.P., 2010. Impact of Climate Change on Groundwater Resources 247667, 1–14. https://doi.org/10.4018/978-1-4666-8814-8.ch010

Somaratne, N., Frizenschaf, J., 2013. Geological Control upon Groundwater Flow and

Major Ion Chemistry with Influence on Basin Management in a Coastal Aquifer , South Australia. J. Water Resour. Prot. 5, 1170–1177.

Srinivasamoorthy, K., Gopinath, M., Chidambaram, S., Vasanthavigar, M., Sarma, V.S., 2014. Hydrochemical characterization and quality appraisal of groundwater from Pungar sub basin, Tamilnadu, India. J. King Saud Univ. - Sci. 26, 37–52. https://doi.org/10.1016/j.jksus.2013.08.001

Srinivasamoorthy, K., Sarma, V.S., 2014. Hydrochemical characterization and quality appraisal of groundwater from Pungar sub basin , Tamilnadu , India. J. King Saud Univ. - Sci. 26, 37–52. https://doi.org/10.1016/j.jksus.2013.08.001

Stephen Foster, Héctor Garduño, Karin Kemper, Albert Tuinhof, M.N. and C.D., 2004. Quality Protection defining strategy and setting priorities. Sustain. Groundw. Manag. 8, 1–6.

Talabi, A.O., Tijani, M.N., 2013. Hydrochemical and stable isotopic characterization of shallow groundwater system in the crystalline basement terrain of Ekiti area, southwestern Nigeria. Appl. Water Sci. 3, 229–245. https://doi.org/10.1007/s13201-013-0076-3

Talabi, A.O., Tijani, M.N., Aladejana, A.J., 2012. Assessment of impact of climatic change on groundwater quality around Igbokoda Coastal area , southwestern Nigeria . J. Environ. Earth Sci. 2, 39–50.

Thilagavathi, R., Chidambaram, S., Thivya, C., Prasanna, M. V., Keesari, T., Pethaperumal, S., 2017. Assessment of groundwater chemistry in layered coastal aquifers using multivariate statistical analysis. Sustain. Water Resour. Manag. 3, 55–69. https://doi.org/10.1007/s40899-017-0078-7

Tijani, M.N., Lapworth, D.J., Macdonald, A.M., 2014. Hydrochemical and isotopes studies of shallow basement aquifers in nigeria: implications for groundwater recharge, in: International Association of Hydrogeologists IAH, the Moroccan Chapter - 41st IAH International Congress “Groundwater : Challenges and Strategies” - Marrakech, September, 15-19, 2014 Hydrochemical. p. 22.

Wang, J., Zhang, F., Kung, H. te, Ren, Y., Zhang, Y., Yu, H., 2017. Linkage analysis of

land use/cover patterns and hydro-chemical characteristics in different seasons in Ebinur Lake Watershed, China. Water (Switzerland) 9. https://doi.org/10.3390/w9110888

CHAPTER 7

7.0 GROUNDWATER ORIGIN AND RESIDENCE TIME

7.1 Preambles

In Chapter 6, rock-water interaction, evaporation, saltwater interaction and sea spraying were suggested to be the dominant hydrogeochemical that controlled the groundwater chemistry of the Eastern Dahomey Basin. Further studies involving origin and residence time of groundwater along flow paths and infiltration through the soil of the vadose zone is necessary to develop a conceptual model. This model provides knowledge of sources and how long it will take potential contaminant and pollutant to reach the groundwater.

The lack of GNIP precipitations isotopes stations in the south coast of Nigeria necessitated using isotopes of precipitation data from the nearest GNIP stations which are situated at both sides of Nigeria along the West African coast. These stations are Douala in Cameroon at the east and Cotonou in the Republic of Benin at the west end of the study area. These two data sets were compared to the $\delta^{18}O$ and δD data obtained from the groundwater samples and with the data set collected from Kano GNIP station at the northern Sahel savannah of Nigeria.

This study led to an article which was submitted for publication in the MDPI; Applied Sciences (Earth Sciences and Geography) as presented below;

- Jamiu A. Aladejana, Robert M. Kalin, Ibrahim Hassan, Philippe Sentenac and Moshood N. Tijani. 2020. Origin and residence time of groundwater in the shallow coastal aquifer of Eastern Dahomey Basin using $\delta^{18}O$ and δD Isotopes. To be submitted to MDPI; *Applied Science (Earth Science and Geography)* [Open access]

The article presents the efforts in characterisation of the groundwater of the shallow aquifer of the basin to identifying the dominant hydrogeological processes that influence the groundwater chemistry. The research was designed under the supervision of my supervisor, Prof. Robert M. Kalin with a further critical review of the manuscript, while technical contributions were made by Dr. Philippe Sentenac, Ibrahim Hassan and Prof. Moshood N. Tijani.

7.2 Paper 4

Jamiu A. Aladejana, Robert M. Kalin, Ibrahim Hassan, Philippe Sentenac and Moshood N. Tijani. 2020. Origin and residence time of groundwater in the shallow coastal aquifer of Eastern Dahomey Basin using $\delta^{18}O$ and δD Isotopes. *Submitted* to MDPI; *Applied Science (Earth Science and Geography)* [Open access]

Origin and residence time of groundwater in the shallow coastal aquifer of Eastern Dahomey Basin using $\delta^{18}O$ and δD Isotopes

Jamiu A. Aladejana [1,2,*], Robert M. Kalin [1], Ibrahim Hassan [1,3], Philippe Sentenac and Moshood N. Tijani[2]

[1] *Department of Civil and Environmental Engineering, University of Strathclyde, Glasgow G1 1XJ, UK*

[2] *Department of Geology, University of Ibadan, Ibadan 200284, Nigeria*

[3] *Department of Civil Engineering Abubakar Tafawa Balewa University Bauchi, Bauchi 740272, Nigeria*

jamiu.aladejana@strath.ac.uk

7.2.1 Abstract

This study employed stable isotopes of $\delta^{18}O$ and $\delta^{2}H$ in conjunction with other hydrological parameters to understand the origin, residence time and seasonal effect of groundwater in the shallow aquifers of the Eastern Dahomey Basin. A total of 230 groundwater samples (97 in the wet season and 133 in the dry season) were collected from the borehole and shallow aquifer between May 2017 and April 2018. The analysed parameters from the groundwater include major ions and $\delta^{18}O$ and $\delta^{2}H$, while isotopes data in precipitation from three selected GNIP stations, Douala, Cotonou and Kano, were collected for comparative analysis. Results of the hydrochemical model revealed Ca-HCO3 and Na-Cl as dominant water types with other mixing water types such as Ca-SO_4, Ca-Cl, Na-SO_4 and K-Mg-HCO_3 which characterised early stage of groundwater transformation in the shallow coastal basin. $\delta^{18}O$ and $\delta^{2}H$ precipitation

data from the three stations plotted along with the groundwater samples indicate recent meteoric water as a source of groundwater recharge in the basin, with little effect of evaporation during the dry season. The plot of Total Dissolved Solids (TDS) against $\delta^{18}O$ showed clustering of the water samples between the recharge and the evaporation zone with dry season samples trending towards the brackish zones, which is an indication of the subtle effect of evaporation during this period. Tracing groundwater types along the flow paths within the basin revealed a none-consistent pattern in groundwater type distribution across the geologic units of the basin which is attributed to the heterogeneity of the aquifer with anthropogenic influence. In addition, a comparison of the $\delta^{18}O$ and $\delta^{2}H$ isotopic compositions of groundwater and precipitation in the three selected stations, with their respective D-excess values established low evapotranspiration induced isotope enrichment which could be due to higher precipitation and humidity in the region resulting in low isotope fractionation, hence, little effect of seasonal variations. The study, therefore, suggested groundwater recharge in the shallow aquifer in the Eastern Dahomey Basin is of meteoric origin with a short residence time of water flows from soils through the vadose zone to the aquifers.

Keywords: Hydrogen and Oxygen isotopes; Groundwater sources; Residence time

7.2.2 Introduction

Rock-water interaction is a process that influences groundwater chemical evolution from recharge along the flow paths through the vadose zone to the phreatic zones. Aquifers' mineral solubility, residence time and intrinsic chemical characteristics of original water determine how quickly groundwater quality changes (Gattacceca et al., 2009; Guendouz et al., 2003). The origin of water also plays a role

before continuous evolution as it flows from recharge zone downgradient within the geological unit of formations (Daniele et al., 2013). Sedimentary basins play a vital role as sources of water supply to meet water demand, especially in developing countries in Africa and Asia. Sub-Saharan African countries depend mostly on groundwater to meet their daily water demand due to infrastructural failure and poor water management (Kashaigili, 2012; Lapworth et al., 2017). Generally, groundwater resources are under stress from natural and human drivers. Coastal basins are more susceptible to these pressures due to their proximity to the sea, increased population, industrialisation, agricultural activities and the effect of global climate change (Edet, 2016; Oke et al., 2016). For coastal basins' the stratigraphical characteristics make aquifers vulnerable to contamination and pollution (Jamiu A Aladejana et al., 2020). Shallow coastal aquifers in some developing countries have been reported to be facing various challenges of groundwater quality deterioration, the causes of which are attributed to both geogenic and anthropogenic influence.

The Eastern Dahomey Basin is one of the eight hydrogeological provinces of Nigeria, providing groundwater demand for about 30% of the country's population. Urbanisation, industrialisation, and agriculture, coupled with the dynamic geology of this basin, continues to pose a significant challenge to understanding groundwater dynamics (Jamiu A. Aladejana et al., 2020; Oke, 2015). In Nigeria, inadequate pipe-borne water leaves individual households to rely on groundwater from shallow boreholes and hand-dug wells to meet water demand for domestic, agriculture and other usages (Ayoade, 1975; Omole, 2013). A unique characteristic of this basin is its complex geology and relief with a drainage system controlled by topography and geology (Jamiu A Aladejana et al., 2020). Most of the major rivers in the basin flow southward across different geologic units and formations and discharge water into

lagoons and the ocean. During the process of groundwater flow from the recharge area at the northern parts (upslope) of the Basin to recharge major rivers through baseflow or recharging the aquifers, the water interacts with aquifer materials which alter the chemistry of the water. Understanding the hydrochemical dynamics at a regional level is critical in the development of a sustainable water resource management regulation (Gagné et al., 2017). As part of understanding the hydrogeochemical dynamics of shallow coastal aquifers of the Eastern Dahomey Basin, this study aimed to apply stable environmental isotopes of $\delta^{18}O$ and $\delta^{2}D$ in combination with key hydrochemical parameters for a conceptual model of how groundwater chemistry changes across different geological units and formation within the EDB. This model adds to the knowledge required by water professionals and policymakers to develop an effective strategy for water resources management and protection for this extensive aquifer.

7.2.2.1 Study area

The Eastern Dahomey Basin is administratively located in the South-Western part of Nigeria. It is bordered to the west, east and north by the Republic of Benin, Okitipupa ridge and the Precambrian Basement Rocks respectively while stretching south into the Atlantic Ocean. Geographically, the EDB is located between Latitudes 2° 41'10.00" and 4° 59'59.00" N and Longitudes 6°21'13.00" and 7°52'42.00"E along the coast of the Gulf of Guinea (Figure7.1). The Nigerian part of this basin is known as the Eastern Dahomey Basin which underlies the three states of Lagos, Ogun and Ondo. The study area is low lying, with several points virtually at or below sea level, which is always saturated with water, and prone to flooding. The highest elevation, 265 m above sea level, is at Abeokuta town, where the basin thins out into the Precambrian basement rocks (Jamiu A. Aladejana et al., 2020). The climate of the basin is characterised by wet and dry seasons, within the tropical rain forest belt.

Precipitation in this area occurs as rainfall ranges between 750 and 1000 mm mostly between April and October (wet season) and 250 mm and 500 mm between November and March (dry season) (Oloruntola et al., 2019).

Most of the hydrogeologic studies in the Eastern Dahomey basin are fragmented, primarily focussing on specific sites and locations, with few including stable isotopes. There is an opportunity to use isotope hydrology to better understand the regional system. Groundwater originates from local atmospheric precipitation (Ahmed and Clark, 2016; Shin et al., 2017), and seasonal effect and variations in precipitation are dampened during infiltration, mixing and isotope effects (Kalin, 1995; Peter Bauer-Gottwein, Bibi N. Gondwe, Lars Christiansen, Daan Herckenrath and A, 2010). Some seasonality may exist depending on the hydrological properties, size and thickness of the vadose zone (Ahmed and Clark, 2016; Joshi et al., 2018; Clark & Fritz 1997). Groundwater may become isotopically distinct from the precipitation by selective recharge or isotopic fractionation effects related to evapotranspiration and runoff (Gat and Tzur 1967; Clark and Fritz 1997).

7.2.2.2 Geology and hydrogeology

Geology

The area is a part of the Dahomey basin which extends from Nigeria to Ghana. The lithological character of the sediments is a result of transgressions and regressions of the sea since the Cretaceous age, the transgressions coming from the south. The stratigraphic description of the sediments has been provided by various authors, including Adegoke, O.S. and Omatsola, 1981; Jones, H. A and Hockey, 1964; Solomon O. Olabode1, 2016 as presented in Figure 7.1. The Coastal Plain Sands (Recent – Oligocene) constitute the main aquifer of the area which is exploited through

hand-dug wells and boreholes. It forms a multi-aquifer system consisting of three aquifer horizons separated by clayey layers (Longe et al., 1987; Oloruntola et al., 2019). Quaternary alluvial sediments cover most of the Lagos coastal areas and river valleys.

Hydrogeology

The hydrostratigraphy of the study area has been explained by several researchers (Adeoti et al., 2010; Jamiu A Aladejana et al., 2020; Faleye and Olorunfemi, 2015; Fatoba et al., 2014; Longe, 2011; Offodile, 1971; Oloruntola et al., 2019; Oteri, A.U., & Atolagbe, 2003). Depth to the aquifer units is in the range of 5–23m for the primary unconfined aquifer while depth to three confined aquifers are in the range of 7–80m, 63-188m and 245–261m respectively while their thicknesses range from 7–26m, 6–67m, 20-143m and 61–117m. The aquifers are bounded by intercalation of shale, tar sands, and layers of sandy clay with relatively low hydraulic conductivity. Two main aquifer units were identified within the Upper Coal Measures. The depths to the top/thicknesses of the aquifer units are 9.8 m (1.7m) and 23 m (5.3m) respectively. The Nkporo Shale had a thickness and depth to the top of the only identified aquifer unit as 10m and 16 m, respectively (Faleye and Olorunfemi, 2015). At the northern parts of the study area where the sedimentary rocks of the Abeokuta formation terminate on the basement complex, most of the wells and boreholes are drilled through the upper sandy layers into the weathered profile of the Precambrian basement rocks tapping water through weathered overburden and sometimes fractured basement rocks depending on locations and weathering status.

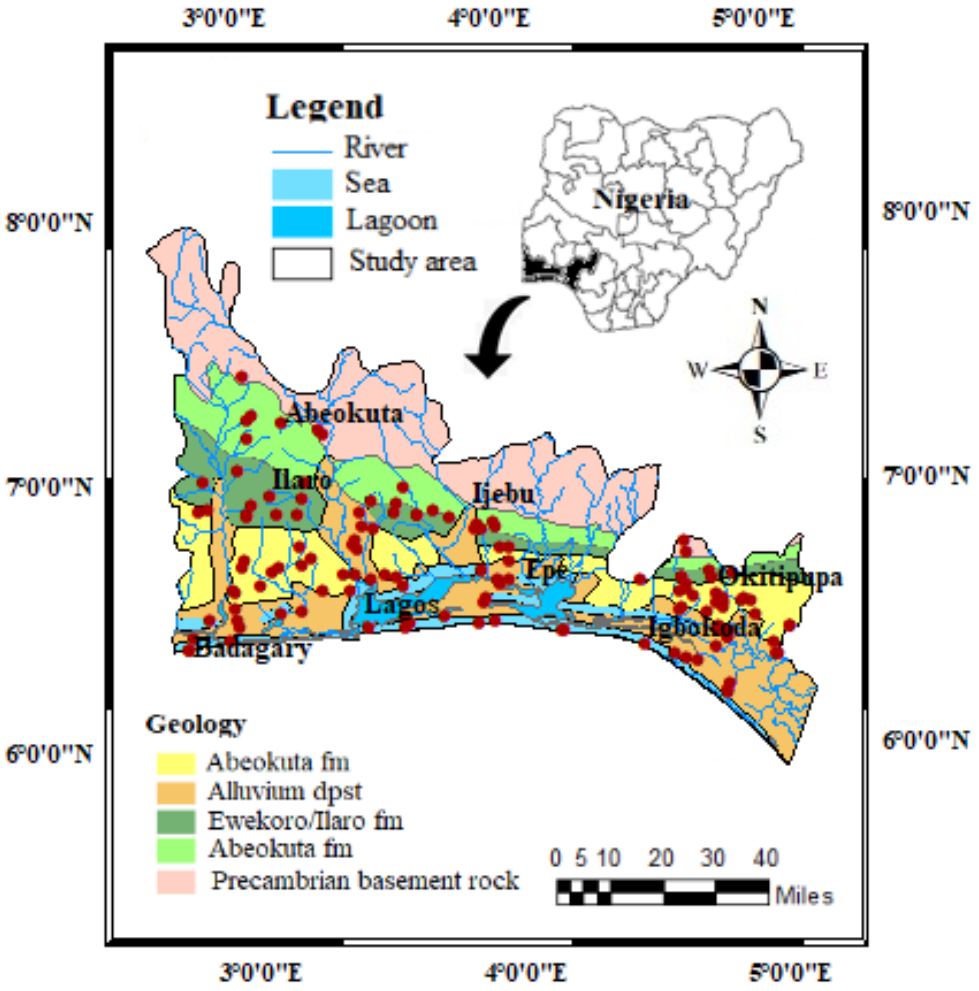

Figure 7.1 Map of the study area showing sampling points and geology

7.2.3 Methodology

7.2.3.1 Field Physicochemical measurement

Well-inventories were carried out on a total number of 230 shallow hand-dug wells, shallow tube wells and boreholes from the Eastern Dahomey Basin (EDB), 96 in the wet season and 134 in the dry season between May 2017 and April 2018. The physicochemical parameters were measured in the field using a Model 99720 pH/Conductivity meter capable of measuring total dissolved solids (TDS), salinity, temperature and Eh/ORP. The depth of the wells and static water level was measured with the aid of a water depth meter while the coordinates of each sampled well were

recorded using GPS. The 230 groundwater samples were collected in three separate sets of 50 ml polypropylene tubes labelled A, B and IS. Samples labelled A were acidified to a pH < 2 after collection with 0.4 ml of concentrated nitric acid (HNO_3). Samples B and IS were filtered with a 0.45µm filter and preserved in an ice-packed cooler to keep the samples' temperature below 4°C before being transported to the laboratory for further analysis.

7.2.3.2 Laboratory Analysis

(a) Major ions and trace metals analysis

Three sets of water samples analysed. Samples labelled (A) were prepared by collecting 10 ml of each sample in a centrifuge polyethylene tube and arranged serially for Inductively Coupled Plasma (ICP-MS) analysis of cations. The same arrangement was used for the sample set labelled (B) for Ion Chromatography (IC) for the anions analysis in the Environmental Laboratory, Department of Civil and Environmental Engineering, University of Strathclyde. Alkalinity (HCO_3^-) was determined using a Digital Titrator (Model: 16900, HACH International) and 1.6 N H_2SO_4 cartridge.

cartridge.

(b) Stable isotopes analysis in groundwater

Samples labelled (IS) were shipped to the Ministry of Agriculture, Irrigation and Water Development Isotope Laboratory, Blantyre, Malawi under a temperature below 4°C for the stable isotope of δ^2H and $\delta^{18}O$ analysis. The groundwater samples and analysis were carried out following the same method of isotope water samples as described in Banda et al., 2019 and analysis which was conducted in line with

International Standard Procedures with appropriate quantification and validation of results.

7.2.3.3 Regional Precipitation Data

Regional precipitation isotope data was needed for this study to identify any possible deviation from the Global Meteoric Water Line (GMWL) to better characterise local meteoric conditions. The closest Global Network of Isotope in Precipitation (GNIP) data stations to the study location in the Eastern Dahomey Basin are Cotonou (Republic of Benin) to the west and Douala (Cameroon) to the east. The only station in Nigeria is situated in Kano, at the northern savannah region of Nigeria. Meanwhile, Cotonou and Douala, located along the coast of West Africa, share similar climate conditions with the study area (Figure 7.2). In light of this, a total of 134 regional and annual precipitation isotope data of $\delta^{18}O$ and $\delta^{2}H$ were collected from the Douala, Cameroon (50), Cotonou, Republic of Benin (50) and Kano, Nigeria (33) meteorological stations during 2009 – 2018. These isotope data were downloaded from the GNIP and are presented in Table 2. The results are expressed as δ-values relative to V-SMOW (Vienna Standard Mean Ocean Water), and the measurement precision is 0.01‰ and 0.2‰ for $\delta^{18}O$ and $\delta^{2}H$, respectively.

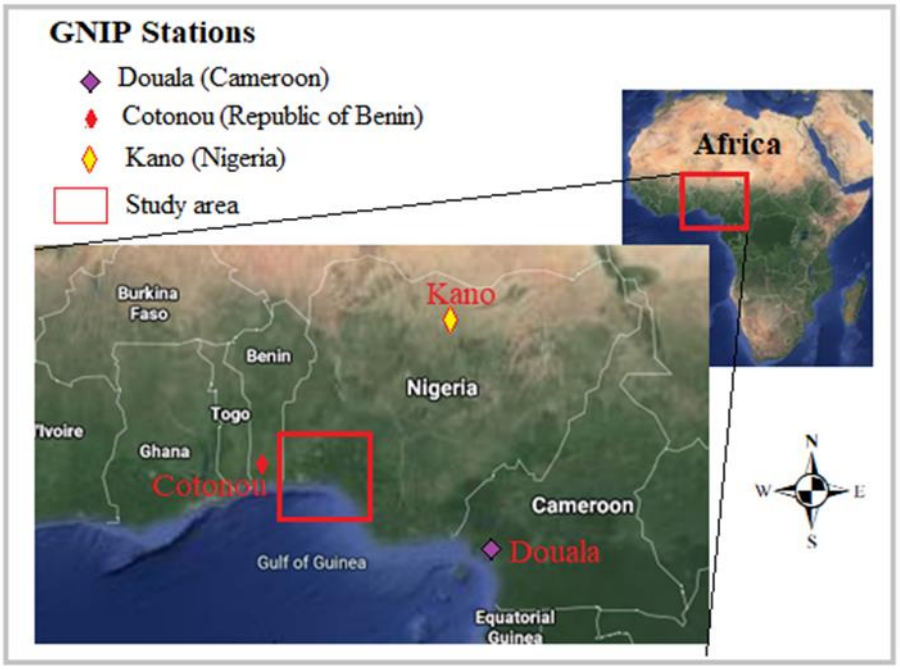

Figure 7.2 Map showing the regional GNIP Stations within West Africa (Adapted from Google Earth Pro)

7.2.3.4 Data analysis and evaluation

Data from the field and laboratory measurements were checked for quality by correlating selected major ions from randomly duplicated samples, of which the correlation values are all above 0.9, indicating low to insignificant analytical errors. Total dissolved solids (TDS), pH, electrical conductivity (EC) temperature and major ions analysed within GeoChemist Work Bench to determine groundwater types for the study area. Piper diagrams for both seasons were also plotted using the same software. Results of water types were used in relation to the major ions for other plots in Excel. At the same time, the spatial distribution maps of the stable isotopes were generated in ArcGIS version 10.6.

7.2.4 Results and discussions

The result The result of the physicochemical parameters and stable isotopes are presented in Table 7.1. pH of the groundwater samples during the wet and dry season range from 4.0 to 8.1 (average of 5.6) and 3.9 to 8.0 (average of 5.7) respectively. The pH of groundwater is slightly higher in the wet season compared to the dry season. TDS ranged from 0.0 to 8500 mg/l (average of 201.8) and 2.3 to 6750 mg/l (average of 236 mg/l) while EC ranges from 0.0 to 12000 µS/cm (average of 295.4 µS/cm) and 5.5 to 10,009 µS/cm (average of 352.4) for wet and dry seasons respectively. The temperature of groundwater ranged from 25.5 to 34.6 °C (average of 39.4 °C) and 26.6 to 37.7 °C (average of 31.2 °C) during wet and dry seasons respectively.

Table 7.1 Statistical summary of physicochemical parameters and stable isotopes in groundwater

	Wet Season				Dry Season			
Parameter	Min	Max	Avg	Stdev	Min	Max	Avg	Stdev
Ca	0.3	374.0	16.5	41.2	0.2	448.5	21.6	55.2
Mg	0.0	1,377.0	18.4	140.4	0.1	1,125.0	16.1	102.2
Na	0.1	8,857.0	106.8	902.8	0.6	10,310.0	112.7	907.4
K	0.1	447.1	10.5	46.2	0.1	590.2	10.1	51.6
HCO3	1.0	8,028.5	142.3	818.7	1.6	8,390.0	139.5	767.6
SO4	0.0	2,210.7	37.0	242.2	0.3	2932.0	39.7	259.8
Cl	0.1	18,970.2	218.1	1,934.3	0.9	18,833.0	206.3	1,677.6
NO3	0.0	258.6	31.8	54.1	0.3	311.9	30.1	54.3
PH	4.0	8.1	5.6	1.0	3.9	8.0	5.6	1.9
TDS	0.0	8,500.0	201.8	863.6	2.3	6750.0	235.8	672.7
EC	0.0	12,000.0	295.4	1,219.4	5.5	10,009.0	352.4	1,002.0
Temp	25.5	34.6	29.4	1.7	26.6	99.9	60.1	28.9
$\delta^{2}H$ (‰)	-32.5	2.3	-13.1	3.6	-19.7	7.5	-12.4	2.8
$\delta^{18}O$(‰)	-5.2	0.3	-3.0	0.6	-4.0	0.8	-3.0	0.5
D-Excess	-0.3	13.8	11.0	1.7	0.9	15.0	11.9	1.6

Major ions and TDS are measured in mg/l, EC in µS/cm and Temperature in °C

7.2.4.1 Hydrochemical characteristics and isotopic relationship

The groundwater types along the flow paths within the basin provides clues to the prevailing hydrochemical processes. The EC values of the groundwater are low in the northern part of the basin, gradually increasing along the groundwater flow paths, a trend probably due to the longer residence time of the water in the stratum or influence of seawater intrusion and sea spraying (Fu et al., 2018; Mohanty and Rao, 2019). Figures 7.4 and 7.5 present pie charts of water type across the geological units to link prevailing groundwater characteristics in each of the aquifers with aquifer mineralogy.

The majority of the shallow groundwater samples are Na-Ca and Ca-HCO_3 type water. The results from Geochemist's Work Bench revealed 8 water types, Ca- HCO_3, Na – Cl, Na – HCO_3, Ca – Cl, B Na – SO_4, Ca – SO_4, K –Cl and Mg – SO_4 across the geologic units of the basin as presented in Figure 7.3 and supported by the piper diagrams (Figure 7.6). Although there is no observed consistency in the pattern of distribution of different water types across the geologic units in the study basin, there is a reflection of the mineralogical composition of the basin sediment and rocks in these water types.

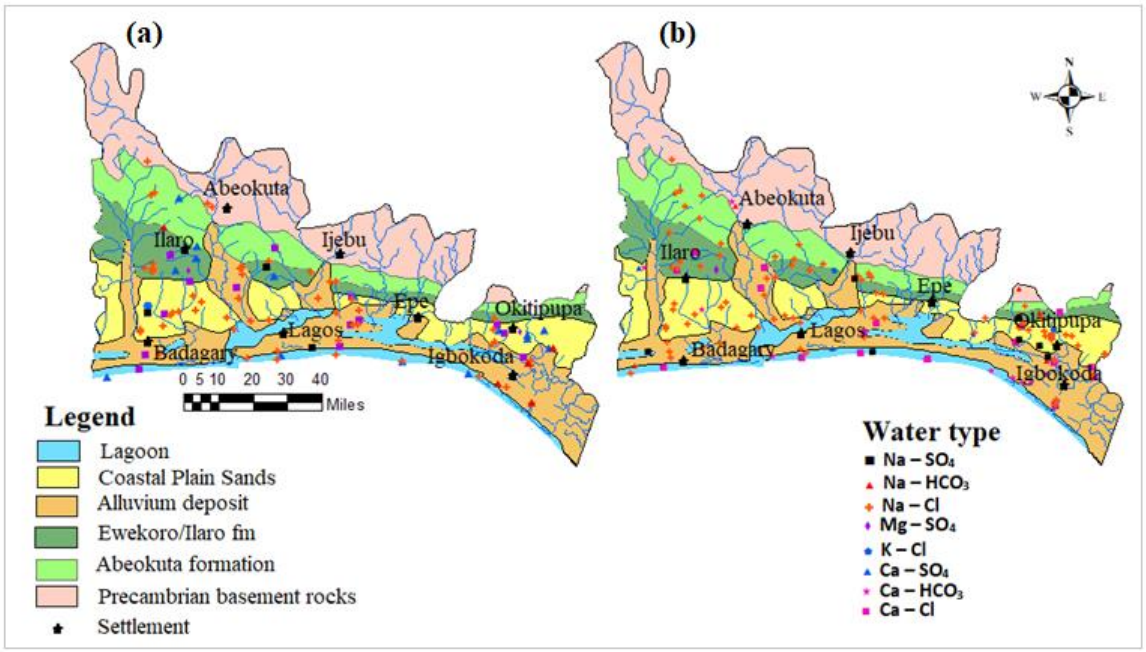

Figure 7.3 Groundwater type distribution (a) Wet season (b) Dry season, across a different geological unit of the Eastern Dahomey Basin

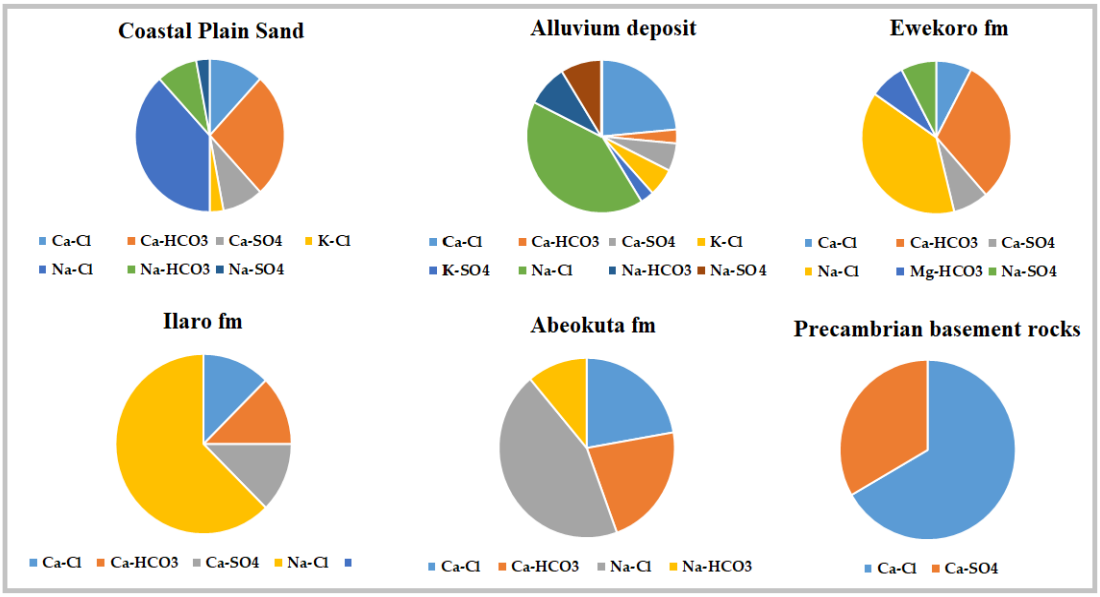

Figure 7.4 Pie chart of percentage water type across the geologic units within the basin for the wet season water samples

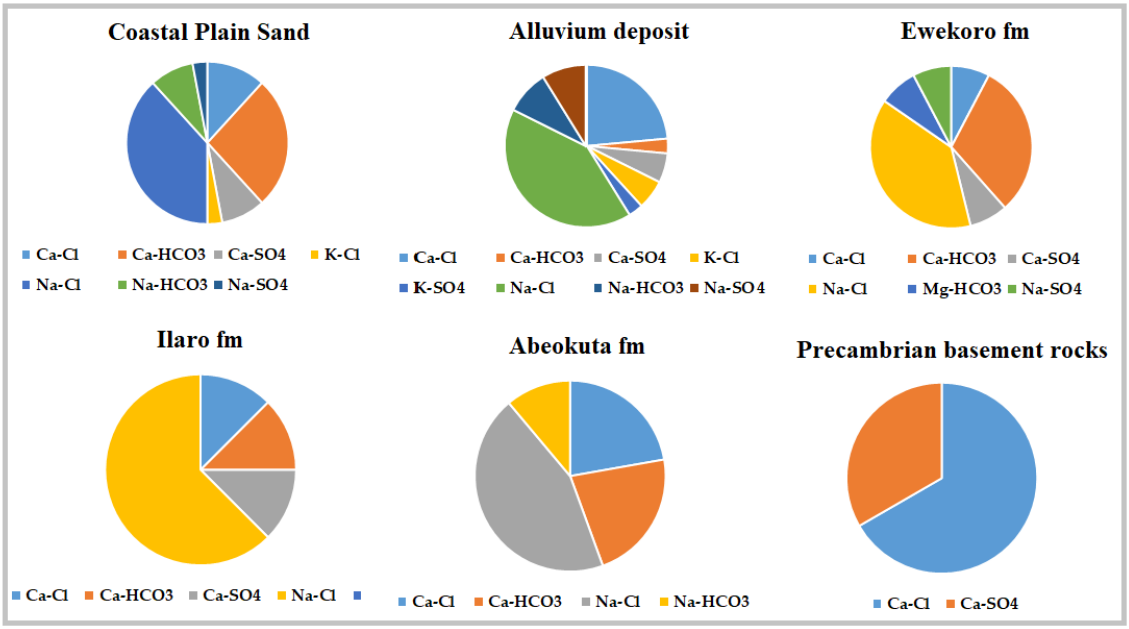

Figure 7.5 Pie chart of percentage water type across the geologic units within the basin for the dry season water samples

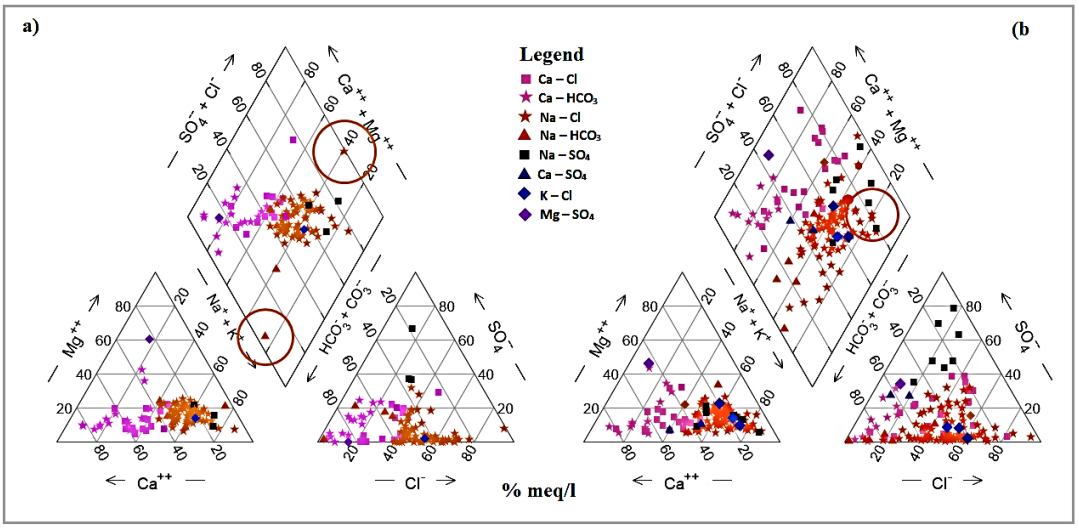

Figure7.6 Piper diagram for groundwater types (a) Wet season (b) Dry season

The hydrochemical process are complex and dynamic that depends on many factors, ranging from the groundwater origin rock/minerals weathering status and mineral composition of the aquifer (Hoque et al., 2014; Joshi et al., 2018). The residence time between precipitation and aquifer recharge zones and impact from humans along the flow paths are compounding factors (Krishnaraj et al., 2012).

Meteoric water is generally dominated by Ca-HCO_3 or Ca-Mg-HCO_3 water types, (Clark and Fritz (1997), with Na^+ and K^+ additions when water interacts with rock-forming minerals as shown in Equations 1 and 2.

Equation 1

$$2KAlSi_3O_8 + 2H^+ + 9H_2O \rightarrow Al_2Si_2O_5(OH)_4 + 2K^+ + 4H_4SiO_4$$

Equation 2

$$2NaAlSi_3O_8 + 2H^+ + 9H_2O \rightarrow Al_2Si_2O_5(OH)_4 + 2Na^+ + 4H_4SiO_4$$

The precipitation / infiltration water carries dissolved gases as it recharges, resulting in a weak acid of mainly carbonic with minor nitric or sulphuric acids (depending on anthropogenic pollution). Hydrolysis, acidolysis and oxidation processes take place as aquifers are recharged through the infiltration of water into soils of the vadose zones (Dehnavi et al., 2011; Fu et al., 2018; Narany et al., 2014). The mineralogy of the Precambrian basement rocks in the study area is heavily weathered along these reactions, resulting in an often thick saprolitic layer dominated by the secondary clay mineral kaolinite, supporting a geogenic source of Na and K in the upland recharge zones of the aquifer system.

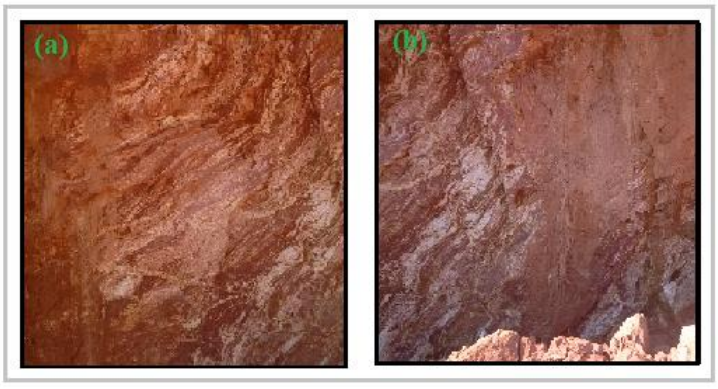

Figure 7.7 Weathering profile of Precambrian basement rocks underlying the oldest Abeokuta formation

At northern boundary of the basin from which aquifer recharge of the basin originates (a road cut along Abiola way, Abeokuta (b) a road cut along Ijebu-Remo and Agowoye road. The weathered profile is known for its richness in kaolinite minerals.

The weathered overburden exposures were documented (Figure 7.7) at the basins northern boundary where exposed Precambrian basement rocks were observed during field mapping and sampling, show feldspar was transformed to Kaolinite as in Equation 1 and 2. This hydrochemical evolution is usually a dynamic process as water moves from recharge to discharge area and is commonly associated with sedimentary basins. Delineating hydrochemical status often becomes a complex multisource process especially in a groundwater basin beneath towns, cities, agricultural and industrial areas from which non-geogenic sources of dissolved ions have entered the groundwater (Hoque et al., 2014). These ions and metals influence the hydrochemical characteristics of groundwater including changes due to saltwater intrusion or sea spray, and heterogeneous reaction between water and minerals, industrial and agricultural waste (Gattacceca et al., 2009; Lapworth1 et al., 2018; Nwankwoala, 2013). In the near-ocean areas of the basin it is most likely the dominant Na-Cl water types are attributed to sea spray or seawater intrusion. Mineral dissolution and hydrochemical evolution of groundwater can be better understood from which the relationship with stable isotopes that provides a clue to the hydrochemical transformation and residence time of water within the groundwater aquifers (Mohanty and Rao, 2019).

7.2.4.2 Oxygen and Deuterium Isotopes of groundwater of EDB

Information on precipitation, evaporation and origin of water can be deduced from the stable isotopes of oxygen ($\delta^{18}O$) and hydrogen ($\delta^{2}H$) values (Al-Charideh and Kattaa, 2016; Carol et al., 2009; Guendouz et al., 2003). The relationship between $\delta^{2}H$ and $\delta^{18}O$ data of any groundwater under investigation is usually defined in relation to Global Meteoric Water Line (GMWL) which is defined by the equation: $\delta^{2}H=8\delta^{18}O + 10$ (Joshi et al., 2018; Kalin, 1995). Stable isotopes of $\delta^{18}O$ and $\delta^{2}H$ have been used to

understand the origin of groundwater in the Eastern Dahomey Basin which suggested recent groundwater from precipitation (Aladejana et al. 2020). In this study, $\delta^{18}O$ and $\delta^{2}H$ were used to explain the hydrochemical evolution of water as it flows from the surface as precipitation and infiltrates into the soil through the vadose zone to the aquifers. Results from isotopes data of groundwater samples during the wet and dry season show $\delta^{18}O$ values range from -5.2 to 0.3 ‰ and -4 to 0.8 ‰ with an average value of -3 ‰ (Table 7.1) for both wet and dry seasons respectively. $\delta^{2}H$ values range from -32 to 2.3 ‰ and -19 to 7.5 ‰ with an average value of -13.1 and -12.4 ‰ (Table 7.1) respectively for wet and dry seasons. In this study, the $\delta D/\delta^{18}O$ diagrams show that the groundwater for both seasons plotted on/close to the Global Meteoric Water Line (GMWL), which implies recent water from precipitation with a slight influence of evaporation (Aladejana et al., 2020). Figure 7.9 and 7.10 show spatial distribution of $\delta^{18}O$ and δD for wet and dry seasons respectively.

The wet season $\delta D/\delta^{18}O$ diagram (Figure 7.8) showed a more extensive range along the Local Meteoric Water Line (LMWL), which indicated precipitation dominant, with rapid infiltration into the shallow coastal aquifers of the basin (Aladejana et al., 2020). Compared to dry season samples plotted within a shorter/narrow range (Figure 7.8) which tend towards mixed water with significant influence of evaporation before infiltrating into the shallow phreatic aquifers of the basin.

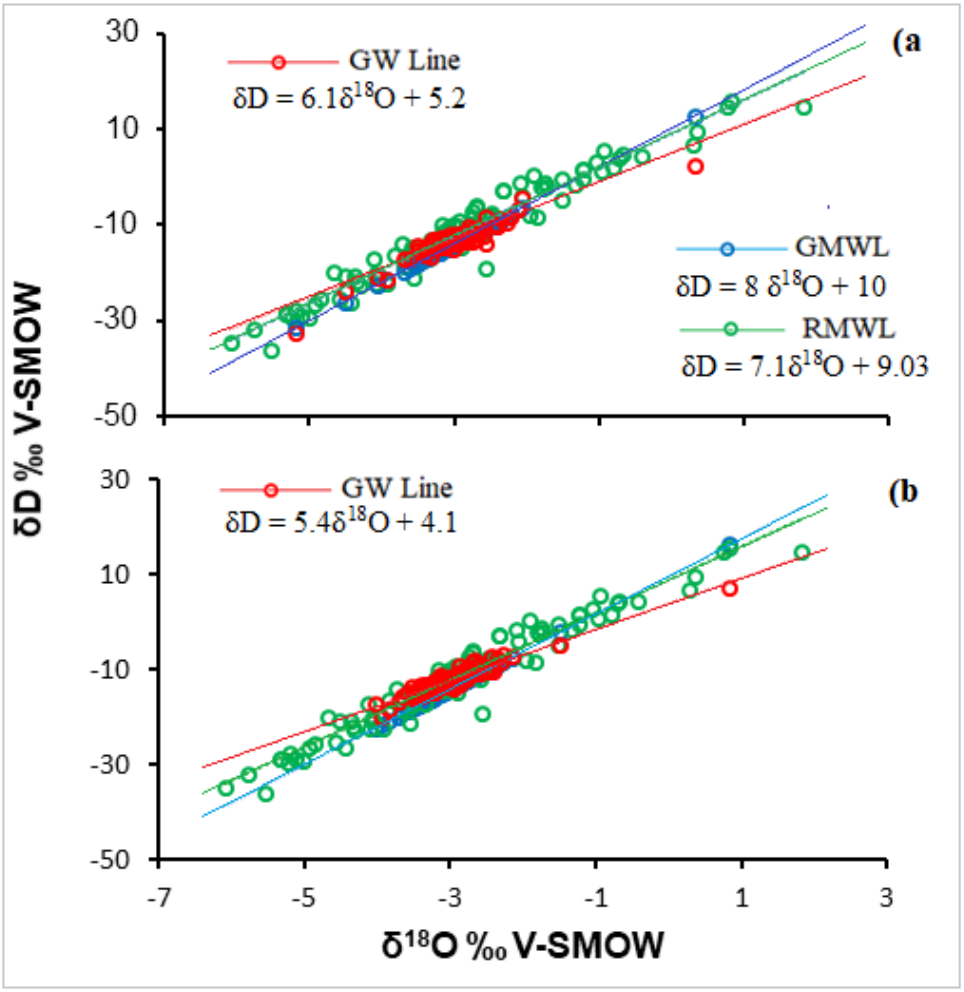

Figure 7.8 $\delta D/\delta^{18}O$ diagram for (a) wet season (b) dry season, groundwater samples

Integrating precipitation $\delta^{2}H$ and $\delta^{18}O$ isotopes data with groundwater from the EDB in understanding the origin of groundwater is necessary to eliminate doubt that could be introduced by the hydrodynamic complexities resulting from the influence of multiple factors from both geology and environment. Unfortunately, the only station of IAEA/WMO GNIP sited in Nigeria is in the northern part in the city of Kano in the Sahel savannah. Due to climate variabilities, it is not ideal to relate such data with the coastal zones groundwater isotopes data. In light of this, two stations, Douala in Cameroon which is in the east of EDB and Cotonou in the Republic of Benin at the west of the studied basin, and all along the West African coast were selected for comparative analysis. The precipitation isotopes data, the statistical summary of which

is presented in Table 2, is part of the continuous temporal record of monthly mean δ^2H and $\delta^{18}O$ for rainfall measurements between 2009 and 2018.

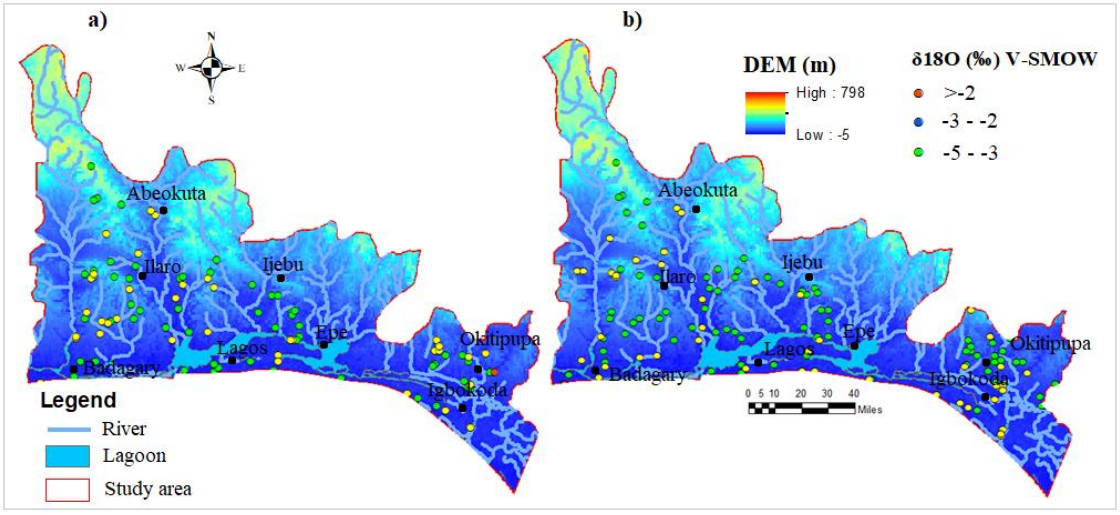

Figure 7.9 Spatial distribution map of $\delta^{18}O$ (‰) for the (a) wet season (b) dry season groundwater samples

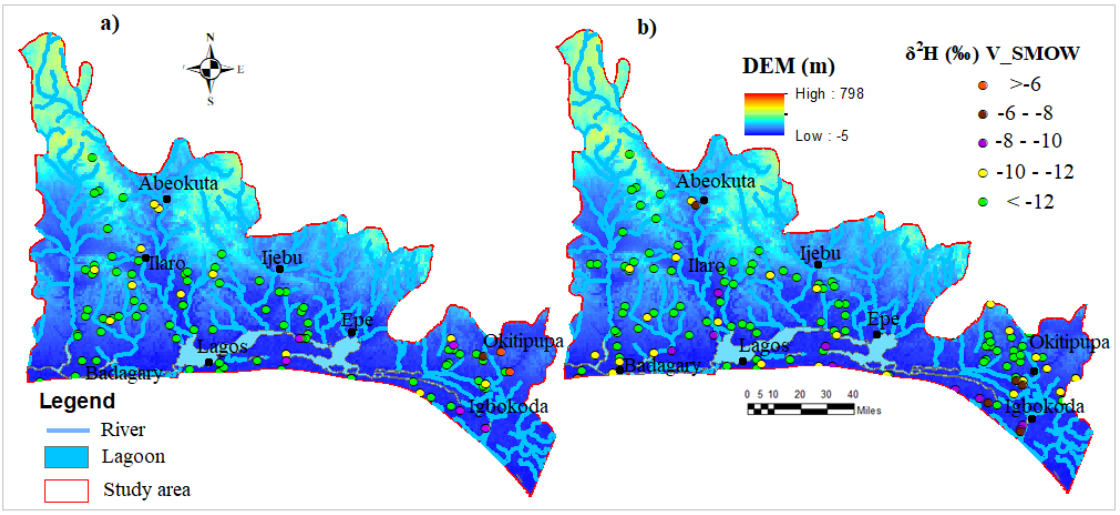

Figure 7.10 Spatial distribution map of δ^2H (‰) for the (a) wet season (b) dry season groundwater.

The groundwater samples for wet and dry seasons plotted along with the meteoric water line for Douala (Cameroon), Cotonou (Republic of Benin) and Kano (Nigeria) and presented in Figures 7.11. The results show all the groundwater samples clustering within the boundaries of the three Regional Meteoric Water Lines (RMWL)

with slope values falling below the GMWL (Figure 10a, b). This further reveals a large number of groundwater samples around the LMWL which indicates that meteoric water is a significant source of groundwater recharge in the study area. The Regional Meteoric Water Line (RMWL) characterising coastal precipitation from Cotonou ($\delta D = 7\ \delta^{18}O + 8.0$) and Douala ($\delta D = 7.2\ \delta^{18}O + 9.3$) are very close to the Global Meteoric Water Line. However, the stable isotopes data from the Kano station ($\delta D = 7.1\delta^{18}O + 4.3$) which has a slope closer to the GMWL but with lower δD intercept, indicates a climate effect of the region with relatively higher temperature and consequently higher evaporation rate with enrichment.

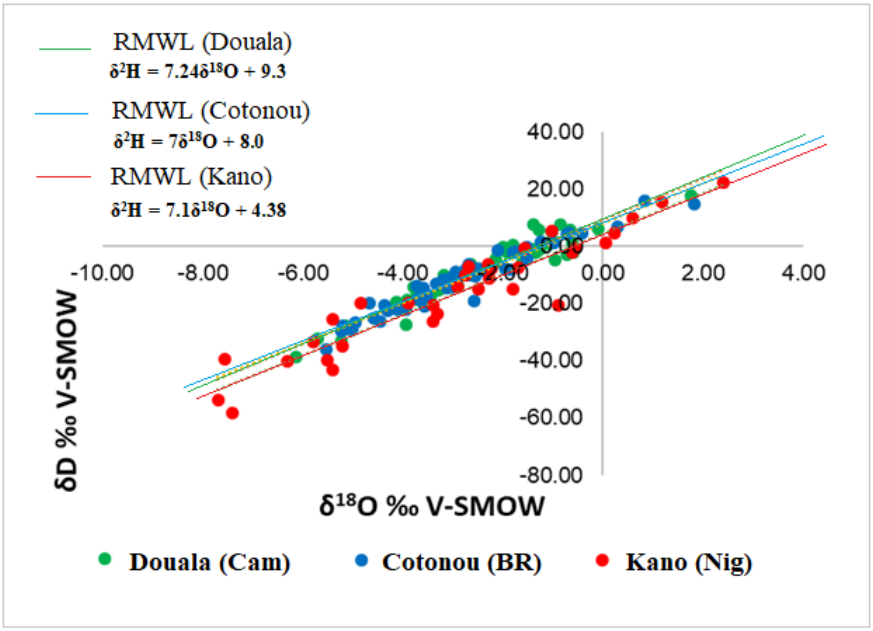

Figure 7.11 δD vs δ18O diagram for the selected regional precipitation data

The δ^2H and $\delta^{18}O$ data for the groundwater collected during the wet ($\delta D = 6.1\delta^{18}O + 5.2$) and dry ($\delta D = 5.4\delta^{18}O + 4.1$) seasons are shown in Figures 7.12). However, groundwater from the EDB for both seasons falls almost along the same meteoric waterline with a slight difference in slopes and deuterium intercepts. The slopes and intercepts of the regression line are lower compared to the LMWL (δD =

$8*\delta^{18}O + 10$) indicating the effect of evaporative enrichment on groundwater driven by seasonal variations in precipitation and temperature.

The results of the stable isotope values of δD, $\delta^{18}O$ and D-Excess of the three selected GNIP stations compared with those of the groundwater from the shallow coastal aquifers of the EDB is presented in Table 7.2. The results of the wet season groundwater show a range of values $\delta^{18}O$ (-5 to 0.3 ‰), δD (-32 to 2.3 ‰) and D-Excess (-0.3 to 13.8 ‰) which are very similar to those of Douala $\delta^{18}O$ (-6.1 to 1.8 ‰), δD (-38 to 17.6 ‰) and D-Excess (2.6 to 18.9 ‰) and Cotonou $\delta^{18}O$ (-5.5 to 1.8 ‰), δD (-36 to 15.8 ‰) and D-Excess (0.3 to 17.4 ‰) which could be a result of similar climatic condition especially temperature, humidity and evaporation. However, the stable isotope values of δD, $\delta^{18}O$ and D-Excess values for the groundwater samples in the dry season show range values $\delta^{18}O$ (-4 to 0.8 ‰), δD (-19.7 to 7.5 ‰) and D-Excess (-0.9 to 15 ‰) with slight deviations from the wet season data. The observed slight variation is an indication of the evaporation effect, which is also responsible for the enhanced values of TDS in dry seasons' groundwater samples. The precipitation isotopes data from the Kano GNIP station in the northern part of Nigeria (Table 7.2) with range values of $\delta^{18}O$ (-7 to 2.4 ‰), δD (-58.3 to 22.3 ‰) and D-Excess (-13.4 to 21 ‰) showed a wide variation from other Douala and Cotonou (Figure 7.11) which is probably an indication of higher elevation and evaporation rate which is characterised by low annual precipitation. The clustering of the groundwater samples around the Douala and Cotonou Regional Meteoric Water Line (RMWL) and Global Meteoric Water Line (GMWL) (Figure 7.11 and 7.12) affirm meteoric water that infiltrates the aquifer within a short time.

Table 7.2 Summary of the stable isotopes data from the three GNIP stations and groundwater samples

Isotopes	Minimum	Maximum	Average	Std dev
	Douala GNIP Station N = 50			
$\delta^{18}O$	-6.14	1.77	-2.54	1.57
$\delta^{2}H$	-38.80	17.68	-9.05	11.89
D-Excess	2.60	18.87	11.26	3.70
	Cotonou GNIP Station N = 50			
$\delta^{18}O$	-5.53	1.82	-2.86	1.63
$\delta^{2}H$	-36.11	15.76	-11.92	11.74
D-Excess	0.30	17.44	10.99	3.30
	Kano GNIP Station			
$\delta^{18}O$	-7.70	2.40	-2.92	2.59
$\delta^{2}H$	-58.30	22.30	-16.30	19.36
D-Excess	-13.38	20.98	7.08	6.69
	Groundwater Samples Wet Season N = 97			
$\delta^{18}O$	-5.2	0.3	-0.3	0.6
$\delta^{2}H$	-32.5	2.3	-13.1	3.6
D-Excess	-0.3	13.8	11.0	1.7
	Groundwater Samples Dry Season N = 133			
$\delta^{18}O$	-4.0	0.8	-3.0	0.5
$\delta^{2}H$	-19.7	7.5	-12.4	2.8
D-Excess	0.9	15.0	11.9	1.6

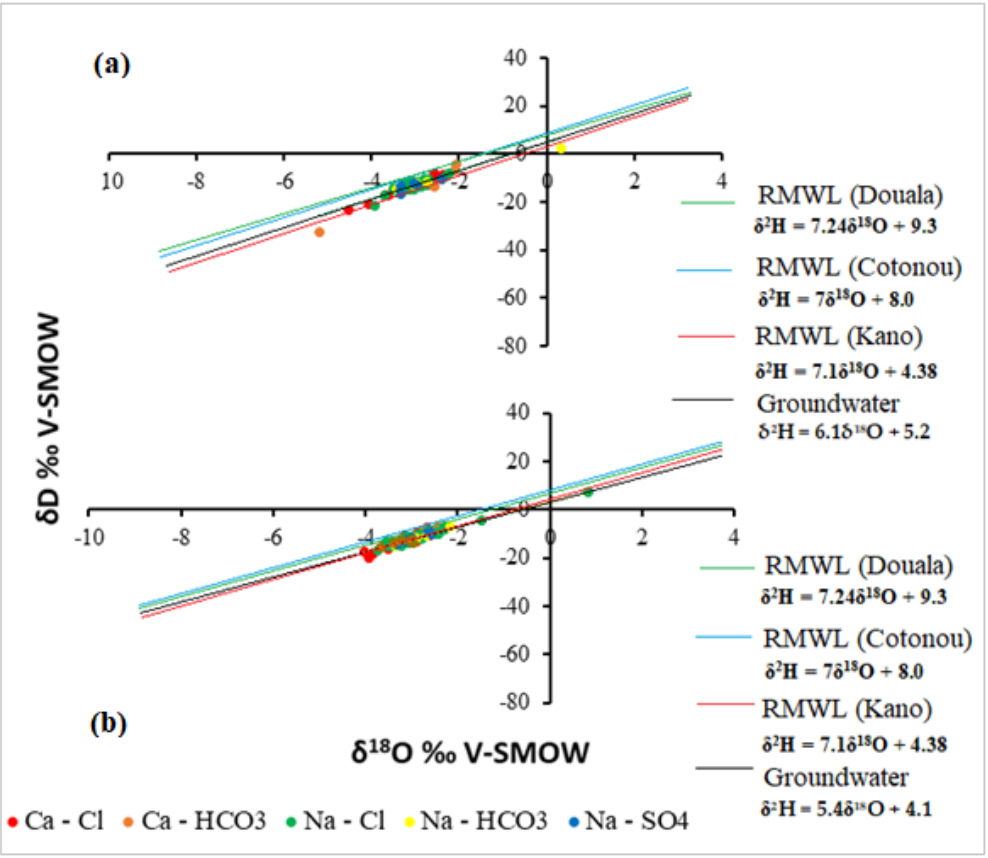

Figure 7.12 δ^2H vs $\delta^{18}O$ diagram for selected precipitation data and the groundwater samples (a) wet season (b) dry season

7.2.4.3 Tracing the origin of groundwater within the EDB using deuterium excess

Deuterium excess (D-Excess) has proven to be a useful tool in tracing the source of groundwater in several hydrological basins across the globe. The D-Excess is defined as D-Excess = $\delta^2H - 8\delta^{18}O$ (Joshi et al., 2018; Kalin, 1995; Vengosh et al., 2007). The deuterium excess is a function of prevailing conditions during primary evaporation, including variation in humidity, ocean surface temperature, wind speed, and thus gives information on the sources of water vapour. The D-Excess does not change with the change in equilibrium processes for any of the phases while non-equilibrium evaporation leads to a decrease in the d-excess which is an indication of an increase in the vapour phase (Banda et al., 2019; Joshi et al., 2018; Kalin, 1995).

In this study, the D-Excess value range of groundwater samples of the wet season (-0.3 – 15.0 ‰) is lower than that of the dry season (0.9 – 15.0 ‰). A higher D-Excess value was observed in the dry season groundwater samples (Figure 7.14), which were collected between the months of February and April 2017. During this period, a dry southerly wind leading to the recycling of moisture from the continental recycling along with the rapid evaporation over warmer seawater was responsible for higher D-Excess which impact the young groundwater of the aquifer of the Eastern Dahomey Basin. This is evident in the relatively lower slope values as observed in the plots of TDS vs D-Excess in Figure 7.13 which also showed the clustering of D-excess in relation to rain, sea and brackish water from the basin. The diagrams showed that most of the groundwater of the wet season plotted closer to the precipitation, which is the source of the groundwater recharge and forms a trend towards the brackish point as evaporation increases.

Finally, the TDS vs D-excess diagram shows that most groundwater samples plot in a region between the recharge and evaporation zones reflecting a meteoric origin of the water with early transformation through evaporation. This suggests precipitation moving towards groundwater storage through the vadose zone is rapid, and that post-precipitation evaporation along these paths is a prolonged process, probably due to higher humidity and precipitation in this region.

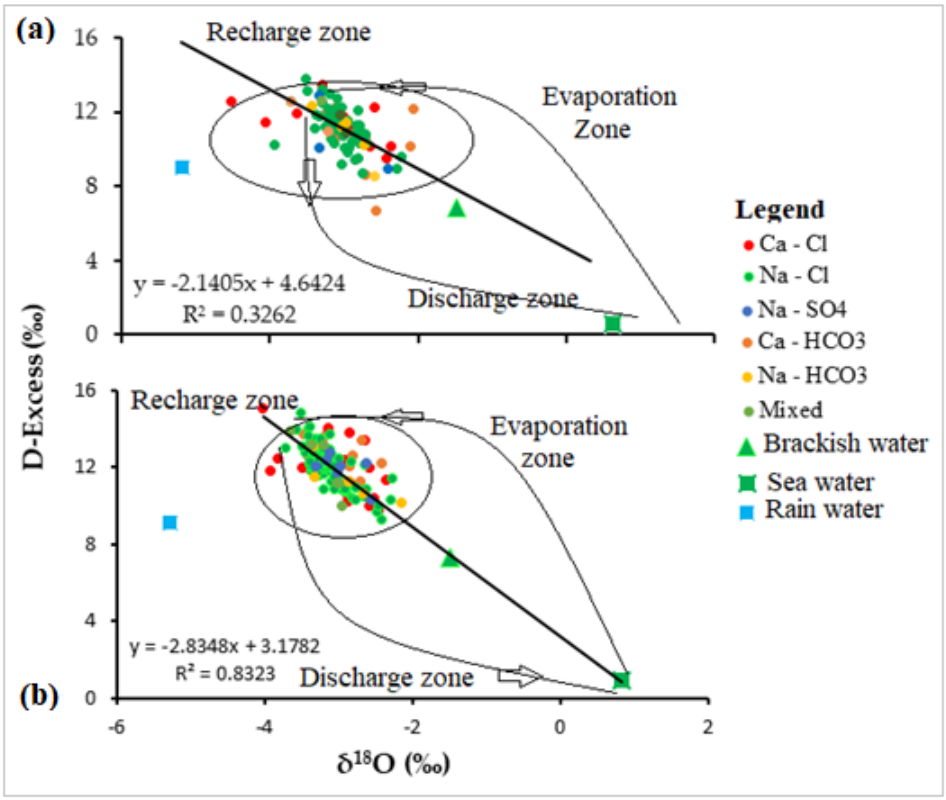

Figure 7.13 18O vs D-Excess for the wet season groundwater samples (a) wet season (b) dry season

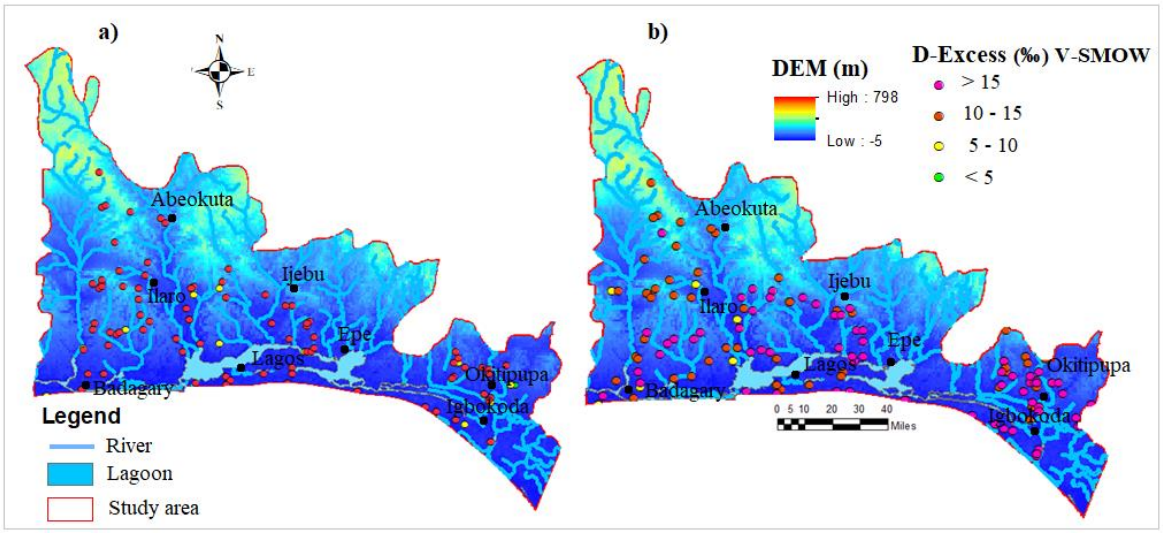

Figure 7.14 Spatial distribution map of D-Excess (‰) for the (a) wet season (b) dry season groundwater.

7.2.4.4 Conceptual model of the hydrological processes controlling isotopic signatures of groundwater

The results from this study have established that the hydrochemical dynamic and processes prevalent in the Eastern Dahomey Basin have revealed a subtle transformation as water moves from the recharge zones in the northern part towards the discharge area in the downstream along the river channels and flood plains. The clustering of groundwater samples between evaporation and recharge and along the seawater line in TDS vs $\delta^{18}O$ diagram confirmed the suggestion of young groundwater in the basin. Also, the slight variations in the distribution of the δD and $\delta^{18}O$ values and clustering along the regional meteoric water line (RMWL) and Global Meteoric Water Line (GMWL) with a slight deviation of the dry season groundwater further confirmed the recent water's short residence time within the soil and vadose zones before recharging the shallow coastal aquifer of the basin. The information from (a) the geological information and field observations (b) groundwater level (c) elevation data (d) aquifer geometry (e) hydrochemical evolution (f) spatial variability of $\delta^{18}O$, δD and D-excess (g) river and static water level and (h) line of cross-section along representative profile were collected. The information listed above was integrated to develop a conceptual model for the prevailing hydrogeological processes within the Eastern Dahomey Basin with well-defined boundary conditions of impermeable basement rock at the north and the ocean line of the Gulf of Guinea in the south enclosed by the flow boundary of the Okitipupa ridge in the east and extended sedimentary deposits (Aladejana et, 2020). The flow systems within this area can be categorised into local and regional, which are mainly driven by gravity influence due to the topography of the basin (Offodile, 1971). It is local where groundwater flows into isolated river valleys and wetlands, while regional flow system relates to the major rivers which cut across the entire basin, with several tributaries, and discharge water

into the ocean through the delta plain. The hydrochemical modelling shows Na-Cl water type as a dominant water type followed by Ca-HCO_3 with other mixed water types such Ca-Cl, Na-SO_4, Na-Cl-HCO_3 and Ca-SO_4 which typifies an early stage of rock-water interactions and possible anthropogenic influence.

This conceptual model helps to explain the lateral and vertical variations in groundwater $\delta^{18}O$, δD and D-Excess concentrations, which are controlled by factors such as high humidity, static water level basin and significant anthropogenic influence from urbanisation, industrialisation and agricultural irrigation in most areas of the study. For example, the D-excess results show comparatively shorter residence time for groundwater moving through the vadose zone to the shallow aquifers of the basin, especially within the alluvium and coastal plain sands geologic units. However, observed hydrochemical characteristics across the basin generally reflect the geology and mineralogy of the area, while the lack of consistencies in groundwater isotopes values and water types distribution could be attributed to heterogeneity and anthropogenic impacts along the flow paths.

Furthermore, as illustrated in the schematic model in Figure 7.15, water recharged in the northern parts of the basin has to travel deeper vertically as the vadose zone thickness is higher in this area to recharge the shallow aquifers, and also rivers inform of baseflow. Higher precipitation and large water bodies in this basin are also responsible for higher humidity which impedes the evapotranspiration rate and buffers the enrichment or depletion of the stable isotopes values, hence rapid recharge of groundwater.

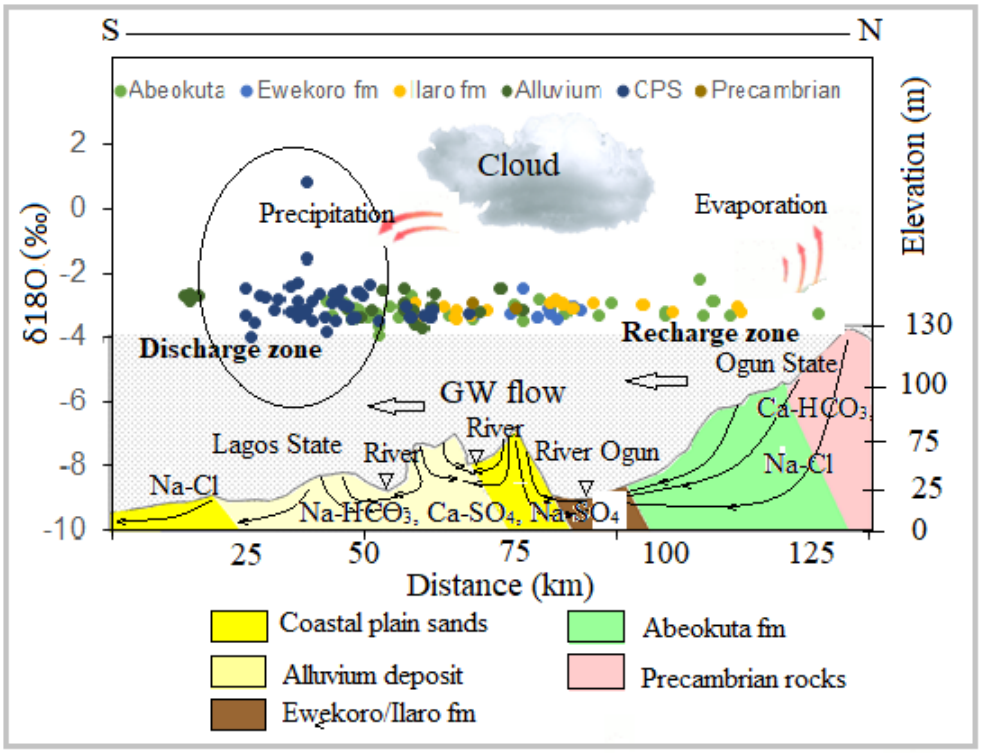

Figure 7.15 A sketch of conceptual model of stable isotopes $\delta^{18}O$ along profile line A-B in North-South direction of the Eastern Dahomey Basin.

7.2.4.5 The implication for EDB groundwater resources management

Sustainable management of groundwater is critical to achieve access to potable water supply, food security, ecosystem/environmental protection and economic growth in sub-Saharan Africa countries (JICA, 2014). Effective groundwater resources management relies on sound hydrogeological skills and knowledge and ultimately on the quality of available data and information necessary for accurate judgement and planning.

In light of the above, this study has advanced the available data, information and knowledge required to better understand the hydrogeology of the Eastern Dahomey Basin, Nigeria. A combination of isotopes, geology and hydrogeochemical approaches have revealed the groundwater are at an early stage of evolution with short residence time. However, the basin has a large volume of water bodies and higher

water level with reasonable aquifer hydraulic characteristics. It is therefore pertinent to emphasise the threat to its water quality as a result of short residence time and rapid recharge. The shallow aquifers of this basin can be described as having a low resilience or higher vulnerability as regards groundwater contamination and pollution from surface water, leakage from septic tanks, waste sites, industrial pipes and leachates from agricultural waste. Groundwater quality is one of the key challenges facing most of the developing countries around the world. Groundwater quality degradation has also been identified in part of this basin especially the urban and agricultural areas by Aladejana et al. (2020a) and Aladejana et al. (2020b). It is, therefore, necessary to ensure enforcement of a proper waste disposal management strategy that will provide protection to groundwater of the shallow aquifers within this basin. Policies and urban planning that ensure best practice from industries and agricultural industries are necessary to protect these vital resources. A review of the existing system is needed to accommodate additional stress and threat imposed on groundwater resources through advancement in technological development in the modern economy.

7.2.4 Conclusion

This study is a novel approach to groundwater hydrodynamic studies which cover all the major towns and cities with the Eastern Dahomey Basin using stable isotopes of $\delta^{18}O$, δD and D-excess. This involves a systematic approach that combined hydrogeochemical modelling with other hydrological parameters including drainage system, topography. Static water level among others, to identify the recharge sources and zones and also characterise groundwater dynamics in relation to stable isotopes in the shallow coastal aquifers of the basin. Hydrochemical modelling shows Na-Cl as the dominant water type followed by Ca-HCO_3, Na-HCO_3, Ca-SO_4, Na-SO_4 with other

mixing water types such as Ca-Cl, K-Cl, and Mg-SO_4. The dominant of the Na-Cl water is thought to have two origins, namely the release of Na^+ and K^+ ions into the groundwater by weathering of feldspars into kaolinite that characterises the recharge zones of the basin and sea spraying and saltwater intrusion. Although, these water types reflect the mineralogical characteristics of the aquifers' units within the basin, the lack of consistency in the pattern of water types distributed across the geologic unit is attributed to the heterogeneity within the aquifers and possible impact of human activities. Relationship between $\delta^{18}O$ and δD revealed that the wet season groundwater data plots along the Global Meteoric Water Line while those of the dry season showed little deviation towards the evaporation line which indicates recent meteoric water with little seasonal effect. The relationship between the TDS and $\delta^{18}O$ further agreed with this by displaying samples clustering between the recharge and evaporation zone. Comparing the results with the regional precipitation data from the selected station of GNIP at Douala (Cameroon), Cotonou (Republic of Benin) and Kano (Nigeria) showed young water recharge with short residence time with little influence of evapotranspiration which is associated with higher static water level and humidity, hence little $\delta^{18}O$ enrichment. However, the variation of $\delta^{18}O$ and $\delta^{2}H$ confirmed this, as no consistent pattern follows along the flow paths. Finally, the results of this study can help in both developing aquifer resilience and vulnerability studies for developing a groundwater quality monitoring strategy for sustainable groundwater management in the Eastern Dahomey Basin.

7.2.6 Reference

Adegoke, O.S. and Omatsola, M.E., 1981. Tectonic Evolution and Cretaceous Stratigraphy of the Dahomey Basin. Niger. J. Min. Geol. 18, 130–137.

Adeoti, L., Alile, O.M., Uchegbulam, O., 2010. Geophysical investigation of saline water

intrusion into freshwater aquifers: A case study of Oniru, Lagos State. Sci. Res. Essays 5, 248–259.

Ahmed, A., Clark, I., 2016. Groundwater flow and geochemical evolution in the Central Flinders Ranges, South Australia. Sci. Total Environ. https://doi.org/10.1016/j.scitotenv.2016.07.123

Al-Charideh, A., Kattaa, B., 2016. Isotope hydrology of deep groundwater in Syria: renewable and non-renewable groundwater and paleoclimate impact. Hidrol. isotópica del agua subterránea profunda en Siria agua subterránea Renov. y no Renov. e impacto paleoclimático. 24, 79–98. https://doi.org/10.1007/s10040-015-1324-4

Aladejana, Jamiu A, Kalin,R.M., Sentenac, P., Hassan, I., 2020. Groundwater Quality Index as a Hydrochemical Tool for Monitoring Saltwater Intrusion into Coastal Freshwater Aquifer of Eastern Dahomey Basin, Southwestern Nigeria. Under Rev. with Groundw. Sustain. Dev. 24.

Aladejana, Jamiu A, Kalin, R.M., Sentenac, P., Hassan, I., 2020. Hydrostratigraphic Characterisation of Shallow Coastal Aquifers of Eastern Dahomey Basin , S / W Nigeria, Using Integrated Hydrogeophysical Approach ; Implication for Saltwater Intrusion. Geoscience 10, 65. https://doi.org/10.3390/geosciences10020065

Aladejana, Jamiu A., Kalin, R.M., Sentenac, P., Hassan, I., 2020. Assessing the Impact of Climate Change on Groundwater Quality of the Shallow Coastal Aquifer of Eastern Dahomey Basin, Southwestern Nigeria. Water 12, 224. https://doi.org/10.3390/w12010224

Ayoade, J.O., 1975. Water Resources and Their Development in Nigeria Recent events of flood , drought and urban water shortages as well as water pollution in Ni- geria and various parts of the world have underlined the need for the rational planning of Nigeria's water reso. Hydrol. Sci. Sci. Hydrol. 4, 581–591.

Banda, L.C., Rivett, M.O., Kalin, R.M., Zavison, A.S.K., Phiri, P., Kelly, L., Chavula, G., Kapachika, C.C., Nkhata, M., Kamtukule, S., Mleta, P., Nhlema, M., 2019. Water-isotope capacity building and demonstration in a developing world context: Isotopic baseline and conceptualization of a Lake Malawi catchment. Water (Switzerland) 11. https://doi.org/10.3390/w11122600

Carol, E., Kruse, E., Mas-Pla, J., 2009. Hydrochemical and isotopical evidence of ground water salinization processes on the coastal plain of Samboromb??n Bay, Argentina. J. Hydrol. https://doi.org/10.1016/j.jhydrol.2008.11.041

Daniele, L., Vallejos, ángela, Corbella, M., Molina, L., Pulido-Bosch, A., 2013. Hydrogeochemistry and geochemical simulations to assess water-rock interactions in complex carbonate aquifers: The case of Aguadulce (SE Spain). Appl. Geochemistry 29, 43–54. https://doi.org/10.1016/j.apgeochem.2012.11.011

Dehnavi, A., Sarikhani, R., Nagaraju, D., 2011. Hydro geochemical and rock water interaction studies in East of Kurdistan, NW of Iran. Int J Env. Sci Res 1, 16–22.

Edet, A., 2016. Hydrogeology and groundwater evaluation of a shallow coastal aquifer, southern Akwa Ibom State (Nigeria). Appl. Water Sci. https://doi.org/10.1007/s13201-

016-0432-1

Faleye, E.T., Olorunfemi, 2015. Aquifer Characterization and Groundwater Potential Assessment of the Sedimentary Basin of Ondo State 1 2. Ife J. Sci. 17, 429–439.

Fatoba, J.O., Omolayo, S.D., Adigun, E.O., 2014. Using geoelectric soundings for estimation of hydraulic characteristics of aquifers in the coastal area of Lagos, southwestern Nigeria. Int. Lett. Nat. Sci. 11, 30–39. https://doi.org/10.18052/www.scipress.com/ILNS.11.30

Fu, C., Li, X., Ma, J., Liu, L., Gao, M., Bai, Z., 2018. A hydrochemistry and multi-isotopic study of groundwater origin and hydrochemical evolution in the middle reaches of the Kuye River basin. Appl. Geochemistry. https://doi.org/10.1016/j.apgeochem.2018.08.030

Gagné, S., Larocque, M., Pinti, D.L., Saby, M., Meyzonnat, G., Méjean, P., 2017. Benefits and limitations of using isotope-derived groundwater travel times and major ion chemistry to validate a regional groundwater flow model: example from the Centre-du-Québec region, Canada. Can. Water Resour. J. 1784, 1–19. https://doi.org/10.1080/07011784.2017.1394801

Gattacceca, J.C., Vallet-Coulomb, C., Mayer, A., Claude, C., Radakovitch, O., Conchetto, E., Hamelin, B., 2009. Isotopic and geochemical characterization of salinization in the shallow aquifers of a reclaimed subsiding zone: The southern Venice Lagoon coastland. J. Hydrol. 378, 46–61. https://doi.org/10.1016/j.jhydrol.2009.09.005

Guendouz, A., Moulla, A.S., Edmunds, W.M., Zouari, K., Shand, P., Mamou, A., 2003. Hydrogeochemical and isotopic evolution of water in the Complexe Terminal aquifer in the Algerian Sahara. Hydrogeol. J. 11, 483–495. https://doi.org/10.1007/s10040-003-0263-7

Hoque, M.A., Mcarthur, J.M., Sikdar, P.K., Ball, J.D., Molla, T.N., 2014. Tracing recharge to aquifers beneath an Asian megacity with Cl / Br and stable isotopes : the example of Dhaka , Bangladesh. J. Hydrol. 22, 1549–1560. https://doi.org/10.1007/s10040-014-1155-8

Jamiu A. Aladejana, Robert M. Kalin, Ibrahim Hassan, M.N.T. and P.S., n.d. Hydrogeochemical and Isotopic Characterization of Coastal Groundwater of Eastern Dahomey Basin, Southwestern Nigeria Title. Under Rev. Results Geochemistry 26.

Jamiu A. Aladejana, Robert M. Kalin, Ibrahim Hassan, P.S. and M.N.T. 2020, 2020. Assessing the Impact of Land Use Patterns on the Groundwater in the Shallow Coastal Aquifer of Eastern Dahomey Basin, Nigeria Using Statistical and Water Quality Analysis. Under Rev. Results African J. Earth Sci. AES8466.

JICA, 2014. Federal Republic of Nigeria the Project for Review and Update of Nigeria National Water Resources. Abuja.

Jones, H. A and Hockey, R.., 1964. The Geology of part of Southwestern Nigeria. GSN Bull. No. 31-10.

Joshi, S.K., Rai, S.P., Sinha, R., Gupta, S., Densmore, A.L., Rawat, Y.S., Shekhar, S., 2018.

Tracing groundwater recharge sources in the northwestern Indian alluvial aquifer using water isotopes (δ18O, δ2H and3H). J. Hydrol. 559, 835–847. https://doi.org/10.1016/j.jhydrol.2018.02.056

Kalin, R.M., 1995. Basic concepts and formulations for isotope-geochemical process investigations, procedures and methodologies of geochemical modelling of groundwater systems, in: Y Yurtsever (Ed.), Manual on Mathematical Models in Isotope Hydrology. IAEA TECHDOC 910, Viena, pp. 155–206.

Kashaigili, J.J., 2012. Ground water Availability and Use in Sub-Saharan Africa, Groundwater availability and use in Sub-Saharan Africa: A review of 15 countries. https://doi.org/10.5337/2012.213

Krishnaraj, S., Murugesan, V., K, V., Sabarathinam, C., Paluchamy, A., Ramachandran, M., 2012. Use of Hydrochemistry and Stable Isotopes as Tools for Groundwater Evolution and Contamination Investigations. J. Geo-sciences 1, 16–25. https://doi.org/10.5923/j.geo.20110101.02

Lapworth, D.J., Nkhuwa, D.C.W., Okotto-Okotto, J., Pedley, S., Stuart, M.E., Tijani, M.N., Wright, J., 2017. Urban groundwater quality in sub-Saharan Africa: current status and implications for water security and public health. Hydrogeol. J. 25, 1093–1116. https://doi.org/10.1007/s10040-016-1516-6

Longe, E.O., 2011. Groundwater Resources Potential in the Coastal Plain Sands Aquifers , Lagos , Nigeria 3, 1–7.

Longe, E.O., Malomo, S., Olorunniwo, M.A., 1987. Hydrogeology of Lagos metropolis. J. African Earth Sci. 6, 163–174. https://doi.org/10.1016/0899-5362(87)90058-3

Mohanty, A.K., Rao, V.V.S.G., 2019. Catena Hydrogeochemical , seawater intrusion and oxygen isotope studies on a coastal region in the Puri District of Odisha , India. Catena 172, 558–571. https://doi.org/10.1016/j.catena.2018.09.010

Narany, T.S., Ramli, M.F., Aris, A.Z., Nor, W., Sulaiman, A., Juahir, H., Fakharian, K., 2014. Identification of the Hydrogeochemical Processes in Groundwater Using Classic Integrated Geochemical Methods and Geostatistical Techniques , in Amol-Babol Plain, Iran. Sci. World J. 2014, 1–15.

Nwankwoala, S.A.N. and H.O., 2013. Salinity Dynamics : Trends and Vulnerability of Aquifers to Contamination in the Niger Delta. Compr. J. Environ. Earth Sci. 2, 18–25.

Offodile, M.E. (1971), 1971. The Hydrogeology of Coastal Areas of Southeastern states of Nigeria., Unpublished Geological survey of Nigeria Report.

Oke, S.A., 2015. Evaluation of the Vulnerability of Selected Aquifer Systems in the Eastern Dahomey Basin, South Western Nigeria.

Oke, S.A., Vermeulen, D., Gomo, M., 2016. Aquifer vulnerability assessment of the Dahomey Basin using the RTt method. Environ. Earth Sci. 75, 1–9. https://doi.org/10.1007/s12665-016-5792-1

Oloruntola, M.O., Adeyemi, G.O., Bayewu, O., Obasaju, D.O., 2019. Hydro-geophysical

mapping of occurrences and lateral continuity of aquifers in coastal and landward parts of Ikorodu, Lagos, Southwestern Nigeria. Int. J. Energy Water Resour. 3, 219–231. https://doi.org/10.1007/s42108-019-00026-8

Omole, D.O., 2013. Sustainable Groundwater Exploitation in Nigeria. J. Water Resour. Ocean Sci. 2, 9. https://doi.org/10.11648/j.wros.20130202.11

Oteri, A.U., & Atolagbe, F.P., 2003. Saltwater Intrusion into Coastal Aquifers in Nigeria, in: The Second International Conference on Saltwater Intrusion and Coastal Aquifers — Monitoring, Modeling, and Management. Mérida, Yucatán, México, March 30 - April 2, 2003. Merida Yucatan, pp. 1–15.

Peter Bauer-Gottwein, Bibi N. Gondwe, Lars Christiansen, Daan Herckenrath, L.K., A, S.Z., 2010. Hydrogeophysical exploration of three-dimensional salinity anomalies with the time-domain electromagnetic method (TDEM). J. Hydrol. 380, 318–329. https://doi.org/10.1007/s12665-014-3130-z

Shin, W.J., Park, Y., Koh, D.C., Lee, K.S., Kim, Yongcheol, Kim, Yongje, 2017. Hydrogeochemical and isotopic features of the groundwater flow systems in the central-northern part of Jeju Island (Republic of Korea). J. Geochemical Explor. 175, 99–109. https://doi.org/10.1016/j.gexplo.2017.01.004

Solomon O. Olabode1, M.Z.M., 2016. Depositional Facies and Sequence. Int J. Geosci. 7, 210–228.

Vengosh, A., Hening, S., Ganor, J., Mayer, B., Weyhenmeyer, C.E., Bullen, T.D., Paytan, A., 2007. New isotopic evidence for the origin of groundwater from the Nubian Sandstone Aquifer in the Negev, Israel. Appl. Geochemistry 22, 1052–1073. https://doi.org/10.1016/j.apgeochem.2007.01.005

CHAPTER 8

8.0 Natural and Anthropogenic Impact on Groundwater Quality

8.1 Preamble

This chapter presents the groundwater quality assessment in relation to natural drivers such as climate change which lead to extreme weather events such high precipitation that characterises the coastal area of West Africa. Due to the vast population and economic importance of this area to Nigeria and West Africa at large, it is necessary to look at the possible impact of urbanisation on the groundwater quality of the basin. This chapter employed some groundwater quality indices and biogeochemical processes like redox reaction which control some of the major groundwater quality parameters such as NO_3^-, SO_4^{2-}, Fe, Mn and As, to investigate the link of these drivers and groundwater quality of Eastern Dahomey Basin.

This lead to two article papers with one of them published while the other one is under review with the *Journal of Africa Earth Sciences*. The two articles are listed below;

- Jamiu A. Aladejana, Robert M. Kalin, Ibrahim Hassan, Philippe Sentenac and Moshood N. Tijani. 2020. Assessing the Impact of Land Use Patterns on the Groundwater in the Shallow Coastal Aquifer of Eastern Dahomey Basin, Nigeria Using Statistical and Water Quality Analysis. *Under review* in Elsevier Journal; *African Journal of Earth Sciences*. Manuscript number AES8466.
- Aladejana, Jamiu A., Kalin, R.M., Sentenac, P., Hassan, I., 2020. Assessing the Impact of Climate Change on Groundwater Quality of the Shallow Coastal Aquifer of Eastern Dahomey Basin, Southwestern Nigeria. *Water* 12, 224. https://doi.org/10.3390/w12010224 [Open access].

The articles established the quality status of the sampled groundwater from the basin with the possible influence of seasonal variations on some of the critical processes that control the behaviours of groundwater quality parameters. The design of these articles was supervised by my supervisor, Prof. Robert M. Kalin, who assisted in designing the research and gave a further critical review which contributed to the improvement in the quality of the manuscript. Technical assistance and relevant suggestion from Ibrahim Hassan, Dr Philippe Sentenac (my second supervisor) and Prof. Moshood N. Tijani also helped in the improvement of the articles.

8.2 Paper 5

Jamiu A. Aladejana, Robert M. Kalin, Ibrahim Hassan, Philippe Sentenac and Moshood N. Tijani. 2020. Assessing the Impact of Land Use Patterns on the Groundwater in the Shallow Coastal Aquifer of Eastern Dahomey Basin, Nigeria Using Statistical and Water Quality Analysis. *Under review* in Elsevier Journal; *African Earth Sciences. Manuscript number AES8466.*

Assessing the Impact of Land Use Patterns on the Groundwater in the Shallow Coastal Aquifer of Eastern Dahomey Basin, Nigeria Using Statistical and Water Quality Analysis

Jamiu A. Aladejana [1,2,*], Robert M. Kalin [1], Ibrahim Hassan [1,3], Philippe Sentenac [1] and Moshood N. Tijani[2]

[1] *Department of Civil and Environmental Engineering, University of Strathclyde, Glasgow G1 1XJ, UK; Robert.Kalin@Strath.ac.uk (R.K.); philippe.sentenac@strath.ac.uk (P.S.); Ibrahim.hassan@strath.ac.uk (I.H.)*

[2] *Department of Geology, University of Ibadan, Ibadan 200284, Nigeria*

[3] *Department of Civil Engineering Abubakar Tafawa Balewa University Bauchi, Bauchi 740272, Nigeria*

jamiu.aladejana@strath.ac.uk

8.2.1 Abstract

Effective monitoring of groundwater quality is difficult in Sub-Saharan Africa countries due to rapid urbanisation and limited financial resources, but is required to meet the challenges of meeting targets for Sustainable Development Goal 6 (SDG6) aimed at providing clean and potable drinking water to all. Science-led policy interventions are needed to set and meet national SDG6 targets, in particular for groundwater resource management. This study used the Groundwater quality index (GWQI) and statistical analysis to assess the impact of land use patterns on groundwater quality in the shallow aquifers of Eastern Dahomey Basin, Nigeria. Selected water quality parameters pH, EC, TDS, TH, Ca, Mg, Na, K, HCO_3, Cl, SO_4, NO_3, F and the trace metals As, Cd, Fe, Mn, Pb and Si were analysed in 230

groundwater samples from boreholes and hand-dug wells between June 2017 and April 2018. The results were used to calculate the GWQI by assigning weight according to adverse impact on human health. A Land use map of the area where irrigation may be of benefit was developed from Landsat image using ArcGIS. Assessing the future use of groundwater for irrigation suggests some parts of the aquifer may have unsuitable quality based on the percentage sodium (%Na), Kelly's ratio (KR), magnesium ratio (MR) and total hardness. Results of GQWI revealed 44.8, 22.9 and 12.5% of water samples during the wet season fell in the class of excellent, good and moderate-quality respectively, while 8.3 %, 1.0 and 10.4 % fell in a class of poor, very poor and non-potable water quality. Correlating the spatial distribution of the GWQI with the land use pattern map of the area revealed the least potable water is clustered around settlement areas, indicating groundwater quality has been impacted by municipal, industrial and agricultural waste. There is a need for waste management policy review and enforcement to support sustainable groundwater resource management and SDG6 goals.

Keywords: Groundwater Quality Index; land use; seasonal effects; water resource management

8.2.2 Introduction

Sustainable water resources management is a broad concept which encompasses water availability, quality and usability. Remedial management of coastal freshwater aquifers that have suffered groundwater depletion, especially in urban centres in the arid region of Asia and Africa, is generating attention by water professionals, NGOs and the international community (Kashaigili, 2012; Lapworth et al., 2017c; Re et al., 2011).

In contrary, there is little attention on shallow coastal aquifer of developing countries of Sub-saharan African, because of large easily accessible volumes of surface water in rivers, wetlands, and lagoons. There is a need to bring groundwater resources to the attention of national/local governments, NGOs and water professional to evaluate water quality degradation of vulnerable coastal freshwater aquifers (Oke, 2015; Oke et al., 2016). Water bodies within and around the urban centres of developing countries tend to be contaminated (Aboyeji and Ogunkoya, 2015) due to high growth rates for population, poverty and poor waste management practice (Babanyara et al., 2010; Biswas and Tortajada, 2019).

The situation in Eastern Dahomey Basin (EDB) in Southwestern Nigeria is similar in this respect. This basin has about 35% of the population of the country. Groundwater is used as an alternative / complementary source of freshwater to meet the daily water demand resulting from the acute shortage of pipe-borne water due to infrastructural decay and incessant power failure (Oteri & Atolagbe, 2003; Longe and Balogun, 2010). The rapid surge in population over the past decade is due to rural-urban migration for people seeking jobs in the metropolitan city of Lagos and other cities within this basin (Aladejana et al., 2020). The quality of groundwater of shallow coastal aquifer of this basin is under threat from several drivers such as Sea Level Rise (SLR), uncontrolled land use, waste from municipal, industrial and agricultural industries, and flooding.

Groundwater quality is influenced by the land use and hydrological parameters such as evaporation, interception infiltration rate, and runoff that may also be altered or controlled by land use patterns (Senthilkumar et al., 2018). Urbanisation and agriculture activities release waste with an adverse effect on groundwater quality.

Inappropriate waste management practice that characterised developing countries of Sub-Sahara African increases the challenge facing groundwater quality.

Groundwater pollution and quality deterioration within EDB has been reported by others including Oteri; 1988, Longe et al.; 1987, Adeoti et al.; 2010, and Ayolabi et al.; 2013. According to the United nation SDG6, "*2 billion people are living with the risk of reduced access to freshwater resources, and by 2050, at least one in four people is likely to live in a country affected by chronic or recurring shortages of freshwater*" (UNDP, (2017). Consequently, more than 2 million people die every year from water-borne related diseases while 4.3 and 6.4 per cent of Sub-Sahara African and India's GDP resulting from adverse economy impacted cost due to inadequate sanitation. Nigeria is ranked poorly in the planning to achieve Sustainable Development Goal 6 (SDG6), a challenge which requires among others proper understanding of relationships between land use and groundwater quality. Monitoring groundwater is necessary to detect contamination early enough to prevent damage to the resource since remediation remains expensive and, in Africa, nearly impossible to implement after water quality deterioration.

In order to improve the quality of freshwater resources, policies that support investment planning for the management of freshwater ecosystems and sanitation facilities at a local level are needed. This study assessed the impact of land use on groundwater quality in the EDB using the groundwater quality index and statistical analysis. The Groundwater quality index (GWQI) has been shown useful for identifying water quality spatial variability (Adimalla and Kumar, 2020; Krishna Kumar et al., 2014; Singh et al., 2011; Verma et al., 2020). Overlaying GWQI results on land-use maps highlights possible sources of contaminants and pollutant of

groundwater. The results should be used to support a science-led policy review of existing integrated water resources management (Akpabio, 2007; Jideonwo, 2014).

8.2.2.1 Study area

The Eastern Dahomey Basin is located in the South-Western part of Nigeria. It lies between Latitudes 2° 41'10.00" and 4° 59'59.00" N and Longitudes 6°21'13.00" and 7°52'42.00"E along the coast of the Gulf of Guinea (Figure 8.1). The Nigerian part of this basin is known as the Eastern Dahomey Basin which underlies the three states of Lagos, Ogun and Ondo. The area of investigation is low lying, with several points virtually at or below the sea level, always saturated with water, and prone to flooding. The highest elevation, 265 m above sea level is at Abeokuta town, where the basin thins out into the Precambrian basement rocks (Jamiu A. Aladejana et al., 2020). The climate of the basin is characterised by wet and dry seasons, within the tropical rain forest belt. Precipitation in this area occurs as rainfall ranges between 750 and 1000 mm mostly between March and October (wet season) and 250 mm and 500 mm between November and March (dry season) (Oloruntola et al., 2019).

8.2.2.2 Geology and hydrogeology

The area is a part of the Dahomey basin which extends from Nigeria to Ghana. The lithological character of the sediments was a result of transgressions and regressions of the sea since the Cretaceous age, the transgressions coming from the south. The stratigraphic description of the sediments has been provided by various authors including (Jones and Hockey, 1964; Adegoke and Omatsola, 1981; Olabode and Mohammed, 2016).

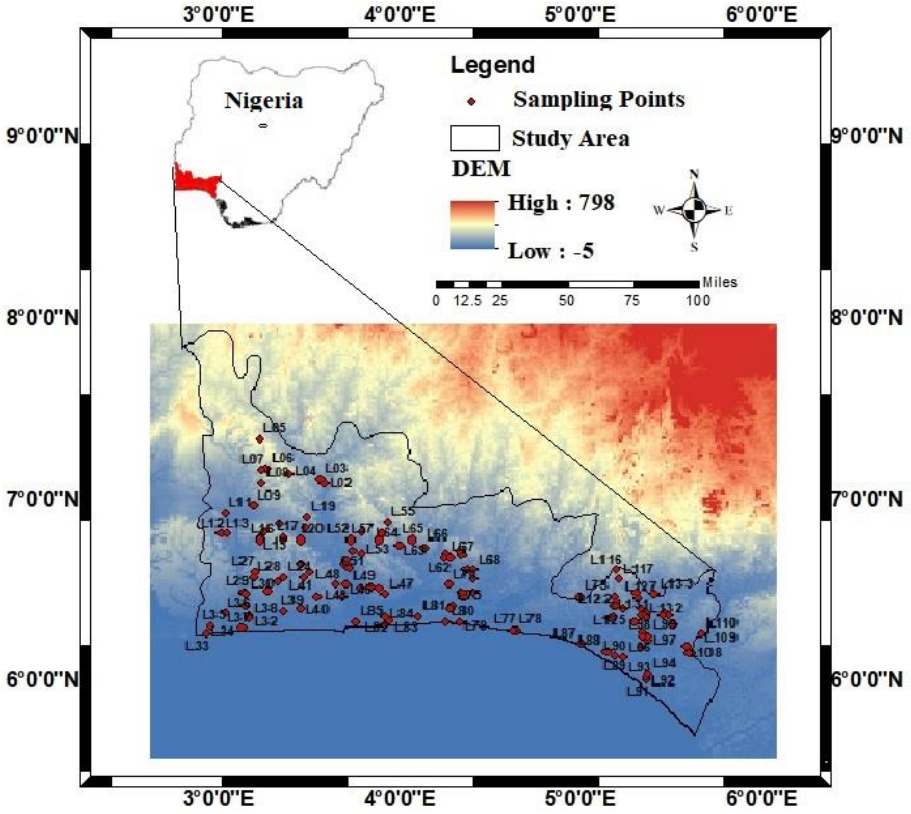

Figure 8.1 Map showing the study area, digital elevation and sampling pints

The Coastal Plain Sands (Recent – Oligocene) constitute the main aquifer of the area and is exploited through hand-dug wells and boreholes. It forms a multi-aquifer system consisting of three aquifer horizons separated by clayey layers (Longe et al., 1987; Oloruntola *et al.*, 2019). Quaternary alluvial sediments cover most of the Lagos Coastal areas and river valleys. Details about the geology and hydrogeology of this area is presented in the work of Aladejana et al., 2020b.

8.2.3 Materials and methods

8.2.3.1 Field Inventory and Laboratory analysis of water samples

A Topographical map of the study area was used to determine accessibilities to different locality within the study area. A well inventory was carried out at each sample location, during which physicochemical measurements of Electrical

conductivity (EC), pH, Total Dissolved Solids (TDS) and temperature were measured using portable hand-held multimeter Hach pH/EC metre. A total of 230 water samples (96 in the wet season and 134 in the dry season) were collected in separate Polyethylene bottles labelled A and B. Filtered samples labelled A, were acidified to a pH<2 after collection with 0.4ml of concentrated Nitric acid (HNO_3). Acidification was necessary to avoid the problem of absorption or precipitation of the metals before hydrochemical analysis while sample B were preserved in a cooler with an ice pack to keep its temperature as low as 4°C before taking to the Laboratory for anions analysis.

Cations and anions analyses were carried out using Inductively coupled plasma - optical emission spectrometry (ICP-OES) and ion chromatography (Metrohm 850 Professional IC) with standard methods after filtering with <0.45µm. Alkalinity and Bicarbonate were determined using HACH digital titrator using Bromcresol Green-Methyl red and Phenolphthalein indicator using 0.16 and 1.6M of sulphuric acid. Results were checked calculated ion balance errors recommended by Appelo and Postma (2005).

8.2.3.2 Data Quality Evaluation

Total Dissolved Ions (TDI) was calculated for each sample and correlated with the Total Dissolved Solids (TDS) measured in the field during the sample collection. The correlation coefficient is 0.96. Duplicate laboratory analysis was conducted on 10 randomly selected water samples. The results were correlated with the coefficient of correlation R ranges from 0.86 to 0.99, indicating analytical precision and consistency on the part of the instrument and analytical procedure. The ion balance (sum of cations versus the sum of anions), was calculated and 87% of the samples analysed fall within

10%, the acceptable limit in standard water chemistry analysis as recommended by WHO (1994).

8.2.3.3 Evaluation and analysis of Groundwater Quality Index (GWQI)

The Groundwater Quality Index (GWQI) is a rating which provides the composite influence of individual water quality parameters for human consumption. This method was developed by Horton (1965) and has been employed in recent studies of groundwater quality assessment at different case studies around the world. GWQI involves three steps. The first step, essential parameters were assigned a weight (wi) according to its relative importance in the quality of potability (Table 8.1). The maximum weight of 5 was assigned to nitrate and fluoride due to their human health impacts and considered major importance in water quality assessment (Kumar *et al.*, 2014). Bicarbonate and phosphate were given the minimum weight of 1 as they play a less significant role in the water quality assessment. In step two, the relative weight (Wi) is being calculated using the equation below (Vasanthavigar et al.,2010)

$$Wi = wi \sum_{i=1}^{n} wi \quad \text{----------(1)}$$

Where wi is the assigned weight to each parameter and n is the number of parameters. In the third step, quality rating scale(qi) for each parameter is assigned by dividing its concentration in each water sample (Ci) by its respective standard (Si) according to WHO (World Health Organization) guidelines in mg/l. The result is then multiplied by 100, as shown in the equation below:

$$qi = \left({}^{Ci}/_{Si}\right) \times 100 \quad \text{----------(2)}$$

To compute the GWQI, the sub-index (SI) of the parameter is first determined for each chemical parameter, which is then used to determine the GWQI using the following equations:

$$SI = Wi \times qi \quad \text{----------(3)}$$

$$GWQI = \sum SIi \quad \text{----------(4)}$$

Where; SIi is the sub-index of ith parameter where i represent the number of parameters used.

Table 8.2 presents the classification of GWQI.

8.2.3.4 Spatial analysis for the distribution of GWQI and some selected water quality parameters

Geographical information system (GIS) and geostatistical techniques provide an integrated tool to investigate the spatial distribution water quality (Adimalla, 2019a; Kumar et al., 2010; Shah and Joshi, 2017). The calculated GWQI with georeferenced coordinates were converted to shapefiles representing each class of water quality.

The shapefile then overlaid on the boundary map, static water level (SWL) contour and river map of the study area. The spatial distribution maps of some selected water quality parameters such as Ca^{2+}, Mg^{2+}, Na^{+} and K^{+} were generated and overlaid on the geological map of the area. Furthermore, results were compared and correlated with the land use map of the study area in order to see the water quality distribution across different land use in the area.

Table 8.1 Water quality parameters, WHO standards and assigned weights

S/N	Parameters	Highest Desirable Limit	Max Permissible Limit	Assigned Weight wi	Weight Index W
1	TDS (mg/l)	500	1500	3	0.051
2	Total Hardness	100	500	4	0.068
3	Calcium (mg/l)	75	200	3	0.051
4	Magnesium (mg/l)	20	150	3	0.051
5	Sodium (mg/l)	200	250	4	0.068
6	Potassium (mg/l)	200	--	2	0.034
7	Bicarbonate (mg/l)	100	500	1	0.017
8	Chloride (mg/l)	200	600	3	0.051
9	Sulphate (mg/l)	250	500	3	0.051
10	Nitrate (mg/l)	10	50	5	0.085
11	Iron (mg/l)	1	1	3	0.051
12	Fluoride (mg/l)	1.5	5	5	0.085
13	Arsenic (ug/l)	0.01	0.01	5	0.085
14	Lead (mg/l)	0.01	0.01	5	0.085
15	Manganese	0.1	0.4	4	0.068
16	Cadmium	0.03	0.03	4	0.068
17	Silica	17	17	2	0.034
	Total Weight			59	1.000

Table 8.2 Summary of classification of groundwater quality index (GWQI) used in this study

Class of Groundwater based on GWQI	GWQI
Very good	0 - 25
Good	25 - 50
Moderate	50 - 75
Poor	75 - 100
Very poor	100 - 125
Unfit	125 and above

8.2.3.5 Land use map of the area

The land-use pattern The Landsat imagery 2017 was downloaded from the DIVAS-GIS site and imported to the ArcGIS 10.6, where it is processed to a shapefile of the study location. The imageries were geometrically corrected, and the projection

was set to Universal Transverse Mercator (UTM) projection system. A false colour composite operation was carried on the different bands and then combined to obtain a composite image followed by supervised classification using the maximum likelihood classification algorithm. Different land use classification map of the Eastern Dahomey Basin (Figure 8.13) revealed Water bodies, Plantation, Bare soil, Agriculture, Agriculture in shallows and recession, Cropland and fallow with oil palms, Forest, Savannah, Wetland-floodplain and settlement. With this diverse outlook of the land-use pattern in the study area, it is necessary to compare how this correlates with the groundwater quality distribution within the Eastern Dahomey basin.

8.2.3.6 Statistical analysis

Principal component analysis (PCA) and factor analysis (FA) method

Geostatistics was used for analysis and interpretation of the geographically referenced data. Multivariate statistics method of R-mode factor analysis has been proven effective for the understanding of hydrochemical association with source, processes and geospatial relationship (Aiuppa *et al.*, 2003; Ako *et al.*, 2013; Kumar *et al.*, 2017; Bodrud-Doza *et al.*, 2019). The dimensionality of the problem is effectively reduced by factor analysis (Morell et al., 1996; Kumar *et al.*, 2017; Shi *et al.*, 2018) (Davis 1986). Principal component analysis (PCA) was carried out for the chemical data from the study area for hydrogeochemical interpretation. Kaiser's varimax rotation was applied to obtain a simple structure in such a way that components are closer to 1, 0 and -1, representing the contributions of corresponding variables to the total variance as a positive contribution, a no contribution and a negative contribution, respectively (Ako et al., 2013). The interpretation can be simplified using specific rotational procedures.

Hierarchical cluster analysis

This classification method groups the results into the classes or clusters based on similarities within a class and dissimilarities between different classes. Clusters are formed sequentially by starting with the most similar pair of objects and forming higher clusters step by step. Hierarchical agglomerative CA was performed on the normalised data set (mean observations over the whole period) employing Ward's method using squared Euclidean distances as a measure of similarity. Based on geochemical characteristics, cluster analysis helps us to find similar sampling location in a region, which optimally helps in future sampling strategy in the monitoring network. Thus, it reduces the cost of sampling in water resource management. In various studies (Ako et al., 2013; Hashmi et al., 2014; Sudheer Kumar et al., 2017), this approach has been used successfully for water quality assessment and monitoring program.

8.2.4 Results and Discussions

8.2.4.1 Results of some selected water quality parameters

Groundwater quality is critical to its suitability for drinking and other purposes. Statistic summary of physicochemical parameters such as pH, EC, TDS and TH and major ions such as Ca^{2+}, Mg^{2+}, Na^{+}, K^{+}, HCO_3, F^{-}, Cl^{-}, SO_4^{2-} and NO_3^{-}, trace metals As, Cd, Fe, Mn, Pb and Si are presented in Table 8.3. The pH of water samples ranges from 4 to 8, with average values of 5.6 and 5.5 for wet and dry seasons respectively indicating acidic to slightly alkaline through neutral groundwater but tending towards acidic in the dry season. The electrical conductivity (EC) range from 0.00 to 12000 µS/cm and 5.50 to 10009 µS/cm with average values of 295 and 348 respectively for the wet and dry seasons. The total dissolved solid values range from 0.00 to 8500 mg/l

and 2.30 to 6750 mg/l with average values of 201 and 232 mg/l. The comparative average values of EC and TDS in wet and dry seasons indicate the effect of evaporation and mineral dissolution through longer travel/residence time of groundwater within aquifers or vadose zones of the study area.

Calcium ions (Ca^{2+})

Figure 8.3 presents the spatial distribution maps of Ca^{2+} (a, b) and Mg^{2+} (c, d) in wet and dry seasons. The Ca^{2+} concentration in the wet season groundwater ranges from 0.3 to 374 mg/l with an average value of 16.5 mg/l while the concentration in the dry season water samples ranges from 0.2 to 428 mg/l with an average value of 21.2 mg/l. In the wet season, the higher concentrations (> 200 mg/l) are observed in locations around Badagary, Lekki and Ode-Mahin which are in the southern part of the study area along the coastline. Other locations fell well within the WHO 2017 standard for drinking water. The relatively higher concentration of Ca^{2+} in the groundwater samples of the dry season could be linked to evaporation and mineral dissolution especially in areas area similar to those of wet season with few locations towards the middle of the study area which are underlain by carbonate rocks such as limestone in Ibese, Ewekoro and Shagamu. Dissolution of carbonate minerals from the remains of carbonate shells of some of the sea animals could also have an influence on observed distribution Ca^{2+} in groundwater within this Basin.

Magnesium (Mg^{2+})

The results of Mg^{2+} concentration in analysed groundwater samples from wet and dry seasons are also presented in spatial distribution map (Figure 8.2c, d) respectively. The concentration of Mg^{2+} in wet season groundwater samples range from 0.0 to 1,377 mg/l with an average value of 18.4 mg/l, while Mg^{2+} for the dry

season water sample ranges from 0.1 to 1,417 mg/l with an average value of 18.5 mg/l. Mg^{2+} concentration in wet season fell well within the WHO 2017 limit (50 mg/l) for drinking water except in the location at the southeast part of the study area. In the wet season, a higher concentration of magnesium is observed in the three locations along the coastline while few locations are also observed along the floodplain of river Ogun running Northwest – Southwest direction at the western part of the study area. Magnesium concentration in groundwater could be control by cations exchange associated with the dissolution of minerals from magnesium-rich carbonates rocks.

Sodium (Na^+)

The concentration of Na in analysed groundwater in wet season ranges from 0.1 to 8,857 mg/l with an average value of 106.8 mg/l while in the samples collected during the dry season concentration ranges from 0.6 to 9,420 mg/l with an average value of 103.4 mg/l. sodium concentration in the groundwater samples follows this same trend with Ca and Mg with a relatively higher concentration in the dry season, which can be attributed to the evaporation effect (Adimalla, 2019b; Bodrud-Doza et al., 2019; Narany et al., 2014). As presented in the spatial distribution map in Figure 8.3 (a, b), High Na concentration was observed in the southern part of the study area along the coastline in both seasons which could be attributed to sea spraying and seawater intrusion into coastal freshwater aquifers (Aladejana et al., 2020b). Na^+ concentrations in sampled groundwater in both seasons fell well within the WHO 2006 standard permissible limit for drinking water except in few locations within the proximity of the sea (Table 8.3 and Figure 8.3).

Table 8.3 Statistical Summary of the water quality parameters and WHO Standard

	Wet Season N = 96				Dry Season N = 134				WHO Max Perm Lmt
Parameter	**Min**	**Max**	**Aver**	**St Dev**	**Min**	**Max**	**Aver**	**Stdev**	
pH	3.97	8.10	5.57	1.0	3.85	8.0	5.5	0.9	6.5 – 8.5
EC	0.0	12,000	295.4	1219	5.5	1,0009	348	995	500
TDS	0.0	8,500	201	863.6	2.3	6,750	222.0	667.3	1500
TH	0.8	6,504	115.6	663	0.0	6750	232	528.6	500
Ca^{2+}	0.3	374	16.5	41.2	0.2	428	21.2	53.7	200
Mg^{2+}	0.0	1,377	18.4	140.4	0.1	1,417	18.5	126.8	150
Na^{+}	0.1	8,857	106.8	902.8	0.6	9,420	103.4	825.7	250
K^{+}	0.1	447	10.5	46.2	0.1	488	9.4	42.8	-
HCO_3	1.0	8,029	142.3	818.7	0.0	8,390	155.8	771.2	500
Cl-	0.1	18,970	218.1	1934.3	0.9	1,289	31.6	115.9	600
SO_4^{2-}	0.0	2,211	32.0	225.4	0.3	576	17.5	56.1	500
NO_3^{-}	0.0	259	31.8	54.1	0.3	312	30.3	54.4	50
F^{-}	0.0	6.1	0.226	0.14	0.01	1.5	0.12	0.2	1
As	0.0	0.0	0.0	0.0	0.0	0.0	0.0	0.0	0.01
Cd	0.0	0.0	0.0	0.0	0.0	0.0	0.0	0.0	0.03
Fe	0.0	6.1	0.3	0.8	0.0	136	1.5	11.9	1
Mn	0.0	1.1	0.1	0.1	0.0	27.7	0.3	2.4	0.4
Pb	0.0	0.1	0.0	0.0	0.0	0.0	0.0	0.0	0.01
Si	0.0	29.8	5.8	4.3	1.1	31.1	6.2	5.6	17

EC in µS/cm while other parameters are in mg/l except for pH with no unit.

Potassium (K^{+})

The concentration of K^{+} in the analysed groundwater samples in wet season ranges from 0.1 to 447 mg/l with an average value of 10.5 mg/l while the concentration ranges from 0.1 to 488 mg/l with an average value of 9.4 mg/l in dry season water samples (Table 8.3). Although, there is no known limit of K^{+} concentration intake for a man in the WHO guidelines as it is considered an essential element for a human nutrient that is part of natural mineral in groundwater at a concentration below those of health concerns (Hashmi et al., 2014; Tirkey et al., 2017). Intake of excess may behave as a laxative but have the possibility of causing diarrhoea when it becomes abnormally high in the body (Tirkey et al., 2017).

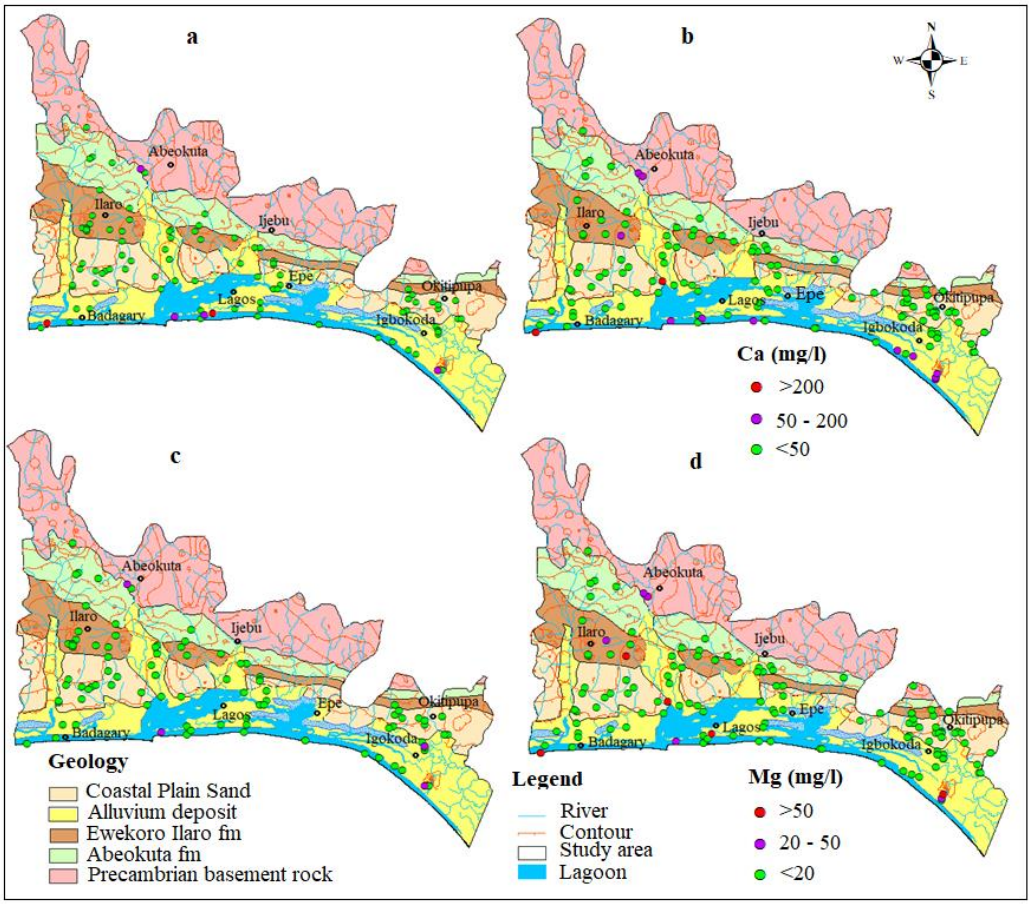

Figure 8.2 Spatial distribution of major Cations in Eastern Dahomey Basin (a) Ca for wet season (b) Ca dry season (c) Mg for wet season (d) Mg for dry season

WHO guidelines for K^+ has not been established as it naturally occurs in drinking water at concentrations well below those of health concern (Pfeiffer et al., 2015) (WHO, 2017). Figure 8.3 (c, d) present the spatial distribution of K^+ for wet and dry seasons. A higher concentration of K^+ only occurred in few locations at the southern part of the study area along the coastline in both seasons groundwater samples.

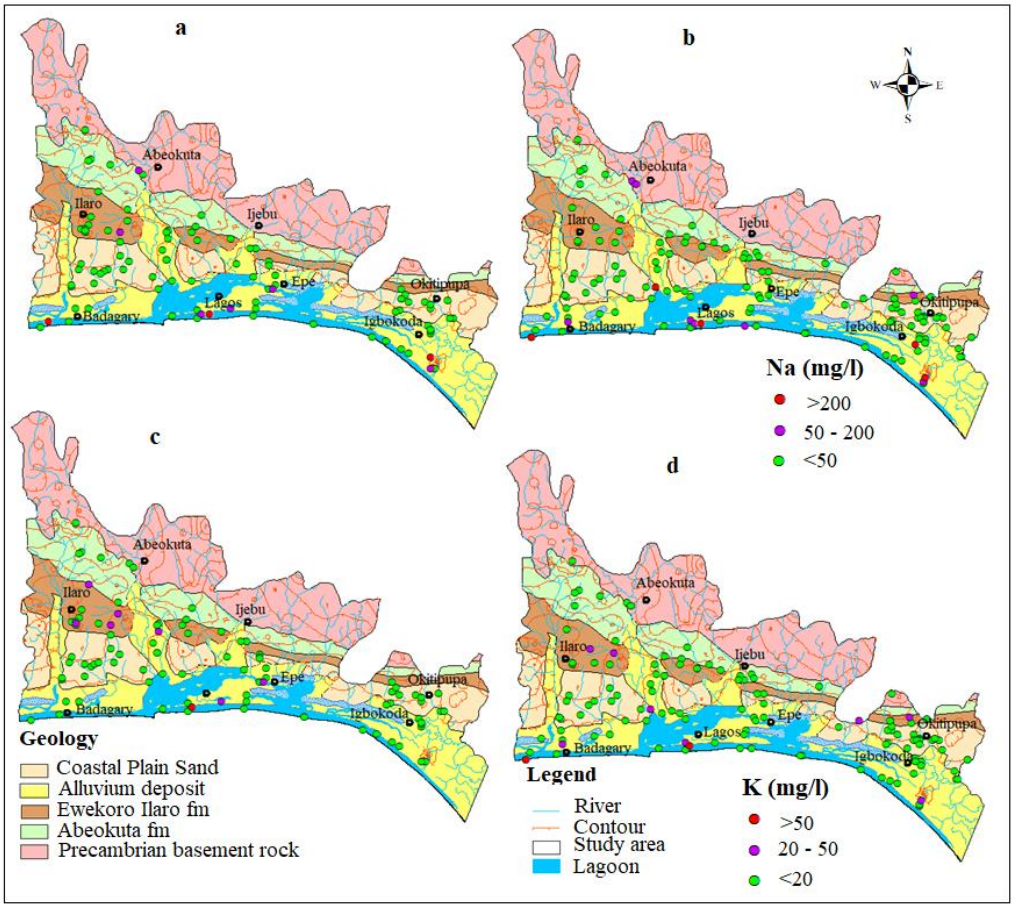

Figure 8.3 Spatial distribution of significant Cations in Eastern Dahomey Basin (a) Na for wet season (b) Na dry season (c) K for wet season (d) K for dry season

Nitrate (NO_3^-)

In recent research, Nitrate in drinking water was linked to a high risk of colorectal cancer resulting from the endogenous transformation into carcinogenic N-nitroso compounds (Schullehner et al., 2018). It also linked to the causes of "blue-baby syndrome" resulting from the methaemoglobinaemia which is caused by the decreased ability of blood to carry vital oxygen around the body. Though there is a suggestion for more research along this line to confirm the link further. This discovery has raised more awareness and fear about the amount, origin and occurrence of Nitrate in groundwater, most notably where people depend on groundwater to meet their daily water demand. The Nitrate concentration in the analysed sample groundwater in this

area as reported in (Aladejana et al., 2020) range from 0.02 to 259 mg/l and 0.3 to 312 mg/l with average values of 32.1 and 30.3 mg/l for the wet and dry seasons respectively. Pollution risk of nitrate concentration in groundwater samples is presented in Table 8.4. The results show that 75 (78.1 %) and 109 (81.3 %) of the sample for the respective wet and dry season fell under low risk of Nitrate pollution. 12 (12.5 %) and 12 (9 %) fell under the high-risk category, while 9 (9.4 %) and 13 (9.7 %) of nitrate concentration in the samples fell in the category of very high risk. Figure 8.4 presents the spatial distribution of nitrate in the Eastern Dahomey Basin is for both seasons of water samples. The trend shows most of the high to very high-risk nitrate concentration is found in water samples from wells along the flood plains of rivers and lakes in the area which could be associated with both agricultural and municipal waste (Aladejana et al., 2020; Jahangir et al., 2012; Lapworth et al., 2017b; Morari et al., 2012).

Table 8.4 Summary of the pollution risk of Nitrate concentration in Eastern Dahomey Basin

		Wet Season (N = 96)		**Dry Season (N = 134)**	
Conc. range	**Risk Category**	**Sample No.**	**% Sample**	**Sample No.**	**% Sample**
< 45	Low risk	75	78.1 %	109	81.3 %
45-100	High risk	12	12.5 %	12	9 %
>100	Very high risk	9	9.4 %	13	9.7 %

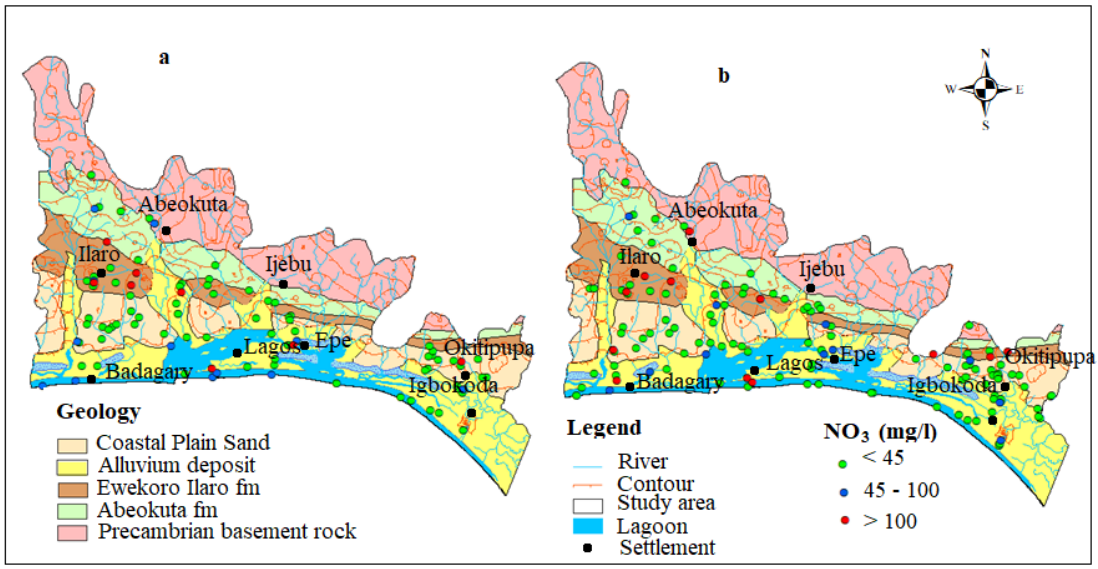

Figure 8.4 Spatial distribution of nitrate (NO_3^-) in Eastern Dahomey Basin (a) NO_3^- for wet season (b) NO_3^- the dry season

Fluoride (F^-)

Fluoride concentration in groundwater is crucial to its quality drinking purpose. While the low concentration of fluoride is beneficial to dental health and often form an essential ingredient in water and dental products, high concentration is a concern globally for safely managed drinking water because of implication on dental fluorosis (Brunt, Vasak et al., 2004; Dar et al., 2011; Kumar *et al.*, 2017; Martins *et al.*, 2018; Addison *et al.*, 2020; Alcaine *et al.*, 2020). In this study, fluoride concentration ranges from 0.0 to 6.1 mg/l and 0.01 to 1.5 mg/l with average values of 0.26 and 0.12 mg/l (Table 8.3) for the wet and dry seasons respectively. Fluoride concentration beyond 1 mg/l WHO (2006) standard for drinking water is found in groundwater samples from L35, L53, L64, L74, L76 and L81in wet season while it is found in samples from wells L3, L34, 43 and L94 in the dry season. Scatter diagram (Figure 8.5) of fluoride against nitrate in the analysed water samples show very low correlation which indicates the geogenic origin of fluoride in groundwater within the Eastern Dahomey Basin.

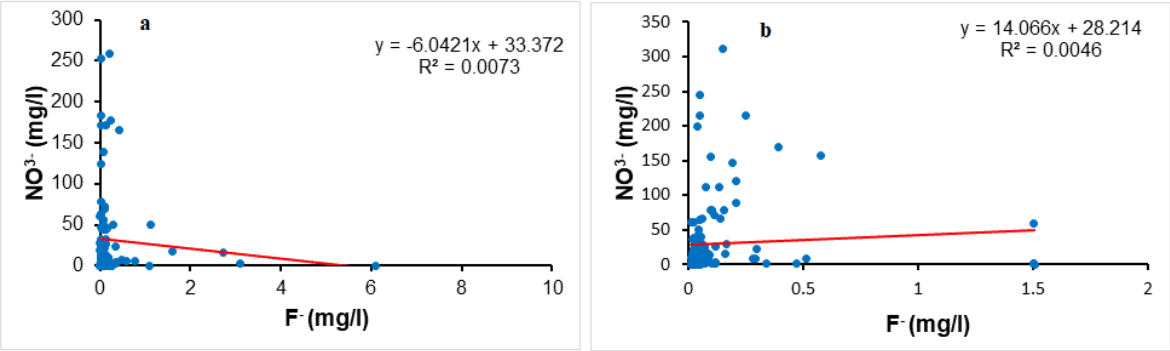

Figure 8.5 Scatter plot between Fluoride and Nitrate in sampled groundwater (a) wet season (b) dry season

8.2.4.2 Cation Exchange Process as a hydrochemical controlling mechanism

Cation exchange process (CEP), as proposed by Schoeller (1965) is another useful approach in understanding natural processes in groundwater which have been employed by several authors such as Li et al., 2016. The CEP describes the ion exchange between Na^+ (and K^+) and Ca^{2+} (or Mg^{2+}) which occur in the groundwater system. This is a crucial process that alters the hydrochemistry of groundwater (Adimalla, 2019b; Li et al., 2015). CAP can be examined in the form of chloro-alkaline indices from which two chloroalkaline indices (CAI-1 and CAI-2) was proposed for the study of cation exchange which is defined in equations 1 and 2 below;

$$\text{CAI} - \text{I} = Cl^- - (Na^+ + K^+)/Cl^- \quad \text{----------} \quad (5)$$

$$\text{CAI} - \text{II} = Cl^- - (Na^+ - K^+)/(HCO3^- + SO4^{2-} + NO3^-) \text{---} \quad (6)$$

In this study, for the wet season groundwater samples, the CAI-1 and CAI-2 values are 11.5 and 24 % for positive values, while 88.5 and 76 % are negative values for CAI-1 and CAl-II, respectively. In the dry season water samples, 14.9 and 29,9 % of analysed groundwater samples are positive for CAI-1 and CAI-2 while 85.1 and 70 .2 % of the samples are negative for CAI-1 and CAI-2, respectively (Table 8.5).

Dominant of negative values in both cases and seasons is an indication that the exchange of Ca^{2+}+Mg^{2+} in groundwater with Na^{+}+K^{+} from an aquifer material while the reverse positive cation exchange occurs probably from locations where carbonate rocks with magnesium mineral predominate which allow Na^{+} + K^{+}. to be exchanged by Ca^{2+} + Mg^{2+} ions within aquifer medium mostly during infiltration and lateral flow.

Table 8.5 Cation exchange table for both wet and dry seasons

	Wet Season N=96		Dry Season N=134	
Cation Exchange	**CAI-I**	**CAI-II**	**CAI-1**	**CAI-II**
Number of positive samples	11	23	20	40
Number negative samples	85	73	114	994
% of positive samples	11.5	24	14.9	29.9
% of negative samples	88.5	76	85.1	70.2

8.2.4.3 Factor and Principal Component Analysis

Groundwater physicochemical parameters of pH, EC, TDS and TH along with major ions including Fluoride (F) and Iron (Fe) were selected as variables in principal component analysis (PCA) to provide an insight as to Hydrogeochemical processes. Hydrochemical data from wet (96 samples) and dry (134 samples) seasons were subjected to factor analysis using the PCA method. Three principal components were detected in hydrochemical data for both seasons as presented in Table 8.6. The factor analysis FA for the groundwater samples in the wet season (May-August 2017) revealed percentage variance 59.3, 11.2 and 8.9 % for component 1, 2, and 3, respectively for the wet season. In the dry season (February – April 2018), the FA revealed percentage variance of 63.1 10.7 and 10.1 % for component 1, 2 and 3 respectively for the dry season samples. The total variance is 79.4 and 83.9 % for wet

and dry season's geochemical data respectively. PCA analysis geochemical data during the wet season, factor 1 showed a strong loading of EC, TDS, TH, Ca, Mg, Na, K, HCO_3, and SO_4 with over 59.3%, indicating that Ca, K, Na and HCO_3 (Table 8.7) were the dominant ions in local groundwater. Factor 2 revealed the loading of Cl, NO_3 and F while factor 3 show loading of pH and Fe. The association observed in factor 2 and 3 show anthropogenic influence on the groundwater.

Table 8.6 Component Matrix for some selected water quality parameters

	PCA (*Wet season*)			**PCA (*Dry season*)**		
Parameters	**1**	**2**	**3**	**1**	**2**	**3**
pH	0.387	0.304	**0.684**	**0.447**	**0.482**	0.141
EC	**0.99**	-0.121	-0.014	**0.966**	-0.154	-0.188
TDS	**0.989**	-0.127	-0.015	**0.967**	-0.159	-0.178
TH	**0.986**	-0.144	0.016	**0.978**	0.152	0.008
Ca	**0.97**	0.112	0.114	**0.91**	0.223	0.247
Mg	**0.977**	-0.189	-0.002	**0.944**	0.086	-0.202
Na	**0.972**	-0.215	-0.026	**0.902**	-0.257	-0.308
K	**0.983**	-0.108	-0.069	**0.588**	-0.477	**0.442**
HCO_3	**0.986**	-0.145	0.015	**0.977**	0.157	0.004
Cl	0.495	**0.64**	-0.248	**0.888**	-0.226	-0.354
SO_4	**0.749**	0.26	-0.019	**0.613**	0.398	**0.416**
NO_3	0.387	**0.597**	-0.552	0.307	**-0.632**	**0.604**
F	0.074	**0.585**	0.151	0.392	0.191	0.304
Fe	0.079	0.234	**0.735**	0.18	**0.496**	0.092
% Variance	59.3	11.2	8.9	63.1	10.7	10.1
Cumulative %	59.2	70.5	79.4	63.1	73.8	83.9

Bold numbers are the correlation values that are significant in explaining the relationship

For the dry season, EC, TDS, TH, Ca, Mg, Na, K, HCO_3, Cl, and SO_4 are the loading parameters in factor 1. Factor 2 contains pH, NO_3 and Fe while only NO_3 loaded in factor 3 (Table 8.7). The association of these parameters in factor 1 signified geogenic influence through the mineral dissolution of aluminosilicates such as feldspars and clay during groundwater infiltration and subsequent subsurface flow into the aquifers (Ako et al., 2012). In addition to Na, Cl and SO_4 present in this group

could also indicate the dissolution of evaporite mineral from coastal sediments and seawater intrusion (Paris et al., 2010). Factor 2 and 3 which contained pH, NO3, F and Fe which could be anthropogenic influence since these ions and metal are commonly found in industrial, agricultural and municipal waste while their enrichment and preservation is sensitive to pH of the environment. The presence of Cl in factor 2 in the wet season and factor 1 in the dry season could be attributed to evaporation, and possible see spraying due to the proximity of the area to the coast. These associations are better projected using component plot rotated space, as shown in Figure 8.6 and 8.7

8.2.4.4 Cluster analysis

Cluster analysis is another statistical tool used to detect similarity among different sampling sites (Bodrud-Doza et al., 2019; Lapworth1 et al., 2018; Sudheer Kumar et al., 2017).

Table 8.7 Factor loading parameters for both seasons water quality parameters

	Wet season	***Dry season***
Factor	**Parameter loading**	**Parameter loading**
1	EC, TDS, TH, Ca, Mg, Na, K, HCO3 and SO4	EC, TDS, TH, Ca, Mg, Na, K, HCO_3 Cl and SO_4
2	Cl, NO_3 and F	pH, NO_3 and Fe
3	pH and Fe	NO_3

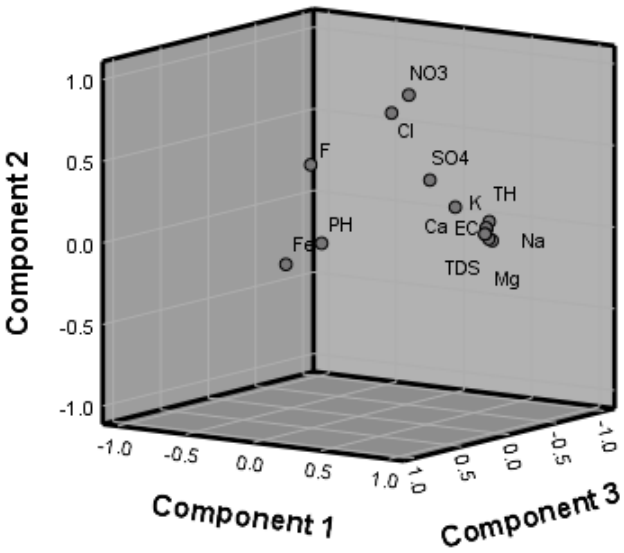

Figure 8.6 Component Plot in rotated space for wet season wet Season

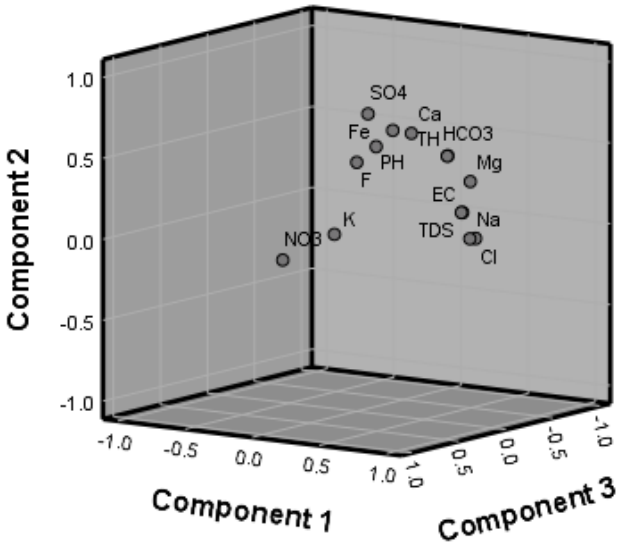

Figure 8.7 Component Plot in rotated space for wet season dry season

In this study, cluster analysis was carried out on the water quality parameters for both wet and dry seasons using Ward's method. The samples were found to be grouped into three main clusters, as seen in the dendrogram (Figure 8.8 and 8.9) for wet and dry seasons, respectively.

In the wet season water samples, most of the samples were classified in cluster 1 with similarity between major ions (Na, EC, Mg, NO_3, K, Ca, Cl, SO_4, Si, pH, Fe, Mn, F, Pb, Cd, As) in association with Na and EC which indicated mixture of processes ranging from weathering, mineral dissolution and anthropogenic which is a reflection of landuse influence. Cluster 2 demonstrate, TDS, HCO3 and Na were associated based on their amount of concentration which is correlated with one another. The third cluster shows the similarity between HCO_3 and TH which is based on similarity in the amount of contribution while cluster 4 contains EC and Na based on their dominant behaviour in the hydrochemistry of the sampled groundwater. In the case of the groundwater samples during the dry season cluster, 1 contains NO_3, SO_4, Mg, Ca. K, Si, K, Si, pH, Fe, F, Mn, Pb, Cd, and As which indicates the influence of the mixed process of geogenic and anthropogenic activities. Cluster 2, Mg, Na and Cl which could be attributed seawater influence. Cluster 3 contains SO_4, TH, and HCO_3. Cluster 4 contains Na, EC, and TDS which implies similarities in their control in hydrochemical processes. This complexity in the hydrochemistry of groundwater from this basin could be attributed to the high recharge rate driven by the short residence time of water from precipitation within the vadose zone which possibly allow surface-groundwater interaction.

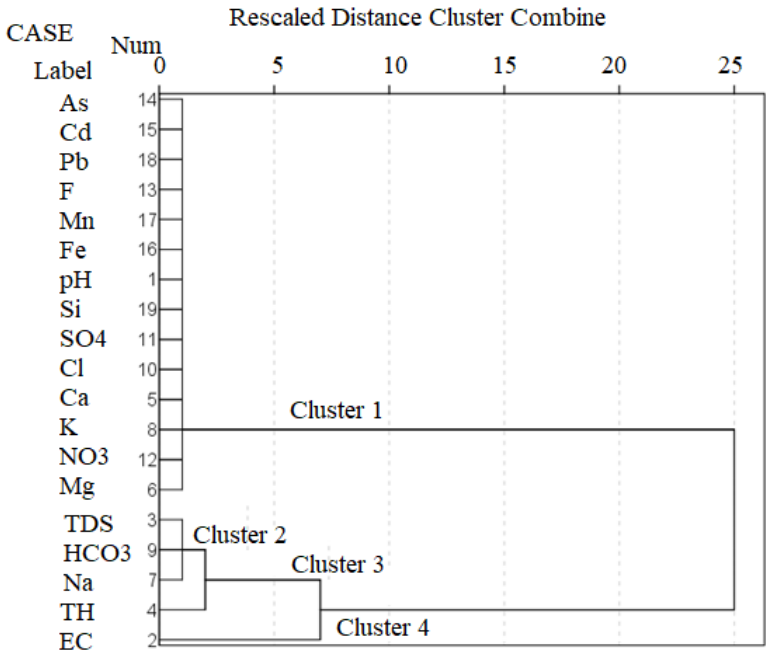

Figure 8.8 Dendrogram using average linkage (between groups) rescaled distance cluster combine for the wet season

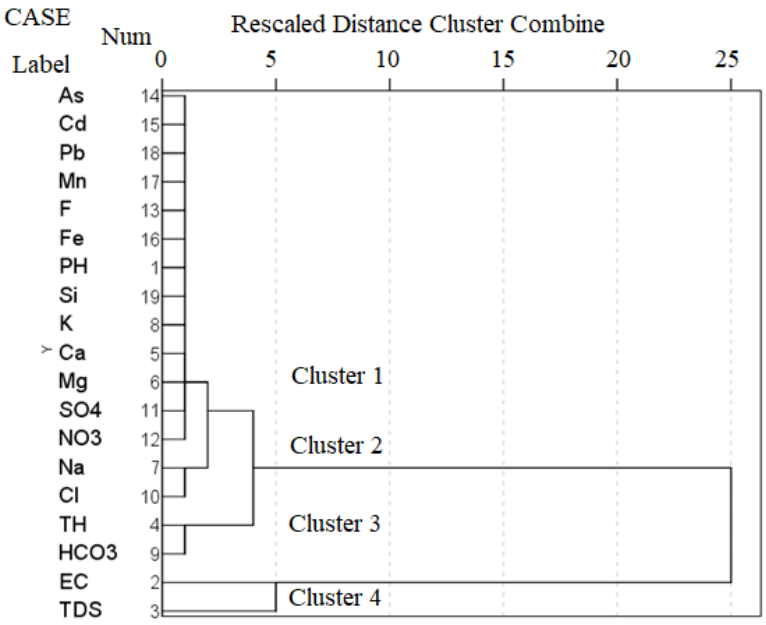

Figure 8.9 Dendrogram using average linkage (between groups) rescaled distance cluster combine for dry season

8.2.4.5 Groundwater quality in relation to Irrigation and other agricultural purposes

Percentage of Sodium (%Na)

Percentage sodium is an index employed in evaluating the suitability of water quality for irrigation in agricultural soils. The percentage sodium ($\%Na^{+}$) is computed concerning relative proportions of cations present in water, where the concentrations of ions are expressed in meq/l, using the equation below while the classification of analysed groundwater for wet and dry seasons are presented in Table 9.

$$\%N = [(Na^{+} + K^{+})/(Ca^{2+} + Mg^{2+} + Na^{+} + K^{+})] * 100 \quad \text{----------(7)}$$

The results showed that the values of percentage sodium range from 8.2 to 86.9 % with an average value of 49.5 % for wet season groundwater samples while the dry season water samples %Na values range from 36.8 to 96.8 % with an average value of 67.2 % (Table 8.8). For the dry season samples, 8.3, 18.8 and 43.8 % fell under excellent, good and permissible respectively while 28.1 and 1.0 % of the samples fell under doubtful and unsuitable for irrigation purpose. 6.7, 11.9, and 35.1 % fell under excellent, good and permissible respectively and doubtful and unsuitable water occupies 41.8 and 4.5 % of the groundwater samples for the dry season (Table 8.9).

Residual Sodium Carbonate (RSC)

RSC is a measure which also revealed sodium hazard in the water meant for irrigation purpose. RSC >5 in water is considered harmful to plants while water with RSC value > 2.5 is considered doubtful for the plant growth while RSC value<2.5 considered suitable for the plant growth (Arulbalaji and Gurugnanam, 2017). Water with a high concentration of bicarbonate caused calcium and magnesium to precipitate as carbonates. This precipitation of Calcium and magnesium is determined by an

experimental parameter known as residual sodium carbonate (RSC). RSC is expressed in meq/1 and calculated using the equation below.

$$RSC = (HCO3^{-} + CO3^{2-}) - (Ca^{2+} + Mg^{2+}) \quad \text{----------(8)}$$

In this study, all the water samples (100%) for the wet and dry season have RSC values below 1.25 which indicate they are suitable for irrigation purpose based on RSC (Table 8.8).

Kelly's Ratio (KR)

The relationship between Na^{+} alkaline earth metals/ions such as Ca^{2+} and Mg^{2+} was proposed by Kelley (1963). This relationship in the form of equation (Equation 9) called Kelly's ratio, and its values are expressed in meq/1. A Kelley's ratio is said to be unsuitable for irrigation when sodium is higher than the alkaline earth. Therefore, Kelly's ratio of less than one is suitable for irrigation.

$$KR = Na^{+}/(Ca^{2+} + Mg^{2+}) \quad \text{---------- (9)}$$

In the analysed groundwater samples from both seasons of the study area, KR values range from 0.1 to 6.6 and 0.1 to 3.5 with the average values of 1.1 and 0.7 (Table 8.8) for wet and dry seasons respectively. Based on KR, 57.3 % of the water from the wet season is suitable for irrigation while 42.7 % remain unsuitable. 42.5 % of dry season water samples are suitable while 57.5 % (Table 8.9) is unsuitable for such agricultural use.

Permeability Index (PI)

Irrigation of soil with water containing Na^{+}, Ca^{2+}, Mg^{2+} and $HCO3^{-}$ for a long time, the soil permeability starts to decline due to reaction of the irrigation water with

the content of the soil. The can affect soil hydraulic characteristics, and soil aeration leads to poor support for plant and growth and hinder the crop yield (Li et al., 2016). Relationship between these ions and possible impact measure was developed by Donnen (1964) as a criterion for assessing the suitability of water for irrigation in term of permeability index(PI). This equation is shown below, where all ions are expressed in meq/l.

$$PI = (Na^{+} + \sqrt{HCO3}) * 100/(Ca^{2+} + Mg^{2+} + Na^{+}) \text{ ----------(10)}$$

PI values range from 50.6 to 663.8 and 5.8 to 136.5 with an average value of 149.4 and 39.7, respectively (Table 8.8) for wet and dry seasons. Based on the PI, irrigation water is classified into excellent (PI > 75), acceptable (75 < PI > 25) and poor (PI < 25). In this study, 89 (92,7 %) and 7 (7.3 %) water samples from the wet season fell under excellent and acceptable categories while none is unsuitable for irrigation. 120 (89.6 %) and 14 (10.4 % (Table 8.9) of the dry season water samples fell under excellent and acceptable categories while none of the samples is unsuitable for irrigation purpose.

Magnesium Ratio (MR)

Generally, Ca^{2+} and Mg^{2+} occur and maintain a state of equilibrium in most groundwater. In the state of this equilibrium, excess Mg^{2+} in groundwater results is called magnesium hazard, which has an adverse effect on the soil quality by increasing its alkalinity. High alkalinity in the soil leads to a decrease in the yield of a crop by plants. MR values are expressed in meq/l. MR is calculated using the equation below, while Table 8 presents the result of the calculated MR from the results of the analysed water sample for wet and dry seasons in the study location.

$$MR = (Mg^{2+}) * 100/(Ca^{2+} + Mg^{2+})$$ ----------(11)

Magnesium ratio (MR) values greater than 50 in groundwater is considered a hazard to plant, which is unsuitable for irrigation (Adimalla and Kumar, 2020). Only magnesium ration values less than 50 is considered suitable for irrigation. In this study, the values of MR range from 7.7 to 728.4 and 6.5 to 84.7 with averages values of 66.8 and 35.1 (Table 8.8) for groundwater samples in wet and dry seasons, respectively. Based on MR, 43 (44.8 %) of groundwater in wet season fell under suitable class while 53 (55.2 %) are unsuitable for irrigation purpose. 113 (84.3 %) and 21 (15.7 %) (Table 8.9) of groundwater sample in the dry season fell under suitable and unsuitable respectively for irrigation purpose. The overall results show that dry season water samples from the eastern Dahomey basin show better quality for irrigation purpose based on Magnesium ratio.

Total hardness (TH)

The sum of the concentration of calcium and magnesium is directly equivalent to what is called water hardness. Because of the interaction of rock/soil minerals and groundwater, hardness in water is commonly associated with water, especially areas underlain with carbonates rocks. In this regards, the surface is generally soft when compared to groundwater. Desirable limit of hardness in drinking water, as stated by WHO (2006) guideline for drinking water is 300 mg/l. High TH in water could lead to waste of soap, scale in the pipes causing the blockage, it can also lead to health complication causing kidney stones (Adimalla and Kumar, 2020).

In analysed sampled groundwater from Eastern Dahomey Basin in wet and dry seasons, TH values range from 0.9 to 6580 mg/l and 0.0 to 5596 mg/l with average values of 116.7 and 118.2 mg/l (Table 8.10) for wet and dry seasons respectively.

Table 8.8 Statistical Summary of the selected indices for Irrigation purpose

	Min	**Max**	**Aver**	**Stdev**	**Min**	**Max**	**Aver**	**Stdev**
Indices	Wet Season N = 96				Dry Season N = 134			
SAR	0.0	16.7	0.5	1.7	0.0	17.3	0.6	1.5
TH	0.9	6580.7	116.7	671.1	0.0	5596.0	118.2	526.7
Na%	8.2	86.9	49.5	16.6	36.8	96.8	67.2	14.9
KR	0.1	6.6	1.1	0.9	0.1	3.5	0.7	0.3
PI	50.6	663.8	149.4	84.7	5.8	136.5	39.7	9.6
RSC	-1.8	0.0	0.0	0.2	-9988.6	110.1	-333.5	988.3
MR	7.7	728.4	66.8	79.3	6.5	84.7	35.1	15.3
CAI-I	-104.1	534.4	3.5	55.8	-99.4	35.4	-1.7	9.3
CAI-II	-6.1	534.2	5.1	54.6	-3.1	35.2	0.1	3.3

According to classification by Sawyer and McCarty as presented in Table 8.10. TH in water is classified by concentration are: <75 mg/L as calcium carbonate is classified as soft water; 75 to 150 mg/L as moderately hard water; 150 to 300 mg/L as hard water; and values greater than 300 mg/L as very hard water. 78 (82.5 %), 10 (10.1 %) of water samples in the wet season fell in soft and moderately hard respectively while 4 (4.2 %) each which comprises water samples from locations L20, L68, L70 and L8, and locations L05, L36, L72 and L77 fell in hard and very hard water respectively. 79.9% and 7.7 % of samples from the dry season classified as soft and moderately hard respectively while 8 (6 %) and 9 (6.7 %) samples from locations (L90, L82, L10, L88, L91, L80, L93 and L85) and locations (L83, L92, L02, L03, L20, L21, L94, L43 and L34) fell in hard and very hard class of water hardness. Figure 8.10 (c, d) present spatial distribution of the Total hardness of the sampled water for both seasons. The map showed that hard water occurs in the west centre of the study location are over Ilaro / Ewekoro formation and alluvium deposit which could be due to weathering of carbonate rock within this geological unit.

Sodium absorption ratio (SAR) plots of the analysed groundwater samples

The high salt concentration is known to cause an increase in soil salinity which could lead to saline soil and when soil is saturated with saline water could lead to a reduction in its infiltration and aeration (Adimalla, 2019a; Minhas et al., 2020). In this study, based on SAR value, the classification of water samples in the study area for both wet and dry seasons is presented in Table 8.8).

Table 8.9 Analysis of the indices for irrigation on the groundwater for wet and dry seasons

Indices	**Classification**		**Wet Season**		**Dry Season**	
			No. of Sample	**% Sample**	**No. of Sample**	**% Sample**
SAR	< 6	Suitable	95	99%	133	99.30%
	6 - 9	Unsuitable	Nil	0%	Nil	0%
	>9	Unfit	1	1%	1	0.7%
% Na	<20	Excellent	8	8.3%	9	6.7%
	20 - 40	Good	18	18.8%	16	11.9%
	40-60	Permissible	42	43.8%	47	35.1%
	60-80	Doubtful	27	28.1%	56	41.8%
	>80	Unsuitable	1	1.0%	6	4.5%
RSC	1.25	Good	96	100%	134	100%
	1.25-2.2.50	Doubtful	0	0%	0	0%
	2.5	Unfit	0	0%	0	0%
KR	<1	Suitable	55	57.3%	57	42.5%
	>1	Unsuitable	41	42.7%	77	57.5%
PI%	>75	Excellent	89	92.7%	120	89.6%
	75-25	Acceptable	7	7.3%	14	10.4%
	<25	Poor	0	0%	0	0%
MR	<50	Suitable	43	44.8%	113	84.3%
	>50	Unsuitable	53	55.2%	21	15.7%

99% of 99 wet season water samples are suitable based on SAR while only 1 % unfit for irrigation purpose. 99.3 % of 134 water samples in the dry season are suitable for irrigation purpose while the remaining 0.7 % is unfit. For further

clarification, sodium absorption ratio (SAR) USSL (Figure 8.11) and Wilcox salinity diagram (Figure 8.12) were employed in order to assess the sodium hazard of water as regards the irrigation usability of the groundwater sample.

The USSL diagram presents, the classification in a graphical form which is in agreement with the evaluation shown in Table 8.9 with only one location in both seasons revealed unfit groundwater sample for irrigation purpose based on SAR. The salinity hazard in groundwater of the Eastern Dahomey basin is generally low based on Wilcox and salinity diagram.

Table 8.10 Classification of Total Hardness for wet and dry season

TH (mg/l)	**Classification**	**Wet Season**	**Dry Season**
0 - 75	Soft	78	107
75 - 150	Moderately Hard	10	10
		4 (L68, L20, L81 and L70)	8 (L90, L82, L10, L88, L91, L80, L93 and L85)
150 - 300	Hard		
>300	Very Hard	4 (L72, L05, L77 and L36)	9 (L83, L92, L02, L03, L20, L21, L94, L43 and L34)

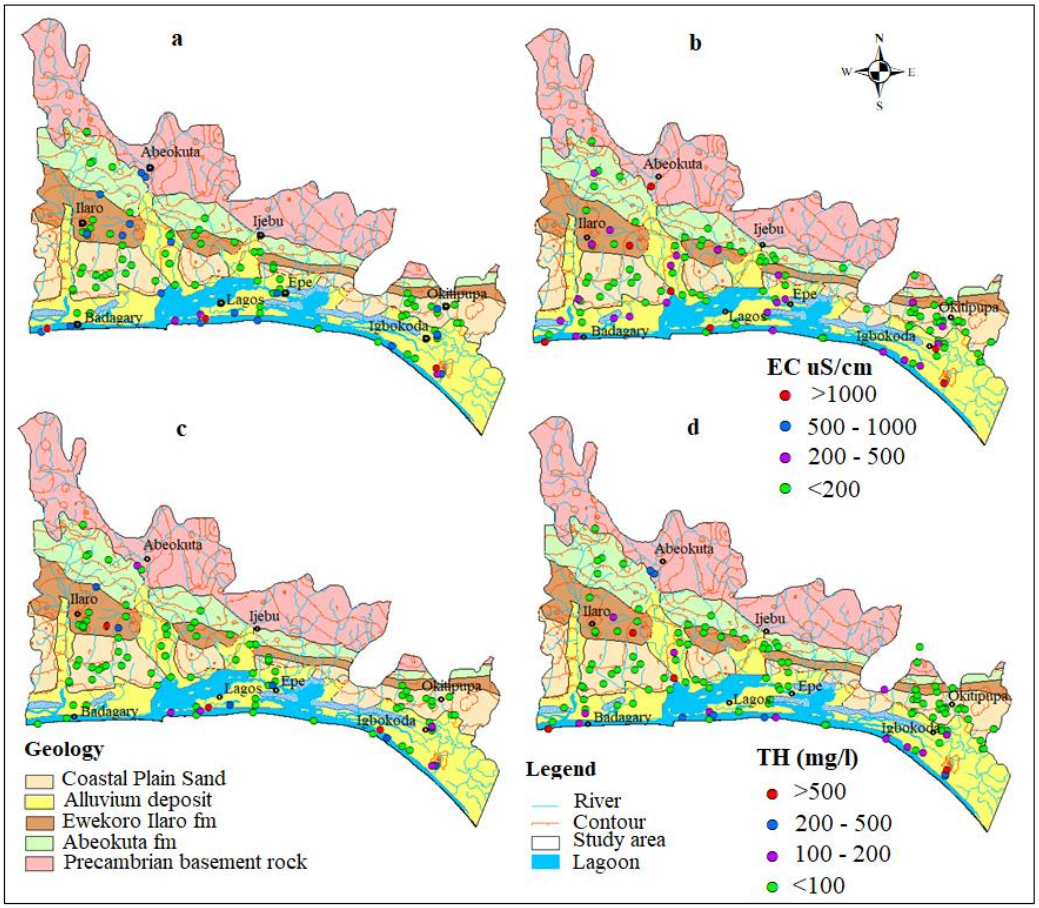

Figure 8.10 Spatial distribution of major Cations in Eastern Dahomey Basin (a) EC for wet season (b) EC dry season (c) TH for wet season (d) TH for dry season

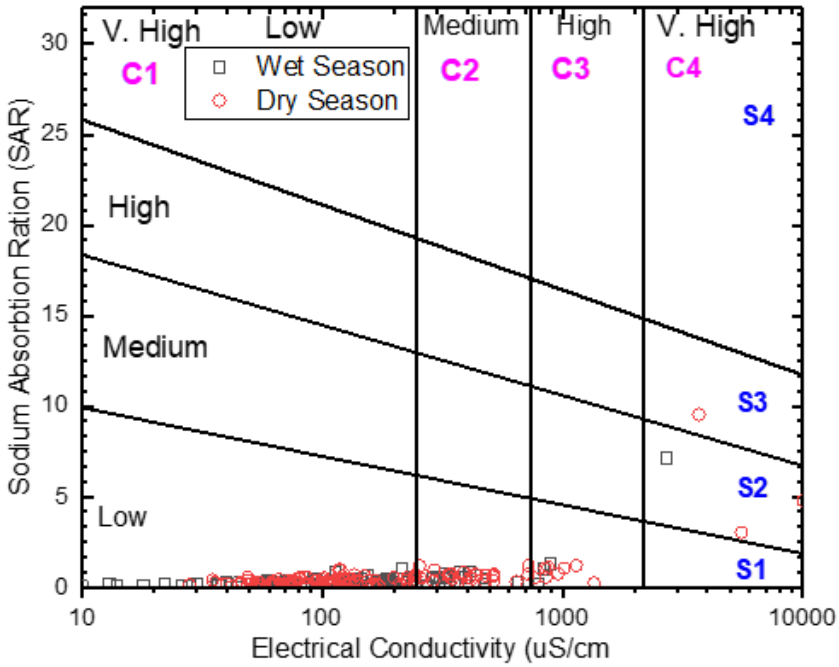

Figure 8.11 USSL diagram for classification of water for irrigation purpose

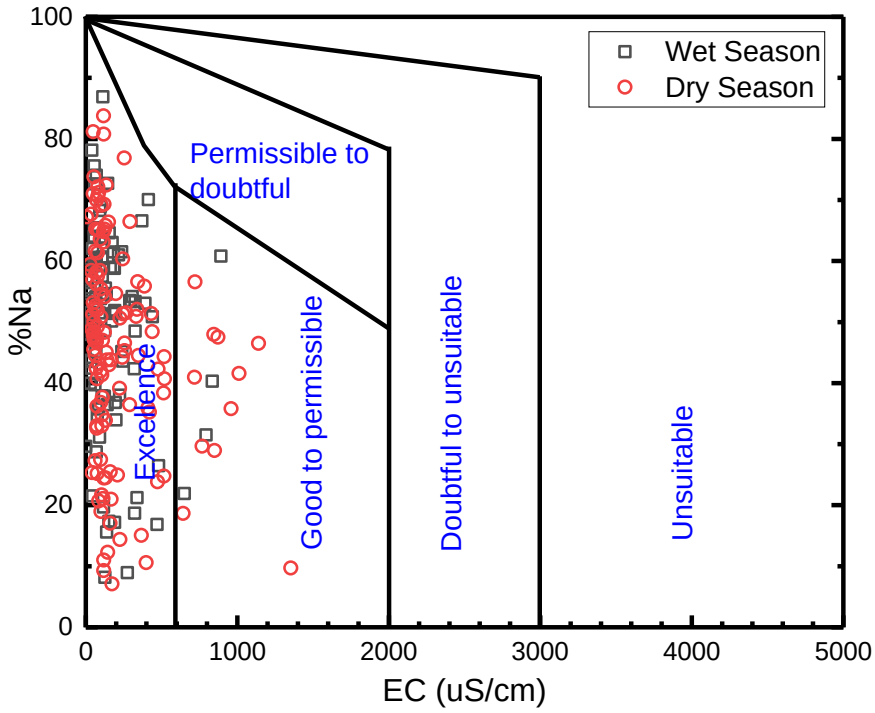

Figure 8.12 Wilcox (1995) diagram for classification groundwater based on EC and Na%

8.2.4.6 Groundwater Quality Index (GWQI)

Groundwater quality Index method is a unified way for assessment and monitoring groundwater quality by bringing together, all the crucial groundwater quality parameters which are most peculiar to a particular location (Krishna Kumar et al., 2014; Singh et al., 2011; Tirkey et al., 2017; Verma et al., 2020). Results of the evaluated GWQI carried out on groundwater samples from wet and dry seasons, as explained in the methodology section is presented in Table 8.11. The calculated GWQI ranges from 4.28 to 1505.36 with an average of 68.66 for the wet season groundwater samples and 4.92 to 3010.07 with an average value of 100.16 for the dry season water samples. The summary of the results of Index classification is presented in Table 8.11. Based on water quality index calculation, for the wet season water samples, 44.8 % fall in Excellent, 22.9 % fall in good, 12.5 % fall in moderate while 8.3, 1.0 and 10.4 % fall under poor, very poor and None potable class. For the dry season GWQI classification, 1.45, 51.5 and 19.4 falls under Excellent, good and moderate class respectively while Poor, very poor and none potable class have 9.7, 4.5 and 13.4 % of water samples respectively. Spatial distribution of the calculated GWQI of groundwater samples for both wet and dry seasons are presented in Figure 8.15. The map of revealed fewer unfit water in locations west centre and southern part of the study location in the wet season while more poor, very poor and unfit water samples are distributed in the west centre and southern part along the coastline of the eastern Dahomey basin (Figure 14).

8.2.4.7 Analysis and description of the land use map of Eastern Dahomey Basin

Landuse map of the Eastern Dahomey Basin, as presented in Figure 14 shows where Agriculture, plantation, Agriculture in shallow and recession, cropland and fallow with oil palm and forest covers 4,567 Km^2. These generally cover the northern

part through the centre of the study area through areas along the flood plain and river channel are cultivated in the southern part, especially for vegetables. The Bare soil covers 2161 $Km^{2,}$ which is common in the northwestern and in few places in the north-eastern part. 4813 Km^2 part of the area is covered by wetland and swamp which dominated the southern parts. Water bodies cover 13688 Km^2 which is the most extensive areas due to lagoon and rivers while settlement in terms of villages, town and cities, which is the second largest area covered 8780 km^2 of the area.

Table 8.11 GWQI rating for both wet and dry seasons

Class	Category	Range	No of Sample	% Sample
Wet Season				
Class 1	Excellent		43	44.8
Class 2	Good		22	22.9
Class 3	Moderate		12	12.5
Class 4	Poor		8	8.3
Class 5	Very Poor		1	1.0
Class 6	None Potable		10	10.4
Dry Season				
Class 1	Excellent		2	1.45
Class 2	Good		69	51.5
Class 3	Moderate		26	19.4
Class 4	Poor		13	9.7
Class 5	Very Poor		6	4.5
Class 6	None Potable		18	13.4

8.2.4.7.1 Correlation of GWQI and Land use pattern maps of Eastern Dahomey Basin

Urbanisation has been listed as one of the major sources of anthropogenic impact on groundwater quality, especially in the shallow coastal aquifers. Many researchers have established a possible impact of urbanisation on groundwater quality across developing countries around Asia and Africa. This occurrence necessitates the correlation of the calculated GWQI spatial distribution map to the Landuse of the Eastern Dahomey Basin. The correlation is presented in Figure 8.13, which show areas

with poor, very poor and unfit groundwater are generally situated within the settlement, agriculture and along the flood plains area of the landuse map. This distribution revealed the impact of urbanisation through indiscriminate waste disposal, with unregulated industrial, municipal and agricultural waste that leached down into the surface and ended up in shallow groundwater (Aladejana et, 2020).

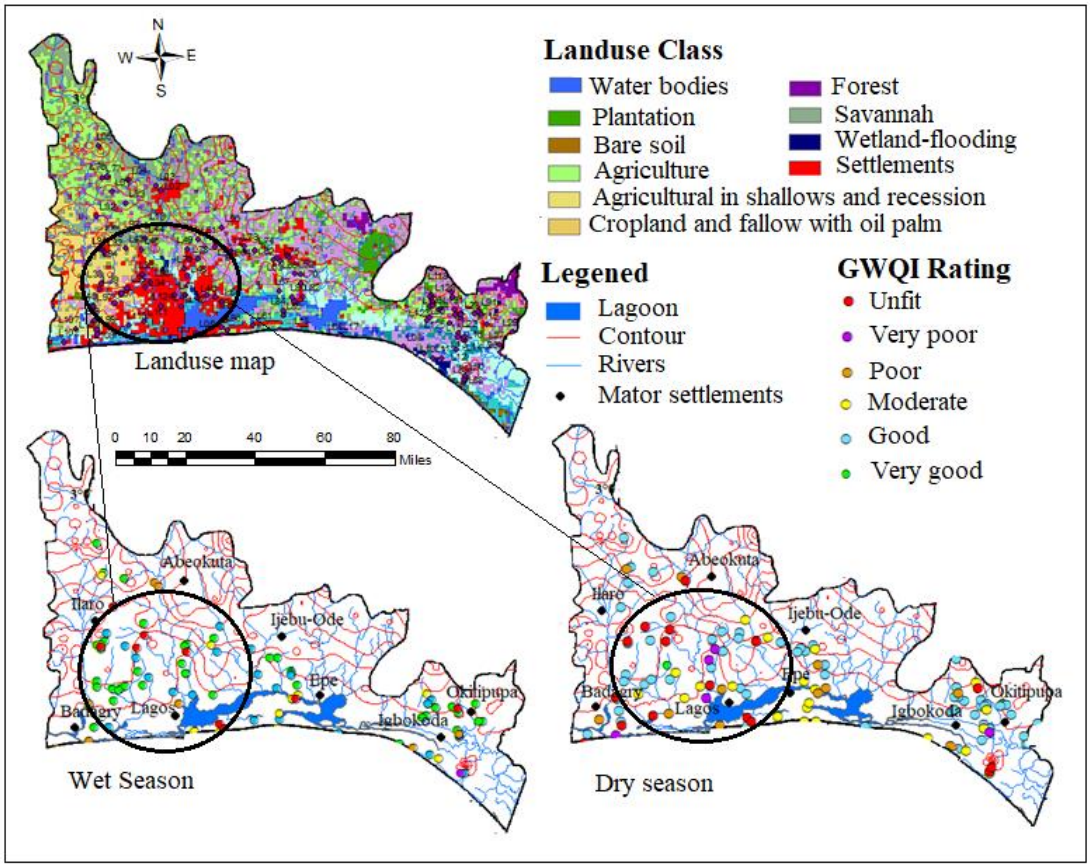

Figure 8.13 Maps showing land use pattern and Groundwater Quality Index (GWQI) of the Eastern Dahomey Basin

8.2.4.8 The implication for integrated water resources management in Nigeria

Nigeria water resources management policy was reviewed in the year 2014 to bring it in-line with the global best practice of Integrated Water Resource Management (IWRM) (JICA, 2014). The structural framework constitutes different action plans

such as water safety plan (WSP), Hydrological Areas, among many others. The National Water Resource Institute (NWRI) was established with other inter-agencies to create a framework for national water resource management, with the mandate of providing safe and sustainable drinking water to all.

The implementation of these new policies has been facing challenges. These challenges include lack of enforcement, inconsistent interpretation of policies, absence of local inclusion, inadequate funding, lack of transparent management practice, weak political commitment, among others (Akpabio, 2007; Jideonwo, 2014; Omole, 2013). The rapid transformation in the agricultural (for food security) and industrial sector, as well as urbanisation in the coastal areas of Nigeria, requires a proper education and data in information on which policy enforcement can be implemented to protect groundwater resource. The findings of this study provide a basis for interpreting the impacts of land use pattern and changes on IWRM, informing policy implementation. Groundwater contamination from urban settlements, agricultural and industrial waste within Eastern Dahomey Basins are evidence of impact from unregulated waste disposal practice on the shallow groundwater aquifers. Results of water quality index assessment in this study show a high concentration of Nitrates beyond the highest permissible limit of WHO standards (WHO, 2006) for drinking water, that confirms agricultural and municipal waste impacts. This deterioration in groundwater quality is a justification for a review of the implementation of policy, in particular as the country sets targets for SDG6.

The trend identified in this study shows that IWRM of the eastern Dahomey Basin requires renewed inclusive strategies in order to achieve sustainable groundwater management. Modern waste recycling plant "waste to wealth" could be employed for waste management. Such an incentive-driven approach to waste

management could be employed to encourage local motivation and commitment to waste collection, promoting a cleaner environment and empowering communities while reducing poverty. Management of fertilisers in farming, especially along flood plains and wetland in the study area, should be encouraged to reduce contamination of surface and groundwater with nitrate, pesticides and herbicides. Finally, enforcement of IWRM policies should be supported.

8.2.5 Conclusion

Early detection of pollution and contamination, which adversely affect groundwater quality is critical for ensuring safe drinking water for proper sanitation and hygiene. Groundwater is needed to meet water demands in most developing countries around the world as an alternative to pipe-borne water, and this study showed that deterioration in groundwater quality is a risk in the EDB. Land-use was found to have an adverse effect on groundwater quality, especially in shallow coastal aquifers where the water level is relatively high. In this study, a combination of Groundwater quality index GWQI and land use pattern map has demonstrated effectiveness tracking groundwater quality.

The hydrochemical analysis showed that ion exchange (Ca/Na) occurs in the study area with the exception of locations underlain by Ewekoro and Ilaro carbonates rock units. PCA and Cluster analysis indicates water-rock reactions primarily control hydrochemical results with variance of 59.2% and 63.1% for PC1 on wet and dry seasons water samples, with anthropogenic (component 2 and 3) playing an integral part with variance of 11.2% and 10.7% (PC2), 8.9% and 10.1%(PC3) for wet and dry seasons water samples. Assessing water quality for irrigation revealed some samples with doubtful and unsuitable quality based on percentage sodium (%Na), Kelly's ratio

(KR), magnesium ratio (MR) and total hardness. The GWQI results revealed 44.8%, 22.9% and 12.5% of water samples during the wet season fell in the class of excellent, kind and moderate-quality respectively, while 8.3%, 1.0% and 10.4% fell in a class of poor, very poor and none potable water quality. For the dry season groundwater samples revealed excellent, excellent and moderate water quality class account for 1.45%, 51.5% and 19.4% samples respectively while poor, very poor and none potable water quality account for 9.7%, 4.5% and 13.4% respectively.

Correlating the spatial distribution map of the GWQI for both seasons with the land use pattern map of the area revealed poor to none potable water clustered more in the settlement, agricultural area and along flood plains where planting is taking place throughout the year. This distribution signifies the groundwater water quality has been impacted by municipal, industrial and agricultural waste within the EDB. The finding revealed how inappropriate waste disposal system and poor agricultural practice are having an adverse effect on groundwater quality. Access to reliable potable water is crucial to achieving many of SDG goals. The study suggests the need for proper waste and agricultural management policy review and enforcement towards sustainable water resource management to ensure Nigeria can meet its targets for SDG6.

8.2.6 References

Aboyeji, O.S., Ogunkoya, O.O., 2015. Assessment of Groundwater Quality of Selected Inland Valley Agro-ecosystems for Irrigation in Southwest Nigeria. Environ. Res. Eng. Manag. 71, 5–15.

Addison, M.J., Rivett, M.O., Robinson, H., Fraser, A., Miller, A.M., Phiri, P., Mleta, P., Kalin, R.M., 2020. Fluoride occurrence in the lower East African Rift System, Southern Malawi. Sci. Total Environ. 712, 1–16. https://doi.org/10.1016/j.scitotenv.2019.136260

Adegoke, O.S. and Omatsola, M.E., 1981. Tectonic Evolution and Cretaceous Stratigraphy of the Dahomey Basin. Niger. J. Min. Geol. 18, 130–137.

Adimalla, N., 2019a. Controlling factors and mechanism of groundwater quality variation in semiarid region of South India: an approach of water quality index (WQI) and health risk assessment (HRA). Environ. Geochem. Health 18–19. https://doi.org/10.1007/s10653-019-00374-8

Adimalla, N., 2019b. Controlling factors and mechanism of groundwater quality variation in semiarid region of South India: an approach of water quality index (WQI) and health risk assessment (HRA). Environ. Geochem. Health 8. https://doi.org/10.1007/s10653-019-00374-8

Adimalla, N., Kumar, A., 2020. Hydrogeochemical investigation of groundwater quality in the hard rock terrain of South India using Geographic Information System (GIS) and groundwater quality index (GWQI) techniques. Groundw. Sustain. Dev. 10.

Aiuppa, A., Bellomo, S., Brusca, L., D'Alessandro, W., Federico, C., 2003. Natural and anthropogenic factors affecting groundwater quality of an active volcano (Mt. Etna, Italy). Appl. Geochemistry 18, 863–882. https://doi.org/10.1016/S0883-2927(02)00182-8

Ako, A., Eyong, G.E.T., Shimada, J., Koike, K., Hosono, T., Ichiyanagi, K., Richard, A.A., Tandia, B.K., Nkeng, G.E., Roger, N.N., 2013. Nitrate contamination of groundwater in two areas of the Cameroon Volcanic Line (Banana Plain and Mount Cameroon area). Appl. Water Sci. 4, 1–15. https://doi.org/10.1007/s13201-013-0134-x

Ako, A.A., Shimada, J., Hosono, T., Ichiyanagi, K., Nkeng, G.E., Eyong, G.E.T., Roger, N.N., 2012. Hydrogeochemical and isotopic characteristics of groundwater in Mbanga, Njombe and Penja (Banana Plain) - Cameroon. J. African Earth Sci. 75, 25–36. https://doi.org/10.1016/j.jafrearsci.2012.06.003

Akpabio, E.M., 2007. Assessing integrated water resources management in Nigeria: Insights and lessons from irrigation projects in the Cross River Basin. Water Policy 9, 149–168. https://doi.org/10.2166/wp.2007.007

Aladejana, J.A., Kalin, R.M., Sentenac, P., Hassan, I., 2020. Assessing the Impact of Climate Change on Groundwater Quality of the Shallow Coastal Aquifer of Eastern Dahomey Basin, Southwestern Nigeria. Water 12, 224. https://doi.org/10.3390/w12010224

Alcaine, A.A., Schulz, C., Bundschuh, J., Jacks, G., Thunvik, R., Gustafsson, J.-P., Mörth, C.-M., Sracek, O., Ahmad, A., Bhattacharya, P., 2020. Hydrogeochemical controls on the mobility of arsenic, fluoride and other geogenic co-contaminants in the shallow aquifers of northeastern La Pampa Province in Argentina. Sci. Total Environ. 715, 136671. https://doi.org/10.1016/j.scitotenv.2020.136671

Appelo, C.A.J., Postma, D., 2005. Groundwater, Geochemistry, and Pollution.

Arulbalaji, P., Gurugnanam, B., 2017. Groundwater quality assessment using geospatial and statistical tools in Salem District, Tamil Nadu, India. Appl. Water Sci. 7, 2737–2751. https://doi.org/10.1007/s13201-016-0501-5

Babanyara, Y.Y., Usman, H.A., Saleh, U.F., 2010. An Overview of Urban Poverty and Environmental Problems in Nigeria. J. Hum. Ecol. 31, 135–143.

Biswas, A.K., Tortajada, C., 2019. Water quality management: a globally neglected issue. Int. J. Water Resour. Dev. 35, 913–916. https://doi.org/10.1080/07900627.2019.1670506

Bodrud-Doza, M., Bhuiyan, M.A.H., Islam, S.M.D.U., Rahman, M.S., Haque, M.M., Fatema, K.J., Ahmed, N., Rakib, M.A., Rahman, M.A., 2019. Hydrogeochemical investigation of groundwater in Dhaka City of Bangladesh using GIS and multivariate statistical techniques. Groundw. Sustain. Dev. https://doi.org/10.1016/j.gsd.2018.11.008

Brunt, R., Vasak, L., Griffioen, J., 2004. Fluoride in groundwater: Probability of occurrence of excessive concentration on global scale. Int. Groundw. Resour. Accessment Centre, UNESCO. Report nr., 20p. https://doi.org/10.1016/j.apgeochem.2003.09.004

Dar, M.A., Sankar, K., Dar, I.A., 2011. Fluorine contamination in groundwater: A major challenge. Environ. Monit. Assess. 173, 955–968. https://doi.org/10.1007/s10661-010-1437-0

Hashmi, M.Z., Yu, C., Shen, H., Duan, D., 2014. Concentrations and Human Health Risk Assessment of Selected Heavy Metals in Surface Water of the Siling Reservoir Watershed in Zhejiang Province , China. Pol. J. Environ. Stud. 23, 801–811.

Horton K. R., 1965. An index number system for rating water quality. J. Water Pollut. Control Fed 37, 300–306.

Jahangir, M.M.R., Johnston, P., Khalil, M.I., Richards, K.G., 2012. Linking hydrogeochemistry to nitrate abundance in groundwater in agricultural settings in Ireland. J. Hydrol. 448–449, 212–222. https://doi.org/10.1016/j.jhydrol.2012.04.054

JICA, 2014. Federal Republic of Nigeria the Project for Review and Update of Nigeria National Water Resources. Abuja.

Jideonwo, J.A., 2014. Ensuring Sustainable Water Supply in Lagos , Nigeria. University of Pennyslyvania.

Jones, H. A and Hockey, R.., 1964. The Geology of part of Southwestern Nigeria. GSN Bull. No. 31-10.

Kashaigili, J.J., 2012. Ground water Availability and Use in Sub-Saharan Africa, Groundwater availability and use in Sub-Saharan Africa: A review of 15 countries. https://doi.org/10.5337/2012.213

Krishna Kumar, S., Bharani, R., Magesh, N.S., Godson, P.S., Chandrasekar, N., 2014. Hydrogeochemistry and groundwater quality appraisal of part of south Chennai coastal aquifers, Tamil Nadu, India using WQI and fuzzy logic method. Appl. Water Sci. 341–350. https://doi.org/10.1007/s13201-013-0148-4

Kumar, K.S., Kumar, P.S., BABU, M.J.R., RAO, C.H., 2010. Assessment and Mapping of Ground Water Quality Using Geographical Information Systems. Int. J. Eng. Sci. Technol. 2, 6035–6046.

Kumar, P., Singh, C.K., Saraswat, C., Mishra, B., Sharma, T., 2017. Evaluation of aqueous

geochemistry of fluoride enriched groundwater: A case study of the Patan district, Gujarat, Western India. Water Sci. 31, 215–229. https://doi.org/10.1016/j.wsj.2017.05.002

Lapworth, D.J., Krishan, G., MacDonald, A.M., Rao, M.S., 2017a. Groundwater quality in the alluvial aquifer system of northwest India: New evidence of the extent of anthropogenic and geogenic contamination. Sci. Total Environ. https://doi.org/10.1016/j.scitotenv.2017.04.223

Lapworth, D.J., Nkhuwa, D.C.W., Okotto-Okotto, J., Pedley, S., Stuart, M.E., Tijani, M.N., Wright, J., 2017b. Urban groundwater quality in sub-Saharan Africa: current status and implications for water security and public health. Hydrogeol. J. 25, 1093–1116. https://doi.org/10.1007/s10040-016-1516-6

Li, W., Wang, M.-Y., Liu, L.-Y., Yan, Y., 2015. Assessment of Long-Term Evolution of Groundwater Hydrochemical Characteristics Using Multiple Approaches: A Case Study in Cangzhou, Northern China. Water 7, 1109–1128. https://doi.org/10.3390/w7031109

Longe, E.O., Balogun, M.R., 2010. Groundwater quality assessment near a municipal landfill, Lagos, Nigeria. Res. J. Appl. Sci. Eng. Technol. 2, 39–44.

Longe, E.O., Malomo, S., Olorunniwo, M.A., 1987. Hydrogeology of Lagos metropolis. J. African Earth Sci. 6, 163–174. https://doi.org/10.1016/0899-5362(87)90058-3

Martins, V.T. d. S., Pino, D.S., Bertolo, R., Hirata, R., Babinski, M., Pacheco, D.F., Rios, A.P., 2018. Who to blame for groundwater fluoride anomaly in São Paulo, Brazil? Hydrogeochemistry and isotopic evidence. Appl. Geochemistry 90, 25–38. https://doi.org/10.1016/j.apgeochem.2017.12.020

Minhas, P.S., Ramos, T.B., Ben-Gal, A., Pereira, L.S., 2020. Coping with salinity in irrigated agriculture: Crop evapotranspiration and water management issues. Agric. Water Manag. https://doi.org/10.1016/j.agwat.2019.105832

Morari, F., Lugato, E., Polese, R., Berti, A., Giardini, L., 2012. Nitrate concentrations in groundwater under contrasting agricultural management practices in the low plains of Italy. Agric. Ecosyst. Environ. 147, 47–56. https://doi.org/10.1016/j.agee.2011.03.001

Morell, I., Giménez, E., Esteller, M. V., 1996. Application of principal components analysis to the study of salinization on the Castellon Plain (Spain). Sci. Total Environ. 177, 161–171. https://doi.org/10.1016/0048-9697(95)04893-6

Narany, T.S., Ramli, M.F., Aris, A.Z., Nor, W., Sulaiman, A., Juahir, H., Fakharian, K., 2014. Identification of the Hydrogeochemical Processes in Groundwater Using Classic Integrated Geochemical Methods and Geostatistical Techniques , in Amol-Babol Plain , Iran. Sci. World J. 2014, 1–15.

Oke, S.A., 2015. Evaluation of the Vulnerability of Selected Aquifer Systems in the Eastern Dahomey Basin , South Western Nigeria.

Oke, S.A., Vermeulen, D., Gomo, M., 2016. Aquifer vulnerability assessment of the Dahomey Basin using the RTt method. Environ. Earth Sci. 75, 1–9.

https://doi.org/10.1007/s12665-016-5792-1

Olabode, S.O., Mohammed, M.Z., 2016. Depositional Facies and Sequence 2016, 210–228.

Oloruntola, M.O., Adeyemi, G.O., Bayewu, O., Obasaju, D.O., 2019. Hydro-geophysical mapping of occurrences and lateral continuity of aquifers in coastal and landward parts of Ikorodu, Lagos, Southwestern Nigeria. Int. J. Energy Water Resour. 3, 219–231. https://doi.org/10.1007/s42108-019-00026-8

Omole, D.O., 2013. Sustainable Groundwater Exploitation in Nigeria. J. Water Resour. Ocean Sci. 2, 9. https://doi.org/10.11648/j.wros.20130202.11

Oteri, A.U., & Atolagbe, F.P., 2003. Saltwater Intrusion into Coastal Aquifers in Nigeria, in: The Second International Conference on Saltwater Intrusion and Coastal Aquifers — Monitoring, Modeling, and Management. Mérida, Yucatán, México, March 30 - April 2, 2003. Merida Yucatan, pp. 1–15.

Paris, G., Gaillardet, J., Louvat, P., 2010. Geological evolution of seawater boron isotopic composition recorded in evaporites. Geology 38, 1035–1038. https://doi.org/10.1130/G31321.1

Pfeiffer, M., Batbayar, G., Hahn-tomer, D.K.S., 2015. Investigating arsenic (As) occurrence and sources in ground , surface , waste and drinking water in northern Mongolia. Environ. Earth Sci. 73, 649–662. https://doi.org/10.1007/s12665-013-3029-0

Re, V., Cissé Faye, S., Faye, A., Faye, S., Gaye, C.B., Sacchi, E., Zuppi, G.M., 2011. Water quality decline in coastal aquifers under anthropic pressure: The case of a suburban area of Dakar (Senegal). Environ. Monit. Assess. 172, 605–622. https://doi.org/10.1007/s10661-010-1359-x

Schullehner, J., Hansen, B., Thygesen, M., Pedersen, C.B., Sigsgaard, T., 2018. Nitrate in drinking water and colorectal cancer risk: A nationwide population-based cohort study. Int. J. Cancer 143, 73–79. https://doi.org/10.1002/ijc.31306

Senthilkumar, S., Gowtham, B., Sundararajan, M., Chidambaram, S., Lawrence, J.F., Prasanna, M. V, 2018. Impact of landuse on the groundwater quality along coastal aquifer of Thiruvallur district , South India. Sustain. Water Resour. Manag. 4, 849–873. https://doi.org/10.1007/s40899-017-0180-x

Shah, K.A., Joshi, G.S., 2017. Evaluation of water quality index for River Sabarmati, Gujarat, India. Appl. Water Sci. 7, 1349–1358. https://doi.org/10.1007/s13201-015-0318-7

Shi, X., Wang, Y., Jiao, J.J., Zhong, J., Wen, H., Dong, R., 2018. Assessing major factors affecting shallow groundwater geochemical evolution in a highly urbanized coastal area of Shenzhen City, China. J. Geochemical Explor. 184, 17–27. https://doi.org/10.1016/j.gexplo.2017.10.003

Singh, C.K., Shashtri, S., Mukherjee, S., Kumari, R., Avatar, R., Singh, A., Singh, R.P., 2011. Application of GWQI to Assess Effect of Land Use Change on Groundwater Quality in Lower Shiwaliks of Punjab: Remote Sensing and GIS Based Approach.

Water Resour. Manag. 25, 1881–1898. https://doi.org/10.1007/s11269-011-9779-0

Sudheer Kumar, M., Dhakate, R., Yadagiri, G., Srinivasa Reddy, K., 2017. Principal component and multivariate statistical approach for evaluation of hydrochemical characterization of fluoride-rich groundwater of Shaslar Vagu watershed, Nalgonda District, India. Arab. J. Geosci. 10. https://doi.org/10.1007/s12517-017-2863-x

Tirkey, P., Bhattacharya, T., Chakraborty, S., Baraik, S., 2017. Assessment of groundwater quality and associated health risks: A case study of Ranchi city, Jharkhand, India. Groundw. Sustain. Dev. https://doi.org/10.1016/j.gsd.2017.05.002

Verma, P., Singh, P.K., Sinha, R.R., Tiwari, A.K., 2020. Assessment of groundwater quality status by using water quality index (WQI) and geographic information system (GIS) approaches: a case study of the Bokaro district, India. Appl. Water Sci. 10, 1–16. https://doi.org/10.1007/s13201-019-1088-4

8.3 Paper 6

Aladejana, Jamiu A., Kalin, R.M., Sentenac, P., Hassan, I., 2020. Assessing the Impact of Climate Change on Groundwater Quality of the Shallow Coastal Aquifer of Eastern Dahomey Basin, Southwestern Nigeria. MDPI; Water (Switzerland), 12(224). https://doi.org/10.3390/w12010224 [Open access]

Assessing the Impact of Climate Change on Groundwater Quality of the Shallow Coastal Aquifer of Eastern Dahomey Basin, Southwestern Nigeria

Jamiu A. Aladejana [1,2,*], Robert M. Kalin [1], Philippe Sentenac [1], and Ibrahim Hassan [1,3]

1 *Department of Civil and Environmental Engineering, University of Strathclyde, Glasgow* [2]
2 *Department of Geology, University of Ibadan, Ibadan, Nigeria*
3 *Department of Civil Engineering, Abubakar Tafawa Balewa University, Bauchi, Nigeria*
***** *Correspondence: jamiu.aladejana@strath.ac.uk; Tel.: +44-7717-651-171*

Received: 22 November 2019; Accepted: 10 January 2020; Published: 13 January 2020

8.3.1 Abstract

Despite the increasing interest in climate change and water security, research linking climate change and groundwater quality is still at an early stage. This study explores the seasonal effect of the change in biogeochemical process for the redox-sensitive ions and metals Fe^{2+}, Mn^{2+}, SO_4^{2-}, and NO_3^- to assess the groundwater quality of the shallow coastal aquifer of Eastern Dahomey Basin in southwestern Nigeria. Field physicochemical measurement of EC, pH TDS, Eh, salinity, temperature, and the static water level (SWL) was carried out on 250 shallow wells; 230 water samples were collected for analysis between June 2017 and April 2018. A spatial distribution map of these ions and metals showed an increasing concentration in the dry season water samples compared to those of the wet season. This higher concentration could be attributed to change in the intensity of hydrochemical processes such as evaporation, redox, and mineral precipitation. Results of linear regression modelling established significant relationships between SWL, SO_4^{2-}, NO_3^-, Fe, and Eh for both wet and dry seasons with the *p*-value falling between 75% and 95%, which can also be seen in the

plots of Eh/ORP against Fe^{2+}, Mn^{2+}, SO_4^{2-}, and NO_3^-. These results revealed the influence of the redox process for both seasons, while also having a higher impact in the dry season while variation of concentration revealed decrease with increase in depth, which could be attributed to a decrease in well hydraulic properties and aeration. An Eh-pH geochemical diagram revealed NO_3^- as the controlling biogeochemical process over Fe in most of the sample wells. Concentrations of NO_3^-, Fe, and Mn are above the World Health Organization's (WHO) standard for drinking water in most water samples. This study has established the link between climate change and groundwater quality in shallow coastal aquifers and suggested the need for strategic groundwater management policy and planning to ameliorate groundwater quality deterioration.

Keywords: biogeochemical processes; coastal aquifer; climate change; redox and metals mobilisation

8.3.2 Introduction

Groundwater remains an important source of freshwater to meet daily water demand, especially in the developing country of sub-Saharan Africa [1–4]. It complements the water supply shortage experienced as a result of failed infrastructure. This water source must meet a certain quality standard to ensure safe consumption, based on the physicochemical composition of groundwater controlled by specific hydrochemical processes such as oxidation-reduction, evaporation, precipitation, and dissolution. The chemical composition of groundwater is not restricted to only its source(s), but also by the biogeochemical processes occurring along the groundwater flow path, particularly within the aquifers where freshwater interacts with several other inorganic and organic substances either geogenic or of anthropogenic origin [5–7].

Floods and drought are the common impacts of climate change on water availability [8]. In shallow coastal aquifers, flooding can also impact the quality of groundwater, especially in the unconfined aquifer with porous overburden characterised by high hydraulic conductivities offering little or no attenuation to contaminants coming from polluted surface water from the flooded river and lagoons. Recently, substantial rainfall has triggered seasonal flooding in the coastal area of the Eastern Dahomey basin, and poses a threat to groundwater quality in shallow coastal aquifers [9,10].

Climate change is expected to result in sea level rise, ocean surge [11], and flooding of the coastal plains. This combined with contamination from urbanization and waste disposal, results in a mixture of waste dumped in open refuse sites being carried along river channels [9]. The result is mineralization and nutrient loading in surface water with dissolution, advection, and absorption, eventually percolating into shallow aquifers [12–14]. In most cases, the recharge of floodwater to groundwater takes between a few days to a few weeks, which facilitates biogeochemical activities that result in ion and metal concentrations that could degrade the quality of groundwater. Notably, among these biogeochemical processes are oxidation and reduction, which drive ion and metal precipitation in surface and groundwater. Nutrient loads in surface water are expected to increase during precipitation and redox process with climate-induced flooding [12]. It may also be possible, via field or modelling experiments [12], to assess the impacts of climate change on individual components contributing to eutrophication.

The relationship between climate change and drinking water is casual and complicated. This is due to the climate change-related effects of extreme precipitation,

temperature rise, and waterborne diseases being systematically interrelated with different types of microorganisms, geographical area, season, type of water supply, water source, and watershed characteristics [15] (Figure 8.14). There are substantial knowledge gaps regarding systemic causes and effects with considerable uncertainty about how heavy rainfall, microbial pollution of water supplies, and increased turbidity are interrelated. Recently, several outbreaks of waterborne diseases were attributed to extreme hydrological events in sub-Saharan Africa and other parts of the world [16–19]. This risk is enhanced in the densely populated coastal areas of a developing country like Nigeria, as waste management is a challenge due to indiscriminate dumping of waste from municipal, industrial, and agricultural activities across the cities [9].

The Intergovernmental Panel on Climate Change (IPCC) Fourth Assessment Report failed to capture, in detail, the impacts of climate change on water quality. Researchers have established the impact of climate change-driven flooding on surface water quality, especially in the coastal zones of the world where extreme precipitation occurs [20–24], whereas research in the area of climate change impact on groundwater quality is still in its early stage [18,24]. This is probably due to the invisibility of groundwater and the fact that groundwater quality monitoring data in the study area is rarely conducted. Previous studies [2,4,25,26] have identified elevated concentrations of ions, heavy, and traced metals in groundwater in shallow aquifers of the coastal cities of Nigeria, many of which attributed groundwater contaminations to indiscriminate waste disposal, effluents from sewage, industrial, and agricultural waste.

The study aimed to delineate the possible origin of a high elevated concentration of some ions that could impact the quality of groundwater within this basin, to serve as a fingerprint of the impact of climate change driven flooding on groundwater of the shallow coastal freshwater aquifer of Eastern Dahomey Basin (EDB). Understanding will guide policy for the Sustainable Development Goals (SDGs), management of these resources, and promotion of resilience in the wake of future climate change impacts.

The objectives of this study were to investigate the impacts of climate change through flooding on groundwater quality of the shallow coastal groundwater of the Eastern Dahomey basin, using seasonal redox biogeochemical process of some selected redox-sensitive ions such as Fe, Mn, NO_3, and SO_4. Understanding the possible impacts of this seasonal flooding on the groundwater quality of the freshwater aquifer is critical to the management of this essential resource. Oxidation and reduction processes have been shown to have a significant influence on the hydrochemical status of groundwater by either removal or addition of dissolved material which controls its overall quality [13,27]. This process also controls the solubility and stability of many dominant species in groundwater. Groundwater redox process can be influenced by various factors such as recharge, presence of contaminants, local groundwater flow, and well construction configuration and development, which determines the available electron acceptors [6]. The redox variation within a basin could establish a relationship with the spatial variability of some of these ions which could be linked to the redox condition. As a result of this, groundwater from areas with a similar redox condition will generally exhibit chemical stability for redox, while groundwater from areas with varied redox conditions relating to different controlling factors display various characteristics regarding redox-influenced groundwater chemistry [28].

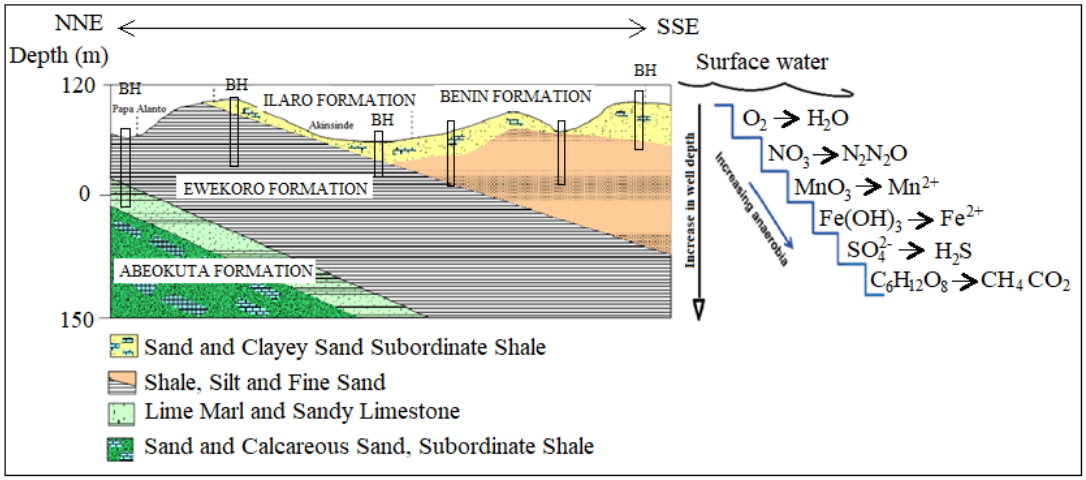

Figure 8.14 Schematic diagram of the biogeochemical process of some selected redox-sensitive ions in a typical coastal aquifer (Modified after [29]).

8.3.3 Description of the Study Area

The Eastern Dahomey Basin (also called Benin or Keta Basin) falls along the western part of Nigeria's south coast (Figure 8.15). It is a transboundary basin that cuts across Ghana, Togo, and Benin to Nigeria. This basin is separated in the east from the Niger Delta basin by Okitipupa Ridge [30]. The basin lies within Latitudes 2°41′10″ N and 4°59′59″ N and Longitudes 6°21′13″ E and 7°52′42″ E along the coast of the Gulf of Guinea. The basin is bounded in the south by the Atlantic Ocean and thin out at the north into the Precambrian basement rocks of south-western Nigeria. The area of investigation towards the south is low lying with several points at or below sea level, which experiences flooding almost annually. The elevation increases towards the northern part with the highest point fall in the location around the city of Abeokuta. This area witnesses two major climatic seasons with a dry period from November to March and the wet season which usually begins around April and ends around October, with a short break in mid-August. Major rivers such as the Ogun, Ose, Oluwa, Oyan, and other smaller river tributaries drain the basin into the delta and the Atlantic Ocean. The basin hosts two major administrative water basins authorities in Nigeria which

include Ogun-Osun and Benin-Owena river basins. It accommodates about 40% of the country's population and underlies one of the most populous cities in Africa along with other large cities, towns, and villages.

8.3.3 Geology and Hydrogeology

8.3.3.1 Geology

The area is part of the Dahomey basin, which extends from Nigeria to Ghana. The lithological character of the sediments is dictated by a southerly transgression and regression of the sea, which has occurred since the Cretaceous period. The stratigraphic description of the sediments has been provided by various authors [30–32]. The Alluvium deposits and coastal plain sands consist of soft, very poorly sorted clayey sands, pebbly sands, sandy clays, and rare thin lignite of Oligocene to recent age [33]. The coastal sands layer is underlain by the Ilaro formation, which consists of massive, yellowish, poorly consolidated, cross-bedded sandstones, which are fine-medium-grained and poorly sorted [32]. The Ilaro formation is followed by the Ewekoro formation, which consists predominantly of Paleocene fossiliferous limestone which becomes arenaceous towards the base [33] and the Abeokuta formation, which consists of lower Cretaceous sandstone and grits with interbedded mudstone unconformity overlying the basement complex fine-grained detrital sandstone, siltstone, and shale overlying the formation in the upperparts. The geology map of the basin is presented in Figure 8.15 with the groundwater sampling points.

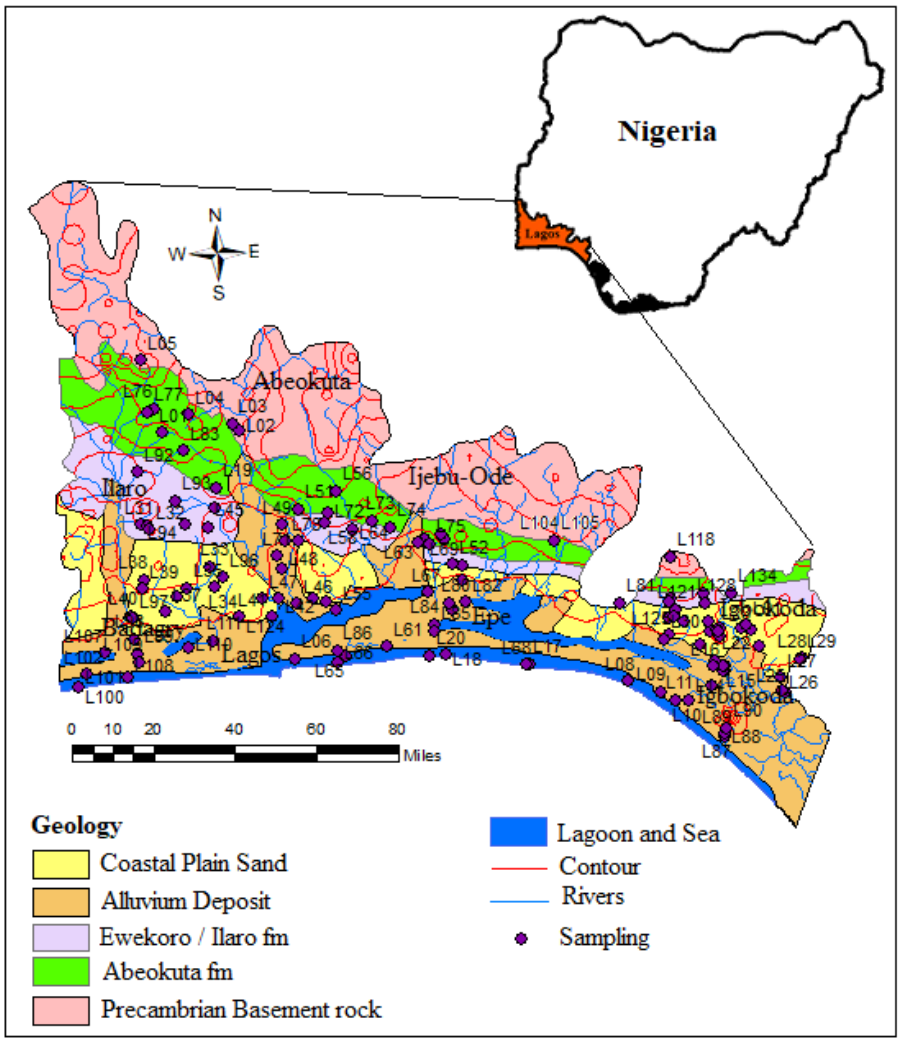

Figure 8.15 Geology map of the Eastern Dahomey basin showing the sampling points.

8.3.3.2. Hydrogeology

Three to four different hydrogeological units have been identified within the Dahomey and Niger Delta Basins. The unconfined alluvial aquifers along the delta line and major rivers (creek lines), shallow coastal plain sands and intercalations of clay, limestone, tar sands, shale, peats, and upper coal measure underlying different locations within the study area defined the layer boundaries because of their relatively low permeability [34–37]. The alternating sequence of low and high permeability layers define the three confined aquifers that define groundwater resources of the study area. The top aquifer is shallow with thickness ranging from 8–45 m. The thickness of

the second aquifer ranges from 10–35 m, while the third aquifer is about 10–35 m with the depth ranging from 150–240 m [29,38]. The fourth aquifer starts from 200 to 250 m below the ground's surface, depending on the locations. Generally, the variation in the aquifer characteristics begins from Abeokuta formation (Figure 8.14) in the North as the lateritic topsoil thins out as it passes through Ilaro, Ewekoro, into Coastal Plain Sand, and Alluvium units towards the sea at the south. Figure 8.16 shows a typical lithological description of the coastal area from a combined X-ray, resistivity logs, and electrical resistivity tomography.

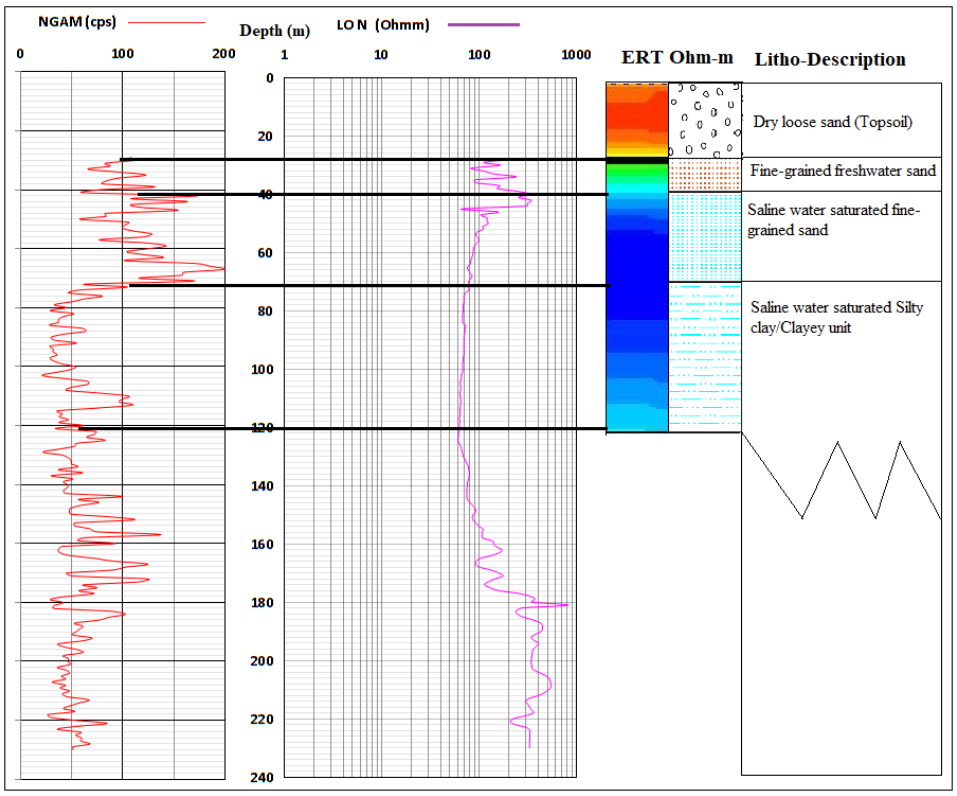

Figure 8.16 A lithological section showing the description of the vadose zone and aquifers of the southwestern coast of Nigeria.

8.3.4 Methodology

8.3.4.1. Field Physicochemical Measurement

Groundwater from shallow hand-dug wells and boreholes across Eastern Dahomey Basin were collected in wet (May to June 2017) and dry (February to March 2018) seasons. Field measurement of the depth of the wells and the static water level (SWL) were carried out using water level meters. Total dissolved solids (TDS), pH, electrical conductivity (EC), temperature, redox potential (Eh), and salinity were measured using a multitester Harch pH/EC meter (Model 99720). Water samples from wells were collected in a bailer and poured into a 3-L plastic from which samples were collected in 25 mL syringes with a 0.45-micron filter and then transferred into the tubes. The water samples were collected in two separate 50 mL polypropylene centrifuge tubes labelled nA and nB for metals and anions (where n stands for sampling well number from 1 to 96 and 1 to 134 for wet and dry season, respectively). Sample A was acidified with two drops of concentrated nitric acid to preserve the metals before laboratory analysis. The bottles were filled to the overflow and quickly covered with an airtight seal to prevent oxygen traps. The samples were then stored in the storage room at 4 °C until laboratory analysis.

8.3.4.2 Laboratory Analysis

Alkalinity was determined as total alkalinity in un-acidified samples by potentiometric titration with a 0.5 M HCl stock solution. Filtered samples Labelled nA which were acidified to pH two were used for cations analysis using Inductively coupled plasma mass spectrometry (ICP-MS). Unacidified samples were used for anions of chloride, bromide, nitrate, and sulphate were analyzed using Ion chromatography (IC).

8.3.4.3 Data Evaluation and Statistical Analysis

Statistical methods have proven to be useful for delineating hydrochemical processes [39–44]. In this study, a statistical method involving a summary of the minimum, maximum, mean and standard deviation was conducted for the physicochemical data to enable basic comparison, while the multivariate method of regression was run using the REGTEL software. Both pH and Eh were separately used as independent variables against which all other variables were dependent. Selection of pH and Eh were chosen based on their direct influence on the biogeochemical processes of redox, which mostly dominate nutrient loading and mineralization in surface water which subsequently infiltrate into coastal groundwater aquifers. The variations of the redox-sensitive ions were tested using the correlation, *p*-value and Significance values of both pH and Eh with the other selected parameters. Eh-pH diagram for Iron and Nitrogen species were plotted using Geochemist Workbench version 6 with activities values of 10^{-6} and 10^{-3} for Iron and Nitrogen, respectively. The general diagram of Eh-pH was plotted using Origin Pro 2017.

8.3.5 Results and Discussion

8.3.5.1 Physicochemical characterisation and desciption

A statistical summary of selected physicochemical parameters of groundwater in the study area during the wet and dry period is presented in Table 8.12. The results revealed that most of the hydrochemical parameters show a wide range and are generally higher in the dry season compared to the wet season. The high standard deviation could be attributed to dilution and mixing in the wet season and the effect of evaporation with its associated hydrochemical processes such as precipitation, oxidation, and reduction, etc. The temperature varied from 25.5 to 34.6 °C with an

average of 29.4 °C during the wet season while 26.6 to 37.7 °C with an average of 31.2 °C was observed in the dry. The higher temperature observed in the dry season may be responsible for a higher rate of evapotranspiration, which probably aids the rate of hydrochemical reactions and triggers a range of hydrochemical dynamics. pH, Eh, and salinity have values ranging from 3.85–7.96, −280–362 mV, and 14–5070 mg/L in the dry season and 3.97–8.10, −136–330 mV and 0.00–5000 mg/L for the wet season with respective averages of 5.5, 208.18 mV and 173 mg/L for the dry season while 5.57, 222 mV and 137 mg/L were recorded for the wet season.

Sulfate (SO_4^{2-})

Sulfate in groundwater occurs from both natural and anthropogenic sources. The natural source is linked with the dissolution sulfate/evaporites minerals such as gypsum while the anthropogenic sources could be from municipal and industrial effluents mainly due to sulfur-based waste products. Unmanaged waste disposal is common within the alluvium aquifer along the rivers within the coastal areas. Seasonal flooding in this area likely triggers a biogeochemical reaction of oxidation and reduction which promotes dissolution of sulfate in water. In this study, SO_4^{2-} concentration in groundwater samples from the dry season range from 0.26–576.3 mg/L with an average of 17.5 mg/L while wet season concentration ranges from 0.08–2.211 mg/L with an average of 37.9 mg/L. The relatively higher average concentration in the dry season water samples revealed the influence of evaporation. The spatial and temporal map, as shown in Figure 8.17 below, shows that most of the higher concentration samples are found within the coastal plain sands and alluvium deposit of the basin.

Table 8.13 Statistical summary of physicochemical parameters from water samples for both seasons.

Param	Wet Season					Dry Season				
	Min	Max	Aver	Stdev	N	Min	Max	Aver	Stdev	N
Elev	−1.00	230.0	46.3	39.8	96	−1.0	230	48.2	41.5	134
pH	3.97	8.10	5.57	1.00	96	3.85	8.0	5.5	0.9	134
EC	0.00	12000	295	1219	96	5.50	10009	348	995	134
TDS	0.00	8500	201	863	96	2.30	6750	232	668	134
ORP	−136	330	222	74	96	−280	326	208	92.1	134
Sal	0.00	5000	137	509	96	14	5070	173	502	134
Temp	25.5	34.6	29.4	1.7	96	26.6	37.7	31.2	1.7	134
SWL	0.20	67.0	18.3	15.4	96	0.3	123	18.8	19.2	134
Cl^-	0.10	18970	218	1934	96	0.9	1289	31.6	116	134
SO_4^{2-}	0.10	2211	37.9	245	96	0.3	576	17.5	56.1	134
NO_3^-	0.02	259	32.2	54	96	0.3	312	30.3	54.4	134
Br^-	0.00	40.8	0.46	4.2	96	0.01	21.7	0.3	1.9	134
Fe	0.00	6.10	0.3	0.8	96	0.01	136	1.5	11.9	134
Mn	0.00	1.11	0.1	0.1	96	0.00	27.7	0.3	2.4	134

Elevation and Static water level in (m), EC in (µS/cm), Eh in (mV), TDS, salinity, and other ions and metals measured in mg/L.

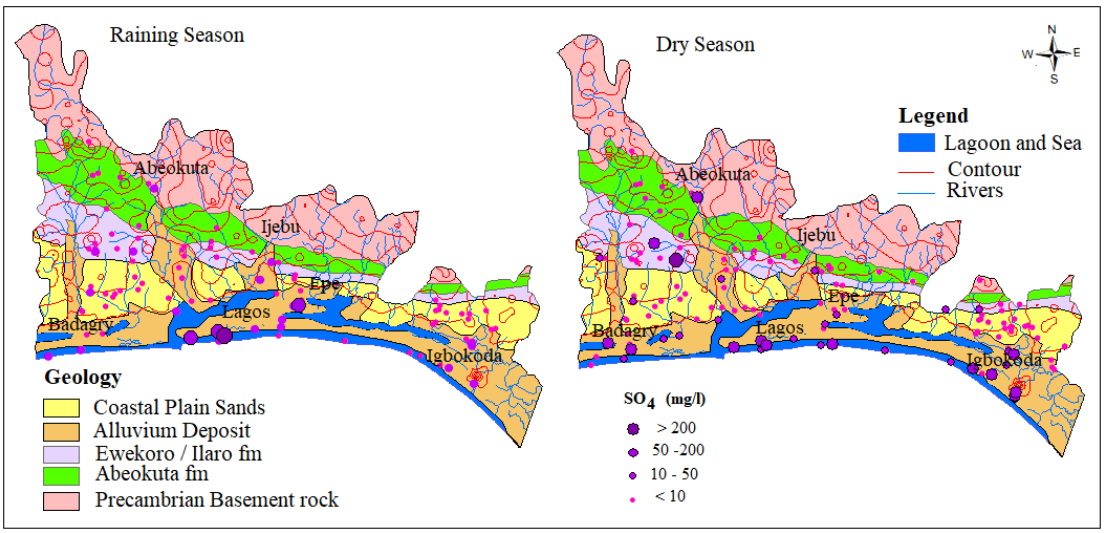

Figure 8.17 Spatial distribution of SO_4^{2-} across the Eastern Dahomey Basin.

Nitrate (NO_3^-)

Nitrogen in surface and groundwater is dominated by nitrate under oxidizing conditions and ammonium ions under reducing conditions. This is common when

water is in direct contact with wastewater, septic tanks and sewage systems. Leachates from farming as a result of fertilizer application and animal waste also form the source of nitrate in the groundwater [7,45–47]. Within the study area, Nitrate concentrations in groundwater range from 0.25 to 312 mg/L and 0.02 to 259 mg/L with an average of 30.3 mg/L and 32.1 mg/L, respectively for both dry and wet seasons. In groundwater samples analyzed during the dry and wet seasons, 82.4 % (131) and 81.2 % (96) fell well within the WHO permissible limit for drinking water standard while 17.6 % and 18.8 % fell beyond the same limit, respectively. The spatial map of nitrogen as shown in Figure 8.18, revealed most of the samples beyond the standard are distributed close to the river channels along with alluvium deposits, which is an indication of the impact of waste from municipal, agriculture, and industries that are commonly transported in water medium along the river channels.

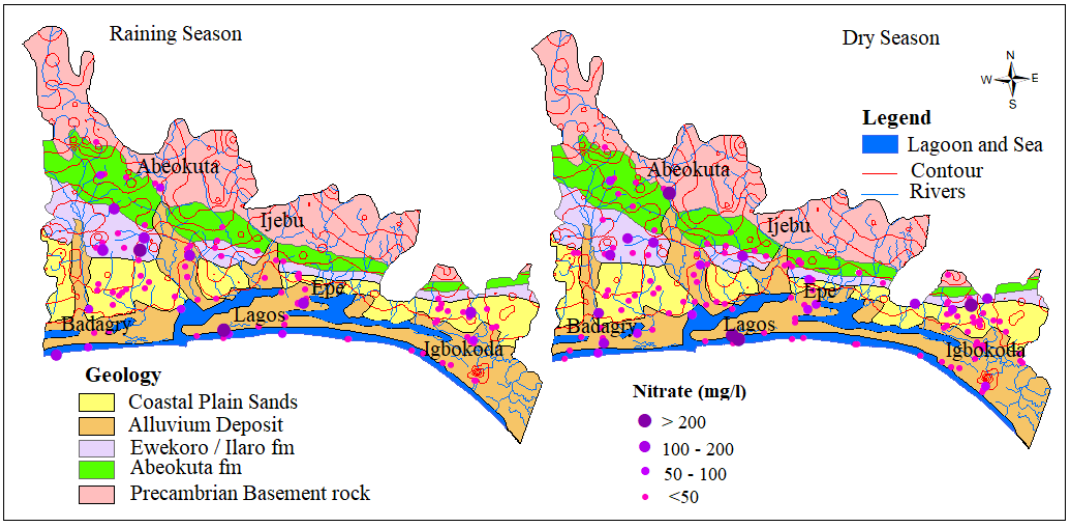

Figure 8.18 Spatial distribution of NO_3^- in mg/L.

Iron (Fe)

Dissolved irons generally have a terrigenous source and are transported towards the coast during which some are precipitated out of solution through oxidation to ferric oxyhydroxides [48]. However, even though most dissolved irons sourced from

catchment precipitates out as the water flow towards the coast, groundwater, and river can still accommodate significant quantities of dissolved iron to coastal environments. The input of fulvic acids can maintain iron in solution in brackish to saline coast waters [47].

Under anaerobic groundwater may contain ferrous iron at concentrations of up to several milligrams per liter without discoloration or turbidity in the water when directly pumped from a well. On exposure to the atmosphere, however, the ferrous iron oxidizes to ferric iron, giving an objectionable reddish-brown colour to the water. In this study, the concentration of Fe ranges from 0.0 to 6.1 mg/L and 0.01 to 136 mg/L and average of 0.3 mg/L and 1.5 mg/L, respectively for wet and dry seasons groundwater samples. The relative higher concentrations and standard deviation observed in the dry season (11.9) compared to wet season (0.8) signifies the possible influence of precipitation/redox driven by evaporations resulting from seasonal variation in precipitation. Scatter plots (Figure 8.19) between Fe and pH indicates that the higher concentration of Fe predominates the Alluvium and coastal plain sands aquifer. This occurrence is hypothesized to be attributed to the preservation of metals in groundwater by organic/fulvic acid, which commonly characterized the alluvium deposits around the coastal areas [5,47]. This trend can also be observed in spatial distribution map in Figure 8.20.

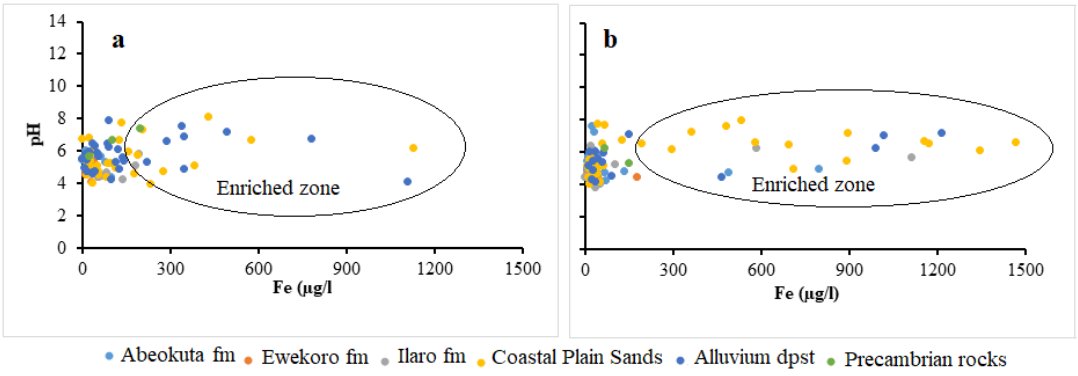

Figure 8.19 Scatter plots of Fe against pH for (**a**) wet and (**b**) dry season.

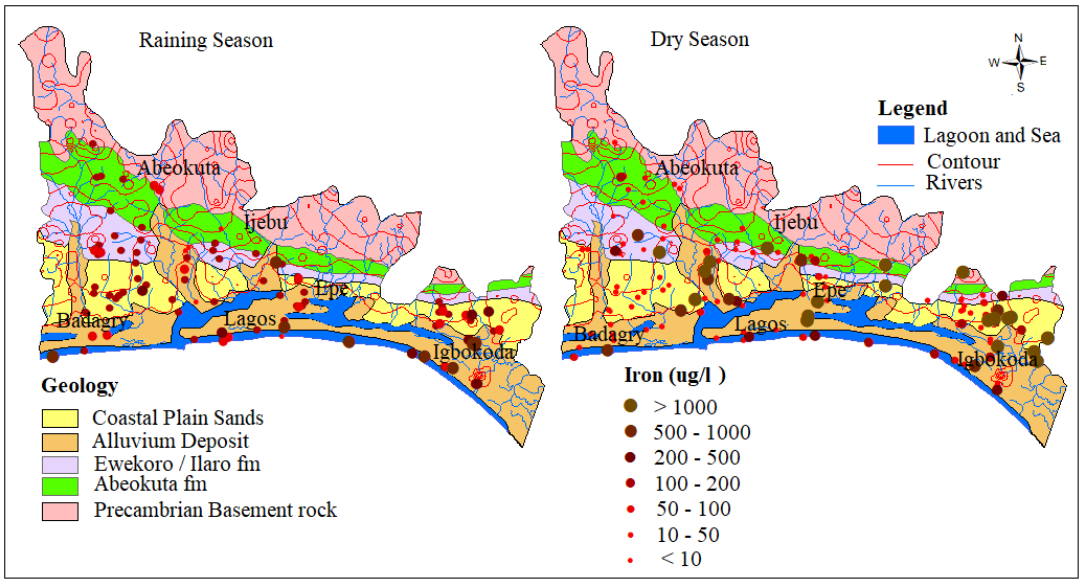

Figure 8.20 Spatial distribution of Fe^{3+} in µg/L.

Manganese (Mn)

Manganese occurs naturally in rocks and soils and finds its way into groundwater through rock-water interaction and is a well-known cause of aesthetic problems in drinking water [3,47,48]. Manganese is seldom found as a lone ion, as it is commonly found in iron-bearing water, though less abundantly than Iron. Most soils and rocks around the world commonly contain manganese. pH and ORP/Eh is one of the environmental parameters that control the behavior of manganese in groundwater. In this study, concentrations of groundwater range from 0.00 to 1.11 mg/L and 0.00 to

27.7 mg/L with an average of 0.1 mg/L and 0.3 mg/L for both wet and dry seasons, respectively. The slightly higher concentration observed in the dry season could be attributed to higher intensity of evaporation and hydrochemical process of reduction. The spatial distribution of Mn across the EDB is presented in Figure 8.21. 81.8% of 133 and 80.2% of the 96 water samples for both dry and wet seasons fell well within the permissible limit of WHO while 18.2% and 19.8%, respectively, exceed the limit.

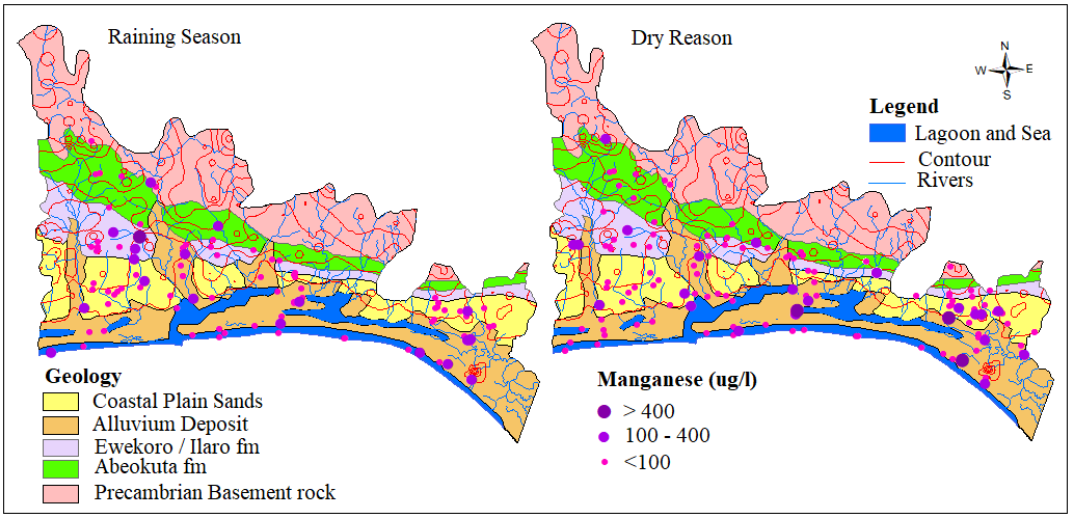

Figure 8.21 Spatial distribution of Mn^{2+} in µg/L.

8.3.5.2 Seasonal Effect of Climate Change on Biogeochemical Processes

The dynamic of mobilization of Fe, Mn, SO_4^{2-}, and NO_3^- at the sediment-water interface in the free water surface, especially along the delta and flood plains of coastal areas can be seasonally dependent (and therefore impacted by changes in climate). High contrast in the seasonal concentration of Fe has been found in coastal wetlands and flood plains [48]. It is well-known that pH in water is affected by the biogeochemical process which occurs either in coastal wetlands or river channels and shallow unconfined aquifers between the period of the end of one season and the beginning of another [5–7]. This process is known for its sensitivity to pH and Eh of the environment. Using changes in Eh and Eh/ORP as drivers for geochemical changes

in the selected redox-sensitive ions and metals allows us to hypothesize factors to link assessing groundwater quality changes with climate change. In order to assess the possible linkage for EDB shallow coastal aquifers, PH, and Eh are selected as dependent variables which control the concentration of redox-sensitive groundwater quality parameters as independent variables.

8.3.5.2.1 Multiple Linear Regression Model

Multiple linear regressions were used to model selected redox-sensitive hydro geochemical parameters related to pH and ORP/Eh as independent variables from both seasons using the REGTEL statistical software package. The results of the multiple linear regression models were used to assess and predict EC, salinity, temperature, static water level (SWL), SO_4^{2-}, Cl^-, NO_3^-, Fe, and Mn. Values of both pH and Eh of the water across different locations within the EDB for both wet and dry seasons were presented in Tables 8.13 and 8.14 for the wet season and Tables 8.15 and 8.16 for the dry season water samples.

For wet season samples, SO_4^{2-}, Cl^-, NO_3^-, Fe, and temperature have a *p*-value of 0.0001 with 99% significance, and with pH a coefficient of 0.0192, −0.0022, −0.0022, 0.2721, and −0.0777, respectively (Table 8.15). This suggests a strong relationship between these variables. In the dry season Temperature, NO_3 and Static water level (SLW) are significantly related to pH (99 percentile) while other parameters such SO_4^{2-}, Cl^-, Fe, and Mn show weak response to pH with no significance. In the rainy season water samples, SO_4^{2-}, Cl^-, NO_3^-, Fe, and temperature show significant change in concentration with change in pH, while only temperature, NO_3^-, and static water level (SWL) show significant change with change in pH of the water sample in the dry season. This relationship could be attributed to relatively higher groundwater recharge

by the contaminated surface water during the wet season with higher water level compared to the dry season when most coastal groundwater aquifers are being recharged through baseflow.

Other groundwater quality parameters such as temperature, SO_4^{2-}, NO_3^-, Cl^-, and Mn show a higher *p*-value well above 0.05 maximum. The Eh showed high predictability with salinity, Fe, and the static water level but little or no sensitivity towards temperature, SO_4^{2-}, NO_3^-, Cl^-, and Mn. This indicates their weak response to fluctuation in Eh resulting from possible dilution effect due to high precipitation in the wet season as presented in Table 4 which can also be observed in the scatter diagram in Figure 8.20. In the dry season, the results show that Eh is well predicted by the independent variables of Salinity, SWL, Cl^- and NO_3^- with 99% significance and regression coefficient −0.6204, 0.9631, −0.2583, and 0.4514.

The temperature has a significance of 95% with coefficient −0.2611 while SO_4^{2-} and Fe each have 75% significance. The observed predictability of Eh with these independent variables in the dry season water samples could be attributed to the effect of evaporation and mineral precipitation and other relevant hydrochemical processes that characterized the dry season.

Lack of Mn significance contrary to other selected parameters could result from anthropogenic influence on the Fe concentration in the groundwater from this area. This nutrient enrichment is higher in Alluvium deposit and Coastal Plain Sands groundwater aquifers, as shown in the scatter diagram in Figures 8.22–8.24.

The overall result of the linear regression analysis indicated that the seasonal flooding possibly resulting from climate change has a significant influence on the quality of the groundwater of EDB. This is more prominent in the shallow coastal

aquifers where the groundwater level is relatively high and consequently vulnerable to contamination from surface water with dissolved ions and metals from a different source.

Table 8.13 Multiple regression statistical model with dependent variables against the pH as independent variables for selected wet season hydrochemical parameters.

Parameters	**Coefficient**	**Std. Error**	***z***	***p*-Value**	
pH(−1)	0.2715	0.0516	5.265	<0.0001	***
const	6.1009	0.9010	6.771	<0.0001	***
SO_4^2	0.0192	0.0036	5.291	<0.0001	***
Cl	−0.0022	0.0004	−5.188	<0.0001	***
NO_3	−0.0022	0.0008	−3.195	0.0014	***
Fe	0.2721	0.0833	3.269	0.0011	***
Mn	−0.0052	0.4067	−0.01280	0.9898	
EC	7.48261×10^{-5}	4.67708×10^{-5}	1.600	0.1096	
Temp	−0.0777	0.0287	−2.711	0.0067	***

Table 8.14 Multiple regression statistical model with dependent variables against the pH as independent variables for selected dry season groundwater quality parameters.

Parameters	**Coefficient**	**Std. Error**	***z***	***p*-Value**	
pH(−1)	0.05621	0.0449	1.252	0.2106	
const	4.9667	0.3383	14.68	<0.0001	***
Sal	4.81623×10^{-5}	0.0002	0.2280	0.8196	
Temp	0.0108	0.00301	3.594	0.0003	***
SO_4	0.0022	0.0020	1.076	0.2819	
Cl	0.0007	0.0011	0.6099	0.5419	
NO_3	−0.0057	0.0019	−2.948	0.0032	***
Fe	0.0125	0.0827	0.1508	0.8801	
Mn	−0.0636	0.4079	−0.1559	0.8761	
SWL	−0.0173335	0.0056	−3.100	0.0019	***

This could stimulate redox reaction that results in mobilization and remobilization of Fe into the particulate form. Iron mobilization is known for his ability to precipitate SO_4, NO_3 Mn^{2+}, and phosphate [49]. Though not a direct linkage between climate change and groundwater quality, this complex linkage chain is a plausible linking mechanism.

Oxidation/reduction (redox) reaction potential of groundwater (Eh) plays a vital role in the geochemical processes that occur in groundwater. Redox is defined as the transfer of electrons. Redox reactions are crucial in aqueous environmental geochemistry. Eh measurements are useful in identifying the redox zones as its value decreases with increases in residence time [28,50]. Change in pH and Eh have been identified as controlling factors in the mobilization and remobilization of ions and metals in surface and groundwater of the shallow aquifer of the EDB basin (Figure 8.22).

8.3.5.3 Analysis of Biogeochemical Processes of Redox Reaction in Groundwater of EDB

Oxidation and reduction of ions and metals is a typical process in an aquifer system, especially SO_4^{2-} and Fe. The Eh-pH geochemical diagram shows how Eh in groundwater is governed in the upper range by oxidation of water to O_2 and lower range by reduction of hydrogen ions to H_2. The groundwater samples of the study area undergo a combination of redox process (under ferrous (Fe^{2+}), i.e., reduction state and $Fe(OH)_2$, i.e., oxidation states. This situation from (Figure 10) revealed a scatter pattern that could be a seasonal effect. Eh values above 300 mV indicate a recharge area where sulphates are commonly stable.

Table 8.15 Multiple regression statistical model with dependent variables against the Eh as independent variables for selected wet season hydrochemical parameters.

Parameters	**Coefficient**	**Std. Error**	***z***	***p*-Value**	
ORP(−1)	0.3181	0.0989	3.215	0.0013	***
const	0.4747	0.6421	0.7393	0.4598	
Sal	−0.2739	0.0872	−3.142	0.0017	***
Temp	5.6701	4.7094	1.204	0.2286	
SWL	1.0481	0.5535	1.894	0.0583	*
SO_4^2	0.4348	0.5958	0.7298	0.4655	
Cl	−0.0530	0.0689	−0.7689	0.4420	
NO_3	0.1468	0.1004	1.462	0.1437	
Fe	−22.0104	10.2563	−2.146	0.0319	**
Mn	−23.3314	31..8584	−0.7323	0.4640	

Table 8.16 Multiple regression statistical model with dependent variables against the Eh as independent variables for selected dry season hydrochemical parameters.

Parameters	**Coefficient**	**Std. Error**	***z***	***p*-Value**	
ORPmV(−1)	0.3596	0.03501	10.27	<0.0001	***
const	143.197	11.3490	12.62	<0.0001	***
Sal	−0.0624	0.0087	−7.178	<0.0001	***
Temp	−0.2611	0.1027	−2.542	0.0110	**
SWL	0.9631	0.2057	4.684	<0.0001	***
SO_4	0.1294	0.0708	1.828	0.0675	*
Cl	−0.2583	0.0347	−7.446	<0.0001	***
NO_3	0.4514	0.0970	4.655	<0.0001	***
Fe	−2.6130	1.4991	−1.743	0.0814	*
Mn	−0.8053	1.5327	−0.5254	0.5993	

High Eh values indicate the regions of good recharge and low Eh values are the regions of less recharge or discharge. Eh and pH diagram (Figure 8.25) of the water samples from the study area in wet seasons which indicates high Eh value (330 mV) in the well L92 around Okitipupa, and the lowest Eh value (−136 mV) in well L77 at Ode-Mahin.

This value indicates groundwater flow recharge area in Okitipupa to the discharge area around the coasts at Igbokoda and Ode-Mahin. In the dry season samples, the highest Eh value (326 mV) was observed in well L59 around Ijebu-Ode and low values (−280 Mv) in well number L94 around Ode-mahin, Igbokoda (−22 mV), Araromi (−8 mV), and Badagry (−6 mV), with respective numbers L97, L86, and L34 all along the coastline of the study basin. These values also show reduction from the recharge zones to the discharge areas. Water from most of the above-mentioned wells with lower Eh values displayed yellowish to brownish color, which is an indication of redox process which transforms ferrous to ferric Iron.

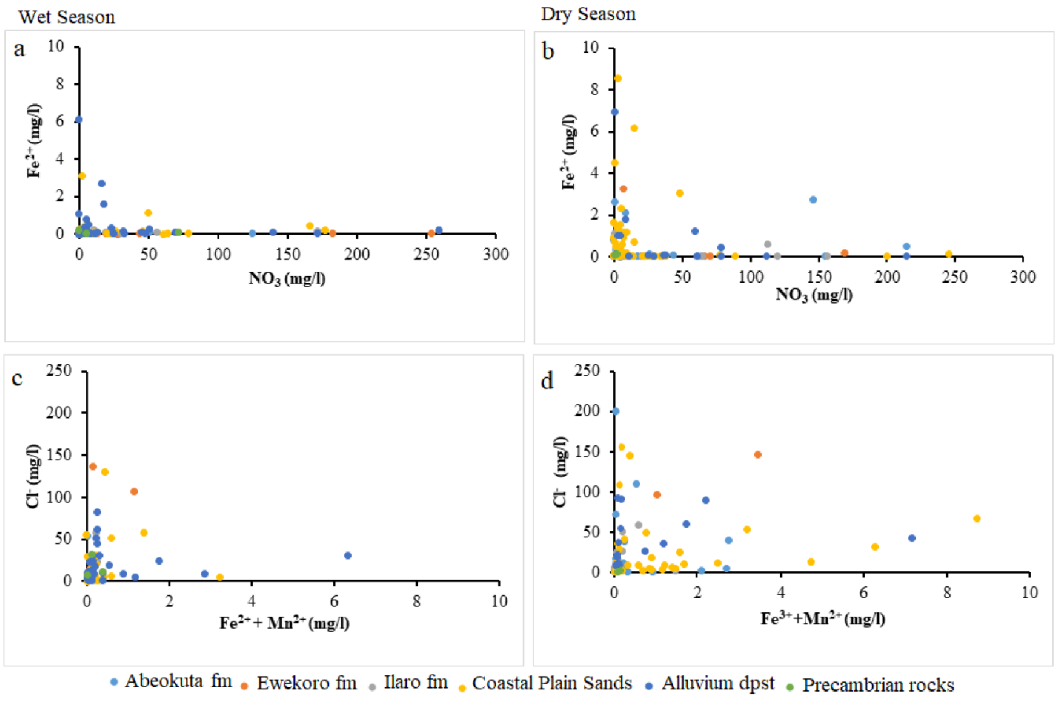

Figure 8.22 Scatter plots NO_3 against Fe^{2+} (a) wet season (b) dry season and Fe^{2+} + Mn^{2+} against Cl^- (c) wet season (d) dry season.

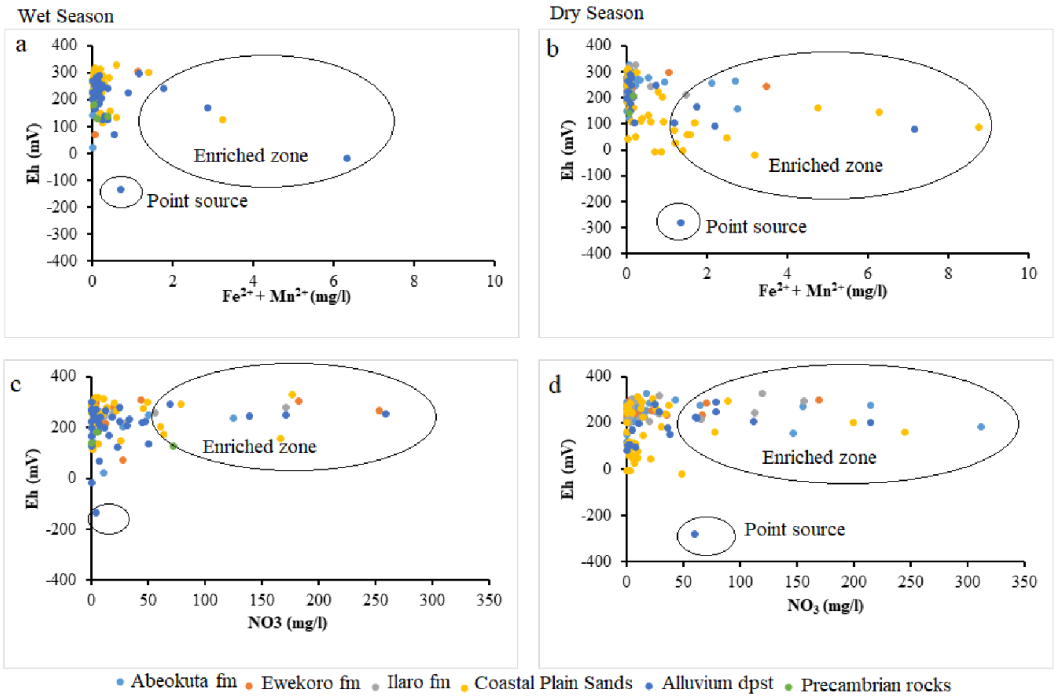

Figure 8.23 Scatter plots (Fe^{2+} + Mg^{2+}) against Eh (a) wet season (b) dry season and NO_3 against Eh (c) wet season (d) dry season.

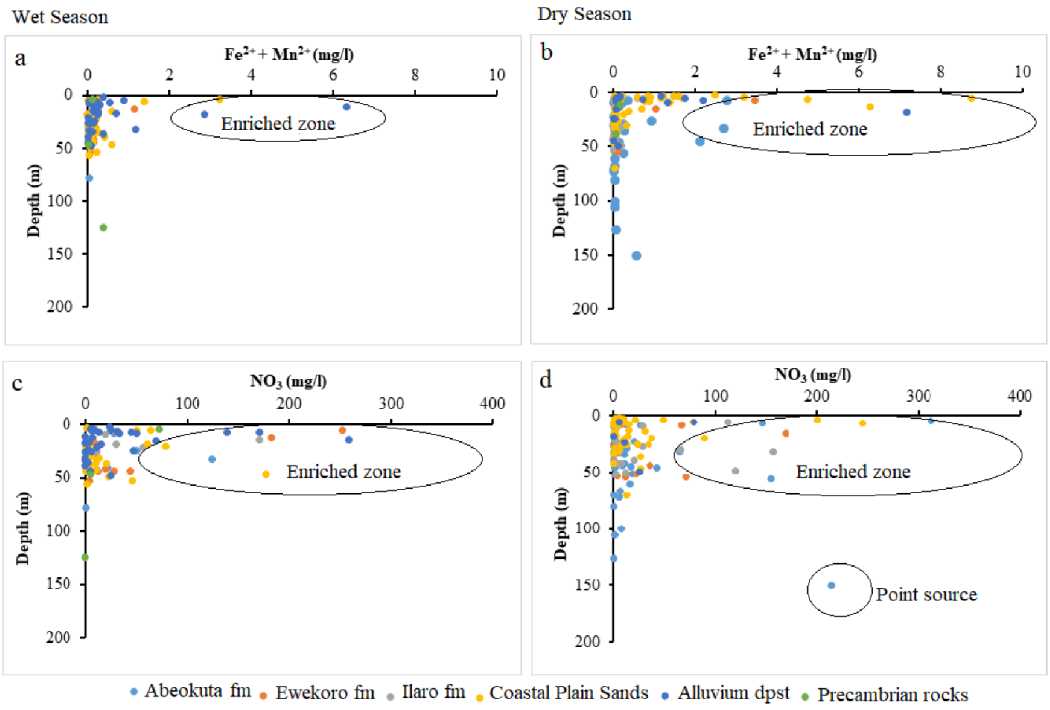

Figure 8.24 Scatter plots (Fe^{2+} + Mn^{2+}) against well depth (a) wet season (b) dry season and NO_3 against well depth (c) wet season (d) dry season.

The general Eh-pH diagram, (Figure 8.25) revealed that the groundwater from the Eastern Dahomey Basin falls within the transitional phase of the redox process, the Iron concentrations in groundwater around the study area showed a higher concentration in locations around the Alluvium deposit and Coastal Plain Sands aquifers. A high concentration of ions was also observed in some locations in other parts of the basin, especially areas within or very close to the flood plains of the major rivers. This type of area is suggested to contain a confined sandy aquifer with sedimentary organic carbon with ferrihydrite coatings on the sands. This is prominent in various locations around Isheri, Eleko, Ibeju Lekki, and Igbokoda. In these areas, the values of dissolved Iron concentration are above 3 mg/L, which have a negative implication on the groundwater quality. The Eh-pH diagram for Iron and Nitrogen species (Figures 8.26 and 8.27) show samples plotted along the boundary between Hematite and Fe^{2+}. This pattern is similar for both seasons and observed among water samples from alluvium deposit and Coastal Plain Sands aquifers. In the case of the

Nitrate species, most samples plotted in the area N_2 had stability between boundary lines NH_4^+ and NO_3^-, indicating likely nitrifying/denitrifying biogeochemical activities. This is prominent in water from the Alluvium and Coastal Plain Sands aquifers, which could be attributed to biogeochemical activities within the flood plain and wetlands of the EDB.

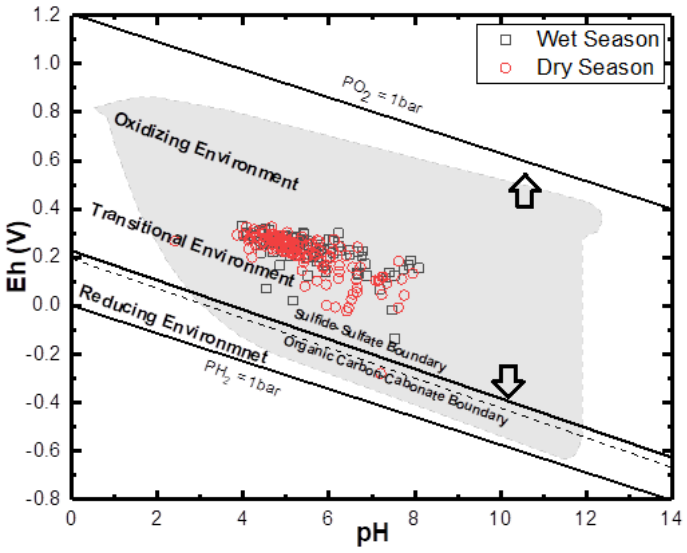

Figure 8.25 General Eh-Ph diagram for both wet and dry season groundwater samples. The upper and lower stability limits of water are given where PO_2 and PH_2 = 1 bar. The dry season shows more extensive variation in the thermodynamic phase, while both are generally plotted within the transitional phase.

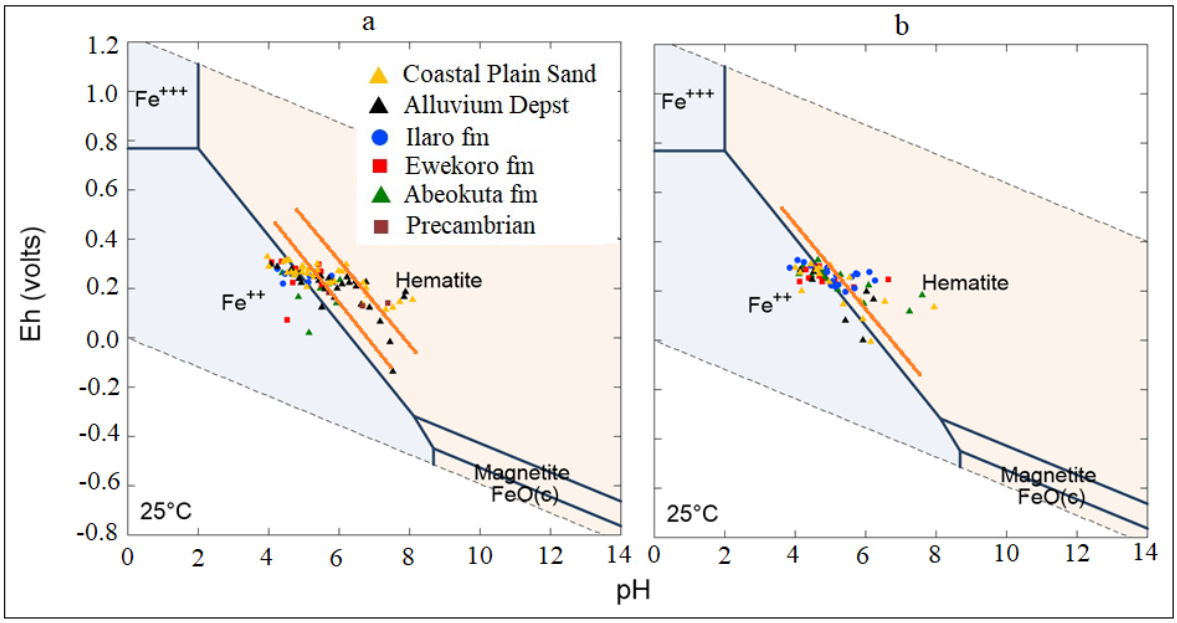

Figure 8.26 Eh-pH diagram for Iron species in the sampled groundwater (**a**) Wet season; (**b**) dry season.

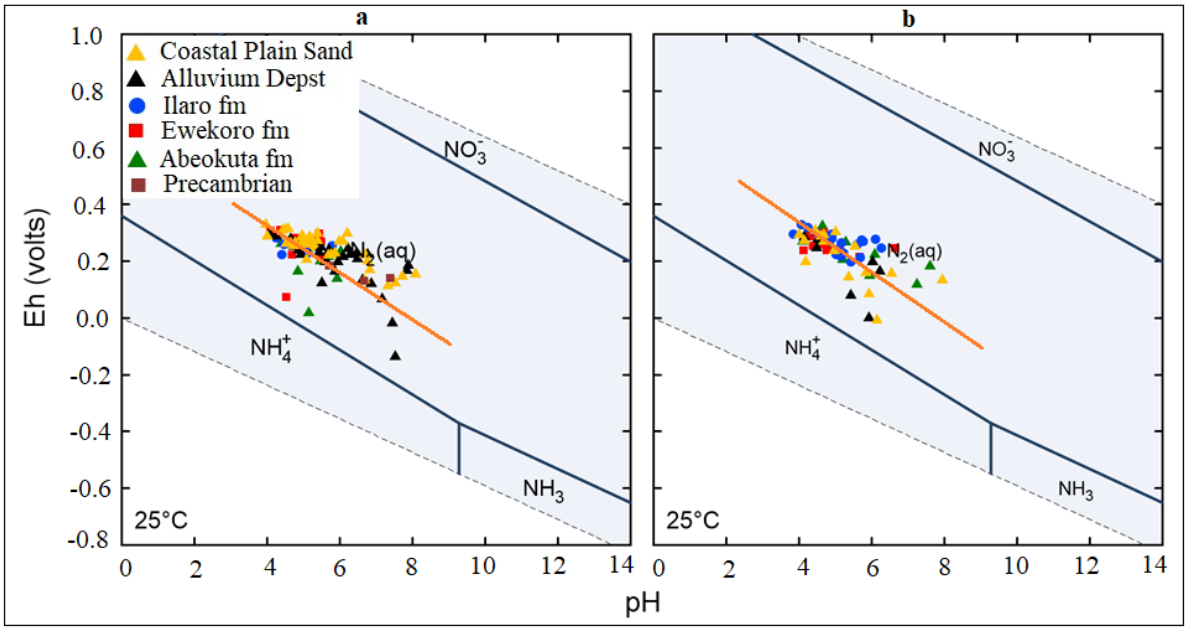

Figure 8.27 Redox plot for Nitrogen species in the sampled groundwater (**a**) Wet season; (**b**) dry season.

8.3.5.4 Implication on the Groundwater Quality and Human Health

Quality assessment was conducted on the selected groundwater quality parameter by directly comparing them with the World Health Organization (WHO) standard for drinking water, as presented in Table 8.17.

For the dry season water samples, Fe^{2+} contamination dominates the groundwater of EDB with 92.55% sample fell above WHO permissible limits. This is followed by Mn^{2+} and NO_3^- with 18.2% and 17.6% samples having concentration beyond the standard. Only 0.4% of the samples show values above the standard limit for both SO_4^{2-} and Cl^-, while 7.7% of samples show both EC and TDS values above the standard. Iron promotes the growth of "iron bacteria," which derive their energy from the oxidation of ferrous iron to ferric iron and in the process deposit a slimy coating on the piping. At levels above 0.3 mg/L, iron stains laundry and plumbing fixtures. There is usually no noticeable taste at iron concentrations below 0.3 mg/liter, although turbidity and colour may develop.

Table 8.17 Comparing some selected ions from the wet season with the World Health Organization (WHO) water quality highest permissible standard.

WHO Standard Classification		Wet Season Groundwater Samples N = 96							
	Parameters	**pH**	**EC**	**TDS**	**Cl**	**SO_4**	**NO_3**	**Fe**	**Mn**
Samples within WHO Limits	No. of Sample	18	95	95	94	95	78	90	77
	% Sample	18.75	98.96	98.96	97.9	98.96	81.3	93.8	80.2
Samples above WHO Permissible Limits	No. of Sample	78	1	1	2	1	18	6	19
	% Sample	81.1	1	1	2.1	1	18.8	6.3	19.8
		Dry Season Groundwater Samples N = 134							
Samples within WHO Limits	No. of Sample	21	123	123	130	133	108	10	109
	% Sample	15.8	92.3	92.3	99.6	99.6	82.4	7.5	81.8
Samples above WHO Permissible Limits	No. of Sample	113	11	11	1	1	23	123	25
	% Sample	84.2	7.7	7.7	0.4	0.4	17.6	92.5	18.2
WHO Permissible Std		6.5–8.5	750	500	200	200	50	0.01	0.1

No health-based guideline value is proposed for iron. Water containing over 50 ug/L dissolved manganese can precipitate in media or storages (aquifer), which could lead to staining laundry and fixtures, and distinct aesthetic effects such as discoloration, odor, or taste. At levels exceeding 0.1 mg/L, Mn in water supplies causes an undesirable taste in beverages and stains sanitary ware and laundry. The presence of manganese in drinking-water, like that of iron, may lead to the accumulation of deposits in the distribution system. Concentrations below 0.1 mg/L are usually acceptable to consumers. The health-based guideline value for manganese is four times higher than this acceptability threshold of 0.1 mg/L. Excessive nitrates and nitrites consumed with drinking water (nitrate is converted to nitrite in the human body) increase the risk of methemoglobinemia and stomach cancer [51].

8.3.6 Conclusions

This study examined possible links between climate change and groundwater chemistry in the shallow coastal aquifers of Eastern Dahomey basin. There is evidence of chemical changes due to seasonal flooding, resulting from extreme precipitation. Thus, we propose the biogeochemical processes of redox and other hydrochemical reactions, which might be influenced by future climate change. These processes are responsible for metals and ions mobilization/remobilization in surface and groundwater of this shallow coastal aquifer. Spatial distribution maps of SO_4^{2-}, NO_3^-, Fe, and Mn revealed higher concentrations within the Alluvium and Coastal Plain Sands aquifer and some wells with the river flood plains of the Basin. The generalized Eh-pH diagram revealed groundwater of the study area are within the transitional (aerobic to anaerobic) phase of the geochemical thermodynamics. It also revealed that Nitrate is a dominant species in the groundwater from both wet and dry seasons, while

Iron occurrence is restricted to the alluvium and coastal plain sands aquifer. This study also revealed that the reduction in concentration and nutrient enrichment of groundwater with the increase in well depth can be attributed to the loss of aeration and possible natural attenuation by the soil and aquifer medium. The linear regression model using both Eh and pH as independent variables against other selected variables such as EC, salinity, SO_4^{2-}, Cl^-, NO_3^-, Fe, and Mn for both season groundwater samples established predictability for both Eh and pH. A possible indication of ions and metals enrichment in groundwater resulting from the effect of seasonal flooding. This enrichment rendered some of the sampled groundwater unsuitable for drinking as the concentration of some of the water quality parameters were above the WHO standard for drinking water. Accumulation could lead to severe contamination of surface and groundwater and render it not potable for drinking or other purposes. This study recommends policy and management enhancements for proper waste management to support SDG planning for sustainable groundwater resource management in the Eastern Dahomey Basin that limits further contamination of the coastal groundwater system in the face of seasonal flooding, especially as predictions suggest more extreme precipitation in the future resulting from climate change.

Author Contributions: J.A.A. and R.M.K. designed the research; J.A.A. wrote the original draft; R.M.K., P.S., and I.H. reviewed and edited the manuscript; R.M.K. gave critical views on the manuscript for further improvement. All authors have read and agreed to the published version of the manuscript.

Funding: This research was funded by the Petroleum Technology and Development Fund (PTDF) under the Overseas PhD scholarship scheme and supported by the Scottish Government under the Climate Justice Fund Water Futures Program, awarded to the University of Strathclyde (R.M. Kalin).

Acknowledgments: The authors would like to gratefully acknowledge Ademola Ologbe, David Akpan, Mara Knapp and Tatyana Peshkur for field and laboratory assistance.

Conflicts of Interest: The authors declare no conflict of interest.

8.3.7 References

1. Omosuyi, G.O.; Oseghale, A. Groundwater vulnerability assessment in shallow aquifers using geoelectric and hydrogeologic parameters at Odigbo, Southwestern Nigeria. *Am. J. Sci. Ind. Res.* **2012**, 501–512, doi:10.5251/ajsir.2012.3.6.501.512.

2. Adegbola, R.; Oseni, S.; Majolagbe, A. The impact assessment of oil spillage and trace metal assessment on groundwater in Baruwa, Lagos Southwest and Nigeria. *Int. Sci. Investig. J.* **2013**, *2*, 12–32.

3. Oyelami, A.C.; Ojo, O.A.; Aladejana,.J.A.; Agbede,.O.O. Assessing the effect of a dumpsite on groundwater quality : A case study of aduramigba estate within osogbo metropolis. *J. Environ. Earth Sci.* **2013**, *3*, 120–131.

4. Edet, A. Hydrogeology and groundwater evaluation of a shallow coastal aquifer, southern Akwa Ibom State (Nigeria). *Appl. Water Sci.* **2016**, *7*, 2397–2412, doi:10.1007/s13201-016-0432-1.

5. Snyder, M.; Taillefert, M.; Ruppel, C. Redox zonation at the saline-influenced boundaries of a permeable surficial aquifer : Effects of physical forcing on the biogeochemical cycling of iron and manganese. *J. Hydrol.* **2004**, *296*, 164–178.

6. Holden, A.A.; Haque, S.E.; Mayer, K.U.; Ulrich, A.C. Biogeochemical processes controlling the mobility of major ions and trace metals in aquitard sediments beneath an oil sand tailing pond: Laboratory studies and reactive transport modeling. *J. Contam. Hydrol.* **2013**, *151*, 55–67.

7. Matiatos, I. Nitrate source identification in groundwater of multiple land-use areas by combining isotopes and multivariate statistical analysis: A case study of Asopos basin (Central Greece). *Sci. Total Environ.* **2016**, *541*, 802–814.

8. Delpla, I.; Jung, A.; Baures, E.; Clement, M.; Thomas, O. Impacts of climate change on surface water quality in relation to drinking water production. *Environ. Int.* **2009**, *35*, 1225–1233.

9. Ojolowo, S.; Wahab, B. Municipal solid waste and flooding in Lagos metropolis, Nigeria : Deconstructing the evil nexus. *J. Geogr. Reg. Plan. Full* **2017**, *10*, 174–185.

10. Ayolabi, E.A.; Epelle, E.S.; Lucas, O.B.; Ojo, A. Geophysical and geochemical site investigation of eastern part of Lagos metropolis, southwestern Nigeria. *Arab. J. Geosci.* **2014**, *8*, 7445–7453.

11. IPCC. *Climate Change 1995. The Science of Climate Cliange*; The Press Syndicate of the University of Cambridge: Camebridge, UK, 1995; Volume 53.

12. Whitehead, P.G.; Wilby, R.L.; Battarbee, R.W.; Kernan, M.; Wade, A.J. A review of the potential impacts of climate change on surface water quality a review of the potential impacts of climate change on surface water quality. *Hydrol. Sci. J. ISSN* **2009**, *54*, 101–123.

13. Guasch, H.; Serra, A.; Corcoll, N.; Bonet, B.; Leira, M. Metal ecotoxicology in fluvial biofilms : Potential influence of water scarcity. *Hdb. Env. Chem.* **2010**, 41–53, doi:10.1007/698.

14. Ezekwe, C.I.; Edoghotu, M.I. Water quality and environmental health indicators in the Andoni River estuary, Eastern Niger Delta of Nigeria. *Environ. Earth Sci.* **2015**, *74*, 6123–6136.

15. Cann, K.F.; Thomas, D.; Salmon, R.; Wyn-Jones, A.; Kay, D. Extreme water-related weather events and waterborne disease. *Epidemiol. Infect.* **2013**, *141*, 671–686.

16. Kasei, R.A. Modelling Impacts of Climate Change on Water Resources in the Volta Basin, West Africa. Ph.D. Dissertation, Mathematisch-Naturwissenschaftlichen Fakultät, Rheinischen Friedrich-Wilhelms-Universität Bonn, Bonn, Germany, 2009.

17. Babanyara, Y.Y.; Usman, H.A.; Saleh, U.F. An overview of urban poverty and environmental problems in Nigeria. *J. Hum. Ecol.* **2010**, *31*, 135–143.

18. Serdeczny, O.; Adams, S.; Baarsch, F.; Coumou, D.; Robinson, A.; Hare, W.; Schaeffer, M.; Perrette, M.; Reinhardt, J. Climate change impacts in Sub-Saharan Africa: From physical changes to their social repercussions. *Reg. Environ. Chang.* **2016**, 1–16, doi:10.1007/s10113-015-0910-2.

19. Pfeiffer, M.; Batbayar, G.; Hahn-tomer, D.K.S. Investigating arsenic (As) occurrence and sources in ground, surface, waste and drinking water in northern Mongolia. *Environ. Earth Sci.* **2015**, *73*, 649–662.

20. Priyantha Ranjan, S.; Kazama, S.; Sawamoto, M. Effects of climate and land use changes on groundwater resources in coastal aquifers. *J. Environ. Manag.* **2006**, *80*, 25–35.

21. Linzey, D. Atlantic climate adaptation solutions association saltwater intrusion and climate change. **2011**, 26.

22. Hiyama, T.; Babiker, I.S.; Mohamed, M.A.A. *Groundwater as a Key for Adaptation to Changing Climate and Society*; Springer: Tokyo, Japan, 2014; ISBN 978-4-431-54967-3.

23. Unsal, B.; Yagbasan, O.; Yazicigil, H. Assessing the impacts of climate change on sustainable management of coastal aquifers. *Environ. Earth Sci.* **2014**, *72*, 2183–2193.

24. Nistor, M.-M.; Dezsi, Ş.; Cheval, S.; Baciu, M. Climate change effects on groundwater resources: A new assessment method through climate indices and effective precipitation in Beliş district, Western Carpathians. *Meteorol. Appl.* **2016**, *23*, 554–561.

25. Ayolabi, E.A.; Folorunso, A.F.; Kayode, O.T. Integrated geophysical and geochemical methods for environmental assessment of municipal dumpsite system. *Int. J. Geosci.* **2013**, *4*, 850–862.

26. Hashmi, M.Z.; Yu, C.; Shen, H.; Duan, D. Concentrations and human health risk assessment of selected heavy metals in surface water of the siling reservoir watershed in Zhejiang Province, China. *Pol. J. Environ. Stud.* **2014**, *23*, 801–811.

27. Bieroza, M.Z.; Heathwaite, A.L. Seasonal variation in phosphorus concentration Discharge hysteresis inferred from high-frequency in situ monitoring. *J. Hydrol.* **2015**, *524*, 333–347.

28. Nick, H.M.; Raoof, A.; Centler, F.; Thullner, M.; Regnier, P. Reactive dispersive contaminant transport in coastal aquifers: Numerical simulation of a reactive Henry problem. *J. Contam. Hydrol.* **2013**, *145*, 90–104.

29. Offodile, M.E. The Hydrogeology of Coastal Areas of Southeastern states of Nigeria. *J. Min. Geol.* **1971**, *14*, 94–101.

30. Adegoke, O.S.; Omatsola, M.E. Tectonic evolution and cretaceous stratigraphy of the dahomey basin. *Niger. J. Min. Geol.* **1981**, *18*, 130–137.

31. Jones, H.A.; Hockey, R. The geology of part of southwestern Nigeria. *GSN Bull.* **1964**, *31*, *87*.

32. Kogbe, C.A. The cretaceous and paleogene sediments of Southern Nigeria. In *Geology of Nigeria*, 2nd ed.; Kogbe, C.A., ed.; Rock View (Nig) Ltd.: Owerri, Nigeria, 1976; pp. 273–282.

33. Reyment, R.A. *Aspects of Geology of Nigeria*; Ibadan University Press: Ibadan, Nigeria, 1965; p. 145.

34. Longe, E.O.; Malomo, S.; Olorunniwo, M.A. Hydrogeology of Lagos metropolis. *J. Afr. Earth Sci.* **1987**, *6*, 163–174.

35. Adeoti, L.; Alile, O.M.; Uchegbulam, O. Geophysical investigation of saline water intrusion into freshwater aquifers: A case study of Oniru, Lagos State. *Sci. Res. Essays* **2010**, *5*, 248–259.

36. Fatoba, J.O.; Omolayo, S.D.; Adigun, E.O. Using geoelectric soundings for estimation of hydraulic characteristics of aquifers in the coastal area of Lagos, southwestern Nigeria. *Int. Lett. Nat. Sci.* **2014**, *11*, 30–39.

37. Faleye, E.T.; Olorunfemi aquifer characterization and groundwater potential assessment of the sedimentary basin of ondo state 1 2. *Ife J. Sci.* **2015**, *17*, 429–439.

38. Offodile, M.E. *Hydrogeology: Groundwater Study and Development in Nigeria*, 3rd ed.; Mecon Geology and Engineering Services Ltd: Jos, Nigeria, 2014; ISBN 978-30956-41.

39. Adhikary, P.P.; Chandrasekharan, H.; Chakraborty, D.; Kumar, B.; Yadav, B.R. Statistical approaches for hydrogeochemical characterization of groundwater in West Delhi, India. *Environ. Monit. Assess.* **2009**, *154*, 41–52.

40. Wu, M.-L.; Wang, Y.-S.; Sun, C.-C.; Wang, H.; Dong, J.-D.; Yin, J.-P.; Han, S.-H. Identification of coastal water quality by statistical analysis methods in Daya Bay, South China Sea. *Mar. Pollut. Bull.* **2010**, *60*, 852–860.

41. Amangabara, G.T.; Ejenma, E. Groundwater quality assessment of Yenagoa and between 2010 and 2011. *Resour. Environ.* **2012**, *2*, 20–29.

42. Thilagavathi, R.; Chidambaram, S.; Thivya, C.; Prasanna, M.V.; Keesari, T.; Pethaperumal, S. Assessment of groundwater chemistry in layered coastal aquifers using multivariate statistical analysis. *Sustain. Water Resour. Manag.* **2017**, *3*, 55–69.

43. Boughariou, E.; Bahloul, M.; Jmal, I.; Allouche, N.; Makni, J.; Khanfir, H.; Bouri, S. Hydrochemical and statistical studies of the groundwater salinization combined with MODPATH numerical model: Case of the Sfax coastal aquifer, Southeast Tunisia. *Arab. J. Geosci.* **2018**, *11*, 69, doi:10.1007/s12517-018-3408-7.

44. Ganiyu, S.A.; Badmus, B.S.; Olurin, O.T.; Ojekunle, Z.O. Evaluation of seasonal variation of water quality using multivariate statistical analysis and irrigation parameter indices in Ajakanga area, Ibadan, Nigeria. *Appl. Water Sci.* **2018**, *8*, 35.

45. White, J.K.; Beaven, R.P.; Powrie, W.; Knox, K. Leachate recirculation in a landfill: Some insights obtained from the development of a simple 1-D model. *Waste Manag.* **2011**, *31*, 1210–1221.

46. Zhang, Y.; Li, F.; Zhang, Q.; Li, J.; Liu, Q. Tracing nitrate pollution sources and transformation in surface- and ground-waters using environmental isotopes. *Sci. Total Environ.* **2014**, *490*, 213–222.

47. Larsen, G.R. Determination of Coastal Ground and Surface Water Processes and Character by Use of Hydrochemistry and Stable Isotopes, Fraser Coast, Queensland. Ph.D. Thesis, Queensland University of Technology, Australia, 2012.

48. Russak, A.; Sivan, O.; Yechieli, Y. Trace elements (Li, B, Mn and Ba) as sensitive indicators for salinization and freshening events in coastal aquifers. *Chem. Geol.* **2016**, *441*, 35–46.

49. Wu, Y.; Prulho, R.; Brigante, M.; Dong, W.; Hanna, K.; Wu, Y.; Prulho, R.; Brigante, M.; Dong, W.; Hanna, K. Activation of persulfate by Fe (III) species : Implications for 4-tert-butylphenol degradation to cite this version : HAL Id : hal-01438110. *J. Hazard. Mater.* **2017**, doi:10.1016/j.jhazmat.2016.10.013.

50. Capaccioni, B.; Didero, M.; Paletta, C.; Didero, L. Saline intrusion and refreshening in a multilayer coastal aquifer in the Catania Plain (Sicily, Southern Italy): Dynamics of degradation processes according to the hydrochemical characteristics of groundwaters. *J. Hydrol.* **2005**, *307*, 1–16.

51. Fan, A.M.; Steinberg, V.E. Health implications of nitrate and nitrite in drinking water: An update on methemoglobinemia occurrence and reproductive and developmental toxicity. *Regul. Toxicol. Pharmacol.* **1996**, *23*, 35–43.

CHAPTER 9

9.0 Implication of the study on the current status of SDG 6 in Sub-Saharan Africa

9.1 Introduction

Sustainable development goals remain at the top of the United Nations' list with much focus on the developing world across the Asian and African continents. Goal 6 is one of most important objectives of this which is set to ensure access to clean water and sanitation with key elements present in Figure 9.1. This is based on believe that access to clean water will ensure healthy society and consequently promote regional and global economic growth. Recent reports acknowledged the significant progress made in some of these countries. Despite this progress, billions of people still lack safe water, sanitation and basic handwashing facilities which implies the need to double the current rate of progress for universal access to basic sanitation service by 2030 to be achieved (United Nations, 2019). Efficient use and management of water are critical to addressing the growing demand for water with numerous challenges threatening global water resources. Relevant information and data on groundwater resources are necessary to develop an inclusive water resources management strategy. This information will be able to quantitatively and qualitatively evaluate the threats to water security and the increasing frequency and severity of droughts and floods resulting from climate change across developing countries especially those in Sub-Saharan Africa where there is the problem of paucity of data on water quantity and quality. With forces such as climate change, population growth, pollution and competition for resources intensifying, the need to develop solutions to ensure clean

and accessible water has never been more urgent. This study on groundwater chemistry of the shallow aquifer of the Eastern Dahomey Basin has helped in contributing information and data regarding the link between the natural and anthropogenic drivers on the groundwater resources of a coastal aquifer in part of West Africa.

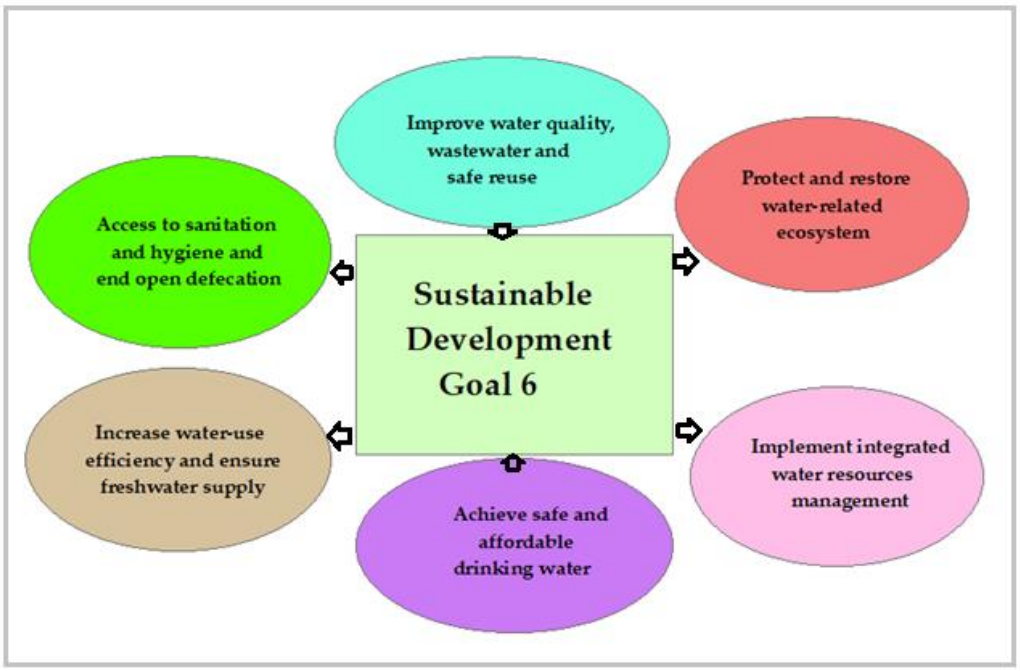

Figure 9.1 Key Elements of Sustainable development goal 6 (SDG6)

9.2 Overview of integrated water resources management in Nigeria

In compliance with the global best practice of Integrated Water Resource Management (IWRM), Nigeria's water resources management policy was reviewed in 2014 in line with JICA, (2004) to achieve Sustainable Development Goals 6 (SDG6). The structural framework constitutes different action plans such as water safety plan (WSP) and Hydrological Areas, among many others. The National Water Resource Institute (NWRI) was also established with other inter-agencies to create a framework for water resource management with the mandate of providing safe and sustainable drinking water to all.

However, the implementation of these new policies has been facing numerous challenges. These challenges include lack of enforcement, inconsistent policies, absence of local inclusion, inadequate funding and lack of transparent management practice, and weak political commitment, among others (Akpabio, 2007; David Omole, 2014; and Jideonwo, 2014). The rapid transformation in the agricultural and industrial sector, as well as urbanisation in the coastal areas of Nigeria, requires a proper education and policy enforcement to protect groundwater resource which is all lacking in the IWRM policy in Nigeria. This accounts for the low rating score for Nigeria's status audit for SDGs achievement.

9.3 Key findings and implication for SDG6 status in Nigeria

The findings of this study, therefore, established the basis for understanding the impacts of land use pattern and changes on IWRM. Groundwater contamination from urban settlements, agricultural and industrial waste within Eastern Dahomey Basin are evidence of possible implications from unregulated waste disposal practice on the shallow groundwater aquifers which harbour freshwater resources of the basin. Results of water quality index assessment in this study show a high concentration of nitrates beyond the highest permissible limit of WHO standard (WHO, 2006) for drinking water which also confirmed possible agricultural and municipal waste impact. The deterioration in groundwater quality revealed a justification for the said set-back for Nigeria on the mandate of achieving the SDG6. The trend identified in this study shows that IWRM of the Eastern Dahomey Basin requires effective and inclusive strategies to achieve sustainable groundwater management.

This study, therefore, suggests that an integrated inter-agency approach through an effective waste management practice should be employed to curtail the

indiscriminate discharge of effluent and solid waste into drainages, rivers and farms within cities. Modern waste recycling plant “waste to wealth” should be employed for effective waste management. An incentive-driven approach to waste management could be used to encourage local communities and motivate their commitment to waste collections. This will promote a cleaner environment and also empower the locals as a strategy to reduce poverty and hunger. Use of pure organic fertiliser in farming, especially along flood plains and wetland in the study area should be encouraged to minimise contamination of surface and groundwater with nitrate, pesticides and herbicides. Finally, enforcement of IWRM policies through penalties should be implemented against any individual and group whose action or inaction negatively impacts the watershed which will, on the other hand, create investment and employment opportunities for locals, improve the wellbeing of people and reduce the cost of health management by the government.

CHAPTER 10

10.0 Conclusion and Recommendations

10.1 Restatement of Research Aim and Objectives

This study employed integrated hydrogeological concepts which have proven effective in groundwater studies in other coastal basins around the world, to assess the hydrogeochemistry of the shallow coastal aquifers of the Eastern Dahomey Basin. This work is necessary for bulking up the amount of hydrogeological data and information available for sustainable groundwater resource management in West African countries. At the conclusion of the research, the following objectives were achieved to accomplish the research aim:

1. Effectiveness of electrical conductivity (EC) in combination with some groundwater quality indices and ionic ratios as a hydrochemical tool for prilimnary studies of fingerprints of salinity and other groundwater quality parameters in shallow coastal aquifers of Eastern Dahomey Basin.
2. Characterised the Hydrostratigraphic units of the shallow coastal aquifers of the Eastern Dahomey Basin with focus on origin and distribution of saltwater intrusion into the coastal freshwater aquifer using a physicochemical approach through the electrical conductivity and geophysical method of Electrical Resistivity Tomography (ERT), Induced Polarisation (IP) complemented with borehole logs.
3. Identified the main Hydrogeochemical processes that control groundwater chemistry across the Eastern Dahomey Basin using GIS and interpolation techniques.
4. Evaluated groundwater chemistry variations across different geological units and formation within the basin using stable environmental isotopes of $\delta^{18}O$ and $\delta^{2}D$ in

combination with key hydrochemical parameters as contribution to the groundwater conceptual model.

5. Assessed the impact of land use on groundwater quality in the EDB using the groundwater quality index and statistical analysis for various water usage.
6. Assessed the impacts of climate change through flooding on groundwater quality of the shallow coastal groundwater of the Eastern Dahomey basin, using variations of

10.2 Conclusion and summary

The following statements therefore summarise the conclusion of the study:

1. Results of HFE-D, Ionic ratios, SMI and GQIswi further identified mixed groundwater of Na+Ca-HCO3 and Na-Cl as dominant water. The relationship among some critical groundwater quality parameters such as Na^{+}, Ca^{2+}, Mg^{2+}, Cl^{-}, HCO_3^{-} and SO_4^{2-} and EC through Pearson correlation analysis revealed the influence of seawater intrusion in some of the water samples from wells that are relatively deeper and located within the proximity of the coastline of Seme, Lekki, Eleko, Okun-Ajjah, Ode-Mahin and Igbokoda. Mixed water type around the alluvium deposits signifies the anthropogenic influence of industrial and municipal effluent. Spatial distribution of groundwater revealed freshening, which increases inland from the coastline towards the northern part of the basin.
2. The results of the ERT and IP revealed intercalation of sand and clay underlying the coastal area. However, the maximum depth delineated along the traverses are 105m and 118 m from which 3 to 4 geoelectrical layers were mapped from which the resistivity and chargeability values indicated lateritic topsoil, unconsolidated sand, sandy clay/ clayey sandy, fine grain sand with clay lenses. Unconsolidated sands at the top constitute the unconfined aquifer which is underlain in most areas by sandy clay /

clayey sand which serves as a semi-aquifer unit with depth ranges between 13m and 45 m while the third layer represents the fine-grained sands with clay lenses in some areas which characterised the Ondo-State axis of the coast. The results reveal the clay lenses in the second and third layers, which could be the trap of saltwater attributed to evaporite deposited within the basin during the ancient transgression and regression that produced deposition sediments. Some clay lenses suspected to contain saltwater also were delineated under the sections in Lakowe while thick sandy aquifer with an average thickness of 25 m saturated with saline water was observed in the Okun-Ajjah profile sections. There is a thin layer of freshwater overlying this unit which is the source of freshwater recharging the shallow wells less than 20 m deep. This layer is highly vulnerable and sensitive to saline water intrusion if groundwater exploitation exceeds the current state. Finally, the methods used have identified two possible sources of saltwater intrusion into the coastal freshwater aquifer of the basin; namely dissolution of evaporite/salt lenses within the clay layer and direct (flow boundary) connection between the sea and the coastal aquifer in areas very close to the sea due to lack of hydraulic boundary.

3. The relative concentrations of the ions occur in the order of Na>K>Ca>Mg and Na>Ca >Mg>K, while anions are in order of HCO_3 >Cl>SO_4 and Cl>SO_4>HCO_3 for both wet and dry seasons respectively. In the multi-aquifer of the EDB, mineral dissolution from the rock weathering, precipitation and evaporation seems to be the major hydrogeochemical processes controlling the concentration of major ions in groundwater. Calcite, dolomite and aragonite have high SI values in some locations especially the area are underlain by limestone and other carbonate rocks, which indicates the influence of precipitation as the result of evaporation, whereas gypsum and anhydrite saturation in areas within coastal sands and alluvium deposits could be

due to the influence of evaporite dissolution. The hydrochemical types in the area can be divided into two major groups. The first group includes mixed Na–Cl, Ca-HCO_3 and Ca–Cl types in both wet and dry seasons, which indicate recent meteoric water in contact with atmospheric CO_2 and water at the intermediate zone of groundwater discharge area which influences rocks mineral dissolution and possible sea spraying due to proximity to the ocean. The other class of water comprises mixed Na–HCO_3, Na-SO_4, Ca-SO_4, K-Cl, K-SO_4 and Mg–HCO_3 types, indicating the groundwater recharge areas within the basin. The stable isotopes analysis from $\delta D/\delta^{18}O$ showed recent groundwater with precipitation having a significant influence on the chemistry of water samples from the wet season from a wide range of clustering along the local meteoric water line (LMWL) and almost on the global meteoric water line (GMWL) with much depletion in their isotopic composition of both δD and $\delta^{18}O$. In the case of water samples from the wet season, the plots displayed a short range of cluster along the water lines which indicates relative influence of evaporation and effect of seasonal variation with accompanying enrichment of δD and $\delta^{18}O$ composition.

4. The relationship between the TDS and $\delta^{18}O$ further agreed with this by displaying samples clustering between the recharge and evaporation zone. Comparing the results with the regional precipitation data from the selected station of GNIP at Douala (Cameroon), Cotonou (Republic of Benin) and Kano (Nigeria) showed young water recharge with short residence time with little influence of evapotranspiration which is associated with higher static water level and humidity, hence little $\delta^{18}O$ enrichment.
5. Land-use was found to have an adverse effect on groundwater quality, especially in shallow coastal aquifers where the water level is relatively high. In this study, a combination of groundwater quality index (GWQI) and land use pattern map has demonstrated effectiveness tracking groundwater quality. Correlating the spatial

distribution map of the GWQI for both seasons with the land use pattern map of the area revealed poor to none potable water clustered more in the settlement, agricultural area and along flood plains where planting is taking place throughout the year. This distribution signifies the groundwater water quality has been impacted by municipal, industrial and agricultural waste within the EDB.

6. The generalized Eh-pH diagram revealed groundwater of the study area is within the transitional (aerobic to anaerobic) phase of the geochemical thermodynamics. It also revealed that nitrate is a dominant species in the groundwater from both wet and dry seasons, while iron occurrence is restricted to the alluvium and coastal plain sands aquifer. Spatial distribution maps of SO_4^{2-}, NO_3^-, Fe, and Mn revealed higher concentrations within the Alluvium and Coastal Plain Sands aquifer and some wells with the river flood plains of the basin. This study also revealed that the reduction in concentration and nutrient enrichment of groundwater with the increase in well depth could be attributed to the loss of aeration and possible natural attenuation by the soil and aquifer medium. The linear regression model using both Eh and pH as independent variables against other selected variables such as EC, salinity, SO_4^{2-}, Cl^-, NO_3^-, Fe, and Mn for both season groundwater samples established predictability for both Eh and pH. A possible indication of ions and metals enrichment in groundwater resulting from the effect of seasonal flooding. This enrichment rendered some of the sampled groundwater unsuitable for drinking as the concentration of some of the water quality parameters were above the WHO standard for drinking water. Accumulation could lead to severe contamination of surface and groundwater and render it not potable for drinking or other purposes.

This study recommends policy and management framework review and enhancements for proper waste management to support SDG planning for sustainable

groundwater resource management in the Eastern Dahomey Basin that limits further contamination of the coastal groundwater system in the face of seasonal flooding, remarkably as predictions suggest more extreme precipitation in the future resulting from climate change.

10.3 Overall impact of the research

This finding has justified the need for investment in research geared towards groundwater resilience in the wake of challenges of climate change which will possibly increase precipitations shortly with more seasonal flooding., systematic waste disposal system, well-engineered sanitary plants and proper drainage system (Ecological control) with a regular and periodic groundwater monitoring system are required for sustainable groundwater resources management in the EDB.

10.4 Recommendation

From the findings of this study, the following recommendation will be helpful to government, NGOs, water professionals and researchers for action and further research:

1. This study founded two scenarios of saltwater intrusion within the 5 km from the coastline of the eastern Dahomey Basin. (a) The saltwater intrusion into the sands aquifer around Lekki, and Okun-Ajjah which are thought to be driven by higher groundwater abstraction and (b) the saltwater trapped in clay lenses within the sandy clay around Lakwe, Igbokoda and Ugbonla. This suggest the need for a proactive measure such as well-representative monitoring wells for regular salinity and relevant physicochemical parameters to ensure early detection of elevated salinity in the coastal area of the basin.

2. With a complex geology in this basin, groundwater was actually based on the existing private wells which largely controlled the sampling pattern. There is need for the government and NGOs to coordinate more boreholes to ensure better sampling spread which could help in improving the quality and coverage of the future hydrogeological research.
3. This has established the connection between the groundwater quality and the climate change-driven flood. There is need for an ecological control that prevent wastewater from the drainages to interact with groundwater, while a well-engineered waste disposal system is required to curtail the indiscriminate municipal waste practice and free waste from river and drainage channels.
4. There is need for 'WASH' education incorporated into the curriculum of the elementary schools and colleges to spread awareness on the important of a clean environment to groundwater protection.
5. Finally, there is need for review of the current Integrated water resources management (IWRM) framework to engage urban planner to ensure agricultural and industrial locations are sited to ensure watershed protection across the basin. Sustainable

10.5 Research Contribution to Knowledge and Future Research

The Hydrochemical evaluation identified the natural variations and changes which are intrinsic to coastal areas, as well as the current alterations resulting from human impacts from urbanisation, agriculture and industrialisation especially around the major cities within the basin. These findings may be valuable for achieving sustainable use of coastal ecosystems in Eastern Dahomey Basin. The future research is suggested to focus on groundwater modelling in relation to saltwater intrusion and contaminants transport with the shallow aquifer to be able to accurately predict

travelling and resident time of possible contaminants and develop a full conceptual hydrogeology model for a sustainable groundwater resources management of the Basin.

REFERENCE

Abdulrahman, A., Nawawi, M., Saad, R., Abu-Rizaiza, A.S., Yusoff, M.S., Khalil, A.E., Ishola, K.S., 2016. Characterization of active and closed landfill sites using 2D resistivity/IP imaging: case studies in Penang, Malaysia. Environ. Earth Sci. 75, 1–17. https://doi.org/10.1007/s12665-015-5003-5

Abimbola, A. F., Tijani M. N and Nurudeen, A., 1999. Some aspect of groundwater quality assessment of Abeokuta. J. Min. Geol. 32, 23–32.

Adegbola, R., Oseni, S., Majolagbe, A., 2013. The Impact Assessment of Oil Spillage and Trace Metal Assessment on Groundwater in Baruwa, Lagos Southwest and Nigeria. Int. Sci. Investig. J. 2, 12–32.

Adeoti, L., Alile, O.M., Uchegbulam, O., 2010. Geophysical investigation of saline water intrusion into freshwater aquifers: A case study of Oniru, Lagos State. Sci. Res. Essays 5, 248–259.

Adepelumi, A.A., Ako, B.D., Ajayi, T.R., Afolabi, O., Omotoso, E.J., 2009. Delineation of saltwater intrusion into the freshwater aquifer of Lekki Peninsula, Lagos, Nigeria. Environ. Geol. 56, 927–933. https://doi.org/10.1007/s00254-008-1194-3

Adimalla, N., 2019. Controlling factors and mechanism of groundwater quality variation in semiarid region of South India: an approach of water quality index (WQI) and health risk assessment (HRA). Environ. Geochem. Health 18–19. https://doi.org/10.1007/s10653-019-00374-8

Adimalla, N., Kumar, A., 2020. Hydrogeochemical investigation of groundwater quality in the hard rock terrain of South India using Geographic Information System (GIS) and groundwater quality index (GWQI) techniques. Groundw. Sustain. Dev. 10.

Ahmed, N., Bodrud-Doza, M., Towfiqul Islam, A.R.M., Hossain, S., Moniruzzaman, M., Deb, N., Bhuiyan, M.A.Q., 2019a. Appraising spatial variations of As, Fe, Mn and NO

3 contaminations associated health risks of drinking water from Surma basin, Bangladesh. Chemosphere. https://doi.org/10.1016/j.chemosphere.2018.11.104

Ahmed, N., Reza, A., Hossain, S., Deb, N., Quaiyum, A., 2019b. Appraising spatial variations of As , Fe , Mn and NO 3 contaminations associated health risks of drinking water from Surma basin , Bangladesh. Chemosphere 218, 726–740. https://doi.org/10.1016/j.chemosphere.2018.11.104

Akinbinu, V.A., 2015. Delineation of saline water intrusion to safe-guide inland groundwater resources. Ocean Coast. Manag. 116, 162–168. https://doi.org/10.1016/j.ocecoaman.2015.07.005

Ako, A.A., Shimada, J., Hosono, T., Ichiyanagi, K., Nkeng, G.E., Eyong, G.E.T., Roger, N.N., 2012. Hydrogeochemical and isotopic characteristics of groundwater in Mbanga, Njombe and Penja (Banana Plain) - Cameroon. J. African Earth Sci. 75, 25–36. https://doi.org/10.1016/j.jafrearsci.2012.06.003

Al-Charideh, A., Kattaa, B., 2016. Isotope hydrology of deep groundwater in Syria: renewable and non-renewable groundwater and paleoclimate impact. Hidrol. isotópica del agua subterránea profunda en Siria agua subterránea Renov. y no Renov. e impacto paleoclimático. 24, 79–98. https://doi.org/10.1007/s10040-015-1324-4

Avrahamov, N., Yechieli, Y., Lazar, B., Lewenberg, O., Boaretto, E., Sivan, O., 2010. Characterization and dating of saline groundwater in the Dead Sea area. Radiocarbon 52, 1123–1140.

Ayolabi, E. a, Folorunso, A.F., Odukoya, A.M., Adeniran, A.E., 2013. Mapping saline water intrusion into the coastal aquifer with geophysical and geochemical techniques : the University of Lagos campus case (Nigeria). Springer plus 2, 1–14. https://doi.org/10.1186/2193-1801-2-433

Ayolabi, Elijah A, Enoh, I.J.E., Folorunso, A.F., 2013. Engineering Site Characterisation

Using 2-D and 3-D Electrical Resistivity Tomography. Earth Sci. Res. 2. https://doi.org/10.5539/esr.v2n1p133

Ayolabi, E.A., Epelle, E.S., Lucas, O.B., Ojo, A., 2014. Geophysical and geochemical site investigation of eastern part of Lagos metropolis, southwestern Nigeria. Arab. J. Geosci. 8, 7445–7453. https://doi.org/10.1007/s12517-014-1688-0

Ayolabi, Elijah Adebowale, Folorunso, A.F., Kayode, O.T., 2013. Integrated Geophysical and Geochemical Methods for Environmental Assessment of Municipal Dumpsite System. Int. J. Geosci. 4, 850–862. https://doi.org/10.4236/ijg.2013.45079

Ayolabi, E.A., Oyelayo, F.J., 2005. Geophysical and hydrochemical assessment of groundwater pollution due to a dumpsite in Lagos state, Nigeria. J. Geol. Soc. India 66, 617–622.

Babanyara, Y.Y., Usman, H.A., Saleh, U.F., 2010. An Overview of Urban Poverty and Environmental Problems in Nigeria. J. Hum. Ecol. 31, 135–143.

Banu, Z., Chowdhury, M.S.A., Hossain, M.D., Nakagami, K., 2013. Contamination and Ecological Risk Assessment of Heavy Metal in the Sediment of Turag River, Bangladesh: An Index Analysis Approach. J. Water Resour. Prot. 05, 239–248. https://doi.org/10.4236/jwarp.2013.52024

Bauer-Gottwein, P., Gondwe, B.N., Christiansen, L., Herckenrath, D., Kgotlhang, L., Zimmermann, S., 2010. Hydrogeophysical exploration of three-dimensional salinity anomalies with the time-domain electromagnetic method (TDEM). J. Hydrol. 380, 318–329. https://doi.org/10.1016/j.jhydrol.2009.11.007

Biswas, A.K., Tortajada, C., 2019. Water quality management: a globally neglected issue. Int. J. Water Resour. Dev. 35, 913–916. https://doi.org/10.1080/07900627.2019.1670506

Bodrud-Doza, M., Bhuiyan, M.A.H., Islam, S.M.D.U., Rahman, M.S., Haque, M.M.,

Fatema, K.J., Ahmed, N., Rakib, M.A., Rahman, M.A., 2019. Hydrogeochemical investigation of groundwater in Dhaka City of Bangladesh using GIS and multivariate statistical techniques. Groundw. Sustain. Dev. https://doi.org/10.1016/j.gsd.2018.11.008

Bouzourra, H., Bouhlila, R., Elango, L., Slama, F., Ouslati, N., 2015. Characterization of mechanisms and processes of groundwater salinization in irrigated coastal area using statistics, GIS, and hydrogeochemical investigations. Environ. Sci. Pollut. Res. 22, 2643–2660. https://doi.org/10.1007/s11356-014-3428-0

Buselli, G., Lu, K., 2001. Groundwater contamination monitoring with multichannel electrical and electromagnetic methods. J. Appl. Geophys. 48, 11–23. https://doi.org/10.1016/S0926-9851(01)00055-6

Oli I. C., Okeke O. C., Abiahu C. M. G., Anifowose F. A. and Fagorite V. I., 2019. A Review of the Geology and Mineral Resources of Dahomey Basin , Southwestern Nigeria. Iternational J. Environ. Sci. Nat. Resour. 21, 556055. https://doi.org/10.19080/IJESNR.2019.21.556055

C. P. Kumar, 2014. Management of groundwater in salt water ingress coastal aquifers. Natl. Inst. Hydrol. 3, 16–25. https://doi.org/10.5923/j.geo.20110101.02

Cann, K.F., Thomas, D.R., Salmon, R.L., Wyn-Jones, A.P., Kay, D., 2013. Extreme water-related weather events and waterborne disease. Epidemiol. Infect. 141, 671–686. https://doi.org/10.1017/S0950268812001653

Cary L., Petelet-Giraud E., Bertrand G., Kloppmann W., Aquilina L., Martins V., Hirata R., Montenegro S., Pauwels H., Chatton E., Franzen, M. and Aurouet A., 2015. Origins and processes of groundwater salinization in the urban coastal aquifers of Recife (Pernambuco, Brazil): A multi-isotope approach. Sci. Total Environ. 530–531, 411–429. https://doi.org/10.1016/j.scitotenv.2015.05.015

Chang, S.W., Clement, T.P., Simpson, M.J., Lee, K.K., 2011. Does sea-level rise have an impact on saltwater intrusion? Adv. Water Resour. 34, 1283–1291. https://doi.org/10.1016/j.advwatres.2011.06.006

Chukwura, U.O., Udom, G.J., Cuthbert, S.J., Hursthouse, A.S., 2015. Evaluation of hydrochemical characteristics and flow directions of groundwater quality in Udi Local Government Area Enugu State, Nigeria. Environ. Earth Sci. 73, 4541–4555. https://doi.org/10.1007/s12665-014-3741-4

Cimino, A., Cosentino, C., Oieni, A., Tranchina, L., 2008. A geophysical and geochemical approach for seawater intrusion assessment in the Acquedolci coastal aquifer (Northern Sicily). Environ. Geol. 55, 1473–1482. https://doi.org/10.1007/s00254-007-1097-8

Coode Blizard Ltd, Akute Geo-Resource Ltd and Rofe, K.& L.L., 1996. Hydrogeological investigation of Lagos State. Final Rep. to Lagos State Water Corp. Volumes 1.

de Franco, R., Biella, G., Tosi, L., Teatini, P., Lozej, A., Chiozzotto, B., Giada, M., Rizzetto, F., Claude, C., Mayer, A., Bassan, V., Gasparetto-Stori, G., 2009. Monitoring the saltwater intrusion by time lapse electrical resistivity tomography: The Chioggia test site (Venice Lagoon, Italy). J. Appl. Geophys. 69, 117–130. https://doi.org/10.1016/j.jappgeo.2009.08.004

Di Maio, R., Fabbrocino, S., Forte, G., Piegari, E., 2013. A three-dimensional hydrogeological–geophysical model of a multi-layered aquifer in the coastal alluvial plain of Sarno River (southern Italy). Hydrogeol. J. 22, 691–703. https://doi.org/10.1007/s10040-013-1087-8

Doug Linzey, 2011. Saltwater Intrusion and Climate Change: A primer for local and provincial decision-makers 1–26.

Duran-Encalada, J.A., Paucar-Caceres, A., Bandala, E.R., Wright, G.H., 2017. The impact

of global climate change on water quantity and quality: A system dynamics approach to the US–Mexican transborder region. Eur. J. Oper. Res. https://doi.org/10.1016/j.ejor.2016.06.016

Ebrahimi, M., Kazemi, H., Ehtashemi, M., Rockaway, T.D., 2016. Assessment of groundwater quantity and quality and saltwater intrusion in the Damghan basin, Iran. Chemie der Erde - Geochemistry 76, 227–241. https://doi.org/10.1016/j.chemer.2016.04.003

Edet, A., 2019. Seasonal and spatio-temporal patterns, evolution and quality of groundwater in Cross River State, Nigeria: implications for groundwater management. Sustain. Water Resour. Manag. 5, 667–687. https://doi.org/10.1007/s40899-018-0236-6

Edet, A., 2016. Hydrogeology and groundwater evaluation of a shallow coastal aquifer, southern Akwa Ibom State (Nigeria). Appl. Water Sci. https://doi.org/10.1007/s13201-016-0432-1

Edet, A.E., Merkel, B.J., Offiong, O.E., 2003. Trace element hydrochemical assessment of the Calabar Coastal Plain Aquifer, southeastern Nigeria using statistical methods. Environ. Geol. 44, 137–149. https://doi.org/10.1007/s00254-002-0738-1

Faleye, E.T., Olorunfemi, 2015. Aquifer Characterization and Groundwater Potential Assessment of the Sedimentary Basin of Ondo State 1 2. Ife J. Sci. 17, 429–439.

Fatoba, J.O., Omolayo, S.D., Adigun, E.O., 2014. Using geoelectric soundings for estimation of hydraulic characteristics of aquifers in the coastal area of Lagos , southwestern Nigeria. Int. Lett. Nat. Sci. 11, 30–39. https://doi.org/10.18052/www.scipress.com/ILNS.11.30

Francés, A.P., Ramalho, E.C., Fernandes, J., Groen, M., Hugman, R., Khalil, M.A., De Plaen, J., Monteiro Santos, F.A., 2015. Contributions of hydrogeophysics to the hydrogeological conceptual model of the Albufeira-Ribeira de Quarteira coastal

aquifer in Algarve, Portugal. Hydrogeol. J. 23, 1553–1572. https://doi.org/10.1007/s10040-015-1282-x

Gattacceca, J.C., Vallet-Coulomb, C., Mayer, A., Claude, C., Radakovitch, O., Conchetto, E., Hamelin, B., 2009. Isotopic and geochemical characterization of salinization in the shallow aquifers of a reclaimed subsiding zone: The southern Venice Lagoon coastland. J. Hydrol. 378, 46–61. https://doi.org/10.1016/j.jhydrol.2009.09.005

Giambastiani, B.M.S., Antonellini, M., Oude Essink, G.H.P., Stuurman, R.J., 2007. Saltwater intrusion in the unconfined coastal aquifer of Ravenna (Italy): A numerical model. J. Hydrol. 340, 91–104. https://doi.org/10.1016/j.jhydrol.2007.04.001

Gime´nez-Forcada, E., 2014. Space/time development of seawater intrusion: A study case in Vinaroz coastal plain (Eastern Spain) using HFE-Diagram, and spatial distribution of hydrochemical facies. J. Hydrol. 517, 617–627. https://doi.org/10.1016/j.jhydrol.2014.05.056

Giménez-Forcada, E., Bencini, A., Pranzini, G., 2010. Hydrogeochemical considerations about the origin of groundwater salinization in some coastal plains of Elba Island (Tuscany, Italy). Environ. Geochem. Health 32, 243–257. https://doi.org/10.1007/s10653-009-9281-2

Günther, T., Dlugosch, R., 2010. Aquifer characterization using coupled inversion of DC/IP and MRS data on a hydrogeophysical test-site. 23rd EEGS Symp. … 302–307. https://doi.org/doi:10.4133/1.3445447

Harcourt, P., Amadi, C.A., 2012. Investigation of Aquifer Quality in Bonny Island , Eastern Niger Delta , Nigeria using Geophysical and Geochemical Techniques Department of Geology , Federal University of Technology , 3, 183–187.

Hashmi, M.Z., Yu, C., Shen, H., Duan, D., 2014. Concentrations and Human Health Risk Assessment of Selected Heavy Metals in Surface Water of the Siling Reservoir

Watershed in Zhejiang Province , China. Pol. J. Environ. Stud. 23, 801–811.

He, J., Ma, J., Zhao, W., Sun, S., 2015. Groundwater evolution and recharge determination of the Quaternary aquifer in the Shule River basin, Northwest China. Hydrogeol. J. 23, 1745–1759. https://doi.org/10.1007/s10040-015-1311-9

He, J., Ma, J., Zhao, W., Sun, S., n.d. Groundwater evolution and recharge determination of the Quaternary aquifer in the Shule River basin, Northwest China.

Helena, B., Pardo, R., Vega, M., Barrado, E., Fernandez, J.M., Fernandez, L., 2000. Temporal evolution of groundwater composition in an alluvial aquifer (Pisuerga River, Spain) by principal component analysis. Water Res. 34, 807–816. https://doi.org/10.1016/S0043-1354(99)00225-0

Hiyama, T., Babiker, I.S., Mohamed, M.A.A., 2014. Groundwater as a Key for Adaptation to Changing Climate and Society, Groundwater as a Key for Adaptation to Changing Climate and Society. https://doi.org/10.1007/978-4-431-54968-0

Hodlur, G.K., Dhakate, R., Andrade, R., 2006. Correlation of vertical electrical sounding and borehole-log data for delineation of saltwater and freshwater aquifers. Geophysics 71, G11. https://doi.org/10.1190/1.2169847

Igboekwe, M.U., Chukwu, G.U., Okengwu, K.O., 2012. Hydrogeophysical Delineation and Hydrogeochemical Characterization of the Aquifer Systems in Umuahia-South Area , 2, 406–432.

Isa, N.M., Aris, A.Z., 2015. Identification of Saltwater Intrusion/Assessment Scheme in Groundwater Using the Role of Empirical Knowledge. Procedia Environ. Sci. 30, 291–296. https://doi.org/10.1016/j.proenv.2015.10.052

Jones, H. A and Hockey, R.., 1964. The Geology of part of Southwestern Nigeria. GSN Bull. No. 31-10.

K. F. CANN, D. RH.THOMAS,R. L. SALMON, A.P.W.-J.A.D.K., 2019. Extreme water-

related weather events and waterborne disease. J. Epidemiol. Infect. 141, 671–686. https://doi.org/10.1017/S0950268812001653

Kalin, R.M., 1995. Basic concepts and formulations for isotope-geochemical process investigations, procedures and methodologies of geochemical modelling of groundwater systems, in: Y Yurtsever (Ed.), Manual on Mathematical Models in Isotope Hydrology. IAEA TECHDOC 910, Viena, pp. 155–206.

Kasei, R.A., 2009. Modelling impacts of climate change on water resources in the Volta Basin , West Africa. PhD Diss. Rheinischen Friedrich-Wilhelms-Universität Bonn.

Khalil, M.H., 2006. Geoelectric resistivity sounding for delineating salt water intrusion in the Abu Zenima area, west Sinai, Egypt. J. Geophys. Eng. 3, 243. https://doi.org/10.1088/1742-2132/3/3/006

Kirsch, R., 2011. Groundwater Geophysics: A Tool for Hydrogeology, Environmental and Engineering Geoscience. https://doi.org/10.2113/gseegeosci.17.1.96

Kouzana, L., Benassi, R., Ben mammou, A., Sfar felfoul, M., 2010. Geophysical and hydrochemical study of the seawater intrusion in Mediterranean semi arid zones. Case of the Korba coastal aquifer (Cap-Bon, Tunisia). J. African Earth Sci. 58, 242–254. https://doi.org/10.1016/j.jafrearsci.2010.03.005

Krishnaraj, S., Murugesan, V., K, V., Sabarathinam, C., Paluchamy, A., Ramachandran, M., 2012. Use of Hydrochemistry and Stable Isotopes as Tools for Groundwater Evolution and Contamination Investigations. J. Geo-sciences 1, 16–25. https://doi.org/10.5923/j.geo.20110101.02

Land, L.A., Lautier, J.C., Wilson, N.C., Chianese, G., Webb, S., 2004. Geophysical Monitoring and Evaluation of Coastal Plain Aquifers. Ground Water 42, 59–67. https://doi.org/10.1111/j.1745-6584.2004.tb02450.x

Lapworth1, L.J., & & D.C.W.N.& J.O.-O.& S.P.& M.E.S., Tijani5, M.N., Wright6, & J.,

2018. Urban groundwater quality in sub-Saharan Africa: current status and implications for water security and public health. Arab. J. Geosci. 8, 290. https://doi.org/10.1007/978-3-319-58538-3_20-1

Longe, E.O., 2011. Groundwater Resources Potential in the Coastal Plain Sands Aquifers , Lagos , Nigeria 3, 1–7.

Longe, E.O., Malomo, S., Olorunniwo, M.A., 1987. Hydrogeology of Lagos metropolis. J. African Earth Sci. 6, 163–174. https://doi.org/10.1016/0899-5362(87)90058-3

McInnis, D., Silliman, S., Boukari, M., Yalo, N., Orou-Pete, S., Fertenbaugh, C., Sarre, K., Fayomi, H., 2013. Combined application of electrical resistivity and shallow groundwater sampling to assess salinity in a shallow coastal aquifer in Benin, West Africa. J. Hydrol. 505, 335–345. https://doi.org/10.1016/j.jhydrol.2013.10.014

Mi, L., Xiao, H., Zhang, J., Yin, Z., Shen, Y., 2016. Evolution of the groundwater system under the impacts of human activities in middle reaches of Heihe River Basin (Northwest China) from 1985 to 2013. Hydrogeol. J. 24, 971–986. https://doi.org/10.1007/s10040-015-1346-y

Mohanty, A.K., Rao, V.V.S.G., 2019. Catena Hydrogeochemical , seawater intrusion and oxygen isotope studies on a coastal region in the Puri District of Odisha , India. Catena 172, 558–571. https://doi.org/10.1016/j.catena.2018.09.010

Narany, T.S., Ramli, M.F., Aris, A.Z., Nor, W., Sulaiman, A., Juahir, H., Fakharian, K., 2014. Identification of the Hydrogeochemical Processes in Groundwater Using Classic Integrated Geochemical Methods and Geostatistical Techniques , in Amol-Babol Plain , Iran. Sci. World J. 2014, 1–15.

Newman, B.D., Land, L., Phillips, F.M., Rawling, G.C., 2016. The hydrogeology of the Sacramento Mountains and Roswell and Salt basins of New Mexico, USA: overview of investigations on dryland groundwater systems using environmental tracers and

geochemical approaches. Hydrogeol. J. 24, 753–756. https://doi.org/10.1007/s10040-016-1404-0

Nistor, M.-M., Dezsi, Ş., Cheval, S., Baciu, M., 2016. Climate change effects on groundwater resources: a new assessment method through climate indices and effective precipitation in Beliş district, Western Carpathians. Meteorol. Appl. 23, 554–561. https://doi.org/10.1002/met.1578

Nowroozi, A.A., Horrocks, S.B., Henderson, P., 1999. Saltwater intrusion into the freshwater aquifer in the eastern shore of Virginia: A reconnaissance electrical resistivity survey. J. Appl. Geophys. 42, 1–22. https://doi.org/10.1016/S0926-9851(99)00004-X

Nwankwo, C.N., Emujakporue, G.O., 2012. Geophysical Method of Investigating Groundwater and Sub-Soil Contamination – A Case Study. Am. J. Environ. Eng. 2, 49–53. https://doi.org/10.5923/j.ajee.20120203.02

Nwankwoala, H.O., 2011. Coastal aquifers of nigeria : an overview of its management and sustainability considerations. J. Appl. Technol. Environ. Sanit. 1, 371–380.

Nwankwoala, S.A.N. and H.O., 2013. Salinity Dynamics : Trends and Vulnerability of Aquifers to Contamination in the Niger Delta. Compr. J. Environ. Earth Sci. 2, 18–25.

Odukoya, A.M., Folorunso, A.F., Ayolabi, E.A., Adeniran, E.A., 2013. Groundwater Quality and Identification of Hydrogeochemical Processes within University of Lagos , Nigeria. J. Water Resour. Prot. 5, 930–940. https://doi.org/10.4236/jwarp.2013.510096

Odunaike, R.K., Laoye, J.A., Fasunwon, O.O., Ijeoma, G.C., Akinyemi, L.P., 2010. Geophysical mapping of the occurrence of shallow oil sands in Idiopopo at Okitipupa area , South-western Nigeria 4, 34–44.

Ofomola, M.O., 2015. Integrated Geophysical and Hydrogeochemical Studies of Shallow

Aquifer Contamination in Osubi , Near Warri ,. J. Earth Sci. Geotech. Eng. 5, 79–102.

Ojolowo, S., Wahab, B., 2017. Municipal solid waste and flooding in Lagos metropolis , Nigeria : Deconstructing the evil nexus. J. Geogr. Reg. Plan. Full 10, 174–185. https://doi.org/10.5897/JGRP2016.0614

Omosuyi, G.O., Ojo, J.S., Olorunfemi, M.O., 2008. Geoelectric Sounding to Delineate Shallow Aquifers in the Coastal Plain Sands of. Pacific J. Sci. Technol. 9, 62–77.

Oteri, A.U., & Atolagbe, F.P., 2003. Saltwater Intrusion into Coastal Aquifers in Nigeria, in: The Second International Conference on Saltwater Intrusion and Coastal Aquifers — Monitoring, Modeling, and Management. Mérida, Yucatán, México, March 30 - April 2, 2003. Merida Yucatan, pp. 1–15.

Oteri, A.U., 1991. Geophysical investigations of sea water intrusion into the Cainozoic aquifers of South Coast Kenya - a review. J. African Earth Sci. 13, 221–227. https://doi.org/10.1016/0899-5362(91)90006-K

Oteri, A.U. and R.A.A., 2008. The Lagos Megacity Project :, Water, Megacities and Global Change.

Oyeyemi, K.D., Aizebeokhai, A.P., Oladunjoye, M.A., 2015. Integrated Geophysical and Geochemical Investigations of Saline Water Intrusion in a Coastal Alluvial Terrain, Southwestern Nigeria. Int. J. Appl. Environ. Sci. ISSN 10, 973–6077.

Pfeiffer, M., Batbayar, G., Hahn-tomer, D.K.S., 2015. Investigating arsenic (As) occurrence and sources in ground , surface , waste and drinking water in northern Mongolia. Environ. Earth Sci. 73, 649–662. https://doi.org/10.1007/s12665-013-3029-0

Post, V.E.A., Vandenbohede, A., Werner, A.D., Maimun, Teubner, M.D., 2013. Groundwater ages in coastal aquifers. Adv. Water Resour. 57, 1–11. https://doi.org/10.1016/j.advwatres.2013.03.011

Prasanna, M. V, Chidambaram, S., Kumar, G.S., 2011. Hydrogeochemical assessment of groundwater in Neyveli Basin , Cuddalore District , South India. Arab J. Geosci. 4, 319–330. https://doi.org/10.1007/s12517-010-0191-5

Priyantha Ranjan, S., Kazama, S., Sawamoto, M., 2006. Effects of climate and land use changes on groundwater resources in coastal aquifers. J. Environ. Manage. 80, 25–35. https://doi.org/10.1016/j.jenvman.2005.08.008

Salami B. M & Olorunfemi M. O, 2014. Hydrogeophysical evaluation of the groundwater potential of the central part of ogun state, nigeria 16, 291–299.

Saravana Kumar, U., Sharma, S., Navada, S. V., Deodhar, A.S., 2009. Environmental isotopes investigation on recharge processes and hydrodynamics of the coastal sedimentary aquifers of Tiruvadanai, Tamilnadu State, India. J. Hydrol. 364, 23–39. https://doi.org/10.1016/j.jhydrol.2008.10.004

Senthilkumar, S., Gowtham, B., Sundararajan, M., Chidambaram, S., Lawrence, J.F., Prasanna, M. V, 2018. Impact of landuse on the groundwater quality along coastal aquifer of Thiruvallur district , South India. Sustain. Water Resour. Manag. 4, 849–873. https://doi.org/10.1007/s40899-017-0180-x

Serdeczny, O., Adams, S., Baarsch, F., Coumou, D., Robinson, A., Hare, W., Schaeffer, M., Perrette, M., Reinhardt, J., 2016. Climate change impacts in Sub-Saharan Africa: from physical changes to their social repercussions. Reg. Environ. Chang. 1–16. https://doi.org/10.1007/s10113-015-0910-2

Shakerkhatibi, M., Mosaferi, M., Pourakbar, M., Ahmadnejad, M., Safavi, N., Banitorab, F., 2019. Comprehensive investigation of groundwater quality in the north-west of Iran: Physicochemical and heavy metal analysis. Groundw. Sustain. Dev. https://doi.org/10.1016/j.gsd.2018.10.006

Shin, W.J., Park, Y., Koh, D.C., Lee, K.S., Kim, Yongcheol, Kim, Yongje, 2017.

Hydrogeochemical and isotopic features of the groundwater flow systems in the central-northern part of Jeju Island (Republic of Korea). J. Geochemical Explor. 175, 99–109. https://doi.org/10.1016/j.gexplo.2017.01.004

Sivan, O., Yechieli, Y., Herut, B., Lazar, B., 2005. Geochemical evolution and timescale of seawater intrusion into the coastal aquifer of Israel. Geochim. Cosmochim. Acta 69, 579–592. https://doi.org/10.1016/j.gca.2004.07.023

Somaratne, N., Frizenschaf, J., 2013. Geological Control upon Groundwater Flow and Major Ion Chemistry with Influence on Basin Management in a Coastal Aquifer , South Australia. J. Water Resour. Prot. 5, 1170–1177.

Talabi, A.O., Tijani, M.N., 2013. Hydrochemical and stable isotopic characterization of shallow groundwater system in the crystalline basement terrain of Ekiti area, southwestern Nigeria. Appl. Water Sci. 3, 229–245. https://doi.org/10.1007/s13201-013-0076-3

Talabi, A.O., Tijani, M.N., Aladejana, A.J., 2012. Assessment of impact of climatic change on groundwater quality around Igbokoda Coastal area , southwestern Nigeria . J. Environ. Earth Sci. 2, 39–50.

Thilagavathi, R., Chidambaram, S., Thivya, C., Prasanna, M. V., Keesari, T., Pethaperumal, S., 2017. Assessment of groundwater chemistry in layered coastal aquifers using multivariate statistical analysis. Sustain. Water Resour. Manag. 3, 55–69. https://doi.org/10.1007/s40899-017-0078-7

Tomaszkiewicz, M., Abou Najm, M., El-Fadel, M., 2014. Development of a groundwater quality index for seawater intrusion in coastal aquifers. Environ. Model. Softw. 57, 13–26. https://doi.org/10.1016/j.envsoft.2014.03.010

Trabelsi, N., Triki, I., Hentati, I., Zairi, M., 2016. Aquifer vulnerability and seawater intrusion risk using GALDIT, GQISWIand GIS: case of a coastal aquifer in Tunisia.

Environ. Earth Sci. 75. https://doi.org/10.1007/s12665-016-5459-y

Tran, L.T., Larsen, F., Pham, N.Q., Christiansen, A. V., Tran, N., Vu, H. V., Tran, L. V., Hoang, H. V., Hinsby, K., 2012. Origin and extent of fresh groundwater, salty paleowaters and recent saltwater intrusions in Red River flood plain aquifers, Vietnam. Hydrogeol. J. 20, 1295–1313. https://doi.org/10.1007/s10040-012-0874-y

Ukhurebor, K.E., Abiodun, I.C., 2018. Variation in annual rainfall data of forty years (1978-2017) for south-south, Nigeria. J. Appl. Sci. Environ. Manag. 22, 511. https://doi.org/10.4314/jasem.v22i4.13

Unsal, B., Yagbasan, O., Yazicigil, H., 2014. Assessing the impacts of climate change on sustainable management of coastal aquifers. Environ. Earth Sci. 72, 2183–2193. https://doi.org/10.1007/s12665-014-3130-z

Usama A. Abu Risha1, 2016. Radiocarbon dating and the chlorine isotopes evolution of three Great. Hygrogeology J. 24, 987–1000.

W. Ali, H. Hötzl, S. Geyer, E. Salameh, A. Flexer, Y. Guttman, A.R.T. (5), 2004. Hydrogeological investigations on the aquifers along the jordan rift valley escarpment. Geothermics 32, 309–335. https://doi.org/10.1016/j.geothermics.2003.08.011

Wang, J., Zhang, F., Kung, H. te, Ren, Y., Zhang, Y., Yu, H., 2017. Linkage analysis of land use/cover patterns and hydro-chemical characteristics in different seasons in Ebinur Lake Watershed, China. Water (Switzerland) 9. https://doi.org/10.3390/w9110888

Werner, A.D., Bakker, M., Post, V.E.A., Vandenbohede, A., Lu, C., Ataie-Ashtiani, B., Simmons, C.T., Barry, D.A., 2013. Seawater intrusion processes, investigation and management: Recent advances and future challenges. Adv. Water Resour. 51, 3–26. https://doi.org/10.1016/j.advwatres.2012.03.004

Werner, A.D., Gallagher, M.R., 2006. Characterisation of sea-water intrusion in the Pioneer

Valley, Australia using hydrochemistry and three-dimensional numerical modelling. Hydrogeol. J. 14, 1452–1469. https://doi.org/10.1007/s10040-006-0059-7

APPENDIX

APPENDIX 1

Field Physicochemical measurements for wet season

Sample ID	Locality	Geological Fm	Lat	Long	Elev	pH	EC	TDS	ORP	Sal	Temp	DTW	DTB
L01	Ijebu Ishiwo	Ilaro fm	6.71	3.96	56	5.8	153	95	251	71	30	3.4	5.1
L02	Ijebu Ishiwo	Ilaro fm	6.70	3.96	63	4.41	136	92	219	69	30.2	7.6	18.5
L03	Ijebu Ishiwo	Ewekoro fm	6.72	3.97	50	4.7	90	59	221	45	31.2	6.5	17.2
L04	Abeokuta (Ogun Radio)	Precambrian	7.17	3.31	90	6.68	326	219	127	165	28.5	0.8	4
L05	Abeokuta Sokoto Rd	Precambrian	7.19	3.29	81	7.4	481	322	137	249	32.2	62	125
L06	Olorunda Village	Abeokuta Fm	7.22	3.15	163	5.93	122	82	140	60	31.8	41.2	44.2
L07	Obada Town	Prcambrian	7.40	3.01	230	5.72	123	82	182	61	31.8	36	47
L08	Aiyetoro	Abeokuta Fm	7.25	3.04	122	5.16	183	122	20	91	32.7	26.2	30.2
L09	Aiyetoro 2	Abeokuta Fm	7.24	3.02	103	5.32	189	126	250	96	34.6	20.7	24.7
L10	Yewa	Abeokuta Fm	7.08	3.08	82	6.04	238	159	234	121	32.1	26.2	32.3
L11	Ibese	Ilaro fm	6.95	3.10	107	4.65	130	88	258	66	29.7	5.1	9.2
L12	Ilaro (Poly)	Ilaro fm	6.89	2.98	86	5.13	30	20	224	15	27.2	28	33.5
L13	Ilaro (Lesley Rd)	Ilaro fm	6.89	3.02	87	4.47	155	104	257	76	28.3	16	22
L14	Ilaro	Ilaro fm	6.88	3.02	66	4.26	298	198	278	149	29.6	11	15
L15	Ilaro	Ilaro fm	6.87	3.01	54	5.77	69	46	242	35	29.3	21	26
L16	Ilaro (Ibese Rd)	Ilaro fm	6.91	3.02	124	5.18	61	40	250	30	29	39.5	43.3
L17	Ewekoro	Ewekoro fm	6.88	3.12	133	5.43	58	38	295	29	30	45.7	53.34
L18	Ewekoro	Ewekoro fm	6.93	3.22	40	4.1	370	250	304	189	29.9	9.14	12.8
L19	Ewekoro	Abeokuta Fm	6.99	3.23	93	5.7	70	46	218	36	31.7	18	26
L20	Ewekoro	Ewekoro fm	6.87	3.19	50	5.5	326	222	267	168	31.5	3.4	5.6
L21	Ifo	Ewekoro fm	6.82	3.19	82	4.77	107	71	279	53	33.1	35	42
L22	Sango otta	CPS	6.75	3.20	75	4.51	72	47	316	36	31.5	31.9	36.6

Field Physicochemical measurements for wet season

Sample ID	Locality	Geological Fm	Lat	Long	Elev	pH	EC	TDS	ORP	Sal	Temp	DTW	DTB
L23	Sango otta	CPS	6.72	3.24	94	4.97	92	61	293	46	30.8	29.6	36.6
L24	Sango otta	CPS	6.68	3.21	73	5.13	67	44	279	33	30.5	29.3	39.1
L25	Sango	CPS	6.68	3.13	62	5.4	60	40	300	29	30.4	34.14	39.6
L26	Atan	CPS	6.67	3.10	55	5.17	45	28	286	21	30.3	34	39.6
L27	Ajibowo	CPS	6.67	3.06	60	6.1	30	20	270	15	29.4	26	30
L28	Atan	CPS	6.66	3.09	62	5.4	22	14	275	10	28.6	24	29
L29	Alago Ado-odo Otta	CPS	6.61	3.05	37	4.53	13	8	263	6	26.3	23.2	25.91
L30	Ishaga Owode	CPS	6.71	2.99	82	5.88	36	26	231	20	28.1	18	22
L31	Owode	CPS	6.68	2.98	55	5.27	162	108	250	81	30.1	36	42.7
L32	Ado-od Town	CPS	6.60	2.94	15	4.01	197	132	290	99	30.4	15	21
L33	Ado-od Town	CPS	6.59	2.94	60	5.11	59	37	262	28	30	31.1	36.6
L34	Ikonga Badagery	Alluvium Deposit	6.48	2.96	18	4.92	69	46	266	34	30.1	6.1	7.62
L35	Gbetomey Badagery	CPS	6.38	2.77	12	6.22	290	194	299	146	30.3	1.1	5.6
L36	Gbetomey Coast	CPS	6.38	5.77	10	8.1	12000	8500	155	5000	29.6		
L37	Idale Badagery	CPS	6.41	2.93	9	6.84	391	262	172	195	30.2	2	5
L38	Oko Afo Badagery	Alluvium Deposit	6.48	3.03	16	5.62	125	82	206	61	29.9	2.44	6.1
L39	Kajola Owode Egba	Abeokuta Fm	6.90	3.57	122	4.85	98	64	167	49	28.4	67	77.7
L40	Ajura Owode Egba	Abeokuta Fm	6.96	3.60	61	5.48	178	118	202	88	30.6	6.7	8.5
L41	Ofada Obafemi Owode	Alluvium Deposit	6.87	3.43	24	5.62	117	71	199	59	30.1	21.3	25.91
L42	Ofada Obafemi Owode	Alluvium Deposit	6.88	3.44	49	4.94	68	45	224	33	30.3	36.6	39.1
L43	Mowe	Alluvium Deposit	6.84	3.44	38	5.49	307	204	250	155	30.9	3	7.4
L44	Orimerunmu	Alluvium Deposit	6.78	3.41	26	5.43	108	72	233	54	30.8	17.1	23.8

Field Physicochemical measurements for wet season

Sample ID	Locality	Geological Fm	Lat	Long	Elev	pH	EC	TDS	ORP	Sal	Temp	DTW	DTB
L45	Ojodu Lagos	CPS	6.64	3.36	55	4.66	113	75	266	56	29.8	41.5	49.3
L46	Majidun Ikorodu	Alluvium Deposit	6.62	3.47	13	5.51	185	123	125	93	30	3	18
L47	Omitoro Ijede	Alluvium Deposit	6.62	3.56	46	4.63	56	37	269	28	29.7	29.3	33.5
L48	Prince Odonga Ogudu	Alluvium Deposit	6.58	3.39	31	4.25	237	158	290	119	28.6	10.7	15.2
L49	Ibafo Rain Water	Alluvium Deposit	6.73	3.42	1	5.88	10	6	165	4	25.6		
L50	Ibafo	Alluvium Deposit	6.73	3.42	1	5.96	109	72	200	54	27.3	1.2	21.3
L51	Shagamu	Ewekoro fm	6.87	3.56	87	5.52	67	45	213	34	29.2	39.6	44.2
L52	Odogbolu	Abeokuta Fm	6.84	3.77	57	4.4	107	72	264	55	30.1	35.1	41.2
L53	Ososa Ijebu	Alluvium Deposit	6.79	3.86	49	4.08	145	96	298	73	31.7	26.2	32
L54	Ijebu Ode	Ewekoro fm	6.83	3.59	86	4.53	94	60	71	45	31.6	51.8	44.2
L55	Ijebu Ode	Abeokuta Fm	6.79	3.89	51	4.67	66	43	266	32	31.3	21.3	29
L56	Ilado Ibefun	Alluvium Deposit	6.71	3.80	20	6.3	108	73	225	55	30.1	1.8	5.8
L57	Ketu Epe	Alluvium Deposit	6.64	3.88	54	4.65	97	64	279	48	30.8	24	48
L58	Epe Lagos	Alluvium Deposit	6.58	3.98	18	6.23	440	294	246	221	30.7	0.3	7
L59	Epe Lagos	Alluvium Deposit	6.60	3.99	38	5.82	171	113	224	84	28.6	17.7	24.4
L60	Eredo Epe Lagos	Alluvium Deposit	6.65	3.99	44	4.74	40	27	268	20	29.1	36.6	44.2
L61	Epe Lagos	Alluvium Deposit	6.58	3.95	1	6.1	195	130	218	97	26	2	7
L62	Epe Lagos	Alluvium Deposit	6.58	3.96	7	4.73	18	11	254	8	26.3	22.9	26.8
L63	Ibeju Lekki	Alluvium Deposit	6.51	3.89	12	6.47	141	93	231	70	28.1	3.5	8.3
L64	Ibeju Lekki	Alluvium Deposit	6.48	3.89	6	4.87	191	126	240	96	27.4		
L65	Ikegun Lekki	CPS	6.40	4.19	9	5.7	0	0	222	0	25.5		
L66	Ikegun Lekki	CPS	6.40	4.19	14	6.7	138	92	134	69	25.8	7	15

Field Physicochemical measurements for wet season

Sample ID	Locality	Geological Fm	Lat	Long	Elev	pH	EC	TDS	ORP	Sal	Temp	DTW	DTB
L67	Oko Olowo Beach	CPS	6.44	3.87	11	6.77	320	214	203	160	26.3	13.7	18.3
L68	Bodije Lekki	Alluvium Deposit	6.48	3.76	13	6.49	216	144	210	109	28.1	6	13
L69	Abraham Adesany Estate, Lekki	Alluvium Deposit	6.47	3.59	15	5.32	794	532	251	399	30.1	3	15
L70	Ogombo Ajjah	CPS	6.45	3.61	13	6.69	892	593	224	448	29.4	2	7
L71	Okun Ajjah	CPS	6.43	3.59	9	6	223	148	272	112	27.9	32	53.3
L72	Admiralty Rd Lekki	Alluvium Deposit	6.44	3.45	16	7.9	650	431	186	324	29.3	18	26
L73	Araromi Sea Side	CPS	6.33	4.50	4	7.33	127	84	114	63	28.4	0.3	3.5
L74	Obinehin	CPS	6.31	4.55	1	7.53	275	182	125	137	29	0.2	3.6
L75	Aiye titun	CPS	6.27	4.64	11	7.74	91	62	148	46	28.6	1	5
L76	Atejire	Alluvum Deposit	6.25	4.68	38	7.86	190	127	168	96	26.7	8	18.6
L77	Ode-mahin	Alluvum Deposit	6.17	4.80	6	7.54	835	558	-136	419	28.2	2.6	17
L78	Ode-mahin Palace	Alluvum Deposit	6.17	4.80	5	7.18	322	214	68	161	27	0.8	6.6
L79	Igbokoda	Alluvium Deposit	6.36	4.79	15	6.78	338	226	226	113	30.6	0.3	4.6
L80	Igbokoda	Alluvium Deposit	6.35	4.80	16	6.88	199	133	123	101	28.5	1.2	2.1
L81	Igbokoda	Alluvium Deposit	6.37	4.80	-1	7.46	470	313	-17	237	28.3	1.2	11.4
L82	Igbokoda	Alluvium Deposit	6.37	4.80	6	6.64	244	160	136	121	28.6	0.8	8.6
L83	Igbokoda	Alluvium Deposit	6.39	4.77	16	4.88	56	38	240	28	29.8	8.6	36
L84	Ilutitun	CPS	6.53	4.65	52	5.77	45	30	225	22	29.3	13.1	22.9
L85	Ugbotako	Ewekoro fm	6.58	4.64	59	4.38	174	116	306	87	28.6	20.4	44.2
L86	Iju-Odo	CPS	6.55	4.65	53	5.24	86	56	278	42	30.1	14.3	32
L87	Ilutitun Osooro	CPS	6.53	4.63	40	4.43	57	37	310	28	30.8	22	33.5
L88	Igboegurin	Alluvium Deposit	6.46	4.62	19	5.71	76	50	240	37	30.3	0.9	4.1

Field Physicochemical measurements for wet season

Sample ID	Locality	Geological Fm	Lat	Long	Elev	pH	EC	TDS	ORP	Sal	Temp	DTW	DTB
L89	Igbinsi Oloto	Alluvium Deposit	6.47	4.63	17	5.34	36	22	264	17	29.4	6.5	34.2
L90	Ikoya	CPS	6.51	4.68	42	4.96	26	17	286	13	28.6	21.6	29.3
L91	Okiyipupa	CPS	6.51	4.76	53	4.6	28	18	314	13	28.6	14	30
L92	Okitipupa	CPS	6.50	4.79	25	3.97	414	276	330	207	28.2	18	47
L93	Okitipupa	CPS	6.48	4.79	40	5.09	14	9	206	6	26.2	44.2	56.4
L94	Ode-Irele	CPS	6.52	4.87	29	4.73	37	24	256	18	28	29.2	35.2
L95	Igbekebo	CPS	6.43	4.89	31	4.77	38	24	266	17	29	11	29.2
L96	Ajagba	CPS	6.43	4.91	14	4.96	36	24	267	18	29	32	44.2

APPEDIX 2

Field Physicochemical measurements for dry season

Sample ID	Locality	Geological Fm	Lat	Long	Elev	PH	EC	TDS	ORP	Sal	Temp	DTW	DTB
L01	Lisabi Crescence Abeokuta	Abeokuta fm	7.17	3.06	124	6.1	338	224	225	128	28	46.3	60.3
L02	Lafenwa Ogun Radio	Abeokuta fm	7.17	3.31	90	7.62	1140	766	184	564	31.6	3	4.8
L03	Igbo-ora Road	Abeokuta fm	7.19	3.29	81	7.26	850	568	119	420	33.3	82	126
L04	Olorunda Abeokuta-Aiyetoro Road	Abeokuta fm	7.22	3.15	163	5.96	100	66	150	50	31.7	40.2	42.2
L05	Obada Town	Abeokuta fm	7.40	3.01	230	5.21	63	42	207	32	31.7	38.6	72.4
L06	Aiyetoro Town	Ilaro Fm	7.25	3.04	122	5.04	66	42	221	32	31.3	24.2	51
L07	Shaala quarter	Ilaro Fm	7.24	3.02	103	5.15	225	152	215	115	33.5	24	30.2
L08	Aiyetoro Town	Ilaro Fm	7.11	3.13	96	5.23	40	27	224	19	31.3	9.8	10.58
L09	Imashae	Ilaro Fm	7.05	2.98	84	5.17	46	31	261	23	30.2	14	33
L10	Ibese Town	Ilaro Fm	6.95	3.10	107	6.27	474	318	242	40	30.9	5	5.4
L11	Ilaro Poly	Ilaro Fm	6.89	2.99	54	5.44	36	2.3	194	18	30.8	36.6	51.8
L12	Oja-Odan	Ilaro Fm	2.83	6.90	63.2	5.7	109	73	209	55	30.6	2	3.4
L13	Oja Odan	Ilaro Fm	2.86	6.90	65.6	6.4	119	79	207	58	89.5	33.2	39.6
L14	Ibese Town	Ilaro Fm	3.03	6.91	132	5.08	76	50	239	38	31.7	8.7	9.2
L15	Lesley Road, Ilaro	Ilaro Fm	6.88	3.01	44	3.85	439	290	292	219	30.8	26	32
L16	Owode Rd, Ilaro	Ilaro Fm	6.87	3.01	51	5.73	75	49	271	36	33.2	26.8	33.5
L17	Ayegunle Town Papalanto	Ewekoro	6.88	3.12	137.11	4.7	94	62	297	46	31.5	38.4	53.34
L18	Oremeji Makt Itori	Ewekoro	6.93	3.22	43.1	4.5	517	388	298	288	33.5	7.9	15.24
L19	Wasinmi	Abeokuta fm	6.99	3.23	148	5.3	49	32	268	27	32.05	21	26
L20	Arigbajo Papalanto	Ewekoro fm	6.87	3.20	59.48	6.66	1353	896	243	695	31.3	5.4	7.2

Field Physicochemical measurements for dry season

Sample ID	Locality	Geological Fm	Lat	Long	Elev	PH	EC	TDS	ORP	Sal	Temp	DTW	DTB
L21	Iyana Ilogbo	Ilaro Fm	6.7458	3.1986	82	4.8	107	71	279	53	33.1	27.13	42.67
L22	Ojuore Sango Ota	Ilaro Fm	6.68	3.21	72	4.92	35	24	276	18	28.6	30	42.6
L23	Iyana Joju	Coastal Plain Sand	6.71	3.24	109.7	5.56	87	58	254	43	27.8	32.2	36.6
L24	Onibukun Junction Idedo	Ilaro Fm	6.68	3.12	94	6.12	118	78	274	58	26.6	23.8	39.62
L25	Agbara-Atan Rd	Ilaro Fm	6.66	3.09	73	5.61	61	41	256	30	28.6	15.6	23.8
L26	Alaako	Ilaro Fm	6.61	3.05	54	4.25	125	84	316	62	29.4	17.1	27.4
L27	Owode, Yewa South	Ilaro Fm	6.71	2.99	73	5.77	73	47	267	35	30.1	20.1	22
L28	Owode Ado-Odo Rd	Ilaro Fm	6.68	2.98	67.93	4.92	136	90	292	67	30.2	38.2	42.7
L29	Owode Ado-Odo Rd	Ilaro Fm	6.60	2.94	73.95	4.07	347	231	325	173	31.2	37.4	48.6
L30	Ado-odo	CPS	6.59	2.95	27.38	5.02	124	84	304	63	32.9	17.7	25.91
L31	Ado-odo Badagary Rd	CPS	6.53	2.95	25	4.45	96	65	311	48	33.3	15.9	21.3
L32	Ado-odo Badagary Rd	CPS	6.48	2.96	61	4.7	116	78	295	58	31.2	24.7	25.84
L33	Keta Seme Lagos	CPS	6.38	2.77	26	5.93	292	193	87	145	28.6	4.7	5.6
L34	Seme sea side	CPS	6.38	2.77	21	7.96			134		31.5		
L35	Bdagary Area	CPS	6.42	2.79	10.05	6.15	154	102	-6	77	30.6	3.7	9.14
L36	Badagary-Seme Rd	CPS	6.49	2.85	21.5	5.85	470	315	160	240	30.3	2.2	5.7
L37	Topo Badagary	CPS	6.41	2.93	20.23	6.55	420	281	158	211	31.2	4.6	5.4
L38	Mowo Badagary	CPS	6.46	2.96	2.6	4.2	873	582	200	433	31.8	2.6	4.2
L39	Ijanikin Lagos	CPS	6.50	3.12	26.15	4.01	333	224	295	167	31.4	7.92	19.8
L40	Iyana Iba Lagos	CPS	6.51	3.20	35	5.37	244	162	146	121	31.5	6	13

Field Physicochemical measurements for dry season

Sample ID	Locality	Geological Fm	Lat	Long	Elev	PH	EC	TDS	ORP	Sal	Temp	DTW	DTB
L41	Idimu Rd Lagos	CPS	6.58	3.28	6.95	4.97	119	78	238	60	30.4	12.8	25.9
L42	Prince Odonga Close, Ojota Lagos	Alluvium	6.58	3.39	7	4.16	343	229	287	172	30.1	12.6	5.6
L43	Isheri Lagos	Alluvium	6.64	3.41	1.7	5.94	10009	6750	2	5070	28.2	1.3	4.7
L44	CSL Rd, Ikorodu	Alluvium	6.62	3.47	28	5.44	198	132	80	99	30.9	6.1	18
L45	Ikorodu-Epe Rd	CPS	6.63	3.52	68.11	4.15	136	91	275	69	30.7	12.8	20.4
L46	Ijede Rd Ikorodu	CPS	6.62	3.56	41	4.7	5.5	36	270	27	29.7	31.4	33.5
L47	Ijede Ikorodu	CPS	6.59	3.59	43.25	4.62	85	56	288	42	32.11	11.6	18.2
L48	Omole Phase 1	Alluvium	6.64	3.36	41	4.54	117	79	278	59	32.2	44.8	49.5
L49	Ibafo	Alluvium	6.73	3.42	10	6.03	100	64	198	50	28.6	6.2	24.1
L50	Orimenumu	Alluvium	6.77	3.41	15	6.24	410	274	167	204	28.3	4.8	5.6
L51	Mowe	Alluvium	6.82	3.44	60.5	4.5	254	167	248	126	30.7	5.4	5.8
L52	Ofada	Ewekoro	6.87	3.43	15	5.67	114	72	213	54	30.5	23.8	27.4
L53	Ofada, Olorunda Rd	Ewekoro	6.81	3.48	39	5.13	77	52	234	39	31.89	38.2	39.1
L54	Shomeke Ogun	Ewekoro	6.91	3.48	112	5.01	99	66	228	49	32.3	34	54
L55	Ajura-Ogere	Abeokuta fm	6.96	3.60	24	4.85	140	93	249	69	32	7.8	8.4
L56	Shagamu-Abeokuta Rd	Abeokuta fm	6.90	3.57	123	4.82	72	48	274	36	31.5	42.1	46
L57	Lagos-Ibadan Exp, Shagamu	Abeokuta fm	6.87	3.56	68	4.76	100	66	285	50	36.7	34	42.7
L58	Ijebu-Ode Express	Abeokuta fm	6.80	3.94	86	4.23	150	100	300	75	32.3	36.6	45.7
L59	Olukoku, Ijebu-Ode	Abeokuta fm	6.82	3.93	130	4.66	81	54	326	40	32.7	34.1	45.1
L60	Ijebu Ishiwo	Ewekoro fm	6.72	3.96	52.4	4.31	245	164	285	123	31.8	33	54

Field Physicochemical measurements for dry season

Sample ID	Locality	Geological Fm	Lat	Long	Elev	PH	EC	TDS	ORP	Sal	Temp	DTW	DTB
L61	Itanrin-Ososa Rd	Abeokuta fm	6.81	3.87	90	4.82	80	53	252	40	31.6	40.2	51.8
L62	Gbawojo, Ososa	Abeokuta fm	6.79	3.86	66.52	4.48	121	80	265	61	31.3	29.3	32.4
L63	Akarigbo Rd	Abeokuta fm	6.85	3.65	82	4.12	387	256	271	196	29.6	37.2	55.6
L64	Aiyepe Community	Ewekoro fm	6.85	3.65	32	4.13	166	110	235	82	30	5.7	8.2
L65	Ikenne, Ogun State	Ewekoro fm	6.87	3.71	155.94	4.77	123	82	235	61	32.3	33.5	44.2
L66	Odogbolu	Ewekoro	6.84	3.77	51	4.4	107	72	251	53	30	33.5	51.82
L67	Odogbolu	Ewekoro	6.79	3.89	59	4.7	45	30	257	22	30.5		
L68	Ijebu-Ode Epe Rd	Abeokuta fm	6.72	3.99	38	4.7	80	53	232	40	86	3.2	4.6
L69	Ijebu-Ode Epe Rd	Abeokuta fm	6.67	3.99	67	4,78	63	42	245	32	89.3	48.1	52.2
L70	Ketu Epe, Lagos	CPS	6.64	3.88	24	4.46	102	68	259	51	94.1	42	47.2
L71	Epe Lagos	Alluvium	6.58	3.95	8.62	5.61	289	192	220	145	90.2	3	7.2
L72	Epe Lagos	Alluvium	6.60	3.94	12	4.29	130	86	249	65	90.3	7.32	13.72
L73	Epe Lagos	Alluvium	6.58	4.48	41	6.02	519	344	204	259	90.6	0.4	4
L74	Iraye oke, Epe Lagos	Alluvium	6.60	3.99	45	5.16	223	148	222	111	92.6	20.6	24.5
L75	Lekki-Epe Express	Alluvium	6.53	3.90	2	5.96	415	278	149	211	82.9	2.2	5.6
L76	Lekki-Epe Express	Alluvium	6.51	3.89	18	5.41	130	86	178	65	84.7	6.7	8.4
L77	Lekki Tropicana	CPS	6.40	4.19	5	6.46	452	302	-8	230	87.1	4.6	15
L78	Lekki Acient Town	CPS	6.40	4.18	5	6.64	162	109	108	81	90	2.4	4.4
L79	Ibeju Lekki	CPS	6.44	3.93	11	4.94	477	316	224	238	88.4	5.6	7.8
L80	Okolowo Beach, Lekki	CPS	6.44	3.87	3	7.23	718	478	118	359	89.1	3.4	17

Field Physicochemical measurements for dry season

Sample ID	Locality	Geological Fm	Lat	Long	Elev	PH	EC	TDS	ORP	Sal	Temp	DTW	DTB
L81	Lakwe, Lekki	CPS	6.47	3.74	15	5.78	620	415	181	315	90.2	6	14
L82	Abraham Adesanya Estate, Ajjah	Alluvium	6.47	3.59	26	5.48	845	561	203	472	91.8	7.2	15.2
L83	Ogombo Lekki	CPS	6.45	3.61	12	6.73	1012	725	160	551	93.9	3.2	7
L84	Okun-Ajjah	CPS	6.43	3.59	12	6.22	567	380	113	288	90.8	7.6	30.2
L85	Admiralty Road, Lekki	CPS	6.44	3.45	4	7.7	642	427	109	320	88.1	4.3	26
L86	Araromi Seaside	CPS	6.35	4.80		7.62	173	115	-8	86	85	1.1	3.5
L87	Araromi Committee	CPS	6.33	4.49	22	7.75	226	148	43	112	89.1	1.2	3.6
L88	Zion Pepe	CPS	6.29	4.60	6	7.23	399	262	46	198	88.8	1.2	1.8
L89	Aiyetitun	CPS	6.27	4.64	5	6.56	105	70	49	53	90.5	2.2	2.7
L90	Abule-Ipara	CPS	6.26	4.68	2	7.18	367	244	107	183	87.1	1.4	4.1
L91	Ugbonla	Alluvium	6.14	4.79	7	7.08	716	480	104	364	90.1	0.3	3.2
L92	Ugbonla	Alluvium	6.15	4.79	6	7.35	959	641	92	480	99.9	3	7.6
L93	Ugbonla	Alluvium	6.15	4.79	4	7.15	768	506	103	383	87.6	0.4	3.2
L94	Ode-Mahin	Alluvium	6.17	4.80	3	7.21	5540	3660	-280	2750	88.6	2.3	9
L95	Aboto Town	CPS	6.31	4.76	2	6.52	161	107	25	81	86.2	2.1	3.4
L96	College Road, Igbokoda	CPS	6.37	4.77	22	6.65	256	171	56	128	86.4	0.7	2.8
L97	Ikuemola Street, Igbokoda	CPS	6.35	4.80	16	6.41	814	545	-22	414	86.7	1.1	4
L98	Alfred Street, Igbokoda	CPS	6.37	4.80	16.8	6.66	145	96	74	72	87.9	2.1	5.6
L99	Igbokoda-Okitipupa Rd	CPS	6.37	4.80	9	5.72	111	74	103	56	86.3	2.1	5.6
L100	Okitipupa-Igbokoda Rd	CPS	6.39	4.77	28	5.01	49	32	242	24	86.3	10.97	30.48

Field Physicochemical measurements for dry season

Sample ID	Locality	Geological Fm	Lat	Long	Elev	pH	EC	TDS	ORP	Sal	Temp	DTW	DTB
L101	Igbekebo	CPS	6.48	4.79	3	5.37	50	33	284	25	83.4	1.3	6.8
L102	Apoi	Abeokuta fm	6.48	4.79	4	5.84	42	28	223	21	88.1	3.66	9.14
L103	Apoi	Abeokuta fm	7.10	4.82	6	4.5	100	67	280	50	87.1	21.95	28.96
L104	Igbotu, Ese-Odo LGA	Abeokuta fm	7.10	4.82	13	5.08	54	37	261	27	90.1	4.2	8.4
L105	Ajagba Town	Abeokuta fm	6.43	4.91	61	4.71	71	46	278	35	94.7	16.46	27.43
L106	Agadagba, Ese-Odo	CPS	6.28	4.99	30.64	5.5	73	49	202	36	90.5	2.6	8.2
L107	Agadagba, Ese-Odo	CPS	6.28	4.98	16	5.19	72	48	241	36	88.5	3.66	16.76
L108	Agadagba, Ese-Odo	CPS	6.32	4.97	22.6	5.08	73	48	267	36	88.7	12	29.2
L109	Akotogbo, Ondo State	CPS	6.38	5.04	34	5.01	106	72	259	53	90.7	46	70
L110	Akotogbo, Irele LGA	CPS	6.38	5.04	42	5.17	74	51	254	37	92.3	32	42.67
L111	Sabomi, Ese-Odo	Alluvium	6.49	4.87	30	4.91	57	40	266	29	96.1	31.09	44.2
L112	Irele Town	Abeokuta fm	6.48	4.89	58	4.93	56	37	272	28	92	42	70
L113	Ebute, Olu-Agbo	Abeokuta fm	0.00	0.00		24	53	36	267	26	85.4	5.6	6.2
L114	Okitipupa	Abeokuta fm	6.48	4.86	54	4.91	54	36	270	27	87.7	15.85	21.34
L115	Okitipupa	Abeokuta fm	6.49	4.79	38	4.98	28	19	225	14	81.2	48.77	67.06
L116	Omotosho, Odigbo LGA	Precambrian Rock	6.72	4.65	117	6.24	74	48	140	36	85	27	38
L117	Omotisho, Odigbo LGA	Precambrian Rock	6.80	4.66	107	5.32	77	52	205	39	86.1	10	10.7
L118	Igbotako	Abeokuta fm	6.58	4.64	27	4.67	117	73	254	58	86.1	25.6	44.2
L119	Igbokoda	Abeokuta fm	6.58	4.64	60	4.74	241	158	265	118	88	3.6	11.4
L120	Iju Odo	Abeokuta fm	6.55	4.65	83	5.01	106	70	275	53	86.1	16.6	32

Field Physicochemical measurements for dry season

Sample ID	Locality	Geological Fm	Lat	Long	Elev	PH	EC	TDS	ORP	Sal	Temp	DTW	DTB
L121	Ilu-Titun	Abeokuta fm	6.53	4.63	42	4.74	77	52	283	39	86.9	15.8	22.8
L122	Ilu-Titun	Abeokuta fm	6.53	4.65	64	5.75	61	40	231	30	89.8	26	33.5
L123	Egbo-Egunrin	CPS	6.46	4.62	6.6	5.17	98	64	245	49	88.4	1.6	4.2
L124	Oloto-Okitipupa	Abeokuta fm	6.47	4.63	27	5.28	68	47	246	34	86	3.6	7.8
L125	Ikoya, Okipupa	Abeokuta fm	6.51	4.68	41.91	5.48	64	42	245	32	92.1	24.3	29.3
L126	Ode-Aye	Abeokuta fm	6.60	4.74	52	5	721	475	260	356	88.6	18.5.6	25.2
L127	Ode-Aye	Abeokuta fm	6.57	4.75	55	4.76	98	65	275	49	89.1	123	150
L128	Ode-Erinje	Abeokuta fm	6.44	4.73	38	4.99	49	36	268	25	89.4	56	80
L129	Ode-Erinje	Abeokuta fm	6.48	4.76	42	5.04	52	36	269	27	88.9	70	105
L130	Ilu-TituN Rd, Okitipupa	Abeokuta fm	6.51	4.76	58	4.86	69	46	289	35	87.1	24.2	32.4
L131	Igodan, Okitipupa	Abeokuta fm	6.48	4.78		5.14	85	57	218	43	83.4	68	100
L132	Okitipupa	Abeokuta fm	6.46	4.79	23	4.46	432	289	265	217	84.1	22.2	34.5
L133	Agbabu	Abeokuta fm	6.59	4.83	54	5.87	85	57	156	42	84.2	6	7.1
L134	College Road, Igbokoda	CPS	6.37	4.77	22	6.65	256	171	56	128	86.4	0.7	2.8

APPENDIX 3

Major ions (mg/l) and Stable Isotopes of Wet season samples

Sample ID	Ca	Mg	Na	K	HCO_3	SO_4	Cl	NO_3^-	F	δ^2H (‰)	$\delta^{18}O$ (‰)
L01	10.57	0.75	2.54	0.54	35.97	1.58	2.60	10.50	0.04	-17.1	-3.63
L02	5.65	1.23	9.04	2.71	23.38	3.48	10.80	30.63	0.01	-13.8	-3.14
L03	1.80	0.64	3.46	0.06	8.69		3.45	9.07	0.01	-12.6	-3.06
L04	27.56	7.13	37.10	9.54	119.74	29.17	31.59	71.73	0.15	-11.3	-2.81
L05	77.01	44.44	59.59	5.00	457.17	4.30	12.02	0.02	1.14	-11.2	-2.69
L06	2.71	0.37	4.46	0.25	10.10	0.16	4.61	2.59	0.01	-14	-3.09
L07	7.52	0.35	5.49	0.30	24.67	0.41	7.10	5.44	0.02	-14.7	-3.13
L08	3.26	0.37	6.90	0.37	11.80	0.16	7.04	11.09	0.01	-14.8	-3.25
L09	7.76	4.23	19.29	8.49	44.85	2.54	26.41	50.38	0.04	-13.7	-3.1
L10	25.52	10.30	24.92	26.35	129.36	7.11	54.71	124.52	0.05	-12.3	-2.97
L11	3.81	2.80	11.38	1.38	25.63	1.70	22.97	19.55	0.02	-13.3	-3.01
L12	1.86	0.66	3.34	0.49	8.99	0.39	4.25	0.86	0.01	-13.4	-3.11
L13	5.73	3.53	21.72	4.53	35.15		23.52	56.00	0.11	-11.9	-2.84
L14	19.87	11.64	30.98	35.09	118.83	31.64	58.42	171.21	0.22	-13.7	-3.14
L15	8.41	0.99	4.52	0.24	30.62		4.97	10.99	0.04	-12.7	-2.89
L16	1.88	0.85	5.49	0.22	9.95	0.19	5.17	11.74	0.01	-13.7	-3.09
L17	2.42	1.04	5.69	2.11	12.58	0.09	13.73	4.08	0.01	-13.3	-3.05
L18	16.26	5.99	42.74	29.42	79.54	0.11	107.13	182.70	0.39	-13.4	-3.14
L19	0.79	0.26	3.94	0.12	3.71	0.13	5.72	0.32	0.01	-11	-2.7
L20	35.35	17.16	61.83	37.76	193.65	15.62	136.39	253.00	0.1	-12.5	-3.04
L21	1.96	1.38	7.15	0.52	12.88		8.39	19.72	0.02	-11	-2.64
L22	0.97	0.61	4.13	0.36	6.03		8.27	3.44	0.08	-14.9	-3.33

Major ions (mg/l) and Stable Isotopes of Wet season samples

Sample ID	Ca	Mg	Na	K	HCO_3	SO_4	Cl	NO_3	F	δ^2H (‰)	$\delta^{18}O$ (‰)
L23	2.99	1.17	11.57	1.11	14.96		12.63	20.31	0.01	-12.6	-3.2
L24	2.21	0.55	5.29	0.38	9.50		5.34	4.04	0.01	-12	-3.03
L25	3.48	0.58	3.23	0.23	13.48	0.14	6.09	1.78	0.01	-13.3	-2.75
L26	1.15	0.46	3.49	0.22	5.83	0.08	6.45	0.82	0.01	-13.9	-3.21
L27	4.52	0.39	3.78	0.29	15.72	0.14	5.97	0.87	0.01	-12	-2.85
L28	1.97	0.50	3.80	0.14	8.50	0.15	6.47	3.38	0.01	-11	-2.79
L29	1.12	0.61	2.86	0.36	6.46	0.20	6.78	4.88	0.09	-12	-2.94
L30	4.21	0.31	3.90	0.20	14.42	0.14	6.58	1.41	0.01	-12.9	-2.97
L31	5.17	3.47	11.77	10.61	33.12	27.29	15.71	9.96	0.05	-13.8	-3.34
L32	10.85	7.10	25.06	4.50	68.59		30.65	78.81	0.17	-13.7	-2.94
L33	0.85	0.43	4.72	0.09	4.74	0.18	4.20	10.79	0	-12.7	-2.98
L34	2.24	0.91	5.97	1.13	11.38	0.55	9.30	13.17	0.04	-12.2	-3
L35	20.67	4.65	32.56	8.57	86.29	17.89	58.48	49.86	0.08	-13.1	-2.71
L36	374.00	1377.00	8857.00	447.10	8028.45	115.61	130.58	166.13	0.02	-12.2	-2.59
L37	22.03	4.25	29.49	14.23	88.45	19.95	29.56	63.57	0.02	-12.9	-3.11
L38	8.79	3.11	12.18	5.09	42.37	7.69	17.63	31.73	0.01	-13.4	-3.01
L39	1.06	0.44	2.34	0.12	5.44		5.61	0.82	0.01	-12.7	-3.11
L40	7.50	2.14	8.56	8.32	33.59	3.82	18.55	28.06	0.09	-12.5	-3.07
L41	8.96	1.75	3.11	0.41	36.08	1.17	6.27	0.50	0.01	-14.3	-3.51
L42	1.09	0.29	2.70	0.05	4.79		4.78	0.34	0.01	-13.6	-3.22
L43	23.41	7.37	36.45	20.46	108.24	8.51	50.97	171.19	0.06	-13.4	-2.85
L44	2.49	1.43	4.66	6.74	14.75	5.44	8.96	2.69	0.02	-11.9	-2.89

Major ions (mg/l) and Stable Isotopes of Wet season samples

Sample ID	Ca	Mg	Na	K	HCO_3	SO_4	Cl	NO_3	F	δ^2H (‰)	$\delta^{18}O$ (‰)
L45	0.68	0.49	11.30	0.18	4.52	0.20	9.24	22.51	0	-13.9	-3.3
L46	4.60	3.45	15.41	2.86	31.26	4.40	44.89	0.11	0.02	-13.7	-3.17
L47	0.60	0.16	1.65	0.19	2.61	0.09	3.14	0.50	0	-12.9	-2.8
L48	11.06	2.92	24.28	8.45	48.33	31.20	31.05	69.53	0.14	-13.8	-2.98
L49	0.61	0.18	0.65	0.26	2.74	0.92	1.20	0.89	0	-17.1	-3.71
L50	4.15	2.34	11.51	1.68	24.33	-	10.24	11.68	0.03	-14	-3.15
L51	5.09	0.99	6.03	0.63	20.50	-	7.79	12.87	0.01	-10.3	-2.4
L52	2.27	0.86	3.38	6.96	11.23	0.31	8.04	21.41	0.02	-13.2	-3.3
L53	1.45	1.11	9.05	1.80	9.97	27.91	4.75	0.14	0.01	-13.2	-3.13
L54	2.53	1.29	8.47	1.78	14.15	0.44	8.13	28.25	0.02	-12	-2.94
L55	0.97	0.48	2.16	0.41	5.36	0.27	2.59	6.08	0.01	-13.2	-3.03
L56	11.70	3.16	6.42	9.32	51.50	16.70	11.09	24.92	0.02	-13	-3.08
L57	1.55	1.07	8.05	0.80	10.09	0.08	6.57	24.85	0.08	-16.1	-3.4
L58	47.86	5.21	50.51	28.52	172.03	53.54	62.12	139.19	0.03	-14.4	-3.22
L59	9.00	4.26	13.88	8.07	48.76	5.93	22.99	47.30	0.16	-23.6	-4.52
L60	0.42	0.15	2.69	0.12	2.04	0.14	2.99	4.63	0	-21.3	-3.94
L61	24.66	1.70	15.30	5.31	83.72	24.74	13.89	44.80	0.03	-9.9	-2.43
L62	0.51	0.18	1.27	0.12	2.49	1.09	2.14	1.14	0	-12	-2.79
L63	17.43	2.96	9.20	9.43	67.96	14.63	11.47	32.99	0.07	-10.3	-2.8
L64	9.74	3.46	15.77	5.87	47.03	33.08	24.67	18.10	0.02	-8.4	-2.58
L65	0.28	0.04	0.07	0.16	1.04	0.14	0.10	0.08	0	-14.8	-3.22
L66	21.52	1.25	3.95	1.79	71.87	9.31	5.90	6.11	0.02	-13	-3.05

Major ions (mg/l) and Stable Isotopes of Wet season samples

Sample ID	Ca	Mg	Na	K	HCO_3	SO_4	C	NO3-	F	δ^2H (‰)	$\delta^{18}O$ (‰)
L67	22.76	8.05	28.28	3.85	109.69	9.11	56.00	60.34	0.01	-12.1	-3.1
L68	46.97	8.32	86.09	39.57	184.87	43.93	13.86	6.84	0	-16.6	-3.33
L69	20.49	1.53	9.71	4.20	70.13	66.80	82.49	258.56	0.01	-12.6	-3.03
L70	68.23	14.65	128.40	62.32	281.38	2210.66	18970.20		0.78	-12.6	-3.11
L71	16.70	2.71	11.60	5.70	64.50	21.91	20.04	46.17	0.01	-13.4	-3.13
L72	55.18	40.10	29.31	17.02	368.88	55.29	24.37	5.95	0.29	-14.9	-3.5
L73	16.27	1.20	1.57	0.50	55.65	2.28	1.42	1.47	0.01	-11.9	-2.85
L74	42.59	2.91	3.63	2.92	144.46	3.37	5.02	2.07	0.08	-15.2	-3.38
L75	11.89	1.34	5.56	3.02	42.98	4.72	6.21	26.32	0.08	-15.1	-3.43
L76	33.26	2.75	7.02	3.39	115.21	33.68	9.53	15.98	0.01	-9.4	-2.29
L77	110.00	45.60	139.60	8.16	563.59	12.20	253.18	4.10	0.11	-8.2	-2.22
L78	41.55	4.87	11.20	3.24	151.09	25.00	19.01	6.72	0.04	-11.6	-2.73
L79	42.50	4.13	11.84	5.87	150.29		8.84	5.18	0.03	-13	-3.03
L80	22.04	1.47	11.27	5.45	74.58	12.13	10.27	23.55	0.02	-15	-3.02
L81	24.28	39.63	14.89	10.40	272.28		30.54	0.02	0.18	-11.3	-2.79
L82	19.94	2.30	16.83	7.26	72.31	19.67	30.93	50.27	0.02	-10.8	-2.7
L83	0.54	0.18	2.75	0.41	2.55	2.18	1.32	3.40	0.01	-12.9	-3.3
L84	2.33	0.38	0.79	0.23	8.98	0.31	0.91	4.43	0.01	-13.8	-2.56
L85	4.53	2.39	9.64	11.92	25.74	3.05	13.72	43.42	0.11	-11.3	-2.82
L86	4.00	1.04	2.63	1.77	17.41		3.36	13.27	0.01	-8.8	-2.37
L87	0.75	0.58	2.93	1.31	5.18	0.32	3.92	11.11	0.01	-13.3	-2.92
L88	4.63	0.38	2.67	0.93	16.01	3.21	5.78	8.40	0	-13.8	-3.15

Major ions (mg/l) and Stable Isotopes of Wet season samples

Sample ID	**Ca**	**Mg**	**Na**	**K**	**HCO_3**	**SO_4**	**Cl-**	**NO_3**	**F**	**δ^2H (‰)**	**$\delta^{18}O$ (‰)**
L89	0.48	0.19	0.63	0.12	2.41	0.65	1.17	**0.16**	**0.01**	-14.80	-3.17
L90	0.40	0.19	0.69	0.12	2.17	0.76	1.15	0.43	0	-21.00	-4.06
L91	0.71	0.33	1.58	0.35	3.83	0.31	1.64	6.44	0.01	-13.90	-3.32
L92	10.99	4.60	39.93	17.39	56.52	1.42	51.75	176.96	0.14	-6.70	-2.11
L93	0.44	0.17	1.11	0.16	2.19	0.31	1.28	1.52	0.01	-13.80	-3.23
L94	0.48	0.25	0.87	0.24	2.72	0.55	1.33	0.47	0.01	-4.30	-2.06
L95	0.56	0.18	0.94	0.12	2.62	0.89	1.39	1.01	0.01	-32.50	-5.19
L96	0.65	0.18	0.92	0.29	2.87	0.20	1.34	0.42	0.01	2.30	0.33

APPENDIX 4

Major ions (mg/l) and Stable Isotopes of Dry season samples

Sample ID	Ca	Mg	Na	K	HCO_3	SO_4	Cl	NO_3	F	δ2H (‰)	δ18O (‰)
L01	11.21	8.49	37.58	9.16	76.66	2.38	72.30	15.73	0.16	-14.4	-3.33
L02	87.60	27.27	142.78	19.16	403.58	70.36	199.86	311.92	0.15	-7.1	-2.16
L03	80.31	35.09	66.11	4.40	420.47	5.21	12.84	0.26	1.50	-11.6	-2.86
L04	2.51	0.32	3.86	0.40	9.26	0.36	2.56	0.92	0.01	-14.5	-3.29
L05	2.88	0.30	6.75	0.52	10.31	0.38	7.60	5.72	0.03	-14.6	-3.27
L06	2.53	0.40	8.01	1.02	9.69	0.28	7.71	11.48	0.04	-14.8	-3.21
L07	7.90	3.82	20.06	5.34	43.18	1.50	25.21	65.34	0.06	-13.3	-3.03
L08	2.40	0.25	3.38	0.52	8.55	0.42	3.73	3.49	0.12	-14	-3.21
L09	1.94	0.43	4.63	0.75	8.05	0.69	6.57	1.98	0.03	-12.8	-2.95
L10	35.79	20.09	28.64	20.12	209.65	68.07	59.16	112.31	0.13	-12.9	-2.89
L11	1.32	0.61	4.22	0.52	7.08	0.45	4.73	2.66	0.03	-12.2	-2.82
L12	8.79	0.73	7.24	0.79	30.48	10.75	2.76	0.79	0.47	-13.7	-2.96
L13	8.23	2.36	4.71	0.96	36.91	0.70	7.09	20.37	0.07	-12.5	-2.92
L14	4.27	1.76	9.47	0.79	21.82	0.36	8.79	28.72	0.06	-12.9	-3.06
L15	13.92	6.75	35.38	14.77	76.22	1.50	51.30	156.42	0.58	-11.9	-2.78
L16	9.48	0.61	4.20	0.67	31.96	0.54	4.67	4.61	0.04	-12.6	-2.88
L17	1.38	0.90	6.49	2.22	8.69	0.29	13.49	3.56	0.06	-13.1	-3.07
L18	22.60	6.78	43.86	27.31	102.86	0.46	96.84	168.93	0.39	-10.1	-2.42
L19	1.09	0.33	5.16	0.37	12.97	0.35	5.96	1.33	0.04	-12.6	-2.91
L20	184.95	118.16	47.49	3.29	1155.10	576.26	146.43	7.40	0.51	-12.8	-3

Major ions (mg/l) and Stable Isotopes of Dry season samples

Sample ID	Ca	Mg	Na	K	HCO_3	SO_4	Cl	NO3	F	δ^2H (‰)	$\delta^{18}O$ (‰)
L21	1.96	1.38	7.15	0.52	12.88	0.00	8.39	19.72		-13.3	-3.16
L22	1.70	0.38	6.27	0.52	56.09	0.34	8.09	2.26	0.03	-14.4	-3.41
L23	3.78	1.26	13.08	0.48	17.81	0.48	12.80	26.41	0.04	-12.9	-3.26
L24	11.61	6.84	3.30	0.35	69.61	0.30	5.51	0.69	0.04	-13.6	-3.37
L25	2.79	0.51	4.73	0.25	11.05	0.41	7.01	2.89	0.04	-11.6	-3.01
L26	2.13	1.08	7.98	3.79	11.91	0.41	12.10	28.56	0.17	-14.5	-3.36
L27	3.30	0.31	4.67	1.33	11.63	0.29	6.86	1.53	0.04	-14.2	-3.32
L28	2.81	1.82	8.56	6.28	17.69	13.93	11.95	7.80	0.08	-13.4	-3.16
L29	12.15	6.97	23.84	4.00	71.94	0.96	27.25	119.50	0.21	-12.7	-2.93
L30	3.11	0.64	10.33	1.22	12.66	0.48	7.29	22.81	0.30	-15.2	-3.38
L31	0.59	0.68	5.08	1.55	5.23	2.40	3.65	9.83	0.03	-14.9	-3.46
L32	2.31	0.82	9.50	2.25	37.16	0.89	12.99	13.01	0.09	-14.1	-3.36
L33	10.58	2.28	37.19	3.79	43.66	8.24	66.99	3.29	0.03	-4.7	-1.5
L34	448.50	1125.00	10310	590	8390	2932	18833	1.56	1.50	7.5	0.83
L35	3.74	5.25	12.66	4.10	37.70	0.41	7.08	2.91	0.02	-13.7	-3.35
L36	15.65	5.53	31.94	2.52	7.37	87.61	13.82	0.73	0.34	-10.3	-2.58
L37	32.09	5.84	30.92	14.82	28.07	29.71	35.77	78.12	0.10	-10.8	-2.6
L38	41.04	9.50	85.83	49.87	98.70	70.18	109.38	199.81	0.04	-10.2	-2.48
L39	15.98	2.84	30.11	8.83	62.92	20.37	41.09	89.18	0.21	-10.6	-2.67
L40	8.24	2.31	24.26	3.46	36.66	21.55	32.02	14.94	0.03	-8.1	-2.3

Major ions (mg/l) and Stable Isotopes of Dry season samples

Sample ID	Ca	Mg	Na	K	HCO_3	SO_4	Cl	NO_3	F	δ2H, in ‰	δ18O, in ‰
L41	1.64	0.78	17.23	1.22	8.91	0.45	13.47	34.37	0.03	-12.6	-3.02
L42	12.85	3.06	33.16	8.07	54.52	28.37	37.84	78.88	0.15	-9.7	-2.46
L43	338.10	285.90	1583.00	11.94	2618.89	10.60	4185.00	1.50	1.50	-10.3	-2.64
L44	5.24	3.22	17.71	4.24	32.09	3.80	43.22	0.41	0.11	-16.8	-3.72
L45	1.86	1.26	13.76	0.49	11.10	0.81	12.10	39.90	0.06	-14.9	-3.39
L46	0.44	0.14	2.44	0.69	15.05	0.31	3.36	0.25	0.05	-13.7	-3.28
L47	0.84	0.60	7.85	1.81	5.54	0.61	7.47	14.07	0.07	-15	-3.37
L48	0.89	0.51	13.30	0.97	5.27	0.41	10.55	25.21	0.04	-12.8	-3.01
L49	4.30	2.05	12.26	1.68	23.35	0.90	9.73	10.70	0.05	-13.4	-3.2
L50	37.21	6.06	36.28	17.49	143.79	18.57	60.45	4.94	0.09	-9.9	-2.46
L51	4.66	1.51	32.31	2.49	51.76	0.62	26.89	78.36	0.10	-13.2	-3.13
L52	8.89	1.57	3.68	0.86	34.98	1.11	6.62	0.75	0.04	-13.7	-3.35
L53	1.13	0.33	3.11	0.63	5.10	0.38	5.00	0.26	0.04	-13.1	-3.27
L54	2.78	1.23	3.99	2.18	14.65	0.76	6.36	11.47	0.03	-14	-3.4
L55	3.88	1.26	7.67	5.01	18.16	1.49	12.04	26.06	0.12	-14.7	-3.3
L56	1.00	0.41	2.74	0.32	15.13	0.31	6.19	0.91	0.06	-13.8	-3.27
L57	2.05	1.01	5.97	1.17	11.29	0.38	8.09	10.64	0.02	-12.8	-3.16
L58	2.68	1.43	14.74	2.80	15.30	0.35	13.49	43.24	0.04	-12.6	-3.03
L59	1.66	0.54	7.59	1.90	7.78	0.41	6.84	17.19	0.02	-14.9	-3.5
L60	6.85	3.76	21.44	8.88	39.71	0.66	27.30	70.50	0.11	-12.7	-3.11

Major ions (mg/l) and Stable Isotopes of Dry season samples

Sample ID	Ca	Mg	Na	K	HCO_3	SO_4	Cl	NO_3	F	δ2H, in ‰	δ18O, in ‰
L61	1.50	0.66	8.25	0.75	7.87	0.35	5.77	17.67	0.04	-13.1	-3.13
L62	1.86	1.16	11.99	1.61	11.47	36.45	5.18	0.35	0.04	-11.9	-2.99
L63	11.25	5.77	38.85	11.34	63.18	0.36	39.22	154.94	0.10	-11.3	-2.78
L64	6.78	2.57	12.50	5.61	33.53	0.71	9.74	66.27	0.14	-12.9	-2.97
L65	4.44	1.84	9.55	2.68	22.75	0.57	9.37	35.78	0.02	-13	-3.24
L66	1.74	0.64	4.45	8.70	8.50	1.43	7.22	22.37	0.02	-13.9	-3.38
L67	0.78	0.37	1.94	0.40	4.24	0.39	2.72	3.62	0.06	-13	-3.26
L68	1.14	0.54	7.84	1.16	36.16	0.73	11.64	6.13	0.02	-13.3	-3.42
L69	1.00	0.46	2.58	2.01	5.35	1.26	3.88	1.78	0.03	-13	-3.31
L70	1.49	0.93	8.94	0.84	9.21	0.26	5.90	25.66	0.07	-12.8	-3.11
L71	25.09	1.74	19.76	3.81	85.25	26.02	22.70	61.44	0.01	-10.8	-2.89
L72	2.08	0.64	9.01	1.80	9.54	0.71	8.80	29.08	0.05	-14.7	-3.58
L73	35.60	3.83	42.50	23.08	127.72	40.80	55.45	111.51	0.07	-12.1	-3.13
L74	9.48	3.77	14.81	8.31	47.77	5.79	20.15	60.89	0.02	-12.5	-3.15
L75	26.29	1.39	11.47	2.78	23.11	27.05	18.73	38.22	0.02	-9.8	-2.52
L76	6.58	1.57	8.31	9.55	27.94	7.45	10.20	36.54	0.02	-13.6	-3.11
L77	15.99	0.88	2.15	1.50	2.17	1.62	2.66	0.77	0.03	-16	-3.5
L78	16.74	0.75	7.59	2.56	54.82	10.34	9.43	6.58	0.05	-10.9	-2.87
L79	34.24	4.85	43.88	19.05	128.68	151.56	50.19	15.05	0.09	-8.9	-2.64
L80	64.82	9.56	66.46	5.08	120.52	29.06	144.93	2.55	0.05	-11.1	-2.93

Major ions (mg/l) and Stable Isotopes of Dry season samples

Sample ID	Ca	Mg	Na	K	HCO_3	SO_4	Cl	NO_3	F	δ2H, in ‰	δ18O, in ‰
L81	8.81	1.61	6.07	16.37	34.94	14.04	7.48	30.46	0.04	-13.1	-3.03
L82	49.48	7.07	83.11	33.33	186.25	94.53	92.55	214.43	0.05	-13.6	-3.06
L83	95.83	15.30	128.90	56.60	132.63	133.82	150.00	244.99	0.05	-10.8	-2.66
L84	10.03	1.41	4.32	3.32	7.94	12.30	9.94	6.47	0.02	-18.3	-3.84
L85	63.03	31.88	33.16	18.69	561.71	72.05	30.04	7.83	0.29	-14.1	-3.48
L86	32.66	2.06	3.23	1.30	109.90	2.55	5.71	1.24	0.05	-12.2	-3.22
L87	34.38	3.07	8.10	4.75	120.21	10.30	10.70	20.99	0.06	-9.9	-2.81
L88	63.12	2.65	9.71	7.29	205.76	61.82	12.69	5.20	0.04	-8.2	-2.7
L89	7.42	0.56	2.87	1.26	25.45	4.03	3.15	9.56	0.01	-7.2	-2.43
L90	50.29	4.85	12.50	5.71	177.64	74.84	19.03	6.87	0.05	-13	-3.28
L91	71.43	3.85	31.32	9.53	23.10	28.18	35.76	2.91	0.09	-7.9	-2.66
L92	77.98	27.53	85.62	18.75	75.54	32.84	90.45	8.46	0.28	-9.2	-2.87
L93	85.25	17.39	56.88	5.88	77.00	54.13	91.93	1.72	0.10	-8.8	-2.6
L94	179.50	190.30	788.80	25.02	320.00	111.00	1378.00	59.52	1.50	-9.1	-2.65
L95	16.50	1.90	5.26	5.05	59.81	15.80	9.20	7.41	0.04	-10.5	-2.72
L96	23.54	1.70	26.95	4.28	69.76	35.70	27.20	5.52	0.04	-6.8	-2.28
L97	48.34	4.81	46.34	18.99	43.66	57.30	54.60	51.00	0.04	-7.6	-2.37
L98	19.70	1.43	3.87	3.79	67.24	4.33	4.29	9.55	0.03	-11.8	-2.87
L99	3.74	1.27	8.08	4.03	17.76	7.11	10.16	0.29	0.04	-12.9	-3.15
L100	0.39	0.17	4.68	0.53	2.03	3.62	1.80	5.07	0.05	-12.3	-3.13

Major ions (mg/l) and Stable Isotopes of dry season samples

Sample ID	Ca	Mg	Na	K	HCO_3	SO_4	Cl	NO_3	F	δ^2H (‰)	$\delta^{18}O$ (‰)
L101	1.48	0.23	2.34	0.69	5.68	0.74	2.22	3.47	0.07	-13.7	-3.42
L102	1.15	0.25	0.63	0.13	4.74	0.99	0.87	0.25	0.01	-14.8	-3.44
L103	1.36	0.94	1.52	5.25	8.40	0.37	8.38	13.80	0.08	-12.5	-3.21
L104	0.58	0.16	0.93	0.05	2.54	0.98	1.44	1.04	0.07	-13.4	-3.32
L105	0.89	0.45	2.06	0.79	4.94	0.58	1.85	7.17	0.04	-10.4	-2.84
L106	1.87	0.53	2.07	1.88	8.33	3.91	3.67	0.25	0.02	-17.2	-4.03
L107	0.44	0.23	3.49	0.94	2.48	3.14	3.48	0.25	0.03	-13.4	-3.53
L108	0.97	0.22	1.08	1.12	4.06	1.20	2.29	1.44	0.07	-11.2	-3.15
L109	1.52	0.72	1.16	0.08	7.65	0.67	2.94	13.90	0.04	-11.3	-3.14
L110	0.67	0.18	0.89	0.30	2.94	0.69	1.85	0.45	0.04	-12.5	-3.25
L111	0.31	0.14	0.93	0.72	1.65	0.00	0.00	0.00	0.00	-13.1	-3.36
L112	0.54	0.24	1.28	0.59	2.82	0.49	1.84	0.45	0.05	-13.1	-3.4
L113	0.53	0.26	1.80	1.16	2.94	0.48	1.92	1.77	0.07	-15.4	-3.66
L114	0.37	0.23	2.67	0.13	2.28	0.63	3.11	1.00	0.04	-11.3	-3.13
L115	0.35	0.17	1.17	0.12	1.92	0.55	1.83	5.94	0.03	-12.2	-3.11
L116	2.20	0.62	3.48	4.10	9.81	0.47	1.35	0.73	0.03	-11.9	-2.89
L117	1.38	0.44	4.32	0.49	6.42	0.88	2.03	2.07	0.06	-13	-3.06
L118	1.31	0.58	5.62	0.75	6.87	0.74	3.17	8.90	0.04	-13.4	-3.21
L119	4.47	2.57	14.10	13.12	26.47	15.50	5.86	0.78	0.01	-12.5	-3.03
L120	2.711	1.355	3.65	2.86	15.10	1.00	17.49	64.12	0.05	-12.1	-3.01

Major ions (mg/l) and Stable Isotopes of Dry season samples

Sample ID	**Ca**	**Mg**	**Na**	**K**	**HCO_3**	**SO_4**	**Cl**	**NO_3**	**F**	**δ^2H (‰)**	**$\delta^{18}O$ (‰)**
L121	0.84	0.58	2.98	1.68	5.47	0.99	5.19	20.28	0.03	-14.1	-3.27
L122	1.58	0.30	1.05	0.73	6.28	0.46	3.76	9.94	0.02	-19.7	-3.94
L123	3.57	0.37	2.05	1.00	12.75	0.65	0.94	3.09	0.04	-12.8	-2.96
L124	0.63	0.30	1.15	0.43	3.43	4.32	2.18	12.08	0.03	-12.9	-3.16
L125	0.24	0.17	0.83	0.24	1.59	0.84	1.54	1.90	0.01	-12.8	-3.22
L126	20.43	8.95	73.32	26.47	107.07	0.61	1.38	0.30	0.04	-10.7	-2.67
L127	1.14	0.68	2.18	0.66	6.91	4.57	110.23	214.11	0.25	-14.8	-3.34
L128	0.32	0.18	1.29	0.71	1.88	9.11	2.87	0.29	0.05	-14.4	-3.31
L129	0.37	0.15	0.84	0.48	1.90	0.74	1.82	0.92	0.03	-12.4	-3.06
L130	0.54	0.34	2.16	0.47	3.35	0.82	1.13	0.25	0.03	-15	-3.39
L131	1.51	0.84	3.26	1.60	8.83	0.69	2.01	7.06	0.02	-14.8	-3.39
L132	12.03	4.58	33.50	15.41	59.58	0.67	4.00	10.98	0.01	-12.5	-2.92
L133	3.43	0.57	2.05	4.74	13.35	2.01	40.57	146.10	0.19	-15.3	-3.4
L134	20.00	1.63	23.90	4.60	69.16	0.79	5.65	2.43	0.05	-15.2	-3.34

APPENDIX 5

Heavy and Trace Metals (µg/l) for wet season groundwater samples

Sample ID	As	Ba	Cd	Co	Cr	Cu	Fe	Hg	Li	Mn	Ni	Pb	Sr	Zn
L01	0.9	10.6	0.3	0.8	1.1	0.7	193.1	2.5	5.1	26.7	1.0	3.4	34.1	15.0
L02	0.9	32.2	0.3	0.8	1.1	12.1	54.5	2.5	5.1	51.6	1.0	3.4	29.3	10.7
L03	0.9	1.0	0.3	0.8	1.1	0.7	43.0	2.5	5.1	10.0	1.0	3.4	11.4	6.9
L04	0.9	138.7	0.3	0.8	1.1	0.7	102.9	2.5	5.1	19.4	1.0	3.4	159.0	5.8
L05	0.9	453.8	0.3	0.8	1.1	14.1	198.2	2.5	43.0	190.2	1.0	3.4	433.2	0.5
L06	0.9	14.1	0.3	0.8	1.1	15.9	16.7	2.5	5.1	4.6	1.0	3.4	13.1	9.6
L07	0.9	21.2	0.3	0.8	1.1	21.6	23.8	2.5	5.1	8.0	1.0	3.4	23.0	26.3
L08	0.9	19.2	0.3	0.8	1.1	22.0	16.6	2.5	5.1	3.9	1.0	3.4	18.4	13.5
L09	0.9	100.2	0.3	0.8	1.1	12.2	79.3	2.5	5.1	49.2	1.0	3.4	59.2	19.2
L10	0.9	90.7	0.3	0.8	1.1	5.9	12.9	2.5	5.1	1.4	1.0	3.4	142.3	0.5
L11	0.9	46.9	0.3	4.0	1.1	0.7	82.9	2.5	5.1	167.8	1.0	3.4	37.1	30.9
L12	0.9	17.8	0.3	0.8	1.1	21.5	180.9	2.5	5.1	14.0	1.0	12.3	16.6	51.9
L13	0.9	128.3	0.3	3.3	1.1	11.7	68.3	2.5	5.1	44.0	1.0	3.4	59.6	12.5
L14	0.9	112.0	0.3	3.4	1.1	8.6	137.5	2.5	5.1	87.0	1.0	3.4	95.1	12.8
L15	0.9	49.2	0.3	0.8	1.1	0.7	43.4	2.5	5.1	7.8	1.0	3.4	42.8	7.4
L16	0.9	31.8	0.3	0.8	1.1	42.5	19.7	2.5	5.1	10.2	1.0	3.4	22.6	88.2
L17	0.9	80.2	0.3	0.8	1.1	265.1	36.8	2.5	5.1	45.4	4.6	17.8	20.6	297.5
L18	0.9	422.9	0.3	42.0	1.1	6.7	31.9	2.5	5.1	1113.0	14.7	16.2	110.3	81.6
L19	0.9	17.8	0.3	0.8	1.1	0.7	61.3	2.5	5.1	5.0	1.0	3.4	6.9	0.5
L20	0.9	264.5	0.3	3.6	1.1	0.7	24.1	2.5	5.1	124.7	1.0	3.4	224.3	11.7
L21	0.9	76.7	0.3	5.1	1.1	15.8	10.1	2.5	5.1	131.2	1.0	3.4	25.8	5.9
L22	0.9	22.6	0.3	0.8	1.1	89.5	54.8	2.5	5.1	24.8	1.0	3.4	8.8	100.8
L23	0.9	39.8	0.3	0.8	1.1	11.4	39.3	2.5	5.1	108.1	1.0	3.4	23.6	29.6
L24	0.9	24.2	0.3	0.8	1.1	0.7	380.3	2.5	5.1	26.0	1.0	3.4	11.3	9.7
L25	0.9	16.2	0.3	0.8	1.1	190.9	25.2	2.5	5.1	10.4	4.7	13.4	11.7	348.7
L26	0.9	18.7	0.3	0.8	1.1	37.3	17.7	2.5	5.1	16.0	1.0	3.4	10.4	32.8
L27	0.9	18.8	0.3	0.8	1.1	17.4	37.0	2.5	5.1	6.2	1.0	3.4	48.4	21.1
L28	0.9	25.0	0.3	0.8	1.1	11.0	13.9	2.5	5.1	7.5	1.0	3.4	10.5	10.3
L29	0.9	16.9	0.3	0.8	1.1	20.0	13.8	2.5	5.1	19.5	1.0	3.4	8.9	22.1
L30	0.9	14.6	0.3	0.8	1.1	29.5	33.2	2.5	5.1	11.5	1.0	3.4	14.9	10.1
L31	0.9	24.1	0.3	0.8	1.1	42.9	98.3	2.5	5.1	29.5	1.0	3.4	21.7	312.8
L32	0.9	97.6	0.3	4.0	1.1	0.7	34.6	2.5	5.1	209.1	1.0	3.4	80.8	22.0
L33	0.9	15.3	0.3	0.8	1.1	8.2	17.3	2.5	5.1	8.2	1.0	3.4	6.9	1.1
L34	0.9	78.9	0.3	0.8	1.1	0.7	125.1	2.5	5.1	18.8	1.0	3.4	26.1	8.0
L35	0.9	71.8	0.3	4.4	3.3	0.7	1126.0	2.5	5.1	262.5	1.0	3.4	117.9	11.9

Heavy and Trace Metals (µg/l) for wet season groundwater samples

Sample ID	As	Ba	Cd	Co	Cr	Cu	Fe	Hg	Li	Mn	Ni	Pb	Sr	Zn
L36	0.9	8.3	0.3	0.8	1.1	9.2	428.7	2.5	822.2	22.1	1.0	3.4	6424.0	0.5
L37	0.9	11.9	0.3	0.8	1.1	10.9	22.0	2.5	5.1	8.6	1.0	3.4	90.5	30.1
L38	0.9	203.8	0.3	0.8	1.1	6.6	136.6	2.5	5.1	77.3	1.0	3.4	77.0	8.8
L39	0.9	16.1	0.3	0.8	1.1	8.0	26.0	2.5	5.1	10.1	1.0	3.4	8.6	6.9
L40	0.9	67.1	0.3	3.0	1.1	0.7	0.9	2.5	5.1	149.0	1.0	3.4	61.0	23.3
L41	0.9	15.1	0.3	0.8	1.1	8.0	6.5	2.5	5.1	2.5	1.0	3.4	28.2	8.5
L42	0.9	18.3	0.3	0.8	1.1	15.9	7.2	2.5	5.1	4.8	1.0	3.4	5.9	12.5
L43	0.9	1239.0	0.3	0.8	1.1	8.0	14.9	2.5	5.1	220.0	8.1	3.4	352.4	37.1
L44	0.9	195.2	0.3	0.8	1.1	39.7	142.2	2.5	5.1	29.3	1.0	11.6	39.5	120.7
L45	0.9	19.4	0.3	0.8	1.1	11.5	25.3	2.5	5.1	37.2	1.0	3.4	6.7	45.6
L46	0.9	103.4	0.3	0.8	1.1	7.0	0.9	2.5	5.1	245.8	1.0	3.4	62.0	5.9
L47	0.9	3.3	0.3	0.8	1.1	69.5	33.5	2.5	5.1	9.4	1.0	3.4	2.5	65.6
L48	0.9	53.7	0.3	1.9	1.1	73.6	96.8	2.5	5.1	65.9	1.0	9.0	46.7	78.7
L49	0.9	5.5	0.3	0.8	1.1	0.7	49.9	2.5	5.1	8.3	1.0	3.4	1.8	23.0
L50	0.9	53.4	0.3	0.8	4.2	24.9	23.6	2.5	5.1	2.0	1.0	3.4	77.0	36.9
L51	0.9	44.4	0.3	0.8	1.1	16.5	29.9	2.5	5.1	14.6	1.0	61.3	30.9	24.7
L52	0.9	77.3	0.3	0.8	1.1	21.8	97.9	2.5	5.1	43.3	1.0	3.4	27.2	17.2
L53	0.9	5.5	0.3	32.6	1.1	18.9	1107.0	2.5	5.1	61.7	54.0	3.4	2.4	606.4
L54	0.9	30.1	0.3	0.8	1.1	15.8	12.9	2.5	5.1	51.8	1.0	3.4	19.8	12.6
L55	0.9	10.1	0.3	0.8	1.1	13.1	31.4	2.5	5.1	16.3	1.0	3.4	4.5	21.8
L56	0.9	26.4	0.3	0.8	1.1	0.7	43.8	2.5	5.1	2.4	1.0	3.4	77.6	0.5
L57	0.9	26.5	0.3	0.8	1.1	45.3	34.9	2.5	5.1	59.5	1.0	3.4	13.0	64.2
L58	0.9	28.1	0.3	0.8	1.1	18.1	90.1	2.5	5.1	173.3	1.0	3.4	142.4	83.4
L59	0.9	15.5	0.3	0.8	1.1	12.7	12.5	2.5	5.1	50.9	1.0	3.4	44.3	42.7
L60	0.9	1.5	0.3	0.8	1.1	10.4	17.0	2.5	5.1	4.8	1.0	3.4	2.4	8.7
L61	0.9	40.9	0.3	0.8	1.1	0.7	119.6	2.5	5.1	23.6	1.0	3.4	55.9	2.5
L62	0.9	2.5	0.3	0.8	1.1	35.5	41.8	2.5	5.1	29.3	1.0	3.4	3.9	131.0
L63	0.9	78.3	0.3	0.8	1.1	5.4	34.2	2.5	5.1	19.8	1.0	18.2	70.8	10.9
L64	0.9	178.6	0.3	0.8	1.1	12.9	1611.0	2.5	5.1	156.7	1.0	3.4	89.9	21.3
L65	0.9	0.6	0.3	0.8	1.1	0.7	22.9	2.5	5.1	3.4	1.0	3.4	0.4	2.8
L66	9.9	7.1	0.3	0.8	1.1	7.8	573.6	2.5	5.1	21.2	1.0	3.4	131.6	9.0
L67	0.9	12.8	0.3	0.8	1.1	0.7	0.9	2.5	5.1	0.2	1.0	3.4	179.9	3.4
L68	0.9	92.6	0.3	1.6	1.1	6.6	85.2	2.5	5.1	80.2	1.0	3.4	162.0	20.0
L69	0.9	46.8	0.3	0.8	1.1	6.4	220.8	2.5	1.5	24.5	1.0	3.4	53.2	27.6
L70	0.9	165.8	0.3	0.8	1.1	33.8	126.3	2.5	7.8	58.2	1.0	3.4	239.2	8.6

Heavy and Trace Metals (µg/l) for wet season groundwater samples

Sample ID	As	Ba	Cd	Co	Cr	Cu	Fe	Hg	Li	Mn	Ni	Pb	Sr	Zn
L71	0.9	29.2	0.3	0.8	1.1	0.7	158.5	2.5	5.1	74.2	1.0	3.4	75.3	8.8
L72	0.9	9.5	0.3	0.8	1.1	6.8	91.0	2.5	10.5	73.8	1.0	3.4	545.2	0.5
L73	0.9	2.6	0.3	0.8	1.1	39.5	205.4	2.5	5.1	40.1	1.0	3.4	53.4	83.0
L74	39.5	7.0	0.3	0.8	1.1	7.1	3102.0	2.5	5.1	133.3	1.0	23.6	249.0	36.8
L75	0.9	13.7	0.3	0.8	1.1	0.7	135.2	2.5	5.1	66.2	1.0	10.5	61.7	12.3
L76	20.1	26.3	0.3	0.8	5.2	11.9	2721.0	2.5	5.1	140.2	1.0	3.4	195.9	459.8
L77	0.9	5.0	0.3	0.8	2.5	8.7	338.5	2.5	16.7	364.7	1.0	3.4	805.6	0.5
L78	0.9	4.7	0.3	0.8	1.1	0.7	490.5	2.5	5.1	49.1	1.0	3.4	250.1	1.7
L79	0.9	7.8	0.3	0.8	1.1	7.8	780.0	2.5	5.1	104.3	1.0	3.4	177.2	69.3
L80	0.9	5.3	0.3	0.8	1.1	7.1	346.6	2.5	5.1	33.9	1.0	3.4	63.0	200.3
L81	0.9	16.7	1.2	0.8	1.1	8.8	6093.0	2.5	5.1	244.0	1.0	3.4	301.6	3.3
L82	0.9	3.7	0.3	0.8	1.1	9.2	285.1	2.5	5.1	14.8	1.0	3.4	57.4	25.6
L83	0.9	6.3	0.3	0.8	1.1	7.5	345.4	2.5	5.1	31.3	1.0	3.4	2.0	55.3
L84	0.9	5.7	0.3	0.8	1.1	50.8	190.4	2.5	5.1	26.0	1.0	36.9	8.5	75.9
L85	0.9	41.5	0.3	0.8	1.1	13.0	56.3	2.5	5.1	86.3	1.0	3.4	24.2	59.0
L86	0.9	10.3	0.3	0.8	1.1	47.4	85.7	2.5	5.1	20.3	1.0	11.0	17.3	123.2
L87	0.9	16.6	0.3	0.8	1.1	13.6	80.1	2.5	5.1	31.1	1.0	3.4	6.1	78.9
L88	0.9	4.8	0.3	0.8	1.1	0.7	53.2	2.5	5.1	81.7	1.0	3.4	16.2	33.3
L89	0.9	6.1	0.3	0.8	1.1	47.9	113.0	2.5	5.1	18.1	1.0	3.4	2.6	80.8
L90	0.9	3.8	0.3	0.8	1.1	20.8	29.8	2.5	5.1	10.5	1.0	3.4	2.3	28.9
L91	0.9	13.3	0.3	0.8	1.1	46.7	177.8	2.5	5.1	29.0	1.0	3.4	6.0	85.8
L92	0.9	92.3	0.3	2.8	1.1	13.5	230.7	2.5	5.1	365.2	1.0	3.4	66.3	65.0
L93	0.9	4.5	0.3	0.8	1.1	9.6	50.2	2.5	5.1	9.0	1.0	3.4	1.8	18.6
L94	0.9	10.8	0.3	0.8	1.1	11.9	274.6	2.5	5.1	18.4	1.0	3.4	2.3	21.4
L95	0.9	3.7	0.3	0.8	1.1	16.6	55.6	2.5	5.1	9.8	1.0	3.4	3.3	30.9
L96	0.9	3.4	0.3	0.8	1.1	45.4	115.4	2.5	5.1	7.0	1.0	3.4	3.4	47.5

APPENDIX 6

Heavy and Trace Metals (µg/l) for dry season groundwater samples

Sample ID	As	Ba	Cd	Co	Cr	Cu	Fe	Hg	Li	Mn	Ni	Pb	Sr	Zn
L1	7	202	0.4	1.2	1.5	0.8	30.5	4	7.5	8.9	5.3	20	114.3	18.8
L2	7	458.7	0.4	7.1	1.5	0.8	23	4	2.9	1.8	3.1	20	471.9	8
L3	7	429.8	0.4	1.2	1.5	0.8	32.1	4	39.8	23.3	1.2	20	416.8	11.6
L4	7	10.9	0.4	1.2	1.5	0.8	13.8	4	2.9	2.8	1.2	20	10.7	38.3
L5	7	19.7	0.4	1.2	1.5	0.8	13.6	4	2.9	4.7	1.2	20	11.8	21
L6	7	19	0.4	1.2	1.5	22.8	31	4	2.9	3.4	1.2	20	16.2	71.7
L7	7	78.3	0.4	1.2	1.5	0.8	13.7	4	2.9	35.1	1.2	20	52.7	41.2
L8	7	20.6	0.4	1.2	1.5	0.8	103.3	4	2.9	13.5	1.2	20	9.4	23.2
L9	7	19.9	0.4	1.2	1.5	44.2	20.7	4	2.9	6.4	1.2	20	11.5	83.2
L10	7	112.8	0.4	1.2	1.5	0.8	581.9	4	2.9	11.4	1.2	20	257.6	36.8
L11	7	16.7	0.4	1.2	1.5	0.8	23.7	4	2.9	5.4	1.2	20	15.1	10.2
L12	7	16.8	0.4	1.2	1.9	0.8	1111	4	2.9	377.4	5.2	20	18.4	29.7
L13	7	106.9	0.4	1.2	1.5	40.4	17.5	4	2.9	7.7	1.2	20	81.6	75.8
L14	7	75.7	0.4	1.2	1.5	31.6	24.3	4	2.9	16.8	1.2	20	51.8	51.5
L15	7	226.5	0.4	5.3	1.5	0.8	33.8	5	7.6	166	4.3	20	130.4	63.4
L16	7	32.5	0.4	1.2	1.5	30.9	41.6	4	2.9	5.1	1.2	20	29.8	58.7
L17	7	66.2	0.4	1.2	1.5	62.1	17.6	4	2.9	32.8	1.2	20	16.7	84.5
L18	7	429.4	0.4	36.9	1.5	0.8	177.8	4	28	869.1	17.4	20	116.9	133.7
L19	7	16	0.4	1.2	1.5	0.8	22.2	4	2.9	3.3	1.2	20	9.6	5.5
L20	7	73.7	0.4	1.2	1.5	0.8	3249	4	291.3	215	5.3	20	1280.4	0.3
L21	0	0	0	0	0	0	0	0	0	0	0	0	0	0
L22	7	17.3	0.4	1.2	1.5	0.8	33.5	4	2.9	7.8	1.2	20	8.7	14.3
L23	7	43.5	0.4	2.7	1.5	0.8	13.7	4	2.9	91.3	1.2	20	26.5	13.7
L24	7	16.1	0.4	1.2	1.5	158.6	21.1	4	2.9	14.5	1.2	20	14.5	261.6
L25	7	27.3	0.4	1.2	1.5	0.8	16.7	4	2.9	6.8	1.2	20	11.4	8.4
L26	7	24.6	0.4	1.2	1.5	98.9	19.3	4	2.9	39.6	1.2	20	14.4	93.4
L27	7	13.5	0.4	1.2	1.5	0.8	23.2	4	2.9	8.8	1.2	20	12.3	10.9
L28	7	18.5	0.4	1.2	1.5	0.8	15	4	2.9	21.8	1.2	20	11.6	10.2
L29	7	86.5	0.4	4.1	1.5	0.8	51.4	4	3.8	163.5	1.2	20	80	24.9
L30	7	18.2	0.4	1.2	1.5	26.3	39	4	2.9	12.1	1.2	20	10.7	46.5
L31	7	11.8	0.4	1.2	1.5	0.8	25.9	4	2.9	9.2	1.2	20	4.5	3.8
L32	7	81.3	0.4	1.2	1.5	0.8	43.2	4	2.9	13.3	1.2	20	25.7	14.8
L33	24.4	35.3	0.4	8.3	3.8	0.8	8566	4	2.9	178.2	1.2	20	63.8	8
L34	7	16.9	0.4	1.2	1.5	0.8	530.5	4	319.6	21.6	1.2	20	7763.2	67.4
L35	7	15.8	0.4	1.2	1.5	0.8	1344	4	2.9	54.5	1.2	20	46.3	77.1

Heavy and Trace Metals (µg/l) for dry season groundwater samples

Sample ID	As	Ba	Cd	Co	Cr	Cu	Fe	Hg	Li	Mn	Ni	Pb	Sr	Zn
L36	7	29.4	0.4	1.2	1.5	0.8	4506	4	72.4	238.5	1.2	20	172	18.3
L37	7	12.7	0.4	1.2	1.5	0.8	57.7	4	2.9	10.6	1.2	20	116	102.8
L38	7	54.6	0.4	1.2	1.5	0.8	30.2	4	2.9	100.1	1.2	20	209	108.8
L39	7	282.7	0.4	3.9	1.5	0.8	13.3	4	5.1	239.2	1.2	20	70	54.2
L40	7	51	0.4	1.2	1.5	0.8	6184	4	2.9	88.7	1.2	20	43.9	71.5
L41	7	23.7	0.4	1.2	1.5	0.8	39.2	4	2.9	38.6	1.2	20	13.2	53.8
L42	7	48.5	0.4	1.2	1.5	0.8	34.5	4	2.9	58.6	4.1	20	49.2	61.3
L43	7	7633	0.4	149	1.5	0.8	#####	4	19.1	27678	19.4	20	4656	48.5
L44	7	91.2	0.4	1.2	1.5	18.3	6951	4	3.3	213.8	1.2	20	60.1	42
L45	7	30.9	0.4	1.2	1.5	0.8	49.4	4	2.9	30.6	1.2	20	21.2	14.1
L46	7	3.5	0.4	1.2	1.5	0.8	32.7	4	2.9	9.1	1.2	20	2.5	12.6
L47	7	6.6	0.4	1.2	1.5	17.7	25.8	4	2.9	15.8	1.2	20	8.2	41.1
L48	7	18.5	0.4	1.2	1.5	0.8	88.9	4	2.9	30.6	1.2	20	7.3	42.7
L49	7	44.2	0.4	1.2	4.1	0.8	16.9	4	2.9	1.9	1.2	20	71.9	30.4
L50	7	497.1	0.4	9.4	1.5	0.8	988	4	6.1	762.3	1.2	20	350	13.5
L51	7	402.1	0.4	16.2	1.5	0.8	462.8	4	4.6	279.9	7.5	20	49.3	28
L52	7	14.5	0.4	1.2	1.7	0.8	29.1	4	2.9	3.3	1.2	20	26.6	10.7
L53	7	20.5	0.4	1.2	1.5	18.5	26.1	4	2.9	5.2	1.2	20	6.7	27.2
L54	7	34	0.4	1.2	1.5	0.8	27.5	4	2.9	11.9	1.2	20	18	15.2
L55	7	49.7	0.4	1.2	1.5	0.8	133.5	4	2.9	93.7	1.2	20	29.9	19.7
L56	7	15.1	0.4	1.2	1.5	0.8	23.8	4	2.9	7.4	1.2	20	8.3	3.4
L57	7	51.7	0.4	1.2	1.5	23.3	17.7	4	2.9	11.2	1.2	20	20.4	21.9
L58	7	42.5	0.4	2.8	1.5	20.4	70.5	4	2.9	58.6	1.2	20	27.5	15.7
L59	7	14	0.4	1.2	1.5	0.8	44.9	4	2.9	24.8	1.2	20	11.7	16
L60	7	65.6	0.4	1.2	1.5	0.8	44.9	4	2.9	77.9	2.7	20	45.9	43.1
L61	7	17.1	0.4	1.2	1.5	0.8	29.4	4	2.9	32.7	1.2	20	14.9	17.1
L62	7	4.3	0.4	16.3	1.5	0.8	2643	4	2.9	48.8	36.4	20	2	401.2
L63	7	246.6	0.4	9.5	1.5	0.8	14.1	4	7.8	235.5	7.3	20	108	17.6
L64	7	74.3	4.6	3.4	1.5	0.8	40.2	4	3.9	100.8	1.2	20	34.4	32.9
L65	7	103.7	0.4	2.4	1.5	21.5	14.1	4	2.9	30.3	1.2	20	43.3	27.6
L66	7	47.9	0.4	1.2	1.5	0.8	11.5	4	2.9	22.2	1.2	20	18.8	13.6
L67	7	8.4	0.4	1.2	1.5	27.8	8.8	4	2.9	9.4	1.2	20	3	26.7
L68	7	14.1	0.4	1.2	1.5	0.8	24.9	4	2.9	32.5	1.2	20	5.4	2.1
L69	7	6.3	0.4	1.2	1.5	0.8	33.5	4	2.9	10.2	1.2	20	5.1	65.3
L70	7	29.3	0.4	1.2	1.5	0.8	11.7	4	2.9	46.9	1.2	20	13.1	51.5

Heavy and Trace Metals (µg/l) for dry season groundwater samples

Sample ID	As	Ba	Cd	Co	Cr	Cu	Fe	Hg	Li	Mn	Ni	Pb	Sr	Zn
L71	7	46.6	0.4	1.2	1.5	0.8	41.5	4	2.9	29.8	1.2	20	60.2	54.8
L72	7	15.8	0.4	1.2	1.5	0.8	24.7	4	2.9	94	1.2	20	11.9	90.8
L73	7	19.5	0.4	1.2	1.5	0.8	36.2	4	2.9	131.1	1.2	20	102	94.7
L74	7	14.4	0.4	1.2	1.5	0.8	9.5	4	2.9	38.5	1.2	20	41.6	24.2
L75	7	62.5	0.4	1.2	1.5	0.8	62	4	2.9	20.2	1.2	20	88.6	30.3
L76	7	95.7	0.4	1.2	1.5	0.8	57.4	4	2.9	22.6	1.2	20	32.4	38.7
L77	7	4.8	0.4	1.2	3.2	0.8	692	4	2.9	16.8	1.2	20	120	43.6
L78	7	4.9	0.4	1.2	2.2	0.8	576.9	4	2.9	33.8	1.2	20	85.5	48.7
L79	7	35.5	0.4	27.1	2.3	0.8	709.2	4	2.9	66.7	13.6	20	121	88.7
L80	7	15	0.4	1.2	1.5	0.8	360.9	4	2.9	27.1	5.2	20	334	56.9
L81	7	51	0.4	1.2	1.6	0.8	30.2	4	2.9	17.9	1.2	20	52.3	34.9
L82	7	59.5	0.4	1.2	1.9	0.8	26.3	4	2.9	48.1	1.2	20	143	59.2
L83	7	95.8	0.4	1.2	4.2	0.8	126.1	4	2.9	55.9	1.2	20	252	18.3
L84	7	13.7	0.4	1.2	2.4	0.8	295.3	4	2.9	54.4	1.2	20	34.6	22.6
L85	7	8.8	0.4	1.2	3.2	27.3	65.6	4	6.9	53.5	1.2	20	540	28.7
L86	7	6.7	0.4	1.2	1.6	71.1	478.8	4	2.9	382.3	1.2	20	135	160.4
L87	7	1.7	0.4	1.2	1.5	0.8	44.1	4	2.9	6.1	1.2	20	154	98.6
L88	7	14	0.4	1.2	1.5	0.8	2326	4	2.9	173.9	1.2	20	241	69.7
L89	7	9.8	0.4	1.2	1.5	0.8	192.1	4	2.9	27.6	1.2	20	29.3	38.2
L90	7	30.7	0.4	1.2	1.5	0.8	892.4	4	2.9	25.9	1.2	20	284	227.3
L91	7	31.4	0.4	1.2	1.5	0.8	1015	4	2.9	168.8	1.2	20	208	404.5
L92	7	2	0.4	1.2	1.5	0.8	1811	4	15.1	390.8	1.2	20	738	285.9
L93	7	4.8	0.4	1.2	1.5	0.8	150.9	4	2.9	39.9	1.2	20	1025	480.8
L94	7	25.95	0.4	1.2	5.3	0.8	1214	4	27.6	119.1	1.2	20	1702	293.7
L95	7	4.6	0.4	1.2	1.5	0.8	1171	4	2.9	49.5	1.2	20	73	384.1
L96	7	14.9	0.4	1.2	1.5	0.8	1555	4	2.9	29.9	1.2	20	96.8	207.6
L97	7	27.8	0.4	1.2	1.5	0.8	3021	4	2.9	168.2	1.2	20	135	301.3
L98	7	6.1	0.4	1.2	1.5	0.8	1155	4	2.9	26.1	1.2	20	55	183.6
L99	7	13.7	0.4	1.2	1.8	0.8	1637	4	2.9	64.1	1.2	20	13.5	166
L100	7	4.6	0.4	1.2	1.5	0.8	16.2	4	2.9	19.7	1.2	20	1.9	99.9
L101	7	5.4	0.4	1.2	1.5	580	34.5	4	2.9	21.2	8.4	20	5.3	1236
L102	7	2.6	0.4	1.2	1.5	0.8	19.6	4	2.9	8.6	1.2	20	3.9	682.3
L103	7	23.6	0.4	1.9	1.5	0.8	17.4	4	2.9	218.3	1.2	20	11.2	814.3
L104	7	2.5	0.4	1.2	1.5	22.4	9.3	4	2.9	5.1	1.2	20	3.2	458.2
L105	7	7.1	0.4	1.2	1.5	0.8	18.2	4	2.9	6.4	1.2	20	8.2	516

Heavy and Trace Metals (µg/l) for dry season groundwater samples

Sample ID	As	Ba	Cd	Co	Cr	Cu	Fe	Hg	Li	Mn	Ni	Pb	Sr	Zn
L106	7	18.7	0.4	1.2	1.5	0.8	890.1	4	2.9	9.1	1.2	20	16	481.4
L107	7	11.2	0.4	1.2	1.5	0.8	61.7	4	2.9	5.1	1.2	20	2.7	1109
L108	7	3.6	0.4	1.2	1.5	56.6	23.1	4	2.9	4.5	1.2	20	5.1	984.4
L109	7	11.5	0.4	1.2	1.5	0.8	9.3	4	2.9	39.1	1.2	20	9.2	77.1
L110	7	2.1	0.4	1.2	1.5	19.7	8.7	4	2.9	5	1.2	20	3.4	99.1
L111	7	3.5	0.4	1.2	1.5	66.2	27	4	2.9	7	1.2	20	2.3	265.7
L112	7	3.7	0.4	1.2	1.5	17.1	13.5	4	2.9	5.8	1.2	20	4.4	190.7
L113	7	29.3	0.4	1.2	1.5	0.8	312.5	4	2.9	31.6	1.2	20	4.3	135
L114	7	4.2	0.4	1.2	1.5	19.4	6.7	4	2.9	5.2	1.2	20	2.6	152.3
L115	7	3.6	0.4	1.2	1.5	0.8	18.2	4	2.9	7	1.2	20	1.7	167.6
L116	7	32.8	0.4	1.2	2.4	26.1	65.4	4	2.9	8.6	1.2	20	26.8	165
L117	7	6.6	0.4	1.2	1.5	0.8	147.5	4	2.9	19.4	1.2	20	9.5	109.2
L118	7	9.8	0.4	15.8	1.5	18.4	2093	4	7.6	21.3	17.3	20	10.1	323.9
L119	7	43	0.4	1.2	1.5	18.8	67.1	4	2.9	85.6	1.2	20	21.4	128.6
L120	7	11.6	0.4	1.2	1.5	0.8	7.7	4	2.9	17.2	1.2	20	22.9	58.7
L121	7	15.3	0.4	1.2	1.5	0.8	10.7	4	2.9	25.1	1.2	20	5.7	191.3
L122	7	2.7	0.4	1.2	1.5	26.9	9.8	4	2.9	18.6	1.2	20	7.2	165.2
L123	7	5.1	0.4	1.2	1.5	0.8	53.2	4	2.9	44.4	1.2	20	12	199.7
L124	7	2.7	0.4	1.2	1.5	0.8	26.4	4	2.9	10.1	1.2	20	5.3	190.9
L125	7	3.2	0.4	1.2	1.5	0.8	7.8	4	2.9	6.9	1.2	20	1.8	178.6
L126	7	122.3	0.4	2.4	2.3	0.8	796.8	4	5.9	140.9	5.4	20	79.1	301.2
L127	7	16	0.4	5.3	1.5	0.8	486.9	4	16.7	63.7	5.5	20	10.5	287.9
L128	7	3.7	0.4	1.2	1.5	0.8	20	4	2.9	5.2	1.2	20	1.8	220
L129	7	4.3	0.4	1.2	1.5	0.8	19	4	2.9	5	1.2	20	1.6	189.3
L130	7	9.4	0.4	1.2	1.5	65.4	26.8	4	2.9	17.9	1.2	20	5.3	321.4
L131	7	7.3	0.4	1.2	1.5	20.1	15	4	2.9	9.6	1.2	20	10.4	380.4
L132	7	87.4	0.4	2.1	1.5	0.8	19.5	4	3.7	246.4	3.5	20	58.7	397.6
L133	7	35.3	0.4	1.2	2.7	16.6	2721	4	5.7	39.3	12.3	20	13.2	763.4
L134	7	15.4	0.4	1.2	1.5	0.8	1464	4	2.9	30.1	1.2	20	92.3	198.8

APPENDIX 7

Mineral Saturation Index for wet season groundwater samples

Sample ID	Anhydrite	Aragonite	Calcite	Dolomite	Gypsum	Halite
L01	0	-5.312	-5.148	-9.727	0	-9.597
L02	-5.948	-8.134	-7.97	-14.9	-5.826	-9.478
L03	-2.609	-0.506	-0.3416	-0.4689	-2.451	-8.254
L07	-5.916	-8.057	-7.893	-14.93	-5.768	-10.47
L04	-5.628	-7.911	-7.747	-14.83	-5.489	-10.41
L06	-4.176	-3.548	-3.384	-6.766	-4.047	-9.731
L05	-6.215	-7.425	-7.261	-13.95	-6.076	-10.44
L08	-4.103	-6.684	-6.52	-12.55	-3.976	-8.561
L09	0	-6.991	-6.827	-12.94	0	-9.462
L10	-2.693	-1.364	-1.2	-1.833	-2.55	-7.515
L11	-4.191	-4.404	-4.24	-8.415	-4.065	-9.357
L12	-5.824	-6.892	-6.728	-12.71	-5.689	-10.66
L13	-5.835	-7.765	-7.601	-14.39	-5.693	-10.63
L14	-5.987	-7.987	-7.823	-14.83	-5.844	-10.12
L15	-4.327	-6.967	-6.802	-12.84	-4.181	-7.255
L16	-6.207	-7.508	-7.344	-13.98	-6.041	-10.37
L17	0	-0.8937	-0.7297	-1.309	0	-8.563
L18	-3.088	-1.367	-1.202	-2.431	-2.944	-8.504
L19	-3.253	0.4623	0.626	2.2	-3.145	-7.774
L20	0	-0.195	-0.0307	1.308	0	-7.943
L21	-2.937	-1.741	-1.577	-2.942	-2.795	-7.855
L22	-4.24	-5.228	-5.064	-9.213	-4.119	-8.928
L23	-6.227	-7.813	-7.649	-14.29	-6.096	-8.524
L24	-4.136	-4.527	-4.363	-7.696	-4.007	-7.721
L25	-6.591	-8.149	-7.985	-15.4	-6.46	-9.819
L26	-2.977	-6.477	-6.313	-12.05	-2.834	-7.691
L27	-5.612	-5.805	-5.64	-10.7	-5.44	-10.63
L28	0	-3.894	-3.729	-6.571	0	-8.475
L29	0	-4.627	-4.463	-8.489	0	-8.873
L30	-5.511	-7.405	-7.241	-13.75	-5.382	-9.109
L31	-3.796	-8.298	-8.134	-15.22	-3.683	-8.923
L32	-5.302	-6.975	-6.811	-12.75	-5.188	-8.71
L33	-5.895	-7.522	-7.358	-13.86	-5.778	-9.789
L34	-3.287	-2.236	-2.073	-3.368	-3.178	-7.453
L35	-3.174	-2.555	-2.391	-4.194	-3.045	-8.711

Mineral Saturation Index for wet season groundwater samples

Sample ID	Anhydrite	Aragonite	Calcite	Dolomite	Gypsum	Halite
L36	-6.266	-7.105	-6.941	-12.89	-6.145	-8.821
L37	-2.236	-1.609	-1.445	-2.683	-2.113	-7.104
L38	-4.602	-6.353	-6.189	-11.36	-4.47	-8.136
L39	-5.701	-4.411	-4.247	-8.202	-5.589	-9.23
L40	-4.871	-3.966	-3.802	-7.78	-4.76	-8.959
L41	-5.517	-6.192	-6.028	-11.37	-5.361	-9.382
L42	0	-6.43	-6.266	-11.6	0	-7.848
L43	-2.785	-5.82	-5.656	-10.39	-2.652	-7.327
L44	0	-3.78	-3.615	-7.01	0	-9.196
L45	-3.743	-3.504	-3.34	-5.858	-3.601	-8.056
L46	-5.82	-6.017	-5.853	-10.91	-5.681	-9.086
L47	-6.052	-5.317	-5.153	-9.519	-5.923	-8.653
L48	-5.313	-6.377	-6.213	-11.7	-5.183	-6.922
L49	-6.299	-5.787	-5.623	-10.56	-6.186	-9.186
L50	-2.896	-2.926	-2.762	-4.666	-2.781	-6.678
L51	-5.255	-7.711	-7.547	-14.42	-5.124	-9.976
L52	-5.604	-5.679	-5.515	-10.81	-5.501	-8.86
L53	0	-6.62	-6.457	-11.9	0	-8.77
L54	-5.474	-4.844	-4.68	-9.005	-5.338	-10.68
L55	-4.104	-4.421	-4.257	-7.598	-4.019	-7.861
L56	0	-7.789	-7.625	-14.29	0	-9.008
L57	0	-6.028	-5.864	-10.98	0	-8.384
L58	0	-6.036	-5.872	-11.19	0	-9.09
L59	-5.671	-5.171	-5.007	-9.64	-5.546	-9.248
L60	-6.367	-6.452	-6.288	-11.82	-6.241	-9.187
L61	-5.559	-3.759	-3.595	-7.107	-5.424	-9.189
L62	-5.893	-5.647	-5.483	-10.42	-5.75	-9.147
L63	-6.032	-7.755	-7.591	-14.31	-5.867	-9.245
L64	-5.62	-4.222	-4.058	-8.102	-5.473	-9.131
L65	-6.556	-8.2	-8.036	-15.38	-6.418	-9.627
L66	-2.773	-2.429	-2.264	-4.555	-2.605	-8.239
L67	-5.61	-8.099	-7.935	-15.19	-5.446	-10.09
L68	-3.309	-4.92	-4.756	-8.528	-3.181	-8.295
L69	0	-6.755	-6.591	-12.21	0	-7.682
L70	-3.102	-2.052	-1.888	-3.401	-2.955	-8.541

Mineral Saturation Index for wet season groundwater samples

Sample ID	Anhydrite	Aragonite	Calcite	Dolomite	Gypsum	Halite
L71	-3.007	-5.333	-5.169	-9.644	-2.853	-7.973
L72	-6.145	-6.794	-6.63	-12.41	-6.016	-9.24
L74	-3.222	-1.652	-1.487	-3.08	-3.053	-9.191
L75	-3.282	-1.388	-1.224	-1.76	-3.117	-7.378
L84	-2.368	-1.246	-1.081	-1.761	-2.221	-7.523
L79	-5.272	-6.374	-6.21	-11.66	-5.144	-8.799
L80	-2.973	-2.241	-2.077	-3.642	-2.847	-7.301
L81	-2.346	2.304	2.468	6.78	-2.213	-4.824
L82	-2.9	-1.343	-1.179	-1.912	-2.773	-7.64
L83	-3.613	-3.909	-3.744	-6.786	-3.483	-8.227
L88	0	-7.177	-7.013	-13.26	0	-9.417
L89	-3.959	-4.317	-4.153	-7.693	-3.836	-8.356
L76	-4.377	-3.943	-3.779	-7.115	-4.249	-9.26
L73	-6.742	-6.873	-6.708	-13.18	-6.569	-12.67
L85	-4.287	-6.833	-6.669	-12.47	-4.144	-8.43
L86	-2.426	-3.956	-3.792	-7.546	-2.298	-7.678
L87	-1.601	-1.359	-1.195	-1.716	-1.481	-4.482
L77	0	-7.005	-6.841	-13.1	0	-9.426
L78	-3.24	-3.342	-3.178	-5.695	-3.12	-7.313
L90	-2.951	-2.835	-2.671	-4.986	-2.801	-8.198
L91	-2.295	0.6993	0.8634	2.761	-2.159	-7.765
L92	-3.895	-1.079	-0.915	-1.815	-3.751	-10.21
L93	-3.419	-0.08325	0.08089	0.1512	-3.28	-9.319
L94	-3.707	-0.8895	-0.7253	-1.251	-3.564	-9.018
L95	-2.553	0.006546	0.171	0.4039	-2.392	-8.751
L96	-2.788	0.7315	0.8957	2.584	-2.642	-6.099

APPENDIX 8

Mineral Saturation Index for dry season groundwater samples

Sample ID	Anhydrite	Aragonite	Calcite	Dolomite	Gypsum	Halite
L01	-4.161	-2.822	-2.657	-4.306	-3.983	-7.137
L02	-2.116	0.5389	0.7038	2.055	-1.938	-6.178
L03	-3.214	0.195	0.3599	1.504	-3.036	-7.687
L04	-5.446	-4.539	-4.374	-8.515	-5.268	-9.537
L05	-5.379	-5.822	-5.657	-11.17	-5.201	-8.826
L06	-5.569	-6.238	-6.073	-11.83	-5.391	-8.746
L07	-4.435	-4.915	-4.75	-8.691	-4.257	-7.85
L08	-5.399	-5.937	-5.772	-11.4	-5.221	-9.432
L09	-5.283	-6.176	-6.011	-11.55	-5.105	-9.051
L10	-2.342	-1.686	-1.521	-2.154	-2.164	-7.366
L11	-5.633	-5.875	-5.71	-10.63	-5.455	-9.232
L12	-3.5	-3.97	-3.805	-7.563	-3.322	-9.246
L13	-4.715	-2.751	-2.586	-4.589	-4.537	-9.022
L14	-5.263	-5.59	-5.425	-10.11	-5.085	-8.621
L15	-4.258	-7.023	-6.858	-12.9	-4.08	-7.309
L16	-4.75	-3.849	-3.684	-7.435	-4.572	-9.25
L17	-5.823	-7.219	-7.054	-13.17	-5.645	-8.595
L18	-4.601	-5.406	-5.241	-9.875	-4.423	-6.95
L19	-5.82	-5.965	-5.8	-10.99	-5.642	-9.044
L20	-1.144	0.06284	0.2277	1.433	-0.966	-6.837
L22	-5.655	-5.88	-5.715	-10.95	-5.477	-8.83
L23	-5.196	-4.816	-4.651	-8.655	-5.018	-8.319
L24	-4.977	-2.775	-2.61	-4.325	-4.798	-9.294
L25	-5.36	-5.046	-4.881	-9.379	-5.182	-9.015
L26	-5.496	-7.792	-7.627	-14.42	-5.318	-8.555
L27	-5.437	-4.66	-4.495	-8.896	-5.259	-9.03
L28	-3.881	-6.193	-6.028	-11.12	-3.703	-8.537
L29	-4.476	-6.653	-6.488	-12.09	-4.298	-7.748
L30	-5.258	-6.075	-5.911	-11.38	-5.08	-8.662

Mineral Saturation Index for dry season groundwater samples

Sample ID	Anhydrite	Aragonite	Calcite	Dolomite	Gypsum	Halite
L31	-5.256	-8.294	-8.129	-15.07	-5.078	-9.266
L32	-5.123	-6.369	-6.204	-11.73	-4.945	-8.449
L33	-3.617	-3.367	-3.202	-5.943	-3.439	-7.169
L34	-1.142	1.998	2.163	6.056	-0.979	-2.625
L35	-5.298	-3.474	-3.309	-5.346	-5.12	-8.596
L36	-2.493	-4.159	-3.994	-7.306	-2.315	-7.93
L37	-2.653	-2.145	-1.98	-3.569	-2.475	-7.533
L38	-2.279	-5.824	-5.659	-10.82	-2.101	-6.626
L39	-3.061	-6.733	-6.568	-12.76	-2.883	-7.474
L40	-3.286	-4.566	-4.401	-8.227	-3.108	-7.669
L41	-5.581	-6.611	-6.446	-12.09	-5.403	-8.176
L42	-3.012	-6.595	-6.43	-12.35	-2.834	-7.468
L43	-2.987	-0.5457	-0.3808	0.4009	-2.812	-3.956
L44	-4.209	-4.67	-4.506	-8.095	-4.031	-7.671
L45	-5.268	-8.083	-7.918	-14.88	-5.09	-8.32
L46	-6.25	-7.457	-7.292	-13.95	-6.072	-9.615
L47	-5.711	-7.784	-7.62	-14.26	-5.533	-8.767
L48	-5.87	-7.944	-7.779	-14.68	-5.692	-8.391
L49	-4.874	-3.81	-3.645	-6.489	-4.696	-8.468
L50	-2.819	-1.836	-1.672	-2.999	-2.641	-7.242
L51	-5.036	-6.342	-6.177	-11.72	-4.858	-7.614
L52	-4.467	-3.95	-3.785	-7.198	-4.289	-9.158
L53	-5.762	-6.679	-6.514	-12.44	-5.584	-9.338
L54	-5.101	-6.076	-5.911	-11.05	-4.923	-9.132
L55	-4.688	-6.162	-5.997	-11.36	-4.51	-8.576
L56	-5.904	-6.867	-6.702	-12.66	-5.726	-9.302
L57	-5.536	-6.812	-6.647	-12.48	-5.358	-8.853
L58	-5.484	-7.631	-7.466	-14.08	-5.306	-8.245
L59	-5.588	-7.262	-7.098	-13.56	-5.41	-8.82
L60	-4.856	-6.671	-6.506	-12.15	-4.678	-7.787

Mineral Saturation Index for dry season groundwater samples

Sample ID	Anhydrite	Aragonite	Calcite	Dolomite	Gypsum	Halite
L61	-5.693	-6.985	-6.82	-12.87	-5.515	-8.858
L62	-3.669	-7.452	-7.287	-13.65	-3.491	-8.758
L63	-4.955	-6.65	-6.485	-12.13	-4.776	-7.381
L64	-4.797	-7.093	-6.928	-13.15	-4.619	-8.462
L65	-5.05	-6.165	-6	-11.26	-4.872	-8.591
L66	-5.032	-7.724	-7.559	-14.43	-4.854	-9.03
L67	-5.903	-7.762	-7.597	-14.39	-5.724	-9.805
L68	-5.504	-6.683	-6.518	-12.24	-5.326	-8.576
L69	-5.302	-	-	-	-5.124	-9.531
L70	-5.841	-7.633	-7.468	-14.02	-5.663	-8.814
L71	-2.766	-3.28	-3.115	-6.259	-2.588	-7.915
L72	-5.26	-7.815	-7.65	-14.69	-5.081	-8.639
L73	-2.501	-2.27	-2.105	-4.045	-2.323	-7.211
L74	-3.774	-4.775	-4.61	-8.495	-3.595	-8.08
L75	-2.721	-3.2	-3.035	-6.219	-2.543	-8.232
L76	-3.788	-4.674	-4.509	-8.515	-3.61	-8.619
L77	-4.07	-3.605	-3.44	-7.015	-3.892	-9.79
L78	-3.287	-1.962	-1.797	-3.815	-3.109	-8.701
L79	-2.013	-4.342	-4.177	-8.063	-1.835	-7.25
L80	-2.484	-0.4412	-0.2763	-0.2442	-2.306	-6.62
L81	-3.408	-3.778	-3.613	-6.838	-3.229	-8.894
L82	-2.082	-2.974	-2.809	-5.324	-1.904	-6.715
L83	-1.767	-0.8896	-0.7247	-1.1	-1.589	-6.338
L84	-3.398	-3.617	-3.452	-6.631	-3.22	-8.916
L85	-2.2	0.6436	0.8085	2.474	-2.022	-7.622
L86	-3.667	-0.2658	-0.1009	-0.2722	-3.489	-9.302
L87	-3.065	-0.08648	0.07842	0.2398	-2.887	-8.635
L88	-2.129	-0.2067	-0.04183	-0.3222	-1.951	-8.501
L89	-3.981	-2.722	-2.557	-5.109	-3.803	-9.587
L90	-2.134	-0.4247	-0.2598	-0.3964	-1.956	-8.214

Mineral Saturation Index for dry season groundwater samples

Sample ID	Anhydrite	Aragonite	Calcite	Dolomite	Gypsum	Halite
L91	-2.397	-1.242	-1.077	-2.291	-2.219	-7.539
L92	-2.398	-0.4455	-0.2806	0.1245	-2.22	-6.721
L93	-2.13	-0.6166	-0.4517	-0.4553	-1.952	-6.888
L94	-1.979	0.1186	0.2835	1.778	-1.802	-4.678
L95	-3.12	-2.101	-1.937	-3.685	-2.942	-8.873
L96	-2.678	-1.743	-1.578	-3.165	-2.5	-7.706
L97	-2.253	-2.008	-1.843	-3.553	-2.075	-7.185
L98	-3.597	-1.774	-1.609	-3.231	-3.419	-9.337
L99	-4.034	-4.534	-4.369	-8.08	-3.856	-8.629
L100	-5.245	-7.774	-7.609	-14.47	-5.067	-9.605
L101	-5.35	-6.049	-5.884	-11.45	-5.172	-9.813
L102	-5.327	-5.367	-5.202	-9.944	-5.149	-10.78
L103	-5.709	-7.631	-7.466	-13.97	-5.531	-9.429
L104	-5.621	-7.359	-7.194	-13.84	-5.442	-10.4
L105	-5.677	-7.617	-7.452	-14.08	-5.499	-9.949
L106	-4.55	-5.548	-5.383	-10.19	-4.372	-9.654
L107	-5.259	-7.288	-7.123	-13.41	-5.081	-9.447
L108	-5.32	-6.935	-6.77	-13.07	-5.142	-10.13
L109	-5.388	-6.606	-6.441	-12.09	-5.21	-9.999
L110	-5.714	-7.058	-6.893	-13.23	-5.536	-10.31
L111		-8.144	-7.979	-15.19	-	-
L112	-5.961	-7.64	-7.475	-14.19	-5.783	-10.15
L113	-19.15	-13.87	-13.71	-27.5	-18.97	-20.8
L114	-6.016	-7.939	-7.774	-14.63	-5.837	-9.61
L115	-6.087	-7.89	-7.725	-14.65	-5.909	-10.19
L116	-5.393	-4.113	-3.948	-7.324	-5.214	-9.862
L117	-5.315	-6.126	-5.961	-11.3	-5.136	-9.589
L118	-5.42	-7.395	-7.23	-13.69	-5.242	-9.281
L119	-3.654	-6.179	-6.014	-11.14	-3.476	-8.634
L120	-5.007	-6.082	-5.918	-11.01	-4.828	-8.735

Mineral Saturation Index for dry season groundwater samples

Sample ID	Anhydrite	Aragonite	Calcite	Dolomite	Gypsum	Halite
L121	-5.483	-7.547	-7.382	-13.8	-5.305	-9.342
L122	-5.533	-5.273	-5.108	-9.82	-5.355	-9.931
L123	-5.045	-5.707	-5.542	-10.94	-4.867	-10.25
L124	-4.958	-6.814	-6.649	-12.5	-4.78	-10.13
L125	-6.063	-7.171	-7.006	-13.05	-5.885	-10.42
L126	-4.508	-4.434	-4.269	-7.771	-4.33	-8.568
L127	-4.788	-7.326	-7.161	-13.42	-4.61	-8.176
L128	-4.944	-7.944	-7.779	-14.68	-4.766	-9.965
L129	-5.935	-7.754	-7.589	-14.44	-5.757	-10.34
L130	-5.737	-7.704	-7.539	-14.16	-5.559	-10.14
L131	-5.383	-6.297	-6.132	-11.4	-5.205	-9.714
L132	-4.626	-5.957	-5.792	-10.88	-4.448	-8.431
L133	-4.624	-4.429	-4.264	-8.18	-4.446	-8.626
L134	-4.347	-1.777	-1.612	-3.186	-4.169	-8.43

APPENDIX 9

Groundwater quality indices and Chloroalkaline Index for wet season groundwater

Sample ID	SAR	TH	Na%	KR	PI	RSC	MR	CAI-I	CAI-II	GWQI
L01	0.07	29.48	17.35	0.19	125.29	0.00	11.81	-1.62	-0.13	21.25
L02	0.32	19.17	54.57	1.02	130.11	0.00	36.47	-1.21	-0.71	38.18
L03	0.20	7.12	51.49	1.05	179.70	0.00	59.58	-1.47	-0.97	14.67
L04	0.57	98.15	48.50	0.82	84.06	-0.01	43.74	-1.20	0.17	87.05
L05	0.47	374.73	26.47	0.34	52.52	-0.06	99.88	-7.69	-0.02	84.59
L06	0.24	8.28	54.66	1.17	166.93	0.00	22.50	-1.41	-1.06	9.94
L07	0.19	20.22	37.84	0.59	135.89	0.00	7.68	-1.03	-0.40	14.03
L08	0.34	9.67	61.47	1.55	149.79	0.00	18.98	-1.36	-1.37	17.59
L09	0.49	36.76	58.78	1.13	107.38	-0.01	91.28	-0.68	-0.60	59.21
L10	0.37	106.03	45.18	0.51	78.93	-0.01	68.13	0.40	0.77	129.54
L11	0.38	21.01	55.57	1.17	124.42	0.00	122.90	-0.17	-0.52	38.62
L12	0.19	7.37	51.56	0.98	180.27	0.00	59.61	-1.20	-0.90	16.69
L13	0.62	28.81	64.61	1.63	111.68	0.00	103.10	-0.94	-1.18	62.91
L14	0.48	97.40	53.36	0.69	82.85	-0.02	98.60	0.28	0.78	177.05
L15	0.14	25.10	28.73	0.39	129.31	0.00	19.76	-1.31	-0.26	19.24
L16	0.29	8.16	59.81	1.45	159.44	0.00	75.34	-1.54	-1.32	17.58
L17	0.27	10.31	59.21	1.19	154.19	0.00	72.07	-0.39	-1.06	26.19
L18	0.81	65.20	66.57	1.42	94.64	-0.01	61.88	2.15	1.02	264.60
L19	0.35	3.04	74.05	2.80	179.75	0.00	55.78	-0.92	-2.59	7.03
L20	0.75	158.73	53.35	0.84	75.95	-0.02	82.34	2.89	2.80	258.88
L21	0.34	10.55	60.36	1.46	147.07	0.00	117.38	-1.14	-1.30	33.52
L22	0.28	4.95	65.44	1.80	176.92	0.00	104.90	-0.58	-1.68	11.59
L23	0.51	12.27	68.28	2.04	133.13	0.00	65.28	-1.14	-1.81	32.53
L24	0.29	7.78	60.52	1.47	161.63	0.00	41.87	-1.44	-1.39	13.73
L25	0.15	11.05	39.71	0.63	168.59	0.00	27.66	-0.68	-0.48	17.68
L26	0.24	4.78	62.05	1.58	185.97	0.00	67.29	-0.68	-1.44	7.87
L27	0.16	12.88	39.98	0.64	159.02	0.00	14.36	-0.85	-0.49	8.27
L28	0.22	6.97	54.67	1.18	176.45	0.00	42.30	-0.74	-1.00	9.55
L29	0.19	5.30	55.60	1.17	194.59	0.00	91.37	-0.51	-1.02	11.80
L30	0.17	11.82	42.42	0.72	161.41	0.00	12.44	-0.76	-0.54	8.97
L31	0.35	27.15	58.87	0.93	117.87	0.00	112.27	-1.33	-0.26	21.83
L32	0.51	56.22	51.52	0.96	96.70	-0.01	109.59	-0.53	-0.21	97.77
L33	0.37	3.88	72.62	2.62	170.71	0.00	84.02	-1.64	-2.43	15.70
L34	0.30	9.33	60.59	1.38	154.56	0.00	67.59	-0.84	-1.20	19.98
L35	0.59	70.73	53.51	1.00	91.84	-0.01	37.87	0.65	0.73	85.70

Groundwater quality indices and Chloroalkaline Index for wet season groundwater

Sample ID	SAR	TH	Na%	KR	PI	RSC	MR	CAI-I	CAI-II	GWQI
L36	16.67	6580.70	74.82	2.89	76.48	-1.84	728.39	-104.13	0.72	1505.36
L37	0.53	72.50	53.08	0.88	90.81	-0.01	32.51	-1.15	-0.05	74.89
L38	0.32	34.73	48.57	0.76	110.97	0.00	59.19	-0.83	-0.28	44.08
L39	0.17	4.46	53.82	1.13	209.16	0.00	70.05	-0.50	-1.02	7.81
L40	0.25	27.53	51.40	0.67	120.38	0.00	47.85	-0.60	-0.41	45.00
L41	0.09	29.57	19.71	0.23	124.04	0.00	32.68	-0.65	-0.06	10.46
L42	0.21	3.93	60.07	1.49	202.55	0.00	44.71	-0.75	-1.38	6.69
L43	0.59	88.72	54.18	0.89	86.58	-0.01	53.05	-0.03	0.36	183.25
L44	0.21	12.09	60.65	0.83	155.59	0.00	95.73	-1.23	-0.80	21.34
L45	0.90	3.71	86.89	6.57	134.89	0.00	121.54	-1.65	-6.07	28.45
L46	0.47	25.63	58.98	1.30	116.74	0.00	125.32	0.68	0.03	29.91
L47	0.17	2.14	64.05	1.67	243.03	0.00	43.87	-0.77	-1.63	6.60
L48	0.59	39.61	61.51	1.33	105.07	0.00	44.22	-0.58	-0.01	83.18
L49	0.07	2.24	43.74	0.63	327.06	0.00	47.80	-1.01	-0.51	5.75
L50	0.39	19.95	57.48	1.24	125.44	0.00	93.99	-1.60	-1.07	24.11
L51	0.23	16.81	45.19	0.78	140.42	0.00	32.57	-1.05	-0.61	69.00
L52	0.17	9.21	63.72	0.79	173.37	0.00	63.71	-1.21	-1.48	28.85
L53	0.48	8.18	72.70	2.38	142.88	0.00	127.97	-3.15	-0.46	17.99
L54	0.38	11.60	63.92	1.58	141.18	0.00	85.06	-1.58	-1.49	35.04
L55	0.16	4.39	54.12	1.06	214.07	0.00	83.08	-1.35	-1.04	12.32
L56	0.15	42.21	37.91	0.33	106.24	0.00	45.29	-1.35	-0.12	32.77
L57	0.43	8.27	68.94	2.10	146.43	0.00	115.28	-1.82	-2.03	32.77
L58	0.65	141.01	50.87	0.78	77.15	-0.01	18.57	0.08	1.01	160.38
L59	0.34	39.97	50.17	0.75	106.32	-0.01	79.24	-0.60	-0.23	56.70
L60	0.32	1.67	78.14	3.48	199.01	0.00	59.01	-1.34	-3.22	9.58
L61	0.28	68.62	36.83	0.48	90.04	0.00	11.63	-1.66	-0.03	56.08
L62	0.14	2.04	58.65	1.34	267.18	0.00	59.77	-0.91	-0.86	8.35
L63	0.19	55.71	36.46	0.36	95.88	0.00	28.54	-1.66	-0.13	55.84
L64	0.39	38.55	51.88	0.88	107.01	0.00	59.51	-0.51	0.12	47.17
L65	0.01	0.86	29.63	0.18	663.76	0.00	21.42	-2.52	-0.36	4.28
L66	0.08	58.91	15.58	0.15	93.02	0.00	9.75	-1.14	0.01	30.38
L67	0.46	89.91	42.34	0.68	84.60	-0.01	59.63	0.74	0.91	72.51
L68	1.07	151.53	61.00	1.23	80.83	-0.01	30.21	-11.79	-0.82	41.06
L69	0.20	57.49	31.51	0.37	94.95	0.00	12.55	2.10	2.12	243.10
L70	1.30	230.64	60.79	1.21	75.68	-0.02	37.01	534.36	534.23	581.84

Groundwater quality indices and Chloroalkaline Index for wet season groundwater

Sample ID	SAR	TH	Na%	KR	PI	RSC	MR	CAI-I	CAI-II	GWQI
L71	0.24	52.87	38.01	0.48	97.91	0.00	27.28	-0.59	0.13	59.24
L72	0.26	302.36	21.90	0.21	50.62	-0.05	124.46	-1.81	0.45	67.66
L73	0.04	45.61	8.18	0.07	104.20	0.00	12.43	-1.99	-0.04	15.97
L74	0.05	118.41	8.94	0.07	67.07	0.00	11.63	-1.51	0.05	97.98
L75	0.14	35.23	31.13	0.34	114.03	0.00	18.92	-1.65	-0.22	43.97
L76	0.11	94.44	17.17	0.16	76.43	0.00	14.02	-1.19	0.12	71.64
L77	1.00	461.96	40.30	0.65	59.27	-0.06	72.89	6.25	6.47	114.64
L78	0.15	123.85	18.67	0.20	69.38	-0.01	19.94	-0.53	0.35	36.26
L79	0.16	123.19	21.22	0.21	69.85	-0.01	16.55	-2.42	-0.02	39.53
L80	0.22	61.13	33.96	0.40	93.07	0.00	11.25	-1.89	-0.14	38.73
L81	0.15	223.18	16.83	0.14	53.45	-0.05	275.34	-0.20	0.66	91.60
L82	0.34	59.27	43.58	0.62	94.81	0.00	19.39	-0.18	0.30	61.42
L83	0.29	2.09	75.58	2.85	200.40	0.00	56.03	-3.48	-1.46	11.96
L84	0.04	7.36	21.50	0.23	229.49	0.00	26.88	-1.56	-0.24	40.68
L85	0.32	21.10	63.02	0.99	126.58	0.00	88.10	-1.49	-1.11	53.05
L86	0.11	14.27	35.74	0.40	161.73	0.00	43.53	-1.59	-0.46	26.60
L87	0.22	4.24	65.24	1.49	196.65	0.00	127.19	-1.34	-1.65	17.62
L88	0.11	13.13	34.73	0.44	165.79	0.00	13.62	-0.70	-0.26	19.54
L89	0.07	1.98	43.52	0.69	336.10	0.00	66.52	-0.89	-0.55	6.86
L90	0.08	1.78	47.98	0.84	332.28	0.00	77.68	-0.99	-0.61	6.09
L91	0.14	3.14	55.12	1.08	242.21	0.00	77.83	-1.63	-1.07	13.36
L92	0.90	46.33	70.06	1.86	101.12	-0.01	70.11	-0.04	-0.82	193.63
L93	0.13	1.79	59.18	1.34	281.55	0.00	62.40	-1.41	-1.20	6.92
L94	0.09	2.23	49.35	0.84	301.33	0.00	87.46	-1.13	-0.74	8.09
L95	0.10	2.14	50.52	0.95	294.98	0.00	54.73	-1.08	-0.68	6.80
L96	0.09	2.35	50.08	0.85	294.17	0.00	44.76	-1.22	-0.89	6.43

APPENDIX 10

Groundwater quality indices and Chloroalkaline Index for dry season groundwater

Sample ID	SAR	TH	Na%	KR	PI	RSC	MR	CAI-1	CAI-2	GWQI
L01	0.73	62.29	56.61	0.65	39.58	-343.39	55.80	1.12	0.84	58.20
L02	1.20	328.00	45.29	0.67	40.11	-1145.35	34.16	4.44	5.12	352.55
L03	0.55	342.60	44.49	0.66	39.97	-854.34	42.14	-7.90	-0.06	91.40
L04	0.22	7.53	67.09	0.62	38.48	-105.93	17.66	-2.40	-0.95	27.26
L05	0.36	8.38	78.50	0.62	38.25	-68.18	14.91	-1.22	-0.93	31.46
L06	0.44	7.87	78.73	0.59	37.32	-71.01	20.70	-1.51	-0.85	36.38
L07	0.52	35.20	61.46	0.66	39.92	-229.83	44.59	-0.71	0.15	90.00
L08	0.20	6.95	84.73	0.60	37.58	-45.21	14.73	-1.42	-0.67	30.68
L09	0.28	6.54	85.09	0.61	37.96	-51.13	26.98	-1.01	-1.05	28.07
L10	0.33	170.60	53.83	0.66	40.00	-478.60	48.34	0.61	1.40	154.31
L11	0.27	5.76	82.57	0.06	5.77	-41.39	43.39	-1.34	-1.04	28.24
L12	0.22	24.75	71.09	0.64	39.02	-114.64	12.23	-4.24	-0.38	64.38
L13	0.13	31.43	69.52	0.63	38.87	-125.20	32.36	-0.95	-0.04	47.83
L14	0.34	17.76	78.09	0.62	38.44	-80.93	40.78	-1.50	-0.27	53.61
L15	0.69	62.01	56.79	0.65	39.67	-442.29	44.70	0.12	0.94	186.02
L16	0.13	25.99	79.85	0.61	37.94	-80.68	9.70	-1.39	-0.20	33.13
L17	0.37	7.08	78.44	0.63	38.75	-98.63	51.95	-0.51	-1.27	31.99
L18	0.73	83.78	56.81	0.74	42.74	-520.93	33.35	1.77	2.14	249.07
L19	0.39	4.05	84.67	0.59	37.27	-54.27	33.64	-1.23	-1.95	27.08
L20	0.24	938.50	45.58	0.66	39.86	-1349.81	51.57	3.60	4.06	220.74
L21	0.24	938.50	89.36	0.57	36.39	-38.46	51.57	0.18	0.18	4.92
L22	0.40	5.76	88.26	0.60	37.83	-39.89	27.32	-1.03	-1.56	28.26
L23	0.52	14.46	77.12	0.63	38.74	-92.46	35.72	-1.25	-0.44	56.16
L24	0.07	56.49	73.93	0.63	38.96	-123.55	49.54	-0.83	0.02	34.56
L25	0.24	8.97	81.68	0.62	38.29	-66.57	23.27	-0.88	-0.70	29.07
L26	0.39	9.68	75.58	0.65	39.53	-129.16	45.88	-0.96	-0.33	54.80
L27	0.23	9.44	79.95	0.60	37.50	-78.74	13.51	-1.03	-0.88	28.24
L28	0.34	14.39	73.05	0.64	39.14	-140.77	51.94	-1.25	-0.42	36.19
L29	0.48	58.56	61.30	0.66	39.82	-350.49	48.89	-0.72	0.40	150.02
L30	0.49	10.31	75.05	0.65	39.54	-128.97	25.52	-2.13	-0.61	48.89
L31	0.37	4.27	78.92	0.65	39.43	-100.39	65.76	-2.44	-0.78	34.70
L32	0.48	9.08	75.55	0.65	39.39	-120.63	37.15	-0.92	-0.78	39.14
L33	0.95	35.43	48.45	0.65	39.40	-297.74	26.40	0.98	0.06	107.36
L34	17.34	5596.00	94.39	0.65	136.49	110.08	84.66	0.98	-3.07	1269.47
L35	0.35	30.71	37.48	0.64	39.16	-159.71	70.06	-3.09	-0.77	43.77

Groundwater quality indices and Chloroalkaline Index for dry season groundwater

Sample ID	SAR	TH	Na%	KR	PI	RSC	MR	CAI-1	CAI-2	GWQI
L36	0.62	61.28	55.33	0.65	39.63	-272.39	37.04	-3.34	-0.08	84.04
L37	0.46	103.30	50.72	0.66	39.81	-426.06	23.26	-0.70	0.57	111.51
L38	1.11	140.40	47.13	0.66	39.95	-876.41	27.84	1.46	2.41	233.73
L39	0.64	51.15	60.63	0.66	40.01	-336.77	22.83	-0.17	0.63	128.75
L40	0.68	29.82	55.26	0.65	39.49	-249.18	31.82	-0.37	0.02	81.98
L41	0.98	7.25	71.82	0.63	38.75	-123.90	44.41	-1.68	-0.72	58.99
L42	0.76	44.29	59.78	0.66	39.83	-346.90	28.44	-0.48	0.47	106.73
L43	4.77	1988.00	40.27	0.67	40.29	-9988.63	60.70	-0.48	-1.48	3010.07
L44	0.53	26.12	51.03	0.65	39.51	-203.17	50.63	0.50	-0.22	83.35
L45	0.68	9.75	72.31	0.65	39.50	-140.05	52.47	-1.61	-0.45	61.67
L46	0.29	1.67	96.77	3.53	78.16	-10.19	34.83	-1.21	-2.71	25.88
L47	0.56	4.51	79.33	0.62	38.61	-89.57	54.17	-1.63	-0.96	39.09
L48	0.98	4.29	74.60	0.65	39.50	-121.50	48.61	-1.73	-0.91	50.34
L49	0.43	18.97	71.19	0.60	37.88	-105.86	44.20	-1.83	-0.73	42.35
L50	0.51	116.60	51.44	0.66	39.80	-415.74	21.34	0.51	0.99	107.98
L51	1.17	17.70	61.62	0.65	39.33	-258.37	35.12	-1.18	-0.14	118.58
L52	0.11	28.42	70.43	0.60	37.75	-119.54	22.75	-0.79	-0.11	30.15
L53	0.23	4.15	77.69	0.63	38.89	-82.10	32.69	-0.94	-1.44	26.32
L54	0.18	11.93	73.87	0.63	39.01	-103.91	42.54	-1.10	-0.34	37.49
L55	0.30	14.78	70.25	0.64	39.24	-144.74	35.15	-1.02	-0.28	57.42
L56	0.20	4.17	80.74	0.62	38.60	-76.79	40.78	-0.55	-1.03	27.06
L57	0.30	9.23	77.01	0.63	38.82	-104.68	44.97	-1.04	-0.57	36.35
L58	0.64	12.46	72.17	0.65	39.47	-154.11	47.08	-1.50	-0.37	68.83
L59	0.46	6.33	81.60	0.63	38.82	-85.61	35.32	-1.77	-0.72	42.36
L60	0.58	32.33	64.30	0.66	39.82	-249.00	47.81	-0.74	0.13	97.58
L61	0.50	6.40	78.24	0.62	38.63	-84.77	42.36	-2.16	-0.73	43.49
L62	0.60	9.34	73.33	0.64	39.08	-125.38	50.90	-3.71	-0.44	44.92
L63	0.83	51.36	57.40	0.65	39.67	-390.64	46.09	-0.69	0.55	184.47
L64	0.37	27.26	66.97	0.65	39.43	-169.92	38.70	-2.23	-0.15	94.48
L65	0.34	18.52	71.27	0.64	39.28	-127.62	40.90	-1.57	-0.24	60.58
L66	0.26	6.91	74.36	0.65	39.38	-111.35	37.98	-1.84	-0.58	46.82
L67	0.16	3.45	85.24	0.60	37.86	-49.67	44.50	-1.16	-0.62	28.97
L68	0.53	5.24	77.09	0.63	38.64	-84.66	44.20	-0.80	-1.39	33.39
L69	0.19	5.24	77.09	0.63	38.64	-84.66	43.22	-1.39	-1.04	27.35
L70	0.50	7.88	75.44	0.64	39.14	-106.38	50.94	-2.30	-0.55	51.67

Groundwater quality indices and Chloroalkaline Index for dry season groundwater

Sample ID	SAR	TH	Na%	KR	PI	RSC	MR	CAI-1	CAI-2	GWQI
L71	0.36	72.54	58.31	0.65	39.53	-294.46	10.38	-0.86	0.31	90.48
L72	0.49	8.13	71.38	0.64	39.14	-134.24	33.72	-1.52	-0.44	57.97
L73	0.64	108.70	51.07	0.66	39.65	-524.70	15.19	0.00	1.05	148.71
L74	0.36	40.81	61.86	0.65	39.49	-227.85	39.86	-0.94	0.11	86.21
L75	0.21	73.66	57.15	0.64	39.26	-215.84	8.07	-0.55	0.31	69.51
L76	0.27	23.68	66.10	0.64	39.01	-135.28	28.47	-1.82	-0.22	61.47
L77	0.05	45.14	36.78	0.65	39.36	-125.39	8.41	-1.69	-0.07	35.64
L78	0.17	46.63	56.27	0.65	39.35	-168.58	6.97	-1.22	-0.06	42.32
L79	0.66	109.40	52.84	0.66	39.68	-481.54	19.09	-0.28	0.98	68.13
L80	0.72	208.80	45.11	0.66	39.80	-724.43	19.73	3.34	3.44	66.69
L81	0.17	29.76	62.77	0.64	39.32	-173.65	23.38	-3.04	-0.29	56.74
L82	1.03	158.70	47.32	0.66	39.80	-849.89	19.22	0.89	2.08	242.17
L83	1.04	314.80	46.49	0.71	41.64	-1017.47	22.54	2.99	3.90	292.33
L84	0.14	32.07	59.48	0.64	39.12	-136.11	19.13	-0.88	-0.07	39.54
L85	0.30	299.10	45.21	0.66	39.81	-647.04	45.74	-1.42	0.59	85.45
L86	0.05	93.09	37.20	0.64	39.04	-180.45	9.50	-0.92	0.07	66.01
L87	0.13	102.20	44.97	0.63	38.90	-233.49	12.95	-1.27	0.11	57.19
L88	0.11	174.80	43.12	0.64	39.28	-406.01	6.53	-1.35	0.23	77.50
L89	0.10	21.66	51.61	0.63	38.67	-111.51	11.24	-1.68	-0.15	38.47
L90	0.16	150.70	48.40	0.65	39.57	-373.78	13.85	-0.75	0.39	59.13
L91	0.35	201.80	46.02	0.65	39.60	-522.76	8.23	-0.59	0.65	74.12
L92	0.75	322.90	43.13	0.66	39.97	-964.06	37.04	0.90	1.95	125.08
L93	0.52	294.80	44.00	0.65	39.59	-773.70	25.37	1.58	2.21	79.00
L94	3.02	1276.00	37.86	0.66	39.80	-5530.39	65.89	35.44	35.21	366.40
L95	0.12	50.74	44.07	0.64	39.12	-167.36	16.08	-1.12	0.01	47.65
L96	0.52	68.12	46.36	0.65	39.51	-262.53	10.88	-0.94	0.09	50.19
L97	0.59	145.50	38.08	0.66	39.73	-520.05	14.25	-0.05	0.99	117.88
L98	0.08	57.11	52.85	0.63	38.90	-151.54	10.80	-2.08	-0.08	48.54
L99	0.32	15.09	60.26	0.63	38.97	-116.61	36.22	-1.30	-0.74	41.09
L100	0.56	1.72	83.53	0.59	37.34	-54.00	41.25	-4.23	-1.09	30.31
L101	0.17	4.81	85.13	0.60	37.50	-55.35	20.61	-1.84	-0.66	29.62
L102	0.05	4.03	83.99	0.59	37.11	-47.82	26.60	-1.23	-0.28	25.47
L103	0.09	7.55	76.85	0.64	39.23	-104.43	52.92	-0.72	-0.39	51.44
L104	0.10	2.17	83.45	0.63	38.63	-59.07	30.87	-0.99	-0.49	26.04
L105	0.16	4.23	81.06	0.61	37.95	-75.67	45.52	-2.06	-0.47	31.55

Groundwater quality indices and Chloroalkaline Index for dry season groundwater

Sample ID	SAR	TH	Na%	KR	PI	RSC	MR	CAI-1	CAI-2	GWQI
L106	0.12	7.10	76.18	0.62	38.60	-78.46	32.03	-1.23	-0.52	31.39
L107	0.37	2.12	78.92	0.62	38.45	-77.17	46.51	-1.70	-1.50	26.10
L108	0.09	3.46	80.14	0.61	38.18	-78.06	27.16	-1.11	-0.60	26.64
L109	0.15	7.02	74.89	0.65	39.47	-110.95	43.67	-1.65	-0.32	38.89
L110	0.09	2.51	79.39	0.64	39.27	-79.15	31.00	-0.83	-0.61	25.51
L111	0.12	1.41	83.17	0.65	39.36	-61.90	42.53	-0.83	-2.18	24.85
L112	0.13	2.41	83.53	0.61	37.93	-60.91	42.10	-1.31	-1.06	25.59
L113	0.18	0.00	79.74	0.47	31.99	-76.98	45.21	-1.94	-1.19	30.06
L114	0.30	1.94	83.86	0.61	38.08	-58.89	51.08	-1.28	-1.70	25.81
L115	0.14	1.62	88.09	0.58	36.78	-32.97	44.08	-1.00	-0.34	29.92
L116	0.19	8.32	70.09	0.60	37.61	-80.19	31.87	-6.71	-1.37	29.28
L117	0.29	5.45	75.74	0.63	38.86	-82.28	34.67	-3.46	-1.22	29.19
L118	0.36	5.84	72.88	0.60	37.61	-121.62	42.44	-2.86	-0.88	45.72
L119	0.46	22.53	63.25	0.64	39.25	-245.53	48.87	-5.59	-1.07	36.42
L120	0.16	12.78	75.66	0.63	38.86	-110.90	45.45	0.02	0.31	82.70
L121	0.22	4.65	80.39	0.64	39.05	-81.69	53.75	-1.04	-0.25	44.28
L122	0.07	5.35	80.24	0.60	37.62	-66.73	23.79	-0.50	-0.13	34.69
L123	0.10	10.84	74.97	0.62	38.39	-103.14	14.75	-4.31	-0.40	31.67
L124	0.10	2.91	79.99	0.64	39.21	-73.26	44.00	-0.93	-0.12	35.87
L125	0.11	1.36	80.51	0.60	37.78	-69.47	53.67	-0.93	-0.52	26.53
L126	1.20	91.16	50.31	0.65	39.62	-725.25	42.20	-99.42	-2.14	57.86
L127	0.14	5.88	76.79	0.63	38.89	-102.70	50.01	3.07	3.07	218.73
L128	0.16	1.60	84.92	0.67	40.14	-53.97	48.60	-0.83	-0.25	25.47
L129	0.10	1.62	84.24	0.63	38.81	-57.03	40.42	-0.90	-0.75	25.65
L130	0.20	2.85	81.94	0.62	38.52	-73.83	51.18	-3.31	-1.36	26.19
L131	0.19	7.49	75.31	0.63	38.92	-90.07	48.14	-3.17	-0.61	32.21
L132	0.73	50.51	55.93	0.66	39.92	-436.08	38.79	-16.33	-1.47	61.00
L133	0.09	11.30	70.10	0.63	38.70	-90.82	21.80	0.96	1.06	169.29
L134	0.49	58.66	46.36	0.65	39.52	-262.51	11.97	-7.11	-0.81	45.79

APPENDIX 11

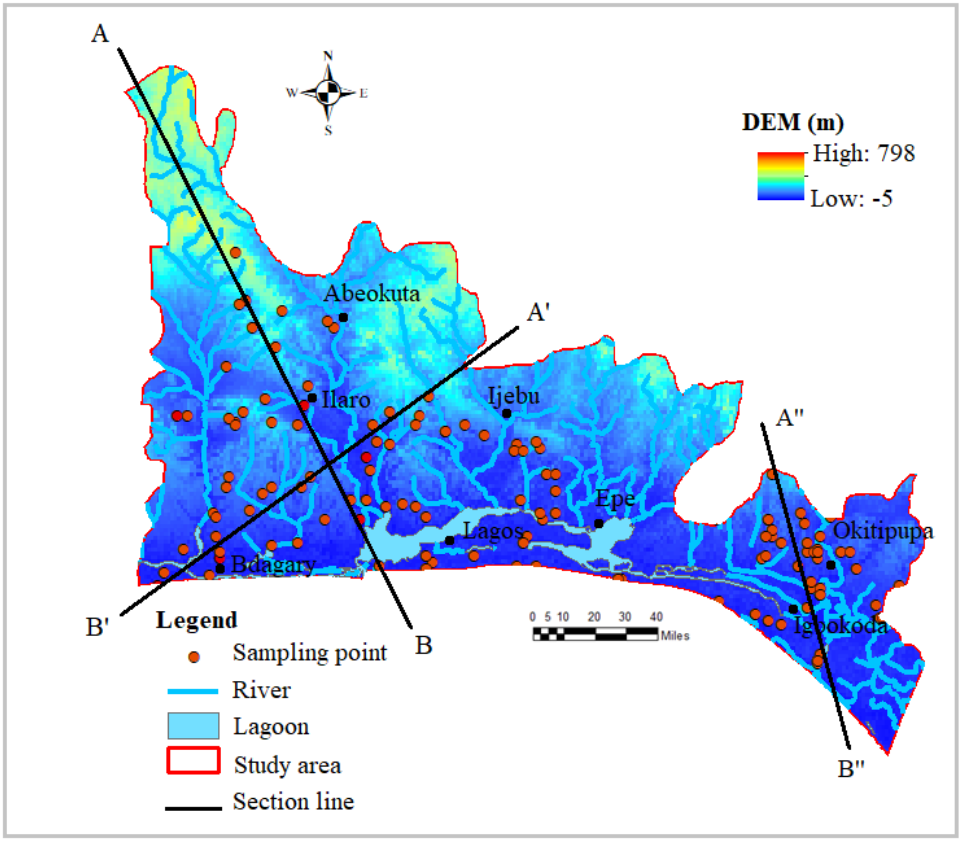

Digital elevation map of the study area

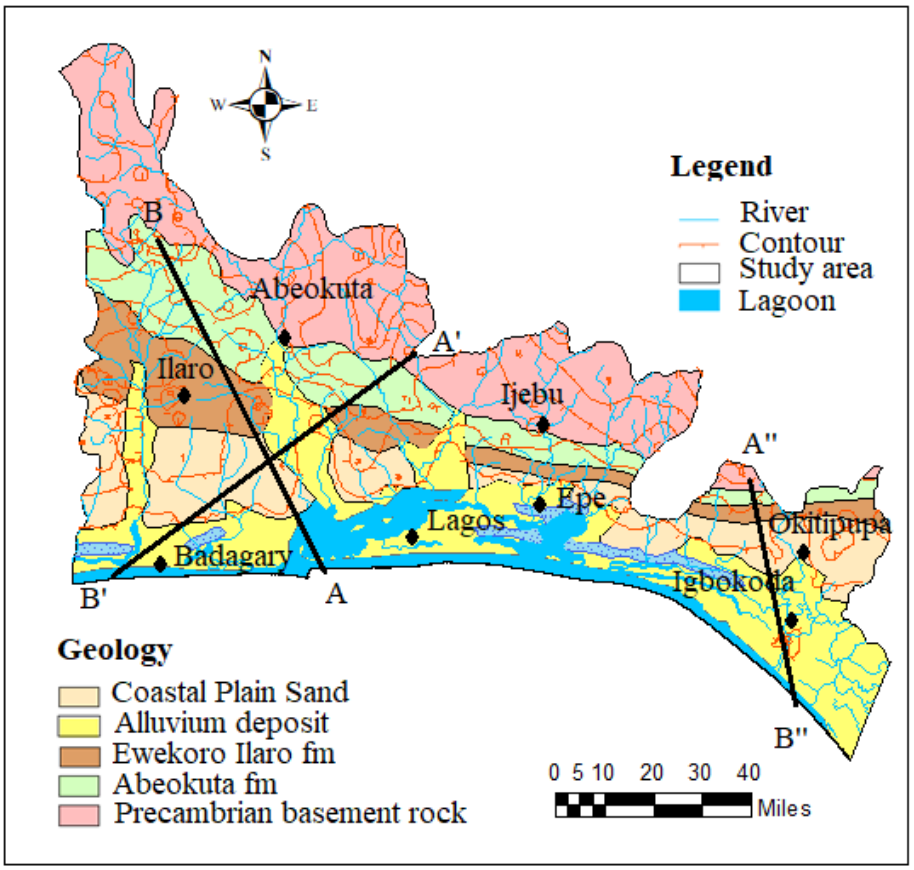

Geology map of the study area with cross section lines

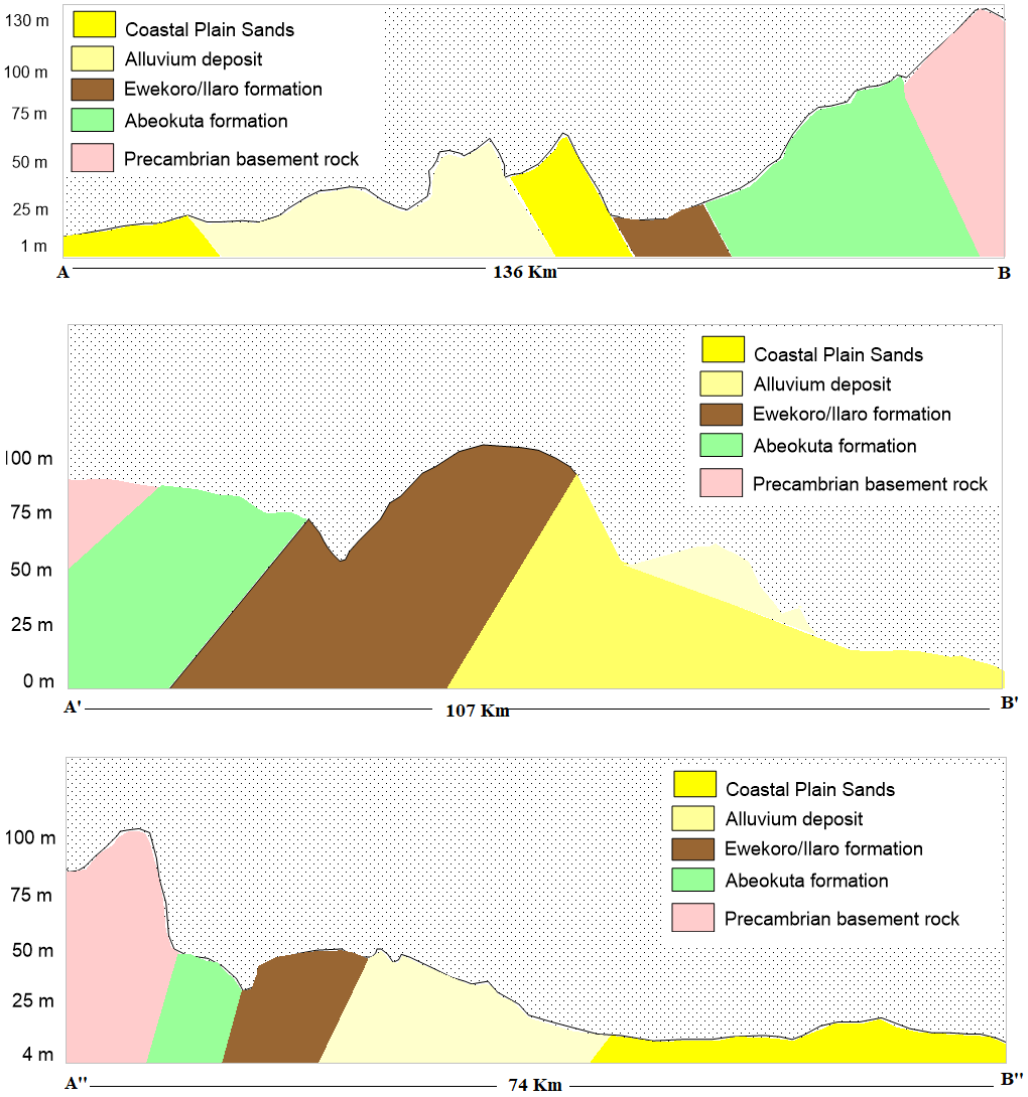

Geology profile along the three lines of cross section

APPENDIX 12

Selected Gamma and resistivity Borehole logs

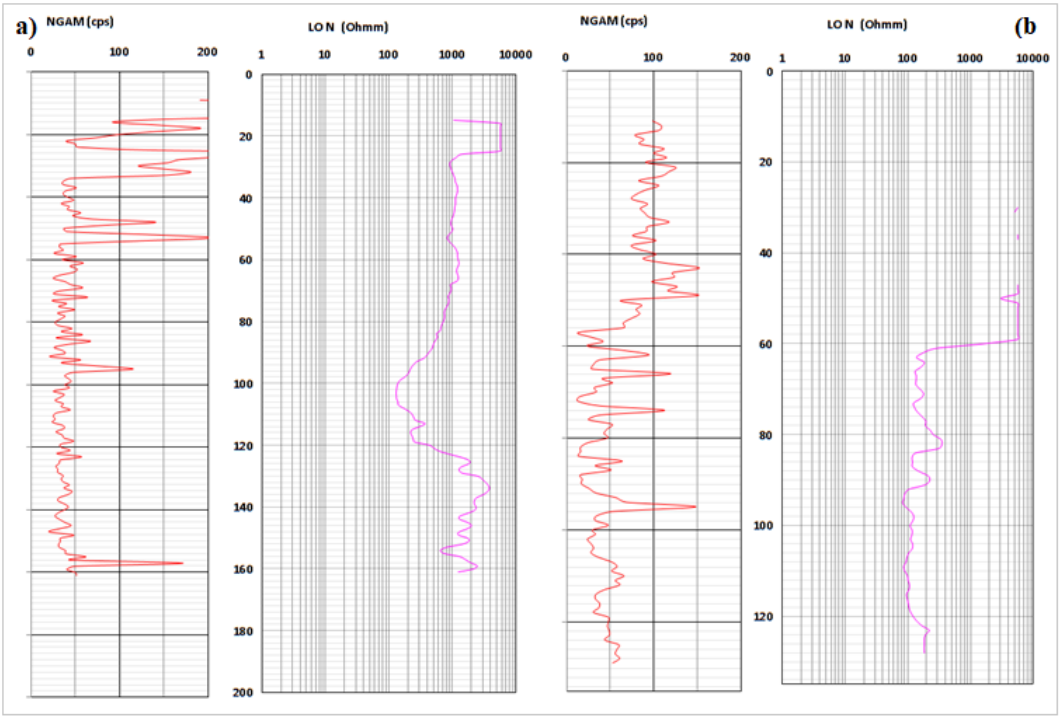

Gamma and resistivity logs (a) Ijebu-Ode (a) NBL Shagamu

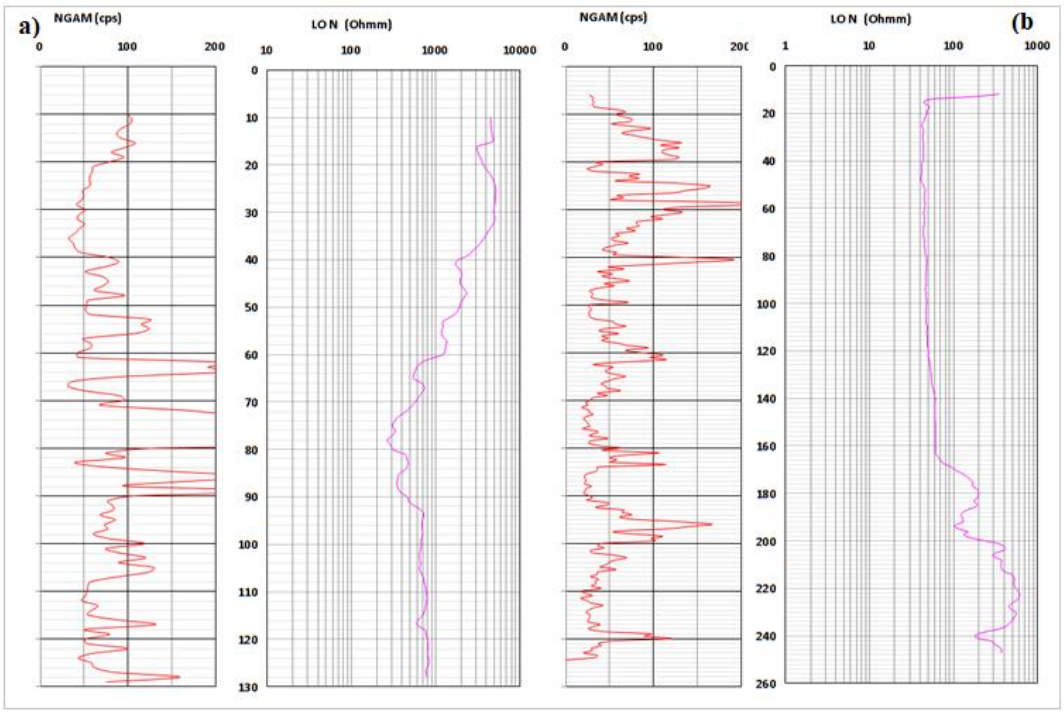

Gamma and resistivity logs (a) Unity Estate (a) Ibeju-Lekki

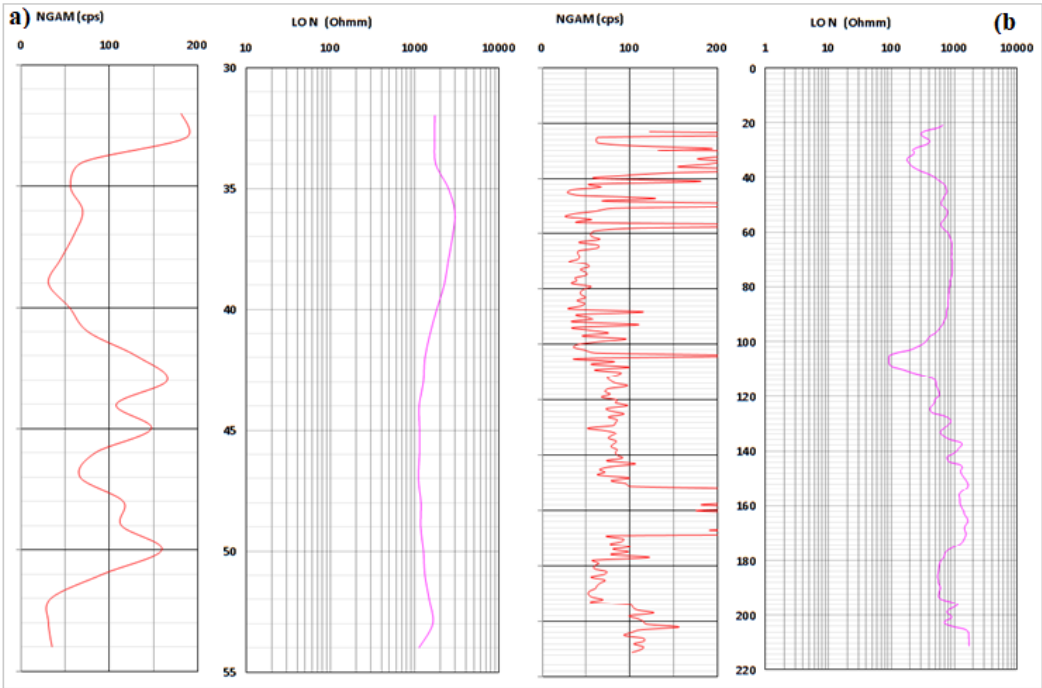

Gamma and resistivity logs (a) NBL Ijebu Ode (a) Ibeju-Lekki